The Relationship Between Hypoxia, Hypoxia Gene Signature and Survival in Patients with Breast Cancer

Suad A. K. Shamis
M.B.B.S, MRes

Submitted in fulfilment of the requirements for the degree of doctor of PhD

School of medicine, College of Medical, Veterinary and Life of Sciences, University of Glasgow

(March 2023)

Author's Declaration

The work presented in this thesis was performed entirely by the author except where acknowledged. This thesis has not been previously submitted for a degree or diploma at this or any other institution.

Suad Shamis
March 2023

Acknowledgement

When I started my PhD four years ago, I underestimated how challenging it would be, both scientifically and personally. I'd like to take this opportunity to thank the many people who have helped me get to this stage.

Firstly, I would like to thank my supervisors, Prof. Donald C. McMillan, and Prof. Joanne Edwards, who have been a cornerstone in my support system. I could always count on them to keep me focused and motivated. I really appreciated them giving me this opportunity and putting their trust in me. Thank you for your advice, patience, understanding and for just caring.

I am also very grateful to Dr Antonia Roseweir for providing valuable guidance and to Dr Elizabeth Mallon and Jennifer Hay, who marked the tumour areas and constructed the tissue microarray, and Hannah Morgan who patiently scanned literally hundreds of slides into NDP to analyse.

Additional thanks must go the members of Professor Edwards' team, specially to Dr Gerard Lynch, Phimmada Hatthakarnkul, Molly McKenzie and Holly Leslie for their assistance with bioinformatics, Sara Al-Badran, Chris Bigley and Hannah Hayman for their help with digital pathology and Dr Kathryn Pennel for help with lab work. I could not have wished for a better team. I would also like to thank Dr Ditte Andersen from BioClavis for help with the TempO-Seq.

Many thanks to all my family and friends here in Glasgow and in Libya for being there when I needed them and providing much needed distraction.

I gratefully acknowledge the financial support from Libyan Government and Libyan Cultural Affairs Bureau.

Thesis Summary

Breast cancer is the most frequently diagnosed cancer in women in the UK. It is a heterogenous disease with subtypes which behave differently. Although several targeted therapies have been approved for patients with oestrogen receptor (ER) positive and Her-2 positive breast cancer, chemotherapy remains the standard systemic option for triple negative breast cancer (TNBC) patients. New prognostic tools for risk stratification and to guide use of the most aggressive treatments and new targeted therapies are desirable. The role of the tumour microenvironment (TME) in tumour progression is increasingly recognised. Features of the TME such as hypoxia have been reported to have a prognostic role in cancer. A better understanding of this feature may lead to identification of new prognostic and predictive tools and of new therapeutic targets for TNBC.

The work of this thesis is carried out in three cohorts of patients with primary operable breast cancer and mature follow up. Data was available from clinical records regarding patient age, tumour pathology, treatment details and survival. Several hypoxic markers have been investigated and were reported to be overexpressed in breast cancer tissue.

The aim of the current study was to investigate the role of hypoxia inducible factors [HIF-1α (1), HIF-1α (2), HIF-2α] and carbonic anhydrases IX (CAIX) in different breast cancer subtypes, to establish biological processes, and key pathways related to cytoplasmic CAIX expression in ER-negative and a node negative subset of ER-negative breast cancer patients, and to identify the mRNA signature associated with CAIX within the tumour and stromal compartments in TNBC.

Immunohistochemistry (IHC) was employed on a tissue microarray (TMA) of patients with breast cancer to assess the expression of HIF-1α (1), HIF-1α (2), HIF-2α and CAIX. Clinical outcomes for the marker's expression were estimated using Kaplan-Meier analysis and compared between groups with the log-rank test. In a cohort of mixed breast cancer subtypes, the expression of cytoplasmic HIF-1α (1), and HIF-2α were only associated with poor overall survival (OS) in luminal A tumours ($P = 0.009$), and poor recurrence free survival (RFS) in Her-2 disease ($P = 0.038$), respectively. However, regardless of cellular localisation, high CAIX expression was associated with poor outcome for the full cohort and in breast cancer subtypes. High cytoplasmic CAIX was associated with decrease RFS in the full cohort ($P<0.001$), and in luminal B tumours ($P = 0.025$), disease-free survival (DFS) in the full cohort ($P<0.001$) in luminal B tumours ($P = 0.035$), and Her-2 disease ($P = 0.016$). Also, high cytoplasmic CAIX was associated with poor OS in the full cohort ($P<0.001$) and

in Her-2 disease (P = 0.001). Moreover, membranous CAIX was associated with decrease RFS (P<0.001), DFS (P = 0.004), and OS (P = 0.003) in the full cohort. In multivariate analysis, cytoplasmic CAIX was an independent prognostic factor for RFS in the entire cohort (HR = 2.24, 95% CI: 1.19–4.22, P = 0.012), DFS in the full cohort (HR = 1.74, 95% CI: 1.08–2.82, P = 0.023) and in luminal B disease (HR = 3.59, 95% CI: 1.23–10.53, P = 0.020), and OS in Her-2 disease (HR = 4.19, 95% CI: 1.37–12.80, P = 0.012).

Furthermore, in the cohort of ER-positive breast cancer, high cytoplasmic HIF-1α (1) expression was associated with shorter DFS (P = 0.032), and OS (P = 0.002) in the full cohort. In addition, high nuclear HIF-1α (1) expression was associated with decrease DFS in the full cohort (P = 0.009) and in luminal A disease (P = 0.013), and OS in the full cohort (P = 0.002) and in luminal A tumours (P = 0.003). Moreover, high cytoplasmic CAIX expression was corelated with worse RFS and DFS in the full cohort (P = 0.014, 0.008, respectively) and with RFS, DFS, and OS in luminal B disease (P = 0.018, 0.001, 0.003, respectively). On multivariate Cox regression analysis, nuclear HIF-1α (1) was an independent prognostic marker for DFS in the full cohort (HR = 1.85, 95% CI: 1.10–3.11, P = 0.019), and in luminal A disease (HR = 1.98, 95% CI: 1.02–3.83, P = 0.042), and for OS in the full cohort (HR = 1.85, 95% CI: 1.08–3.19, P = 0.026), and in luminal A disease (HR = 2.08, 95% CI: 1.11–3.89, P = 0.022). Moreover, high cytoplasmic CAIX expression was an independent prognostic marker for RFS and DFS in the full cohort (HR = 2.09, 95% CI: 1.17–3.75, P = 0.013; HR = 1.74, 95% CI: 1.08–2.82, P = 0.023), and in luminal B disease (HR = 2.57, 95% CI: 1.29–5.12, P = 0.007; HR = 2.75, 95% CI: 1.66–4.55, P<0.001), respectively.

In TNBC cohort, high cytoplasmic expression of CAIX had lower RFS (P = 0.038). Multivariate analysis showed that cytoplasmic CAIX remained as factor contributing significantly to RFS (HR = 6.59, 95% CI: 1.47–29.58, P = 0.014).

Next, Templated Oligo assay with Sequencing readout (TempO-Seq) (bulk RNAseq) was carried out in ER-negative and a node negative subset of ER-negative breast cancer patients to identify gene signatures that associated with CAIX expression to provide further information on biological processes, and key pathways related to cytoplasmic CAIX expression. Whole transcriptome analysis using TempO-Seq identified 10 significant genes within ER-negative cohort (OR8B2, SERHL2, KRT6A, MMP7, SPINK8, TMEM150C, CEACAM6, MUCL1, PITX2, and GALNT6), and 3 genes in node negative group

(PCSK1N, SERHL2 and SPNS2). In node negative patients SPNS2 was of particular interest.

Further, GeoMx Digital Spatial Profiler (DSP) analyses in TNBC cohort was performed to inform if gene signatures were associated with tumour epithelia or TME. 3 upregulated gene expression signatures, CD68, HIF1A, VSIR, and one down-regulated gene, pan-melanocyte, were identified in tumour compartment. In contrast, 9 downregulated genes, CD86, CD3E, MS4A1, BCL2, CCL5, NKG7, PTPRC, CD27 and FAS were identified in the TME in comparison of high and low CAIX expression groups. Among all 4 selected genes, HIF-1α, BCL2, CD68, and CD3, were further validated by IHC at protein level. Univariate Kaplan-Meier analysis showed high expression of CD68 and HIF-1α was associated with poor prognosis and high expression of BCL2 and CD3 was associated with good prognosis. By performing multivariate analysis for OS, high levels of CD68 cells in tumour nests and in TME were independent prognostic factor for poorer OS (HR = 2.42, 95% CI: 1.05−5.59, P = 0.038; HR = 3.34, 95% CI: 1.28−8.69, P = 0.014), respectively.

In conclusion, this thesis has demonstrated a prognostic role of nuclear HIF-1α (1) and cytoplasmic CAIX in breast cancer. However, their prognostic values were different depending on cellular locations and tumour subtypes. Furthermore, TempO-Seq identified the pathways and genes associated with the CAIX in ER-negative breast cancer. Then, GeoMx DSP technology identified stromal/immune-related genes that were associated with TNBC patients' survival in comparison of high and low CAIX expression groups that might serve as a potential prognostic biomarker for TNBC.

Overall, the results from this thesis provide new evidence to warrant the further investigation of HIF-1α (1) and CAIX in a large contemporaneous cohort of patients with breast cancer and in particular in patients with TNBC.

Publications and Presentations

Publications relating to this thesis

Shamis, S.A., McMillan, D.C. and Edwards, J., 2021. The relationship between hypoxia-inducible factor 1α (HIF-1α) and patient survival in breast cancer: Systematic review and meta-analysis. Critical reviews in oncology/hematology, 159, p.103231.

Shamis, S.A., Quinn, J., Mallon, E.E., Edwards, J. and McMillan, D.C., 2022. The relationship between the tumor cell expression of hypoxic markers and survival in patients with ER-positive invasive ductal breast cancer. Journal of Histochemistry & Cytochemistry, 70(7), pp.479-494.

Shamis, S.A., Edwards, J. and McMillan, D.C., 2023. The relationship between carbonic anhydrase IX (CAIX) and patient survival in breast cancer: systematic review and meta-analysis. Diagnostic Pathology, 18(1), pp.1-16.

Accepted. Shamis, S.A., Savioli, F., Ammar, A., Al-Badran, S. S.F., Hatthakarnkul, P., Leslie, H., Mallon, E., Jamieson, N. B., McMillan, D. C. and Edwards, J. (2023) Spatial transcriptomic analysis of tumour with high and low CAIX expression in TNBC tissue samples using GeoMx™ RNA assay. Histology and Histopathology: Cellular and Molecular Biology.

Submitted to Journal of Cancer Medicine. Suad A. K. Shamis, Jean A Quinn, Sara SF Al-Badran, Molly McKenzie, Phimmada Hatthakarnkul, Gerard Lynch, Laszlo Romics, Ditte Andersen, Elizabeth A Mallon, Donald C McMillan, and Joanne Edwards. Differential gene expression profiles associated with CAIX expression in patients with ER-negative breast cancer.

Poster presentations

Suad A. K. Shamis, Elizabeth Mallon, Joanne Edwards, Donald C. McMillan. The role of hypoxic markers in predicting survival in patients with early-stage invasive breast cancer.

6th Edition-Webinar on Breast Cancer, USA, March 2021.

Suad A. K. Shamis, Elizabeth Mallon, Joanne Edwards, Donald C. McMillan. The role of hypoxic markers in predicting survival in patients with early-stage invasive breast cancer. SoMDN PG Research Day, University of Glasgow, UK, May 2021.

Suad A. K. Shamis, Elizabeth Mallon, Joanne Edwards, Donald C. McMillan. The role of hypoxic markers in predicting survival in patients with early-stage invasive breast cancer. International PhD Student Conference Europe, University of Glasgow, UK, Jun 2021.

Table of Contents

List of Tables

List of Figures

Definitions/Abbreviations

AOI	Area of illumination
AR	Androgen receptor
ARNT	Aryl hydrocarbon receptor nuclear translocator
ASC	Adipose tissue-derived stem cells
AUC	Area under the ROC curve
α-SMA	α-smooth muscle actin
BBD	Benign breast disease
BC	Breast cancer
BCL2	B-cell lymphoma-2
bHLH	basic helix-loop-helix
BMI	Body mass index
BL1	Basal-like type 1
BL2	Basal-like type 2
BLBC	Basal-like breast cancer
BRCA1	Breast cancer type 1
BRCA2	Breast cancer type 2
BSA	Bovine serum albumin
BT	Bicarbonate transporters
CA	Carbonic anhydrase
CAF	Cancer associated fibroblast
CAIX	Carbonic anhydrase IX
CBP	CREB binding protein
CCL5	C-C motif chemokine ligand 5
CD3	Cluster of differentiation 3
CD8	Cluster of differentiation 8
CD27	Cluster of differentiation 27
CD68	Cluster of differentiation 68
CD86	Cluster of differentiation 86
CEACAM6	Carcinoembryonic antigen cell adhesion molecule 6
CI	Confidence interval
Co^{2+}	Cobalt
$CoCl_2$	Cobalt chloride
CRUK	Cancer research UK
CT	Chemotherapy

DAB 3	3'-diaminobenzidine
DEGs	Differentially expressed genes
DFS	Disease-free survival
DNA	Deoxyribonucleic acid
DO	Detector oligonucleotides
DSP	Digital Spatial Profiler
EC	Endothelial cell
ECM	Extracellular matrix
EDTA	Ethylenediamine tetra-acetic acid
EGFR	Epidermal growth factor receptor
EMT	Epithelial mesenchymal transition
EndoMT	Endothelial mesenchymal transition
ER	Oestrogen receptor
ERα	Oestrogen receptor α
FBP1	Fructose 1,6-bisphophatase
FBS	Fetal bovine serum
FDR	False discovery rate
FFPE	Formalin-fixed paraffin-embedded
FIH-1	Factor inhibiting HIF-1
GALNT6	Polypeptide N-acetyl galactosaminyl transferase 6
Glut-1	Glucose transporter 1
GM-CSF	Granulocyte-macrophage colony-stimulating factor
GO	Gene ontology
H&E	Haematoxylin and Eosin
HeLa	Henrietta Lacks
Her-2	Human epidermal growth factor receptor 2
HIER	Heat induced epitope retrieval
HIF-1α	Hypoxia inducible factor-1α
H_2O_2	Hydrogen peroxide
HR	Hazard ratio/Hormone receptor
HREs	Hypoxia response elements
HRP	Horse radish peroxidase
HRT	Hormone replacement therapy
IC	Intracytoplasmic
ICCC	Interclass correlation coefficient

IFN-γ	Interferon-γ
IHC	Immunohistochemistry
IL-6	Interleukin-6
IL-8	Interleukin-8
IL-10	Interleukin-10
IM	Immunomodulatory subtype
IV	Inverse variance
KEGG	Kyoto Encyclopedia of Genes and Genomes
KRT6A	Keratin 6A
LAR	Luminal androgen receptor
LDH-A	Lactate dehydrogenase A
LN	Lymph node
Log2 FC	Logarithm base 2-fold change
LOX	Lysyl oxidase
LOXL	LOX-like proteins
LPA2	Lysophosphatidic acid receptor 2
Lum A	Luminal A
Lum B	Luminal B
LVD	Lymphatic vessel density
LVI	Lymphovascular invasion
M	Mesenchymal
mAbs	Monoclonal antibodies
MAI	Mitotic activity index
MAPK	Mitogen-activated protein kinase
MCT	Mono-carboxylate transporter
MDSC	Mesenchymal derived stem cell
MMP7	Matrix metalloproteinase 7
MS4A1	Membrane spanning 4-domains A1
MSCs	Mesenchymal stem cells
MSL	Mesenchymal stem-like
MUCL1	Mucin like 1
MV	Multivariate analysis
MVD	Microvessel density
NAC	Neoadjuvant chemotherapy
NAF	Normal tissue derived fibroblast

NHERF1	Na+/H+ exchanger regulatory factor 1
NHG	Nottingham histological grade
NK	Natural killer
NKG7	Natural killer cell granule protein 7
NLSs	Nuclear localization signals
NPI	Nottingham prognostic index
NRF2	Nuclear factor erythroid 2-related factor 2
OCs	Oral contraceptives
ODD	Oxygen-dependent degradation domain
OR8B2	Olfactory receptor family 8 subfamily B member 2
OS	Overall survival
OXPHOS	Oxidative phosphorylation
Padj	Adjusted P value
PanCK	Pan-cytokeratin
PARP	Poly-ADP-ribose polymerase
PBS	Phosphate buffered saline
PC	Principal component
PCA	Principal component analysis
PCR	Polymerase chain reaction
pCR	pathological complete response
PCSK1N	Proprotein convertase subtilisin kexin type 1 inhibitor
PD1	Programmed death protein 1
PDL1	Programmed death ligand 1
PFA	Paraformaldehyde
PG	Proteoglycan
PHD	Prolyl hydroxylase
PI3K	Phosphoinositide 3 kinase
PITX2	Paired like homeodomain 2
PPI	Protein-protein interaction
PR	Progesterone receptor
PTPRC	Protein tyrosine phosphatase receptor type C
PVDF	Polyvinylidene fluoride
PVI	Peritumoural vascular invasion
QC	Quality control
RevMan	Review Manager

RFS	Recurrence free survival
RNA	Ribonucleic acid
ROC	Receiver operating characteristic curve
ROI	Region of interest
ROS	Reactive oxygen species
RPM	Revolutions per minute
SDF-1	Stromal cell derived factor 1
SERHL2	Serine hydrolase-like protein 2
SphK1	Sphingosine kinase 1
S1P	Sphingosine 1-phosphate
SPINK8	Serine peptidase inhibitor kazal type 8
SPNS2	Sphingolipid transporter 2
STAR	Spliced transcripts alignment to reference
STAT1	Signal transducer and activator of transcription 1
STRING	Search Tool for the Retrieval of Interacting Genes
STWS	Scott's Tap Water Substitute
TAD	Transactivation domains
TAMs	Tumour-associated macrophages
TB	Tumour budding
TBS	Tris-buffered saline
TBST	Tris-buffered saline plus Tween
TempO-Seq	Templated Oligo-Sequencing
TGF-β	Transforming growth factor-β
TH	T helper
TEMs	TIE2-expressing monocytes
TIL	Tumour infiltrating lymphocyte
TM	Transmembrane
TMAs	Tissue microarrays
TME	Tumour microenvironment
TMEM150C	Transmembrane protein 150C
TNBC	Triple negative breast cancer
TNF-α	Tumour necrosis factor-α
TNM	Tumour, Node, Metastasis
TOP2A	Topoisomerase II-alpha
TRS	Target retrieval solution

TSP	Tumour stroma percentage
3′UTR	3' untranslated region
UV	Univariate analysis/ Ultraviolet
UVQ	UltraVision Quanto
VEGF	Vascular endothelial growth factor
VHL	von Hippel Lindau
VSIR	V-Set immunoregulatory receptor
WCRF/AICR	World Cancer Research Fund/American Institute for Cancer Research

Chapter 1 Introduction

Cancer can be considered as heterogeneous diseases that cause a breakdown in the homeostatic mechanisms that control cell growth and division with the potential to metastasize to distant organs in the body and cause death (1). Breast cancer mainly affects the lobules (milk producing glands) and milk ducts of breast tissue which carry milk to the nipples. Figure 1.1 shows a normal human mammary tissue and structure breaks down in breast cancer.

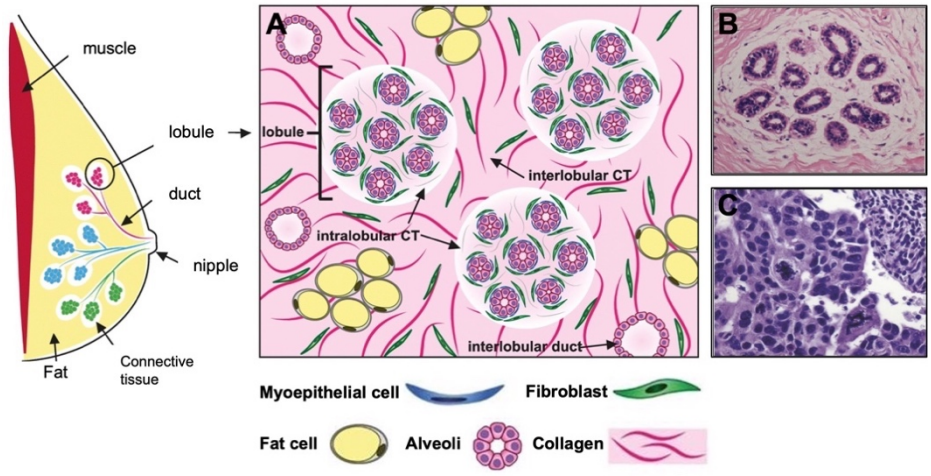

Figure 1.1 Schematic model of normal and malignant human breast tissue.

Anatomy of female breast. Normal breast tissue consisting of lobes, each lobe containing a series of branched ducts that drain into the nipple [A], histopathology of normal tissue shows multiple acini embedded in the stroma with uniform oval nuclei [B], histopathology of invasive breast cancer shows highly pleomorphic nuclei and structure breaks down [C]. Adapted from (2, 3).

1.1 Breast cancer epidemiology

1.1.1 Breast cancer incidence, mortality, and survival

Breast cancer is one of the most life-threatening diseases in women (4). 2.3 million new breast cancer cases were recorded globally in 2020, with a third of them ending in death, making it the second cause of death in women (5), with 1,898,160 new cases and 608,570 deaths projected in the United States by the end of 2021 (6). In the United Kingdom, breast cancer remains the most frequent cancer in women, with an estimated 54,700 new cases in 2017 (7). Over the last decade, the death rate from breast cancer has decreased by 21% in the UK. Screening mammography, advances in surgical techniques, radiation therapy, and systemic therapies for breast cancer have contributed to this decline by increasing 5-year survival rate (8, 9).

1.2 Molecular subtypes of breast cancer

Based on the gene expression profile of biological markers, breast cancer has been classified into four molecular subtypes: luminal A, luminal B, Her-2 enriched, and triple negative (TN) or basal like (10).

1.2.1 Luminal A breast cancer

Luminal A is the most common subtype and comprises around 30−70% of all breast cancer. This disease has a high expression of luminal epithelial genes, oestrogen receptor (ER), progesterone receptor (PR), and low expression of human epidermal growth factor receptor-2 (Her-2) or low ki67 proliferation index (<15%) (11). It is identified as low histological grade, low degree of nuclear pleomorphism, and low mitotic activity (12). Luminal A tumours generally have a good prognosis and respond well to hormone/endocrine treatment (13). The relapse rate is significantly lower than the other subtypes (14) (Table 1.1).

1.2.2 Luminal B breast cancer

Luminal B tumours comprise 10−20% of breast cancers. They are identified as Her-2-positive or Her-2-negative with high ER, PR, and ki67 (>15%) expression (11). Her-2-positive luminal B tumours are associated with a worse overall outcome than luminal B tumours that are Her-2-negative (11) (Table1.1). Compared to luminal A, luminal B tumours have more aggressive phenotype, higher histological grade, mitotic activity and have worse prognosis (15). However, in comparison to all the subtypes, luminal B tumours have intermediate prognosis (13, 16). Because this subtype is more proliferative, treatments that involve both hormonal and chemotherapy will be beneficial (11). If the tumour expresses Her-2, an anti-Her-2 therapy will be an effective measure as well (11, 16).

1.2.3 Human epidermal growth factor receptor-2 (Her-2)

Approximately 5−15% of breast cancers worldwide exhibit amplification and/or overexpression of the Her-2 gene (also known as ERBB2). Her-2-Enriched tumours generally exhibit high expression of Her-2 and are negative for luminal epithelial genes (non-luminal) (11) (Table 1.1) Her-2 positivity confers more aggressive biological and clinical behaviour. These tumours are highly proliferative and are associated with high mitotic count, high tumour grade, and positive lymph nodes (17), and worse clinical outcomes (14). These

tumours respond poorly to chemotherapy (18) and endocrine therapy (19), but they are candidates for anti-Her-2 antibodies or small molecule inhibitors (16).

1.2.4 Triple negative breast cancer (TNBC)/Basal-like breast cancer (BLBC)

TNBC subtype represents from 15−20% of all breast cancers. TNBC is clinically defined as a type of breast cancer with negative expression of the three commonly targeted biomarkers, ER, PR, and Her-2 (20) (Table 1.1). It is associated with high histological and nuclear grade, poor tubule formation, presence of central necrotic or fibrotic zones, high proliferative index, and conspicuous lymphocytic infiltrate. Most of these tumours are infiltrating ductal tumours with aggressive clinical behaviour and high rate of metastasis to the brain and lung (21). Therefore, is considered an interesting and challenging topic for breast cancer research. Chemotherapy is the recommended treatment for TNBC (11).

It is important to clarify that the terms TNBC and basal-like breast cancer (BLBC) are not entirely synonymous and there is a difference of about 20−30% across studies. The term TN refers to the immunohistochemistry (IHC) classification of breast tumours lacking ER, PR and Her-2 protein expression while the basal-like breast cancer (BLBC) is defined by a distinct gene expression signature characterized by strong expression of basal markers such as cytokeratin. Gene expression analysis often classifies TNBC as a subtype of BLBC. Approximately 80% of TNBCs are classified as BLBC, and about 80% of BLBC are ER-negative/Her-2-negative (22) (Figure 1.2). The basal-like classification is available only in the research setting to date and thus the TN phenotype currently is a reliable surrogate in the clinical setting (23).

All these subtypes of breast cancer have shown significant differences in their risk factors (24), different natural histories (25) and diverse responses to targeted therapies, endocrine therapy, Her-2 targeted therapy and chemotherapy (26).

Table 1.1 Subtypes of breast cancer based on routine IHC markers

Intrinsic subtype		Clinicopathologic surrogate definition	Frequency	Outcome	Treatment
Luminal A		ER and PR+, Her-2−, low Ki67 (<15%)	30–70%	Good	Endocrine therapy alone or with chemotherapy
Luminal B	Her-2−	ER and PR+, Her-2−, high Ki67 (>15%)	10–20%	Intermediate	Endocrine therapy and chemotherapy
	Her-2+	ER and PR+, Her-2+, any Ki67		Poor	Anti-Her-2 therapy
Her-2 enriched		ER and PR−, Her-2+	5–15%	Poor	Chemotherapy and anti-Her-2 therapy
Triple negative breast cancer		ER, PR, and Her-2−	15–20%	Poor	Chemotherapy

Table outlining the subtypes of breast cancer and relative frequency, prognosis, and treatment of each subtype (13, 16).

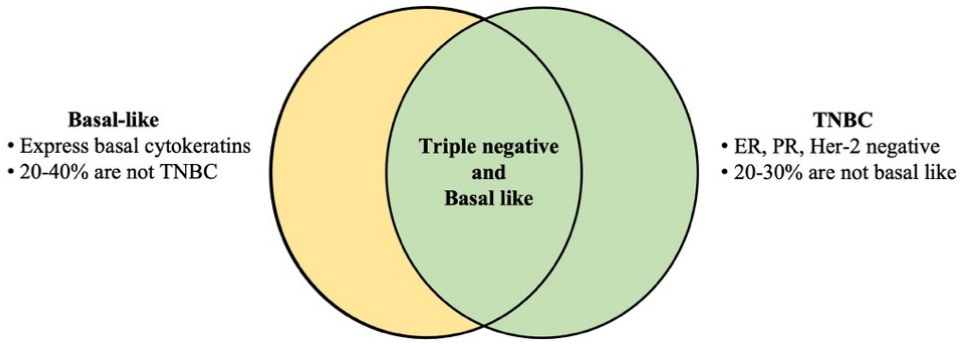

Figure 1.2 Diagram showing the relationship between the TNBC and the basal-like molecular subtype.

One fourth of TNBCs are not basal-like by gene expression, and some non TNBCs are BLBC by molecular profiling. Adapted from (27).

1.3 Triple negative breast cancer

1.3.1 Clinicopathological characteristics of TNBC

TNBC develops early, is diagnosed more often in premenopausal women and has a higher prevalence in the African American population (28). TNBC has early onset, large tumour size, high proliferative index, and high density of lymphocytic infiltrate (28, 29). TNBC is highly invasive with high lymph node metastasis rate (30), and distant metastasis mainly involves the brain and visceral organs which mostly occurs in the 3rd year after diagnosis (31). Once metastasis occurred, the sensitivity to chemotherapy was dramatically decreased, and the median survival time was reduced to less than 6 months (32). TNBC patients have high clinical stage and high recurrence rate (28). After recurrence, TNBC patients have short survival (30).

1.3.2 Classification of TNBC

1.3.2.1 Histological classification

82–90% of TNBC were histologically defined as invasive ductal carcinoma. Within TNBC there are numerous other and mostly rare histological types including less aggressive subtypes; lobular (5%), metaplastic (4%), medullary (2.3%), apocrine (1.6%), papillary (1.4%), neuroendocrine (0.9%), cribriform (0.5%) and mucinous (0.5%) (33). In different histological subtypes, 35% had lymph node involvement (34) which exhibits distinct prognosis of TNBC (35). Medullary and apocrine types had excellent prognosis while

lobular TNBC had the worst prognosis (33). TNBC patients with invasive ductal carcinoma and invasive lobular carcinoma predicted poorer overall survival (OS) (36).

1.3.2.2 Molecular classification

To better demonstrate TNBC-specific tumour heterogeneity, Lehmann et al. (37) used gene expression profiling to subclassify TNBC into six molecular subtypes, each displaying unique ontologies and differential response to standard-of-care chemotherapy. The TNBC subtypes include two basal-like (BL1 and BL2), mesenchymal (M), mesenchymal stem-like subtype (MSL), immunomodulatory subtype (IM) and luminal androgen receptor subtype (LAR). The gene expression patterns of each TNBC subtype are listed in Table 1.2.

Table 1.2 Gene expression in different subtypes of TNBC

Subtypes of TNBC (%)	Gene expression
BL1 (10%)	Proliferation-related genes DNA damage response genes
BL2 (20%)	Growth factor signalling related genes Cell growth factor receptor related genes
M (20%)	Cell differentiation pathways related genes Epithelial mesenchymal transition (EMT) related genes
MSL (10%)	Growth factor signalling pathways Cell differentiation and stem cells related genes Mesenchymal stem cell-specific markers EMT and angiogenesis related genes
IM (20%)	Immune cell signalling related genes
LAR (10%)	Hormonally regulated mediated by androgen receptor (AR)

Data from Lehmann (37).

TNBC subtypes display different clinical characteristics with BL1 subtype displaying higher grade, lower stage, and increased patient survival. TNBC subtypes displayed different patterns of progression with patients with LAR subtype having increased bone metastasis while M tumours preferentially metastasize to lung. Clinical differences were complimented by histological differences, with lobular carcinomas exclusive to the LAR subtype and metaplastic carcinomas either M or BL2. Each subtype differed in their response to standard neoadjuvant chemotherapy, with BL1 tumours displaying the greatest probability of achieving a pathological complete response (pCR) (38). Indeed, research has shown that AR

could be a promising therapeutic target. However, AR phosphorylation rather than total AR expression would present new population of tumours appropriate for anti-androgen therapy (39).

1.3.3 TNBC risk factors

Although approximately half of the women with breast cancer have no known risk factors beyond female sex and increasing age, several well-established risk factors that have been found to increase the risk of TNBC.

1.3.3.1 Age at diagnosis

Besides being female, age is the commonest risk factor for breast cancer. In general, it is a disease of ageing, with the highest incidence rates in older women (40). However, TNBC constitutes a clinically challenging subtype of breast cancer that occurs more frequently in younger women <50 years (30).

1.3.3.2 Family history and genetic predisposition

Up to 10% of women who develop breast cancer in Western countries have a hereditary predisposition, including mutations in the breast cancer susceptibility genes BRCA1 and BRCA2 (41). TNBCs with germline BRCA1/2 mutations are detected in 10–20% of patients with early-stage TNBC (42). TNBC is more likely to be found in BRCA1 mutation carriers than BRCA2 carriers or those who are mutation negative (43). However, the association of BRCA2 mutations with TNBC has been also reported, with prevalence of mutations varying from 4 to 16%, depending on the patient population studied (44). BRCA1 mutation carriers tend to be younger at diagnosis than non-mutation carriers. A study in TNBC reported that the median age of diagnosis among BRCA1 carriers was 39 years old and that the prevalence of BRCA1 mutations among women diagnosed at age younger than 40 was 36% (45).

1.3.3.3 Hormonal factors

1.3.3.3.1 Endogenous hormones exposure

A long exposure to female reproductive hormones, particularly endogenous oestrogens increase the risk of developing TNBC as does early age at menarche and being younger age at first pregnancy (24). Among parous women, multiparity (the number of births) appears to increase the risk of TNBC (24, 41).

Breastfeeding has been most consistently associated with a lower risk of TNBC (46), and the greater protection is associated with longer duration. It has been estimated that breastfeeding for at least 4−6 months decreases the risk of TNBC among parous women (24, 47). Further, a pooled analysis in African American and white women that concluded 40−50% risk reductions correlated with breastfeeding for ≥12 months (48).

1.3.3.3.2 Exogenous hormones exposure

Oral contraceptives (OCs) may increase the relative risk of breast cancer in current users (49) due to their oestrogen content taken later in reproductive age (50). Recently, a systematic review and meta-analysis reported that women who use OCs have a high risk of TNBC compared with women who do not (51). OC use ≥1 year was associated with a 2.5-time increased risk of TNBC (52).

For ER-positive breast cancer, randomized controlled trials have showed an increased risk of breast cancer recurrence with hormone replacement therapy (HRT) use after successful primary treatment, leading to the premature termination of the trials (53). However, no significant negative effect of HRT in ER-negative subgroup (54).

1.3.3.4 Dietary and lifestyle factors

Lifestyle factors such as diet, alcohol consumption, obesity, and regular physical activity play an important role in the development of breast cancer. These significant modifiable breast cancer risk factors can change over time and are important for breast cancer prevention.

1.3.3.4.1 Type of diet

A significant association between an increased TNBC risk with increased consumption of animal fat (55) whereas patients with the highest intake of vegetable fat had a significantly lower TNBC risk than those with the lowest intake of vegetable fat. In addition, a positive association was found between risk of TNBC and the total consumption of red meat and eggs whereas intake of nuts and vegetables was negatively associated (55). Therefore, the World Cancer Research Fund/American Institute for Cancer Research (WCRF/AICR) recommends limiting the consumption of red and processed meats (56).

1.3.3.4.2 Alcohol consumption

Alcohol consumption is a well-established risk factor for breast cancer (57). Approximately 4% of breast cancer patients in developed countries are at least partially due to alcohol intake (58). The risk of TNBC significantly increased with alcohol intake (59). The mechanism for increased TNBC risk is unclear. Recently, Zhao et al. suggested that alcohol promotes TNBC progression through the induction of oxidative stress and the activation of NF-κB signalling (60).

1.3.3.4.3 Physical activity and obesity

Regular physical activity is associated with a considerably lower risk of breast cancer (61). Ma et al. (62) have shown that both long-term and baseline strenuous physical activity were inversely associated with TNBC. The physical activity reduces the exposure to endogenous sex hormones (63). An exercise-induced decrease in tumour hypoxia may affect the efficacy of immunotherapy (64).

Being overweight is now recognized to be one of the breast cancer risk factors and varies according to breast cancer subtype (65). Obesity has been implicated as a risk factor for the development of TNBC (66) that might be through chronic inflammation and secretion of inflammatory cytokines include IL-6, TNF-α, and leptin (67). Obesity has been also reported as a prognostic factor effect on poor survival in obese TNBC patients (66).

1.3.3.5 Benign breast disease (BBD)

Benign breast diseases can be classified into non-proliferative or proliferative disease (68). Only proliferative disease is associated with an increased breast cancer risk. Atypical hyperplasia has been shown to confer high risk for future breast cancer in studies with long-term follow-up (69), with an absolute risk of almost 1–2% per year of developing invasive breast carcinoma (70). With regards to racial-ethnic identity, the 10-year probability for developing TNBC following BBD was 0.56% for African Americans compared to 0.25% for white American patients (71).

Overall, risk factors of breast cancer are summarised in Table 1.3

Table 1.3 Summary of selected risk factors for breast cancer

Risk factor	High risk group hormonal dependent breast cancer	High risk group TNBC	High risk group Her-2 disease
Age	Postmenopausal age	Premenopausal age	Postmenopausal age
Genetic mutation	Women <40 and BRCA1and/or BRCA2	57–88% of BRCA1 and/or BRCA2	Her-2 cancer is uncommon in patients with BRCA2 mutation
Early menarche	12 years of age	Before 12 years	12 years of age
Late menopause	>55 years of age	No association	>50 years of age
Late onset childbearing	First full term >33 years	No association	No association
Breastfeeding	Ever breastfeed a child	Parous women who had never breastfed	>1 year breastfeeding
Bodyweight: Premenopausal Postmenopausal	BMI >35 kg/m^2 for both group	Premenopausal BMI ≥30 kg/m^2	Postmenopausal BMI >27.3 kg/m^2
Exogenous hormones OC HRT	 Recent use ≥5 years use	 OC ≥1 year No association	 Starting at ≦20 years of age No association
Alcohol consumption	Dose-dependent	Dose-dependent	Dose-dependent
Racial groups	American/Northern European women	African American women	American/Northern European women
Benign breast disease	Atypical hyperplasia	Atypical hyperplasia	Atypical hyperplasia

1.3.4 TNBC prognostic and predictive factors

Prognostic factors aim to predict patient clinical outcome independent of treatment, whereas predictive factors provide information on the response of a patient to a definite therapeutic intervention and are associated with tumour sensitivity or resistance to that therapy which allow clinicians to predict therapeutic outcomes and decide future treatment plans (72). Several prognostic and predictive factors are routinely used in clinical practice purely as a prognostic or predictive, or as both (Table 1.4).

Table 1.4 Summary of breast cancer prognostic and predictive factors

Factor	Hormone receptor-positive breast cancer		TNBC	
	Prognostic	Predictive	Prognostic	Predictive
Age	Yes		Yes	
Histological grade	Yes		Yes	Yes
Tumour size	Yes		Yes	
Nodal status	Yes		Yes	
Proliferation marker	Yes	Yes	Yes	Yes
Lymphovascular invasion	Yes		Yes	
Hormone receptors	Yes	Yes	No	No
Her-2 overexpression	Yes	Yes	No	No

Table outlining breast cancer prognostic and predictive factors including, age, histological grade, tumour size, nodal status, proliferation marker, lymphovascular invasion, hormone receptors, and Her-2 overexpression.

1.3.4.1 Patient age

Patient age at the time of diagnosis is an important prognostic factor for breast cancer in general (73). Previous studies could not confirm the independent prognostic impact of age in all breast cancer subsets; instead, the prognostic significance of young age was found to depend on molecular subtype. Patients aged <35 years have a worse prognosis with 75% absolute 5-year survival compared to 84–88% for patients aged 35–69 years (74). This group of patients frequently present at an advance stage and have ER-negative disease.

1.3.4.2 Histological grade

TNBC had high histological grade (75), and the majority were grade III (28, 76), and only 10% were grade I (30). The histological grade of the TNBC is used to decide the treatment, and it is commonly established according to the histological grading system (77). The components of tumour grade include tubule formation (refers to how much of the tumour tissue has normal milk ducts), nuclear pleomorphism (evaluation of the size and shape of the nucleus in tumour cells), and mitosis (This refers to the quantity of dividing cells seen with microscopic magnification) (78) (Table 1.5).

Table 1.5 Summary of method for assessing tumour grade in breast cancer

Feature	Score
Tubular formation	
Majority of tumour (>75%)	1
Moderate degree (10–75%)	2
Little or none (<10%)	3
Nuclear pleomorphism	
Small, regular uniform cell	1
Moderate increase in size and variability	2
Mark variation	3
Mitotic counts	
Fewer than 10 mitotic cells were seen	1
Between 10 to 19 mitotic cells were seen	2
At least 20 mitotic cells were seen	3

Table outlining the clinical description for tumour grade.

The three scores are combined to determine the tumour grade. When a grade is higher, it is more aggressive and is more likely to metastasize (Table 1.6).

Table 1.6 Summary of method for assessing tumour grade in breast cancer

Total Feature Score	Tumour Grade	Appearance of Cells
3–5	Grade I	Well differentiated
6–7	Grade II	Moderately differentiated
8–9	Grade III	Poorly differentiated

The Nottingham prognostic index (NPI) is a scoring system that is used to classify patients with primary operative breast cancer into three prognostic groups (79). This prognostic index is based on tumour grade, tumour size, and lymph node involvement (78).

Lymph node involvement is defined as follows: no lymph node involvement, 1; 1−3 axillary lymph nodes or 1 internal mammary lymph node involved, 2; and ≥4 axillary lymph nodes or an axillary and internal mammary lymph node involved, 3. NPI can be calculated as follows: (Tumour size in cm x 0.2) + stage (based on lymph node involvement) + tumour grade. Based on NPI, patients can be classified into three groups: good prognostic group, NPI <3.5; moderate prognostic group, NPI = 3.5−5.5; and poor prognostic group; NPI >5.5.

1.3.4.3 Tumour size

TNBC women had relatively larger tumours than other subtypes of breast cancer (75), and about two thirds of tumours were >2 cm at presentation (30). Research on TNBC reported that larger tumours were associated with poor survival (80). Lymph node metastasis was more frequent in TNBC with large size, which was also associated with late stage at presentation (76). Yin et al. have found that tumour size had an effect on survival when lymph nodes were extensively involved (81).

1.3.4.4 Nodal status

Highest rates of nodal metastases were in the TNBC patients (30, 76), and it was associated with worse clinical outcomes (29). The higher the number of nodes involved, the worse the prognosis (81). However, Hernandez-Aya et al. reported that in TNBC, the worse prognosis associated with lymph node involvement might not be greatly affected by the absolute number of positive lymph nodes (82).

1.3.4.5 Tumour proliferation marker (Ki67)

Ki67 is a marker of proliferation that measure the percentage of cells in the G1 phase of the cell cycle (83). Ki67 could play an important role to classify subgroups of TNBC (84). Ki67 is currently utilised to distinguish between luminal A and luminal B subtypes and physicians frequently use Ki67 index for making a decision on adjuvant treatment (85, 86). Using of Ki67 as a prognostic marker in TNBC has been widely investigated (87). Higher Ki67 score is an independent risk factor for disease-free survival (DFS) and OS in TNBC (84). A positive association between Ki67 expression and tumour response to neoadjuvant

chemotherapy has been reported. TNBC patients with non-pathological complete response, a significant decrease of Ki67 after treatment could indicate a good prognosis (84), and high Ki67 was a poor prognostic factor for TNBC who received neoadjuvant or adjuvant chemotherapy (88).

1.3.4.6 Lymphovascular invasion (LVI)

LVI is defined as presence of tumour emboli within blood vessels (vascular invasion), lymphatic vessels (lymphatic invasion) or both (lymphovascular invasion) in the breast surrounding invasive carcinoma (89). LVI is more commonly observed in patients with TNBC than in those with non-TNBC (28, 76). LVI has been found to be an independent prognostic factor for both DFS and OS in TNBC (90). Liao et al. reported a significant difference in OS according to the lymph node positive, and LVI positive TNBC (91). However, not all studies have shown LVI to impact survival. Urru et al found that LVI was not significantly associated with survival in multivariate analysis (92). Regardless of the implications for survival, several studies have shown that the presence of LVI predicts the development of distant metastasis (92, 93).

1.3.4.7 Tumour necrosis

Necrosis is uncontrolled cell death which lacks the features of apoptosis and autophagy; it is a non-physiologically regulated cause of cell loss (like apoptosis) and can initiate a local inflammatory response (94). The commonest cause of necrosis during tumour development is inadequate oxygen and nutrient supply (defined as metabolic stress) of fast-growing tumour cells (95). The influence of necrotic cell content on cancer cells and tumour microenvironment (TME) cues has been examined when nutritional deficit and hypoxia were combined (96). Their findings demonstrated that signals released by necrotic cells had an impact on cancer cells function and increased the angiogenic capacity. Several studies have shown that tumour necrosis is associated with aggressive tumour characteristics and poor prognosis (97). Necrosis has been correlated with BLBCs (98), had a higher rate of lung and brain metastasis (99), and it is usually seen in advanced stage at diagnosis. Studies showed that TNBC had central necrotic zones and pushing borders (28, 100), and was related to lower rate of 10-year disease-free survival (DFS) (99).

1.3.5 Treatment of TNBC

TNBC is extremely aggressive disease making its therapy an arduous task resulting in a higher mortality rate than other subtypes of breast cancer (30). Because there is a lack of molecular targets (oestrogen, progesterone and Her-2 receptor), TNBCs are not curable with hormonal treatment and Her-2 therapies (101, 102).

TNBC is normally treated with a combination of surgery, radiotherapy, and chemotherapy. To improve the prognosis and survival of patients with TNBC, some new therapies have been developed and improved, such as new targeted therapies, and immunotherapy.

1.3.5.1 Lumpectomy

Several different surgical methods can be used according to the size of the tumour. For the wide local excision (breast-conserving surgery), only the tumour and some parts of the para-carcinoma tissue are removed. Adjuvant radiotherapy and chemotherapy after breast-conserving surgery was associated with better TNBC patient's survival (103, 104). However, a study shows that TNBC is independently associated with increased risk of residual disease after lumpectomy (105).

1.3.5.2 Chemotherapy and radiotherapy

Chemotherapy is used as an anti-cancer drug to kill tumour cells and could decrease the recurrence rate of cancer. Chemotherapy is the primary systemic treatment at the early and late stages of TNBC. It has been reported that the response rate of TNBC patients to neoadjuvant chemotherapy (NAC) was higher than that of non-TNBC patients (102). Several combinations of chemotherapy regimens have been studied, defining that the response rate increased using a combination of chemotherapeutic drugs compared with using of a single drug. Most guidelines recommend anthracycline and taxane-based neo/adjuvant chemotherapy. Although clinical outcomes for TNBC patients are significantly improved by chemotherapy, recurrence rates remain relatively high and TNBC tumours often develop resistance to chemotherapeutic drugs (101) and increasing cytotoxicity (106).

Radiotherapy is usually conducted after surgery and chemotherapy. The advantages of chemotherapy and radiotherapy are the killing of tumour cells and the inhibition to their growth and proliferation; however, these treatment methods can destroy the immune system and the regeneration of bone marrow.

Therefore, considering the limited treatment options and aggressive phenotypes of TNBC, it is important to discover potential therapeutic targets to aid in the development of effective therapies.

1.3.5.3 Targeted therapy

Compared with that of chemotherapy, there is no damage to the healthy cells by using targeted therapy. However, some targeted therapies, such as endocrine therapy for ER-positive and trastuzumab for Her-2-overexpressed breast cancer are not effective in the treatment of TNBC. Therefore, the search for new and effective target therapies is of great significance for TNBC. Some inhibitors have been used as potential medicines for TNBC therapy, including the poly-ADP-ribose polymerase (PARP) inhibitors, epidermal growth factor receptor (EGFR) inhibitors, MEK inhibitors, vascular endothelial growth factor (VEGF) inhibitors, and phosphoinositide 3 kinase (PI3K) inhibitors (107) (Figure 1.3).

Immunotherapy has been one of the most promising and rapidly progressing areas of cancer therapy. Cancer cells can evade immune responses by regulating T cell activity. Programmed death-ligand 1 (PD-L1) is a cell membrane protein expressed on cancer cells and immune cells. PD-L1 binds to PD-1 on T cells to inhibit their antitumour function (108). PD-L1 expression on cancer cells appears to be higher in TNBC than non-TNBC and has been shown to be correlated with higher numbers of tumour infiltrating lymphocytes (TILs) (109, 110). High PD-L1 expression associated with significantly shorter survival (109). Preclinical studies concluded that suppression the activity of the PD-1/PD-L1 might be used for TNBC therapy. Both anti PD-1 inhibitor (nivolumab and pembrolizumab) and an anti-PD-L1 inhibitor (atezolizumab) exhibited promising results with a potentially acceptable safety and tolerability in preclinical studies (111) (Figure 1.3). Initial phase I trials of monoclonal antibodies (mAbs) to pembrolizumab and atezolizumab on extensively pre-treated PD-L1-positive TNBC cases gave promising results (112). Both PD-1 inhibitor and PD-L1 inhibitor are now being assessed in many phases III clinical trials to assess their benefit in metastatic TNBCs, with or without chemotherapy (113).

Even though the patient's OS has been improved by these treatment plans, later phases of survival are still fatal because TNBC is not effectively targeted. Therefore, developing novel biomarkers are needed to combat TNBC.

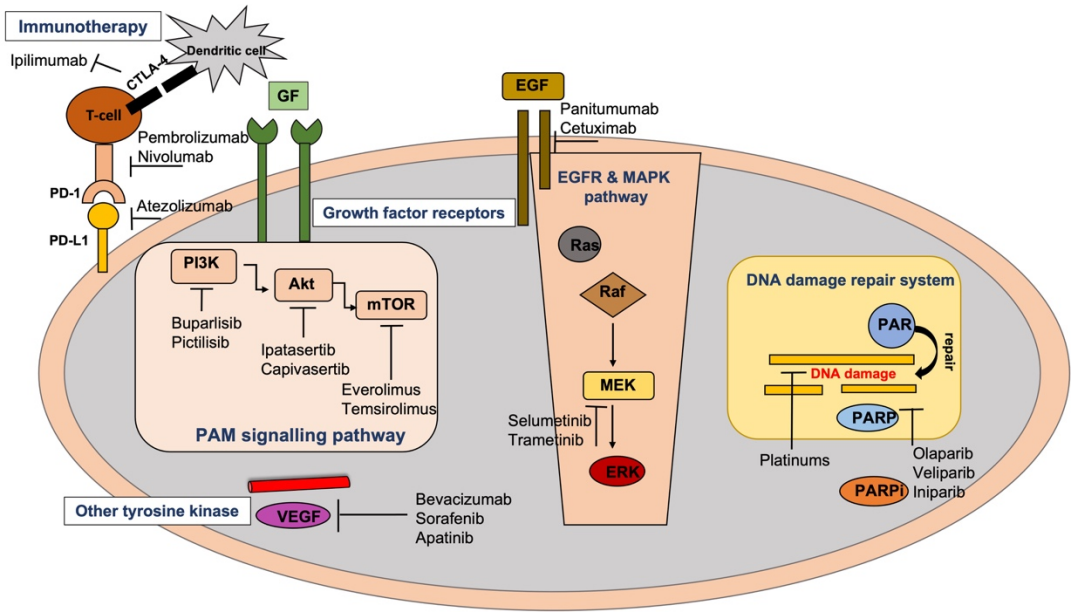

Figure 1.3 Summary of the novel potential agents under development for the treatment of TNBC.

PARPi prevents the repair of single-strand breaks that occur during cell cycle especially in BRCA-mutated cells. EGFR inhibitors bind to EGFR and turn off the uncontrolled growth of cancer cells with EGFR mutations. MEK inhibitors attenuate tumour growth and proliferation by inhibiting MAPK/ERK pathway. Angiogenesis inhibitors block the growth of new blood vessels by inhibiting VEGF. mTOR inhibitors suppress cancer cell growth and proliferation through targeting the PI3K/Akt/mTOR signalling pathway. Targeting PD-1, PD-L1 and CTLA-4 can enhance the adaptive immune reaction. Adapted from (107).

1.3.6 TNBC outcome

TNBC has a poorer prognosis compared to other intrinsic subtypes of breast cancers (16, 29, 102). The survival time of TNBC patients is shorter, and the mortality rate is 40% within the first 5-years after diagnosis (30). TNBC is highly invasive, and about 46% of TNBC patients have distant metastasis. Distant metastasis mostly occurs in the 3rd year after diagnosis (31). The median survival time after metastasis is only 13 months, and the recurrence rate after surgery is as high as 25%. The average time of recurrence in TNBC patients is only 19–40 months while in non-TNBC patients is 35–67 months. The mortality rate of TNBC patients within 3 months after relapse is as high as 75% (114). There are two reasons for the low survival rate of patients with TNBC. First, the lack of therapeutic targets, and there is still no effective therapy for TNBC until now, and the other reason is that it is easier to metastasize and recur compared with other breast cancer with high mortality rate. Therefore, preventing recurrence and metastasis is critical to improving the survival of TNBC patients.

It has been widely believed that the TME is critical for carcinogenesis, and the association between the TME and tumorigenesis as well as disease progression have been well studied; it is helpful to identify new biomarkers to predict the clinical outcomes and will also benefit the treatment of TNBC (115).

1.4 Tumour microenvironment (TME)

The TME is essential for the induction and development of TNBC. Initiation of angiogenesis, proliferation, inhibition of apoptosis, suppression of the immune system, and avoidance of immune surveillance are associated with TME (115). TME is heterogeneous and highly complex (116) composed of cells such as carcinoma-associated fibroblasts (CAFs), mesenchymal stem cells (MSCs), endothelial cells, adipocytes, pericytes, and immune cells such as T lymphocytes, macrophages, natural killer (NK) cells, and cytokines as well as extracellular matrix components (117) (Figure 1.4). The interactions among these compartments may be mediated by secreted factors, cell-matrix interactions, as well as cell-cell direct contact.

TME enabling rapid proliferation of cancer cells, subsequent development of hypoxia, and simultaneous reprogramming of cancer cells to adapt to changes within TME. TME creates a habitat for cancer cells to interact with noncancerous cells include immune cells, endothelial cells, and fibroblasts and can provide potential targets for TNBC (118).

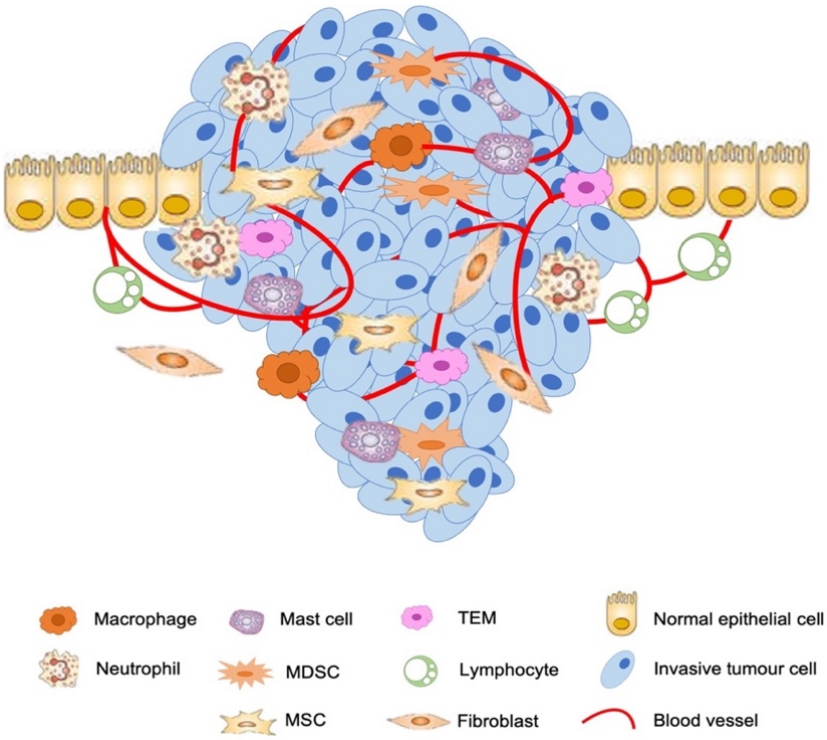

Figure 1.4 Schematic diagram of primary tumour microenvironment.

Tumour cells are surrounded by a complex microenvironment comprising numerous cells including, stromal fibroblasts, macrophages, myeloid-derived suppressor cells (MDSCs), TIE2-expressing monocytes/ macrophage (TEMs), mesenchymal stem cells (MSCs), neutrophil, and lymphocyte. Adapted from (119).

TNBC is characterized with unique TME, which differs from other subtypes, including high infiltration of TILs, tumour associated macrophages (TAMs), and high expression of VEGFs and other molecules that promote tumour cell growth and migration, have been shown to play a role in TNBC initiation, growth and metastasis (120, 121). TME is associated with response to treatment and prognosis of TNBC (122, 123). Therefore, an increasing number of studies have focused on the TME to identify new biomarkers or target in stromal components to predict clinical outcome and guide therapy in TNBCs (124).

Lotfinejad et al. revealed that the TNBC immune microenvironment plays a role in TNBC initiation, growth, and metastasis. Increased tumour antigen expression sets the stage for the immune system to recognize, destroy and remove the tumour, and TILs play a role in tumour cell killing and removal, but the high expression of immune checkpoints inhibits immune cell function and promotes tumour immune escape (120). Therefore, understanding the immune microenvironment of TNBC is important for the prognosis and treatment of TNBC.

1.4.1 Immune cells in TNBC microenvironment

The biological and clinical importance of immune system in TNBC have been explored by several studies (125, 126). Recent studies conducted by Romero-Cordoba et al. showed extensive immune heterogeneity in TNBC. The prognostic value of immune infiltrates varies among TNBC cells, and it has been related with systemic inflammatory parameters that can be identified by a simple blood test such as whole blood count, platelet-lymphocyte ratio, and neutrophil-lymphocyte ratio (127).

TNBC is the most immunogenic subtype of breast cancer, with higher PD-1 expression levels and more TILs. PD-1 is an important immune checkpoint receptor and when it binds to its ligands, PD-L1 and PD-L2, it attenuates T-cell function within tissues (128). PD-L1 is expressed on activated T cells within the TME, however, tumours can also express PD-L1, which has been demonstrated in TNBC (129). It plays an essential role in the clinics for TNBC, and it was a significant predictor of OS in the basal-like subtype (130). PD-1/PD-L1 inhibitory treatment in neoadjuvant setting in TNBC is becoming more important (131).

1.4.1.1 Tumour infiltrating lymphocytes (TILs)

1.4.1.1.1 Significance of TILs

A large number of TILs infiltrate the TNBC microenvironment compared to other breast cancer subtypes (132). TILs have intrinsic immunogenicity in TNBC (107), and was used to induce favourable TME, inhibit tumour progression, and improve TNBC patients' survival. TILs are currently considered a prognostic factor and a predictive marker in TNBC patient. High TIL level was significantly associated with a better survival outcome (122, 133, 134), and associated with increased pCR following neoadjuvant chemotherapy in TNBC (111, 122). Also, it was found that TNBC patients with high TIL levels may have lower Ki67 levels and less proliferation of cancer cells (135). These findings have indicated the use of immunotherapy in TNBC patients (125, 136). Clinically, the evaluation of TILs as a prognostic marker was recommended by an International TILs Working Group (137) with minor modifications added in 2017 by Hendry and colleagues such as assessment of TIL separately in the stromal and tumour compartment, evaluated TIL within the borders of invasive tumour, and excluded the TIL at a distance outside the tumour borders (138).

1.4.1.1.2 Subpopulations of TILs

TILs include CD3+ T and CD20+ B cells, and CD38+/CD138+ plasma cells (subtype of B lymphocytes). With regards to subtypes of TILs, T-lymphocytes are the most predominant type of lymphocytes in the TME, representing up to 75% of TILs (139). The strongest evidence for effect on outcome has been found for T-lymphocytes. The CD3+ T cell population was further divided into CD8+ T lymphocytes (cytotoxic T cells) and CD4+ T lymphocytes (helper T cells).

CD8+ T lymphocytes

CD8+ infiltrates are estimated in 60% of TNBCs (132). It has revealed that TNBC rich in CD8+ T cells are correlative with a better prognosis (140) and increase neoadjuvant chemotherapy sensitivity (141).

CD4+ T lymphocytes

The main subgroups are T-helper cells (Th1, Th2), and regulator T-lymphocytes (Treg). CD4+ helper T lymphocytes play a regulatory role in the immune system by regulating B cell, CD8+ T lymphocytes and macrophages (142). The expression of Th1 predicted an improved OS in breast cancer patients (132). Moreover, the higher levels of Th2 cytokines, IL-5 and GM-CSF (Granulocyte-macrophage colony-stimulating factor), related with a good outcome, may have play a vital role in suppression of carcinogenesis, preventing differentiation into a more aggressive breast cancer phenotype (143). The Th1/Th2 ratio is a prognostic factor for breast cancer and was statistically significant in luminal A and BLBC survival analysis (144). High levels of Tregs TILs are correlated with high histological grade and ER-negativity (145). Tregs induce an immunosuppressive microenvironment, inhibit the activation of CD8+, and prevent the body's antitumour immune response (146), and can predict poor prognosis (132).

B lymphocytes

Several studies reported that TIL-B carry positive prognostic value in TNBC (122), while others found no significant effect (147), or even poorer survival with CD138+ plasma cell infiltrates (148). High expression of CD20+, marker used to assess B lymphocytes was significant predictor of pCR in TNBC (147).

1.4.1.2 Tumour associated macrophages (TAMs)

Macrophage polarization into M1 or M2 phenotypes leads to varied cytokine secretion and function (149). M1 macrophages are associated with an inflammatory response and induce a Th1 immune response by liberating proinflammatory cytokines including interleukin-12 (IL-12) and tumour necrosis factor (TNF). M2 macrophages produce cytokines, including IL-10, IL-1, and associated with tumour growth and progression by stimulating angiogenesis and suppressing other immune responses (150) or facilitating invasion and metastasis (151). Several immunohistochemical (IHC) markers are available to evaluate TAMs. CD68 is known as a pan-macrophage marker and facilitates identification of both M1 and M2 macrophages (152). In TNBC, a higher degree of CD68+ macrophage infiltration was associated with poor prognosis (153). However, Medrek et al. have reported no significant difference in outcome based on TAMs in TNBC, but intratumour macrophages were positively associated with larger size, high histological grade, Ki67 positivity, hormone receptor negativity and TNBC (152). TAMs in BLBCs have been reported to show difference in macrophage polarisation, cytokine profile and migratory function compared with TAMs in luminal cancer (154) suggesting that immune response mediated by TAMs in BLBC may be different from that of non-basal breast cancer.

1.4.2 Cytokines in TNBC microenvironment

TNBC exists in a variety of cytokines and chemokines, including IFN-γ, TNF-α, IL-1β, TGF-β, IL-6, IL-8, IL-2, IL-15, and IL-18, which enhance tumour growth, metastasis, drug resistance, mediated immune suppression and antitumour activity, and plays a vital role in microenvironment.

IFN-γ (interferon-γ) associated mRNA profiles have been proposed as predictors of PD-1 blocking clinical responses (155). It was found that the expression of PD-L1 in breast cancer was induced by IFN-γ, which was regulated by the JAK/STAT signalling pathway (156). A recent study by Singh et al. showed the metastatic role of IFN-γ in TNBC (157).

TNF-α (tumour necrosis factor-α) and IL-1β stimulate co-cultures of TNBC and MSCs *in vitro* has increased the aggressiveness of the cancer cells *in vivo* leading to increase lung metastases in mice through induce the expression of the pro-metastatic chemokines CXCL8 (158).

TGF-β is a cytokine belonging to the TGF superfamily which is involved in the production of Tregs and suppress the effector function of cytotoxic T cells in the TME of mice model. TGF-β can also increase the inhibitory activity of TAMs and stimulate tumour escape by enhancing M1 to M2 phenotype polarization and inducing PD-L1 up-regulation (159).

IL-6 is an inflammatory cytokine that interferes with the expression of cell adhesion and surface molecules, regulates a variety of cell functions, such as proliferation, differentiation and immune defence, participates in TNBC growth, and associated with TNBC prognosis (160, 161). TNBC cells secrete a large amount of IL-6 which activate the JAK2-STAT3 signalling pathway and stimulate CCL5 synthesis in lymphatic endothelial cells and lung lymphocytes (162). In TNBC, MSCs contribute to higher aggressiveness by stimulating the expression of angiogenic factors and pro-metastatic chemokines such as CCL2, CCL5 and CXCL8 (162-164).

IL-8, IL-2, IL-15 are important indicators of immune response in breast carcinoma. IL-8, an immune-related cytokine and inflammatory mediator, has tumorigenic and angiogenic properties. IL-8 is highly expressed in the TNBC and associated with poor prognosis (161). IL-8 secreted by tumour cells, invasive neutrophils and tumour-related macrophages participates in the angiogenesis, proliferation and migration of tumour cells in the TME (162). Stimulation of IL-2 or IL-15 cytokine can improve the antitumour ability of NK cells in TNBC (165).

IL-18 is a cytokine member of the IL-1 family. It is produced by various cells such as macrophages and plays a pro- and anti-inflammatory role. IL-18 is involved in regulating the expression of PD-1 in TNBC microenvironment. IL-18 in TME increases the number of immunosuppressive NK cells and stimulates expression of PD-1 in a subset of NK cells. Tumour-derived IL-18 levels were significantly associated with reduced survival in TNBC patients (166).

1.4.3 Tumour stroma percentage (TSP)

Study of tumour to stroma ratio indicates that increased expansion of tumour stroma is crucial for prompting the prognostic outcome. TSP is fast emerging as a significant prognostic indicator in different tumour types. Many studies document an association of high stromal content with worse prognosis in breast cancer (167). In TNBC, a high percentage of stroma predicts poor prognosis (167, 168), and was found to be an independent prognostic factor for recurrence free survival (RFS) (167).

CAFs make up the bulk of cancer stroma, especially in breast cancer, and have been found to play a critical role in the TME (169). The source of CAFs is complex and debated. CAFs may activated and proliferated from resident fibroblasts, mesenchymal derived stem cells, neighbouring adipose tissue, endothelial cells (endothelial-mesenchymal transition, EndoMT), and epithelial cells (epithelial-mesenchymal transition, EMT) (Figure 1.5). The activation of resident fibroblasts is induced by many factors, such as TGF-β (transforming growth factor-β) and SDF-1 (stromal cell-derived factor-1). The most widely used marker to detect CAFs in the tumour is α-smooth muscle actin (α-SMA) (169). The percentage of positively α-SMA stained cells was graded on a scale of 0–3, with less than 5% representing grade 0, 5-25% representing grade 1, 26-50% representing grade 2, and more than 50% representing grade 3. The intensity of staining was also graded on a scale of 0–2, with negative to weak intensity representing grade 0, weak-moderate intensity representing grade 1, and moderate to strong intensity representing grade 2. The score of percentage and intensity was multiplied. The final score between 0 and 2 was determined as low expression, and a score higher than 2 was determined as high expression (170).

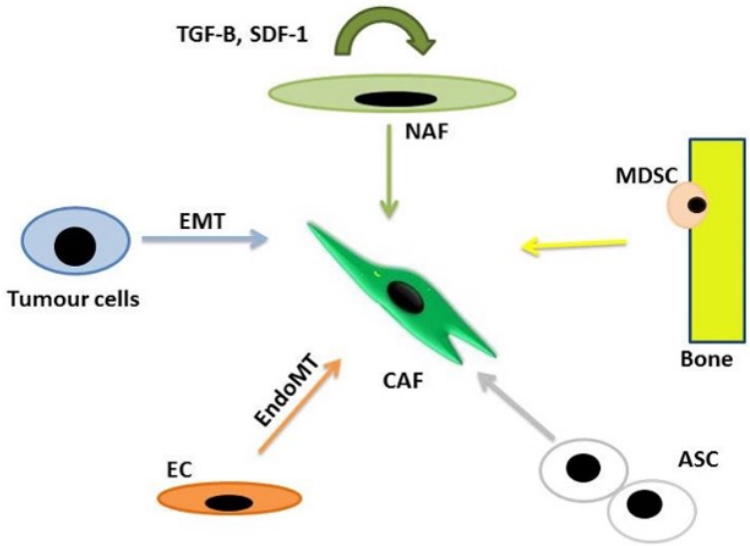

Figure 1.5 Outline of potential progenitor cells for cancer associated fibroblasts in the tumour microenvironment

Illustrative diagram showing origins CAFs from several cells such as normal tissue derived fibroblast (NAF), mesenchymal derived stem cell (MDSC), adipose tissue-derived stem cell (ASC), endothelial cell (EC) (through endothelial mesenchymal transition, EndoMT), and epithelial tumour cell (through epithelial mesenchymal transition, EMT). Adapted from (169).

CAFs reduce antitumour immunity, enhance cancer cell proliferation and invasion, stimulate neo-angiogenesis of tumour cells, reshape the extracellular matrix, and contribute to the formation of an immunosuppressive microenvironment (171). Studies have demonstrated that CAFs autophagy can improve the *in vitro* migration of TNBC cell lines (172), and promote lung metastasis via TGF-β activation in TNBC mouse model (173). Furthermore, Galectin-1, which is highly expressed in CAFs regulates CAF activation and enhances TNBC cells metastasis by stimulating matrix metalloproteinase 9 (MMP9) expression (174). Also, podoplanin expression in CAFs was associated with higher tumour grade and TNBC (175). Metabolically, co-cultured BLBC cells and CAFs has been shown to exhibit higher glucose up-take, glucose oxidation and glycogen synthesis than luminal cells (176). High CAF infiltration in TNBC tissues was significantly correlated with high infiltration of TAMs and lymphatic metastasis which correlated with poor outcome and might be a potential therapeutic target in TNBC patient (177).

1.4.4 Tumour budding (TB)

Tumour budding is defined as isolated single tumour cells or clusters of up to four tumour cells located at the invasive tumour front (178). TB is likely to be an early step in cancer metastasis as budding cells are proposed to reflect the process of an EMT in breast cancers which is an important step during carcinoma progression and metastasis (178). TB has been identified as a poor prognostic factor in breast cancer (179) mainly in TNBC (180). High breast cancer budding was associated with necrosis (181). Budding cells have been shown to escape hypoxia by expressing a hypoxia-inducible factor-1α (HIF-1α) mediated hypoxic tumour phenotype which increases their malignant potential (182).

1.5 Tumour hypoxia

Tumour hypoxia results from an imbalance between the cellular oxygen consumption and the oxygen supply to the cells (183). Approximately 50–60% of solid tumour have been shown to exhibit regions of hypoxia (184). A previous study has demonstrated that about 25–40% of locally advanced breast cancers exhibit hypoxia (185). Hypoxia can be caused by perfusion, or diffusion related factors. Perfusion-related (acute) hypoxia arises due to inadequate blood flow in tissues which caused by structurally and functionally abnormal cancer vessels while diffusion-related (chronic) hypoxia arises due to increased diffusion distances with tumour expansion (183). Cancer cells are exposed to a continuum of oxygen concentrations and consequently solid tumours are comprised of three tissue regions: the

normoxic, hypoxic and necrotic (Figure 1.6). Located nearby functional blood vessels normoxic cells are typically viable and proliferative while at distances of 150μm from patent blood vessels cells may become anoxic, giving rise to areas of necrosis.

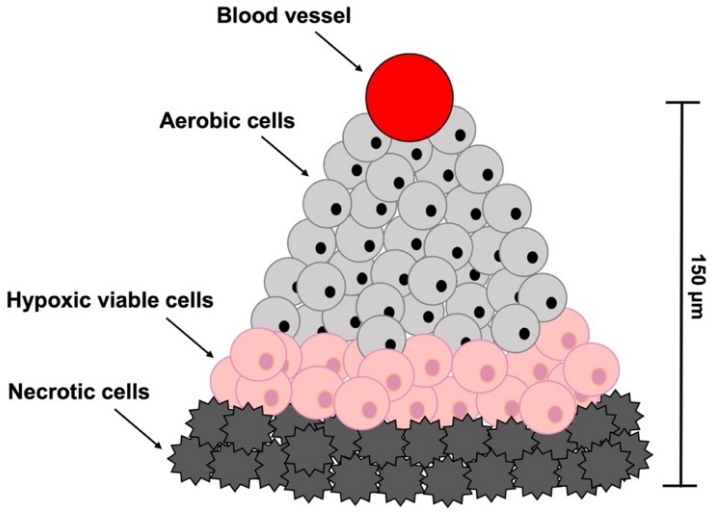

Figure 1.6 Schematic representation of hypoxic regions of solid tumours.

Regions of tumours containing of oxygenated cells situated near to blood vessels, becoming increasingly hypoxic with increased distance from a functional blood supply. Adapted from (186).

1.5.1 Cellular responses and adaptations to hypoxia

Hypoxia stimulates both proteomic and genomic changes within tumour cells (Figure 1.7). Cancer cell responses to hypoxic stress include adaptive proteomic changes permitting the cells to escape their hostile environment by facilitating anaerobic glycolysis, increased proliferation, angiogenesis, decreased sensitivity to apoptotic and other cell death signals, evasion of immune attack, confers limitless replicative potential allowing invasion, or metastatic spread (187). Furthermore, hypoxia promotes genomic instability, thereby increasing the number of mutations. At a molecular level, the adaptation of tumour cells to hypoxic stress is regulated largely by hypoxia-inducible factors (HIFs), key regulators of the hypoxic-induced stress response.

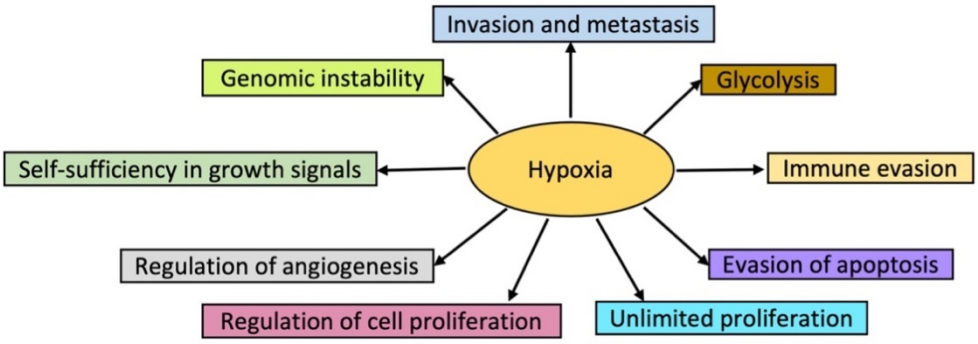

Figure 1.7 The role of hypoxia in the cancer-specific biological pathways.

Schematic diagram showing numerous effects of hypoxia on cancer progression including switch to a glycolytic metabolism, maintenance of proliferation, resistance to apoptosis, obtain unlimited replication potential, genetic instability, evade immune attack, stimulate angiogenesis, invade and metastasize.

1.5.2 Hypoxia inducible factors (HIFs)

Three human HIF family members have been identified, HIF-1, HIF-2, and HIF-3, these heterodimers comprise of α subunit and β subunit (188). Of the three isoforms, HIF-1 is frequently overexpressed in tumour cells (189).

1.5.2.1 Hypoxia inducible factors domain structure

HIF-1 is a heterodimer composed of a constitutively expressed nuclear HIF-1β subunit, aryl hydrocarbon receptor nuclear translocator (ARNT) and an O_2-regulated HIF-1α subunit (190). Both HIF-1 subunits belong to the protein family of the basic-helix-loop-helix (bHLH)/PER-ARNT-SIM (PAS) domain-containing transcription factors (Figure 1.8). The bHLH and PAS motifs facilitate DNA-specific binding and dimerization. HIF-1α subunit contains two transactivation domains (C-TAD and N-TAD). C-TAD can interact with co-activators such as CREB binding protein (CBP)/P300 to regulate the transcription of HIF-1α target genes. N-TAD participates in stabilizing HIF-1α against degradation. Moreover, HIF-1α but not HIF-1β contains an oxygen-dependent degradation domain (ODD) that mediates the O_2-dependent degradation of HIF-1α. Two nuclear localization signals (NLSs) have been identified as determining the nuclear localization of HIF-1α, however, the C-terminal NLS motif is considered to be more important in the nuclear translocation induced by hypoxia (191, 192). HIF-1α was the first HIF family member to be described by Semenza and Wang (193).

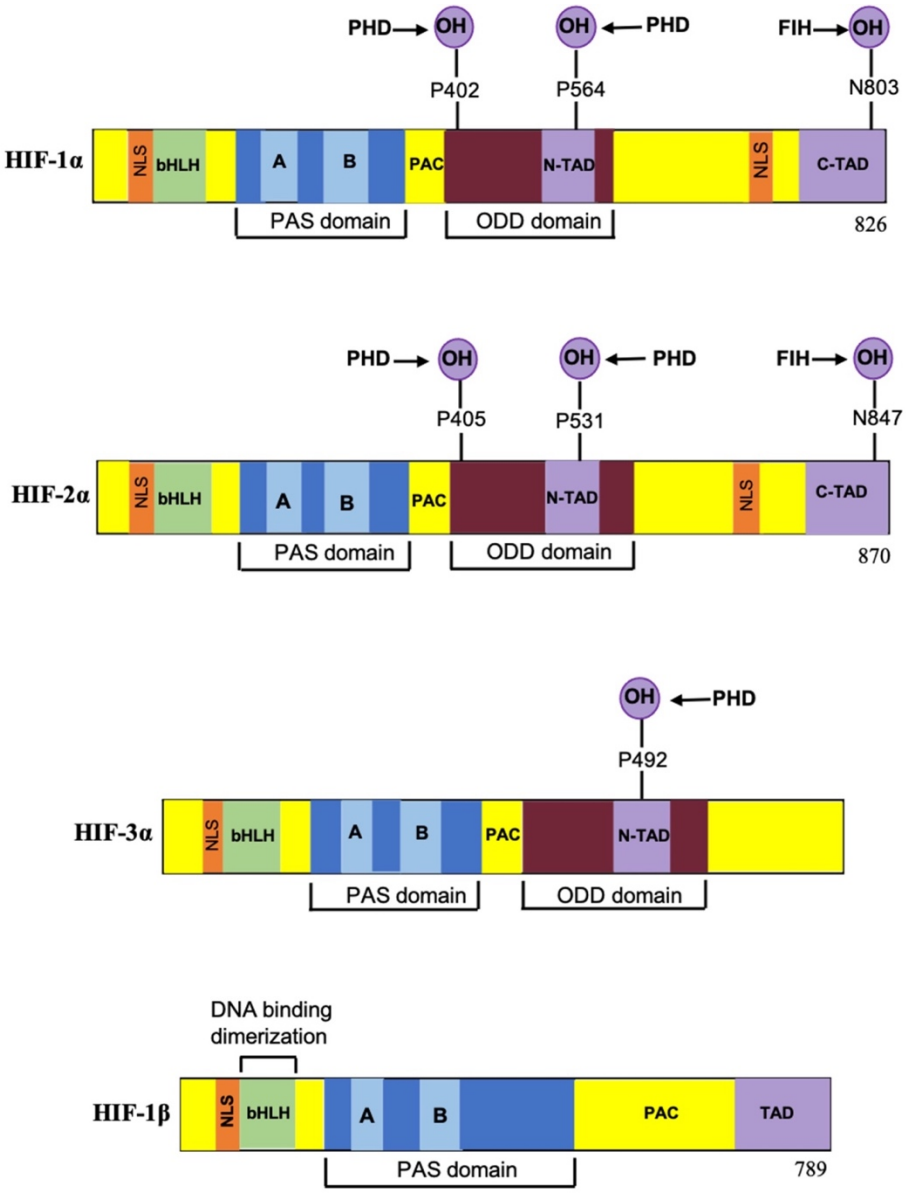

Figure 1.8 Schematic representation of domain structures of hypoxia inducible factors isoforms.

Most isoforms contain a bHLH (Basic helix–loop–helix) domain for DNA-specific binding and two sequential PAS domains (PAS-A and PAS-B) which facilitate dimerization with HIF-1β. Two transcription-activation domains (TADs), one N-terminal domain (N-TAD), and one C-terminal domain (C-TAD). The N-TAD is located in the oxygen-dependent degradation domain (ODD). HIF-3 lacks C-TAD domains, and HIF-1β lacks ODD. Numbers indicate the amino-acid residues of each domain or special amino sites. The figure has been adapted, with some modifications from (194).

HIF-2α was the second HIF family member to be identified and shares about 48% amino acid sequence homology with HIF-1α (195). This identity resemblance could explain their common capability of hetero-dimerization with HIF-β and binding with hypoxia response elements (HREs) and induce gene expression (196). While the DNA binding and dimerization domains of HIF-1α and HIF-2α are similar from a structural view, the transactivation domains of these two forms are different. Another difference is that HIF-1α has all-pervasive expression, while HIF-2α expression is more limited to specific tissues (196). In general, the two forms react to hypoxia through different biological actions. HIF-1α mediated mechanisms favour tumour growth, malignant progression, and regulation of genes (197) while HIF-2α stimulates some, but not all genes stimulated by HIF-1α (198). For example, HIF-1α and HIF-2α share several common targets such as VEGF. HIF-1α mediates transcription of glycolytic enzyme and the proapoptotic gens while erythropoietin production and cyclin D1 is regulated by HIF-2α (196). Furthermore, HIF-1α responds in transient manner to severe hypoxia with rapid stabilization and stimulation of target genes, while HIF-2α responds to moderate levels of hypoxia and accumulates over time (199).

The third HIF family member, HIF-3α, like HIF-1α and HIF-2α, it can dimerize with ARNT and bind to HREs *in vitro*, but the role of HIF-3α in the hypoxic regulation of target gene expression *in vivo* is not well understood (200). HIF-3α lacks the transactivation domain which means that this form possesses a suppressive effect, preventing HIF-1α from initiating transcription by binding to it (201). As result, HIF-3α is referred to as the inhibitory Per-Arnt-Sim PAS domain (189).

Besides ARNT, another HIF-β subunit, ARNT2 and ARNT3 can heterodimerize with HIF-1α proteins (202) (Table 1.7). ARNT2 has 57% amino acid sequence identity to ARNT. Even though the two proteins may share similar functions, the expression patterns of ARNT and ARNT2 differ. While ARNT mRNA is ubiquitously expressed, ARNT2 expression is limited to the brain and kidney tissues (203).

Table 1.7 Members of HIF family

α Subunits	β Subunits
HIF-1α	HIF-1β (ARNT)
HIF-2α	ARNT2
HIF-3α	ARNT3

Each α subunit may dimerize with any β subunit, and each β subunit may dimerize with any α subunit.

1.5.2.2 HIF-1α regulation and its function in cancer

While HIF-1β is stable and constitutively expressed regardless of oxygen availability, HIF-1α levels are regulated via both O_2-dependent and independent pathways.

1.5.2.2.1 HIF-1α versus oxygen-dependant regulation

Under normoxic conditions, HIF-1α is rapidly degraded (half-life of less than 5 minutes) through the ubiquitin-proteasomal pathway (Figure 1.9A). This involves hydroxylation of proline residue 402 and/or 564 within ODD by prolyl hydroxylases (PHDs) in a reaction that requires oxygen as a substrate, ferrous iron (Fe^{2+}) and ascorbate as cofactors, and 2-oxoglutarate (alpha-ketoglutarate) as an electron donor co-substrate (204, 205). This allows recognition hydroxylated HIF-1α through the von Hippel-Lindau (VHL) tumour suppressor protein and is tagged for ubiquitylation and subsequent proteasomal degradation (206). Hydroxylation of asparagine residue 803 located within the HIF-1α C-TAD by the factor inhibiting HIF-1 (FIH-1) provides another regulatory layer by blocking the binding of HIF-1α to coactivator P300 and CREB binding protein (CBP) thus inhibiting HIF transcriptional activation under normal oxygen conditions (206).

Under hypoxic condition, the oxygen-dependent hydroxylation of HIF-1α does not occur resulting in HIF-1α stabilization, accumulation, and subsequent translocation to the nucleus where it dimerises with HIF-1β and binds to HRE to regulate transcription of the target genes (Figure 1.9B). HIF-1α induces a wide variety of biological changes associated with glucose metabolism, pH regulation, cell proliferation, angiogenesis, metastasis, and therapy resistance (206). HIF-1α was also shown to increase the expression of an anti-apoptotic protein, BCL2 (B-cell lymphoma-2) in breast cancer cell lines which may promote cell survival (207).

Hypoxia predicts a poor patient outcome due to increased expression of related genes (208). Up to 1.5% of the human genome is evaluated to be transcriptionally responsive to hypoxia (209). Recent years brought insights into several additional genes and pathways which have been identified as being responsive to hypoxia and might serve as predictive or prognostic markers (210). Since increased activity of the HIF-1α pathway is associated with a more profound intratumoural hypoxia in BLBC compared with other subtypes, gene signatures might direct treatment decisions for potential application of anti-hypoxic drugs within the future (211) .

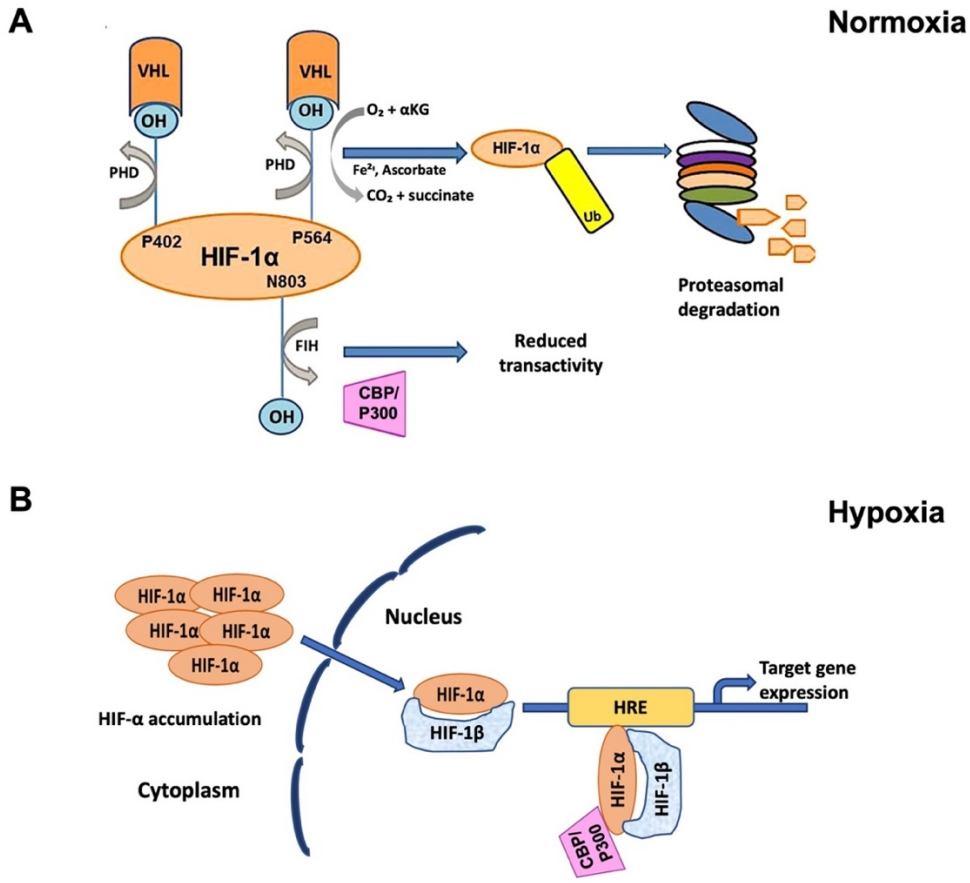

Figure 1.9 Activation and degradation of the hypoxia inducible factor-1α.

Schematic diagram showing molecular mechanism of hypoxia-inducible factor 1 (HIF-1) signalling. In normoxia, HIF-1α is rapidly degraded via the pVHL proteosome pathway. This results in the inactivation of HIF-α subunit transcriptional activity [A]. Under hypoxic conditions, HIF-1α associates with HIF-1β and the resulting heterodimer binds to the hypoxia response element (HRE) of target genes [B]. Adapted from (212).

1.5.2.2.2 HIF versus oxygen-independent regulation

According to an earlier survey of cancer cell lines, there was almost a 50% incidence of HIF-1α stabilizing under normoxic conditions in tumours (213). HIF-1α can be stabilised independently of hypoxia by accumulation of Krebs cycle metabolites such as succinate and fumarate which inhibit PHD activity and in turn increase HIF-1α stabilization (214, 215). Intracellular pyruvate and lactate accumulation also enhance HIF-1α stabilization (216) (Figure 1.10).

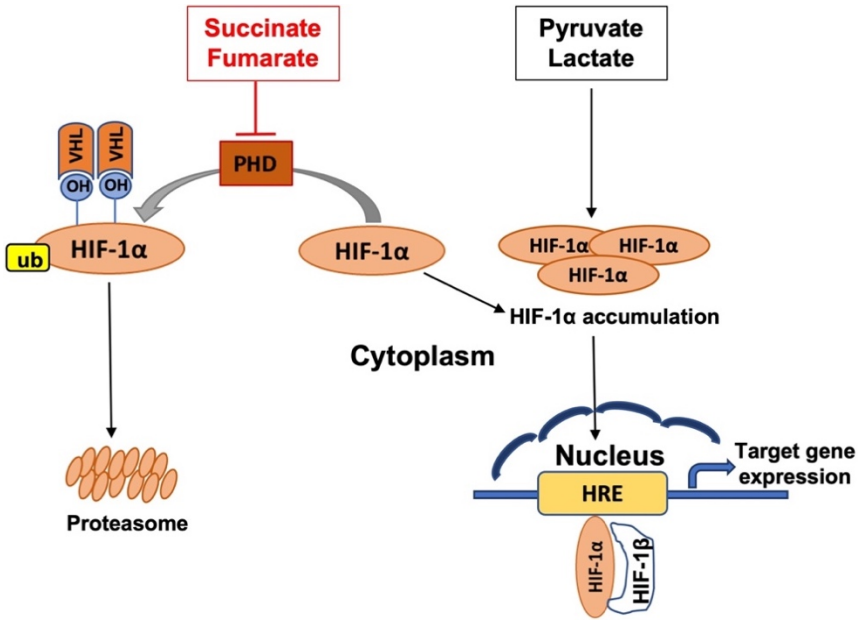

Figure 1.10 Oxygen-independent HIF-1α stabilization via oncometabolite.

Schematic diagram showing oncometabolite stimulates HIF-1α stability. Succinate and fumarate inhibit prolyl hydroxylase (PHD) activity. Pyruvate and lactate enhance HIF-1α stabilization.

Furthermore, HIF-1α can be stabilised independently of hypoxia by dysregulation of oncogenes, such as the amplification of C-Myc in cancer cells. C-Myc has been found to prevents HIF-1α degradation via reducing HIF-1α binding to the pVHL complex, eventually leading to normoxic HIF-1α stabilization in breast tumour cells (217) (Figure 1.11).

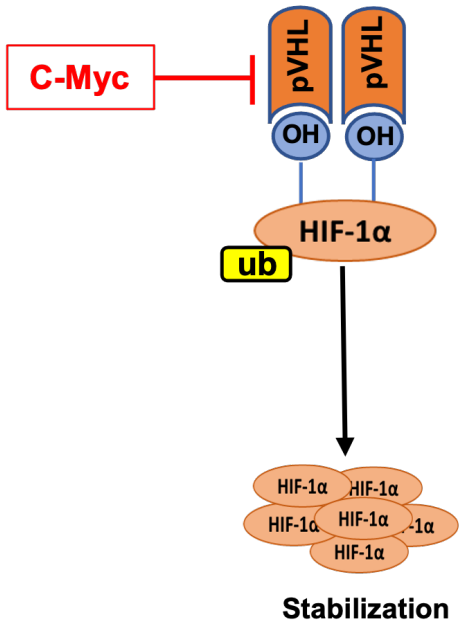

Figure 1.11 PHD-independent pathways regulating HIF-1α stability.

Schematic diagram showing C-Myc inhibit HIF-1α binding to pVHL complex which promotes HIF-1α degradation in hypoxic environment.

HIF-1α may also be regulated through mRNA transcription and protein synthesis. Activation of the PI3K/Akt/mTOR pathway leading to increased mTOR-dependent HIF-1α transcription and translation (218). Consequently, any aberrant stimulation of this pathway in cancer often occurs via hormones, growth factors, and increased reactive oxygen species (ROS) concentrations leads to stimulation of HIF-1α even in normoxic conditions (218-220) (Figure 1.12).

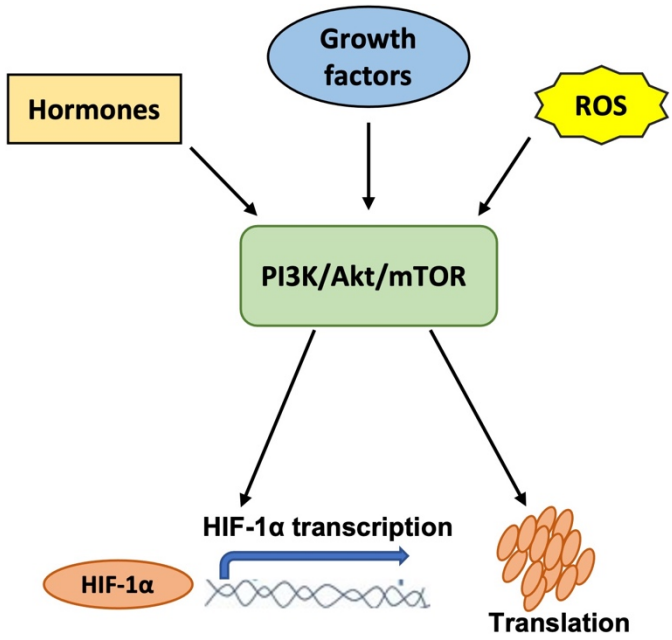

Figure 1.12 Regulation of HIF-1α on transcriptional and translational level.

Schematic diagram showing PI3K/Akt/mTOR axis which is the major pathway involved in promoting HIF-1α transcription and translation, regardless of O_2 concentrations and upon numerous pro-tumourigenic stimuli such as hormones, growth factors, increased ROS concentrations were shown to promote HIF-1α transcription and translation.

Cancer cells must be able to maintain an intracellular pH at or near physiological levels in order to survive in the acidic microenvironment. Therefore, hypoxia-associated enzyme carbonic anhydrase IX, a direct transcriptional target of HIF-1α, is a key in this regulatory process (221, 222).

1.5.3 Carbonic anhydrase IX (CAIX)

In addition to HIFs, CAIX has been proposed to be a potential intrinsic marker of hypoxia (222). It was first detected in human cervix carcinoma HeLa cells and initially named the

MN protein by Pastoreková et al. (223) There are 15 different CAs isoforms differing in physiological roles and expression patterns but only CAIX and CAXII have been implicated in cancer (224) CAIX is of particular interest due to its high expression in solid tumours while displaying low expression in normal tissues (mainly the gastrointestinal tract and biliary tree) (225) suggesting its potential to function as a promising tumour biomarker (226)

1.5.3.1 CAIX domain structure

CAIX is a transmembrane protein belongs to the class of zinc metalloenzymes, consisting of four distinct domains. An N-terminal proteoglycan (PG) domain, a CA catalytic domain, a transmembrane segment (TM), and an intracytoplasmic (IC) tail at the C-terminal (227) (Figure 1.13). A signal peptide domain is removed prior to enzyme maturation (228). The extracellular PG-like domain immediately adjacent to the CA domain allows the enzyme to act efficiently at acidic pH values (227), and it is the distinctive feature of CAIX differing from the other known CAs. It has been suggested that the PG domain is involved to cell adhesion and tumour invasion via its interaction with β-catenin which leads to a decrease in E-cadherin mediated cell-cell adhesion, therefore, promoting cell motility and invasion (229). The intracellular tail contains potential phosphorylation sites which results in increased catalytic activity of CAIX (230).

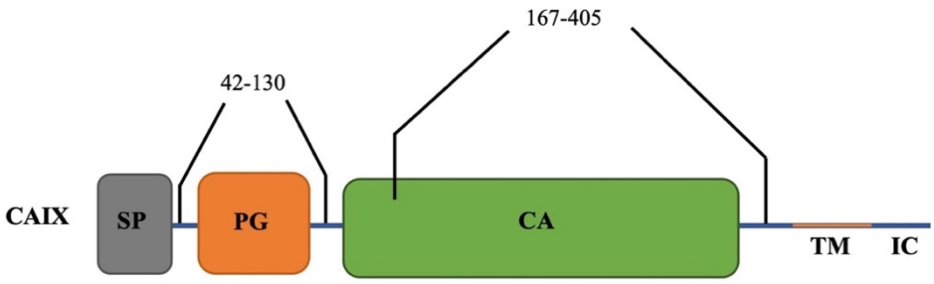

Figure 1.13 Domain organization of CAIX protein.

Schematic diagram showing domain organization of CAIX. The proteoglycan-like domain (PG); the catalytic domain (CA); the transmembrane segment (TM) and the intracytoplasmic tail (IC). SP: signal peptide. Adapted from (227).

CAIX is involved in pH regulation that catalyses the reversible hydration of carbon dioxide to bicarbonate and a proton: $CO_2 + H_2O \rightleftharpoons HCO_3^- + H^+$ maintained a more alkaline and uniform intracellular pH whereas making a more acidic extracellular pH (231) (Figure 1.14).

The extracellular HCO_3^- generated by CAIX is transported by bicarbonate transporter (BT) across the plasma membrane to the cytoplasm, where it contributes to intracellular neutralisation, which is important for cell survival and proliferation. However, protons remain at the cell surface lowering the extracellular pH and support extracellular acidification (232), which facilitates cell migration and invasion (233). Thus, it plays a major role in maintaining the pH gradient between cells and their extracellular space (234).

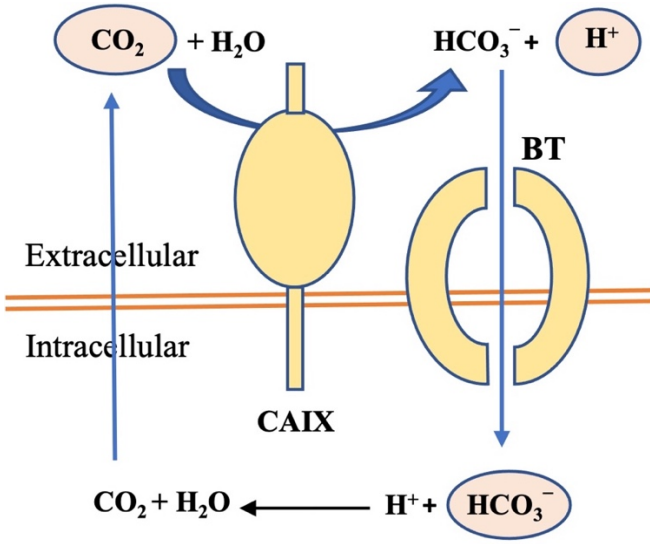

Figure 1.14 Schematic illustration of the catalytic role of CAIX in pH regulation in tumour cells.

Pericellular CO_2 is hydrated to bicarbonate ions and protons by CAIX. Protons remain on the outer side of the plasma membrane and contribute to extracellular acidification while bicarbonate ions transport across the plasma membrane through bicarbonate transporters (BTs) to neutralize intracellular pH. This results in production of CO_2 that leaves the cell by diffusion and may enter a new round of hydration. Adapted from (234).

1.5.3.2 CAIX regulation and its function in cancer

When hypoxic environment advances, HIF-1α is overexpressed and promotes upregulation of various target genes, including CAIX to prevent intracellular acidosis, and allowing breast cancer cells to undergo metabolic adaptation to hypoxia (235, 236). CAIX also contributes to several specific biological process critical for tumour progression including migration, invasion, cell survival, maintenance of cancer stem cell function and chemotherapy and radiotherapy resistance (237) (Figure 1.15). Cancer stem cells (CSCs) are a small subpopulation of tumour cells capable of self-renewal and the ability to differentiate into multiple cell types. These cells are associated with development of metastases and exhibit

enhanced invasiveness. Hypoxia increases the number of CSCs, which are essential for disease progression and recurrence (238). Analysis of CSC markers in invasive breast cancer showed an association with CAIX-positive tumour. Inhibition of CAIX results in reduced the stemness properties and survival of CSCs and decrease migration and invasion (237).

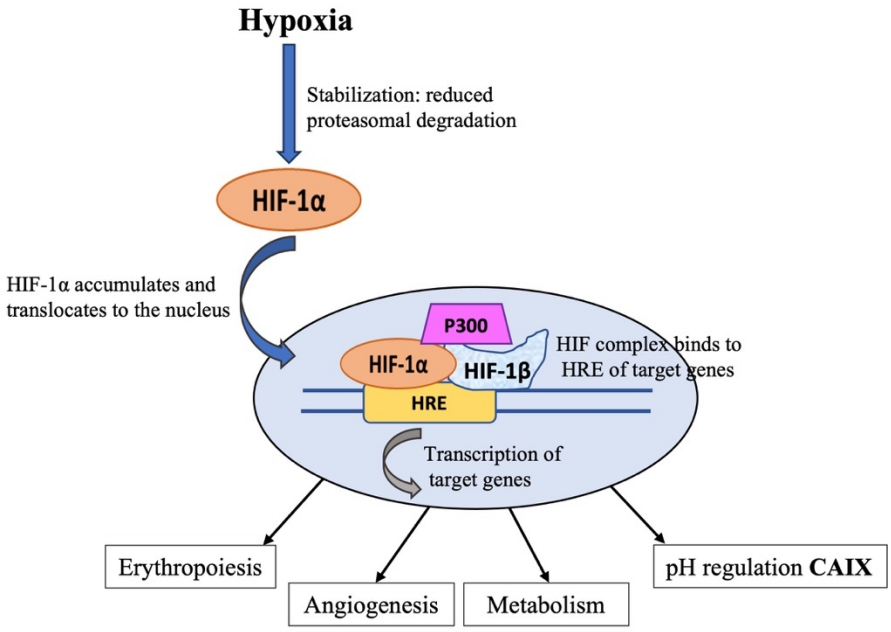

Figure 1.15 Schematic illustration of CAIX regulation.

Hypoxia induces a HIF-1α mediated signalling cascade that results nuclear translocation of HIF-1α and activation of hypoxia-regulated genes, including erythropoiesis, angiogenesis, metabolism, and pH regulation (CAIX).

1.5.4 Hypoxia prognostic factors in breast cancer

Associations between microenvironmental hypoxia, activation of hypoxia pathways, and aggressively malignant phenotypes are observed across a range of cancers. It was previously reported that HIF-1α and HIF-2α were frequently upregulated in a variety of human tumours (239). These finding suggest that HIF may play a role in tumorigenesis. It has been reported that overexpression of HIF-1α in breast cancer was positively associated with large tumour size, advanced tumour stage and high histological grade (240), metastasis (241, 242) and mortality in lymph node positive (243), lymph node negative (244), Her-2-positive (245), ER-positive (246). Clinically, high levels of HIF-1α expression positively correlate with tumour progression and poor prognosis in breast cancer (240, 241, 246-248). Overexpression of HIF-1α is an independent prognostic factor in ER-positive breast cancer with decrease DFS (249). Since TNBC frequently shows central fibrosis and necrosis which are morphologic evidence of hypoxia (100, 250), a high expression of HIF-1α in TNBC may be anticipated. Indeed, this had been confirmed through the preferential expression of HIF-1α in peri-necrotic cancer cells in TNBC and BRCA1 mutated breast tumours (251). TNBC more often has higher HIF-1α expression than non-TNBC, and it is associated with nodal metastasis, histological grade, Ki67 expression (252), and large tumour size (250). Preclinical study showed that, inhibition of HIF in TNBC cell lines was associated with reduction in their growth (253). It was suggested that targeting HIF-1α might provide a new therapeutic option for patients with TNBC (254). Combination of cytotoxic chemotherapy and HIF inhibitors in treatment of patients with TNBC will improve patient survival (255).

Furthermore, elevated HIF-2α expression also associated with poor prognosis in breast cancer patients (256). Combined HIF-1α and HIF-2α downregulation in TNBC xenograft have provided a wealth of information on cell metabolism and significantly affected tumour growth (253).

Moreover, CAIX has been described as a useful marker to identify cancer cell hypoxia (257, 258). Increased CAIX expression is associated with high tumour grade (259), ER-negative (260), metastasis (261), chemotherapy and radiotherapy resistance (258, 262). Clinically, high level of CAIX expression is an independent prognostic factor in ER-positive breast cancer (249), and in TNBC compared to other subtypes of breast cancer (263, 264). Trastour et al. concluded that both HIF-1α and CAIX are markers of poor prognosis of breast cancer patients (248). Jin and colleagues reported that combined expression of HIF-1α and CAIX predicts poor prognostic factor in early stage TNBC particularly in basal type (265).

However, two studies have demonstrated that in TNBC an increase of CAIX expression without HIF-1α being detected (235, 264). It is important to note that HIF-1α has a very short half-life in normoxic conditions, but CAIX protein is relatively stable and persisted much longer than HIF-1α.

1.5.5 Hypoxia and tumour metastasis

EMT is a process promoted by hypoxia which increases the aggressiveness and metastatic potential of cancer cells (266). HIF-1α activates EMT through expression of the transcription factors like SNAIL, and ZEB1 (267). Additionally, hypoxia has been shown to stimulate lysyl oxidase (LOX) and LOX-like proteins (LOXL) secretion by breast cancer cells. LOX and LOXL are collagen-stabilizing enzymes that are implicated in remodelling the ECM in metastatic sites to promote metastasis niche formation. LOX/LOXL expression remodels the ECM at metastatic sites to accelerate recruitment of bone marrow-derived cells, an effect dependent on HIF-1α and HIF-2α activity in cancer cells (268). Consequently, LOX inhibitors are being examined as potential agents that may overcome chemoresistance and decrease metastasis in TNBC (269).

1.5.6 Hypoxia and tumour metabolism

The process of glycolysis is carried out in the cytoplasm and produces two ATPs. Glucose is broken down into pyruvate that is a fuel for oxidative phosphorylation (OXPHOS). In aerobic conditions, pyruvate enters the mitochondria to be further catabolised via the tricarboxylic acid cycle and OXPHOS which can produce 36 ATPs. In anaerobic conditions, cells favour glycolysis, and pyruvate is reduced to lactate by lactate dehydrogenase A (LDH-A) in the cytoplasm and then lactate is exported into the extracellular space through monocarboxylate transporters (MCTs) (270) (Figure 1.16). In contrast to non-malignant tissue, hypoxic tumours tend to increase rate of glycolysis to support their energy demands even when oxygen is plentiful, a phenomenon termed aerobic glycolysis or the Warburg effect. This phenomenon was first observed by Warburg in the 1920s (271), and it was hypothesized that cancer results from impaired mitochondrial metabolism. However, new findings suggest controversy over Warburg hypothesis. The experimental observations of increased glycolysis in tumours even in the presence of oxygen have been repeatedly confirmed (272). Aerobic glycolysis produces lactate which contributes to extracellular acidification which provides a growth advantage to cancer tissues over normal tissues and enhances the invasion and metastasis of tumour cells (273).

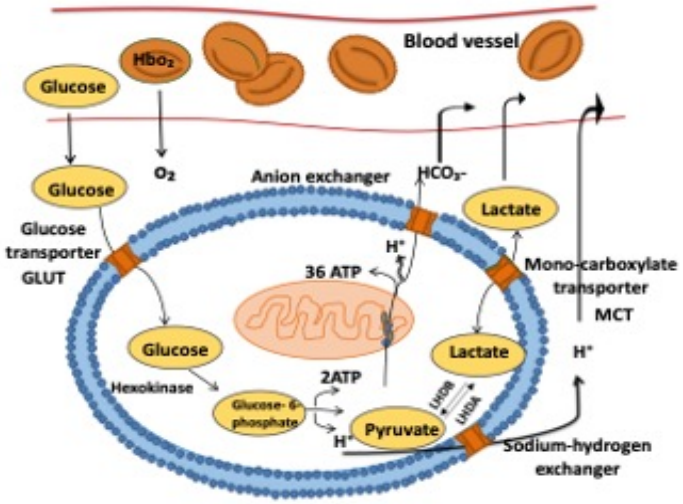

Figure 1.16 Schematic diagram of glucose metabolism in mammalian cells.

Glucose is taken up by specific transporters, where it is converted first to glucose-6-phosphate by hexokinase and then to pyruvate, generating 2 ATP per glucose. In the presence of oxygen, pyruvate is oxidized to HCO_3- generating 36 additional ATP per glucose. In the absence of oxygen, pyruvate is fermented to lactate which is exported from the cell. HbO_2: oxygenated haemoglobin, LDH-A: lactate dehydrogenase A. Modified from (270).

Certain factors contributing to the switch to aerobic glycolysis in various tumour types were reported by Zheng including oncogene activation, tumour suppressor loss, and hypoxic microenvironment (274) (Figure 1.17).

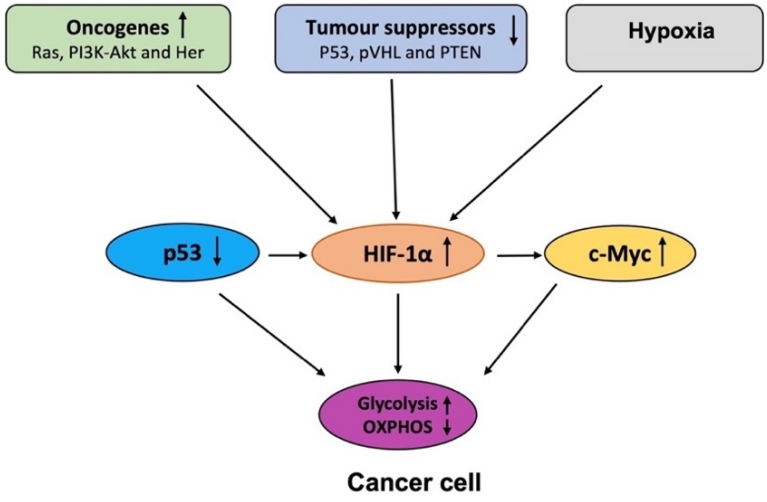

Figure 1.17 Alterations of oncogene and tumour suppressor and hypoxia drive cancer cells to aerobic glycolysis.

Schematic diagram showing HIF-1α and c-Myc, p53 transcription factors responsible for glycolysis in cancer. HIF-1α is induced by hypoxia or activated oncogenes (Ras, PI3K-Akt and Her) or inactivated tumour suppressors (p53, pVHL and PTEN) under normoxia, HIF-1α also stimulates Myc expression. OXPHOS: oxidative phosphorylation. Adapted from (274).

Tumours with high histologic grade, high mitotic index, poor differentiation, and poor outcome have been previously characterized with high metabolic activity (275). Compared to ER-positive breast cancer cell lines, TNBC cell models are shown to harbour high glycolytic flux and low OXPHOS activity (276) and are more primed to switch to aerobic glycolysis in the presence of limited oxygen than non-transformed cells (277).

The effect of HIF-1α on glycolytic metabolism is well established (278). HIF-1α maximizes the efficiency of the glycolytic shift through changes in the expression of glucose transporter (279), and glycolytic enzymes genes (270). Both the maximal glucose uptake and high efficiency of glucose utilization enables cancer cells to grow and proliferate under such conditions.

Additionally, HIF-1α enables cancer cells to maintain intracellular pH that occurs as a result of increased aerobic glycolysis and the resulting lactic acid production through increased activation and expression of HIF-1-dependent genes (280). HIF-1α activation promotes the expression of several hypoxia adaptation genes such as monocarboxylate transporter which removes lactate along with hydrogen ions from tumour cells, or CAIX which facilitates the formation of bicarbonate and hydrogen ions from CO_2 and H_2O (281).

1.5.7 Clinical relevance of hypoxia in breast cancer

Hypoxia is a poor prognostic factor in breast cancer and may cause a more aggressive malignant phenotype (282). Also, it is proposed to promote resistance to cancer therapy (246, 282). Therefore, it is a longstanding goal in experimental cancer research and clinical oncology to develop reliable markers to detect hypoxia. IHC is a reliable approach to assess endogenous hypoxia markers such as HIF-α in combination with CAIX in tumour biopsies. In the era of personalized precision medicine, clinical trials are warranted to determine whether anti-hypoxia drugs may improve the survival of breast cancer patients alone or in combination with current therapeutic regimens. It is essential to explore the crucial influence of hypoxia in the development of breast cancer in order to gain a deeper understanding of individual disease trajectories and to better anticipate them. This knowledge can then be used in the future to develop and implement adequate therapy for each individual patient.

1.6 Research aims and hypothesis

It was hypothesised that hypoxic markers are associated with development of breast cancer, resistance to endocrine therapy and are potentially a novel therapeutic target for breast cancer

treatment. Thesis aims were to investigate the prognostic role of hypoxic markers in breast cancer. In order to address the hypothesis, the main objectives were as follows:

- Investigate expression of hypoxic markers within tumour cells of breast cancer patient tissue microarrays and assess association with prognosis, and clinicopathological features.

- Investigate expression of hypoxic markers in TNBC patient tissue microarrays and assess association with prognosis, and clinicopathological features.

- Establish which biological processes, and key pathways related to hypoxic markers expression in ER-negative and a node negative subset of ER-negative breast cancer patients using TempO-Seq technology.

- Identify the mRNA signature associated with hypoxic markers expression within tumour and stromal compartments in TNBC tissue microarrays based on the NanoString technology.

Chapter 2 Materials and Methods

2.1 Tissue studies

To test whether the hypoxic markers are associated with clinical outcome measure, their expression was assessed using IHC on a tissue microarray (TMA) of breast cancer patients. Formalin-fixed paraffin-embedded tissue (FFPE) blocks were retrieved from the archives of the Department of Pathology, Glasgow Royal Infirmary, Western Infirmary and Stobhill Hospitals, in the West of Scotland, and were used to construct a TMA. Tumour-rich areas on full Haematoxylin and eosin (H&E)-stained sections were identified and marked by a qualified pathologist and were matched to FFPE blocks. Three different 0.6 mm cores per patient from each carcinoma were punched from FFPE tissue blocks and distributed in three pre-prepared holes in three new recipient paraffin array blocks (Beecher Instruments, Silver Spring, Maryland, USA). TMA blocks contained multiple tumour cores, with known coordinates to allow easy linkage to clinicopathological data. Patients were excluded from the cohort if tissue blocks were not available or had insufficient tumour tissue as determined by the pathologist.

There are several advantages of using TMAs as a research tool for the investigation of putative prognostic molecular targets. Because of the small amount of tissue required for construction, the remaining valuable tissue can be preserved for other experiments. TMAs are cost-effective and time saving as the amount of reagents was reduced and a large amount of tumour core can be stained in one run. TMAs enable standardisation for the entire cohort as they are stained in one run with the same conditions. However, due to the small size of TMA cores, the tissue cores can be vulnerable to loss while performing experiments when compared to the full sections (283). Heterogeneity and loss of cores is mitigated by having multiple cores for each tumour specimen.

Ethical approval for this study was approved by the Research Ethics Committee of the West Glasgow University Hospitals NHS Trust (NHS GG&C REC reference: 16/WS/0207).

2.1.1 Patient TMA cohorts

2.1.1.1 Cohort 1: Glasgow breast TMA (Mixed breast cancer cohort)

This retrospective TMA of patients with breast cancer was constructed by Clare Orange (TMA and Image Analysis Unit manager, University Department of Pathology, Queen Elizabeth University Hospital). Sections were marked up by pathologist (E.M). The cohort included 850 breast cancer patients presenting with invasive breast cancer in the West of

Scotland at Royal Infirmary, Western Infirmary and Stobhill Hospitals, Glasgow dating from the years 1995 and 1998. Patients were included in this study based on the selection of ductal histological subtype and having HIF-1α (2) expression available (n = 575). Therefore, 275 patients were excluded from the study as they did not have ductal carcinoma or HIF-1α (2) expression was unavailable (Figure 2.1).

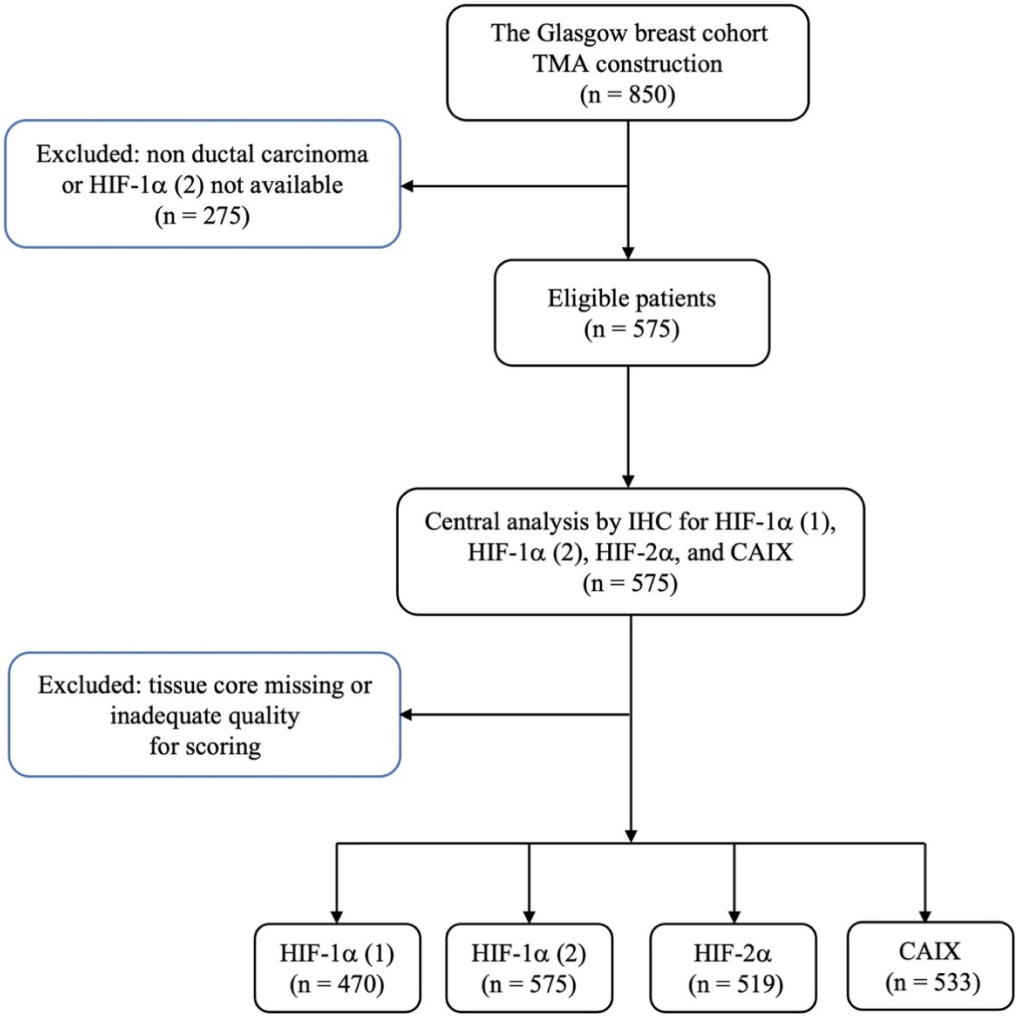

Figure 2.1 Consort diagram in the Glasgow breast cohort.

Consort diagram showing the number of patients included in analysis for each marker based on exclusion criteria of not having ductal histological subtype and HIF-1α (2) expression and missing or damaged cores. There were 850 patients in the full cohort prior to exclusions. After exclusions there were 470 patients analysed for HIF-1α (1), 575 patients for HIF-1α (2), 519 for HIF-2α, and 533 patients analysed for CAIX staining.

A database was available in the Glasgow Safe Haven (database number GSH/18/ON/008) which included clinicopathological details, adjuvant treatment and survival and recurrence data. The patients included in this study did not receive neoadjuvant therapy or adjuvant anti-Her-2 therapy. Details of proteins previously examined in Professor Edwards' laboratory in this cohort were also available in the database. ER, PR and Her-2 staining, and scoring had been previously carried out in the Edwards' lab using current diagnostic protocols. This was to ensure standardisation of technique, as techniques had changed in diagnostic labs over the time period of this cohort and routine Her-2 testing had not been established. Characteristics of the cohort are summarised in Table 2.1.

Table 2.1 Patient tissue microarrays characteristics

Clinicopathological characteristics	The Glasgow breast cohort (n = 850)	The ER-positive cohort (n = 456)	The TNBC cohort (n = 207)
Age (50/>50 years)	248(29)/602(71)	82(18)/361(82)	66(32)/140(68)
Histological status (ductal/lobular/other)	736(87)/68(8)/46(5)	350(82)/49(11)/32(7)	190 (97)/2(1)/9(2)
Size (20/21–50/>50)	496(59)/309(36)/44(5)	220(53)/176(42)/23(5)	82 (42)/100(51)/15(7)
Grade (I/II/III)	161(19)/382(45)/305(36)	102(25)/202(49)/109(26)	2(1)/15(7)/184(92)
Lymph node (negative/positive)	490(59)/348(41)	216(54)/188(46)	141(70)/62(30)
ER status (negative/positive)	276(33)/570(67)	20(5)/392(95)	-
PR status (negative/positive)	448(53)/396(47)	169(41)/238(59)	-
Her-2 status (negative/positive)	699(85)/128(15)	407(91)/39(9)	-
Ki67 (proliferative index) (low/high)	567(61)/228(29)	248(61)/159(39)	-
Molecular subtype (lum A/lum B/TNBC/Her-2)	371(47)/178(22)/176(22)/73(9)	221(57)/90(23)/0(0)/0(0)	-
Adjuvant endocrine therapy (no/yes/ATAC trial)	141(20)/528(75)/32(5)	0(0)/456(100)/0(0)	-
Adjuvant chemotherapy (no/yes)	516(61)/331(39)	338(76)/105(24)	30(15)/176(85)
Adjuvant radiotherapy (no/yes)	446(53)/401(47)	317(70)/139(30)	45(22)/161(78)
Alive/cancer death/non-cancer death	482(58)/174(21)/157(19)	243(55)/116(26)/84(19)	128(62)/69(34)/9(4)
No recurrence/local/distant/both	648(78)/50(6)/123(15)/8(1)	310(70)/118(27)/12(2)/3(1)	136(67)/31(15)/28(14)/7(4)

Table showing the number of patients with clinical characteristics in each cohort including age, histological status, tumour size, grade, lymph node, ER, PR, Her-2 status, Ki67, molecular subtype, adjuvant endocrine therapy, adjuvant chemotherapy and adjuvant radiotherapy.

Clinical end points used were RFS (was measured from the date of primary surgery until the date of the first loco-regional or systemic recurrence), DFS (was measured from the date of primary surgery to the date of the first loco-regional or systemic relapse, or mortality in the absence of relapse) and OS (was defined from the day of surgery until death of the patient either from cancer or a cause other than breast cancer).

Patients were routinely followed up after surgery for minimum of 10-years. Date and cause of death were checked with the cancer registration system and the Registrar General (Scotland).

The follow up for the whole cohort ranged from 1−183 months with a median follow up time was 150.37 (73−165) months. There were 482 patients alive at the last follow up, and median follow up was 162.7 months (range 153−170.98 months). At the last follow up 174 patients had died of their disease and 157 had died of other causes. Follow up of recurrence status found 181 patients had relapsed.

Subtypes in the Glasgow breast cohort

The Glasgow breast cohort includes both ER-positive and ER-negative patients, PR status, Her-2 status and Ki67 index. It was possible to categorise the cohort into four distinct subtypes. 15 (3%) of the 575 patients were missing and were excluded from analysis. Of the remaining 560 patients, 238 (43%) were categorised as luminal A and 130 (23%) as luminal B, 62 (11%) as Her-2 enriched, and 130 (23%) as TNBC as shown in Table 2.2.

Table 2.2 Subtyping of the Glasgow breast cohort

Subtype	IHC markers	Patients number n = 560 (%)
Luminal A	ER or PR+, Her-2−, low Ki67 (< 14%)	238 (43)
Luminal B	ER or PR+, Her-2+ and/or high Ki67 (≥ 14%)	130 (23)
Her-2 enriched	ER, and PR−, Her-2+	62 (11)
Triple negative	ER, PR and Her-2−	130 (23)

Table outlining IHC description and the number of patients for each breast cancer subtype in Glasgow breast cohort including luminal A, luminal B, triple negative and Her-2 enriched.

2.1.1.2 Cohort 2: ER-positive TMA

In order to confirm the results from the Glasgow breast cohort, ER-positive cohort was stained for HIF-1α (1), HIF-1α (2), HIF-2α, and CAIX. This retrospective TMA of breast cancer was constructed by Dr Sian Tovey, and sections were marked up by pathologist (B.D). The TMA included 456 patients presenting with invasive breast cancer and undergoing curative surgery between 1980 and 1999 within Western Infirmary, Victoria Hospital, and Stobhill Hospital, Glasgow. Patients were included in this cohort base on initial ER-positive pathological reports. 20 were found to be ER-negative and 44 were of unknown ER status and were excluded from the study. 107 patients were excluded from analysis as they did not have ductal carcinoma or HIF-1α (2) expression was unavailable remained 285 patients available for analysis as shown in Figure 2.2.

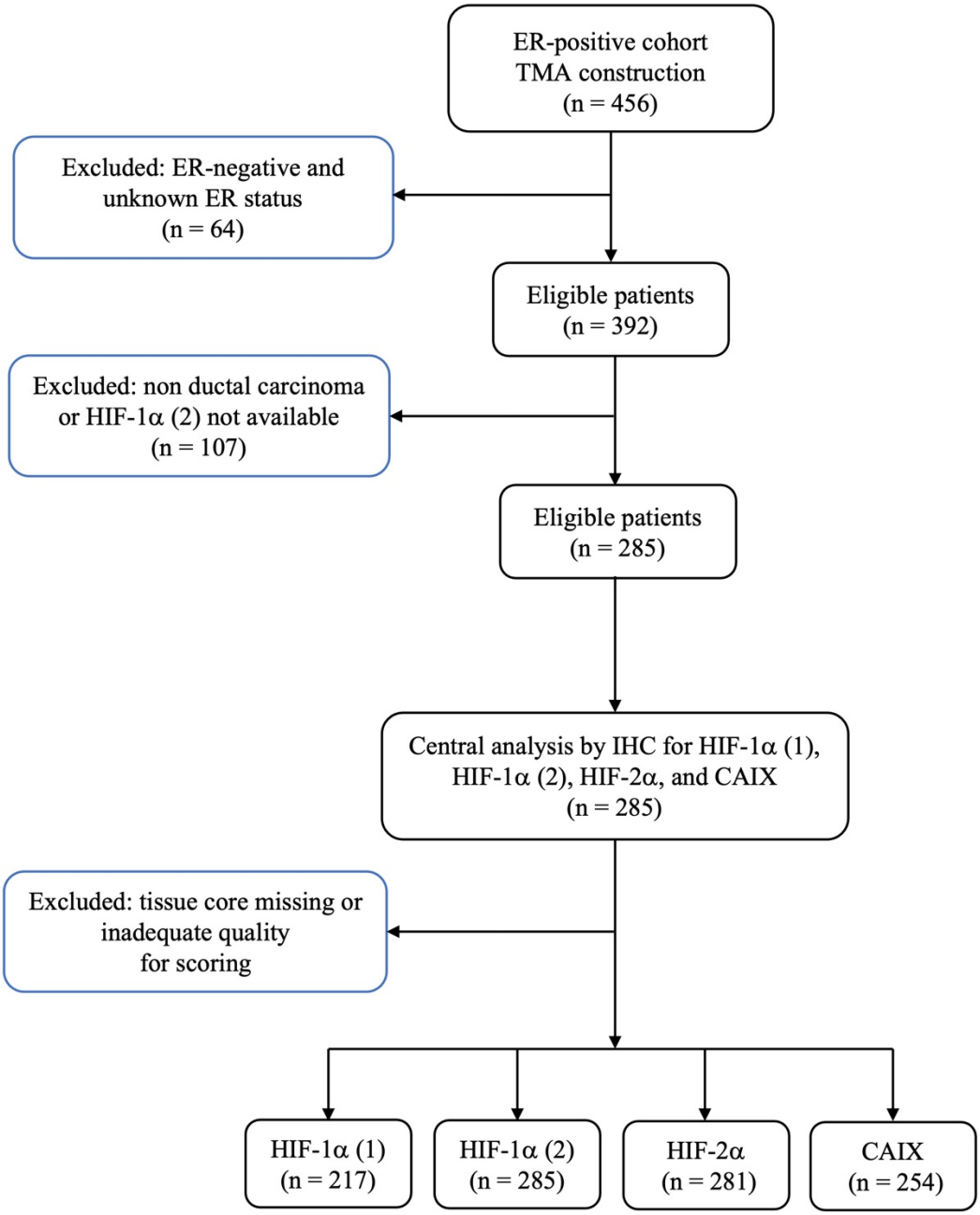

Figure 2.2 Consort diagram in the ER-positive cohort.

Consort diagram showing the number of patients included in analysis for each marker based on exclusion criteria of having ER-negative status, not having ductal histological subtype and HIF-1α (2) expression and missing or damaged cores. There were 456 patients in the full cohort prior to exclusions. After exclusions there were 217 patients analysed for HIF-1α (1), 285 patients for HIF-1α (2), 281 for HIF-2α, and 254 patients analysed for CAIX staining.

The clinicopathological data available via Glasgow Safe Haven (database number GSH/21/ON/011) and including patient's age, histological tumour type, tumour size, tumour grade, involved lymph node status, PR status, Her-2 status, and Ki67 proliferation index. In this cohort patients were treated with adjuvant tamoxifen and time on tamoxifen was available in the database, as well as recurrence and survival follow up. This pathological information was previously retrieved from the pathology routine reports and recorded in SPSS database. The key characteristics of this cohort are summarised in Table 2.1.

Clinical end points used were again RFS, DFS and OS. The follow up for the whole cohort ranged from 0−311.2 months with a median follow up time was 85.44 months (range 58.65−119.13) months. There were 243 patients alive at the last follow up, and median follow up was 97.44 (68.88−119.64) months. At the last follow up date, the number of patients who had died from cancer was 116 and those who died from other causes was 84. The number of patients who experienced local and distance recurrence was 118 and 12, respectively.

Subtypes in the ER-positive TMA cohort

This cohort was an ER-positive cases. The cohort was subdivided into luminal A and luminal B subtypes using Her-2 status and Ki67 index. 47 (17%) of the 285 patients were missing and were excluded from analysis. Of the remaining 238 patients, 169 (71%) were categorised as luminal A and 69 (29%) as luminal B, as detailed in Table 2.3.

Table 2.3 Subtyping of the ER-positive cohort

Subtype	IHC markers	Patients number n = 238 (%)
Luminal A	ER or PR+, Her-2−, and low Ki67 (< 15%)	169 (71)
Luminal B	ER or PR+, Her-2+ and/or high Ki67 (≥ 15%)	69 (29)

Table outlining IHC description and the number of patients for each subtype in ER-positive cohort including luminal A and luminal B.

2.1.1.3 Cohort 3: Triple negative breast cancer (TNBC) cohort

The results from the Glasgow breast cohort were confirmed in a newer cohort with relevance to modern clinical practice. This retrospective TMA TNBC was constructed by Dr Jennifer Hay (University Department of Pathology, Queen Elizabeth University Hospital), tumour and stromal regions were identified by a consultant pathologist (E.M). This cohort included 207 patients presenting with invasive TNBC between 2011 and 2019 in the West of Scotland at Greater Glasgow and Clyde. TNBC cohort was stained for CAIX. After excluding patients who did not have ductal carcinoma or CAIX expression was unavailable (n = 30), and who received neoadjuvant chemotherapy (n = 41), 136 patients remained for downstream analysis (Figure 2.3).

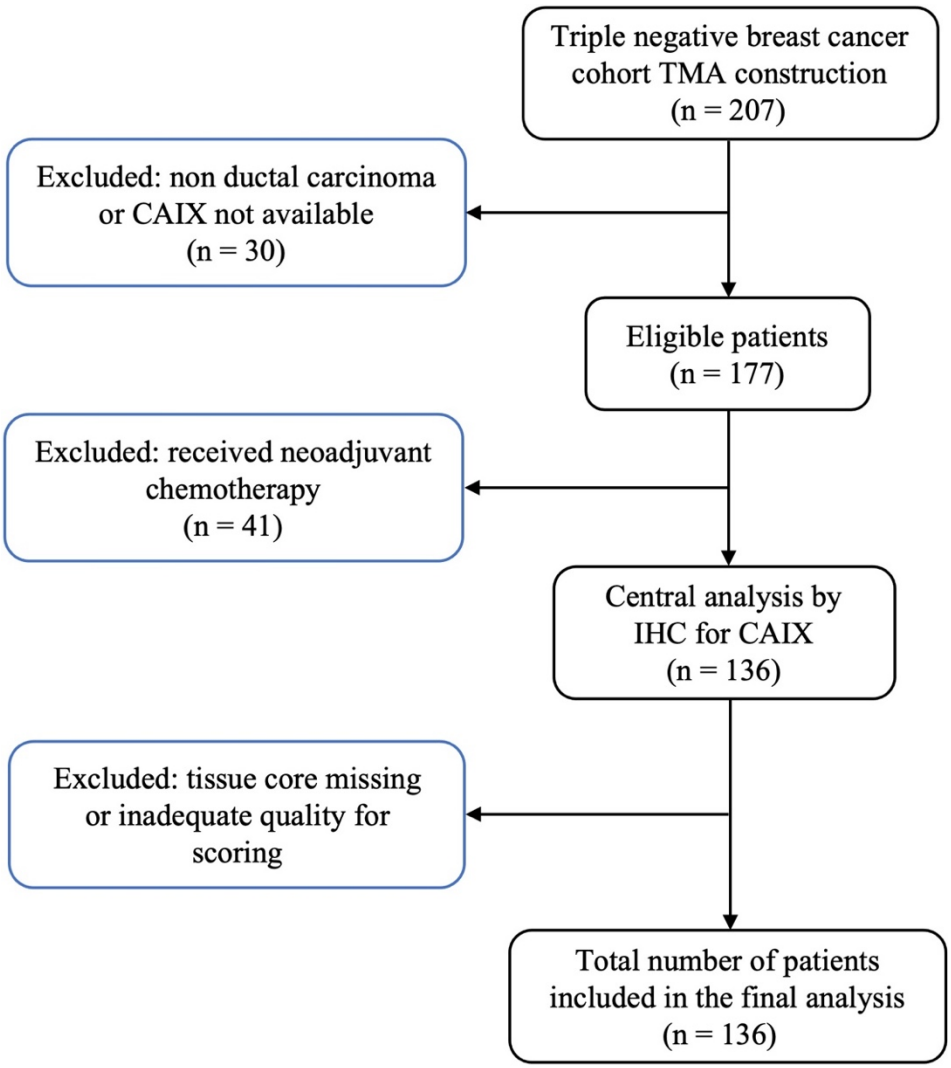

Figure 2.3 Consort diagram showing patient exclusions in TNBC cohort.

Consort diagram showing the number of patients included in analysis for CAIX based on exclusion criteria of not having ductal histological subtype, CAIX expression, administration of neoadjuvant therapy, and missing or damaged cores. There were 207 patients in the full cohort prior to exclusions. After exclusions there were 136 patients analysed CAIX staining.

A database of clinicopathological features was available, including patient age, tumour size, grade, lymph node status and treatment the patient received. Clinical information of the patients was held by Professor Joanne Edwards and in Glasgow Safe Haven (GSH/21/ON/008). The key characteristics of this cohort are summarised in Table 2.1. Patients with insufficient tumour tissue or incomplete follow up were excluded.

Clinical endpoints included RFS, DFS, and OS. The follow up for the whole cohort ranged from 0–112 months with a median follow up time was 52.6 (33–69) months. There were 112 patients alive at the last follow up, and median follow up was 64.20 months (range 49.38–

77.47 months). At the last follow up date, the number of patients who had died from breast cancer was 69 and those who died from other causes was 9. The number of patients who experienced recurrence was 66 patients.

2.1.2 Control tissue

TMAs of breast cancer patients without associated clinical data were available for optimisation of antibodies. These were included as positive and negative controls in IHC experiments. Positive controls were included in every step of the IHC procedure and incubated in identical solutions as to the TMAs of patients. Cores of liver, kidney, prostate, lung, colon, tonsil and pancreas tissue were included as positive controls in the Glasgow breast cohort, and cores of lung, liver, gut, smooth muscle, pancreas and tonsil were included as positive controls in the ER-positive cohort for the various antibodies. Tonsil, colon, liver, prostate, spleen, lung, breast and skin were used as positive controls in TNBC cohort. Negative controls were included in every step with the exception of primary antibody, and slides were instead incubated in antibody diluent for the duration of primary antibody incubation.

2.1.3 Antibody validation

To ensure antibodies utilised were specific for the target protein, specificity testing was performed.

2.1.3.1 Western blotting for antibody specificity

Western blotting was used to validate the specificity of HIF-1α (1), HIF-1α (2) HIF-2α, and CAIX antibodies. Running buffer was prepared by diluting 100mL 10x running buffer, tris/glycine/SDS in 900mL distilled water. Precast protein gels (4–20% Mini-PROTEAN TGX) were utilised (Bio-Rad #4561023). The gel tank was assembled, added to the Bio-Rad tank, and tested for leakage when the reservoir was filled with running buffer.

HeLa hypoxic/normoxic cell lysates (Novus NBP2-36452) were purchased. Ladder (10µL) was loaded into lane 1 and 15µL samples were added to remaining 4 wells plate onto precast gels. Gels were run for 90 minutes or until the samples reached the edge of the gel at a constant 120 Volts. Transfer buffer was prepared by adding 200mL methanol and 100mL 10x transfer buffer (tris/glycine) to 700mL distilled water. Polyvinylidene fluoride (PVDF) membranes (Amersham Pharmacia Biotech, Buckinghamshire, UK) were soaked in

methanol for 5 minutes. Sponges and filter paper were soaked in transfer buffer. Sandwich was prepared as outlined in Figure 2.4 and rolled using to remove any air bubbles. The assembled cassette was added to the tank and run at constant 300mA for 90 minutes to transfer protein from gels to the membranes.

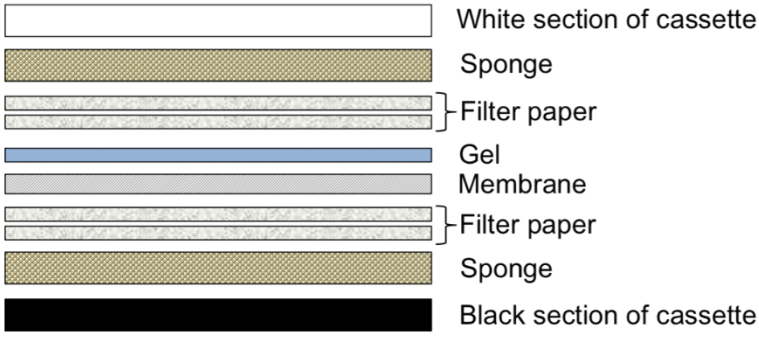

Figure 2.4 Assembly of the sandwich for Western blot transfer.

Diagram showing the makeup of gel membrane sandwich utilised in Western blot transfer step. The cassette is opened, and a piece of sponge is placed at both ends. Two pieces of filter paper are added to each side and the membrane is placed on the side nearest the black end of the cassette. The gel is carefully added on top of the membrane and the sandwich is assembled.

The sandwich was removed from the tank and membranes were blocked depending on the antibody, either with 3% bovine serum albumin (BSA) in tris-buffered saline plus 0.05% Tween-20 (TBST) for HIFs or with 5% non-fat dry milk dissolved in TBST for CAIX for 1 hour on a platform shaker at room temperature. Membranes were incubated in appropriate primary antibody (diluted in 0.3% BSA for HIFs antibodies or in 0.5% dry milk dissolved in TBST for CAIX antibody) overnight at 4^{o}C and then washed three times in TBST for 10 minutes. Conditions for each antibody are listed in Table 2.4. Secondary antibodies were diluted either in 0.3% BSA or in 0.5% non-fat dry milk dissolved in TBST (1:5000 for anti-rabbit and 1:10000 for anti-mouse antibodies) with anti-ladder at 1:50000. Membranes were incubated for 90 minutes in secondary antibodies at room temperature and then washed three times for 10 minutes in TBST. After washing, membranes were incubated in horse radish peroxidase (HRP) substrate enhanced chemiluminescence reagent (Pierce ECL) (Thermo Fisher Scientific, Waltham, MA, USA) for 5 minutes at room temperature. Membranes were blotted on blue roll and then imaged using Syngene Gene Sys (Syngene International Ltd, India). All experiments were repeated three times.

Table 2.4 Antibodies used for Western blot and optimal conditions

Protein of interest	Antibody	Species	Manufacturer	Blocking conditions	Primary antibody	Secondary antibody
HIF-1α (1)	Monoclonal anti-HIF-1α 67 antibody (Novus Biologicals, Abingdon, UK)	Mouse	Novus Biologicals	3% BSA in TBST, 60 minutes	1:2000 (0.3% BSA), overnight 4ºC	1:10000 (0.3% BSA), 90 minutes
HIF-1α (2)	Polyclonal anti-HIF-1α antibody (Novus Biologicals, Abingdon, UK)	Rabbit	Novus Biologicals	3% BSA in TBST, 60 minutes	2.5:10000 (0.3% BSA), overnight 4ºC	1:5000 (0.3% BSA), 90 minutes
HIF-2α	Polyclonal anti-HIF-2α antibody (Novus Biologicals, Abingdon, UK)	Rabbit	Novus Biologicals	3% BSA in TBST, 60 minutes	1:10000 (0.3% BSA), overnight 4ºC	1:5000 (0.3% BSA), 90 minutes
CAIX	Monoclonal anti-CAIX antibody (Bioscience, Slovakia)	Mouse	Bioscience	5% milk in TBST, 60 minutes	1:4000 (0.5% milk in TBST), overnight 4ºC	1:10000 (0.5% milk in TBST), 90 minutes

Table showing the species for each antibody and the optimal conditions for Western blotting.

2.1.3.2 Cell pellets for antibody specificity

Human cell lines are an important resource for research and are often used as *in vitro* models of human diseases. The cells commonly used in the lab include MCF-7 and MDA-MB-231 breast cancer cell lines.

2.1.3.2.1 Culturing of breast cancer cell lines

MCF-7 (ER-positive) and MDA-MB-231 (ER-negative) breast cancer cells were routinely cultured in GlutaMAX^{TM} medium supplemented with 10% (v/v) fetal bovine serum (FBS, Sigma-Aldrich, Gillingham, UK). Cells were grown in T-75 flasks and maintained in 5% CO_2 at 37°C, with media changed twice per week and cells passaged once a confluency of around 70% was reached. To passage cells, flasks were washed once with 1.5ml of phosphate-buffered saline (PBS) to remove traces of serum and 1ml trypsin was added to detach cells from the flask and then incubated at 37°C in 5% CO_2 for 5 minutes. Once cells had detached, medium was added to inactivate the trypsin. Cells were carefully pipetted on the side of the flask to break any clusters, before being split 1: 6 into new T-75 flasks with fresh medium.

2.1.3.2.2 Cell culture and $CoCl_2$ treatment

In order to activate the hypoxia and stimulate expression of certain hypoxic proteins, cells were treated with hypoxia-mimetic agent, cobalt chloride ($CoCl_2$) (Cat no. C8661; Sigma-Aldrich, St. Louis, MO, USA). $CoCl_2$ was used as a chemical hypoxia mimetic agent, because of its property to mimic hypoxic conditions. $CoCl_2$ strongly stabilizes HIF-1α and HIF-2α for several hours under normoxic conditions (284). Therefore, this $CoCl_2$ model permits users to modify and analyse their samples over a longer period of time under normoxia. The $CoCl_2$-hypoxia model is based on blocking PHDs activity, the key enzymes that link O_2 concentration to the degradation of HIF under normoxic conditions, by substitution of Fe^{2+} in PHD by Co^{2+} (cobalt), thus increasing HIF-1α protein levels and inducing its transcriptional activity (284). Because $CoCl_2$ is a reliable HIF-1α inducer, and hypoxia response mimicker, this chemically induced hypoxia is widely used in hypoxia-related research (285, 286).

A stock solution of 100μM $CoCl_2$ was prepared in PBS (1.29mg $CoCl_2$ in PBS to a total volume of 10mL). 10μL of this was added to 9.99mL growth medium to give a final concentration of 100μM. Cells were incubated in this medium for 4 hours and 24 hours in

5% CO_2 and then harvested. Then, the effect of $CoCl_2$ treatment was examined on the expression of HIF-1α, HIF-2α, and CAIX in cultured cells (MCF-7).

2.1.3.2.3 Preparation of cell pellets

After exposed to treatment with 10μL $CoCl_2$ to mimic hypoxia, cells were trypsinised and added to a 15mL falcon tube with medium up to 10mL. Tubes were centrifuged for 3 minutes at 1200 RPM. Supernatant was removed using an aspirator and the pellet resuspended in PBS. Cells were spun for 3 minutes at 1200 RPM. Supernatant was removed and cells were resuspended in 1mL 4% paraformaldehyde (PFA) at room temperature and transferred to Eppendorf tubes. After 20 minutes fixation cells were spun at 1200 RPM for 3 minutes and washed in PBS twice. Once dry, the pellet was resuspended in 1% agarose and left overnight at 4ºC. The embedded pellet was removed, transferred to a labelled cassette. The pellet was dehydrated through a series of graded alcohols (50% once for 15 minutes, 75% once for 15 minutes and 100% twice for 15 minutes), then submersed in Histoclear twice for 15 minutes. Finally, the pellet was removed from the cassette, placed in a mould, embedded in paraffin wax and left on a cold block for 1 hour.

2.1.3.2.4 Cutting cell pellets

Following setting overnight, 4μm thick sections from embedded pellets were obtained with a Leica microtome, transferred onto adhesive slides, dried at 50ºC overnight and baked at 62°C for 30 min.

2.1.3.2.5 Immunohistochemistry of cell pellets

After cutting onto slides, pellets were then stained using the same IHC method outlined in section 2.2 for respective proteins, aside from heating at pressure for 2 minutes and 30 seconds as opposed to 5 minutes for TMAs.

2.2 Immunohistochemistry

Immunohistochemistry utilizes antigen-antibody recognition in detecting specific antigens within breast cancer tissues. A variety of markers has been evaluated for their role in the prognosis. IHC expression of hypoxic markers, HIF-1α (1), HIF-1α (2), HIF-2α, CAIX, anti-apoptotic marker, BCL2, and immune markers, CD3 and CD68, were carried out using a previously constructed TMA. HIF-1α (1), HIF-1α (2) are from different suppliers. The technique uses a specific antibody to the target antigen of interest. A labelled secondary

antibody is then used which reacts with the primary antibody, then DAB chromogen is applied as a signal enhancer so that expression of the antigen can be visualised under a light microscope as a brown stain. The slides are then counterstained with Haematoxylin so that the primary stain is more distinct. The various steps of IHC are described in more details below. There was some variation between antibodies in terms of specific timings of stages of the protocol and types of reagents used, because of variability in the optimal conditions for certain antibodies or changed suppliers to the laboratory. These variations are summarised in Table 2.5.

Table 2.5 Optimal antibody conditions for immunohistochemistry

Target	Clone	Origin	Manufacturer SAME COMPANY	Dilution	Antigen retrieval buffer	Expected staining	Blocking conditions
HIF-1α (1) (anti-HIF-1α 67, NB 100-105; Abingdon, UK)	Monoclonal	Mouse	Novus Biologicals	1:150	Tris-EDTA pH9	Cytoplasmic and nuclear	1.5% horse serum 60 minutes
HIF-1α (2) (anti-HIF-1α, NB 100-449; Abingdon, UK)	Polyclonal	Rabbit	Novus Biologicals	1:400	Tris-EDTA pH9	Cytoplasmic and nuclear	1.5% horse serum 60 minutes
HIF-2α (anti-HIF-2α, NB 100-122; Abingdon, UK)	Polyclonal	Rabbit	Novus Biologicals	1:1000	Tris-EDTA pH9	Cytoplasmic and nuclear	1.5% horse serum 60 minutes
CAIX (anti-CAIX, Slovakia)	Monoclonal	Mouse	Bioscience	1:500	Citrate pH6	Cytoplasmic and membrane	10% casein 60 minutes
BCL2 (anti-BCL2, Cheadle, UK)	Monoclonal	Mouse	Agilent	1:150	Tris-EDTA pH9	Cytoplasmic	-
CD68 (anti-CD68, Newcastle, UK)	Monoclonal	Mouse	DAKO	1:200	HIER Buffer	Cytoplasmic	200µl of UVQ protein 5 minutes
CD3 (anti-CD3, Newcastle, UK)	Monoclonal	Mouse	Leica	1:100	HIER Buffer	Cytoplasmic	200µl of UVQ protein 5 minutes

Table outlining the clone, origin, manufacture, dilution, antigen retrieval buffer, blocking solution for each protein. HIER: heat-induced epitope retrieval/ UVQ: UltraVision Quanto.

2.2.1 Slides preparation

Tissue TMA sections were requested from NHS Research Scotland GGC Biorepository. Tissue was cut at 2.5µm thick paraffin wax sections and mounted onto slides. They were baked overnight at 56ºC prior to being stored at 4ºC.

2.2.2 Immunostaining of markers

2.2.2.1 HIFs and CAIX immunostaining

Immediately before staining TMA sections were baked at 56ºC for 20 minutes to minimise the risk of core loss, then immersed in Histoclear twice for 3 minutes to deparaffinized them. Slides were then rehydrated through a decreasing gradient of alcohols (100% twice for 3 minutes, 90% once for 2 minutes then 70% once for 2 minutes) before being rinsed in water for 10 minutes.

Subsequently, to unmask epitopes blocked during formalin fixation, antigen retrieval was performed using Tri-EDTA buffer (pH9) or citrate buffer (pH6) depending on the antibody. The Tris/EDTA buffer is made up of 0.55g Tris Base (BP152-1, Fisher Scientific, Loughborough, UK) and 0.37g sodium EDTA (Ethylenediamine tetra-acetic acid) (27285, Sigma-Aldrich, St Louis, USA) in 1L distilled water. The citrate buffer is made up of 2.41g tri-sodium citrate dihydrate (S/3320/53, Fisher Scientific, Loughborough, UK) and 0.34g citric acid (27109, Sigma-Aldrich, St Louis, USA) in 1L distilled water. The buffer was adjusted to the required pH using 0.1M hydrochloric acid or 0.1M sodium hydroxide. The buffer and pH used for each antibody is detailed in Table 2.5.

Prior to antigen retrieval 1L of buffer was heated in an open pressure cooker in a microwave for 14 minutes. Slides were added to the buffer and the pressure cookers seal, lid and topper were secured. The slides were heated for around 3 minutes until pressure reached and then heated for a further 5 minutes. After heating sections were left to cool for 30 minutes in buffer and then rinsed in running water.

Then, slides were placed in 3% hydrogen peroxide (H_2O_2) (23619.297 30% hydrogen peroxide VWR Chemicals) for 30 minutes to quench endogenous peroxidases, thus reducing background staining, then slides were rinsed in running water.

To prevent off-target non-specific binding sections were incubated in a blocking solution by using either 5% horse serum (Vector Laboratories, USA) or 10% casein (Vector

Laboratories, USA) for 1 hour at room temperature. Blocking solutions were diluted in antibody diluent (S0809, Dako, Agilent Technologies, Stockport, UK). Antibodies specific for HIFs and CAIX were diluted to respective concentrations in antibody diluent (S0809, Dako, Agilent Technologies, UK). Blocking solution was tapped off, diluted antibodies were added, and sections were incubated at 4ºC overnight. Details of the used blocking solution, and primary antibodies are listed in Table 2.5.

After incubation sections were washed twice in Tris-buffered saline (TBS) for 5 minutes and incubated in ImmPRESS™ Reagent Kit (MP-7500, Vector, Burlingame, CA, USA) which detects both mouse and rabbit primary antibodies for 30 minutes at room temperature. The slides were washed twice again with TBS for 5 minutes.

Antibodies were detected with 3-3'-diaminobenzidine substrate (DAB) as the chromogen (Vector Laboratories) for 5 minutes at room temperature and subsequently rinsed in running water for 10 minutes.

Slides were counterstained in Haematoxylin Gill III (Leica Microsystems, Milton Keynes, UK cat. No. 3801540E) for 5 minutes, dipped in 1% acid alcohol (396 ml 70% ethanol and 4ml hydrochloric acid) for 3 seconds to remove excess Haematoxylin then blued in Scott's Tap Water Substitute (80mM Magnesium sulphate, 40mM sodium hydrocarbonate in distilled water) for 45 seconds. After counterstaining, the slides were dehydrated in increasing alcohol gradients (1 minute in 70%, 1 minute in 90%, and 100% twice for 1 minute) followed by Histoclear twice for 2 minutes. Finally, slides were then mounted with coverslips using DPX mountant (06522, Sigma-Aldrich, St Louis, USA) and allowed to dry.

2.2.2.2 BCL2 immunostaining

FFPE sections were loaded into an Agilent pre-treatment module to be dewaxed and heated to 97ºC for 20 minutes in target retrieval solution (TRS) (K8004, Agilent) using EDTA buffer (pH9). Sections were rinsed in flex wash buffer (K8007, Agilent) prior to being loaded onto a Dako Autostainer. The sections underwent peroxidase blocking (S2023, Agilent) for 5 minutes and rinsed with flex buffer. The BCL2 antibody was applied to sections for 35 minutes. Antibody details are shown in Table 2.5. After incubation, sections were washed with flex wash buffer and then incubated in mouse envision secondary antibody (K4001, Agilent) for 30 minutes. Slides were rinsed with flex wash buffer before applying liquid DAB (K3468, Agilent) for 10 minutes, then washed in water and counterstained with Haematoxylin z (RBA-4201-00A, CellPath). To complete the IHC staining, sections were

dehydrated in a series of graded alcohols and placed in xylene. The stained sections were cover slipped in xylene using DPX mountant (SEA-1300-00A, CellPath). BCL2 staining was performed by Beatson Institute of Cancer Research histological services.

2.2.2.3 CD68 and CD3 immunostaining

Slides were incubated at 97ºC for 30 minutes with dewax and antigen retrieval buffer H (Epredia) using PT module. CD3 and CD68 IHC staining was performed by A.A using the UltraVision Quanto (UVQ) kit (Epredia) according to manufacturer instructions. In brief, endogenous peroxidase was blocked using 200µl of UVQ H_2O_2 block for 10 minutes then rinsed in TBST, and non-specific binding blocked by 200µl of UVQ protein block for 5 minutes. After incubation with primary antibodies for 30 minutes, an amplifier treatment for 10 minutes, and HRP treatment for 10 minutes was performed. Details of antibodies, and dilution factors can be found in Table 2.5. Subsequently, sections were stained for 5 minutes with Quanto DAB chromogen, counterstained with Haematoxylin Gill III using the Myreva Autostainer, dehydrated, and mounted using Pertex.

For each antibody, optimal dilution was optimised on practice tissue before being applied to the cohort. The negative control slides were covered with antibody diluent only to assess the degree of non-specific staining, and these were all negative. The TMAs included appropriate positive control tissues.

2.2.3 Scanning and visualisation of slides

Stained TMAs were scanned by Hannah Morgan (Pathology Department Queen Elizabeth University Hospital) using Hamamatsu NanoZoomer Digital Slide Scanner (Hamamatsu Photonics K.K., Shizuoka, Japan) and visualised in NDP serve 3 image viewer platform system. Slides were visualised at 20x magnification (total 400x magnification).

2.3 Pathological scoring of immunohistochemistry

Assessment of IHC-stained TMA cores for all markers by the presence of brown coloured reaction in the membrane/nucleus and/or cytoplasm was considered a positive reaction. Cores with <20% of the core missing by visual assessment were scored. Different scoring methods were required to be most appropriate to the biomarkers. For all antibodies, expression of protein levels was assessed at each cellular compartment separately. Expression of HIF-1α (1), HIF-1α (2), HIF-2α and CAIX was assessed in tumour cells to evaluate hypoxia, BCL2 expression was used to evaluate apoptosis, CD3 expression

identified lymphocytes, CD68 expression was used to detect macrophages, and D2-40 and Factor VIII was used to identified tumour invasion and metastasis.

2.3.1 Manual weighted Histoscore

Tumour cell expression of HIF-1α (2), HIF-2α, and CAIX in the Glasgow breast cohort and ER-positive cohort and membranous CAIX in TNBC cohort was assessed using the weighted Histoscore method (287, 288). The weighted Histoscore was calculated as follows: (% of unstained tumour cells × 0) + (% of weakly stained tumour cells × 1) + (% of moderately stained tumour cells × 2) + (% of strongly stained tumour cells × 3) to give a range from 0–300. Scoring was performed by a single observer (S.S) blinded to patient clinical and survival data. 10% of cores were co-scored independently by a second scorer (J.E) and the correlation coefficient calculated to ensure good agreement.

2.3.2 QuPath scoring

HIF-1α (1) levels in the Glasgow breast cohort and ER-positive cohort and cytoplasmic CAIX, HIF-1α (1), BCL2, and CD3 in TNBC cohort were scored digitally using QuPath by a single observer (S.S). In brief, after using the TMA Dearrayer function to create a TMA grid with cores in their correct positions, stain vectors were estimated during pre-processing by the visual stain editor available in QuPath, to increase staining quality. Then, cells were detected using a watershed cell detection method, and annotations were made to allow QuPath to recognise different tissue types which are tumour and stroma (Figure 2.5). Then, a random trees classifier was trained using over 40 features such as perimeter, area, and optical density. Three intensity thresholds were used to represent negative, weak, moderate, and strong staining, and after the classifier was built, the auto-update feature was used to re-validate the classifier's accuracy in real-time. The classifier was then saved and applied to all TMA slides that were subjected to QuPath analysis (289). Manual scoring was used to score 10% of cores to ensure reliability and objectivity of QuPath scoring by a second observer (S.A).

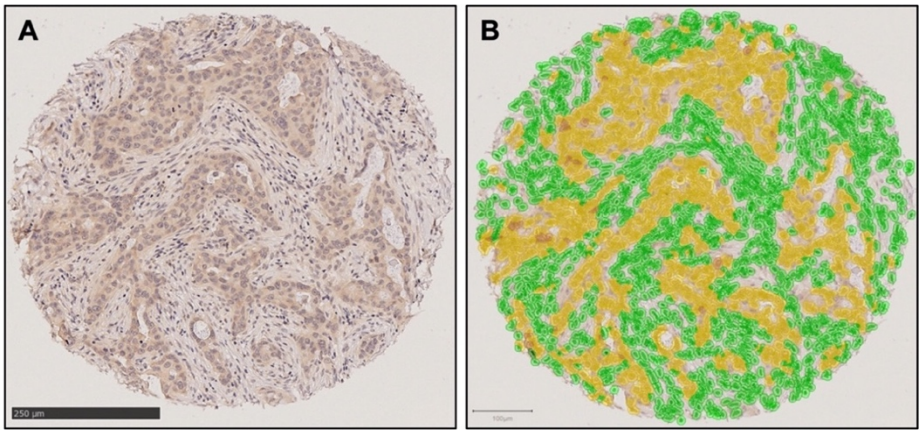

Figure 2.5 Cytoplasmic scoring using QuPath digital platform.

Representative images show original IHC image of cytoplasmic HIF-1α (1) staining [A], and annotation for tumours and stroma [B]. Green indicates regions classified as stroma, and brown indicates tumour epithelium.

2.3.3 Manual quantification method

QuPath method was inappropriate to score macrophages due to shape irregularity, therefore, cytoplasmic CD68 were quantified manually in IHC-stained TMAs from TNBC cohort by the single observer (S.S). CD68 cells were counted in each tumour/stroma core within the tumour nests and the TME separately. The total number of CD68 cells was the sum of the cells in the tumour nest and the TME. Scores were rechecked randomly by a second observer (A.A) to ensure reproducibility.

Expression of each marker within the three cohorts was assessed in the three separate tumour cores. Then, values from three cores were averaged for each patient. If one core was uninformative (either lost or contained no tumour tissues), the overall score applied was that of the remaining core.

2.3.4 Scoring of lymphatic endothelial marker D2-40 and vascular endothelial marker Factor VIII

Two consecutives full TNBC IHC slides were stained by J.Q according to standard protocol and used to assess lymphovascular invasion (LVI) for lymphatic marker, D2-40 and for vascular marker, Factor VIII. Full TNBC Haematoxylin and Eosin (H&E) sections were also used to assess and review the presence of LVI. D2-40 and Factor VIII-H&E-stained sections were scanned at objective magnification 20x. Assessment of $LVI_{D2\text{-}40}$ and BVI_{FVIII} were carried out on a computer monitor using the NDP serve 3 image viewer platform system.

For the assessment of LVI, in serial IHC sections similar to that of H&E sections, $LVI_{D2\text{-}40}$ and BVI_{FVIII} were identified at peritumoural, invasive front or intratumoural areas using criteria previously described (290), as the presence of tumour cell emboli within a vessel space, which was identified by associated fibrin clot and/or an endothelial cell lining. $LVI_{D2\text{-}40}$ was identified by tumour cells within D2-40-positively stained vessels whereas BVI_{FVIII} was counted only when tumour cells were identified in D2-40-negative, Factor VIII-positive vessels (Figure 2.6). $LVI_{D2\text{-}40}$ was generally more extensive than BVI_{FVIII} and lymphatic tumour emboli were larger than blood vessel emboli. A total of 30% of stained sections for LVI and BVI were independently scored by H.W blinded to patient outcome and the other observer's score (S.S).

Reliability analysis was performed with SPSS software to ensure consistency and objectivity between the main scorer and the co-scorers giving an interclass correlation coefficient (ICCC) for all markers. Values above 0.75 are indicative of good reliability (291).

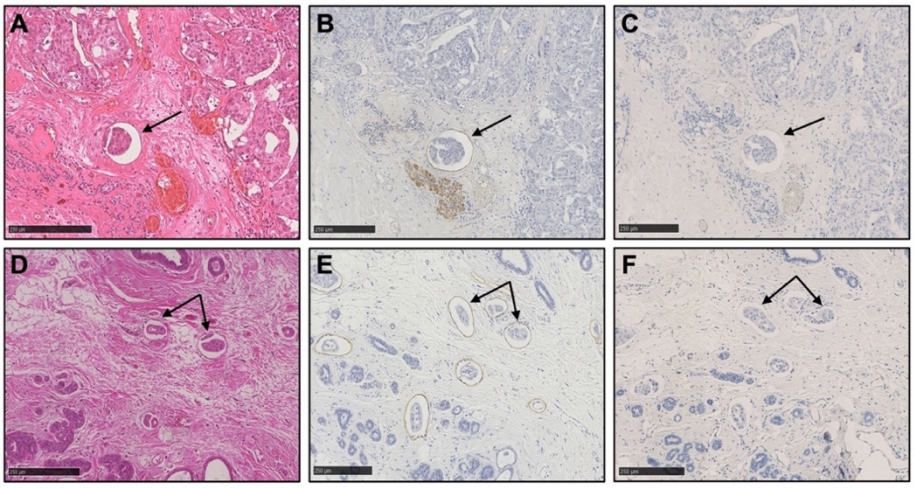

Figure 2.6 Histologic and immunohistochemical features in representative cases of LVI and BVI in TNBC sections stained with H&E, D2-40, and Factor VIII.

H&E conspicuous carcinoma emboli in large vascular spaces (arrow) [A, D]. Similar H&E sections stained with D2-40 confirming that these are LVI (arrow) [B, E]. Similar H&E sections treated with Factor VIII, but they are negative (arrow) [C, F].

2.4 Statistical analysis of IHC tissue-based studies

To set threshold values for categorizing expression of each protein into two groups, “low” and “high”, log-rank statistics were performed in R Studio (RStudio, Boston, MA, USA) using survminer and maxstat packages based on OS (detailed in chapter 5). IBM SPSS software version 28 (SPSS Inc., Chicago, IL, USA) was utilised for statistical analysis. Kaplan-Meier’s plot and log-rank test were constructed RFS, DFS, and OS. Univariate Cox regression survival analysis was used to calculate hazard ratio (HR) and 95% confidence interval (95% CI). Multivariable Cox regression survival analysis was carried out using a backward conditional elimination model. Inter-relationships between variables were assessed using Chi-square testing. Statistical significance was set to $P<0.05$. Consistency between the observers was analysed using an ICCC value by using reliability analysis. This analysis was carried out in the ductal carcinoma only as different pathological subtypes are known to behave differently, and ductal cancers are the most common pathological subtype. All statistical analysis was performed by (S.S) and repeated by a second investigator (J.E) in order to validate methods used and results obtained.

2.5 Gene expression profiling

2.5.1 Transcriptomic

Transcriptomics is the study of the transcriptome, the complete number of RNA transcripts encoded by the genome. Comparison of the transcriptome of different populations can lead to the identification of RNA transcripts, especially mRNA, which correlated with a specific phenotype or function. We performed RNA sequencing for a small sub-cohort of the Glasgow breast cohort (n = 50), with the aim of identifying specific sequences associated with tumour hypoxia.

The RNA sequencing was performed by BioClavis (BioClavis Ltd, Glasgow, UK) using their Templated Oligo assay with Sequencing readout (TempO-Seq). Volcano plots and MA plots were constructed to visualise differentially expressed genes (DEGs). Significance was set to adjusted P-value (padj.) <0.10 and fold change (FC) ≥ 1 or ≤ -1. Principal component analysis (PCA) was carried out to identify any clustering and heatmap was constructed to visualise patterns of gene expression profiles between low and high CAIX groups. Over-representation analyses were performed in R Studio to analyse pathway enrichment and associations of DEGs.

2.5.1.1 Patient selection

A cohort of 50 patients was selected from within the Glasgow breast cohort to undergo whole transcriptome sequencing. These patients had tissue blocks which were easily accessible. Only ER-negative patients were selected for reasons related to tumour hypoxia. Within these specifications, 37 had linked cytoplasmic CAIX protein expression data available (16 samples had high expression and 21 samples had low expression) (Figure 2.7). 20 of these 37 had lymph node negative disease and were selected specifically to identify a gene expression signature associated with tumour hypoxia.

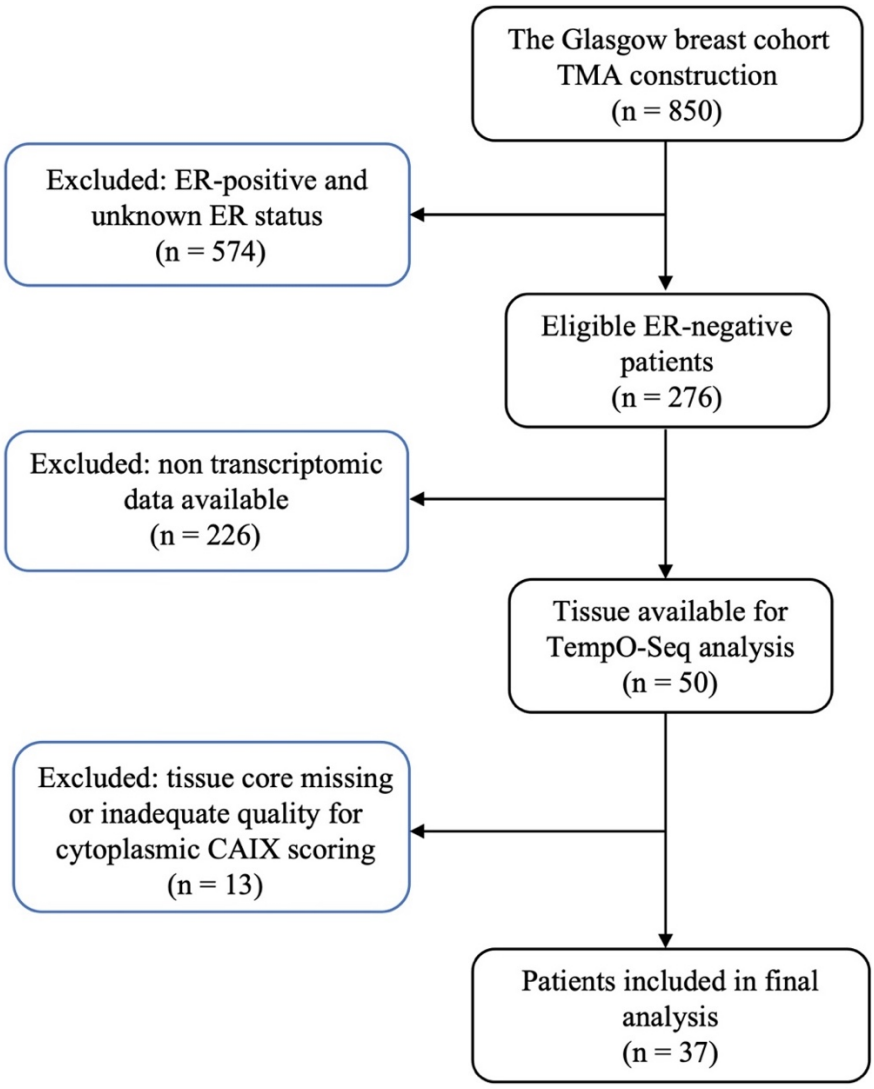

Figure 2.7 Selection of ER-negative breast cancer for analysis.

Consort diagram showing the number of patients included in transcriptomic analysis for cytoplasmic CAIX based on exclusion criteria of having ER-positive status, not having transcriptomic data, and missing or damaged cores. There were 850 patients in the full cohort prior to exclusions. After exclusions there were 37 patients for transcriptomic analysis.

2.5.1.2 Preparation of slides

One 2.5µm full tissue section per patient was cut from the tissue blocks by Jennifer Hay using a Finesse microtome. They were fixed to glass slides and passed on immediately to Ditte Anderson (Scientist, BioClavis Ltd) untreated and unbaked for sequencing. This was to ensure the tissue was as fresh as possible to reduce oxidation.

2.5.1.3 Whole transcriptomic profiling using TempO-Seq®

Whole sections were excised from FFPE slides of ER-negative breast cancer samples and determined using TempO-Seq (n = 37) according to manufacturer's instructions. Briefly, FFPE tissue was deparaffinised prior to tissue digestion. The tissue lysate was combined with detector oligos (DOs) which were annealed in immediate juxtaposition to each other on the targeted RNA template and ligated (292). Amplification of ligated oligos was performed using a unique primer set for each sample, introducing a sample-specific barcode and Illumina adaptors (Figure 2.8). Barcoded samples were pooled into a single library and run on an Illumina HiSeq 2500 High Output v4 flowcell. Sequencing reads were demultiplexed using BCL2FASTQ software (Illumina, USA). FASTQ files were aligned to the Human Whole Transcriptome v2.0 panel, which consist of 22,537 probes, using STAR (Spliced transcripts alignment to reference) (293). Up to two mismatches were allowed in the 50-nucleotide sequencing read.

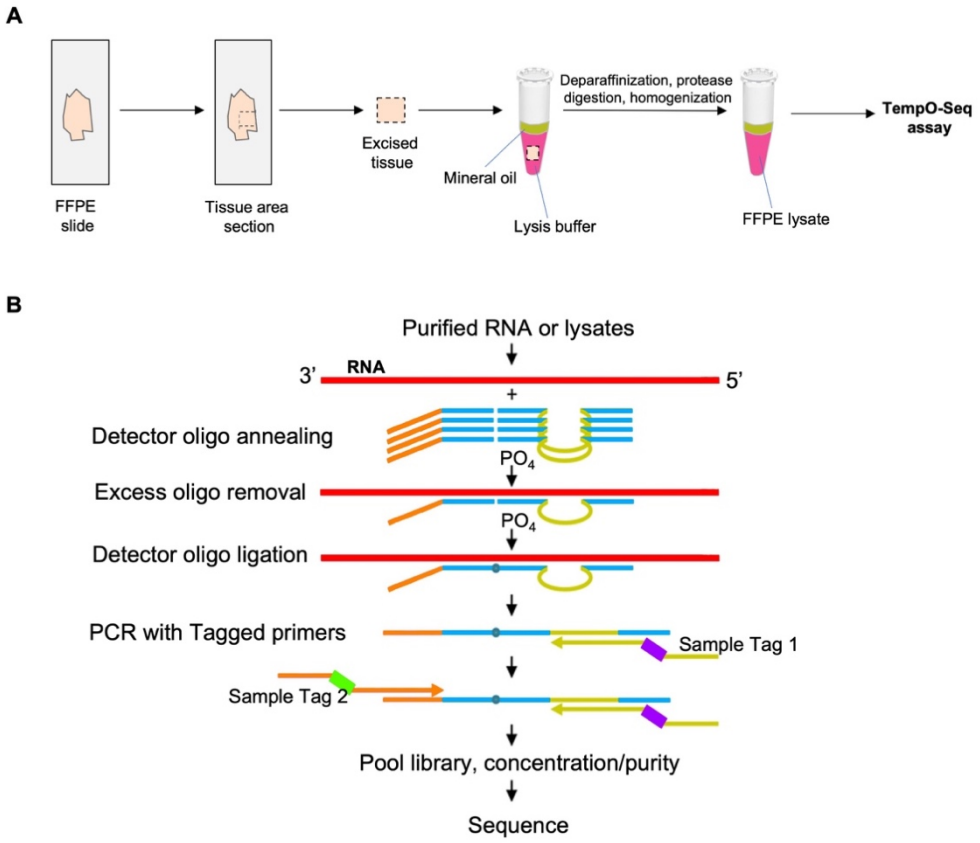

Figure 2.8 Processing FFPE samples for the TempO-Seq assay.

An interest area is manually scraped from mounted FFPE sections. The tissue is added directly into FFPE lysis buffer, overlaid with mineral oil, and then heated at 95°C for 5 minutes. FFPE Protease is added, and the sample is incubated for 30 minutes and manually homogenized. The processed lysate is then ready for input directly into the annealing step of the TempO-Seq assay [A]. Schematic of the TempO-Seq detector oligo annealing and ligation process [B]. Adapted from (292).

2.5.1.4 Data analysis

Initial analysis was carried out by BioClavis using the TempO-Seq data analysis program (BioSpyder technologies, USA). BioClavis then provided the raw gene counts file which were normalised for further analysis. Analysis was performed using R Studio Team (2020) (RStudio: Integrated Development for R. RStudio, PBC, Boston, MA). DEGs analysis were carried out using DESeq2 package (v1.30.0) in R Studio (294). Gene expression was compared between tumours which exhibited either low or high expression of CAIX as determined by IHC. Genes were deemed significantly differentially expressed with a threshold of +/−1 log2 FC and padj <0.10. Volcano plots and MA were constructed using ggplot in R Studio. PCA plot and heatmaps was drawn using DESeq2 and ComplexHeatmap, respectively in R Studio to visualise patterns of gene expression for the top 20 most significantly DEGs.

The search tool for the retrieval of interacting genes (STRING) database 11.5 was utilised to identify the DEGs regarding their Gene Ontology (GO) and relating pathway (295). The DEGs were analysed and categorised into the three categories including cellular component, biological process and molecular function. STRING database and GO were utilised to identify biological pathways associated with DEGs in the high cytoplasmic CAIX expression group.

Protein-protein interaction (PPI) network was constructed and visualised using the STRING online database which integrates both known and predicted PPIs, can be applied to predict functional interactions of proteins. Species limited to "Homo sapiens" and an interaction score >0.4 (medium confidence), a false discovery rate (FDR) <0.05 and PPI enrichment P-value <0.05 were applied to construct the PPI networks (296). Maximum number of interactors to show the first shell was limited to no more than 10 interactions.

2.5.2 GeoMx digital spatial profiling

The GeoMx digital spatial profiling (DSP) platform enables robust detection of high-plex protein and RNA expression from user-defined compartments within FFPE tissues. GeoMx DSP was performed, and data was analysed in RStudio (RStudio, Boston, MA, USA). DSP technique was used to study gene expression according to pan-cytokeratin (PanCK) mask in TNBC samples. Data analysis including volcano plots and heatmap were constructed using ggplot and ComplexHeatmap packages, respectively in R Studio to visualise DEGs. Significance was set to P-value <0.05.

2.5.2.1 Tissue microarray and patient selection

GeoMx data analysis was conducted using archival FFPE microarray data from TNBC samples that was obtained at the department of pathology at Queen Elizabeth University Hospital. From 207 TNBC samples, 98 cores were selected from more than 1 core from each patient and then the results were averaged leaving 52 patients were utilised for GeoMx DSP analysis. Additionally, UV-light subdividing ROI into distinct cellular compartments called areas of illumination (AOI, n = 155) that can be profiled and readout separately. The use of the epithelial cell-specific marker pan-cytokeratin (PanCK) assists pathologic identification of breast tumour tissue within a sample. Each PanCK-positive or PanCK-negative compartment can be profiled separately, there were 73 pan-cytokeratin positive and 82 pan-cytokeratin negative (Figure 2.9).

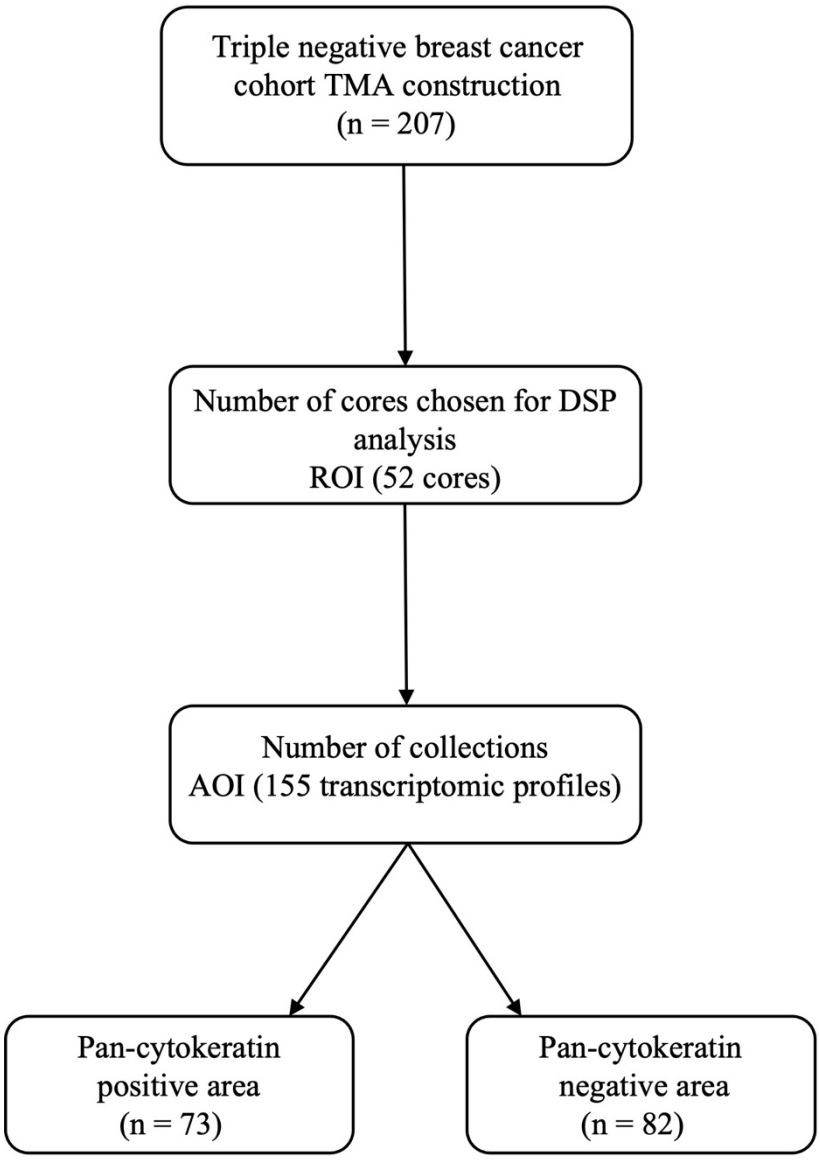

Figure 2.9 Selection of TNBC cohort for analysis.

Consort diagram showing the number of patients included in GeoMx DSP analysis. There were 207 patients in the full cohort prior to selection. After selections there were 52 patients (155 readouts) for GeoMx analysis, 73 pan-cytokeratin positive and 82 pan-cytokeratin negative.

2.5.2.2 Preparation of slides

Sections from the TNBC TMA were cut at 2.5µm and baked for 30 minutes at 60°C. The Leica BOND Autostainer was employed to perform epitope retrieval (ER2, pH9, 100°C) for 10 minutes to expose RNA targets. Protein digestion using proteinase K (0.1µg/ml) for 15 minutes is then performed to remove protein bound to RNA and further expose transcripts. The slides were then stored until required in 1x PBS (phosphate-buffered saline).

In situ hybridisation of RNA-directed DNA oligo probes (Immune Pathways Panel, NanoString) was performed as per manufacturer's protocol. HybriSlip hybridization covers were applied prior to overnight incubation at 37°C for at least 16 hours (Thermo fisher). The following day, slides were washed twice to remove unbound probe with a 1:1 ratio of 100% deionized formamide (Ambion) and 4x SSC (saline-sodium citrate) (Sigma-Aldrich) at 37°C for 25 minutes.

Immunofluorescence staining was performed using primary conjugated antibodies including PanCK, CD45 and DNA marker (SYTO 13) for 1 hour as per manufacturers protocol. Slides were then stored at 4°C for up to 6 hours in 2x SSC before being loaded on the GeoMx DSP instrument for region selection and collection (Figure 2.10).

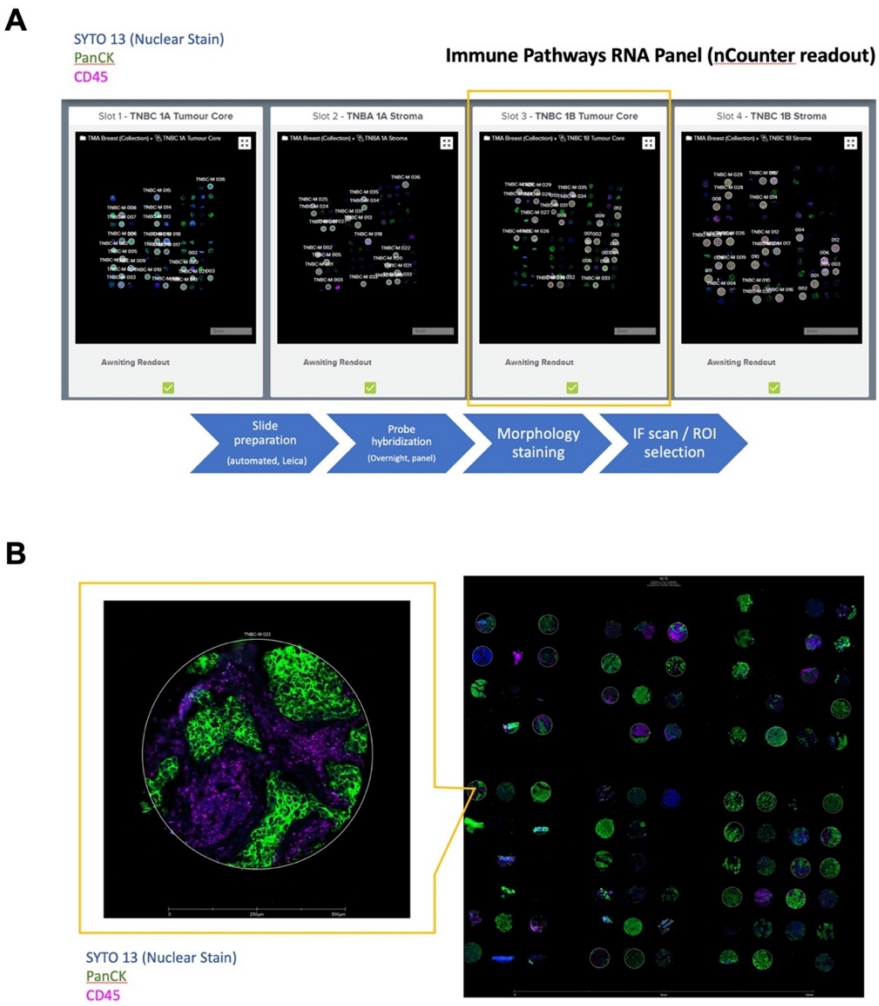

Figure 2.10 TNBC sample preparation and staining.

The picture showed sample preparation and staining [A]. The tissue morphology was delineated by the immunofluorescence detection of PanCK (epithelial cytokeratin, green), CD45+ (immune cells, magenta) proteins and SYTO 13 (nuclei, blue) [B].

2.5.2.3 Region of interest selection (ROI)

Once the incubation is complete, slides are loaded onto the DSP instrument, and scanned to produce a digital image. Circular ROIs were then selected for further analysis based on successful 3-plex immunofluorescence staining of PanCK, CD45 and SYTO 13 (Figure 2.11). PanCK-positive used to select tumour-rich regions that were enriched for PanCK, and PanCK-negative to identify stroma-rich regions that were enriched for CD45 and lacked PanCK staining. After ROIs were selected, the GeoMx platform employs an automatically controlled UV laser to illuminate each ROI in turn, specifically cleaving DSP barcodes within the ROI but not in surrounding tissue. A microcapillary collection system collected the liberated barcodes from each region and plated them into an individual well on a microtiter plate. This process was repeated in turn for each ROI before processing using NanoString MAX/FLEX nCounter system.

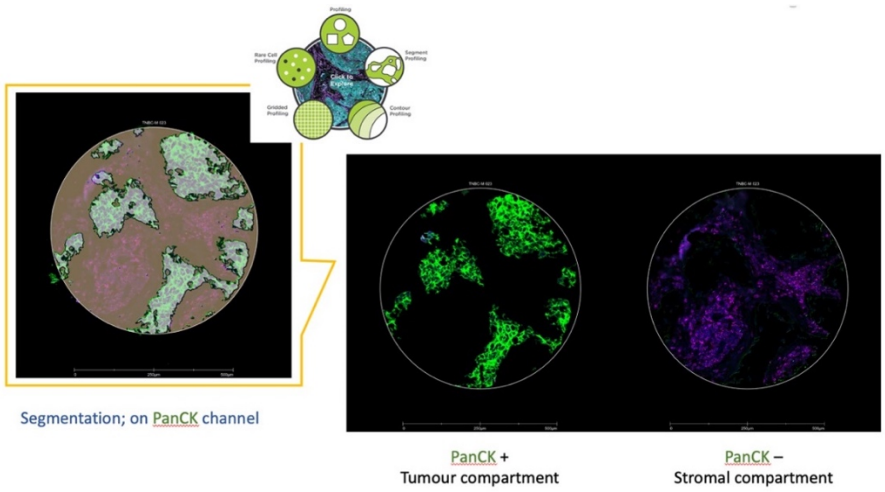

Figure 2.11 Region of interest selection according to the PanCK mask in TNBC.

The picture showed the GeoMx suit where region of interested (ROI) has been selected. PanCK-positive for tumour compartment, and PanCK-negative for stromal compartment.

2.5.2.4 nCounter hybridization assay for photocleaved oligo counting

nCounter readout of GeoMx DSP-collected probes was performed according to manufacturer's protocol (NanoString, MAN-10089-08). In brief, samples were resuspended in dH_2O prior overnight incubation (16–24 hours) with hybridisation codes (Hyb Codes) at 65°C and heated lid (70°C). These hyb codes include reporter and capture probes to enable formation of a tripartite hybridization complex with the DNA oligo probes in the panel. Samples were then pooled by column into 12-well strip tube before processing on NanoString's MAX/FLEX system, using the high sensitivity protocol (NanoString, MAN-10089-08). Data acquisition was performed by using the NanoString's Digital Analyser (FOV, 555). DSP platform overview is shown in Figure 2.12.

2.5.2.5 GeoMx data analysis

GeoMx DSP analysis suite was used to perform preliminary analysis and quality control (QC) checks on transcriptomic data follow quantification by NanoString's nCounter system. Using the GeoMx data analysis suite, the sequenced data underwent technical QC to exclude regions with suboptimal binding density (<0.1, >2.25) and/or high positive control normalisation (>3). Most correlated normalisation method was used following assessment using custom script. The counts also underwent normalisation with negative probes using the geometric mean. Data analysis was performed to identify differences in gene expression between high CAIX tumours versus low CAIX tumours. DEG was performed using the GeoMx analysis suite, which utilises the GeoMxTools R package (tool: 'mixedModelDE' in R package 'lmerTest'). Volcano plots were created using a plugin script, available at: (https://github.com/NanoStringBiostats/DSPPlugins/tree/master/DSPPlugVolcanoPlot).
Heatmaps were created using negative probe-normalised counts as input to R package, ComplexHeatmap (RStudio, Boston, MA, USA). The DEGs screened out with the criteria of log2 FC > ± 0.25/0.3 within tumour and stromal compartment, respectively, and P-value <0.05. The number of genes assessed in the RNA panel was 84 genes.

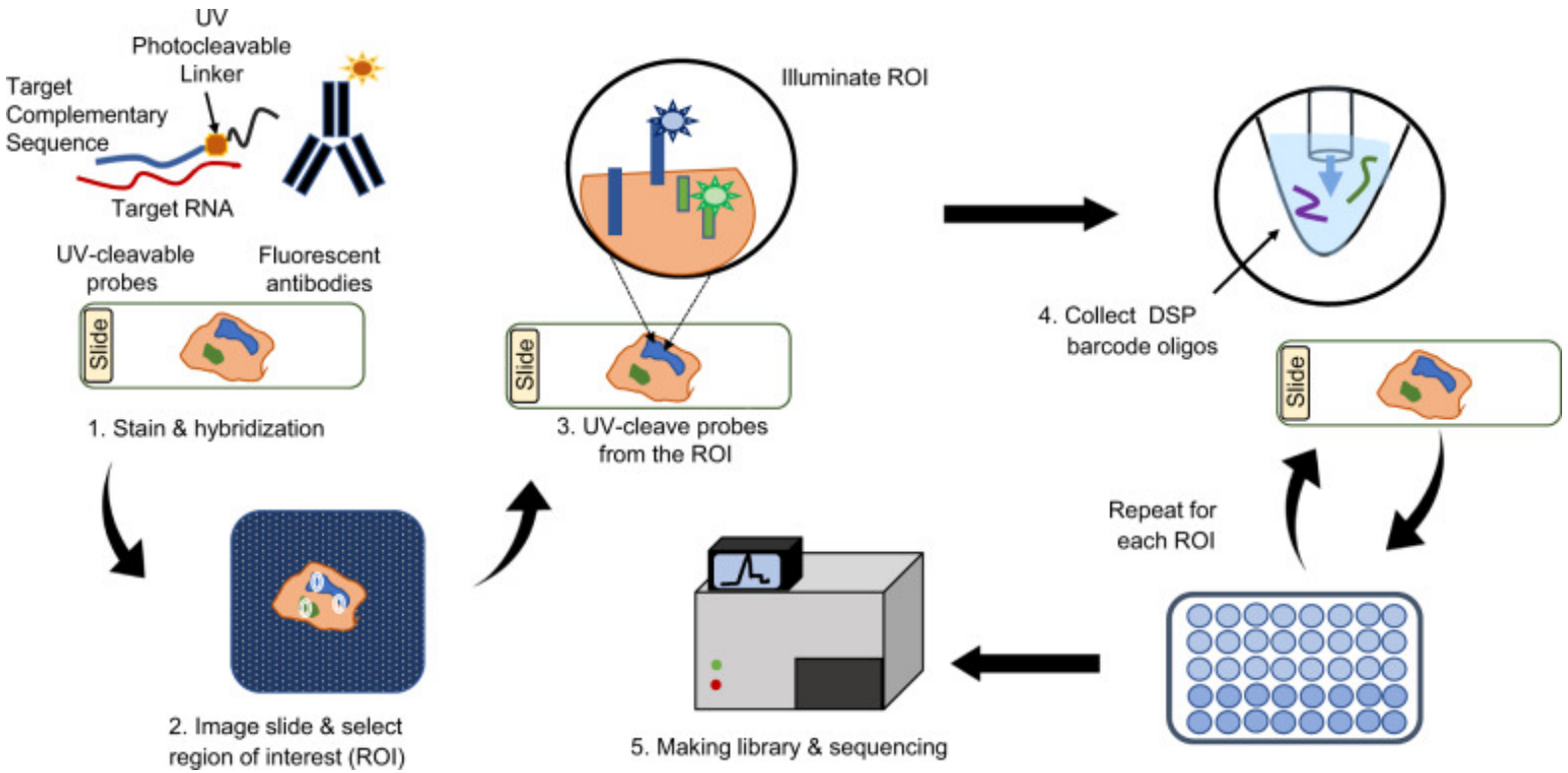

Figure 2.12 Overview of GeoMx system and workflow

Formalin-fixed paraffin-embedded tissue slide preparation involves incubation with an antibody mixture which contains visualization markers and DSP probes. Load prepared slides onto the GeoMx DSP instrument. Following imaging, regions of interest (ROIs) are selected based on visualization of the tissue. Sequential ultraviolet (UV) light exposure of each ROI results in the release of indexing oligos from the DSP probes, allowing their quantification on NanoString's nCounter® system. Adapted from (297).

Chapter 3 The relationship between hypoxia markers and patient survival in breast cancer: systematic review and meta-analysis

3.1 Introduction

Cellular responses to low oxygen tension are mainly mediated by the activation of hypoxia-inducible factors (HIFs), which consist of a constitutively expressed subunit (HIF-β) and an oxygen-regulated subunit, these mainly include HIF-1α and HIF-2α (199). HIF-1α is overexpressed in a number of primary and metastatic human cancers and has been associated with survival (298, 299). Clinical studies have also evaluated the association between HIF-1α expression and patient survival in breast cancer. However, results have been conflicting with HIF-1α being both associate with good and poor prognosis. Schindl et al. (243) reported that HIF-1α was an independent prognostic factor for OS in patients with lymph node positive breast cancer. In contrast, Gruber et al. (300) reported that high HIF-1α expression was associated with DFS but not OS, and Huang et al. (301) reported no association between HIF-1α expression and breast cancer survival.

Hypoxia-associated enzyme CAIX is a direct transcriptional target of HIF-1α and is one of the most commonly up-regulated genes in response to hypoxia. Since HIF-1α is rapidly degraded in normoxic conditions and just as rapidly stabilized in hypoxic conditions and CAIX expression less transient, CAIX expression is a robust biomarker of tumour hypoxia (302, 303). CAIX facilitates the reversible hydration of carbon dioxide to bicarbonate and protons (302), therefore, it plays a major role in maintaining the pH gradient between cells and their extracellular space (222). CAIX is normally expressed in few tissues including the gut epithelium and biliary tree (225) but appears to be upregulated in response to tumour hypoxia in many tumour types including breast cancer (258, 304). The majority of studies in the literature suggest that CAIX can serve as a biomarker and therapeutic target in different tumour types (305). Published breast cancer data supports CAIX as a marker of aggressive tumour behaviour, and high CAIX expression correlates with high tumours grade (248, 264) and loss of ER and PR expression (264, 306). CAIX has also been reported to be positively associated with necrosis (307), larger tumour size and basal-like tumours (264, 308). Indeed, overexpression of CAIX protein in TNBC is associated with a BRCA1 mutant signature and loss of BRCA1 function (309). Several studies have reported that CAIX overexpression in breast cancer is a poor prognostic marker for RFS and OS (259, 264, 308, 310). However, several other studies did not report a significant association of CAIX with RFS or OS (311, 312). It seems likely that these contradictory findings at least partially may be explained by its differential expression in various subtypes of breast cancer, power of the studies and techniques employed to assess expression levels (264, 308). It is of interest that

a meta-analysis of CAIX in renal cell carcinoma showed that high CAIX expression was associated with an improved OS (313). In contrast, a meta-analysis in head and neck cancer patients concluded high CAIX expression was associated with poorer OS and DFS (314). A meta-analysis of the association between CAIX expression and outcome in breast cancer has not been performed.

Therefore, due to conflicting results, it was necessary to perform a meta-analysis to establish the main trend.

3.2 Materials and methods

3.2.1 Search strategy

The present review was performed according to guidelines for systematic reviews and meta-analysis of tumour marker prognostic studies. Studies that examined the prognostic significance of HIF-1α and CAIX in breast cancer were identified by searching the electronic databases PubMed, Web of Science, and Google Scholar, using the following search terms: "breast cancer" or "breast carcinomas" or "breast neoplasm", "HIF-1α" or "hypoxia-inducible factor-1α", "CAIX" or "carbonic anhydrase IX" "prognosis" or "survival" or "outcome", without language limitations. The bibliographies of the included studies were also searched to identify additional studies.

3.2.2 Study selection

Studies were considered eligible if they fulfilled the following criteria: (1) were in breast cancer, (2) determined HIF-1α and CAIX expression in breast cancer using IHC, (3) examined the relationship between HIF-1α and CAIX expression and clinical outcome, (4) provided sufficient data to estimate hazard ratios (HRs) for survival rates and their 95% confidence intervals (CIs). The studies were excluded if they were: (1) not in English, (2) animal studies, (3) cell culture-based studies, (4) had insufficient data for analysis or critical information that could not be extracted.

3.2.3 Data extraction

Three investigators (S.S, D.M and J.E) screened eligible studies and extracted the following information: name of first author, year of publication, country, sample size, detection method, expression pattern, scoring method, threshold values, cellular localization, and

clinical endpoints. From this search, the titles and abstracts of articles were initially examined to determine the relevance of these publications. Then, the full texts of the remaining articles were obtained and carefully reviewed. The reference lists of all relevant articles were also examined manually to identify additional studies that may not have been identified by the strategy outlined above. Discrepancies between the reviewers were resolved by discussion. Finally, 30 articles for HIF-1α and 23 articles for CAIX were considered eligible for inclusion in the meta-analysis.

3.3 Statistical analysis

The effects of HIF-1α and CAIX expression on outcome of breast cancer were described as HRs with an estimate of 95% CIs. The multivariate estimate was used in preference to the univariate analysis (if both were available for the studies) because inter-mixed factors were included in the multivariate analyses. When it was not possible to extract HR directly from the article, survival curves were used to extract data to estimate HR following the method of Tierney et al. (315). The heterogeneity of the data from eligible studies was evaluated by I^2 statistic, which is a quantitative measure of inconsistency across studies (316) using a random effects model. The I^2 varies from 0% (no observed heterogeneity) to 100% (maximal heterogeneity). I^2 value of ≥50% is considered to represent substantial heterogeneity among studies. Statistical significance was defined as P-value <0.05. All analyses were performed using Review Manager (RevMan) version 5.4 (The Nordic Cochrane Centre, The Cochrane Collaboration, Copenhagen, Denmark).

3.4 Results

3.4.1 The relationship between HIF-1α and patient survival in breast cancer

3.4.1.1 Studies selection process

A flow diagram of the study selection process for HIF-1α is summarised in Figure 3.1. The initial literature search returned 745 articles of potential interest. Duplicates (n = 145) were removed. After reviewing the titles and abstracts of these articles, full text was obtained for 218 studies. Of these, 192 were excluded (122 did not examine the prognostic value HIF-1α, 5 were review articles or meta-analysis, 55 were animal studies, 9 studied cell lines, and one was not available in English). Then, careful review of the full texts of these articles and

manually inspecting their bibliographies and reference lists identified 4 additional studies. Finally, a total of 30 independent studies from 16 countries were included in the review.

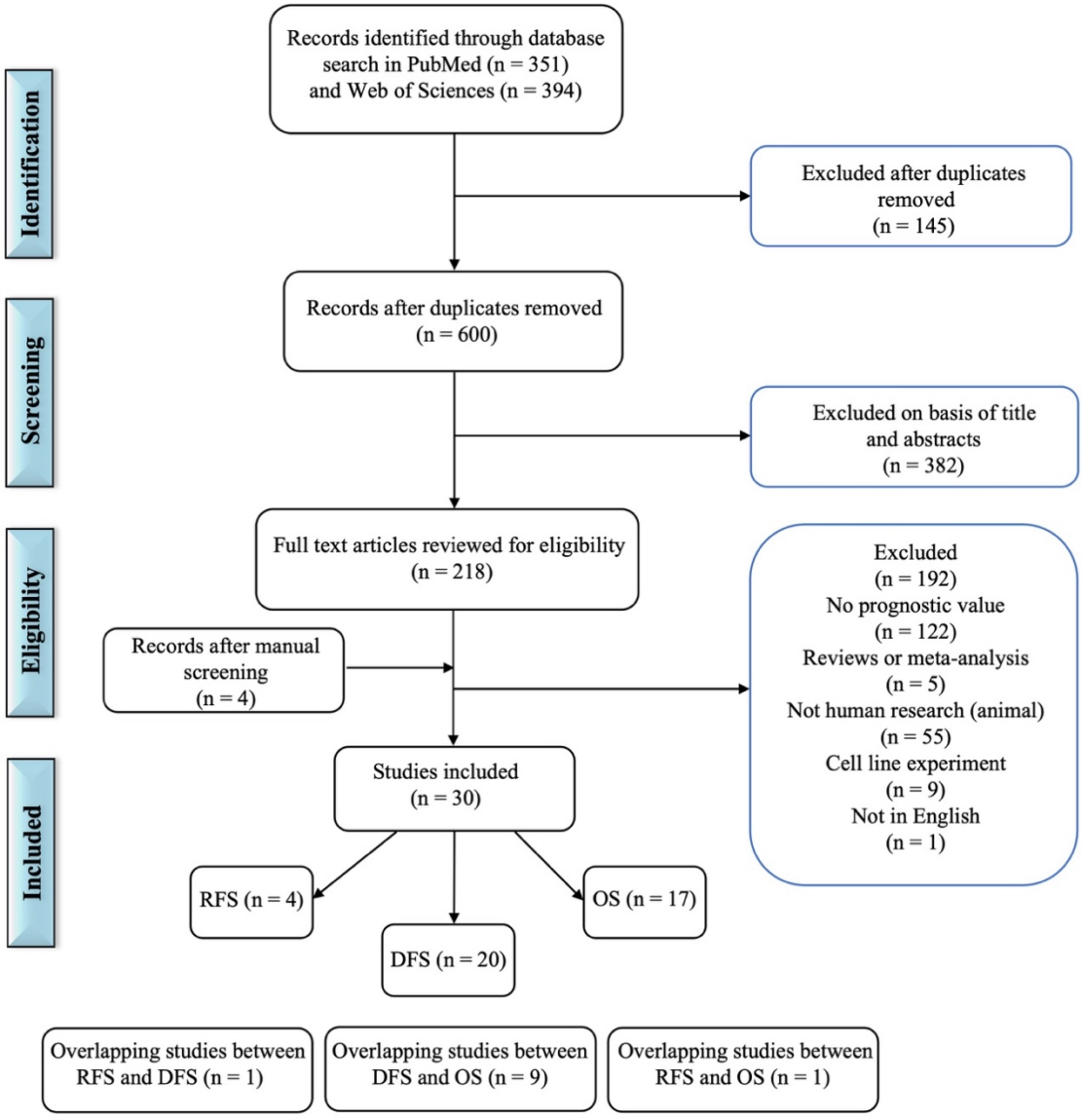

Figure 3.1 PRISMA flow diagram detailing the process of selecting articles describing the association between HIF-1α expression and patient's prognosis.

3.4.1.2 Study characteristics

A total of 30 studies involving 6,201 patients addressing HIF-1α expression in breast cancer met the criteria for this review. Characteristics of all eligible studies are provided in Tables 3.1, 3.2, and 3.3. The majority of studies were carried out in early-stage breast cancer and mainly in patients with ductal disease. Many studies (n = 19) included only a small number of patients (range 31–200). The follow-up of these studies ranged from 30 to 166.8 months. HIF-1α expression was assessed by IHC, and there were 12 different antibodies used. Three different scoring methods had been applied to stratify patients into groups with low and high tumour HIF-1α expression. The definition of positive HIF-1α staining varied among the studies from 1% to 10% or a score of 1–6.

Of the clinical endpoints, RFS, DFS and OS were the only outcome measured. In 25 of 30 studies (n = 4,555 patients), the useful data for calculation of HR were obtained directly from the original articles. These data were not provided in two studies containing 404 patients, and they were calculated from available numerical data extrapolated from Kaplan-Meier survival curve. In three studies (n = 1,242 patients), it was not possible to derive HR.

3.4.1.3 Quantitative data synthesis

The pooled HR and 95% CI was calculated according to survival data including DFS and OS. With RFS end point, the relationship between HIF-1α and RFS was only evaluated in three studies (Table 3.1), and this precluded meaningful meta-analysis. The detailed results for DFS and OS were provided in Tables 3.2 and 3.3, and the forest plots were provided in Figures 3.2 and 3.3, respectively.

Table 3.1 Studies characteristics and the impact of HIF-1α on recurrence free survival

Author(s)	Country	Patients (n)	Median follow up (months)	Cancer death n (%)	High HIF-1α expression n (%)	Tumour type	Scoring method	Score range and location	Definition of positive	Antibody for IHC/dilution	Tumour stage	Multivariate variables	HR (95% CI)	P-value	HR estimation
Nie et al. 2018 (317)	China	220	30	NA	150 (68.2)	Mixed BC	Percentage & intensity	Score 0-9 Location not stated	Score ≥1	NA	II&III	Primary and residual LN involvement, residual tumour size, Ki67 and HIF-1α expression	MV analysis 4.17 (1.01–17.17)	0.048	Reported in text
Yan et al. 2009 (251)	Australia	125	64	31 (24.8)	55 (49)	BRCA	Absence or presence	Score 0-1 Nuclear	Score 1	NeoMarkers 1:50	NA	NA	UV analysis 3.25 (1.01–10.51)	0.049	Survival curve
Kronblad et al. 2006 (247)	Sweden	377	166.8	NA	91 (24)	Mixed BC	Percentage	0-100 Nuclear	>2%	NB100-123H2 1:500	II	Her-2, LN status, tumour size, NHG, Ki67 and HIF-1α expression	MV analysis 1.4 (0.9–2.3)	0.18	Reported in text
Dales et al. 2005 (241)	France	745	162	191 (25.6)	543 (72.89)	Mixed BC	Percentage	0-100 Location not stated	>10%	H206 1:400	NA	Tumour grade, tumour size and HIF-1α expression	MV analysis NA	0.023	NA

Table detailing papers which investigated the prognostic role of HIF-1a on recurrence free survival. NA: Not available.

.

3.4.1.3.1 Analysis of HIF-1α expression and disease-free survival

Twenty studies (n = 3,878 patients) provided the data regarding the HIF-1α expression and DFS in breast cancer, three of which provided incomplete data to estimate HR (Table 3.2).

Table 3.2 Studies characteristics and the impact of HIF-1α on disease-free survival

Author(s)	Country	Patients (n)	Median follow up (months)	Cancer death n (%)	High HIF-1α expression n (%)	Tumour subtype	Scoring method	Score range and location	Definition of positive	Antibody for IHC/dilution	Tumour stage	Multivariate variables	HR (95% CI)	P-value	HR estimation
Cui and Jiang 2019 (318)	China	87	NA	NA	36 (41.4)	TNBC	Absence or presence	Score 0-1 Cytoplasmic and nuclear	Score ≥1	ab51608 1:100	I-II&III	Tumour size, tumour grade, LN status, TNM stage, c-Myc expression and HIF-1α expression	UV analysis 2.03 (1.36–3.51) MV analysis 2.22 (1.47–3.77)	<0.001 <0.001	Reported in text
Shi et al. 2017 (319)	China	60	60	33 (55)	20 (33.3)	Mixed BC	Percentage	0-100 Nuclear	≥5%	NA 1:500	T1-3 N0-3	FBP1, T-stage, LN status, and HIF-1α expression	UV analysis NA MV analysis 1.01 (0.41–2.40)	<0.001 0.797	Reported in text
Jin et al. 2016 (265)	South Korea	270	NA	NA	39 (14.4)	TNBC	Percentage	1-100 Nuclear	≥1%	Novus biologicals 1:50	I-II	LVI, LN metastasis, HIF-1α, CAIX and combined HIF-1α and CAIX expression	UV analysis 1.26 (1.04–1.52) MV analysis 2.62 (1.33–5.15)	0.017 0.005	Reported in text
Huang et al. 2014 (301)	Taiwan	96	NA	NA	29 (30)	Mixed BC	Percentage and intensity	Score 1-4 Cytoplasmic and nuclear	Score ≥3	NA	T1-T4	Age, 1772 C > T genotype, MVD, T-stage, N-stage, VEGF and HIF-1α expression	UV analysis NA MV analysis 2.18 (0.93–11)	NA 0.073	Reported in text
Choi, Jung, and Koo 2013 (235)	South Korea	276	67	23 (8.3)	13 (4.7)	Mixed BC	Percentage	0-100 Nuclear	>10%	EP1215Y 1:100	T1-3 N0-3	Age, T stage, Glut-1 and HIF-1α expression	UV analysis NA MV analysis 5.21 (1.84–14.78)	<0.001 0.002	Reported in text
Dong et al. 2013 (320)	China	378	NA	NA	195 (51)	ER^+, $Her\text{-}2^-$	Percentage and intensity	Score 0-8 Cytoplasmic and nuclear	Score 4	MAB5382 1:100	NA	NA	UV analysis NA	0.963	NA
Marton et al. 2012 (321)	Croatia	31	58.7	NA	7 (22.6)	Neuroendocrine BC	Scored both intensity and percentage but for analysis only used intensity	Score 0-3 Location not stated	Score ≥1	NA 1:25	T1-3 N0-3	Her-2, VEGF-C, PR, ER, age, tumour grade and HIF-1α expression	UV analysis NA MV analysis 145.92 (2.22–919.5)	0.066 0.019	Reported in text
Peurala et al. 2012 (322)	Finland	102	NA	NA	30 (29.41)	Mixed BC	Percentage and intensity	Score 0-4 Cytoplasmic and nuclear	Score ≥2	NA 1:100	T1-4	NA	UV analysis 2.4 (0.75–7.5)	0.126	Reported in text
Koo and Jung 2010 (323)	South Korea	224	89.6	13 (5.8)	2 (1)	Mixed BC	Percentage	0 1-30 >30 Nuclear	≥1%	EP1215Y 1:100	NA	Radiotherapy and HIF-1α expression	UV analysis 2.78 (1.42–5.46) MV analysis 7.6	0.003 0.018	Reported in text
Yamamoto et al. 2008 (240)	Japan	171	60	15 (8.77)	63 (36.8)	Mixed BC	Percentage	0-100 Nuclear	>5%	H1α67 1:1000	I-II&III	Tumour size, LN status, ER status and HIF-1α expression	UV analysis 1.7 (1.67–1.7) MV analysis 1.59 (1.05–2.43)	< 0.0001 0.017	Reported in text

Chen et al. 2007 (324)	Taiwan	104	45.6	NA	47 (45)	Mixed BC LN -ve	Percentage and intensity	0-7 Nuclear	Score 3	H1α67 1:100	T1-2 N0 M0	NA	UV analysis 7.70 (3.19–18.60)	<0 .001	Reported in text
Tan et al. 2007 (325)	United Kingdom	332	89.4	107 (32.2)	NA	Mixed BC	Intensity	0-2 Nuclear	Score 2	ESEE 122 1:40	NA	Nuclear BNIP3, tumour grade, tumour size, LN status and HIF-1α expression	UV analysis NA MV analysis 2.47 (1.14–5.38)	NA 0.02	Reported in text
Trastour et Al. 2007 (248)	France	132	138	20 (15.2)	59 (45)	Mixed BC	Percentage	0-100 Nuclear	>1%	Antiserum 2087 1:500	NA	Tumour size, LN status, tumour grade, CAIX and HIF-1α expression	UV analysis 1.64 (1.28–2.1) MV analysis 4.2 (2.1–8.5)	0.0001 <0.001	Reported in text
Generali et al. 2006a (246)	Italy	187	53	22 (11.7)	138 (80.7)	Mixed BC	Intensity	0-2 Location not stated	Score ≥1	ESEE 122 1:40	T2-4 N0-1	NA	UV analysis 1.83 (1.10–3.04)	0.02	Survival curve
Schoppmann et al 2006 (326)	Austria	119	110	43 (36.1)	30 (25.2)	Mixed BC	Percentage and intensity	0-7 Nuclear	Score 3	H1α67 1:60	T1-2	Tumour grade and HIF-1α expression	UV analysis NA MV analysis NA	0.029 0.035	NA
Dales et al. 2005 (241)	France	745	162	191 (25.6)	543(72.89)	Mixed BC LN-ve	Percentage	0-100 Location not stated	>10%	H206 1:400	NA	Tumour grade, tumour size and HIF-1α expression	UV analysis NA MV analysis NA	NA 0.158	NA
Vleugel et al. 2005 (327)	The Netherlands	200	NA	NA	88 (44)	Mixed BC	Percentage	0-100 Nuclear	≥1%	NA 1:500	NA	NA	UV analysis 2.23 (1.18–4.21)	0.01	Reported in text
Gruber et al. 2004 (300)	Switzerland	77	36	NA	43 (56)	Mixed BC LN +ve	Percentage and intensity	0-4 Nuclear	Score 1	H1α67 1:5000	T1-4	Age, T stage, ER status, LN status and HIF-1α expression	UV analysis 1.55 (1.02–2.35) MV analysis 1.68 (0.62–4.47)	0.04 0.30	Reported in text
Bos et al. 2003 (244)	The Netherlands	150	106	24%	51 (34)	Mixed BC LN -ve (81)	Percentage	0-100 Nuclear	>5%	H1α67 1:500	I-II	MAI, tumour size and HIF-1α expression	UV analysis 1.38 (1.11–1.72) MV analysis 4.20 (1.46–12.08)	0.004 0.008	Reported in text
Schindl et al. 2002 (243)	Austria	206	87	73 (35.4)	48 (23.3)	Mixed BC LN +ve	Percentage and intensity	0-7 Nuclear	Score 3	H1α67 1:60	I-II	Tumour stage, tumour grade, age, ER, Her-2 and HIF-1α expression	UV analysis 2.83 (1.54–5.19) MV analysis 1.4 (1.14–1.72)	0.0008 0.001	Reported in text

.

In the remaining 17 studies, tumours with high HIF-1α expression had a significantly shorter DFS (HR = 2.37, 95% CI: 1.76–3.20, P<0.00001) (Figure 3.2). A random-effect model was adopted due to the existence of significant heterogeneity (I^2 = 83%, P<0.00001). Therefore, subgroup analysis was performed to explore the potential sources of heterogeneity based on survival analysis, study region, antibodies used, scoring methods, and threshold selection criteria.

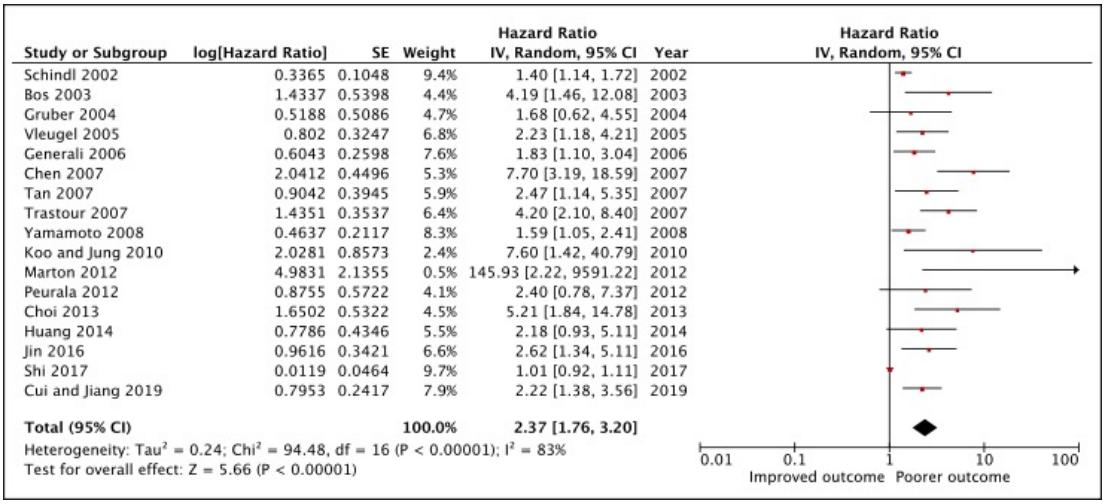

Figure 3.2 Forest plot for the relationship between HIF-1α expression and disease-free survival in breast cancer patients.

The pooled HR for univariate analysis was (HR = 2.78, 95% CI: 1.53–5.08, P = 0.0008) with non-significant heterogenicity (I^2 = 62%, P = 0.05). The HR for multivariable analysis was (HR = 2.22, 95% CI: 1.60–3.08, P<0.00001) and heterogeneity was significant (I^2 = 83%, P<0.00001) (Table 3.4).

Stratified analysis by study region suggested a poor DFS for eight studies with Asian subjects (HR = 2.55, 95% CI: 1.51–4.30, P = 0.0004) and for eight studies from Europe (HR = 2.28, 95% CI: 1.55–3.36, P<0.0001). A significant heterogenicity was observed among two subgroups (I^2 = 87%, P = 0.00001; I^2 = 63%, P = 0.009, respectively) (Table 3.4).

There was variation in the antibody for IHC used in the studies, the most common being H1α67 (n = 5) followed by EP1215Y (n = 2). Other antibodies (n = 8) were used in only

very few studies and therefore meta-analysis was not carried out. In subgroup analysis a significant association was observed in H1α67 antibody (HR = 2.29, 95% CI: 1.35–3.88, P = 0.002) and poor DFS in patients with breast cancer. A substantial degree of heterogeneity was detected (I^2 = 77%, P = 0.002) (Table 3.4).

Variation was observed in the scoring methods of HIF-1α used in the studies, with the most common method being used depending on percentage of antibody-expressing tumour cells regardless of staining intensity (n = 8). On the other hand, 5 studies combined staining intensity and percentage of positive cells as their scoring method of choice. The least common scoring method was based on staining intensity (n = 2). On meta-analysis, a statistically significant effect of HIF-1α on DFS was observed when stratified by percentage of staining cells (HR = 2.58, 95% CI: 1.52–4.37, P = 0.0004), and by combination percentage and intensity (HR = 2.36, 95% CI: 1.25–4.46, P = 0.008), with considerable heterogeneity (I^2 = 86%, P < 0.00001; I^2 = 73%, P = 0.005, respectively) (Table 3.4).

To further explore the relationship between HIF-1α expression and DFS of patients with breast cancer, subgroup analysis of threshold methods was performed. HIF-1α threshold of ≥1% was considered positive in 4 studies, and threshold of ≥5% was used in 3 studies. Also, threshold of score ≥1 was reported in 4 studies and score ≥3 was shown in 3 studies. Stratification by threshold methods showed a poorer DFS for threshold group of ≥1% (HR = 3.00, 95% CI: 2.05–4.39, P<0.00001), and threshold of score ≥1 (HR = 2.06, 95% CI: 1.31–3.24, P = 0.002), and heterogeneity was not significant (I^2 = 2%, P = 0.38; I^2 = 32%, P = 0.22, respectively). In contrast, no association was found between HIF-1α expression and DFS in subgroup analysis of threshold of ≥5% (HR = 1.54, 95% CI: 0.87–2.72, P = 0.14), and threshold of score ≥3 (HR = 2.69, 95% CI: 0.99–7.26, P = 0.05). A significant heterogeneity was observed among two groups (I^2 = 82%, P = 0.004; I^2 = 86%, P = 0.0008, respectively) (Table 3.4).

3.4.1.3.2 Analysis of HIF-1α expression and overall survival

Effect of HIF-1α expression on OS could be evaluated in 14 studies comprising 2,732 patients. The complete data to estimate the HR could not be retrieved from three papers and were therefore not included in the analysis (Table 3.3).

Table 3.3 Studies characteristics and the impact of HIF-1α on overall survival

Author(s)	Country	Patients (n)	Median Follow up (months)	Cancer death n (%)	High HIF-1α expression n (%)	Tumour subtype	Scoring method	Score range and location	Definition of positive	Antibody for IHC dilution	Tumour stage	Multivariate variables	HR (95% CI)	P-value	HR estimation
Jögi et al. 2019 (328)	Sweden	688	NA	NA	111 (18)	Mixed BC	Scored both intensity and percentage but for analysis only used percentage	1-100 Location not stated	≥1%	BD610959 1:50	I&III	ER status, EGFR and HIF-1α expression	UV analysis 1.6 (1.2–2.2) MV analysis 1.6 (1.0–2.5)	0.001 0.03	Reported in text
Li et al. 2016b (329)	China	156	NA	NA	83 (53)	Mixed BC	Percentage and intensity	Score 0-12 Location not stated	Score 6	ab82832 1:200	I-II-III& IV	Age, menopausal status, tumour site, tumour diameter, ER, PR, Her-2 status, nodal metastasis, tumour grade, TNM stage, LPA2 and HIF-1α expression	UV analysis 2.07 (1.58–2.71) MV analysis 2.37 (1.09–5.15)	<0.001 0.029	Reported in text
Laurinavicius et al. 2015 (330)	Lithuania	107	84	18 (16.8)	NA	HR+	Percentage	Factor 1-5 Location not stated	Factor 1	EP1215Y NA	T1-2 N0-1	NA	UV analysis 0.23 (0.08–0.62)	0.002	Reported in text
Huang et al. 2014 (301)	Taiwan	96	NA	NA	29 (30)	Mixed BC	Percentage and intensity	Score 1-4 Cytoplasmic and nuclear	Score ≥3	NA	I-II&III T1-4	Age, 1772 C > T genotype, T-stage, N-stage, microvessel density, VEGF and HIF-1α expression	UV analysis NA MV analysis 1.61 (0.63–4.13)	0.963 0.322	Reported in text
Rajkovic-Molek et al. 2014 (331)	Croatia	208	NA	72 (36)	82 (41)	Mixed BC	Percentage	0-100 Nuclear	≥10%	NB100-131 1:1500	I-II-III &IV	Tumour size, grade, stage, LN, ER, PR, Her-2 status, Ki67, molecular subtype and HIF-1α	UV analysis 1.63 (1.03–2.60)	0.039	Reported in text
Choi, Jung, and Koo 2013 (235)	South Korea	276	67	23 (8.3)	13 (4.7)	Mixed BC	Percentage	0-100 Nuclear	>10%	EP1215Y 1:100	T1-3 N0-3	Age, T stage and HIF-1α expression	UV analysis 1.95 (1.49–2.54) MV analysis 4.54 (1.46–14.11)	<0.001 0.009	Reported in text
Dong et al. 2013 (320)	China	378	NA	NA	195 (51)	ER^+, $Her\text{-}2^-$	Percentage and intensity	Score 0-8 Cytoplasmic and nuclear	Score 4	MAB5382 1:100	-	NA	UV analysis NA	0.714	NA
Ni et al. 2013 (332)	China	75	60	36 (48)	52 (69.3)	Mixed BC	Percentage and intensity	Score 0-9 Location not stated	Score ≥1	NA 1:200	I-II&III	LN metastasis, histological differentiation, TNM stage, VEGF-C expression, LVD, MVD and HIF-1α expression	UV analysis 1.88 (1.01–3.5) MV analysis 2.25 (1.38–6.45)	0.045 0.037	Reported in text
Malfettone et al. 2012 (333)	Italy	187	NA	NA	58 (37)	Mixed BC	Absent or present	0-1 Nuclear	≥1%	H206 1:100	NA	PVI, ER status, MIB1, membranous NHERF1and HIF-1α expression	UV analysis NA MV analysis 1.40 (0.46–1.87)	0.011 0.178	Reported in text

Koo and Jung 2010 (323)	South Korea	224	89.6	13 (5.8)	2 (1)	Mixed BC	Percentage	0 1-30 >30 Nuclear	≥1%	EP1215Y 1:100	NA	Radiotherapy and HIF-1α expression	UV analysis 2.94 (1.98–4.37) MV analysis 13.7	<0.0001 0.002	Reported in text
Yamamoto et al. 2008 (240)	Japan	171	60	15 (8.8)	63 (36.8)	Mixed BC	Percentage	0-100 Nuclear	>5%	H1α67 1:1000	I-II&III	LN status, ER status and HIF-1α expression	UV analysis 1.39 (1.17–1.65) MV analysis 2.15 (1.15–5.76)	0.0002 0.016	Reported in text
Schoppmann et al. 2006 (326)	Austria	119	110	43 (36.2)	30 (25.2)	Mixed BC	Percentage and intensity	0-7 Nuclear	Score 3	H1α67 1:60	T1-2	Tumour grade and HIF-1α expression	UV analysis NA MV analysis NA	0.028 0.025	NA
Dales et al. 2005 (241)	France	745	162	191(25.6)	543 (72.89)	Mixed BC	Percentage	0-100 Location not stated	>10%	H206 1:400	NA	Tumour grade, size and HIF-1α expression	UV analysis 1.15 (1.02–1.29) MV analysis NA	0.019 0.030	NA
Giatromanolaki et al. 2004 (245)	Greece	180	NA	NA	89 (49.44)	Mixed BC	Percentage and intensity	Descriptive Cytoplasmic and nuclear	Score 3	ESEE 122 1:20	T1-3	NA	UV analysis NA	0.0008	Survival curve
Gruber et al. 2004 (300)	Switzerland	77	36	NA	43 (56)	Mixed BC LN +ve	Percentage and intensity	0-4 Nuclear	Score 1	H1α67 1:5000	T1-4	Age, T stage, ER status, LN status and HIF-1α expression	UV analysis 3 (0.54–16.72) MV analysis 2.66 (0.83–8.51)	0.21 0.09	Reported in text
Bos et al. 2003 (244)	The Netherlands	150	106	24%	51 (34)	Mixed BC LN -ve (81)	Percentage	0-100 Nuclear	>5%	H1α67 1:500	I-II	MAI, tumour size and HIF-1α expression	UV analysis 1.21 (1.05–1.39) MV analysis 6.37 (1.32–30.67)	0.008 0.021	Reported in text
Schindl et al. 2002 (243)	Austria	206	87	73 (35.4)	48 (23.3)	Mixed BC LN +ve	Percentage and intensity	0-7 Nuclear	Score 3	H1α67 1:60	I-II	Age, histological grade, tumour stage, ER, Her-2 status and HIF-1α expression	UV analysis 1.89 (1.01–3.53) MV analysis 1.41 (1.12–1.77)	0.045 0.003	Reported in text

Table detailing papers which investigated the prognostic role of HIF-1a on overall survival.

As indicated in Figure 3.3, high HIF-1α expression was associated with a poorer OS in breast cancer (HR = 1.88, 95% CI: 1.41–2.50, P<0.0001), with substantial degree of heterogeneity (I^2 = 61%, P = 0.001). To further explore the sources of high heterogeneity, subgroup analysis for OS data was conducted according to survival analysis, study region, antibodies used, scoring methods and threshold.

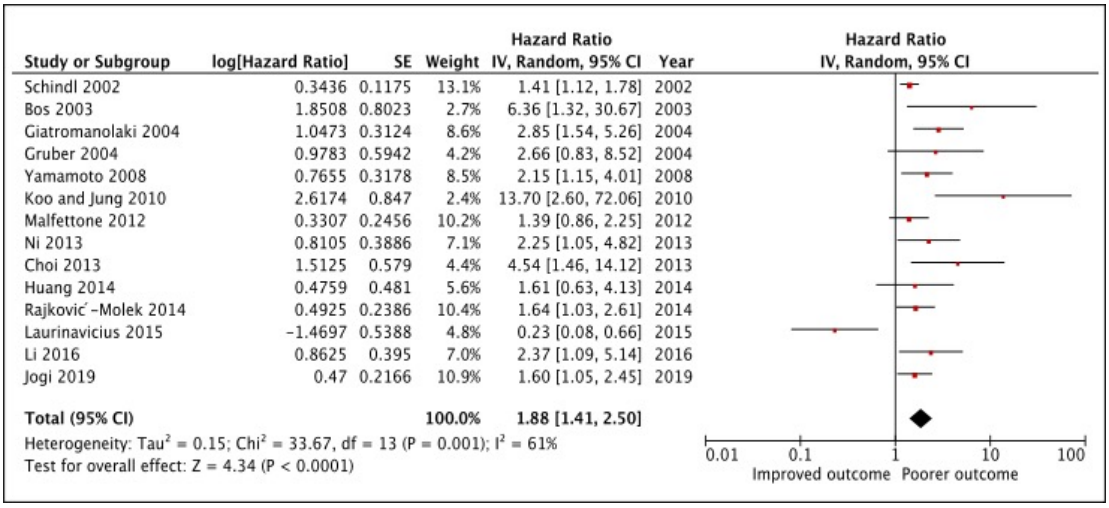

Figure 3.3 Forest plot for the relationship between HIF-1α expression and overall survival in breast cancer patients.

As shown in Table 3.4, the pooled HR for univariate analysis was (HR = 1.13, 95% CI: 0.37–3.41, P = 0.83) and heterogeneity was significant (I^2 = 88%, P = 0.0003). The HR for multivariate analysis was (HR = 1.96, 95% CI: 1.50–2.56, P<0.0001) and heterogeneity was non-significant (I^2 = 42%, P = 0.07).

Stratified analysis by study region suggested a poor OS for six studies with Asian subjects (HR = 2.48, 95% CI: 1.75–3.51, P<0.00001), and for eight studies from Europe (HR = 1.51, 95% CI: 1.29–1.78, P<0.00001). A significant heterogenicity was observed among Europe subgroup (I^2 = 67%, P = 0.004) but not in Asia subgroup (I^2 = 20%, P = 0.28) (Table 3.4).

There were variations in the antibodies used for IHC in the studies, the most common being H1α67 (n = 4) followed by EP1215Y (n = 3). Other antibodies (n = 6) were used in only few studies and therefore meta-analysis was not carried out. In subgroup analysis by antibody,

significant effect of HIF-1α on OS was observed in H1α67 subgroup (HR = 1.95, 95% CI: 1.21–3.15, P = 0.006) but not in EP1215Y (HR = 2.30, 95% CI: 0.20–26.22, P = 0.50). A significant heterogeneity was detected in the group of EP1215Y (I^2 = 91%, P < 0.0001). In contrast, non-significant heterogeneity was observed in H1α67 group (I^2 = 47%, P = 0.13) (Table 3.4).

A stratification based on scoring methods was performed. Six studies used a percentage as scoring method, and seven studies used combined percentage and intensity. The least common scoring method was based on absent or present of staining (n = 1). On meta-analysis, a statistically significant effect of HIF-1α on OS was observed when stratified by combined percentage and intensity (HR = 1.73, 95% CI: 1.39–2.15, P<0.00001) with non-significant heterogeneity (I^2 = 14%, P = 0.32). On the other hand, no association was observed in the subgroup of percentage of staining cells (HR = 2.26, 95% CI: 0.96–5.31, P = 0.13) with considerable heterogeneity (I^2 = 84%, P<0.0001) (Table 3.4).

Twelve studies examined the relationship of various threshold methods and OS (n = 2,469). Percentage of positive cells ≥1% method was used by 3 studies. The scores ≥3 were calculated as the product of combination staining intensity and percentage of positive cells (n = 3). In the subgroup analysis of threshold of score ≥3, HIF-1α overexpression showed poor OS (HR = 1.78, 95% CI: 1.11–2.86, P = 0.02). A non-significant heterogeneity was observed (I^2 = 55%, P = 0.11). In contrast, no association was observed in the subgroup of threshold of ≥1% (HR = 1.99, 95% CI: 1.00–3.96, P = 0.05) with considerable heterogeneity (I^2 = 70%, P = 0.03) (Table 3.4).

Table 3.4 Results of subgroup meta-analysis of analysis methods, study region, different antibodies, scoring and threshold methods reported for HIF-1α

Stratified analysis	Number of studies	Number of patients	Test for association		Test for heterogeneity	
			Pooled HR (95% CI)	P-value	I^2(%)	P-value
Disease-free survival	21	2653	2.37 (1.76–3.20)	<0.00001	83%	<0.00001
Analysis methods						
Univariate	4	593	2.78 (1.53–5.08)	0.0008	62%	0.05
Multivariate	13	2112	2.22 (1.60–3.08)	<0.00001	83%	<0.00001
Study region						
Asia	8	1288	2.55 (1.51–4.30)	0.0004	87%	0.00001
Europe	8	1315	2.28 (1.55–3.36)	<0.0001	63%	0.009
Antibody for IHC						
H1α67	5	708	2.29 (1.35–3.88)	0.002	77%	0.002
Scoring methods						
Percentage	8	1483	2.58 (1.52–4.37)	0.0004	86%	<0.00001
Percentage and intensity	5	585	2.36 (1.25–4.46)	0.008	73%	0.005
Threshold methods						
Percentage ≥ 1%	4	826	3.00 (2.05–4.39)	<0.00001	2%	0.38
Percentage ≥ 5%	3	381	1.54 (0.87–2.72)	0.14	82%	0.004
Score ≥1	4	382	2.06 (1.31–3.24)	0.002	32%	0.22
Score ≥3	3	406	2.69 (0.99–7.26)	0.05	86%	0.0008
Overall survival	14	2801	1.88 (1.41–2.50)	<0.0001	61%	0.001
Analysis methods						
Univariate	3	495	1.13 (0.37–3.41)	0.83	88%	0.0003
Multivariate	11	2306	1.96 (1.50–2.56)	<0.0001	42%	0.07

Study region						
Asia	6	998	2.48 (1.75–3.51)	<0.00001	20%	0.28
Europe	8	1803	1.51 (1.29–1.78)	<0.00001	67%	0.004
Antibody for IHC						
H1α67	4	604	1.95 (1.21–3.15)	0.006	47%	0.13
EP1215Y	3	607	2.30 (0.20–26.22)	0.50	91%	<0.0001
Scoring methods						
Percentage	6	1136	2.26 (0.96–5.31)	0.13	84%	<0.0001
Percentage and intensity	7	1478	1.73 (1.39–2.15)	<0.00001	14%	0.32
Threshold methods						
Percentage ≥ 1%	3	1099	1.99 (1.00–3.96)	0.05	70%	0.03
Score ≥ 3	3	482	1.78 (1.11–2.86)	0.02	55%	0.11

3.4.2 The relationship between CAIX and patient survival in breast cancer

3.4.2.1 Studies selection process

The search yielded 1,294 articles in Google Scholar, 1,079 articles in PubMed and 84 articles in Web of Science. After removal of 530 duplicates, 1,927 unique articles were left for evaluation. Of these, 1,620 articles were excluded based on title and abstract, and 307 remaining articles were identified through full paper review. Subsequently, 284 studies were excluded for the following reasons: 181 lacked survival outcomes, 60 were animal studies, 35 were cell line studies, 5 were non IHC based methods, two of them were review or meta-analysis, and one was non-English studies.

The reference list of each study was examined and did not identify any further studies for inclusion in this analysis. Finally, a total of 23 independent studies from 15 different countries were considered eligible for inclusion in the meta-analysis. The study flow diagram is shown in Figure 3.4.

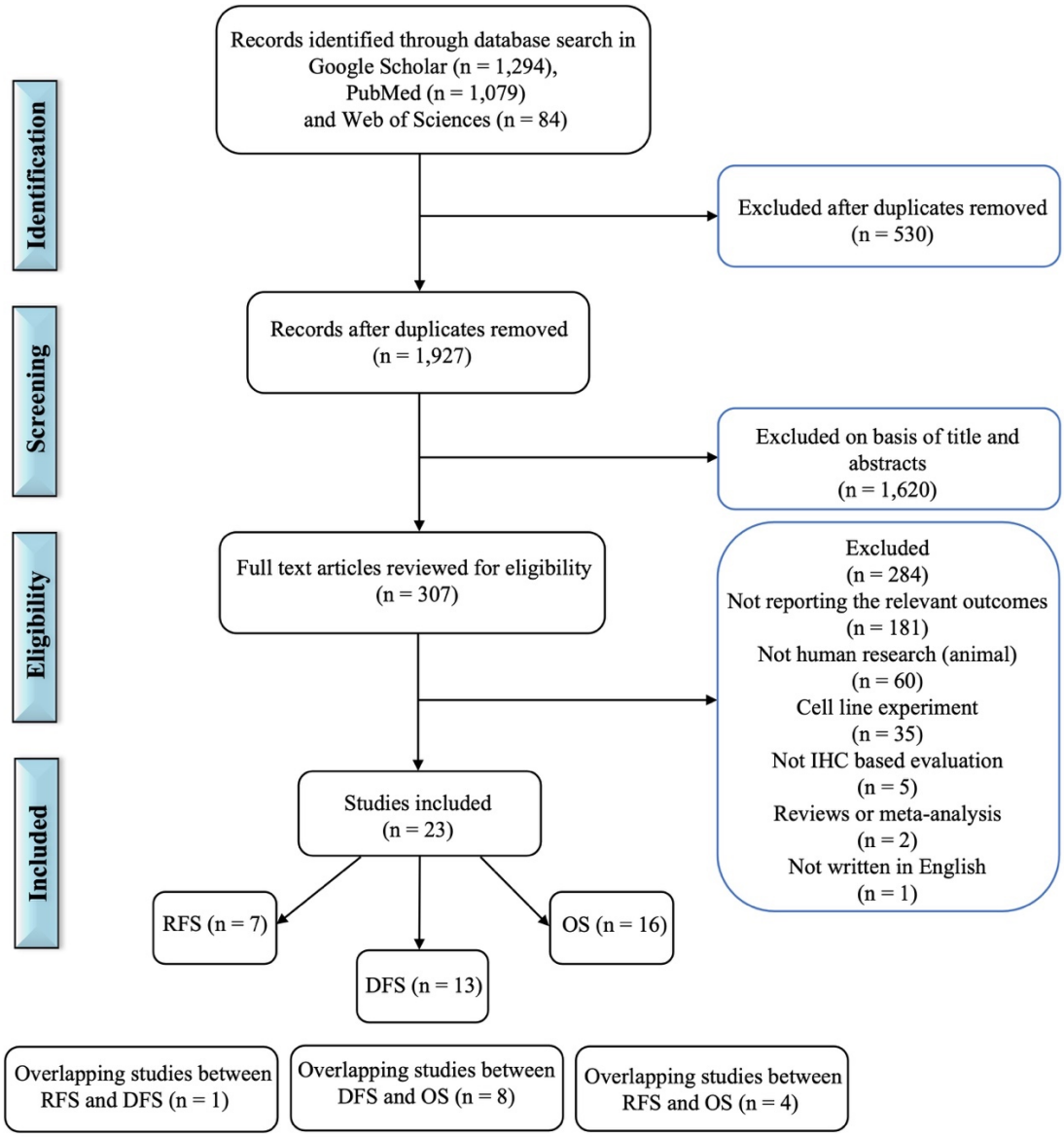

Figure 3.4 PRISMA flow diagram detailing the process of selecting articles describing the association between CAIX expression and patient's prognosis.

3.4.2.2 Study characteristics

A total of 23 studies involving 8,390 participants addressing CAIX expression in breast cancer met the criteria for this review and the characteristics of eligible studies are summarised in Tables 3.6, 3.7, and 3.8. The majority of studies were carried out in early-stage breast cancer and mainly in patients with ductal disease with minimum and maximum sample sizes of 40 and 3,630, respectively. Most of the studies reported the length of the follow-up period, and 13 of them exhibited a sufficiently long follow-up (defined as a median follow-up time >60 months) for the outcomes to be determined.

IHC methodology varied between the studies. Four different antibodies were used. Also, different localizations for protein expression and different quantification methods were reported. Thresholds have been applied to stratify patients into groups with low and high tumour CAIX expression and varied among the studies from 1−10% or a score of 1−52.5.

3.4.2.3 Quantitative data synthesis

The pooled HR and 95% CI was calculated according to survival data including RFS, DFS, and OS. Studies with small number of patients <100 were excluded from the analysis (n = 3). The detailed results were provided in Tables 3.5, 3.6, and 3.7, and the forest plots were provided in Figure 3.5, 3.6, and 3.7, respectively.

3.4.2.3.1 Analysis of CAIX expression and recurrence free survival

RFS was reported in 7 studies, of which one study provided incomplete data to estimate the HR and was therefore not included in the analysis (Table 3.5). One study was also excluded from the analysis because of small sample sizes.

Table 3.5 Studies characteristics and the impact of CAIX on recurrence free survival

Author(s)	Country	Patients (n)	Median follow up (months)	Cancer death n (%)	High CAIX expression n (%)	Tumour subtype	Scoring method	Score range and location	Definition of positive	Antibody for IHC/ dilution	Tumour stage	Multivariate variables	HR (95% CI)	P-value	HR estimation
Beketic-Oreskovic et al. 2011 (310)	Croatia	40	55.8	24 (60)	24 (60)	Mixed BC	Percentage and intensity	Score1-3 Membranous and cytoplasmic	Score >52.5	NA 1:100	NA	Necrosis, tumour size, LN, histological grade and CAIX expression	MV analysis 3.99 (1.38–11.59)	0.011	Reported in text
Lou et al. 2011 (308)	Canada	3,630	126	NA	566 (16)	Mixed BC	Absent or present	0-1 Location not stated	Score ≥1	M75 1:50	NA	NA	UV analysis 1.4	$< 10^{-17}$	Reported in text
Lancashire et al. 2010 (334)	United Kingdom	244	67	NA	29 (18)	Mixed BC (n =160)	Absent or present	0-1 Membranous	Score ≥1	Abcam 15086 1:2,500	NA	NA	UV analysis NA	0.097	Reported in text
Crabb et al. 2008 (335)	Canada	313	NA	NA	47 (15)	Mixed BC	Absent or present	0-1 Location not stated	Score ≥1	M75 1:50	NA	ER, PR, Her-2 status, EGFR, Ki67, p53, CK5/6 and CAIX expression	MV analysis 1.67 (1.06–2.64)	0.03	Reported in text
Trastour et al. 2007 (248)	France	132	138	20 (15)	38 (29)	Mixed BC	Percentage	0-100 Membranous	>1%	MN75 1:10,000	NA	Tumour size, LN status, tumour grade, HIF-1α and CAIX expression	MV analysis 2.7 (1.2–6.1)	0.01	Reported in text
Brennan et al. 2006 (262)	Sweden	400	166.8	NA	42 (11)	Mixed BC LN+ve (n =104) premenopausal	Absent or present	0-1 Membranous	Score ≥1	M75 1:2000	II	NA	UV analysis NA	0.032	Reported in text
Chia et al. 2001 (263)	United Kingdom	103	74.4	32 (31)	49 (48)	Mixed BC	Percentage and intensity	Score 0-300 Membranous	Score ≥1	M75 1:50	NA	LN status, grade, size, ER, necrosis and CAIX expression	MV analysis 2.13	0.06	Reported in text

Table detailing papers which investigated the prognostic role of CAIX on recurrence free survival.

In the remaining 5 studies (n = 4,578), patients with high tumour CAIX expression had a significantly worse RFS (HR = 1.42, 95% CI: 1.32–1.51, P<0.00001), with mild non-significant heterogeneity (I^2 = 4%, P = 0.38) (Figure 3.5A). 3,630 participants from 4,578 was came from the report of Lou and co-workers (308). Thus, further analysis was performed with this study excluded and the result was proven to be stable, the exclusion of this report did not significantly alter the results (HR = 1.62, 95% CI: 1.28–2.05, P<0.0001) and no heterogeneity was shown (I^2 = 0%, P = 0.43) (Figure 3.5B).

Since few studies examined the association between tumour CAIX expression and RFS (n = 5), subgroup analysis was not carried out. The majority of studies were associated with poor prognosis and similar antibodies were used.

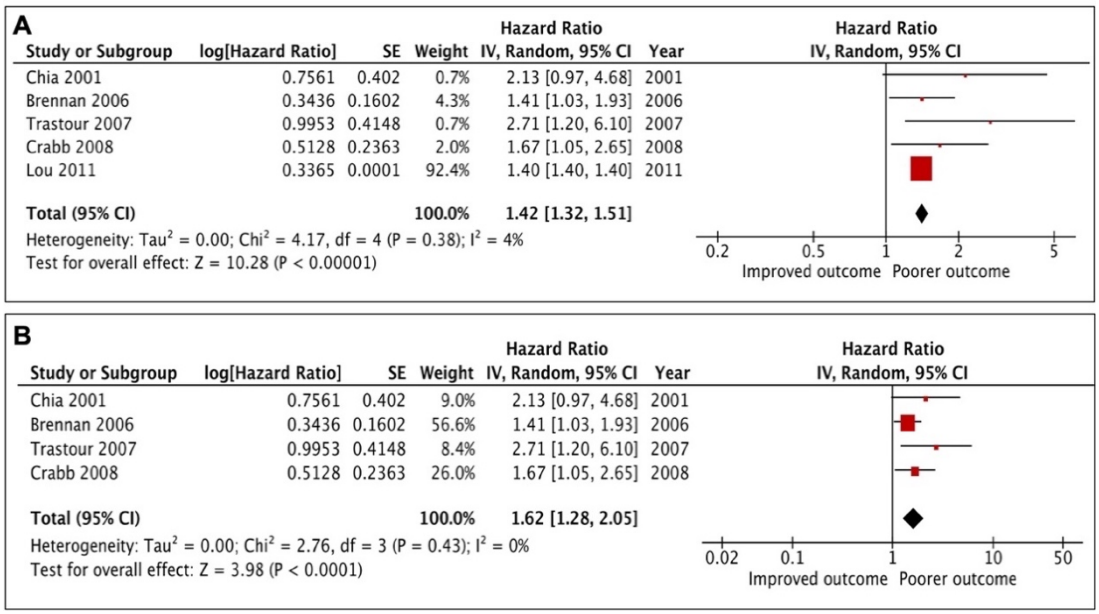

Figure 3.5 Forest plot for the relationship between CAIX expression and recurrence free survival in breast cancer patients.

Including Lou's study [A], after excluding Lou's study [B].

3.4.2.3.2 Analysis of CAIX expression and disease-free survival

Effect of CAIX expression on DFS in breast cancer could be evaluated in 13 studies (n = 2,356 patients). Due to a small observational number, one further study was excluded from the analysis. The complete data to estimate the HR could not be retrieved from two studies and were therefore not included in the analysis. HR for 3 studies was calculated from available numerical data (Table 3.6).

Table 3.6 Studies characteristics and the impact of CAIX on disease-free survival

Author(s)	Country	Patients (n)	Median follow up (months)	Cancer death n (%)	High CAIX expression n (%)	Tumour subtype	Scoring method	Score range and location	Definition of positive	Antibody for IHC/ dilution	Tumour stage	Multivariate variables	HR (95% CI)	P-value	HR estimation
Alves et al. 2019 (312)	Brazil	196	73.9	NA	13 (7)	Mixed BC	Percentage and intensity	Score 0-6 Membranous	Score >2	ab15086 1:200	T1-4 N0-3 M0	NA	UV analysis NA	0.005	Reported in text
Jin et al. 2016 (265)	South Korea	270	NA	NA	59 (22)	TNBC	Percentage	1-100 Membranous and cytoplasmic	≥10%	Abcam 1:75	I-II	LVI, LN metastasis, HIF-1α, CAIX and combined HIF-1α and CAIX expression	MV analysis 2.65 (1.41–4.97)	0.002	Reported in text
Aomatsu et al. 2014 (336)	Japan	102	6.2	NA	47 (46)	Mixed BC	Intensity	Score 0-3 Membranous	Score ≥2	M75 1:1000	IIA-IIB or IIIA	ER, PR, molecular subtypes (HR+/Her-2) and CAIX expression	MV analysis 2.39 (1.04–5.49)	0.041	Reported in text
Noh, Kim, and Koo 2014 (337)	South Korea	334	NA	31 (9.3)	96 (29)	AR+/ER− BC	Percentage and intensity	Score 0-6 Location not stated	Score ≥2	Abcam 1:100	T1-3	T stage, LN status, histologic grade and CAIX expression	MV analysis 2.23 (0.67–7.43)	0.191	Reported in text
Choi, Jung, and Koo 2013	South Korea	276	67	23 (8)	90 (33)	Mixed BC	Intensity	Score 0-3 Cytoplasmic	Score ≥2	NA 1:100	T1-3 N0-3	-	UV analysis NA	0.271	Reported in text
Currie et al. 2013 (338)	New Zealand	87	NA	NA	43 (49)	Mixed BC	Percentage and intensity	Score 0-8 Membranous	Score ≥3	Novus Biologicals 1:1000	NA	-	UV analysis NA	0.47	Reported in text
Betof et al. 2012 (339)	USA	209	99.6	32 (16.6)	182 (88)	Mixed BC based on CT	Percentage and intensity	Score 0-300 Membranous and cytoplasmic	Score ≥50	M75 NA	NA	NA	UV analysis 1.82	0.014	Reported in text
Kaya et al. 2012 (340)	Turkey	111	110	NA	62 (65)	Group1:HR +, Her-2-ve Group2:HR-, Her-2+ve	Absent or present	0-1 Membranous	Score ≥1	H-120 1:100	T1-4 N0-3 M0	-	UV analysis NA	0.344	Survival curve
Pinheiro et al. 2011 (306)	Portugal and Brazil	122	NA	NA	22 (18)	Mixed BC	Percentage and intensity	Score 0-6 Membranous	Score ≥3	ab15086 1:2000	T1-3	NA	UV analysis NA	0.045	Survival curve
Tan et al. 2009 (264)	UK and Australia	182	131.9	99 (21.7)	59 (14)	Mixed BC Patients treated with CT (n=182)	Percentage	0-100 Membranous	≥10%	NA	NA	NA	UV analysis 3.20 (1.79–5.70)	<0.001	Reported in text
Trastour et al. 2007 (248)	France	132	138	20 (15)	38 (29)	Mixed BC	Percentage	0-100 Membranous	>1%	MN75 1:10,000	NA	Tumour size, LN status, tumour grade, HIF-1α and CAIX expression	MV analysis 2 (1.0–4.2)	0.05	Reported in text
Generali et al. 2006a (246)	Italy	166	53	22 (11.7)	41 (24.7)	Mixed BC	Intensity	Score 0-2 Location not stated	Score ≥1	M75 1:50	T2-4 N0-1	NA	UV analysis NA	0.02	Reported in text

Generali et al. 2006b (258)	Italy	169	NA	21 (12.5)	41 (24)	Mixed BC	Intensity	Score 0-2 Location not stated	Score ≥1	M75 1:50	T2–4 N0–1	LN status, tumour size, BCL2, Her-2, PR, ER, Ki67, p53 and CAIX expression	MV analysis 1.6 (0.8–3.2)	0.2	Reported in text

Table detailing papers which investigated the prognostic role of CAIX on disease-free survival.

Overall, high CAIX expression in 10 studies (n = 1,882) was associated with a worse DFS (HR = 1.64, 95% CI: 1.34–2.00, P<0.00001). Mild heterogeneity was detected across these studies (I^2 = 49%, P = 0.04) (Figure 3.6). Therefore, subgroup analysis was performed to explore the potential sources of heterogeneity based on survival analysis, study region, antibodies used, cellular localization, and scoring methods.

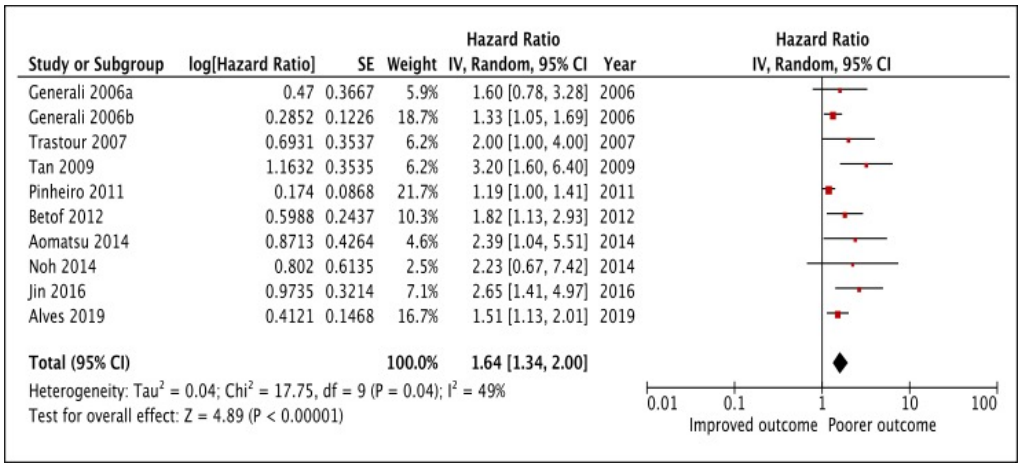

Figure 3.6 Forest plot for the relationship between CAIX expression and disease-free survival in breast cancer patients.

The pooled HR for univariate analysis was (HR = 1.48, 95% CI: 1.19–1.85, P = 0.0005) with significant heterogenicity (I^2 = 61%, P = 0.04). The HR for multivariable analysis was (HR = 2.14, 95% CI: 1.53–3.01, P<0.0001), with no heterogenicity detected (I^2 = 0%, P = 0.88) (Table 3.8).

Stratified analysis by study region suggested a poor DFS for three studies with Asian subjects (HR = 2.50, 95% CI: 1.57–3.98, P = 0.0001) and for five studies from Europe (HR = 1.50, 95% CI: 1.15–1.96, P = 0.003). Heterogenicity was observed only among subgroup of Europe (I^2 = 57%, P = 0.05) (Table 3.8).

There were variations in the antibodies used for IHC in the studies. Five studies (n = 778) used M75 antibody, and four studies (n = 922) used ab50186. Other studies used anti-CAIX antibodies obtained from different suppliers and were used in few studies (n = 2), therefore meta-analysis was not carried out. In subgroup analysis by antibody, significant effect of CAIX on DFS was observed in M75 subgroup (HR = 1.51, 95% CI: 1.25–1.83, P<0.0001),

with no heterogeneity was observed (I^2 = 0%, P = 0.48). A similar association was found in ab50186 (HR = 1.53, 95% CI: 1.12–2.10, P = 0.008) with moderate heterogeneity (I^2 = 61%, P = 0.05) (Table 3.8).

Diverse cellular localization was observed between studies. A membranous expression of CAIX was described in five studies (n = 734) whereas cytoplasmic staining was only reported in one study. Combination of the membranous and cytoplasmic staining was also reported in two studies (n = 479) whereas the rest did not state the staining localization. In subgroup analysis, membranous staining had a significant effect on DFS (HR = 1.69, 95% CI: 1.22–2.34, P = 0.002). A significant heterogeneity was detected (I^2 = 66%, P = 0.02) (Table 3.8).

Eleven studies examined the relationship of various scoring methods and DFS. Percentage of positive cells method was used by three studies (n = 584), and intensity of staining was showed in three studies (n = 437). While in the remaining four studies (n = 861), the scores were calculated as the product of combination of percentage of positive cells and staining intensity. Subgroup analysis of the different scoring revealed a similar significant association between tumoural CAIX expression and DFS in subgroup analysis of percentage of staining cells (HR = 2.57, 95% CI: 1.75–3.79, P<0.00001), intensity of staining (HR = 1.41, 95% CI: 1.13–1.76, P = 0.002), and the combination of two methods (HR = 1.40, 95% CI: 1.13–1.74, P = 0.002). Mild heterogeneity was only observed in subgroup analysis of combination of percentage and staining intensity (I^2 = 37%, P = 0.19) (Table 3.8).

3.4.2.3.3 Analysis of CAIX expression and overall survival

A total of 16 from the selected 23 studies examined the association between CAIX expression and OS. Three studies with small number of patients were excluded from the analysis. Three studies could not be included in this analysis due to incomplete reporting (Table 3.7). HR was calculated from available numerical data extrapolated from Kaplan-Meier survival curve and summary Table for 3 studies.

Table 3.7 Studies characteristics and the impact of CAIX on overall survival

Author(s)	Country	Patients (n)	Median follow up (months)	Cancer death n (%)	High CAIX expression n (%)	Tumour subtype	Scoring method	Score range and location	Definition of positive	Antibody For IHC /dilution	Tumour stage	Multivariate variables	HR (95% CI)	P-value	HR estimation
Alves et al. 2019 (312)	Brazil	176	73.9	NA	13 (7.4)	Mixed BC	Percentage and intensity	Score 0-6 Membranous	Score ≥3	ab15086 1:200	T1-4 N0-3 M0	-	UV analysis NA	0.143	Reported in text
Ozretic et al. 2018 (311)	Croatia	64	55.5	10 (15.6)	49 (77)	TNBC	Percentage and intensity	NR Membranous	NA	ab15086 1:100	NA	-	UV analysis NA	0.493	Reported in text
Noh, Kim, and Koo 2014 (337)	South Korea	334	NA	31 (9.3)	96 (28.7)	AR+/ER− BC	Percentage and intensity	Score 0-6 Location not stated	Score ≥2	NA 1:100	T1-3	T stage, LN status, histologic grade and CAIX expression	MV analysis 15.89 (1.82–131.6)	0.010	Reported in text
Choi, Jung, and Koo 2013 (235)	South Korea	276	67	23 (8.3)	90 (32.6)	Mixed BC	Intensity	Score 0-3 Cytoplasmic	Score ≥2	NA 1:100	T1-3 N0-3	-	UV analysis NA	0.195	Reported in text
Currie et al. 2013 (338)	New Zealand	87	NA	NA	43 (49)	Mixed BC	Percentage and intensity	Score 0-8 Membranous	Score ≥3	NA 1:1000	NA	-	UV analysis NA	0.91	Reported in text
Betof et al. 2012 (339)	USA	209	99.6	32 (16.6)	182 (88)	Mixed BC based on CT	Percentage and intensity	Score 0-300 Membranous and cytoplasmic	Score ≥50	M75 NR	NA	NA	UV analysis 3.77	0.010	Reported in text
Kaya et al. 2012 (340)	Turkey	111	110	NA	62 (65)	Group1:HR+, Her-2-ve Group 2:HR-, Her-2+ve	Absent or present	0-1 Membranous	Score ≥1	H-120 1:100	T1-4 N0-3 M0	-	UV analysis NA	0.109	Survival curve
Beketic-Oreskovic et al. 2011 (310)	Croatia	40	55.8	24 (60)	24 (60)	Mixed BC	Percentage and intensity	Score 1-3 Membranous and cytoplasmic	Score >52.5	NA 1:100	NA	Necrosis, tumour size, LN status, histological grade and CAIX expression	MV analysis 4.14 (1.28–13.35)	0.018	Reported in text
Jubb et al. 2010 (341)	United Kingdom	151	120	NA	49 (32)	Mixed BC	Percentage	0-100 Membranous and cytoplasmic	>10%	M75 NA	NA	-	UV analysis 0.88 (0.43–1.81)	0.73	Reported in text
Lancashire et al. 2010 (334)	United Kingdom	244	67	NA	29 (18.1)	Mixed BC (n=160)	Absent or present	0-1 Membranous	Score ≥1	Abcam 15086 1:2,500	NA	-	UV analysis NA	0.085	Reported in text
Tan et al. 2009 (264)	UK and Australia	182	131.9	99 (21.7)	59 (14)	Mixed BC treated with CT (182)	Percentage	0-100 Membranous	≥10%	NA	NA	LN status, tumour grade, tumour size and CAIX expression	MV analysis 3.20 (1.79–5.70)	<0.001	Reported in text
Kyndi et al. 2008 (342)	Denmark	945	204	NA	151 (16)	Mixed BC	Percentage	0-100 Membranous	≥10%	M75 1:2,500	NA	LN status, tumour size, grade, HR and Her-2 status, menopausal status/systemic treatment	UV analysis 1.30 (1.06–1.60)	NA	Reported In text

Hussain et al. 2007 (259)	United Kingdom	144	48	28 (19.4)	37 (26)	Mixed BC	Intensity and pattern	Score 1-5 Membranous	Score ≥ 2	M75 1:100	NR	Vascular invasion and CAIX expression	MV analysis 2.43 (1.07–5.53)	0.035	Reported in text
Brennan et al. 2006 (262)	Sweden	400	166.8	NA	42 (11)	Mixed BC 1-3 +ve LN Premenopausal	Absent or present	0-1 Membranous	≥1%	M75 1:2000	II	NA	UV analysis NA	0.022	Reported in text
Generali et al. 2006b (258)	Italy and UK	169	NR	21 (11.5)	41 (24)	Mixed BC	Intensity	Score 0-2 Location not stated	Score ≥1	M75 1:50	T2–4 N0–1	NA	UV analysis NA	0.001	Reported in text
Chia et al. 2001 (263)	United Kingdom	103	74.4	32 (31)	49 (48)	Mixed BC	Percentage and intensity	Score 0-300 Membranous	Score ≥50	M75 1:50	NA	LN status, grade, size, ER, necrosis and CAIX expression	MV analysis 2.61 (1.01–6.75)	0.05	Reported In text

Table detailing papers which investigated the prognostic role of CAIX overall survival.

Based on 10 studies (n = 2,813), high CAIX expression was statistically significantly associated with a poorer OS (HR = 1.48, 95% CI: 1.22–1.80, P<0.0001) (Figure 3.7). Moderate heterogeneity was detected across these studies (I^2 = 59%, P = 0.009), therefore, further subgroup analysis was performed.

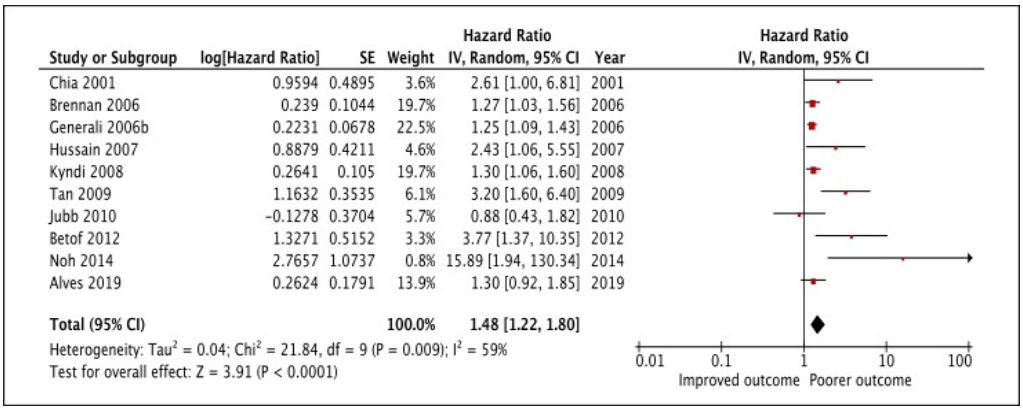

Figure 3.7 Forest plot for the relationship between CAIX expression and overall survival in breast cancer patients.

As shown in Table 3.8, the pooled HR for univariate analysis was (HR = 1.27, 95% CI: 1.16–1.40, P<0.00001) and heterogeneity was non-significant (I2 = 10%, P = 0.35). The HR for multivariate analysis was (HR = 3.03, 95% CI: 1.93–4.77, P<0.00001) and heterogeneity was not reported.

IHC staining of CAIX was predominantly performed using the M75 antibody targeting CAIX (n = 7, including 2,121 patients). The negative association between high CAIX expression in breast cancer and worse OS revealed to be associated with M75 antibody (HR = 1.34, 95% CI: 1.14–1.57, P = 0.0004), with moderate heterogeneity (I^2 = 40%, P = 0.13) (Table 3.8).

In addition, subgroup analysis based on cellular location was performed. A membranous expression of CAIX was described in five studies (n = 1,774). Although combination of the membranous and cytoplasmic staining was also reported in two studies (n = 360), cytoplasmic staining was only reported in one study (n = 276). Whereas two studies did not state the staining localization. Interestingly, the results of the subgroup analysis demonstrate

a significant prognostic value of CAIX in membranous location (HR = 1.62, 95% CI: 1.21–2.17, P = 0.001), with significant moderate heterogeneity (I^2 = 60%, P = 0.04) (Table 3.8).

There was variation in the scoring methods. The most common method being used depending on percentage of antibody-expressing tumour cells (n = 3, containing 1,278 patients) and combined staining intensity and percentage of positive cells (n = 4, containing 822 patients). On the other hand, the least common scoring method was based on staining intensity (n = 2). On meta-analysis, statistically significant effect of CAIX on OS was observed when stratified by combination percentage and intensity (HR = 2.70, 95% CI: 1.18–6.20, P = 0.02), with significant heterogeneity (I^2 = 69%, P = 0.02). However, no association was detected in other subgroups of percentage (HR = 1.51, 95% CI: 0.83–2.74, P = 0.17), with significant heterogeneity (I^2 = 73%, P = 0.02) (Table 3.8).

Table 3.8 Results of meta-analysis and subgroups of analysis methods, study region, different antibodies, cellular location, and scoring methods reported for CAIX

Stratified analysis	Number of studies	Number of patients	Test for association		Test for heterogeneity	
			Pooled HR (95% CI)	P-value	I^2 (%)	P-value
Recurrence free survival	5	4,578	1.42 (1.32–1.51)	<0.00001	4%	0.38
Disease-free survival	10	1,882	1.64 (1.34–2.00)	<0.00001	49%	0.04
Analysis methods						
Univariate	5	875	1.48 (1.19–1.85)	0.0005	61%	0.04
Multivariate	5	1,007	2.14 (1.53–3.01)	<0.0001	0%	0.88
Study region						
Asia	3	706	2.50 (1.57–3.98)	0.0001	0%	0.96
Europe	5	771	1.50 (1.15–1.96)	0.003	57%	0.05
Antibody for IHC						
M75 antibody	5	778	1.51 (1.25–1.83)	<0.0001	0%	0.48
Ab15086 antibody	4	922	1.53 (1.12–2.10)	0.008	61%	0.05
Cellular location						
Membranous	5	734	1.69 (1.22–2.34)	0.002	66%	0.02
Scoring methods						
Percentage	3	584	2.57 (1.75–3.79)	<0.00001	0%	0.64
Intensity	3	437	1.41 (1.13–1.76)	0.002	0%	0.39
Percentage and intensity	4	861	1.40 (1.13–1.74)	0.002	37%	0.19
Overall survival	10	2,813	1.48 (1.22–1.80)	<0.0001	59%	0.009
Analysis methods						
Univariate	6	2,050	1.27 (1.16–1.40)	<0.00001	10%	0.35
Multivariate	4	763	3.03 (1.93–4.77)	<0.00001	0%	0.43

Antibody for IHC						
M75 antibody	7	2,121	1.34 (1.14–1.57)	0.0004	40%	0.13
Cellular location						
Membranous	5	1,774	1.62 (1.21–2.17)	0.001	60%	0.04
Scoring methods						
Percentage	3	1,278	1.51 (0.83–2.74)	0.17	73%	0.02
Percentage and intensity	4	822	2.70 (1.18–6.20)	0.02	69%	0.02

To reduce heterogeneity, we only included studies utilizing IHC. However, no consensus was used with how the scoring was dichotomised into low and high expression. Patient stratification into groups with low and high tumoural HIF-1α and CAIX expression was performed using different thresholds. Even within the same methods of scoring there was no consensus on what cellular locations should be scored. For HIF-1α expression, some studies (n = 17) considering only nuclear staining and a few (n = 5) considering both cytoplasmic and nuclear staining, and eight studies did not mention cellular compartment. Moreover, for CAIX scoring, 13 studies considering only membranous staining, 4 studies considering both cytoplasmic and membranous staining, only one study considering cytoplasmic staining while five studies did not mention cellular location.

3.5 Discussion

The present systematic review and meta-analysis is the first to our knowledge to perform a meta-analysis for the prognostic value of both HIF-1α and CAIX expression in breast cancer. Overall, the results clearly show that high HIF-1α and CAIX expression is an adverse prognostic marker in breast cancer independent of the antibody used, tumour localisation, scoring methods and clinical endpoints evaluated. Therefore, HIF-1α and CAIX expression confirms the hypothesis that hypoxia is an important determinant of clinical outcome in patients with breast cancer.

HIF-1α, is one of the most important transcription factors in mediating cellular adaptation to hypoxia and has been linked with poor prognosis in a variety of tumours. A previous meta-analysis of 14 studies (including 2,933 patients) reported an association between HIF-1α expression and survival outcomes in breast cancer (343). However, the prognostic value of HIF-1α in breast cancer remains unclear due to the variety of methodological approaches used. The present larger meta-analysis of 30 studies (including 6,201 patients) confirms the prognostic significance of HIF-1α and through meta-analysis clarifies consistent methodology showing the independent prognostic value of HIF-1α.

The results of the present meta-analysis showed a consistent association between a high expression level of HIF-1α and poorer DFS (HR = 2.37, 95% CI: 1.76−3.20, P<0.00001), and OS (HR = 1.88, 95% CI: 1.41−2.50, P<0.0001) in patients with breast cancer. Moreover, in those studies in which multivariate analysis was carried out, HIF-1α overexpression was consistently independently associated with unfavourable survival outcomes in breast cancer.

Significant heterogeneity was found in analysis of the correlation between HIF-1α expression and DFS (I^2 = 83%, P<0.00001) and OS (I^2 = 61%, P = 0.001). This appeared to reflect the significant interaction between the type of IHC antibody, the scoring methods used, threshold selection criteria and DFS and OS. Therefore, it would appear that consideration of technical factors and breast cancer stage are important in the prognostic value of HIF-1α of patients with breast cancer.

For instance, two main types of antibodies for IHC were used, H1α67 and EP1215Y. The H1α67 antibody had significant prognostic value for DFS and OS. Stratified analysis by threshold selection criteria showed that a poor DFS was noted for studies using staining percentage of ≥1% and combination of staining intensity and percentage of score ≥1. However, only combination of staining percentage and intensity of score ≥3 was significantly associated with poor OS. Therefore, depending on the survival endpoint there would appear to be differences in the optimal HIF-1α antibody and scoring methods to be used. These factors should be taken into account in future studies of HIF-1α in patients with breast cancer. In the future, a clear definition of HIF-1α overexpression should be based on an international standardised practice. For example, the clinical practice guideline from American Society of Clinical Oncology, College of American Pathologists, and Association for Molecular Pathology provides recommendations on the analysis of epidermal growth factor receptor in lung cancer (344). In particular, further work is required to standardise the IHC protocol for HIF-1α expression.

Overexpression of HIF-1α occurs during the onset, development, and progression of human cancers (345). In respect to breast cancer in prospective studies, Nalwoga et al. reported that HIF-1α is highly expressed in patients with breast cancer and they showed significant correlations between HIF-1α expression and features of aggressive tumours (346). Indeed, Kronblad et al. (247) reported an association of HIF-1α level correlated positively to tumour size, NHG, Ki67, Her-2 and cyclin E expression, and correlated negativity to lymph node, cyclin D1, ER and PR. Malfettone et al. (333) showed a significant association between HIF-1α expression and grade II tumour, negative PR status and moderate NPI. Then, Cai et al. (347) found that HIF-1α expression was significantly increased with tumour size and LN metastasis. Recently, Peng et al. (348) concluded that HIF-1α was significantly increased with increasing primary tumour stage. The data suggest that breast cancer patients with high HIF-1α levels express more aggressive cancer characteristics and advanced stages. It is recognised that a hypoxic microenvironment in the tumour represents one of the main obstacles for effective tumour therapies (349). Therefore, inhibition of HIF-1α shows

promise as an anticancer therapy. For example, it may be hypothesised that breast cancer subtypes have a differential susceptibility to hypoxia and the effect of treatment. To date, this has not been examined in detail in patients with breast cancer.

On the other hand, the basis of the association between CAIX expression and poor clinical outcome is not clear. However, given that the CAIX enzyme is important in neutralising tumour cell acidification and contributing to extracellular acidification (232). CAIX is involved in promoting tumorigenesis and leads to a more aggressive phenotype of cancer cells (350). This can partially be explained by the association between CAIX expression and the induction of metastatic or invasive phenotype by reducing cell adhesion (229), increasing cell invasiveness (351), migration, stimulating angiogenesis, and activating proteases (352) which could be caused by the reduction in extracellular pH (261). CAIX also contributes to several specific biological process critical for tumour progression including cell survival, maintenance of cancer stem cell function and chemo and radiotherapy resistance (237). In addition to serving as a prognostic marker, CAIX may also potentially serve as a promising marker for targeted therapy. In particular, CAIX appears to be highly expressed in breast cancer and has relatively low expression in normal tissues (236, 353) and expression is located on the extracellular surface of cell membranes, allowing for efficient targeting by monoclonal antibodies or small molecule inhibitors. Therefore, CAIX constitutes an attractive and promising candidate marker for systemic anticancer therapy. Indeed, carbonic anhydrase inhibitors such as indisulam, which was investigated in phase II clinical trials, is considered one of the most potent anticancer sulfonamides and has showed high antitumour activity in various preclinical tumour models (354). The combination of CAIX inhibitors with conventional chemotherapy may yield improved efficacy (355). Also, one of several potent bis-sulfonamide CAIX inhibitors identified by screening 1 million compounds in a DNA-encoded chemical library has exhibited high and specific accumulation in cancer models (356).

Similar to HIF-1α expression, CAIX has been proposed as a marker of an aggressive malignant phenotype in a variety of common solid tumours. However, given that CAIX is less suspectable to degradation, it is perhaps not surprising that there would appear to be a more consistent association with poor clinical outcome compared with HIF-1α. In the present meta-analysis of approximately 8,390 patients, CAIX expression was significantly associated and all endpoints, RFS (HR = 1.42, 95% CI: 1.32−1.51, P<0.00001), DFS (HR = 1.64, 95% CI: 1.34−2.00, P<0.00001), and OS (HR = 1.48, 95% CI: 1.22−1.80, P<0.0001) whereas HIF-1α expression in approximately the same number of patients was only strongly

associated with DFS and OS (357). Moreover, the degree of heterogeneity associated with the HIF-1α expression meta-analysis was greater than that observed for the present CAIX expression meta-analysis. Therefore, the present study would suggest that CAIX expression is more consistently associated with clinical outcomes and may be considered the preferred prognostic marker for tumour hypoxia.

However, in the present study, there was significant heterogeneity in the DFS and OS according to survival analysis, subcellular localization and scoring methods. Therefore, it would appear that careful consideration of technical factors is required when examining the prognostic value of CAIX of patients with breast cancer. Moreover, comparative studies of HIF-1α and CAIX protein expression in the same large mature breast cancer cohort, using optimal methodological approaches, are required to be carried out to confirm this or if whether a combination of these markers should be employed.

With regards to antibody used, two main types of antibodies for IHC were used, M75 and ab50186. The M75 antibody had more consistent prognostic value for DFS and OS. Although different antibody concentrations were reported, subgroup analysis could not be made due to limited number of studies.

The prognostic value of CAIX expression has been reported in both cytoplasmic and membranous locations, however, it is not clear which location has the greater prognostic value. In addition, the relationship between the expression of CAIX in both locations is not clear.

With reference to the scoring methods used, percentage of positive cells, intensity of staining, and combination of percentage of positive cells and staining intensity were consistently associated with DFS whereas only combined percentage and intensity was consistently associated with OS. Therefore, the above potential sources of heterogeneity require further investigation.

In spite of efforts to comprehensively evaluate the effect of HIF-1α and CAIX expression on survival outcomes, limitations of the current meta-analysis should be acknowledged. The majority of studies included had relatively small sample sizes which would limit the detection of an association with clinical endpoints. Furthermore, the antibodies used, cellular localisation, scoring methods varied considerably in the analysis. Therefore, although we are able to conclude that high CAIX expression is an adverse prognostic factor and that antibodies have consistent prognostic value using standard scoring methods in patients with

breast cancer, it is not clear what is the optimal prognostic cellular localisation. Further work using the validated antibodies and scoring methods derived from the present review is required to tease out the importance of CAIX localisation expression. Furthermore, meta-analysis may overestimate associations due to publication bias.

The present systematic review and meta-analysis results highlight the importance of a high HIF-1α and CAIX expression being associated with poor survival in patients with breast cancer independent of the antibody used, tumour localisation and clinical endpoints evaluated. This information may be useful for future studies, leading to the incorporation of HIF-1α and CAIX inhibitors in treatment regimens for patients with breast cancer. High-quality studies with larger homogeneous samples are required to determine the prognostic role of both markers in different breast cancer subtypes. This will be further investigated in the following chapters.

Chapter 4 Antibody specificity

4.1 Introduction

Hypoxia has been implicated in the progression of breast cancer. However, studies with large numbers of patients exploring the role of hypoxia markers are lacking. Antibodies are one of the most commonly used tools in research, particularly in translational tissue-based research. In order to produce reliable results, antibodies must be demonstrated to be specific and immunostaining reproducible. Selection of appropriate antibodies and verification of specificity are extremely important steps before use in patient tissue. This study aimed to investigate the expression of hypoxic markers in breast cancer patient tissue and assess the clinical significance of each marker. Before use in valuable patient tissue, each antibody was validated to confirm it specifically targeted the protein of interest.

4.2 Antibody validation for each protein

To ensure antibodies utilised were specific for the target protein, specificity testing was performed as outlined in Table 4.1.

Table 4.1 Antibody validation

Protein	Antibody	Validation method
HIF-1α (1)	Novus Biologicals, Abingdon	• IHC on wild type and MDA-MB-231 NRF2 knockdown cell lines • IHC on TMA control cores
HIF-1α (2)	Novus Biologicals, Abingdon	• IHC on MCF-7 cell pellets treated with $CoCl_2$ • IHC on wild type and MDA-MB-231 NRF2 knockdown cell lines • IHC on TMA control cores
HIF-2α	Novus Biologicals, Abingdon	• IHC on MCF-7 cell pellets treated with $CoCl_2$ • IHC on wild type and MDA-MB-468 NRF2 knockdown cell lines • IHC on TMA control cores
CAIX	Bioscience, Slovakia	• Single band on Western blot detected at 57kDa in HeLa cell lysates • IHC on MCF-7 cell pellets treated with $CoCl_2$ • IHC on wild type and MDA-MB-231 NRF2 knockdown cell lines • IHC on TMA control cores

The antibody with method of validation outlined for each protein of interest. For each antibody either Western blotting to detect a single band in a positive control, staining of cell pellets treated with $CoCl_2$, staining of cell pellets known to be positive/negative for protein of interest or staining TMA control cores or all were performed.

4.2.1 Validation of HIFs antibodies

To validate the HIF-1α (1) antibody for *in situ* use, lysates were prepared from MCF-7 and MDA-MB-231 breast cancer cell lines treated with $CoCl_2$, but these lysates showed no result with Western blot. Hence, normoxic and hypoxic HeLa cell protein lysates were purchased and separated by Western blot (n = 3). HIF-1α (1) antibody was investigated using HeLa cells lysates that were purchased. Unfortunately, several repeat experiments were done to ensure reliable and reproducible results, but no conclusions can be drawn from this with no bands detected at 132 kDa for HIF-1α (1) antibody. Therefore, it was decided that Western blot experiments would be stopped, and specificity would continue using other experiments. Wild MDA-MB-231 cell lines revealed higher expression of HIF-1α (1), and no expression was observed in MDA-MB-231 NRF2 (nuclear factor erythroid 2-related factor 2) knockdown cell lines, which is reported in the literature to stop induction of a hypoxic response. No expression was observed in negative control (Figure 4.1A, B).

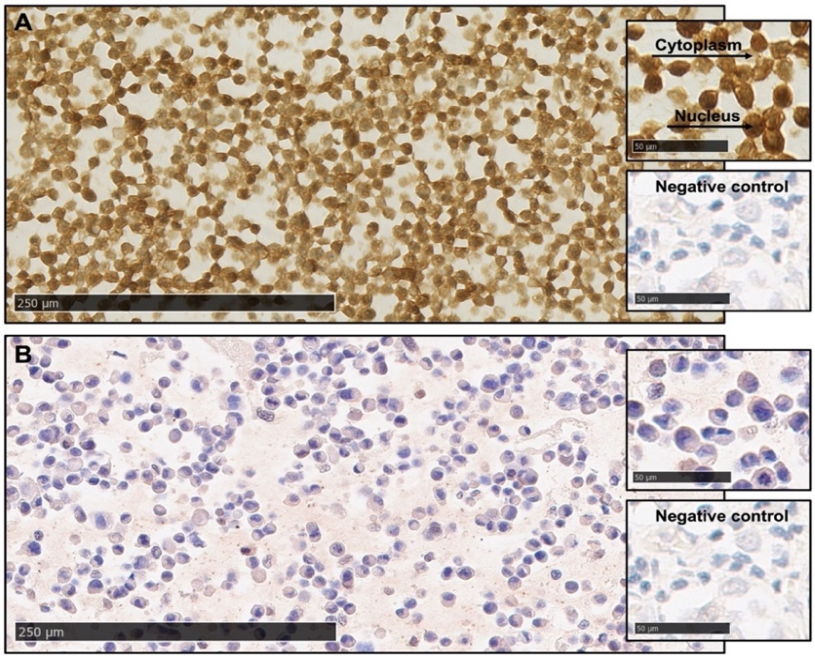

Figure 4.1 HIF-1α (1) expression detected by immunohistochemistry in wild and NRF2 knockdown cell lines.

Staining levels for HIF-1α (1) in MDA-MB-231 cells. Strong HIF-1α (1) staining in wild type MDA-MB-231 cells [A], and negative HIF-1α (1) staining in MDA-MB-231 NRF2 knockdown cell lines [B]. The bottom right boxes show no antibody negative control.

Further, IHC staining on different types of tissues was performed as additional controls, these exhibited large differences in the cytoplasmic/nuclear HIF-1α (1) staining intensity. No expression of HIF-1α (1) was observed in liver tissues. In contrast, light, moderate and strong expression of HIF-1α (1) was observed in colon, renal, and pancreatic tissue, respectively. Examples of staining are shown in Figure 4.2 (A-D).

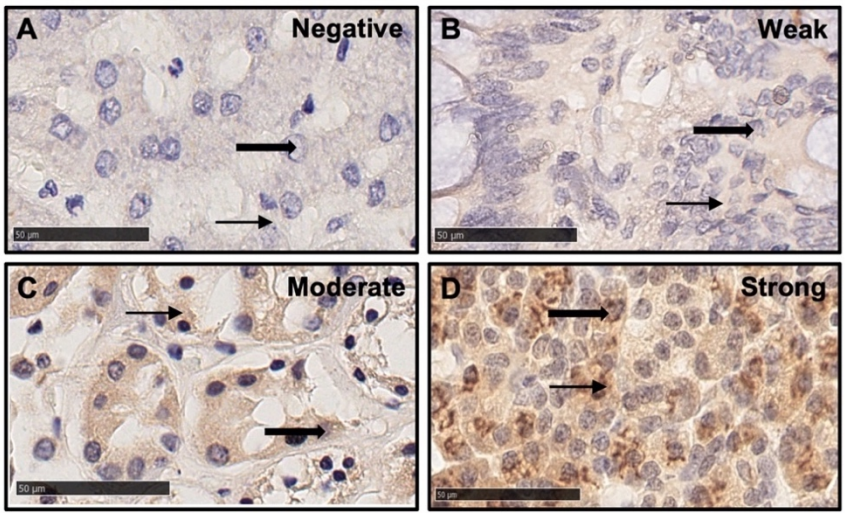

Figure 4.2 HIF-1α (1) expression detected by immunohistochemistry in tissue microarray control cores.

Staining levels for HIF-1α (1) in different tissues. Negative HIF-1α (1) staining in liver tissue [A], low staining in colon tissue [B], intermediate staining in kidney tissue [C], and strong staining in pancreatic tissue [D]. Cytoplasmic expression (thin arrow), and nuclear expression (thick arrow).

Furthermore, to validate the HIF-1α (2) antibody, normoxic and hypoxic HeLa cell protein lysates were purchased and utilised in Western blotting (n = 3). However, no results were obtained after several repeat experiments with no bands detected at 93 kDa for HIF-1α (2) antibody.

In IHC of cell pellets of MCF-7 breast cancer cells, the levels of HIF-1α (2) expression were examined after treatment with 10µL $CoCl_2$ to mimic hypoxia. Cells were cultured in parallel in untreated and treated conditions for 4 and 24 hours. Brown staining to the nucleus/cytoplasm after short $CoCl_2$ treatment (4 hours) is seen in MCF-7 breast cancer cells (Figure 4.3A). In contrast, negative staining is shown with prolonged treatment (24 hours) under the same conditions (Figure 4.3B). Blue (negative) nuclei are observed in the untreated control MCF-7 breast cancer cells (Figure 4.3C).

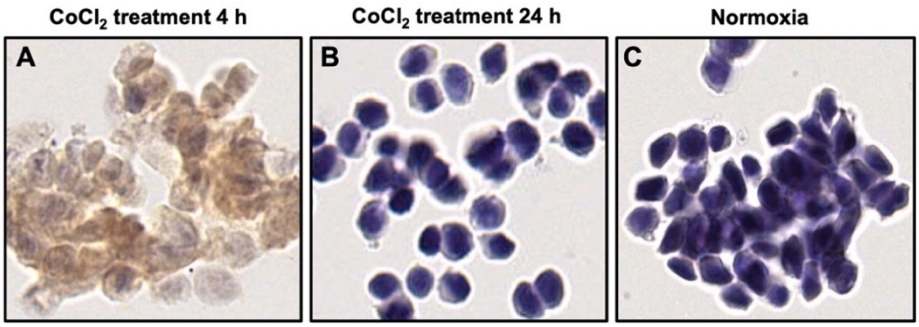

Figure 4.3 Expression of hypoxic and normoxic HIF-1α (2) proteins in MCF-7 cell lines.

Representative images of positive HIF-1α (2) immunoreactivity in MCF-7 cells were captured after $CoCl_2$ treatment for 4 h [A], negative HIF-1α (2) expression was shown in MCF-7 cells after 24 h $CoCl_2$ treatment [B], and normoxic control [C].

Further validation of HIF-1α (2) was performed by IHC staining of cell lines. No difference in staining intensity of HIF-1α (2) between MDA-MB-231 wild type and MDA-MB-231 NRF2 knockdown cells. Examples of staining with negative control are shown in Figure 4.4A, B.

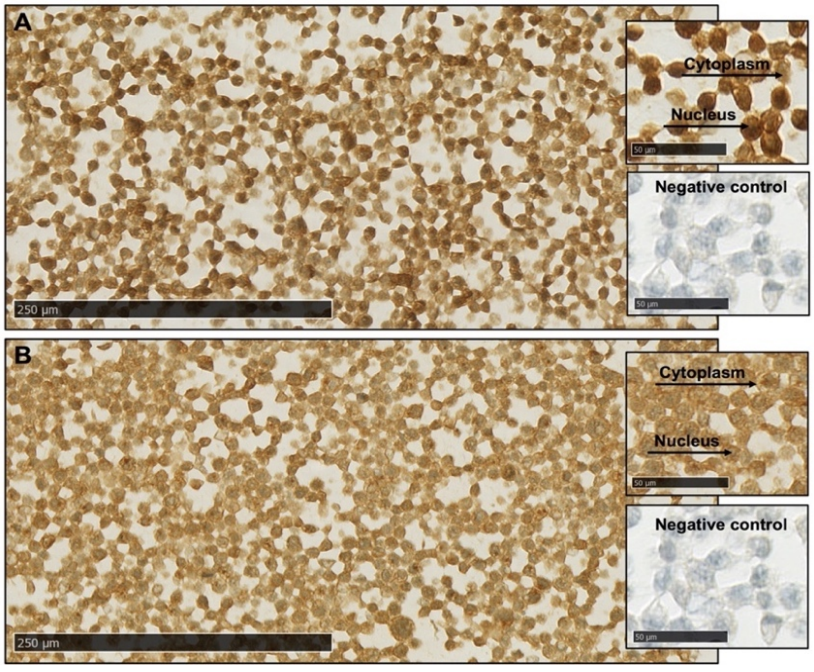

Figure 4.4 HIF-1α (2) expression detected by immunohistochemistry in wild and NRF2 knockdown cell lines.

Staining levels for HIF-1α (2) in MDA-MB-231 cells. Strong HIF-1α (2) staining in wild type MDA-MB-231 cells [A], and weak HIF-1α (2) staining in MDA-MB-231 NRF2 knockdown cell lines [B]. The bottom right boxes show no antibody negative control.

Furthermore, IHC staining on different control TMAs was performed. Representative images of negative, weak, moderate, and strong cytoplasmic/nuclear HIF-1α (2) staining are shown in Figure 4.5. Sections from prostate remained negative (Figure 4.5A). A light HIF-1α (2) staining was seen in lung tissues, and moderate increase in an expression of HIF-1α (2) was observed in colon tissues (Figure 4.5B, C). A strong positive reaction was showed in the tonsil tissues (Figure 4.5D).

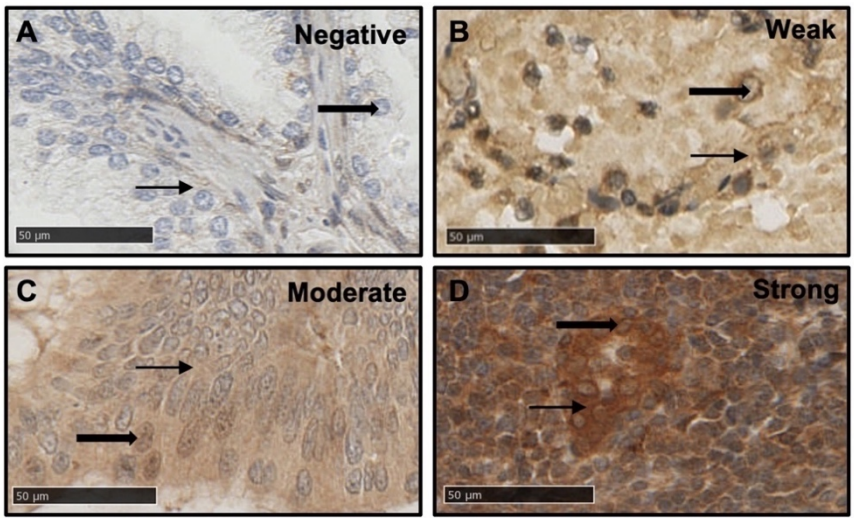

Figure 4.5 HIF-1α (2) expression detected by immunohistochemistry in tissue microarray control cores.

Staining levels for HIF-1α (2) in different tissues. Negative HIF-1α (2) staining in prostatic tissue [A], low staining in lung tissue [B], intermediate staining in colon tissue [C], and strong staining in tonsil tissue [D]. Cytoplasmic expression (thin arrow), and nuclear expression (thick arrow).

Moreover, normoxic and hypoxic HeLa cell protein lysates were purchased and used in Western blotting (n = 3) to validate the HIF-2α antibody. Several repeat experiments yielded no results, with no bands detected at 118 kDa for HIF-2α antibody.

The effect of treatment with 10µL $CoCl_2$ on HIF-2α was also tested and was found to be similar to that of HIF-1α (2). $CoCl_2$-treated MCF-7 cells showed cytoplasmic/nuclear expression of HIF-2α at 4 hours with no detectable expression at later times (24 hours) as shown in Figure 4.6.

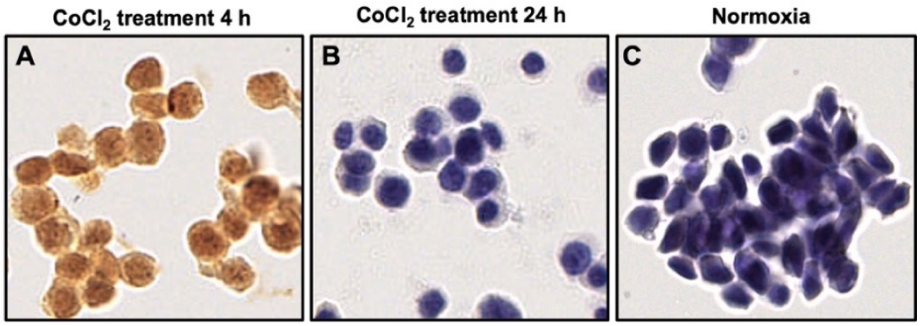

Figure 4.6 Expression of hypoxic and normoxic HIF-2α proteins in MCF-7 cell lines.

Representative images of positive HIF-2α immunoreactivity in MCF-7 cells were captured after $CoCl_2$ treatment for 4 h [A], negative HIF-2α expression was shown in MCF-7 cells after 24 h $CoCl_2$ treatment [B], and normoxic control [C].

Moreover, whereas wild MDA-MB-468 cell lines revealed relatively higher staining of HIF-2α expression, weak expression was observed in MDA-MB-468 NRF2 knockdown cell lines (Figure 4.7A, B). No staining was found in negative control.

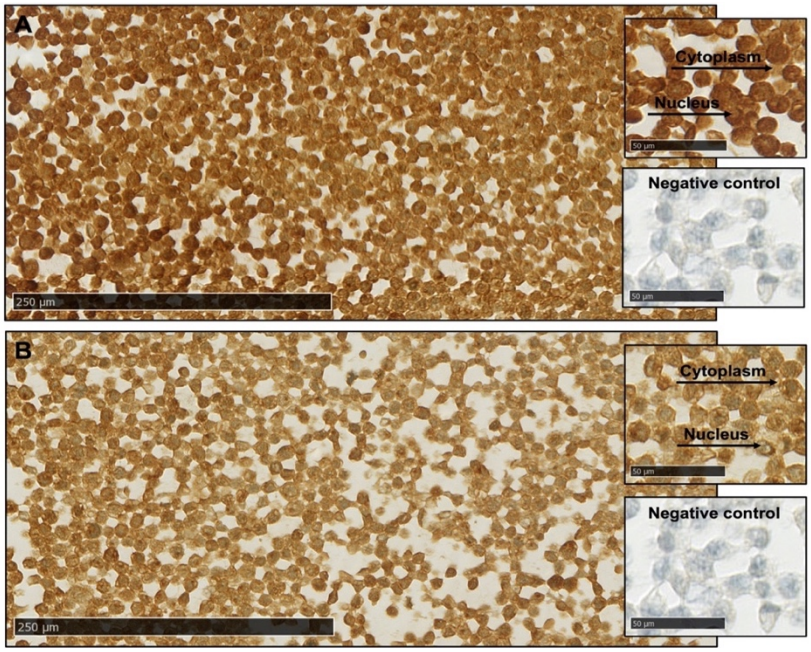

Figure 4.7 HIF-2α expression detected by immunohistochemistry in wild and NRF2 knockdown cell lines.

Staining levels for HIF-2α in MDA-MB-468 cell lines. Strong HIF-2α staining in wild MDA-MB-468 cell lines [A], and weak HIF-2α staining in MDA-MB-468 NRF2 knockdown cell lines [B]. The bottom right boxes show no antibody negative control.

Additionally, immunostaining intensity pattern was observed for HIF-2α expression on different TMA control tissues. While lung tissues showed negative staining, tonsil tissues were weakly stained. Moderate staining was seen in heart tissues and liver tissues exhibited strong staining for HIF-2α (Figure 4.8A-D).

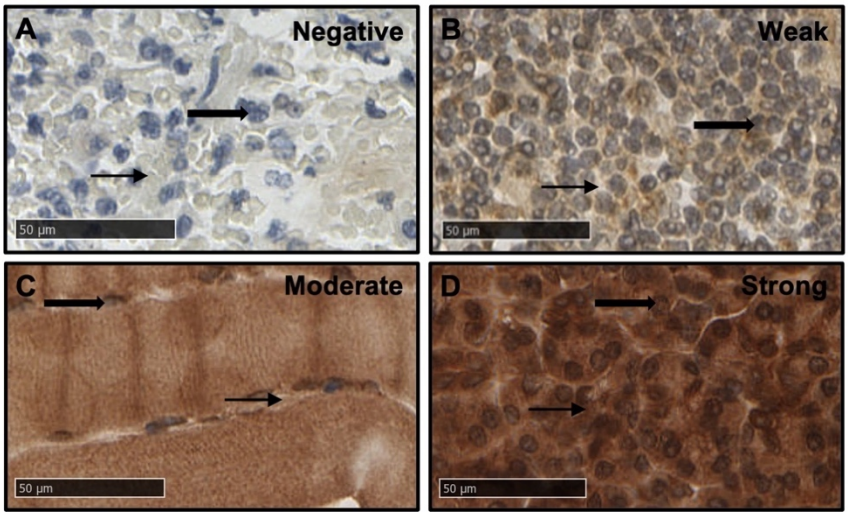

Figure 4.8 HIF-2α expression detected by immunohistochemistry in tissue microarray control cores.

Staining levels for HIF-2α in different tissues. Negative HIF-2α staining in lung tissue [A], low staining in tonsil tissue [B], intermediate staining in heart tissue [C], and strong staining in liver tissue [D]. Cytoplasmic expression (thin arrow), and nuclear expression (thick arrow).

4.2.2 Validation of CAIX

The specificity of the anti-CAIX antibody was confirmed by Western blot analysis. HeLa cell lysates were purchased and separated by Western blot (n = 3). The anti-CAIX antibody recognized a single band at 57 kDa in HeLa cells with consistent bands at 57 kDa when probed for Tubulin (Table 4.1; Figure 4.9). This result, showed bands at the correct size on Western blot, supporting the specificity of this antibody.

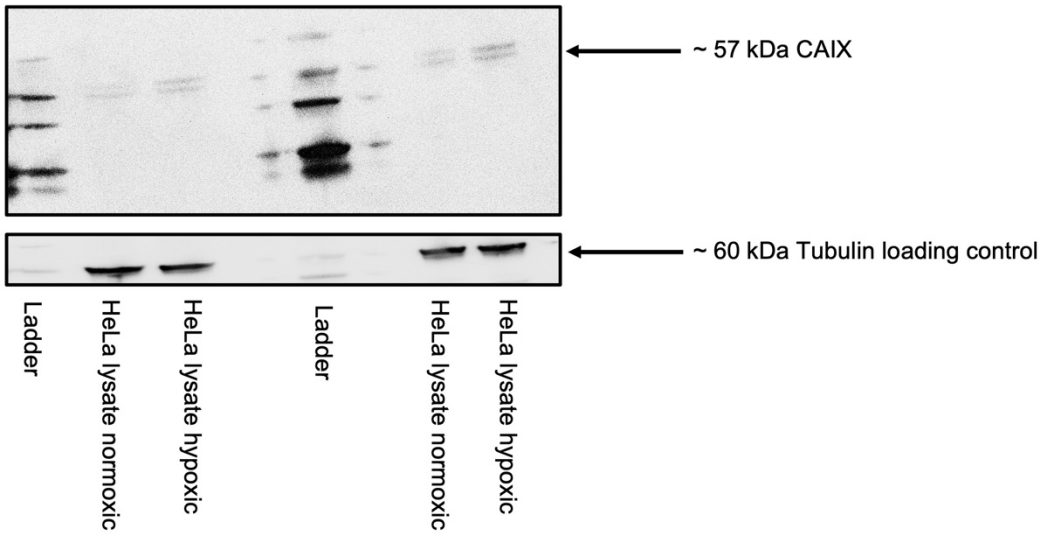

Figure 4.9 Western blots showing specificity of CAIX.

Western blot analysis of CAIX expression in hypoxic HeLa cells and normoxic control shows two bands of appropriate size (57 kDa) for HeLa normoxic and hypoxic cell lysates (15µL loaded per well). Tubulin was used as a loading control. The original Western blots before they were cropped are in the appendix.

Further validation was performed by IHC staining MCF-7 cell pellets treated with $CoCl_2$. Expression of CAIX was detected in treated MCF-7 cell lines for 4 and 24 hours when compared to untreated normoxic cells (Figure 4.10). Again, a change in expression as expected supporting the specificity of the CAIX antibody.

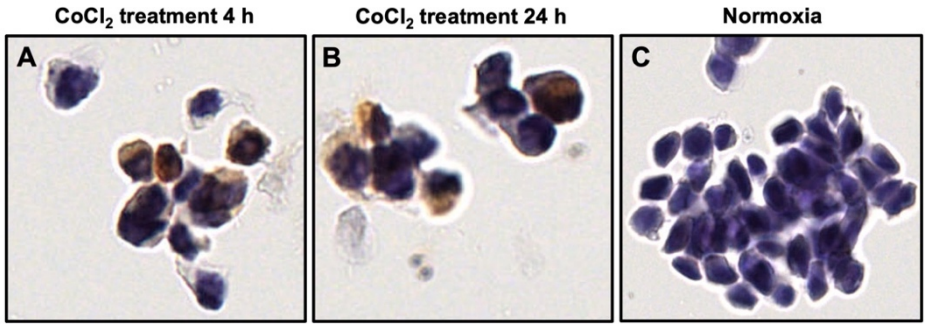

Figure 4.10 Expression of hypoxic and normoxic CAIX proteins in MCF-7 cell lines.

Representative images of positive CAIX immunoreactivity in MCF-7 cells were captured after $CoCl_2$ treatment for 4 h [A], positive CAIX expression was shown in MCF-7 cells after 24 h $CoCl_2$ treatment [B], and normoxic control [C].

In further investigations, IHC analysis of CAIX expression was also performed on MDA-MB-231 cell lines. Wild type and NRF2 knockdown cells were stained. Observation of high cytoplasmic/membranous CAIX expression in wild MDA-MB-231 cell lines and no expression in NRF2 knockdown cells (Figure 4.11A, B). This evokes the assumption that the MDA-MB-231 cell line expresses CAIX only under hypoxic conditions and provides an additional layer of evidence of the specificity of the CAIX antibody. A negative control antibody was used to rule out nonspecific staining.

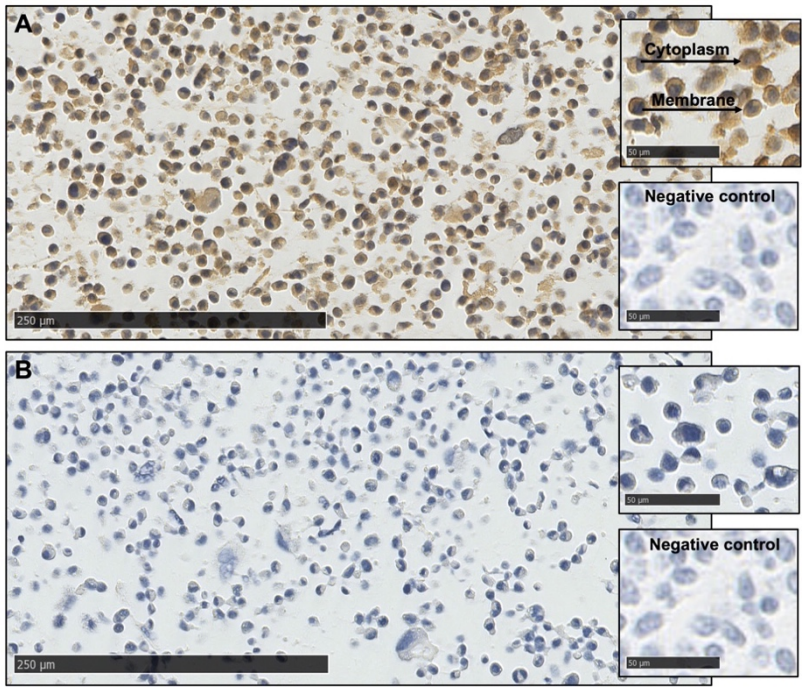

Figure 4.11 CAIX expression detected by immunohistochemistry in wild and NRF2 knockdown cell lines.

Staining levels for CAIX in MDA-MB-231 cell lines. Strong CAIX staining in wild MDA-MB-231 cell lines [A], and negative CAIX staining in MDA-MB-231 NRF2 knockdown cell lines [B]. The bottom right boxes show no antibody negative control.

Additionally, IHC staining on different TMA control tissues exhibited large differences in the staining intensity (Figure 4.12A-D). A negative staining of CAIX was shown in tonsil tissues. In contrast, the lowest expression of CAIX was observed in pancreatic tissue, moderate expression in liver tissue, and marked expression in the intestinal epithelium which is an important source of CAIX expression.

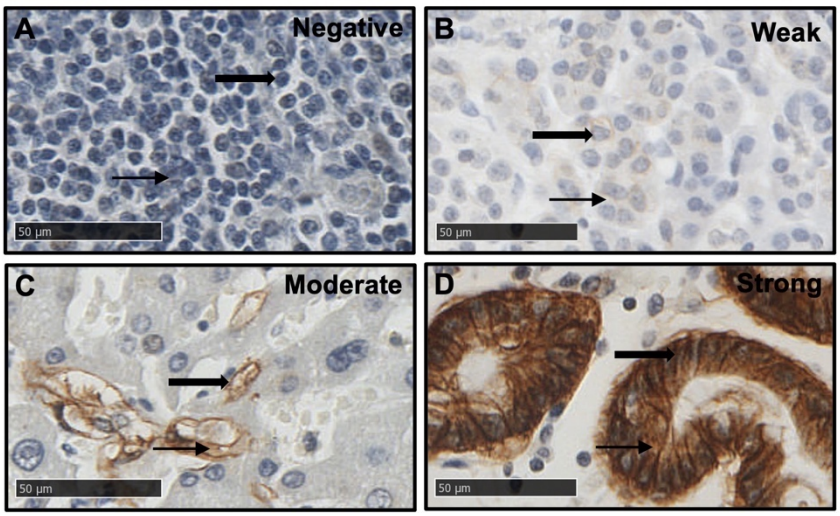

Figure 4.12 CAIX expression detected by immunohistochemistry in tissue microarray control cores.

Staining levels for CAIX in different tissues. Negative CAIX staining in tonsil tissue [A], low staining in pancreatic tissue [B], intermediate staining in liver tissue [C], and strong staining in intestinal tissue [D]. Cytoplasmic expression (thin arrow), and membranous expression (thick arrow).

Contrary to other studies that have been reported that HIF-1α is detectable in Western blot (358, 359), this study failed to obtain result from Western blot for HIFs antibody. This lack of result was consistent with the fact that HIF-1α is unstable and is rapidly degraded under normoxia conditions with a half-life of less than 5 minutes (360). Furthermore, HIF-1α (1) had very good antibody specificity but HIF-1α (2) was normal lab antibody and is not specific. Therefore, HIF-1α (2) was not explored beyond this point.

The results from this chapter indicate that although HIFs antibodies appeared specific in the cell pellet and cell line experiments, it was only CAIX antibody that all levels of evidence were acquired. Western blot experiments and cell pellet experiments provide good evidence of the specificity of CAIX antibody, suggesting that CAIX is reliable biomarker of tumour hypoxia.

Chapter 5 Comparison of threshold analysis for outcome in primary operable invasive ductal breast cancer

5.1 Introduction

Recent systematic review and meta-analyses studied an association between HIF-1α with breast cancer patient's survival and reported that even though several studies used the same antibody and a survival endpoint, they reported different threshold levels (357), suggesting variability in the selection of optimal clinical threshold. It is likely that discordance between the methods used to classify staining into positive/high versus negative/low may largely be responsible for these results.

There are number of approaches to determine clinically important thresholds in IHC, one is ROC (Receiver operating characteristic) and other is the R suite (RStudio, Boston, MA, USA) of statistical tools. Therefore, the aim of the present chapter was to compare these two statistical approaches on the determination of a clinically significant threshold level for OS in patients with primary operable invasive breast cancer.

5.2 Patients and methods

5.2.1 Patient TMA cohorts

5.2.1.1 Cohort 1: Glasgow breast TMA

850 patients presenting with invasive breast cancer at Royal Infirmary, Western Infirmary and Stobhill Hospital, Glasgow dating from the years 1995 and 1998 were studied. Patients were included in this study based on the selection of ductal histological subtype and having HIF-1α (2) expression available (n = 575). Therefore, 275 patients were excluded from the study as they did not have ductal carcinoma or HIF-1α (2) expression was unavailable. Although HIF-1α (2) was used for patients' selection, it was not explored beyond this point because it was not fully specific as showed in chapter 4.

Cohort 2: ER-positive TMA

456 patients presenting with invasive breast cancer at Western Infirmary, Victoria and Stobhill Hospitals, Glasgow between 1980 and 1999. However, when this was verified using current technologies, it was found although the majority of cases were ER-positive (n = 392), 20 were found to be ER-negative and 44 were of unknown ER status and were excluded from the study. 107 patients were excluded from analysis as they did not have ductal

carcinoma or HIF-1α (2) expression was unavailable remained 285 patients available for investigation.

5.2.2 Immunohistochemistry

IHC was performed as described in chapter 2.

5.2.3 Slide scanning and scoring

Hypoxic markers expression, HIF-2α, and CAIX was assessed using the weighted Histoscore method while HIF-1α (1) was scored digitally on QuPath. Slides were scanned using NDP serve 3 image viewer platform system as previously described in chapter 2.

5.2.4 Statistical analysis

ROC curve and R analysis (RStudio, Boston, MA, USA) were used to define of clinically important threshold values for HIF-1α (1), HIF-2α and CAIX expression for categorizing expression data into two groups, “low” and “high”. We investigated different outcomes, RFS, DFS, and OS, to obtain threshold values for hypoxic markers, but nice results were obtained from using OS. Since OS is often the most relevant endpoint, Kaplan-Meier’s plot and log-rank test were constructed based on OS.

5.3 Result

5.3.1 Comparison of different methods for threshold optimization in Glasgow breast TMA

5.3.1.1 ROC curve analysis

Because there are no generally accepted prognostic thresholds for HIF-1α (1), HIF-2α and CAIX, ROC curve was used to generate decision thresholds values, and classify patients as low and high according to OS in breast cancer (Figure 5.1).

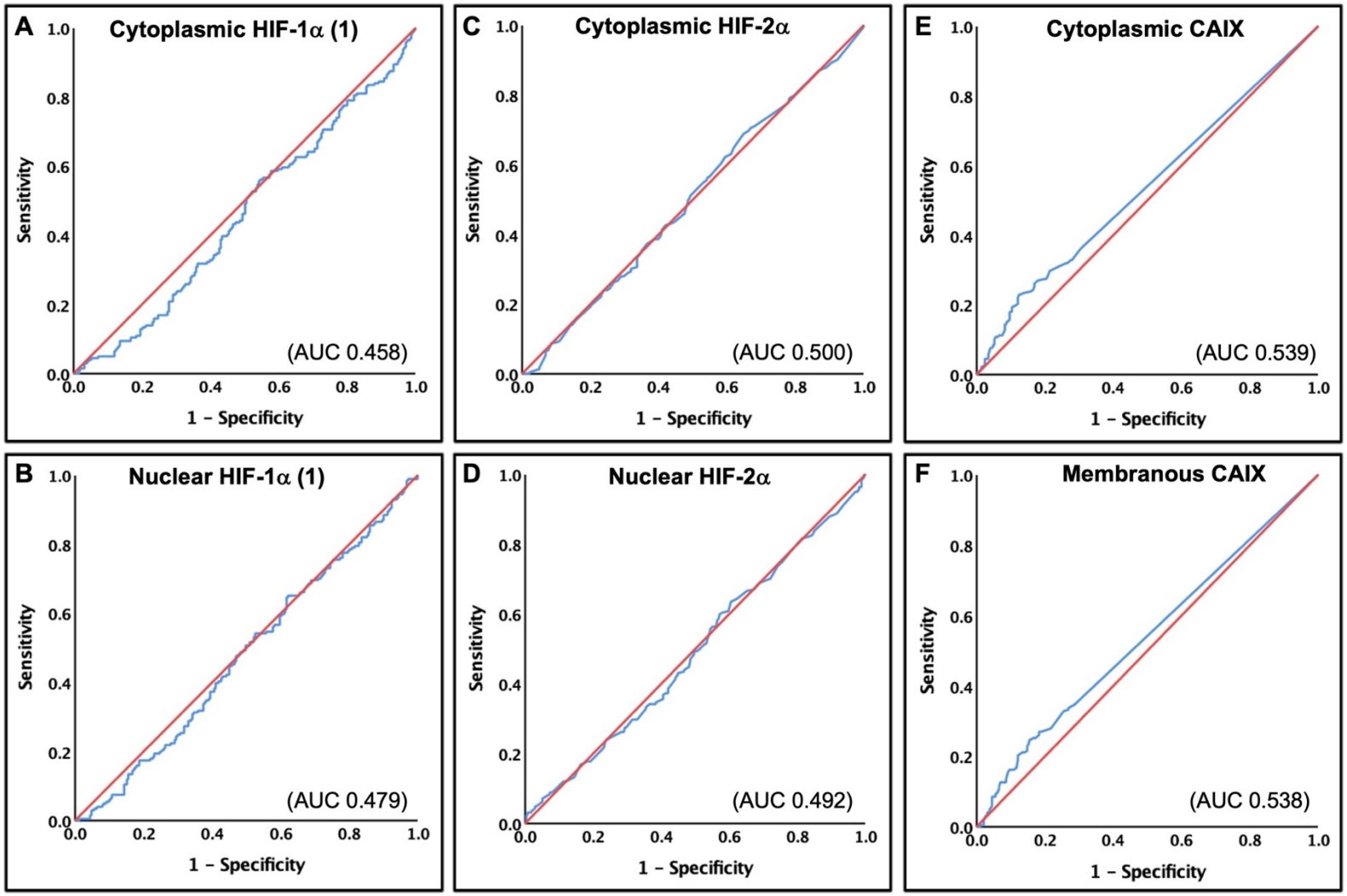

Figure 5.1 Receiver operating characteristics curves of hypoxic markers describing the threshold in Glasgow breast cohort.

Cytoplasmic and nuclear HIF-1α (1) [A, B], cytoplasmic and nuclear HIF-2α [C, D], and cytoplasmic and membranous CAIX [E, F].

The ROC curve threshold levels of low and high cytoplasmic and membranous CAIX were 17. The median threshold was chosen when there were no obvious threshold values from ROC curve to dichotomize cytoplasmic and nuclear [HIF-1α (1), and HIF-2α]. The median threshold values for cytoplasmic and nuclear HIF-1α (1) were 96 and 117, and 127 and 148 for cytoplasmic and nuclear HIF-2α, respectively (Table 5.1).

Table 5.1 Threshold values calculated by ROC curve analysis and median for overall survival in Glasgow breast cohort

Markers	Cytoplasmic		Nuclear		Membranous ROC threshold
	ROC threshold	Median threshold	ROC threshold	Median threshold	
HIF-1α (1)	-	96	-	117	-
HIF-2α	-	127	-	148	-
CAIX	17	-	-	-	17

Table outlining threshold values based on ROC curve for each hypoxic marker.

5.3.1.2 R analysis

Optimizing threshold values for the three hypoxic markers for each cellular location is shown in Figure 5.2. Survminer and maxstat packages in R studio were utilised to classify patients as low and high according to OS.

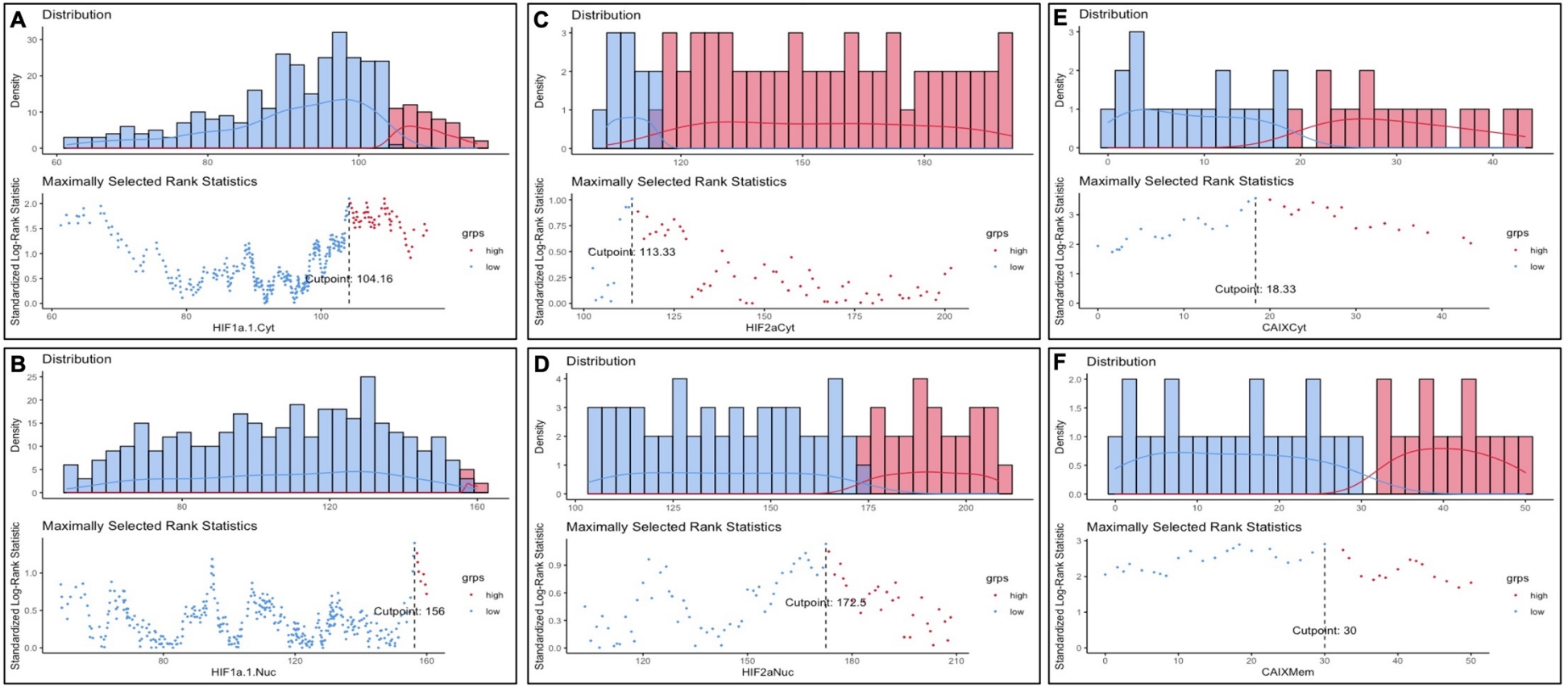

Figure 5.2 Plots showing threshold optimization using R analysis in Glasgow breast cohort.

Cytoplasmic and nuclear HIF-1α (1) [A, B], cytoplasmic and nuclear HIF-2α [C, D], and cytoplasmic and membranous CAIX [E, F].

As shown in Table 5.2, R threshold values for cytoplasmic and nuclear HIF-1α (1) were 104 and 156, respectively. R threshold values for cytoplasmic and nuclear HIF-2α were 113, and 173, and for cytoplasmic and membranous CAIX were 18, and 30, respectively.

Table 5.2 Threshold values calculated by R analysis for overall survival in Glasgow breast cohort

Markers	Cytoplasmic	Nuclear	Membranous
HIF-1α (1)	104	156	-
HIF-2α	113	173	-
CAIX	18	-	30

Table outlining threshold values based on R analysis for each hypoxic marker.

5.3.1.3 Kaplan-Meier analysis

5.3.1.3.1 Cytoplasmic HIF-1α (1)

Kaplan-Meier's plot with the optimal threshold point demonstrated that 225 patients had high cytoplasmic HIF-1α (1) and 236 had low cytoplasmic HIF-1α (1) using median, while 107 patients were high for cytoplasmic HIF-1α (1) and 354 were low for cytoplasmic HIF-1α (1) using R. No significant difference was observed for mean survival between high and low cytoplasmic HIF-1α (1) patients (129.5 months for high, versus 129.8 mean survival for low) using median threshold value (P = 0.868; Figure 5.3A). However, a mean survival of 136 for high cytoplasmic HIF-1α (1) patients and 127.4 mean survival for low cytoplasmic HIF-1α (1) observed when employing the R threshold value (P = 0.031; Figure 5.3B; Table 5.3).

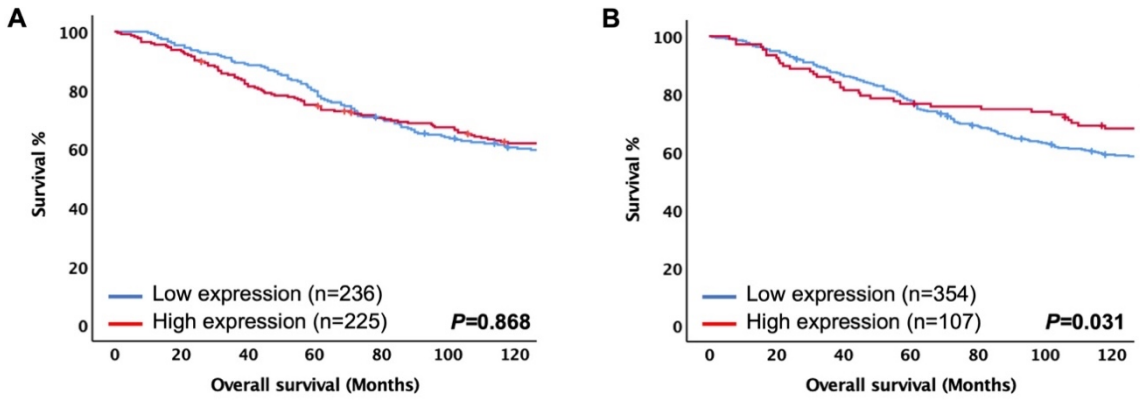

Figure 5.3 Comparison of Kaplan-Meier survival curves (log-rank) for overall survival of cytoplasmic HIF-1α (1) expression in Glasgow breast cohort according to different threshold values.

OS according to median threshold value [A], and OS according to R threshold value [B].

5.3.1.3.2 Nuclear HIF-1α (1)

Threshold levels were generated for both methods, median and R, were used for Kaplan-Meier construction for OS. 206 patients had high nuclear HIF-1α (1) and 255 had low nuclear HIF-1α (1) using median, while 54 patients were high for nuclear HIF-1α (1) and 407 were low for nuclear HIF-1α (1) using R. No significant difference was observed for mean survival between high and low nuclear HIF-1α (1) patients (127.7 months for high versus 131 mean survival for low) using median threshold value (P = 0.717; Figure 5.4A). However, a mean survival of 142 for high nuclear HIF-1α (1) patients and 128 mean survival for low nuclear HIF-1α (1) with using R threshold level (P = 0.053; Figure 5.4B; Table 5.3).

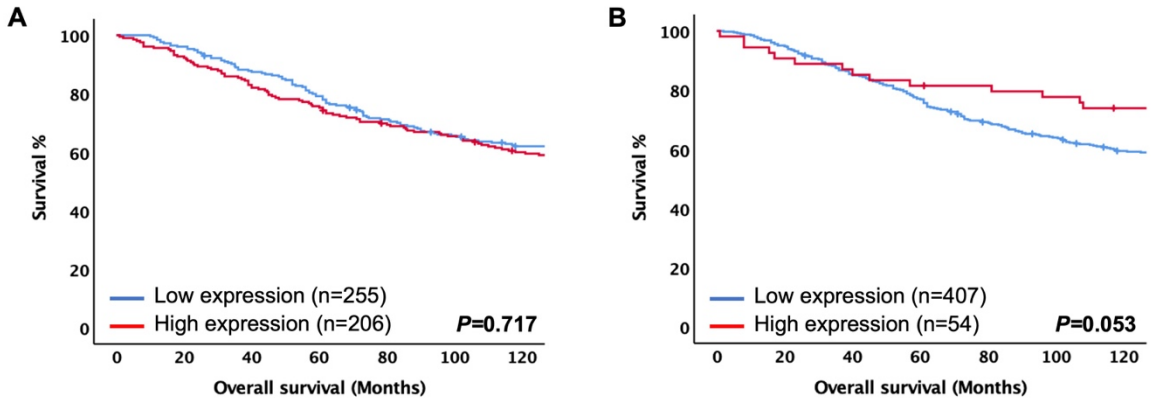

Figure 5.4 Comparison of Kaplan-Meier survival curves (log-rank) for overall survival of nuclear HIF-1α (1) expression in Glasgow breast cohort according to different threshold values.

OS according to median threshold value [A], and OS according to R threshold value [B].

5.3.1.3.3 Cytoplasmic HIF-2α

252 patients had high cytoplasmic HIF-2α and 257 had low cytoplasmic HIF-2α with using median threshold point while 344 patients were high for cytoplasmic HIF-2α and 165 were low for cytoplasmic HIF-2α using R. With a median threshold, a mean survival of 125.4 months for high cytoplasmic HIF-2α patients and 132.8 mean survival for low cytoplasmic HIF-2α. Likewise, a mean survival of 126.9 for high cytoplasmic HIF-2α patients and 133.7 mean survival for low cytoplasmic HIF-2α with using R threshold. Kaplan-Meier curves showed statistically insignificant P-values of 0.465, and 0.295 with an using of median and R threshold, respectively (Figure 5.5A, B; Table 5.3).

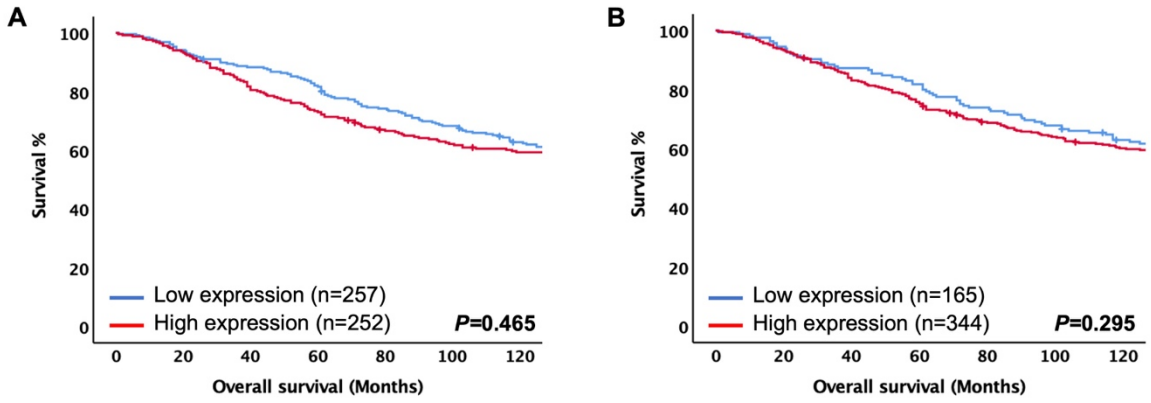

Figure 5.5 Comparison of Kaplan-Meier survival curves (log-rank) for overall survival of cytoplasmic HIF-2α expression in Glasgow breast cohort according to different threshold values.

OS according to median threshold value [A], and OS according to R threshold value [B].

5.3.1.3.4 Nuclear HIF-2α

Patients with high nuclear HIF-2α expression were 243, and 266 had low nuclear HIF-2α using median threshold. In contrast, 196 patients had high nuclear HIF-2α and 313 had low nuclear HIF-2α using R thresholds. Median threshold showed a mean survival of 130 months for high nuclear HIF-2α patients and 128.4 mean survival for low nuclear HIF-2α. R showed a mean survival of 133.6 for high nuclear HIF-2α patients and 126.4 mean survival for low nuclear HIF-2α. Kaplan-Meier curves and the log-rank test data using median and R thresholds showed P-value of 0.760, and 0.237, respectively (Figure 5.6A, B; Table 5.3).

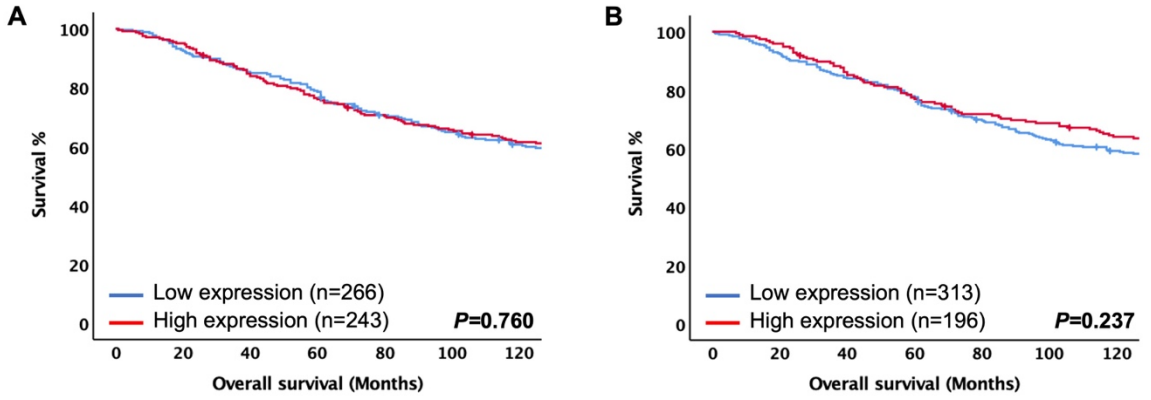

Figure 5.6 Comparison of Kaplan-Meier survival curves (log-rank) for overall survival of nuclear HIF-2α expression in Glasgow breast cohort according to different threshold values.

OS according to median threshold value [A], and OS according to R threshold value [B].

5.3.1.3.5 Cytoplasmic CAIX

With ROC curve threshold optimization, 94 patients had high cytoplasmic CAIX and 427 had low cytoplasmic CAIX. 90 patients had high cytoplasmic CAIX and 431 had low cytoplasmic CAIX using R thresholds. ROC showed a mean survival of 111.2 months for high cytoplasmic CAIX patients and 135.7 mean survival for low cytoplasmic CAIX. R analysis showed a mean survival of 108.5 for high cytoplasmic CAIX patients and 136 mean survivals for low cytoplasmic CAIX. Kaplan-Meier curves and log-rank test for both methods, ROC and R, showed a significant association with worse OS (P = 0.001, P <0.001, respectively; Figure 5.7A, B; Table 5.3).

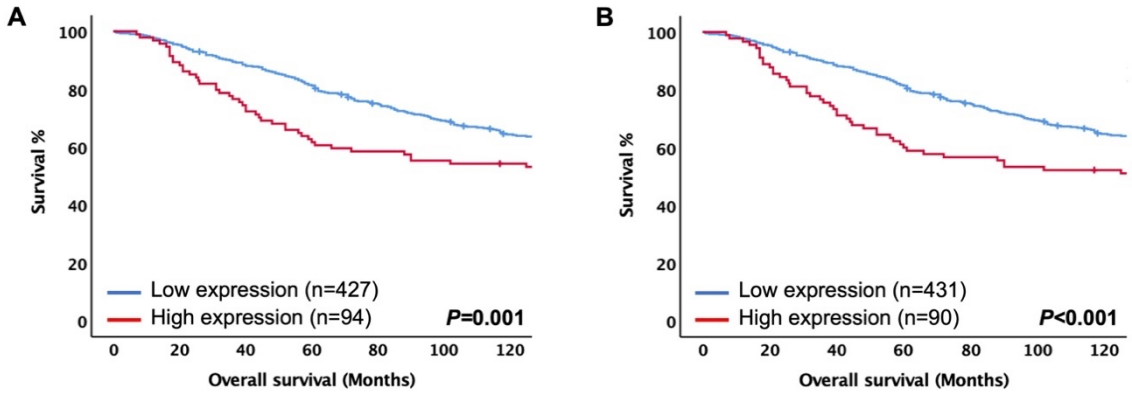

Figure 5.7 Comparison of Kaplan-Meier survival curves (log-rank) for overall survival of cytoplasmic CAIX expression in Glasgow breast cohort according to different threshold values.

OS according to ROC threshold value [A], and OS according to R threshold value [B].

5.3.1.3.6 Membranous CAIX

106 patients had high membranous CAIX, and 415 patients had low membranous CAIX using ROC. 82 patients had high membranous CAIX, and 439 patients had low membranous CAIX using R thresholds. ROC analysis showed a mean survival of 115.3 for high membranous CAIX patients and 135.3 mean survival for low membranous CAIX, with a P-value of 0.006 (Figure 5.8A). R analysis showed a mean survival of 110.8 for high membranous CAIX patients and 135.1 mean survival for low membranous CAIX, with a P-value of 0.003 (Figure 5.8B, Table 5.3).

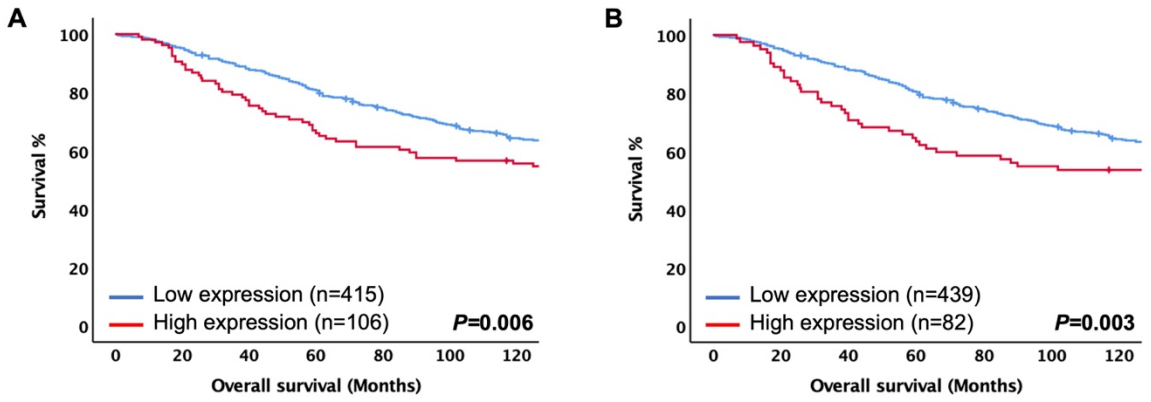

Figure 5.8 Comparison of Kaplan-Meier survival curves (log-rank) for overall survival of membranous CAIX expression in Glasgow breast cohort according to different threshold values.

OS according to ROC threshold value [A], and OS according to R threshold value [B].

Table 5.3 Comparison of different threshold levels and P-values in Glasgow breast cohort

Makers	Survival endpoint	Obtained threshold ^{ROC}	P-value ^{ROC}	Obtained threshold ^{median}	P-value ^{median}	Obtained threshold ^{R}	P-value ^{R}
Cytoplasmic HIF-1α (1)	OS	-	-	96	0.868	104	**0.031**
Nuclear HIF-1α (1)	OS	-	-	117	0.717	156	0.053
Cytoplasmic HIF-2α	OS	-	-	127	0.465	113	0.295
Nuclear HIF-2α	OS	-	-	148	0.760	173	0.237
Cytoplasmic CAIX	OS	17	**0.001**	-	-	18	**<0.001**
Membranous CAIX	OS	17	**0.006**	-	-	30	**0.003**

Table outlining summary of different threshold values based on median, ROC curve and R analysis for each hypoxic marker.

5.3.2 Comparison of different methods for threshold optimization in ER-positive cohort

5.3.2.1 ROC curve analysis

When used in the Glasgow breast cohort, the R approach was deemed to be similar to ROC curve approach. To validate this observation, ROC curves and R methods were then compared in an ER-positive cohort. Low and high protein expression were dichotomised according to the threshold level generated by ROC using IBM SPSS, with OS as an endpoint (Figure 5.9).

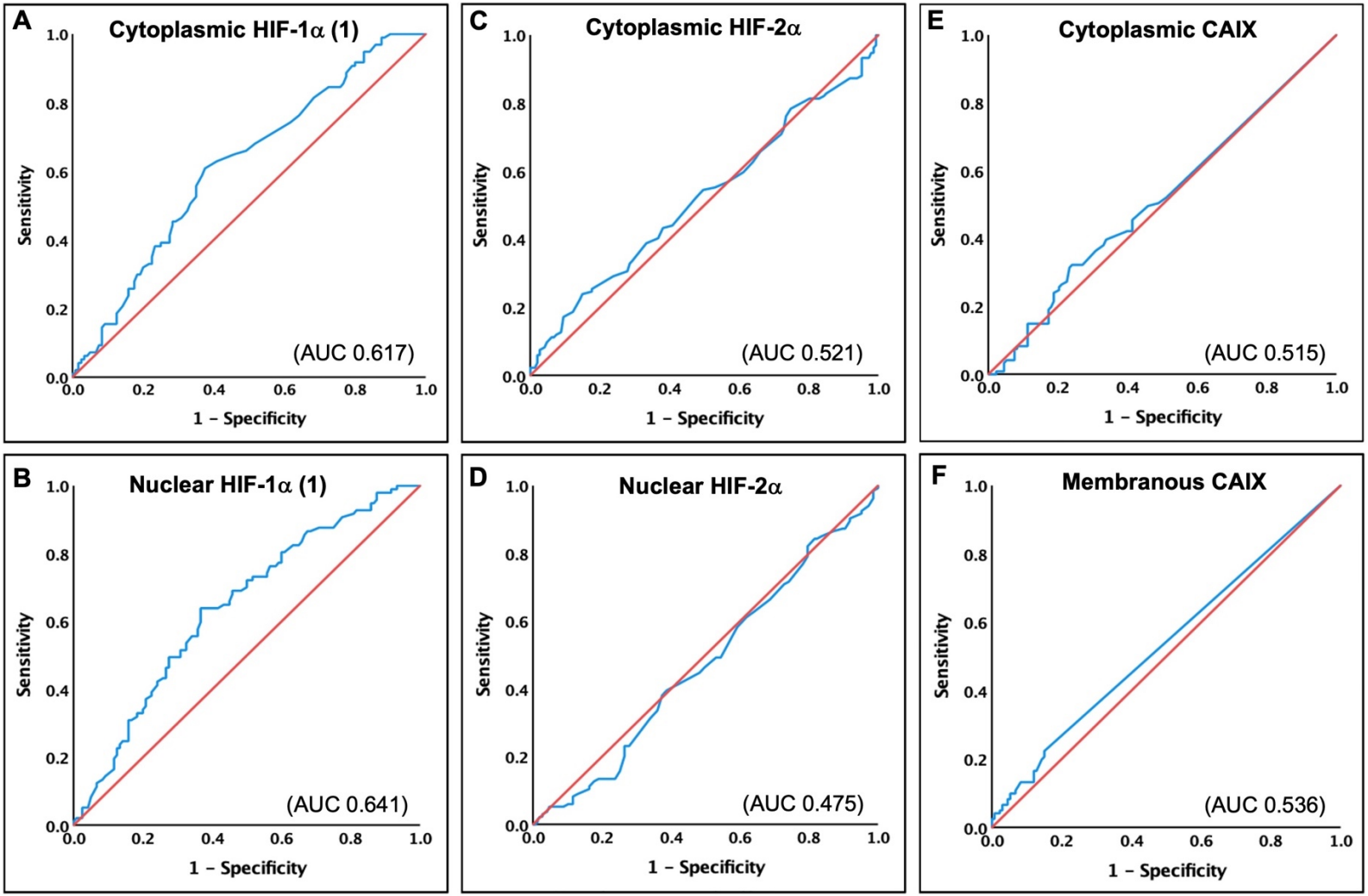

Figure 5.9 Receiver operating characteristics curves of hypoxic markers describing the threshold in ER-positive cohort.

Cytoplasmic and nuclear HIF-1α (1) [A, B], cytoplasmic and nuclear HIF-2α [C, D], and cytoplasmic and membranous CAIX [E, F].

The ROC curve threshold levels of low and high marker expression for cytoplasmic and nuclear HIF-1α (1) were 96 and 97 respectively, and for membranous CAIX was 1 (Table 5.4). However, because there was no obvious threshold value from ROC curve to dichotomize cytoplasmic and nuclear HIF-2α and cytoplasmic CAIX into two groups, low and high, the median values were chosen and were 220, 143, and 3, respectively (Table 5.4).

Table 5.4 Threshold values calculated by ROC curve analysis and median for overall survival in ER-positive cohort

Markers	Cytoplasmic		Nuclear		Membranous [ROC threshold]
	ROC threshold	Median threshold	ROC threshold	Median threshold	
HIF-1α (1)	96	-	97		-
HIF-2α	-	220	-	143	-
CAIX	-	3	-	-	1

Table outlining threshold values based on ROC curve analysis for each hypoxic marker.

5.3.2.2 R analysis

Survminer and maxstat packages in R studio were utilised to determine an optimal threshold for high and low expression of hypoxic markers according to OS (Figure 5.10).

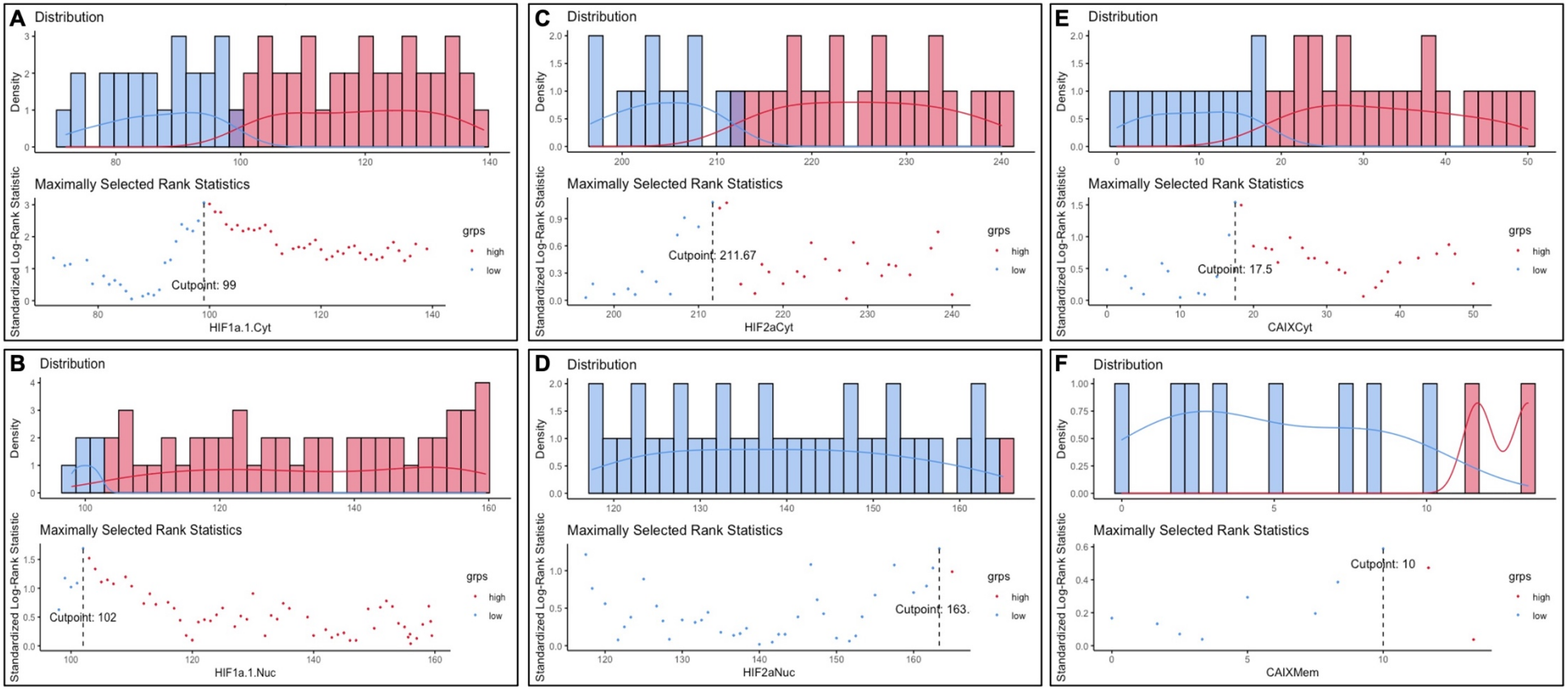

Figure 5.10 Plots showing threshold optimization using R analysis in ER-positive cohort.

Cytoplasmic and nuclear HIF-1α (1) [A, B], cytoplasmic and nuclear HIF-2α [C, D], and cytoplasmic and membranous CAIX [E, F].

Based on R, the thresholds using OS as an endpoint were 99 and 102 for cytoplasmic and nuclear HIF-1α (1), 212 and 163 for cytoplasmic and nuclear HIF-2α, and 18 and 10 for cytoplasmic and membranous CAIX, respectively (Table 5.5).

Table 5.5 Threshold values calculated by R analysis for overall survival in ER-positive cohort

Markers	Cytoplasmic	Nuclear	Membranous
HIF-1α (1)	99	102	-
HIF-2α	212	163	-
CAIX	18	-	10

Table outlining threshold values based on R analysis for each hypoxic marker.

5.3.2.3 Kaplan-Meier analysis

5.3.2.3.1 Cytoplasmic HIF-1α (1)

Threshold values generated for both methods, ROC and R, were used for Kaplan-Meier construction for OS. 114 patients had high cytoplasmic HIF-1α (1) and 103 patients had low cytoplasmic HIF-1α (1) expression using ROC threshold. Also, using R threshold showed 108 patients with high cytoplasmic HIF-1α (1) and 109 patients had low cytoplasmic HIF-1α (1). ROC and R analysis showed the same mean survival of 107 months for high cytoplasmic HIF-1α (1) patients and 171 mean survival for low cytoplasmic HIF-1α (1), with a P-value of 0.002 (Figure 5.11A, B; Table 5.6).

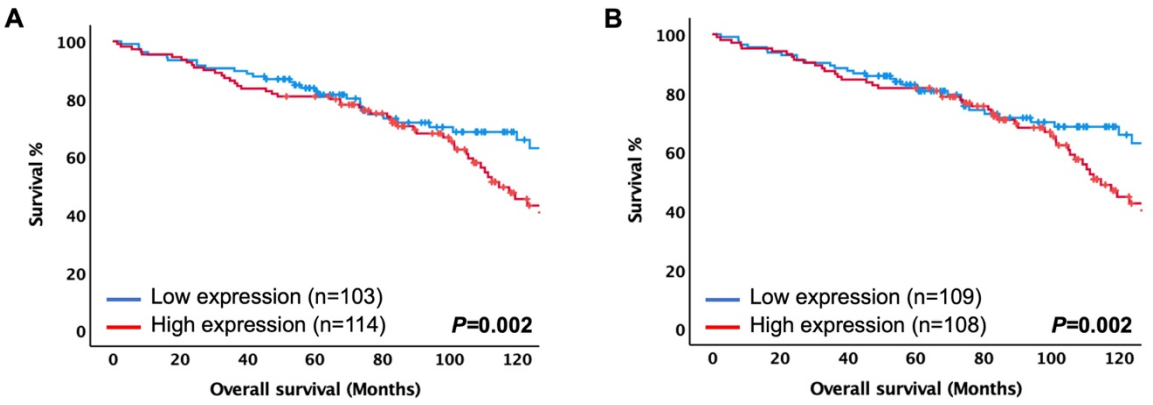

Figure 5.11 Comparison of Kaplan-Meier survival curves (log-rank) for overall survival of cytoplasmic HIF-1α (1) expression in ER-positive cohort according to different threshold values.

OS according to ROC threshold value [A], and OS according to R threshold value [B].

5.3.2.3.2 Nuclear HIF-1α (1)

142 patients had high nuclear HIF-1α (1) and 75 patients had low nuclear HIF-1α (1) expression using ROC threshold. Also, using R threshold showed 138 patients with high nuclear HIF-1α (1) and 79 patients had low nuclear HIF-1α (1). ROC showed a mean survival of 109.2 months for high nuclear HIF-1α (1) patients and 172.4 mean survival for low nuclear HIF-1α (1). Similarly, using R thresholds showed a mean survival of 107.6 for high nuclear HIF-1α (1) patients and 175.9 mean survival for low nuclear HIF-1α (1). Kaplan-Meier curves showed a significant P-value with both ROC and R threshold values (P = 0.008, 0.003, respectively) (Figure 5.12A, B; Table 5.6).

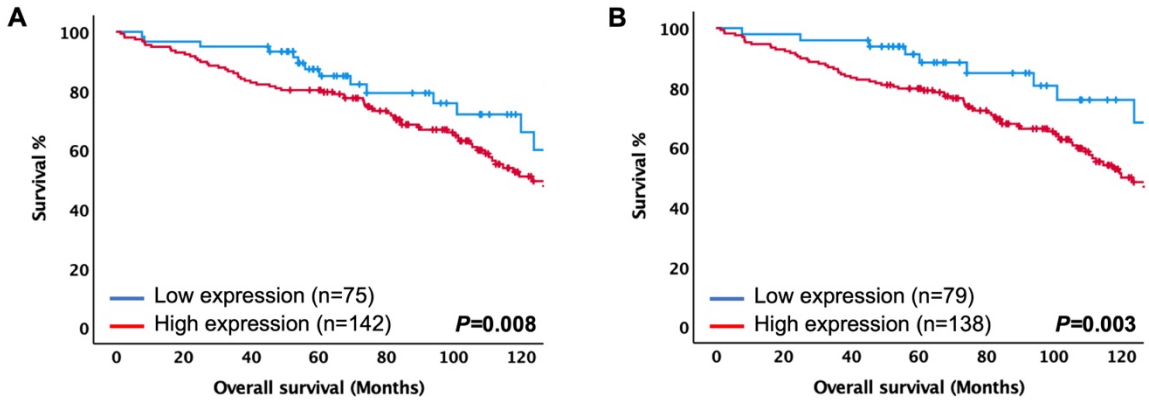

Figure 5.12 Comparison of Kaplan-Meier survival curves (log-rank) for overall survival of nuclear HIF-1α (1) expression in ER-positive cohort according to different threshold values.

OS according to ROC threshold value [A], and OS according to R threshold value [B].

5.3.2.3.3 Cytoplasmic HIF-2α

119 patients had high cytoplasmic HIF-2α and 162 had low cytoplasmic HIF-2α with using median threshold point while 178 patients were high for cytoplasmic HIF-2α and 103 were low for cytoplasmic HIF-2α using R. With a median threshold, a mean survival of 131.3 months for high cytoplasmic HIF-2α patients and 132.4 mean survival for low cytoplasmic HIF-2α. Furthermore, a mean survival of 137.7 months for high cytoplasmic HIF-2α patients and 123.5 mean survival for low cytoplasmic HIF-2α with using R threshold. Kaplan-Meier analysis using optimal threshold value generated from R method and median value showed non-significant P-value in predicting OS for cytoplasmic HIF-2α (P = 0.855, and P = 0.270, respectively) (Figure 5.13A, B; Table 5.6).

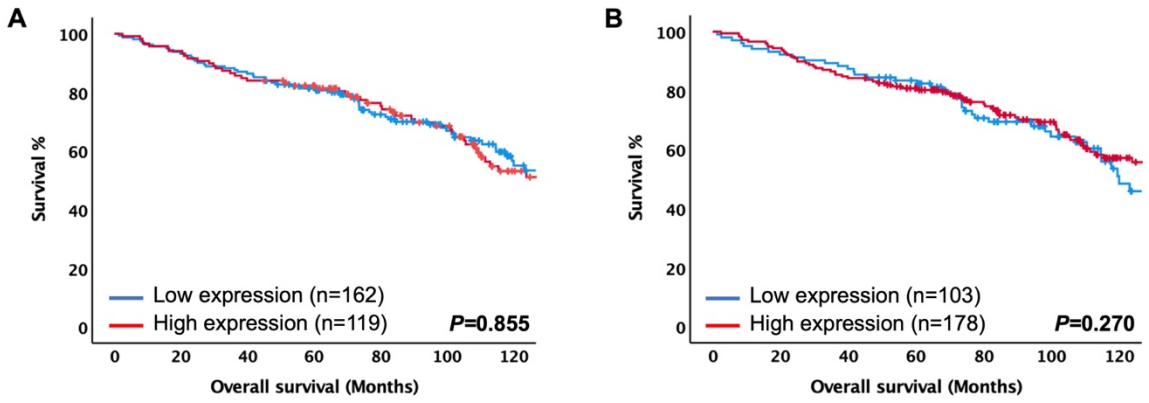

Figure 5.13 Comparison of Kaplan-Meier survival curves (log-rank) for overall survival of cytoplasmic HIF-2α expression in ER-positive cohort according to different threshold values.

OS according to median threshold value [A], and OS according to R threshold value [B].

5.3.2.3.4 Nuclear HIF-2α

Patients had high nuclear HIF-2α expression were 131, and 150 had low nuclear HIF-2α using median. In contrast, 39 patients had high nuclear HIF-2α and 242 had low nuclear HIF-2α using R. A mean survival of 138.8 months for high nuclear HIF-2α patients and 130 months for low nuclear HIF-2α was seen using median threshold values. Also, the mean survival for high and low nuclear HIF-2α using R was observed to be 155.8 and 128.7 months, respectively. Kaplan-Meier curves and the log-rank test data using median and R threshold value showed non-significant P-values (P = 0.879, P = 0.310, respectively) (Figure 5.14A, B; Table 5.6).

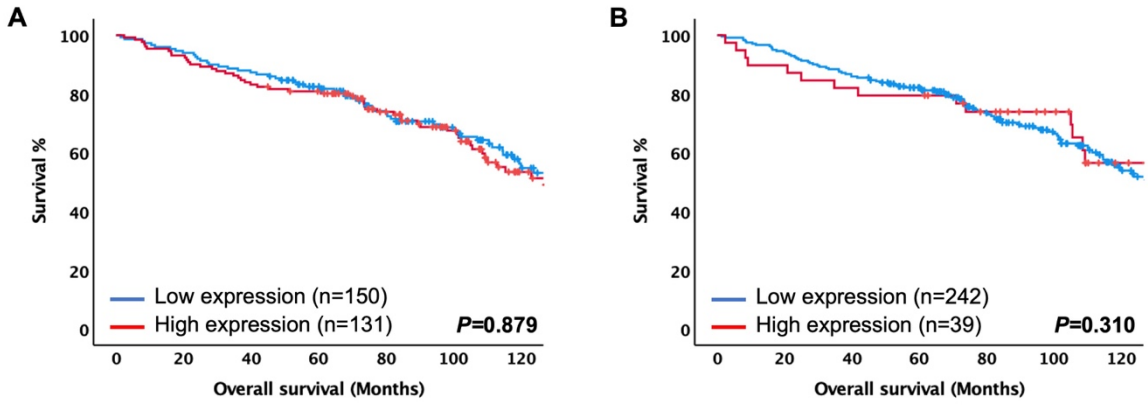

Figure 5.14 Comparison of Kaplan-Meier survival curves (log-rank) for overall survival of nuclear HIF-2α expression in ER-positive cohort according to different threshold values.

OS according to median threshold value [A], and OS according to R threshold value [B].

5.3.2.3.5 Cytoplasmic CAIX

With median threshold value optimisation, 126 patients had high cytoplasmic CAIX and 128 had low cytoplasmic CAIX while 71 patients had high cytoplasmic CAIX and 183 had low cytoplasmic CAIX using R. A median threshold value showed a mean survival of 139.8 for high cytoplasmic CAIX patients and 126.5 mean survival for low cytoplasmic CAIX. However, R analysis showed a mean survival of 121 months for high cytoplasmic CAIX patients and 137.9 mean survival for low cytoplasmic CAIX. Kaplan-Meier analysis using optimal threshold value generated from median and R methods was non-significant (P = 0.705, and P = 0.118, respectively) (Figure 5.15A, B; Table 5.6).

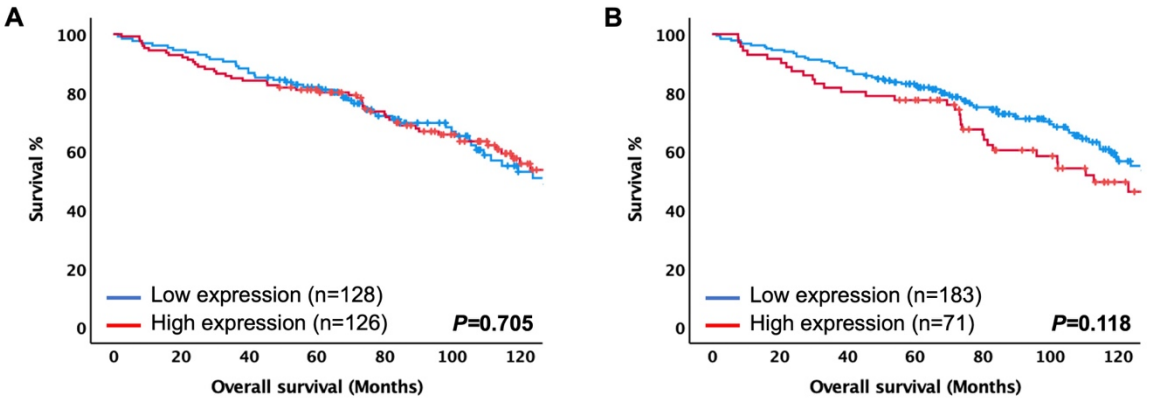

Figure 5.15 Comparison of Kaplan-Meier survival curves (log-rank) for overall survival of cytoplasmic CAIX expression in ER-positive cohort according to different threshold values.

OS according to median threshold value [A], and OS according to R threshold value [B].

5.3.2.3.6 Membranous CAIX

47 patients had high membranous CAIX and 207 had low membranous CAIX using ROC curve. Similarly, 32 patients were high for membranous CAIX and 222 were low for membranous CAIX using R. ROC showed a mean survival of 129.9 months for high membranous CAIX patients and 134 mean survival for low membranous CAIX. However, a mean survival of 146.7 for high membranous CAIX patients and 130 mean survival for low membranous CAIX with using R thresholds. Kaplan-Meier curves and the log-rank test data showed that patients with a high membranous CAIX-expressing tumour had insignificantly poorer OS with ROC curve threshold and R threshold (P = 0.872, and P = 0.573, respectively) (Figure 5.16A, B; Table 5.6).

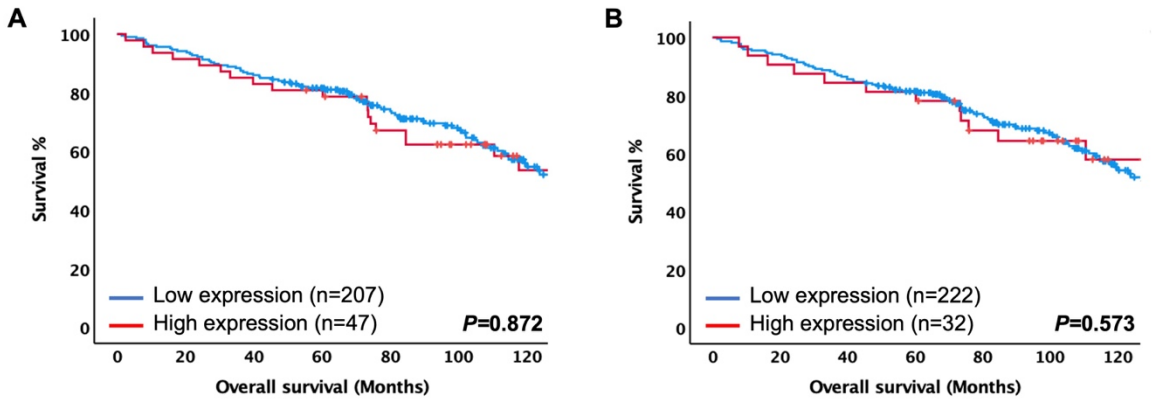

Figure 5.16 Comparison of Kaplan-Meier survival curves (log-rank) for overall survival of membranous CAIX expression in ER-positive cohort according to different threshold values.

OS according to ROC threshold value [A], and OS according to R threshold value [B].

Table 5.6 Comparison of different threshold levels and P-values in ER-positive cohort

Makers	Survival endpoint	Obtained threshold ^{ROC}	P-value ^{ROC}	Obtained threshold ^{median}	P-value ^{median}	Obtained threshold ^{R}	P-value ^{R}
Cytoplasmic HIF-1α (1)	OS	96	**0.002**	-	-	99	**0.002**
Nuclear HIF-1α (1)	OS	97	**0.008**	-	-	102	**0.003**
Cytoplasmic HIF-2α	OS	-	-	220	0.855	212	0.270
Nuclear HIF-2α	OS	-	-	143	0.879	163	0.310
Cytoplasmic CAIX	OS	-	-	3	0.705	18	0.118
Membranous CAIX	OS	1	0.872	-	-	10	0.573

Table outlining summary of different threshold values based on median, ROC curve and R analysis for each hypoxic marker.

5.4 Discussion

Data from previous systematic review chapter has highlighted that although several studies used the same antibody and a survival endpoint, different threshold levels have been applied to dichotomize patients into low and high groups based on protein expression. In the present chapter, using the same IHC approach and the same clinical endpoint, thresholds derived from two statistical approaches were similar for some antibodies and varied for others in patients with primary operable breast cancer. For example, in mixed breast cancer subtype, thresholds were similar for cytoplasmic CAIX. Additionally, there were similarities in threshold for nuclear and cytoplasmic HIF-1α (1) in ER-positive breast cancer subtype. In contrast, for some antibodies the thresholds were different between two statistical approaches such as membranous CAIX in both cohorts. The basis of such differences is not clear, however, where there is not a clear threshold, subjective approaches such as the ROC method may be more variable in determining a clinically important threshold. Mixed breast cancer subtype within Glasgow breast cohort may be contributing to poor trade-off between sensitivity and specificity.

For cytoplasmic/ nuclear HIF-1α (1) and HIF-2α in Glasgow breast cohort, and cytoplasmic/ nuclear HIF-2α, and cytoplasmic CAIX in ER-positive cohort, the values from ROC curves were unable to be used to determine optimal threshold. Therefore, the median histoscore was used as the optimal threshold. However, maybe using quartiles would have shown better effects than median.

Furthermore, although the same antibody and same statistical approach were used, there were different threshold levels between different locations such as nuclear and cytoplasmic expression of HIFs. For example, in mixed breast cancer subtype, cytoplasmic HIF-1α (1) expression was more prominent than in the nucleus. This observation was consistent with a previous report that IHC expression of HIF-1α was observed mainly in the cytoplasm with some cases exhibiting weak nucleus staining (361). The basis of this observation is of interest since active HIF-1α is thought to readily translocate from the cytoplasm to the nucleus where it upregulates the expression of several hypoxia response genes, including erythropoiesis, angiogenesis, and glucose metabolism (362, 363). Therefore, accumulation of cytoplasmic HIF-1α is not expected (191). Some authors have considered that since HIF-1α is only active when located in the nucleus and that cytoplasmic staining is of little importance (247). It should be noted that the HIF protein is synthesized and degraded in the cytoplasm and therefore, expression in this cellular location should not be ignored. Moreover, it has been

reported that there is an HIF-1α variant that is stable even in normoxia and does not translocate to the nucleus under hypoxic conditions (364). Therefore, it is relevant to examine nuclear and cytoplasmic HIF-1α separately.

HIF-1α (1) expression in the present study had different results on both cohorts, while it associated with poorer OS in ER-positive breast cancer subtype, it also correlated with improved OS in mixed breast cancer subtype. An association with strong expression of HIF-1α and adverse prognosis in breast cancer has been reported (328, 329), there are also contrary reports, including association of low HIF-1α expression and poor prognosis in breast cancer (327). An explanation is that breast cancer subtypes may be differentially affected by HIF-1α. One study has shown that HIF-1α preferentially stimulates cancer stem differentiation in ER-positive but not ER-negative breast cancer cells (365).

IHC is an indispensable research tool frequently used to study tumour progression and prognosis in breast cancer. However, the clinical utility of its findings is largely dependent on the methods used to evaluate immunoreactivity. A common problem faced by researchers and pathologists using IHC is the determination of the extent of tumour positivity for a given marker that has biological and clinical significance. The choice of scoring method, and particularly the selection of a threshold for tumour marker positivity is rarely addressed. The lack of a standardised scoring system has led to a varied range of methods among published studies (357). For example, a number of studies have used percentage expression rather than actual expression score for evaluating HIF-1α and CAIX IHC in breast cancer (265, 319, 323, 341, 366) while other studies have used scores of a combination of percentage and intensity of staining (301, 311, 312, 320, 322). Finally, in other studies threshold levels were based on the absence or presence of staining (308, 318, 334, 335, 340) or on the median staining index (346). Therefore, a number of approaches have been used to quantitate IHC staining, and few have been validated in relation to survival in patients with breast cancer.

In clinical practice, stratification of patients is often useful for risk assessment or customized treatment plans. The role of IHC biomarkers in such risk assessment and treatment plans is primarily to dichotomize patients into those with low versus high expression levels. The methods used to identify a threshold value are rarely detailed in the literature, and optimal threshold values are often chosen using a subjective approach, sometimes selected strategically to minimize the P-value and thus improve the statistical significance (367, 368). The present comparison of approaches to determine the thresholds in two IHC methods shows the utility of subjective and objective (non-bias) approaches (ROC and R methods,

respectively). Both these methods gave comparable results and therefore would suggest that the R method being the more objective, and it is the preferred approach for the IHC methods examined in the present chapter (R software, The R V.4.0.3, 2020).

The present chapter given that it is a reliable objective approach to determine IHC hypoxia product expression thresholds related to survival, the use of R analysis is recommended in future studies. Therefore, the next IHC chapters of this thesis will go on using threshold based on R analysis.

Chapter 6 The role of hypoxic markers in predicting survival in patients with primary operable ductal breast cancer

6.1 Introduction

Tumour hypoxia is one of TME factors that has been linked to aggressive phenotypes in several cancer types, including breast cancer (212, 369). Numerous studies have demonstrated that intratumoural hypoxia leading to tumour progression and metastasis mediated by a family of HIFs (370, 371). Hypoxic conditions lead to HIF-1α stabilization. Once stabilized, HIF-1α translocate to the nucleus where it upregulates the expression of several hypoxia response genes, including erythropoiesis, angiogenesis, glucose metabolism, and pH regulation (363, 372). HIF-1α is a master transcription factor produced by most solid tumours when are diminished of oxygen supply (206), and it plays an essential role in oxygen homeostasis that mediates cellular response to hypoxia (373). There are strong suggestions that HIF-1α may play a vital role in the pathogenesis of breast cancer, and its overexpression is significantly associated with an adverse clinical outcome in breast cancer patients (357). Therefore, HIF-1α may have important therapeutic potential, and its inhibitors, such as echinomycin, have been clinically attempted (374). However, HIF-1α expression is transient and therefore difficult to assess through routine techniques such as IHC.

Overexpression of HIF-2α is strongly correlated with poorer OS (375), RFS and CSS (256) of patients with breast cancer.

CAIX, gene that is up-regulated by HIF-1α (257). It is a pH regulation enzyme that enhances metastasis by stimulating the acidification in the TME. It regulates pH by reversible hydration of carbonic dioxide to carbonic acid ($CO_2 + H_2O = HCO_3^- + H^+$). The extracellular HCO_3^- generated by CAIX is transferred into the cytosol where it maintains a slightly alkaline intracellular pH, while protons remain at the cell surface lowering extracellular pH (232), thereby potentiating extracellular matrix breakdown and cell invasion (376). Therefore, CAIX might increase metastatic potential by allowing aggressive cancer cells to survive the hostile environment imposed by hypoxia, and may further function to potentiate extracellular acidosis, facilitating growth and invasion of surviving tumour cells (377). Indeed, CAIX is very stable protein of about 38 hours half-life so easier to measure through techniques such as IHC, it is perhaps not surprising that there would appear to be a more consistent association with poor clinical outcome compared with HIF-1α. CAIX is a marker for hypoxic regions of breast cancers (353), an indicator of poor patient prognosis, associated with ER-negative (260, 263), and ER-positive tumour tissue (249), and contributes to the growth advantage of cancer cells (308, 378, 379).

Traditionally, pathological determination of the tumour size, tumour grade, lymph node involvement, ER, PR and Her-2 status have driven prognostic predictions for patients with breast cancer. However, hypoxic markers are not recognized as a prognostic factor for breast cancer. Therefore, the aim of the current chapter was to investigate the association between hypoxic markers expressions (HIF-1α (1), HIF-2α, and CAIX) with respect to various clinical and pathological features and survival in 850 paraffin-embedded archival tissue block specimens from breast cancer patients.

6.2 Material and methods

6.2.1 Patient cohort

For this study, Glasgow breast cohort was used with characteristics as described in chapter 2. In all, 850 female patients with invasive breast cancer operated on at Royal Infirmary, Western Infirmary, and Stobhill Hospital, Glasgow, in the period from 1995 to 1998 were included in this study. Selection criteria of specimens having ductal histological subtype (n = 736) and HIF-1α (2) expression available for analysis (n = 575) were applied, resulting in the exclusion of 275 patients.

The follow up for the selected patients ranged from 1−181 months with a median follow up time was 149 months (range 67.94−165 months). There were 309 patients alive at the last follow up, and median follow up was 164 months (range 153−171 months). Clinicopathological data including patient's age, tumour size, grade, lymph node status, PR status, Her-2 status, and Ki67 was available.

6.2.2 TMA slide staining and scanning

Previously constructed TMAs were employed, that had three 0.6 mm cores per tumour block/patient to combat tumour heterogeneity. IHC was performed and resulting stained slides scanned using Hamamatsu slide scanner and visualised using NDP serve 3 image viewer platform system as described in chapter 2.

6.2.3 Scoring of hypoxic markers

Tumour cell expression of HIF-1α (2), HIF-2α, and CAIX was assessed using the weighted Histoscore method while HIF-1α (1) was scored digitally on QuPath digital pathology software v0.2.3 (QuPath, Edinburgh, UK) by a single observer (S.S) blinded to the clinical

data as previously described in chapter 2. To ensure reproducibility of scoring, 10% of cores for each marker was co-scored manually by a second observer (J.E) blinded to the previous observer score as well as patient clinical and survival data. Reliability analysis was performed with SPSS software to ensure consistency and objectivity between the main scorer and the co-scorers giving an ICCC for all markers. Values above 0.75 are indicative of good reliability.

Manual interpretation of IHC can be subjective if accessors are not adequately trained and may produce conflicting results among studies, automated digital image analysis of IHC could serve as an alternative method in presenting reproducible, objective, and quantitative measurements for labs without pathologists available to train. In the current study we work closely with pathologists to train and ensure scoring is accurate, but we also employed QuPath for one marker to ensure we could also have reproducibility using digital pathology platforms.

6.2.4 Statistical analysis

To set threshold values for categorizing the expression of each protein into low and high groups, survminer and maxstat packages in R studio were used based on OS as described in chapter 5. Analysis of associations with clinicopathological characteristics and with survival outcomes was carried out as described in chapter 2.

6.3 Result

6.3.1 Clinicopathological characteristics of invasive ductal carcinoma

Of the total number of cases (n = 850), patients with invasive ductal breast cancer and having HIF-1α (2) expression available (n = 575) were selected for analysis. Table 6.1 shows clinicopathological characteristics of selected patients. The majority of patients (70%) were over 50 years of age, had small tumours ≤20mm (56%), grade II (41%) or grade III (43%), and negative lymph node (56%). A total of 575, 373 (65%) had ER-positive tumours and 315 (55%) patients had PR-negative tumours. 464 (81%) patients had Her-2 negative tumours. 334 (75%) patients received adjuvant tamoxifen, 245 (43%) received adjuvant chemotherapy, and 288 (50%) received adjuvant radiotherapy while only 151 (26%) patients received both adjuvant chemotherapy radiotherapy. 131 (23%) patients experienced

recurrences. Of these patients, 34 (6%) had local recurrence, 91 (16%) had distant recurrence and 6 patients had both.

Table 6.1 The clinicopathological characteristics of patients with primary operable invasive ductal carcinoma (n = 575)

Clinicopathological characteristics	Patients, n (%)
Age (≤50/>50 years)	175(30)/400(70)
Size (≤20/21–50/>50 mm)	324(56)/224(39)/26(5)
Grade (I/II/III)	92(16)/233(41)/250(43)
Lymph node (negative/positive)	321(56)/248(44)
ER status (negative/positive)	202(35)/373(65)
PR status (negative/positive)	315(55)/260(45)
Her-2 status (negative/positive)	464(81)/106(19)
Ki67 (proliferative index) (low/high)	379(69)/174(31)
Molecular subtype (lum A/lum B/TNBC/Her-2)	238(43)/130(23)/130(23)/62(11)
Adjuvant endocrine therapy (no/yes/ATAC trial)	100(22)/334(75)/14(3)
Adjuvant chemotherapy (no/yes)	328(57)/245(43)
Adjuvant radiotherapy (no/yes)	285(50)/288(50)
Combined adjuvant chemotherapy and radiotherapy (no/yes)	422(74)/151(26)
Alive/cancer death/non-cancer death	309(55)/129(23)/125(22)
No recurrence/local/distant/both	428(77)/34(6)/91(16)/6(1)

Table showing the number of patients with clinical characteristics and survival outcomes in patients from the Glasgow breast cohort including age, tumour size, grade, lymph node, ER, PR, Her-2 status, Ki67, molecular subtype, adjuvant endocrine therapy, adjuvant chemotherapy and adjuvant radiotherapy.

6.3.2 Expression of HIF-1α (1)

6.3.2.1 Immunohistochemistry of HIF-1α (1)

Expression of HIF-1α (1) was assessed in 470 patients from 575 patients. Positive staining of HIF-1α (1) was observed mainly in epithelial tumour cells, and occasionally in infiltrating lymphocytes and fibroblasts. HIF-1α (1) was clearly expressed in the nuclei and cytoplasm of tumour cells. Representative images of cytoplasmic and nuclear HIF-1α (1) staining which was performed using QuPath digital image analysis software, are shown in Figure 6.1A. Cytoplasmic HIF-1α (1) scores ranged from 0 to 167.75 with a mean score of 92.32, and nuclear scores ranging from 0 to 205.55 with a mean score of 106.51. A histogram was plotted to visualise the range of scores and data were relatively normally distributed (Figure 6.1B). An ICCC of 0.842 and 0.898 for cytoplasmic and nuclear HIF-1α (1), respectively was obtained between QuPath and manual scores and data were visualised in the form of a scatter plot and a Bland Altman plot (Figure 6.1C). Threshold values for high and low expression were determined using R Studio packages as described in chapter 5. The optimal threshold determined was 104 and 156 for cytoplasmic and nuclear HIF-1α (1) expression, respectively. Based on R threshold levels, low cytoplasmic HIF-1α (1) expression was detected in 361 (77%) samples, while 109 (23%) samples had high cytoplasmic expression. 416 (89%) patients showed low nuclear HIF-1α (1) expression, and 54 (11%) showed high nuclear expression (Table 6.2).

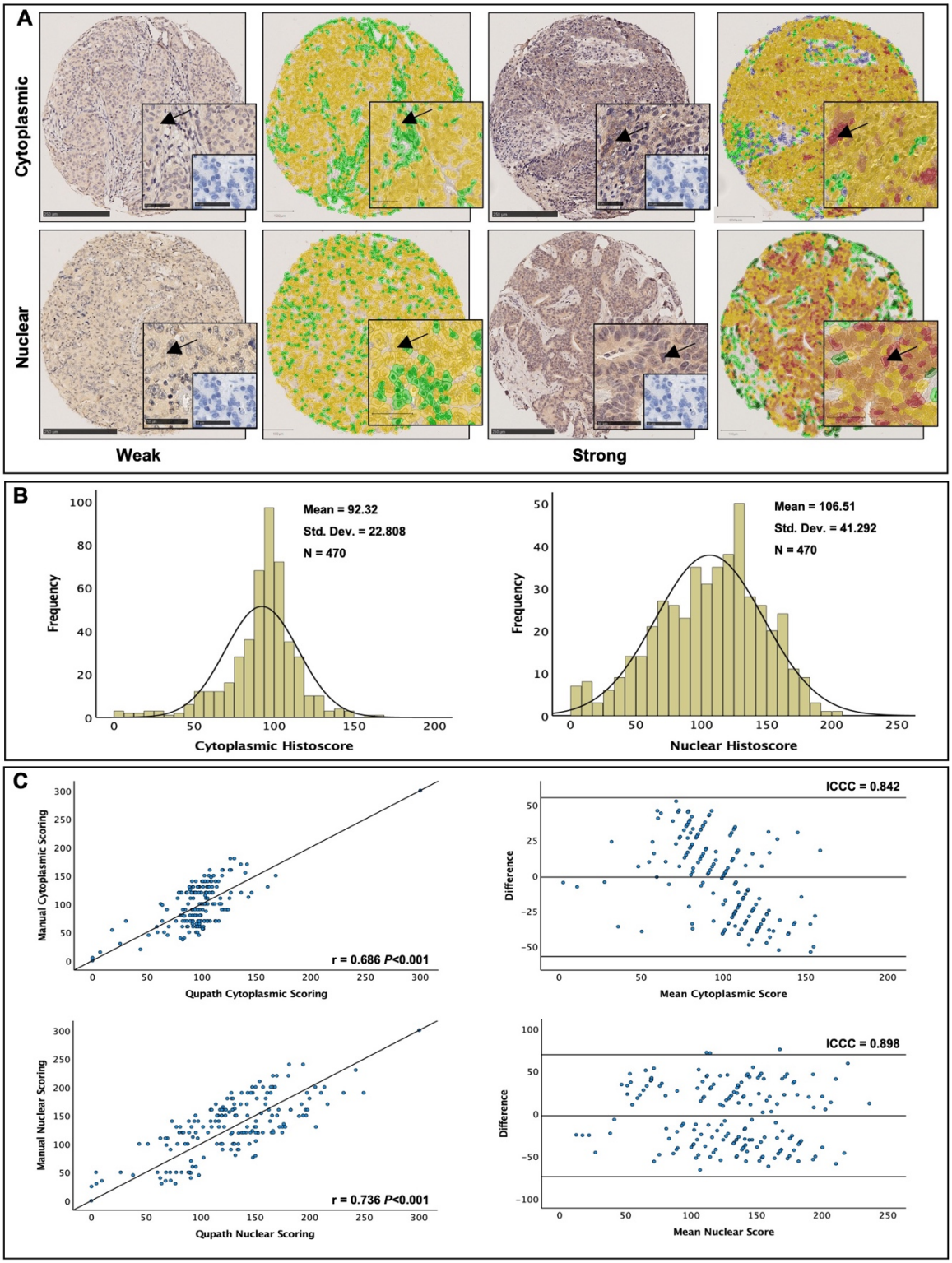

Figure 6.1 Representative immunohistochemical images and scoring distribution for HIF-1α (1).

Representative images of weak and strong cytoplasmic and nuclear staining of HIF-1α (1) within tumour cells with positive cell detection image using QuPath digital platform [A]. Representative images of histogram showing the range of scores obtained for cytoplasmic and nuclear tumour HIF-1α (1) expression and distribution pattern of data [B]. Left: Scatter plot showing correlation between tumour weighted Histoscores, and right: Bland Altman plot showing difference between QuPath and manual scores for HIF-1α (1) in tumour cytoplasm and nucleus [C].

Table 6.2 Hypoxic markers expression in Glasgow breast cohort patients (n = 575)

Markers	Cytoplasmic n (%)	Membrane/Nuclear n (%)	Missing cases n (%)
HIF-1α (1)			
Low	361 (77)	416 (89)	105 (18)
High	109 (23)	54 (11)	
HIF-2α			
Low	169 (33)	319 (62)	56 (10)
High	350 (67)	200 (38)	
CAIX			
Low	442 (83)	450 (84)	42 (7)
High	91 (17)	83 (16)	

Table showing the number of patients and the percentage for each hypoxic marker selected for analysis in Glasgow breast cohort.

6.3.2.2 Association of HIF-1α (1) with clinical outcome in Glasgow breast cohort

To determine whether HIF-1α (1) expression was associated with clinical outcome, Kaplan-Meier survival curves for cytoplasmic and nuclear expression of HIF-1α (1) were plotted. The log-rank test was performed for comparisons between the survival curves. Patients with low immunostaining for cytoplasmic HIF-1α (1) had significantly poorer OS (P = 0.031) as compared with those who had a high expression but low levels of nuclear HIF-1α (1) showed a marginal association with decreased OS (P = 0.053) (Figure 6.2E, F). However, neither cytoplasmic nor nuclear HIF-1α (1) was associated with RFS (P = 0.652, P = 0.885), or DFS (P = 0.126, P = 0.227), respectively (Figure 6.2A-D). Based on text life table analysis, the 10-year OS was 47% for low cytoplasmic HIF-1α (1) expression versus 66% for high protein expression (P = 0.104) (Table 6.3).

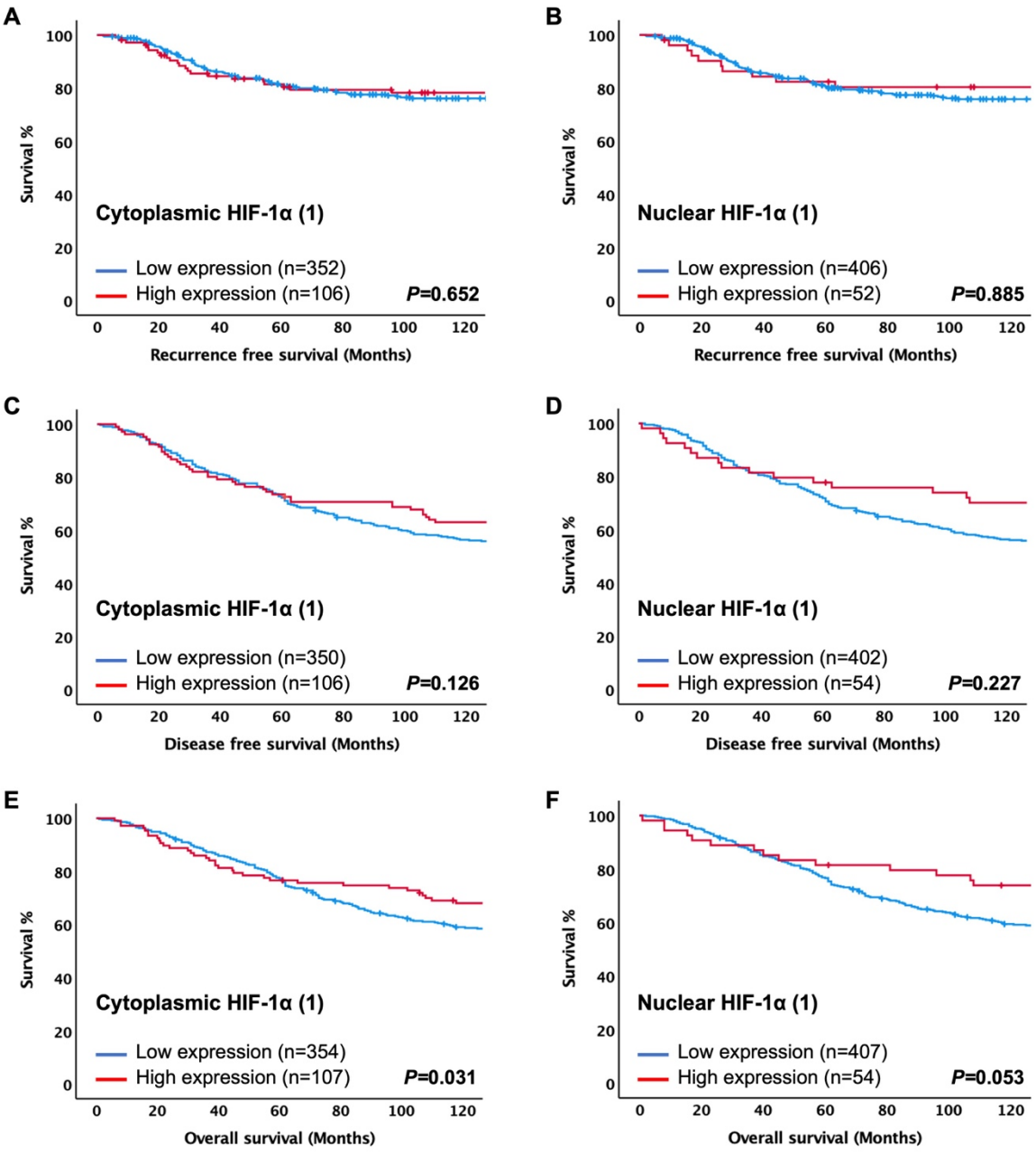

Figure 6.2 Expression of HIF-1α (1) and clinical outcome in Glasgow breast cohort.

Kaplan-Meier curves showing associations between cytoplasmic and nuclear HIF-1α (1) with recurrence free survival [A, B], disease-free survival [C, D], and overall survival [E, F].

6.3.2.3 Association of HIF-1α (1) and clinical outcome in different breast cancer subtypes

Expression of cytoplasmic HIF-1α (1) was assessed by Kaplan-Meier method and compared by log-rank test in different breast cancer subtypes. High cytoplasmic HIF-1α (1) levels showed an association with poorer OS in luminal A disease (P = 0.009), however, no association was found in luminal B disease (P = 0.890), TNBC (P = 0.773) and Her-2 disease (P = 0.386) (Figure 6.3).

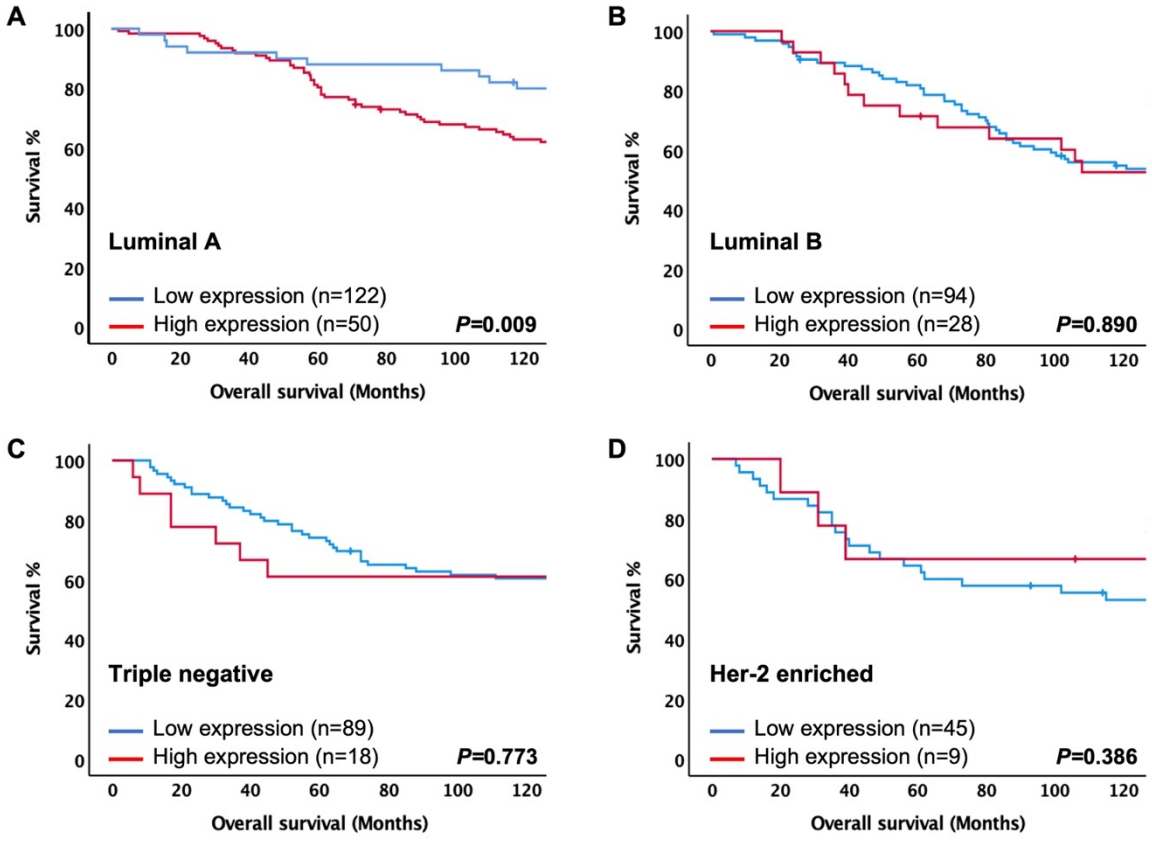

Figure 6.3 Expression of cytoplasmic HIF-1α (1) and overall survival in different breast cancer subtypes.

Kaplan-Meier curves showing associations between cytoplasmic HIF-1α (1) and overall survival in luminal A disease [A], luminal B disease [B], triple negative [C], and Her-2 enriched [D].

6.3.3 Expression of HIF-1α (2)

6.3.3.1 Immunohistochemistry of HIF-1α (2)

Expression of HIF-1α (2) was assessed in 575 patients. Immunoreactivity of HIF-1α (2) proteins was distributed in both nuclei and cytoplasm of tumour cells (Figure 6.4A). Histograms showing relatively normally distributed pattern of cytoplasmic HIF-1α (2) scores, the mean score was 159.71 and scores ranged from 0 to 245. A histogram plot was constructed to visualise the distribution pattern of nuclear HIF-1α (2) scores which was positively skewed, the mean score was 52.80 with a range of 0 to 220 (Figure 6.4B). An ICCC values of 0.885 and 0.942 for cytoplasmic and nuclear HIF-1α (2), respectively was obtained between both observer scores and data were visualised in the form of a scatter plot and a Bland Altman plot (Figure 6.4C).

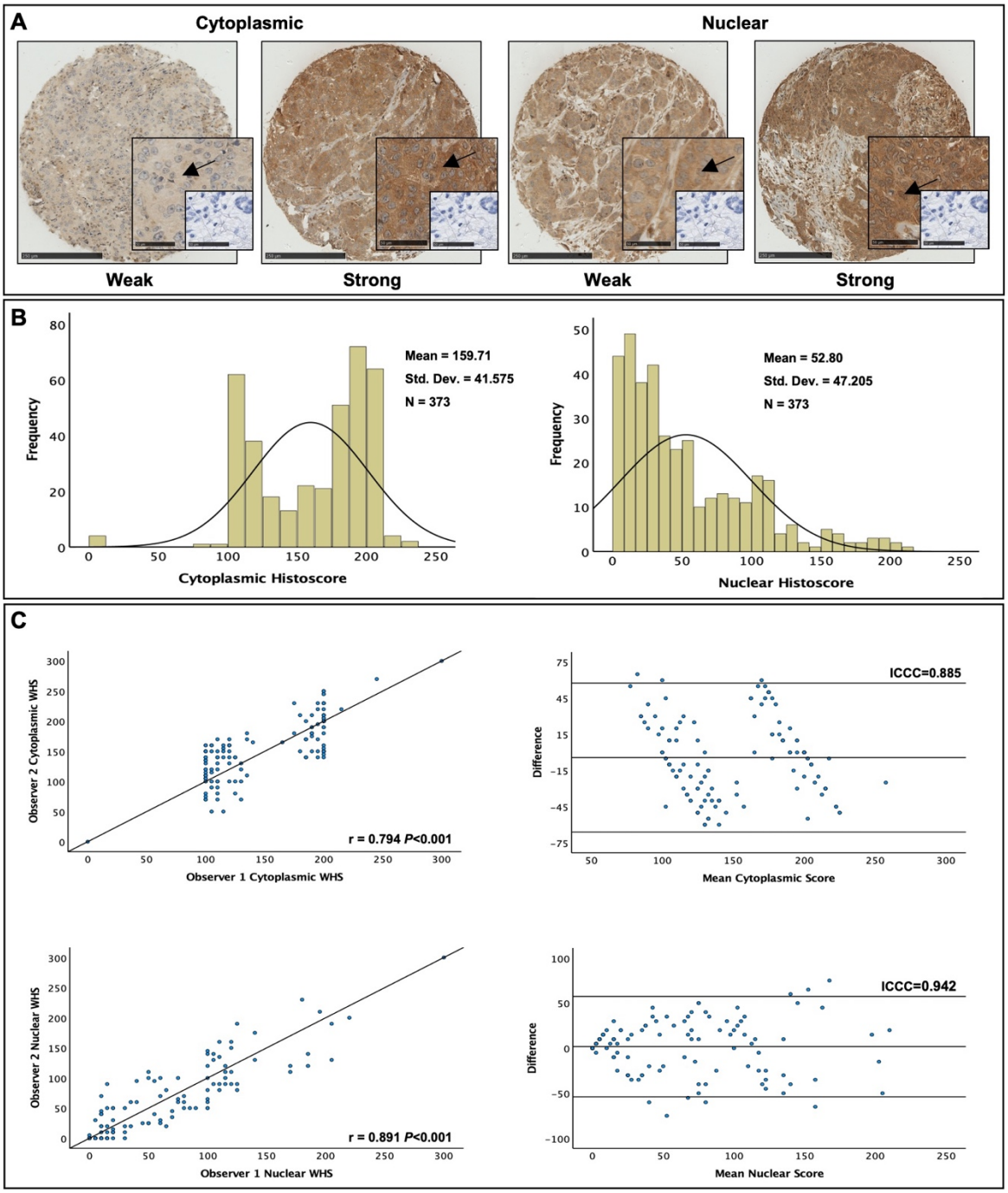

Figure 6.4 Representative immunohistochemical images and scoring distribution for HIF-1α (2).

Representative images of weak and strong cytoplasmic and nuclear staining of HIF-1α (2) [A]. Representative images of histogram showing the range of scores obtained for cytoplasmic and nuclear tumour HIF-1α (2) expression and distribution pattern of data [B]. Left: Scatter plot showing correlation between tumour weighted Histoscores, and right: Bland Altman plot showing difference between manual scores for HIF-1α (2) in tumour cytoplasm and nucleus [C].

6.3.4 Expression of HIF-2α

6.3.4.1 Immunohistochemistry of HIF-2α

Expression of HIF-2α in tumour cell was scored in in 519 patients from 575 patients. Nuclear and cytoplasmic staining was detected in tumour cells with HIF-2α expression. Representative profiles of immunostainings of cytoplasmic and nuclear HIF-2α with examples of weak and strong staining can be seen in Figure 6.5A. Histograms showing the distribution of histoscores for cytoplasmic HIF-2α ranged from 0 to 235 with a mean score of 142.54 for nuclear ranged from 0 to 295 with a mean score of 153.15 and data were relatively normally distributed as shown in histogram plot (Figure 6.5B). An ICCC values of 0.884 and 0.867 for cytoplasmic and nuclear, respectively was obtained between both observers scores and data were visualised in the form of a scatter plot and a Bland Altman plot (Figure 6.5C). R Studio was used to determine an optimal threshold. The optimal threshold determined was 113 and 173 for cytoplasmic and nuclear HIF-2α expression, respectively. Immunoreactive low cytoplasmic HIF-2α was observed in 169 (33%), and high cytoplasmic HIF-2α in 350 (67%). Whereas low nuclear expression was seen in 319 (62%), high nuclear expression was detected in 200 (38%) (Table 6.2).

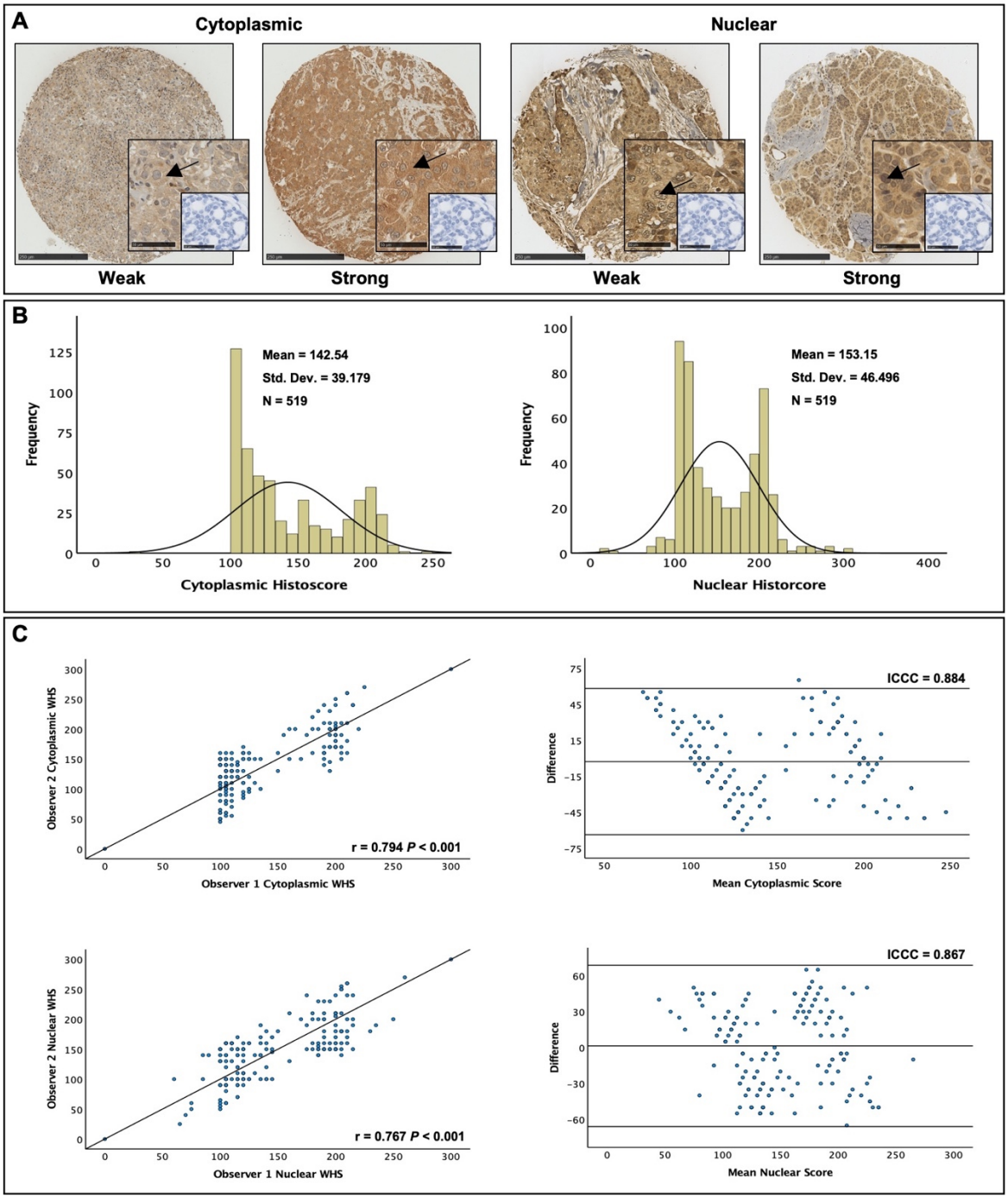

Figure 6.5 Representative immunohistochemical images and scoring distribution for HIF-2α.

Representative images of weak and strong cytoplasmic and nuclear staining of HIF-2α [A]. Representative images of histogram showing the range of scores obtained for cytoplasmic and nuclear tumour HIF-2α expression and distribution pattern of data [B]. Left: Scatter plot showing correlation between tumour weighted Histoscores, and right: Bland Altman plot showing difference between manual scores for HIF-2α in tumour cytoplasm and nucleus [C].

6.3.4.2 Association of HIF-2α with clinical outcome in invasive ductal carcinoma

Clinical outcomes for cytoplasmic and nuclear HIF-2α expression were estimated using Kaplan-Meier analysis and compared between groups with the log-rank test as shown in Figure 6.6A-F. The log-rank test was used to compare low and high protein expression. Patients with a high cytoplasmic HIF-2α expression were observed to have worse RFS as compared with those who had a low expression (P = 0.022). However, no association was detected with DFS and OS (P = 0.174, 0.295, respectively). In contrast, overexpression of nuclear HIF-2α was not associated with RFS (P = 0.320), DFS (P = 0.433), or OS (P = 0.237). Based on text life table analysis, the 10-year RFS was reduced from 81% for low to 70% for high cytoplasmic HIF-2α expression (P = 0.037) (Table 6.3).

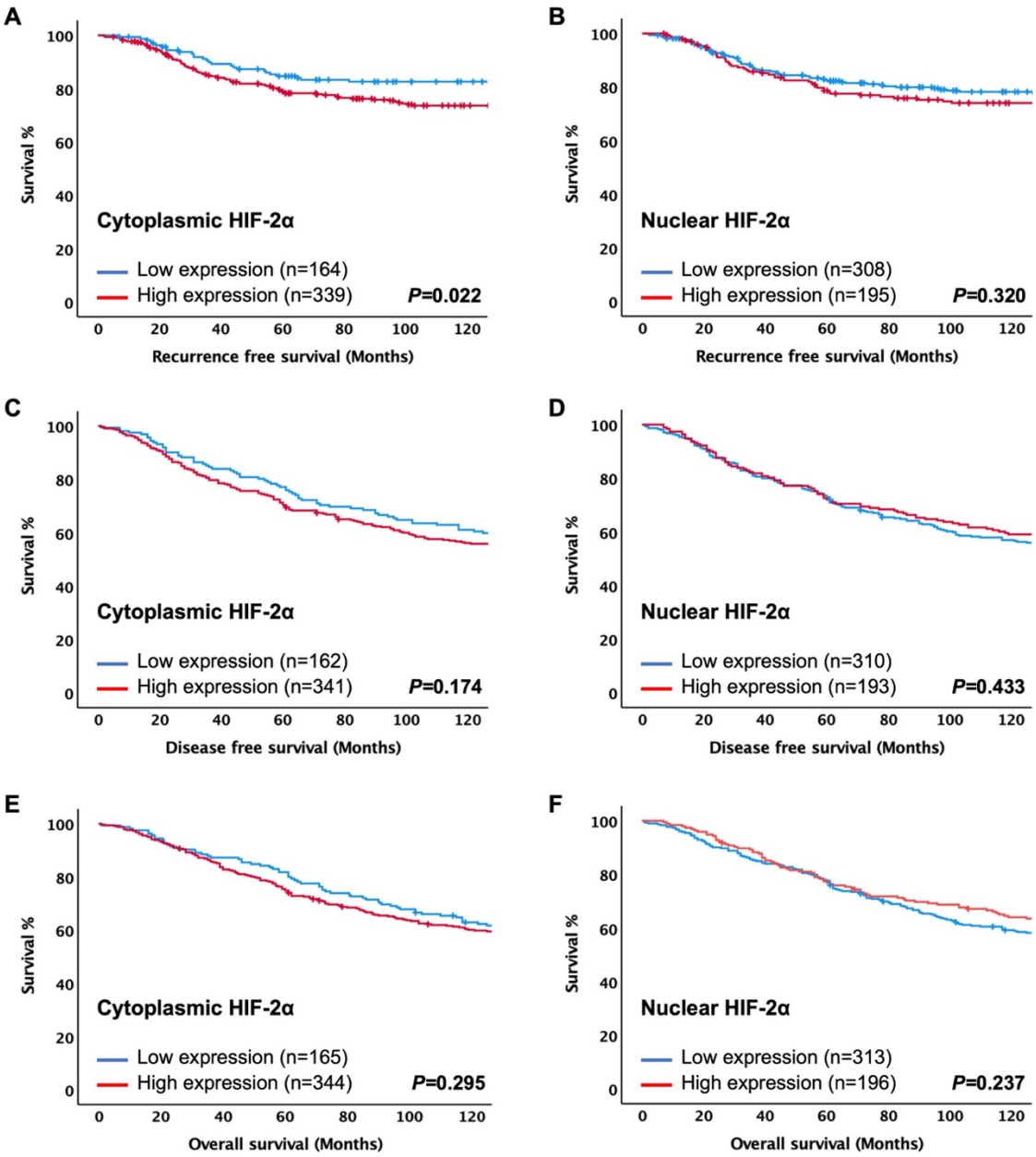

Figure 6.6 Expression of HIF-2α and clinical outcome in Glasgow breast cohort.

Kaplan-Meier curves showing associations between cytoplasmic and nuclear HIF-2α with recurrence free survival [A, B], disease-free survival [C, D], and overall survival [E, F].

6.3.4.3 Association of HIF-2α and clinical outcome in different breast cancer subtypes

Association between expression of cytoplasmic HIF-2α and clinical outcome was assessed in four breast cancer subtypes (Figure 6.7). Cytoplasmic expression of HIF-2α was associated with RFS in Her-2 disease (P = 0.038). Furthermore, a trend toward significance was observed between decreased RFS in tumours with high expression of cytoplasmic HIF-2α in TNBC (P = 0.055). No association was observed between cytoplasmic HIF-2α expression and RFS in luminal A (P = 0.376), and luminal B (P = 0.199).

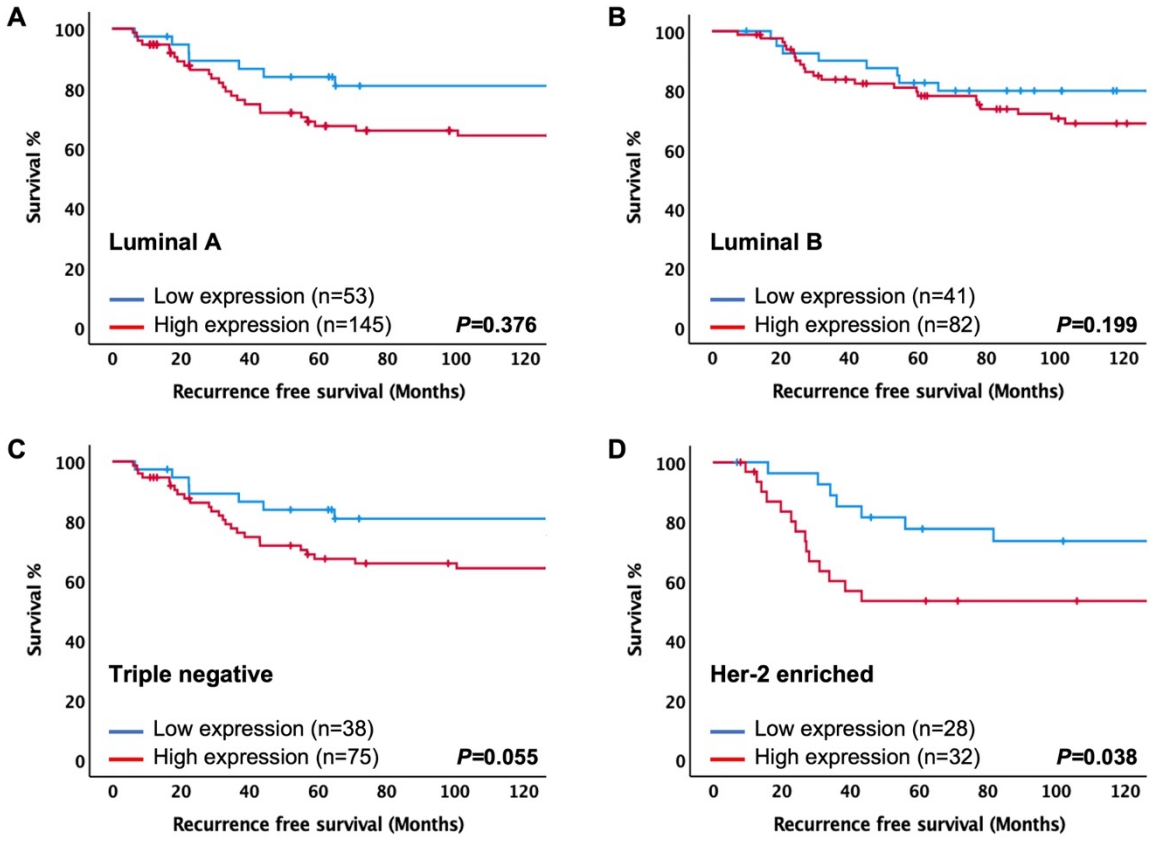

Figure 6.7 Expression of cytoplasmic HIF-2α and recurrence free survival in different breast cancer subtypes.

Kaplan-Meier curves showing associations between cytoplasmic HIF-2α and recurrence free survival in luminal A disease [A], luminal B disease [B], triple negative [C], and Her-2 enriched [D].

6.3.5 Expression of CAIX

6.3.5.1 Immunohistochemistry of CAIX

The expression of CAIX was analyse in 533 (93%) patients. Cytoplasmic and membranous staining was detected in tumour cells with CAIX expression. Representative profiles of immunostainings can be seen in Figure 6.8A. Weighted Histoscores for cytoplasmic expression ranged from 0 to 245 with a mean score of 12.16, and for membranous scores ranged from 0 to 290 with a mean score of 15.26. A histogram was plotted to visualise the range of scores and data showed a positively skewed pattern (Figure 6.8B). There was good correlation between observers with ICCC score of 0.986 for cytoplasmic and 0.987 for membranous expression. Validation was visualised by plotting a scatterplot, and a Bland Altman plot (Figure 6.8C). R studio was utilised to determine an optimal threshold for cytoplasmic CAIX (18) and membranous CAIX expression (30). Based on R threshold, low cytoplasmic CAIX expression of malignant cell was observed in 442 (83%) and high cytoplasmic protein was 91 (17%). Low membranous CAIX expression was detected in 450 (84%), and only 83 patients (16%) with high protein expression (Table 6.2).

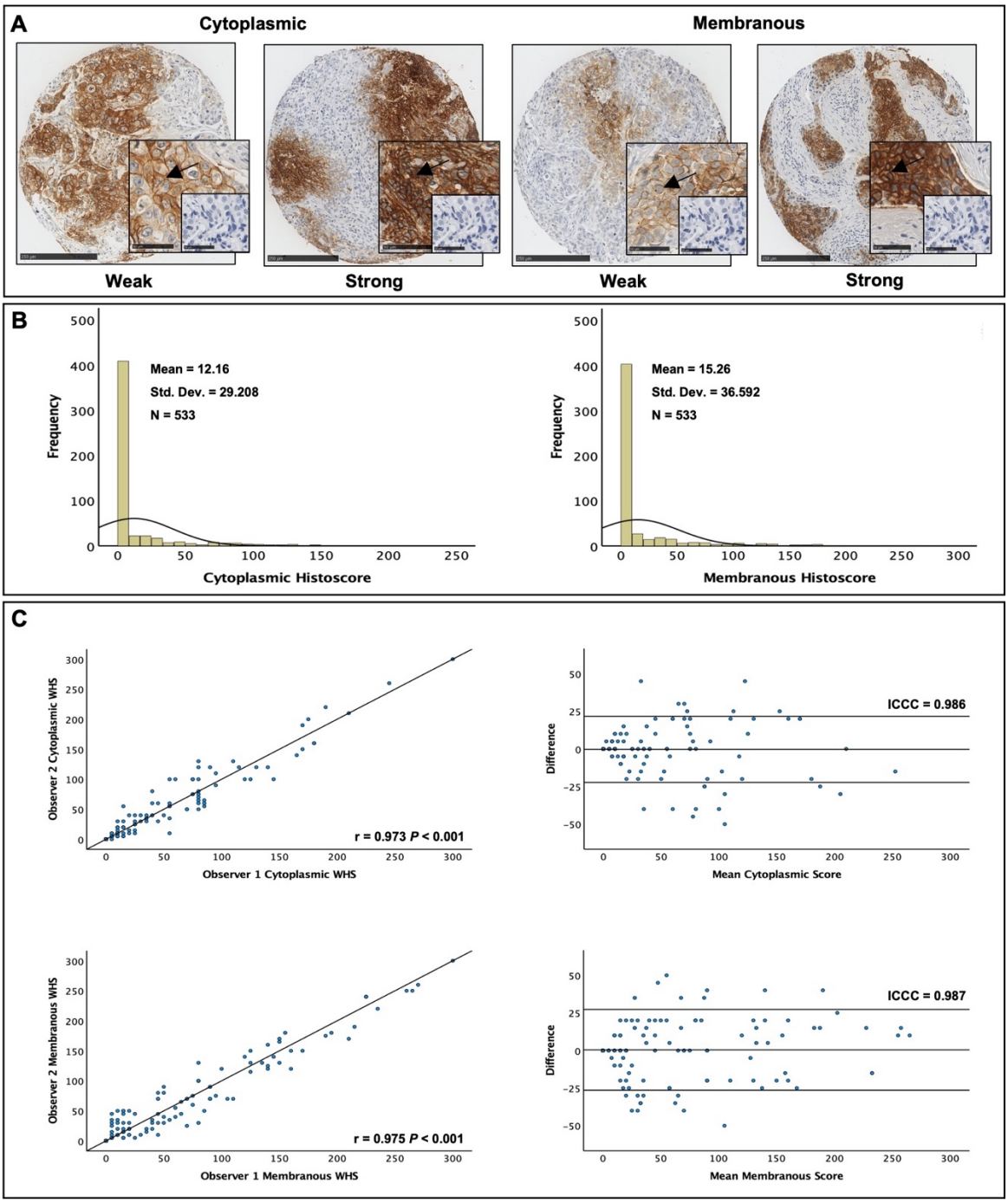

Figure 6.8 Representative immunohistochemical images and scoring distribution for CAIX.

Representative images of weak and strong cytoplasmic and membranous staining of CAIX [A]. Representative images of histogram showing the range of scores obtained for cytoplasmic and membranous tumour CAIX expression and distribution pattern of data [B]. Left: Scatter plot showing correlation between tumour weighted Histoscores, and right: Bland Altman plot showing difference between manual scores for CAIX in tumour cytoplasm and membrane [C].

6.3.5.2 Association of CAIX with clinical outcome in an invasive ductal carcinoma

Kaplan-Meier survival curves for cytoplasmic and membranous expression of CAIX were plotted as shown in Figure 6.9. The log-rank test was used to compare low and high expression. Regardless of cellular localisation, high CAIX expression was consistently associated with poorer outcome in term of RFS, DFS and OS. High cytoplasmic expression of CAIX was significantly associated with worse RFS (P<0.001), DFS (P<0.001), and OS (P<0.001). Similarly, high membranous CAIX expression was associated with decrease RFS (P<0.001), DFS (P = 0.004), and OS (P = 0.003) (Figure 6.9A-F).

As shown in Table 6.3 based on text life table analysis, the 10-year RFS of patients with high cytoplasmic CAIX expression was 58% versus 78% of patients with low cytoplasmic CAIX expression (P<0.001), and the 10-year RFS of patients with membranous CAIX expression was reduced from 77% (low) to 61% (high) (P<0.001). The 10-year DFS was reduced from 53% with low cytoplasmic expression to 31% with high cytoplasmic expression (P<0.001), and the 10-year DFS was decreased from 51% with low membranous expression to 35% with high expression (P = 0.003). The 10-year OS of patients with high cytoplasmic CAIX expression was 37% versus 56% of patients with low cytoplasmic CAIX expression (P<0.001), and 10-year OS of patients with high membranous CAIX expression was 39% versus 55% of patients with low membranous CAIX expression (P = 0.002).

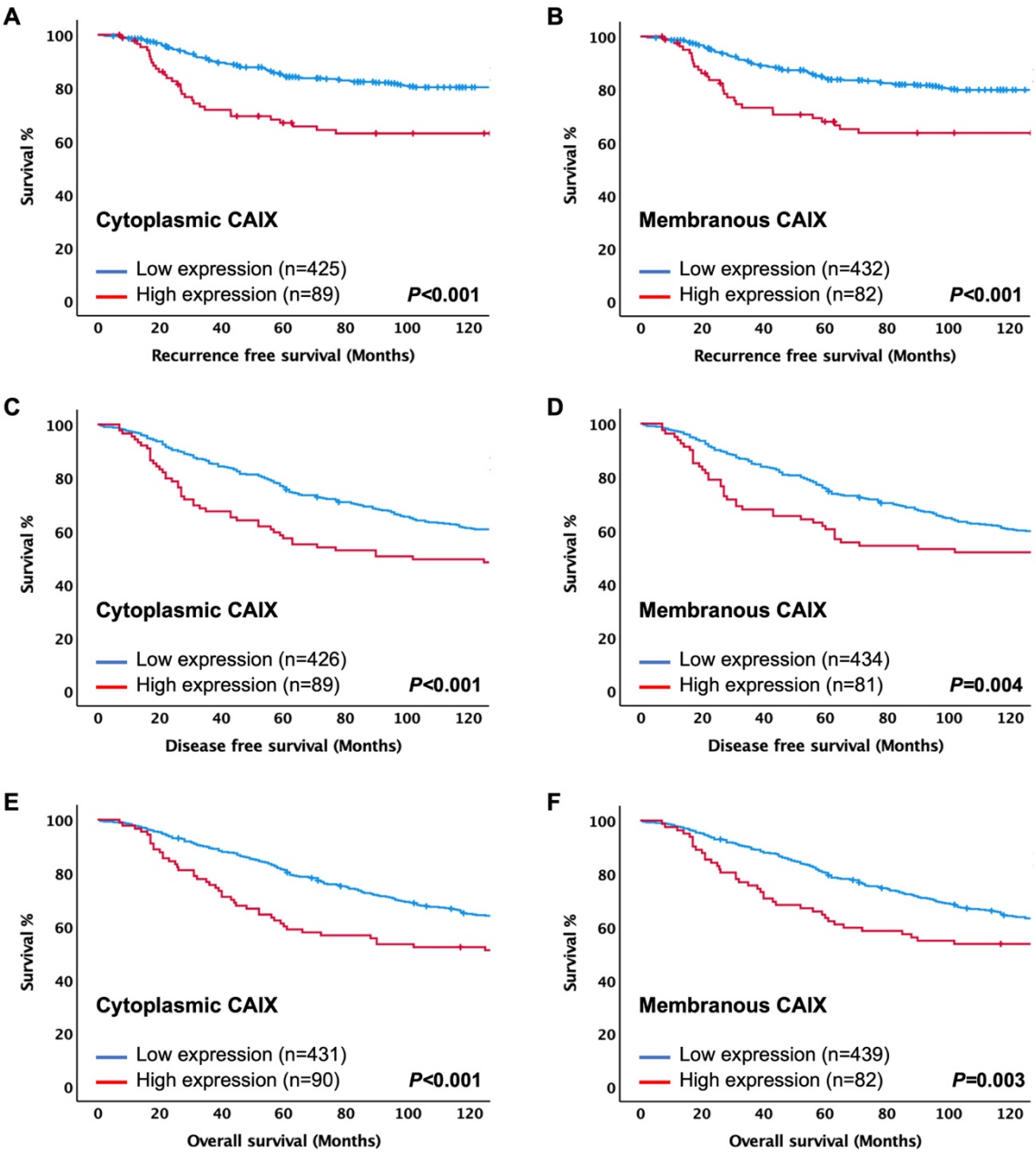

Figure 6.9 Expression of CAIX and clinical outcome in Glasgow breast cohort.

Kaplan-Meier curves showing associations between cytoplasmic and membranous CAIX with recurrence free survival [A, B], disease-free survival [C, D], and overall survival [E, F].

Table 6.3 Association between hypoxic markers expression and survival in Glasgow breast cancer patients (n = 575)

Markers	Recurrence free survival (RFS)						Disease-free survival (DFS)						Overall survival (OS)					
	Cytoplasmic			Membrane/Nuclear			Cytoplasmic			Membrane/Nuclear			Cytoplasmic			Membrane/Nuclear		
	n (%)	10yr-RFS (SE)	P-value	n (%)	10yr-RFS (SE)	P-value	n (%)	10yr-DFS (SE)	P-value	n (%)	10yr-DFS (SE)	P-value	n (%)	10yr-OS (SE)	P-value	n (%)	10yr-OS (SE)	P-value
HIF-1α (1)			0.652			0.885			0.126			0.227			**0.031**			0.053
Low	352(77)	72(3)		406(89)	73(3)		350(77)	45(3)		402(88)	47(3)		354(77)	47(3)		407(88)	50(3)	
High	106(23)	76(5)		52(11)	72(7)		106(23)	58(5)		54(12)	53(8)		107(23)	66(5)		54(12)	66(7)	
HIF-1α (2)			0.279			0.637			0.302			0.397			0.370			0.350
Low	312(56)	73(3)		182(33)	76(3)		307(55)	47(3)		179(32)	44(4)		313(56)	51(3)		183(33)	47(4)	
High	244(44)	76(3)		374(67)	73(3)		249(45)	48(4)		377(68)	49(3)		250(44)	52(4)		380(67)	53(3)	
HIF-2α			**0.022**			0.320			0.174			0.433			0.295			0.237
Low	164(33)	81(3)		308(61)	75(3)		162(32)	52(4)		310(62)	45(3)		165(32)	55(4)		313(61)	48(3)	
High	339(67)	70(3)		195(39)	70(4)		341(68)	45(3)		193(38)	50(4)		344(68)	49(3)		196(39)	54(4)	
CAIX			**<0.001**			**<0.001**			**<0.001**			**0.004**			**<0.001**			**0.003**
Low	425(83)	78(2)		432(84)	77(2)		426(83)	53(3)		434(84)	51(3)		431(83)	56(3)		439(84)	55(3)	
High	89(17)	58(6)		82(16)	61(6)		89(17)	31(6)		81(16)	35(6)		90(17)	37(6)		82(16)	39(6)	

Table showing the number of patients and associations with survival for each hypoxic marker in Glasgow breast cohort.

In term of RFS, cytoplasmic CAIX has prognostic value. When entered into multivariate analysis, cytoplasmic CAIX retained an independent prognostic marker (HR = 2.24, 95% CI: 1.19–4.22, P = 0.012) when combined with tumour size, grade, lymph node status, ER status, PR status, Her-2 status, Ki67, molecular subtype, lymphatic vessel invasion, blood vessel invasion, tumour necrosis, CD8+, CD138+, tumour stroma percentage, tumour budding, adjuvant endocrine therapy, and adjuvant chemotherapy in Glasgow breast cohort (Table 6.4).

Table 6.4 Univariate and multivariate analysis for recurrence free survival of CAIX and clinicopathological characteristics in Glasgow breast cohort (n = 575)

Clinicopathological characteristics	Univariate analysis		Multivariate analysis	
	HR (95% CI)	P-value	HR (95% CI)	P-value
Age (≤50/>50 years)	0.96 (0.66–1.39)	0.810	-	-
Tumour size (≤20/21–50/>50 mm)	1.84 (1.39–2.44)	**<0.001**	0.82 (0.49–1.34)	0.417
Grade (I/II/III)	1.91(1.44–2.54)	**<0.001**	0.88 (0.55–1.42)	0.604
Lymph node (negative/positive)	3.33 (2.28–4.86)	**<0.001**	2.21 (1.22–4.00)	**0.009**
ER status (negative/positive)	0.50 (0.36–0.72)	**<0.001**	6.79 (1.61–28.74)	**0.009**
PR status (negative/positive)	0.52 (0.36–0.76)	**0.001**	0.52 (0.25–1.10)	0.087
Her-2 status (negative/positive)	1.95 (1.32–2.88)	**0.001**	0.47 (0.19–1.14)	0.096
Ki67 index (low/high)	1.55 (1.08–2.23)	**0.018**	0.91 (0.38–2.16)	0.827
Molecular subtype (lum A/lum B/TNBC/Her-2)	1.49 (1.27–1.75)	**<0.001**	3.02 (1.43–6.36)	**0.004**
Lymphatic vessel invasion (no/yes)	3.07 (1.96–4.80)	**<0.001**	1.73 (0.97–3.06)	0.062
Blood vessel invasion (no/yes)	2.64 (1.54–4.52)	**<0.001**	1.71 (0.89–3.31)	0.109
Tumour necrosis (low/high)	3.11 (2.06–4.69)	**<0.001**	2.25 (1.16–4.37)	**0.017**
Klintrup-Mäkinen grade (0/1/2/3)	0.99 (0.79–1.24)	0.911	-	-
CD68+ (low/moderate/high)	0.94 (0.70–1.26)	0.685	-	-
CD8+ (low/moderate/high)	0.73 (0.55–0.97)	**0.030**	0.86 (0.62–1.19)	0.376
CD138+ (low/moderate/high)	1.35 (1.05–1.73)	**0.019**	1.22 (0.88–1.68)	0.240
Tumour stroma percentage (low/high)	1.88 (1.32–2.68)	**0.001**	3.20 (1.86–5.52)	**<0.001**
Tumour budding (low/high)	1.49 (1.04-2.14)	**0.029**	1.29 (0.73–2.31)	0.381
Adjuvant endocrine therapy (no/yes/ATAC trial)	0.62 (0.41–0.94)	**0.025**	1.34 (0.64–2.81)	0.443
Adjuvant chemotherapy (no/yes)	1.90 (1.34–2.71)	**<0.001**	1.17 (0.56–2.45)	0.675
Adjuvant radiotherapy (no/yes)	1.17 (0.83–1.67)	0.373	-	-
Cytoplasmic CAIX (low/high)	2.30 (1.54–3.45)	**<0.001**	2.24 (1.19–4.22)	**0.012**

Multivariate Cox regression model was adjusted for age, tumour size, grade, lymph node, ER, PR, Her-2 status, Ki67, molecular subtype, lymphatic vessel invasion, blood vessel invasion, tumour necrosis, Klintrup-Mäkinen grade, CD68+, CD8+, CD138+, tumour stroma percentage, tumour budding, adjuvant endocrine therapy, adjuvant chemotherapy and adjuvant radiotherapy.

Similar to RFS, when entered into multivariate analysis, cytoplasmic CAIX was an independent prognostic marker for DFS (HR = 1.74, 95% CI: 1.08–2.82, P = 0.023) when combined with patient's age, tumour size, grade, lymph node status, ER status, PR status, Her-2 status, Ki67, molecular subtype, lymphatic vessel invasion, blood vessel invasion, tumour necrosis, CD8+, CD138+, tumour stroma percentage, and tumour budding (Table 6.5).

Table 6.5 Univariate and multivariate analysis for disease-free survival of cytoplasmic CAIX and clinicopathological characteristics in Glasgow breast cohort (n = 575)

Clinicopathological characteristics	Univariate analysis		Multivariate analysis	
	HR (95% CI)	P-value	HR (95% CI)	P-value
Age (≤50/>50 years)	1.58 (1.18–2.10)	**0.002**	1.65 (1.05–2.58)	**0.029**
Tumour size (≤20/21–50/>50 mm)	1.70 (1.39–2.07)	**<0.001**	1.11 (0.79–1.57)	0.535
Grade (I/II/III)	1.23 (1.04–1.47)	**0.018**	0.95 (0.69–1.30)	0.745
Lymph node (negative/positive)	2.31 (1.79–2.96)	**<0.001**	1.99 (1.34–2.97)	**0.001**
ER status (negative/positive)	0.78 (0.61–0.99)	**0.046**	2.23 (0.97–5.11)	0.059
PR status (negative/positive)	0.78 (0.61–0.99)	**0.046**	0.95 (0.58–1.56)	0.835
Her-2 status (negative/positive)	1.50 (1.12–2.01)	**0.006**	0.67 (0.36–1.24)	0.202
Ki67 proliferative index (low/high)	1.39 (1.08–1.81)	**0.011**	1.12 (0.62–2.03)	0.716
Molecular subtype (lum A/lum B/TNBC/Her-2)	1.21 (1.08–1.35)	**0.001**	1.83 (1.28–2.62)	**0.001**
Lymphatic vessel invasion (no/yes)	2.39 (1.75–3.26)	**<0.001**	1.99 (1.35–2.93)	**<0.001**
Blood vessel invasion (no/yes)	2.29 (1.55–3.40)	**<0.001**	1.30 (0.79–2.13)	0.298
Tumour necrosis (low/high)	1.60 (1.25–2.06)	**<0.001**	1.39 (0.91–2.12)	0.131
Klintrup-Mäkinen grade (0/1/2/3)	0.88 (0.75–1.04)	0.132	-	-
CD68+ (low/moderate/high)	0.92 (0.75–1.13)	0.436	-	-
CD8+ (low/moderate/high)	0.76 (0.62–0.93)	**0.007**	0.73 (0.56–0.94)	**0.014**
CD138+ (low/moderate/high)	1.25 (1.05–1.49)	**0.014**	1.26 (1.01–1.57)	**0.040**
Tumour stroma percentage (low/high)	1.78 (1.39–2.29)	**<0.001**	2.02 (1.36–2.99)	**<0.001**
Tumour budding (low/high)	1.53 (1.19–1.97)	**0.001**	1.28 (0.86–1.89)	0.224
Adjuvant endocrine therapy (no/yes/ATAC trial)	0.99 (0.73–1.33)	0.923	-	-
Adjuvant chemotherapy (no/yes)	0.99 (0.78–1.27)	0.964	-	-
Adjuvant radiotherapy (no/yes)	0.85 (0.66–1.08)	0.182	-	-
Cytoplasmic CAIX (low/high)	1.78 (1.32–2.41)	**<0.001**	1.74 (1.08–2.82)	**0.023**

Multivariate Cox regression model was adjusted for age, tumour size, grade, lymph node, ER, PR, Her-2 status, Ki67, molecular subtype, lymphatic vessel invasion, blood vessel invasion, tumour necrosis, Klintrup-Mäkinen grade, CD68+, CD8+, CD138+, tumour stroma percentage, tumour budding, adjuvant endocrine therapy, adjuvant chemotherapy and adjuvant radiotherapy.

Comparable with RFS and DFS, when entered into multivariate analysis, cytoplasmic CAIX was not significant independently associated with reduce OS (P = 0.064) when combined with patient's age, tumour size, grade, lymph node status, Her-2 status, Ki67, molecular subtype, lymphatic vessel invasion, blood vessel invasion, tumour necrosis, CD8+, CD138+, tumour stroma percentage, and tumour budding (Table 6.6).

Table 6.6 Univariate and multivariate analysis for overall survival of cytoplasmic CAIX and clinicopathological characteristics in Glasgow breast cohort (n = 575)

Clinicopathological characteristics	Univariate analysis		Multivariate analysis	
	HR (95% CI)	P-value	HR (95% CI)	P-value
Age (≤50/>50 years)	1.65 (1.22–2.23)	**0.001**	1.98 (1.24–3.15)	**0.004**
Tumour size (≤20/21–50/>50 mm)	1.75 (1.43–2.15)	**<0.001**	1.12 (0.78–1.61)	0.541
Grade (I/II/III)	1.22 (1.02–1.46)	**0.031**	1.12 (0.78–1.60)	0.545
Lymph node (negative/positive)	2.28 (1.76–2.95)	**<0.001**	1.81 (1.18–2.77)	**0.006**
ER status (negative/positive)	0.79 (0.62–1.04)	0.089	-	-
PR status (negative/positive)	0.85 (0.66–1.09)	0.196	-	-
Her-2 status (negative/positive)	1.37 (1.01–1.86)	**0.046**	-	-
Ki67 proliferative index (low/high)	1.35 (1.04–1.76)	**0.027**	1.52 (1.00–2.30)	0.050
Molecular subtype (lum A/lum B/TNBC/Her-2)	1.17 (1.04–1.32)	**0.009**	1.21 (0.99–1.49)	0.068
Lymphatic vessel invasion (no/yes)	2.39 (1.73–3.30)	**<0.001**	2.09 (1.38–3.19)	**0.001**
Blood vessel invasion (no/yes)	2.57 (1.72–3.85)	**<0.001**	1.47 (0.88–2.45)	0.143
Tumour necrosis (low/high)	1.60 (1.23–2.08)	**<0.001**	1.50 (0.96–2.35)	0.073
Klintrup-Mäkinen grade (0/1/2/3)	0.88 (0.75–1.05)	0.150	-	-
CD68+ (low/moderate/high)	0.92 (0.74–1.14)	0.455	-	-
CD8+ (low/moderate/high)	0.71 (0.57–0.88)	**0.001**	0.66 (0.50–0.86)	**0.003**
CD138+ (low/moderate/high)	1.27 (1.05–1.53)	**0.013**	1.31 (1.04–1.66)	**0.023**
Tumour stroma percentage (low/high)	1.79 (1.38–2.31)	**<0.001**	1.83 (1.22–2.76)	**0.004**
Tumour budding (low/high)	1.58 (1.22–2.05)	**<0.001**	1.24 (0.82–1.89)	0.312
Adjuvant endocrine therapy (no/yes/ATAC trial)	1.07 (0.78–1.46)	0.696	-	-
Adjuvant chemotherapy (no/yes)	0.95 (0.74–1.23)	0.693	-	-
Adjuvant radiotherapy (no/yes)	0.82 (0.64–1.06)	0.122	-	-
Cytoplasmic CAIX (low/high)	1.76 (1.29–2.41)	**<0.001**	1.59 (0.97–2.60)	0.064

Multivariate Cox regression model was adjusted for age, tumour size, grade, lymph node, ER, PR, Her-2 status, Ki67, molecular subtype, lymphatic vessel invasion, blood vessel invasion, tumour necrosis, Klintrup-Mäkinen grade, CD68+, CD8+, CD138+, tumour stroma percentage, tumour budding, adjuvant endocrine therapy, adjuvant chemotherapy and adjuvant radiotherapy.

6.3.5.3 Associations between cytoplasmic CAIX expression and clinicopathological characteristics

The relationship between the clinicopathological parameters and cytoplasmic CAIX protein was tested using Chi-square test as shown in Table 6.7. Significant associations were found between CAIX positivity in tumour cells and clinicopathological features such as tumour size ($P = 0.012$), high tumour grade ($P<0.001$), ER-negativity ($P<0.001$), PR-negativity ($P<0.001$), Her-2-negativity ($P = 0.003$), low Ki67 ($P = 0.001$), molecular subtypes ($P<0.001$), high tumour necrosis ($P<0.001$), Klintrup-Mäkinen grade ($P = 0.001$), adjuvant endocrine therapy treated cases ($P = 0.004$), and adjuvant chemotherapy treated cases ($P = 0.016$). No other associations were observed, but high levels of CAIX had an association of borderline significance with lymph node positivity ($P = 0.096$) and low tumour budding ($P = 0.06$).

Table 6.7 Association between cytoplasmic CAIX expression and clinicopathological parameters in Glasgow breast cohort (n = 575)

Clinicopathological characteristics	Cytoplasmic CAIX		
	Low expression n = 442 (83%)	High expression n = 91(17%)	P-value
Age (≤50/>50 years)	135(30)/307(70)	27(30)/64(70)	0.869
Tumour size (≤20/21–50/>50 mm)	262(59)/162(37)/18(4)	40(44)/46(51)/5(5)	**0.012**
Grade (I/II/III)	81(18)/189(43)/172(39)	5(5)/26(29)/60(66)	**<0.001**
Lymph node (negative/positive)	252(58)/185(42)	44(48)/47(52)	0.105
ER status (negative/positive)	120(27)/322(73)	60(66)/31(34)	**<0.001**
PR status (negative/positive)	219(49)/223(51)	66(73)/25(27)	**<0.001**
Her-2 status (negative/positive)	368(84)/70(16)	63(70)/27(30)	**0.003**
Ki67 proliferative index (low/high)	304(71)/122(29)	44(52)/41(48)	**0.001**
Molecular subtype (lum A/lum B/TNBC/Her-2)	208(49)/108(25)/79(18)/34(8)	15(17)/17(19)/37(42)/20(22)	**<0.001**
Lymphatic vessel invasion (no/yes)	191(68)/89(32)	31(65)/17(35)	0.621
Blood vessel invasion (no/yes)	249(89)/31(11)	39(81)/9(19)	0.154
Tumour necrosis (low/high)	231(53)/205(47)	17(19)/74(81)	**<0.001**
Klintrup-Mäkinen grade (0/1/2/3)	52(12)/247(57)/95(22)/40(9)	2(2)/41(45)/42(46)/6(7)	**0.001**
CD68+ (low/moderate/high)	58(23)/95(39)/92(38)	17(39)/12(27)/15(34)	0.153
CD8+ (low/moderate/high)	73(29)/87(36)/85(35)	16(36)/11(24)/18(40)	0.973
CD138+ (low/moderate/high)	125(51)/36(15)/84(34)	18(41)/5(11)/21(48)	0.117
Tumour stroma percentage (low/high)	312(71)/127(29)	58(64)/33(36)	0.166
Tumour budding (low/high)	295(67)/144(33)	70(77)/21(23)	0.069
Adjuvant endocrine therapy (no/yes/ATAC trial)	63(18)/277(79)/12(3)	19(35)/34(63)/1(1)	**0.004**
Adjuvant chemotherapy (no/yes)	264(60)/176(40)	42(46)/49(54)	**0.016**
Adjuvant radiotherapy (no/yes)	217(49)/223(51)	47(52)/44(48)	0.686

Chi-squared table of associations for cytoplasmic CAIX expression and clinical prognostic factors including age, tumour size, grade, lymph node, ER, PR, Her-2 status, Ki67, molecular subtype, lymphatic vessel invasion, blood vessel invasion, tumour necrosis, Klintrup-Mäkinen grade, CD68+, CD8+, CD138+, tumour stroma percentage, tumour budding, adjuvant endocrine therapy, adjuvant chemotherapy and adjuvant radiotherapy.

6.3.5.4 Expression of cytoplasmic CAIX and clinical outcome in different breast cancer subtypes

Expression of cytoplasmic CAIX was also assessed by Kaplan-Meier method and compared by log-rank test in different breast cancer subtypes (Figure 6.10). In terms of RFS, subgroup analysis based on molecular subtypes indicated that high cytoplasmic CAIX levels showed an association with poorer RFS in luminal B disease (P = 0.025), and a trend towards worse RFS was observed in patients with Her-2 disease (P = 0.075). In contrast, no association was found between expression of cytoplasmic CAIX and RFS in luminal A disease (P = 0.488), and TNBC (P = 0.137) (Figure 6.10A-D).

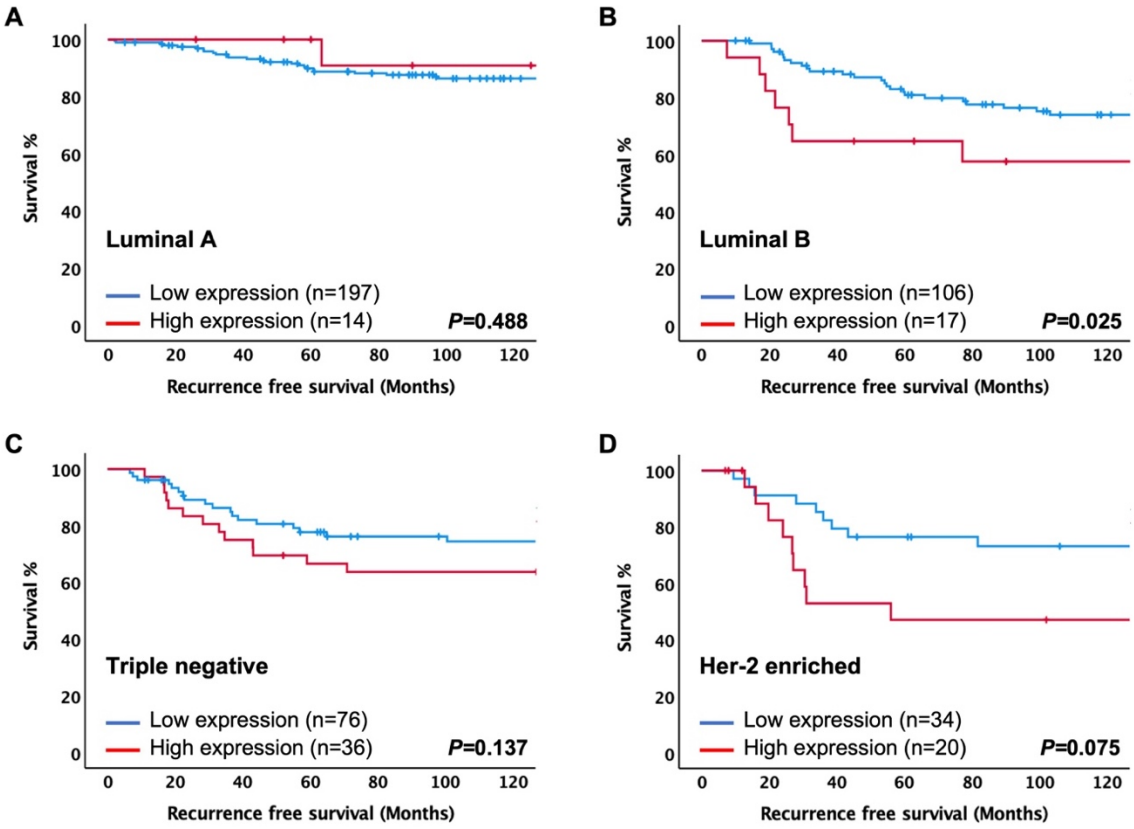

Figure 6.10 Expression of cytoplasmic CAIX and recurrence free survival in different breast cancer subtypes.

Kaplan-Meier curves showing associations between cytoplasmic CAIX and recurrence free survival in luminal A disease [A], luminal B disease [B], triple negative [C], and Her-2 enriched [D].

Multivariate analysis suggested that cytoplasmic expression of CAIX was not an independent prognostic marker for RFS (P = 0.196) when combined with lymph node status, lymphatic vessel invasion, tumour necrosis, CD8+ and adjuvant endocrine therapy in luminal B disease (Table 6.8).

Table 6.8 Univariate and multivariate analysis for recurrence free survival of cytoplasmic CAIX and clinicopathological characteristics in luminal B tumours

Clinicopathological characteristics	Luminal B			
	Univariate analysis		Multivariate analysis	
	HR (95% CI)	P-value	HR (95% CI)	P-value
Age (≤50/>50 years)	0.96 (0.42–2.16)	0.919	-	-
Tumour size (≤20/21–50/>50 mm)	0.96 (0.55–1.68)	0.892	-	-
Grade (I/II/III)	1.42 (0.81–2.48)	0.220	-	-
Lymph node (negative/positive)	3.19 (1.56–6.53)	**0.001**	6.27 (1.79–21.88)	**0.004**
ER status (negative/positive)	0.64 (0.09–4.65)	0.656	-	-
PR status (negative/positive)	0.74 (0.38–1.44)	0.377	-	-
Her-2 status (negative/positive)	1.21(0.60–2.43)	0.593	-	-
Ki67 proliferative index (low/high)	1.03 (0.40–2.66)	0.948	-	-
Lymphatic vessel invasion (no/yes)	2.83 (1.12–7.16)	**0.029**	1.85 (0.69–4.93)	0.220
Blood vessel invasion (no/yes)	1.79 (0.59–5.38)	0.299	-	-
Tumour necrosis (low/high)	3.31 (1.50–7.29)	**0.003**	1.09 (0.32–3.74)	0.884
Klintrup-Mäkinen grade (0/1/2/3)	0.89 (0.59–1.35)	0.599	-	-
CD68+ (low/moderate/high)	1.51 (0.73–3.11)	0.269	-	-
CD8+ (low/moderate/high)	0.39 (0.20–0.75)	**0.005**	0.46 (0.24–0.85)	**0.013**
CD138+ (low/moderate/high)	1.63 (0.97–2.75)	0.064	-	-
Tumour stroma percentage (low/high)	1.62 (0.79–3.29)	0.189	-	-
Tumour budding (low/high)	0.96 (0.47–1.97)	0.916	-	-
Adjuvant endocrine therapy (no/yes/ATAC trial)	0.32 (0.11–0.96)	**0.042**	1.13 (0.14–9.02)	0.909
Adjuvant chemotherapy (no/yes)	1.66 (0.86–3.23)	0.133	-	-
Adjuvant radiotherapy (no/yes)	0.78 (0.40–1.51)	0.455	-	-
Cytoplasmic CAIX (low/high)	2.41 (1.09–5.32)	**0.030**	2.53 (0.62–10.32)	0.196

Multivariate Cox regression model was adjusted for age, tumour size, grade, lymph node, ER, PR, Her-2 status, Ki67, lymphatic vessel invasion, blood vessel invasion, tumour necrosis, Klintrup-Mäkinen grade, CD68+, CD8+, CD138+, tumour stroma percentage, tumour budding, adjuvant endocrine therapy, adjuvant chemotherapy and adjuvant radiotherapy.

Additionally, poorer DFS was observed in patients with high cytoplasmic CAIX expression in luminal B (P = 0.035), and Her-2 disease (P = 0.016) using Kaplan-Meier analysis and compared between groups with the log-rank test as shown in Figure 6.11 (B, D). However, this association was not found in luminal A (P = 0.590), and TNBC (P = 0.485) (Figure 6.11A, C).

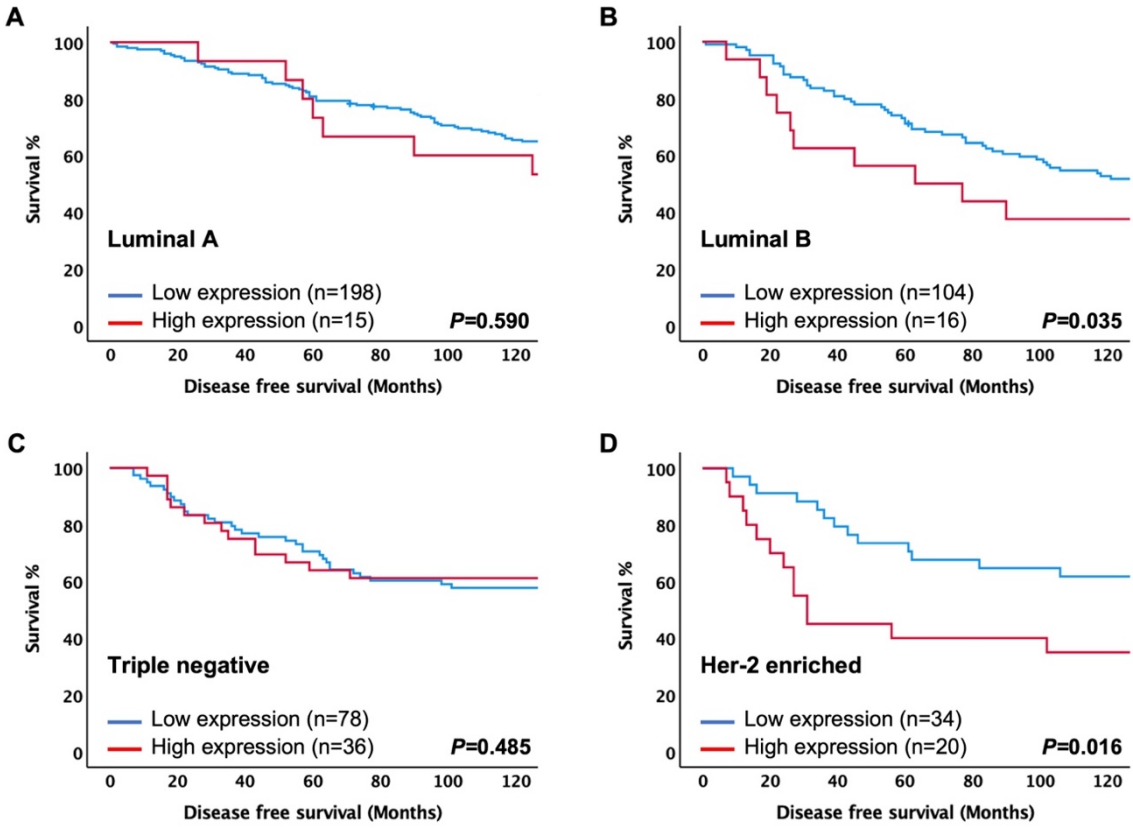

Figure 6.11 Expression of cytoplasmic CAIX and disease-free survival in different breast cancer subtypes.

Kaplan-Meier curves showing associations between cytoplasmic CAIX and disease-free survival in luminal A disease [A], luminal B disease [B], triple negative [C], and Her-2 enriched [D].

Multivariate analysis proposed that cytoplasmic CAIX expression was an independent prognostic marker for DFS (HR = 3.59, 95% CI: 1.23–10.53, P = 0.020) when combined with lymph node status, lymphatic vessel invasion, tumour necrosis, and CD8+ in luminal B disease (Table 6.9).

Table 6.9 Univariate and multivariate analysis for disease-free survival of cytoplasmic CAIX and clinicopathological characteristics in luminal B tumours

Clinicopathological characteristics	Luminal B			
	Univariate analysis		Multivariate analysis	
	HR (95% CI)	P-value	HR (95% CI)	P-value
Age (≤50/>50 years)	1.55 (89–2.68)	0.117	-	-
Tumour size (≤20/21–50/>50 mm)	1.10 (0.75–1.62)	0.628	-	-
Grade (I/II/III)	0.98 (0.67–1.41)	0.896	-	-
Lymph node (negative/positive)	2.36 (1.44–3.87)	**0.001**	3.48 (1.63–7.42)	**0.001**
ER status (negative/positive)	0.65 (0.16–2.64)	0.545	-	-
PR status (negative/positive)	0.93 (0.57–1.49)	0.757	-	-
Her-2 status (negative/positive)	1.03 (0.62–1.70)	0.920	-	-
Ki67 proliferative index (low/high)	1.17 (0.58–2.35)	0.668	-	-
Lymphatic vessel invasion (no/yes)	2.28 (1.21–4.27)	**0.011**	2.01 (0.97–4.19)	0.062
Blood vessel invasion (no/yes)	1.65 (0.76–3.58)	0.205	-	-
Tumour necrosis (low/high)	1.85 (1.13–3.03)	0.014	1.16 (0.51–2.65)	0.727
Klintrup-Mäkinen grade (0/1/2/3)	0.85 (0.63–1.13)	0.256	-	-
CD68+ (low/moderate/high)	1.06 (0.67–1.68)	0.808	-	-
CD8+ (low/moderate/high)	0.49 (0.32–0.75)	**0.001**	0.59 (0.38–0.91)	**0.017**
CD138+ (low/moderate/high)	1.14 (0.80–1.61)	0.472	-	-
Tumour stroma percentage (low/high)	1.63 (0.98–2.70)	0.060	-	-
Tumour budding (low/high)	1.38 (0.85–2.23)	0.191	-	-
Adjuvant endocrine therapy (no/yes/ ATAC trial)	0.57 (0.26–1.27)	0.171	-	-
Adjuvant chemotherapy (no/yes)	0.99 (0.61–1.62)	0.990	-	-
Adjuvant radiotherapy (no/yes)	0.66 (0.41–1.06)	0.084	-	-
Cytoplasmic CAIX (low/high)	1.94 (1.03–3.63)	**0.039**	3.59 (1.23–10.53)	**0.020**

Multivariate Cox regression model was adjusted for age, tumour size, grade, lymph node, ER, PR, Her-2 status, Ki67, lymphatic vessel invasion, blood vessel invasion, tumour necrosis, Klintrup-Mäkinen grade, CD68+, CD8+, CD138+, tumour stroma percentage, tumour budding, adjuvant endocrine therapy, adjuvant chemotherapy and adjuvant radiotherapy.

In Her-2 disease, when multivariate analysis was performed, cytoplasmic CAIX was not independent prognostic marker for DFS (P = 0.069) when combined with lymphatic vessel invasion, and tumour budding (Table 6.10).

Table 6.10 Univariate and multivariate analysis for disease-free survival of cytoplasmic CAIX and clinicopathological characteristics in Her-2 tumour

Clinicopathological characteristics	**Her-2 disease**			
	Univariate analysis		Multivariate analysis	
	HR (95% CI)	P-value	HR (95% CI)	P-value
Age (≤50/>50 years)	0.76 (0.37–1.57)	0.457	-	-
Tumour size (≤20/21–50/>50 mm)	1.08 (0.62–1.89)	0.783	-	-
Grade (I/II/III)	1.43 (0.63–3.28)	0.395	-	-
Lymph node (negative/positive)	1.69 (0.86–3.33)	0.130	-	-
Ki67 proliferative index (low/high)	0.91 (0.45–1.83)	0.785	-	-
Lymphatic vessel invasion (no/yes)	2.87 (1.27–6.49)	**0.011**	3.01 (1.17–7.73)	**0.022**
Blood vessel invasion (no/yes)	1.27 (0.29–5.46)	0.745	-	-
Tumour necrosis (low/high)	0.97 (0.38–2.51)	0.957	-	-
Klintrup-Mäkinen grade (0/1/2/3)	0.83 (0.52–1.32)	0.424	-	-
CD68+ (low/moderate/high)	0.89 (0.55–1.42)	0.612	-	-
CD8+ (low/moderate/high)	0.69 (0.42–1.16)	0.163	-	-
CD138+ (low/moderate/high)	1.16 (0.75–1.80)	0.494	-	-
Tumour stroma percentage (low/high)	1.87 (0.97–3.61)	0.062	-	-
Tumour budding (low/high)	2.71 (1.35–5.42)	**0.005**	1.25 (0.39–3.91)	0.702
Adjuvant endocrine therapy (no/yes/ATAC trial)	0.72 (0.31–1.64)	0.428	-	-
Adjuvant chemotherapy (no/yes)	1.53 (0.74–3.19)	0.255	-	-
Adjuvant radiotherapy (no/yes)	1.20 (0.62-2.33)	0.590	-	-
Cytoplasmic CAIX (low/high)	2.32 (1.41-4.71)	**0.020**	2.57 (0.93–7.08)	0.069

Multivariate Cox regression model was adjusted for age, tumour size, grade, lymph node, Ki67, lymphatic vessel invasion, blood vessel invasion, tumour necrosis, Klintrup-Mäkinen grade, CD68+, CD8+, CD138+, tumour stroma percentage, tumour budding, adjuvant endocrine therapy, adjuvant chemotherapy and adjuvant radiotherapy.

In terms of OS, Kaplan-Meier survival curves for cytoplasmic expression of CAIX were plotted and compared between groups with the log-rank test. High cytoplasmic CAIX expression was associated with worse OS in Her-2 disease (P = 0.001), but no association was found between expression of cytoplasmic CAIX and this outcome in any of the other three breast cancer subtypes, luminal A (P = 0.745), luminal B (P = 0.286), and TNBC (P = 0.516) (Figure 6.12A-D).

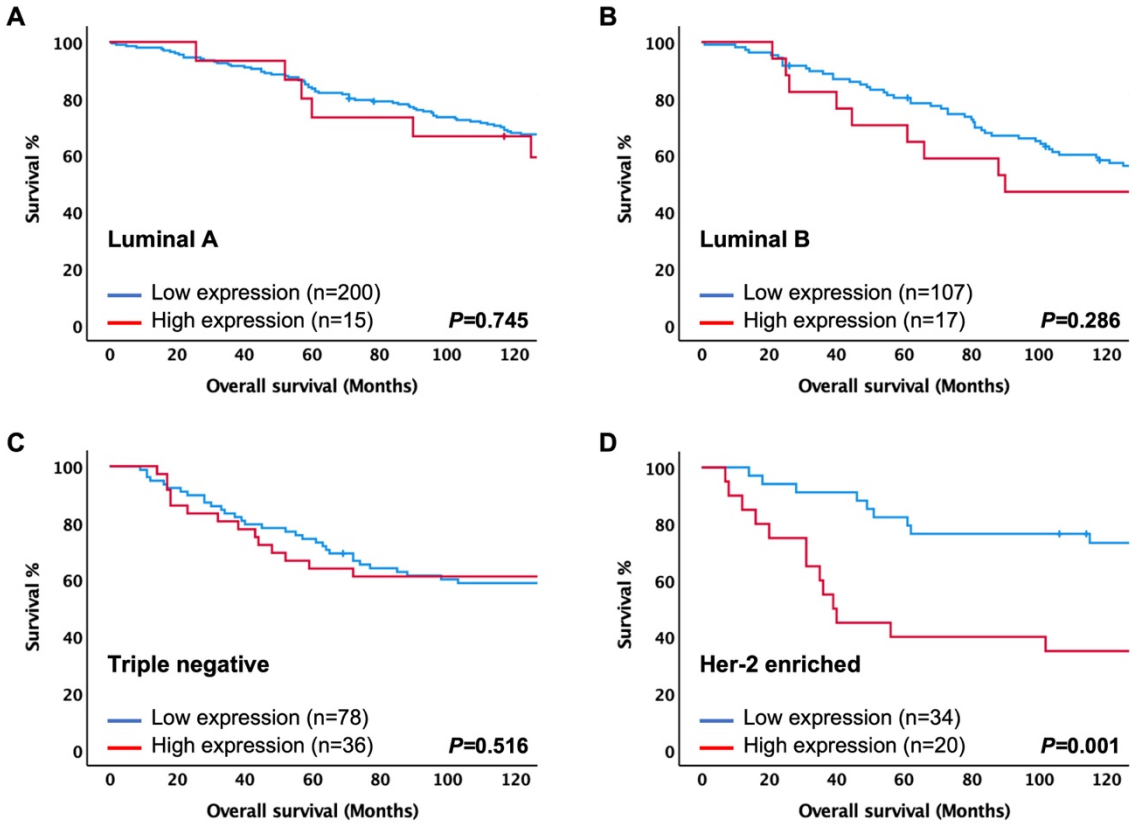

Figure 6.12 Expression of cytoplasmic CAIX and overall survival in different breast cancer subtypes.

Kaplan-Meier curves showing associations between cytoplasmic CAIX and overall survival in luminal A disease [A], luminal B disease [B], triple negative [C], and Her-2 enriched [D].

When multivariate analysis was performed, cytoplasmic CAIX remained as a factor contributing significantly to OS (HR = 4.19, 95% CI: 1.37–12.80, P = 0.012) when combined with lymphatic vessel invasion, tumour stroma percentage, and tumour budding in Her-2 disease (Table 6.11).

Table 6.11 Univariate and multivariate analysis for overall survival of cytoplasmic CAIX and clinicopathological characteristic in Her-2 tumour

Clinicopathological characteristics	Her-2 disease			
	Univariate analysis		Multivariate analysis	
	HR (95% CI)	P-value	HR (95% CI)	P-value
Age (≤50/>50 years)	1.03 (0.46–2.31)	0.949	-	-
Tumour size (≤20/21–50/>50 mm)	0.98 (0.52–1.83)	0.948	-	-
Grade (I/II/III)	1.32 (0.54–3.22)	0.549	-	-
Lymph node (negative/positive)	1.79 (0.86–3.73)	0.118	-	-
Ki67 proliferative index (low/high)	1.04 (0.49–2.21)	0.913	-	-
Lymphatic vessel invasion (no/yes)	3.05 (1.22–7.62)	**0.017**	2.25 (0.62–8.19)	0.220
Blood vessel invasion (no/yes)	1.76 (0.41–7.69)	0.450	-	-
Tumour necrosis (low/high)	0.81 (0.31–2.13)	0.673	-	-
Klintrup-Mäkinen grade (0/1/2/3)	0.79 (0.47–1.34)	0.389	-	-
CD68+ (low/moderate/high)	0.86 (0.50–1.49)	0.600	-	-
CD8+ (low/moderate/high)	0.66 (0.37–1.19)	0.173	-	-
CD138+ (low/moderate/high)	1.36 (0.82–2.26)	0.236	-	-
Tumour stroma percentage (low/high)	2.13 (1.03–4.39)	**0.041**	4.74 (1.49–15.13)	**0.009**
Tumour budding (low/high)	3.22 (1.53–6.77)	**0.002**	1.46 (0.38–5.61)	0.583
Adjuvant endocrine therapy (no/yes/ATAC trial)	0.91 (0.36–2.25)	0.831	-	-
Adjuvant chemotherapy (no/yes)	1.20 (0.55–2.65)	0.643	-	-
Adjuvant radiotherapy (no/yes)	0.90 (0.44–1.85)	0.778	-	-
Cytoplasmic CAIX (low/high)	3.51 (1.60–7.69)	**0.002**	4.19 (1.37–12.80)	**0.012**

Multivariate Cox regression model was adjusted for age, tumour size, grade, lymph node, ER, PR, Her-2 status, Ki67, molecular subtype, lymphatic vessel invasion, blood vessel invasion, tumour necrosis, Klintrup-Mäkinen grade, CD68+, CD8+, CD138+, tumour stroma percentage, tumour budding, adjuvant endocrine therapy, adjuvant chemotherapy and adjuvant radiotherapy.

6.3.6 Association between hypoxia regulated proteins in patients with mixed breast cancer

The association between hypoxia-related protein biomarkers was tested using Chi-square test. The expression of cytoplasmic HIF-1α (1) showed a positive correlation with nuclear HIF-1α (1), cytoplasmic and nuclear HIF-2α ($P<0.001$). Also, nuclear HIF-1α (1) was associated with cytoplasmic and nuclear HIF-2α ($P<0.001$, $P = 0.001$, respectively). Cytoplasmic HIF-2α was associated with nuclear HIF-2α expression ($P<0.001$), and cytoplasmic CAIX was significantly associated with membranous CAIX ($P<0.001$) (Table 6.12).

Table 6.12 Association between hypoxic markers in Glasgow breast cohort

Hypoxic markers	Nuclear HIF-1α (1)	Cytoplasmic HIF-2α	Nuclear HIF-2α	Cytoplasmic CAIX	Membranous CAIX
Cytoplasmic HIF-1α (1)	**<0.001**	**<0.001**	**<0.001**	0.628	0.879
Nuclear HIF-1α (1)	-	**<0.001**	**0.001**	0.892	0.677
Cytoplasmic HIF-2α	-	-	**<0.001**	0.951	0.406
Cytoplasmic CAIX	-	-	-	-	**<0.001**

Chi-squared table of associations between hypoxic markers including cytoplasmic/nuclear HIF-1α (1), cytoplasmic/nuclear HIF-2α, and cytoplasmic/membranous CAIX.

6.4 Discussion

In the present chapter, of 575 patients with invasive ductal breast cancer, both HIF-1α and HIF-2α expression, irrespective of cellular location, were not consistently associated with survival. These results are in contrast to a recent meta-analysis that concluded high HIF-1α expression was consistently associated with poor DFS and OS in breast cancer patients (357). However, in the present analysis CAIX expression was consistently associated with survival and was in agreement with the results of a recent systematic review of CAIX expression in patients with breast cancer (380). Therefore, in this chapter, CAIX was a superior predictor of survival in patients with invasive ductal breast cancer and may be a useful independent indicator of clinical outcome in these patients. The basis of the relatively poor performance of HIF-1α and HIF-2α expression compared with CAIX in the present analysis is not clear, however, it might be due to the sample size and different breast cancer subtypes. High cytoplasmic HIF-1α (1) expression was associated with poor OS in luminal A disease, high cytoplasmic HIF-2α expression was associated with poor RFS in Her-2 disease while high cytoplasmic CAIX levels was associated with poor RFS in luminal B disease, poor DFS in luminal B, and Her-2 disease, poor OS in Her-2 disease.

In accordance with previous studies, a similar pattern of cytoplasmic and nuclear expression of HIF-1α (1) on malignant cells has recognised (301, 320, 322). However, HIF-1α immunoreactivity was detected only in the nucleus (235, 265, 319). In this chapter, cytoplasmic HIF-1α (1) was overexpressed in 109 of 470 (23%). Similarly, Dales et al. showed HIF-1α expression in about 25% of invasive breast cancers (241). While cytoplasmic HIF-2α was expressed in 350 of 519 (67%) cases in this study, Giatromanolaki et al. reported only 35.9% of cytoplasmic HIF-2α was expressed in breast specimens (381). Previous work on CAIX has identified a similar pattern of cytoplasmic and membranous expression on malignant cells (306, 339, 366), however, Tan et al. have showed only membranous protein expression (264), and Choi showed only cytoplasmic CAIX expression (235). Cytoplasmic CAIX in this work was found in 17% whereas Choi and co-workers reported that CAIX was expressed in 33% of the cases (235). Membranous expression was observed in 16% which is in line with other studies showed CAIX expression in 18% (306), 15% (366), and 14% of the cases (264). The large variation of protein positive tumours in the different studies might be explained due to the difference in experimental methods, scoring methods or threshold used.

In this chapter, high cytoplasmic CAIX expression was found to be an independent prognostic predictor of poor RFS in the entire cohort. This result is in agreement with other studies (248, 310, 335). Also, using DFS as an endpoint, cytoplasmic CAIX expression was shown to be independent predictors of DFS in the entire cohort. This finding is consistent with previous reports (265, 336).

With reference to CAIX, more data has been published in breast cancer, which identifies CAIX as a marker of aggressive tumour behaviour which was consistent with this study. This protein was positively correlated with larger tumour size (262, 306), high grade tumours (235, 248, 260, 263, 264, 306), high tumour necrosis (263, 310), loss of ER (248, 260, 263, 264) and loss of PR (260), suggesting CAIX expression was closely associated with indicators of aggressive phenotype. Therefore, the present results of this chapter showed that CAIX could potentially be used as a factor in predicting poor response to treatment in patients with ductal breast cancer.

The mechanism by which CAIX expression influences survival in these patients is not clear. The relationship between tumour CAIX and histological grade is consistent with the hypothesis that high grade tumours have a higher proliferation rate. Such high proliferation rates result in neo-angiogenesis lagging behind tumour growth (382) with subsequent inadequate oxygen supply and nutrients activating the hypoxia pathway (345, 383). Similarly, larger tumours may also express hypoxia markers more frequently.

The association between the expression of CAIX and ER and PR negativity may be explained by several mechanisms. Since it has been reported that hypoxia decreases the expression of hormone receptors (384), it is possible that the loss of hormone receptors is caused by hypoxia induced CAIX expression. Another explanation is related to the fact that aggressive breast cancer with high proliferative activity is known to have hormone receptor loss, which tends to produce hypoxic areas where the expression of CAIX is elevated (248). This inverse association could also explain the endocrine therapy resistance in tumours expressing high levels of CAIX. Most tumours in this group that had been treated with endocrine and chemotherapy were CAIX high staining intensity, and this could be, in part, result in therapy resistance. Indeed, this would suggest that the predictive value of CAIX may be helpful in deciding clinical treatment. For example, CAIX can predict doxorubicin resistance in early-stage breast cancer independent of Her-2 and TOP2A amplification (339). It may also predict chemosensitivity to neoadjuvant taxane and anthracycline treatment in breast cancer patients (336). Further work is required to detail this clinical role.

A significant interaction between CAIX expression and Ki67 was reported in the present chapter. This is consistent with prior reports on breast carcinoma (262). These findings suggest at least the presence of proliferating tumour cells in the tumour areas with high expression of CAIX. This further supports the concept that proliferating cancer cells under hypoxic conditions may develop more aggressive phenotype.

In this chapter, CAIX expression predicted survival in luminal B and Her-2-enriched patients. However, surprisingly, the link between TNBC patients and CAIX expression was not found as anticipated. The Kaplan-Meier plot was separating in the recurrence plots but due to only having just over 100 cases may have been insufficiently powered and therefore further work in a larger cohort should be carried out. For example, a study of more than 3000 breast cancer patients showed that a high CAIX level was significantly associated with poor survival in patients with luminal B, and TNBC, but not luminal A and Her-2 enriched (385). An IHC-based TMA study of invasive breast carcinoma (n = 276) reported that CAIX expression was associated with TNBC (235). Irrespective, the present results indicate a need for further work to understand the prognostic value of cytoplasmic CAIX in subgroups of breast cancer.

While membranous CAIX expression in our patients was significantly associated with nuclear expression of HIF-1α (2), there was no significant association between cytoplasmic HIF-1α (2) and cytoplasmic CAIX. This absence of an association is consistent with other studies (307, 386, 387) and may reflect that rather than being regulated by hypoxia, HIF-1α expression may be modified by other factors. These factors include alterations in tumour suppressor genes and oncogenes (218, 388, 389). HIF-1α may also lose its transcriptional ability such that CAIX induction does not happen despite high expression of HIF-1α (390). Moreover, CAIX expression may be correlated with HIF-1α expression in tumours where HIF-1α expression is perinecrotic, but not in tumours in which HIF-1α expression is diffuse throughout the tumour (327, 386). Also, it may be that the difference in tissue half-lives of HIF-1α (degraded in minutes) and CAIX (degraded in 2–3 days) (391) accounts for the present results. Expression of CAIX may also be increased in the absence of HIF-1α by the PI3K pathway (392) and the MAPK pathway (393). Increased expression of CAIX in the absence of hypoxia may also occur with hypomethylation of the CAIX gene promoter (394). However, there was a consistent association between cytoplasmic and nuclear HIF-1α (1), cytoplasmic and nuclear HIF-2α, and between cytoplasmic and membranous CAIX indicating reliable methodology.

CAIX is functionally involved in diverse aspects of cancer progression and development. Choi and colleagues (235) have reported that cytoplasmic CAIX exhibited an acid-resistant tumour phenotype which depend on pH regulation to prevent intracellular acidosis, allowing breast cancer cells to undergo metabolic adaptation to hypoxia. Acidic microenvironment can be toxic to normal cells, but tumour cells adapt and survive (395-397). In fact, studies indicate that while the proliferation rate of normal cells is maximal at pH 7.3, cancer cell proliferation is highest at pH 6.8 (395).

CAIX is under consideration, by both academic and pharmaceutical entities, as a potential target for intervention in breast carcinoma (398). A preclinical study showed that the natural compound carnosine efficiently inhibits the ability of CAIX to regulate pH and shows anticancer properties in a mouse model (399). Other CAIX specific inhibitors have been previously developed, such as imidazole-substituted benzene sulfonamides, and their application in tumour cells has been described by Mboge et al. (379). Therefore, assessment of CAIX in tumours before or during therapy may represent a more powerful prognostic and predictive biomarker as well as important targets for breast cancer especially in advanced stages with limited treatment options, which warrants further investigation.

In conclusion, the main findings of this chapter were that high cytoplasmic HIF-1α (1) expression was associated with poor survival in luminal A disease, and high cytoplasmic HIF-2α expression was associated with poor survival in Her-2 disease. Also, demonstrated that patients with high cytoplasmic CAIX was an independent prognosticator in the entire cohort and in the patient subpopulation of luminal B disease and Her-2 disease. Because the association of these biomarker expression with survival varies between subtypes, each subtype should be analysed individually and validated in a larger cohort that consists of an adequate number of patients per each. The following chapter of this thesis will go on to assess staining of hypoxic markers in ER-positive breast cancer to validate their prognostic role in different cohorts.

Chapter 7 Validation of cellular hypoxic markers in predicting survival in patients with ER-positive breast cancer

7.1 Introduction

Oestrogen receptor (ER)-positive breast cancer represents approximately 70% of all breast cancers (400). Endocrine therapy is critical to the success of controlling hormone positive breast cancers including tumours bearing the ER for early-stage and metastatic breast disease (401, 402). However, approximately 30% of patients either present with initial resistance called intrinsic (de novo resistance) or with resistance that arises during treatment (acquired resistance) (403).

TME influences the behaviour of cancer cells including characteristics of aggressiveness, such as angiogenesis, invasiveness, metastasis, and therapy resistance (404). A number of factors have been implicated in hormone resistance mechanism including altered ER-binding and cross-talk with other pathways, for example, the PI3K-AKT-mTOR pathway (403). Hypoxia, a condition commonly occurring in solid tumours, is a major driver of invasiveness and metastasis in breast cancer, and it is associated with chemotherapy and radiotherapy resistance (405, 406).

HIFs have been demonstrated to be involved in the resistance mechanism (407, 408). Significantly, the response to tamoxifen is decreased in hypoxic breast cancer cells compared with cells grown under normoxic environments (247, 384). Clinically, HIF-1α expression is associated tamoxifen resistance in breast cancer (328). The possibility of using HIFs and CAIX as prognostic and predictive markers in breast cancer has already been discussed by several authors (240, 256, 262, 339). The prognostic role of these proteins was dependent on cellular distribution and luminal subtypes.

It was previously demonstrated that expression of HIF-1α (1), HIF-2α and CAIX were associated with poor clinical outcome. The prognostic role of these proteins was dependent on cellular distribution and luminal subtypes. Therefore, these findings require validation in an expanded cohort including ER-positive breast cancer. This will provide the potential prognostic significance of these proteins in particular subtypes.

7.2 Material and methods

7.2.1 Patient cohort

For this study, ER-positive cohort was used with characteristics as described in chapter 2. The cohort included 456 patients presenting with invasive breast cancer between 1980 and

1999 within the Glasgow Royal Infirmary. Patients with unknown ER status (n = 44) and ER-negative status (n = 20) were excluded, leaving 392 patients. Selection criteria of specimens having ductal histological subtype (n = 314) and HIF-1α (2) expression available for analysis (n = 285) was applied resulting in exclusion of 107 patients. The clinicopathological data available on the database included patient's age, histological tumour type, tumour size, tumour grade, involved lymph node status, PR status, Her-2 status, and Ki67. The strength of this cohort is that the patients were treated with adjuvant tamoxifen and time on tamoxifen was available.

The follow up for the selected patients ranged from 1.32–282 months with a median follow up time was 87.84 months (range 60.66–118.14 months). There were 149 patients alive at the last follow up, and median follow up was 96.24 months (range 70.62–117.72 months). Clinicopathological data including patient's age, tumour size, grade, lymph node status, PR status, Her-2 status, and Ki67 was available.

7.2.2 TMA slide staining and scanning

Previously constructed TMAs were employed, that had three 0.6 mm cores per tumour block/patient to combat tumour heterogeneity. IHC was performed and resulting stained slides scanned using Hamamatsu slide scanner and visualised using NDP serve 3 image viewer platform system as described in chapter 2.

7.2.3 Scoring of hypoxic markers

Each TMA core of HIF-1α (2), HIF-2α, and CAIX expression was scored using the weighted Histoscore method whereas HIF-1α (1) was scored digitally on QuPath as described in chapter 2. To ensure reproducibility of scoring, 10% of cores for each marker was co-scored manually by a second observer (J.E) blinded to the previous observer score as well as patient clinical and survival data. Reliability analysis was performed with SPSS software to ensure consistency and objectivity between the main scorer and the co-scorers giving an ICCC for all markers. Values above 0.75 are indicative of good reliability.

7.2.4 Statistical analysis

The thresholds from the previous Glasgow breast cohort were applied for analysis of ER-positive cohort. Analysis of associations with clinicopathological characteristics and with survival outcomes was carried out as described in chapter 2.

7.3 Results

7.3.1 Clinicopathological characteristics of ER-positive breast cancer

A total of 285 patients who presented with ER-positive early-stage invasive ductal carcinoma were included in the study. Table 7.1 shows clinicopathological characteristics of patients. The majority of patients (82%) were aged above 50 years, had tumours size ≤20 (48%), and had grade II carcinoma (51%). There were 137 patients with axillary lymph node involvement (52%). A total of 168 patients (61%) had PR-positive tumours and 263 patients (93%) had Her-2 negative tumours. In all, 169 (71%) patients had luminal A disease and 69 (29%) had luminal B disease. All patients were treated with adjuvant tamoxifen. 71 (25%) patients received adjuvant chemotherapy and 86 (30%) patients received adjuvant radiotherapy while only 29 (10%) patients received both chemotherapy and radiotherapy. Two hundred two patients (71%) had no recurrences, and 82 patients (29%) experienced recurrences. Of these patients, 7 (3%) had bilateral recurrence, 76 cancer-associated deaths and 60 non-cancer deaths.

Table 7.1 The clinicopathological characteristics of patients with ER-positive cohort (n = 285)

Clinicopathological characteristics	Patients, n (%)
Age (≤50/>50 years)	50(18)/234(82)
Size (≤20/21–50/>50 mm)	131(48)/128(47)/14(5)
Grade (I/II/III)	60(22)/141(51)/75(27)
Lymph node (negative/positive)	126(48)/137(52)
NPI (<3.5/3.5–5.5/>5.5)	83(34)/116(47)/47(19)
PR status (negative/positive)	109(39)/168(61)
Her-2 status (negative/positive)	263(93)/19(7)
Ki67 (proliferative index) (low/high)	180(76)/58(24)
Molecular subtype (lum A/lum B)	169(71)/69(29)
Adjuvant endocrine therapy (no/yes)	0(0)/285(100)
Adjuvant chemotherapy (no/yes)	213(75)/71(25)
Adjuvant radiotherapy (no/yes)	199(70)/86(30)
Combined adjuvant chemotherapy and radiotherapy (no/yes)	256(90)/29(10)
Alive with no recurrence/recurrence/bilateral	202(71)/75(26)/7(3)
No recurrence on tamoxifen/recurrence/bilateral	223(79)/55(19)/6(2)
Alive/cancer death/non-cancer death	149(52)/76(27)/60(21)

Table showing the number of patients with clinical characteristics in patients from the ER-positive cohort including age, tumour size, grade, lymph node, NPI, PR status, Her-2 status, Ki67, molecular subtype, adjuvant endocrine therapy, adjuvant chemotherapy, and adjuvant radiotherapy.

7.3.2 Expression of HIF-1α (1)

7.3.2.1 Immunohistochemistry of HIF-1α (1)

In 68 (24%) patients, there was a tissue core missing, therefore, HIF-1α (1) expression was analysed in 217 (76%) of the patients from the ER-positive cohort (n = 285). HIF-1α (1) was expressed in the nuclei and cytoplasm of tumour cells (Figure 7.1A). Histograms showing the distribution of histoscores for cytoplasmic HIF-1α (1) ranged from 0 to 180 with a mean score of 103.59, for nuclear HIF-1α (1) ranged from 0 to 183 with a mean score of 101.73 and data were relatively normally distributed (Figure 7.1B). A correlation coefficient of 0.843 and 0.850 for cytoplasmic and nuclear HIF-1α (1), respectively was obtained between QuPath and manual scores. Threshold from the previous cohort was applied for HIF-1α (1) expression. The optimum threshold scores for high and low cytoplasmic and nuclear HIF-1α (1) expression groups were 104 and 156, respectively. Based on R threshold levels, low cytoplasmic HIF-1α (1) expression was detected in 113 (52%) samples, while 104 (48%) samples had high cytoplasmic expression. 87 (40%) patients showed low nuclear HIF-1α (1), and 130 (60%) showed high nuclear expression.

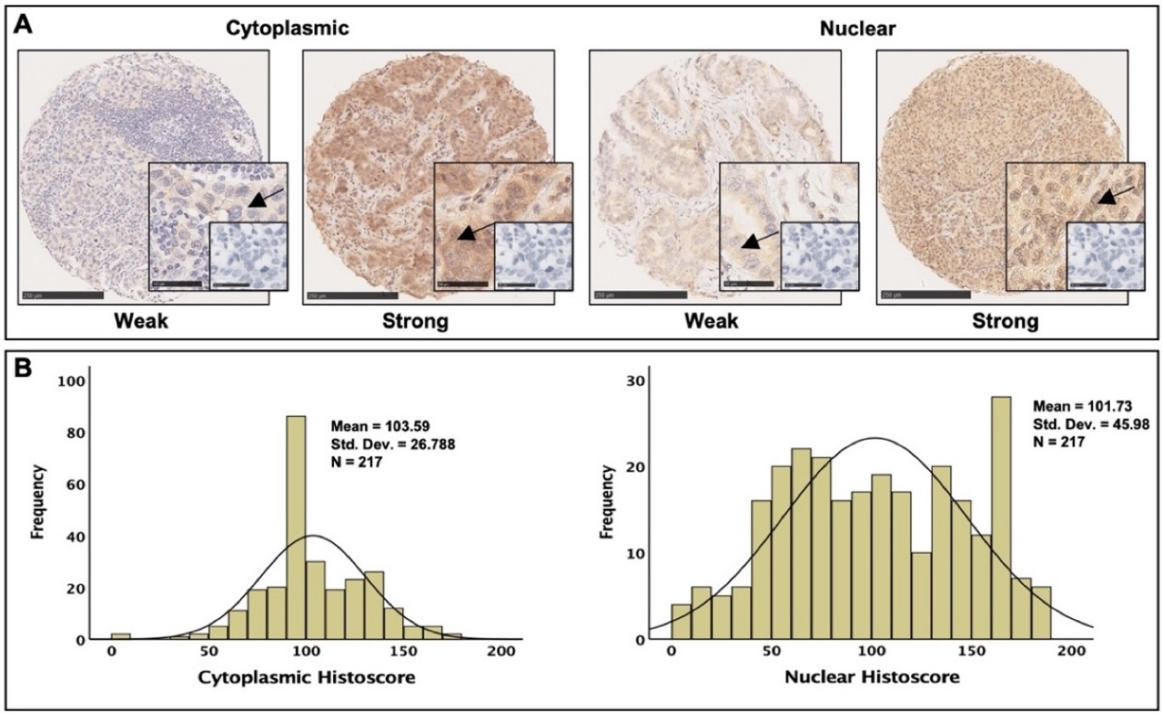

Figure 7.1 Representative immunohistochemical images and scoring distribution for HIF-1α (1).

Representative images of weak and strong cytoplasmic and nuclear staining of HIF-1α (1) [A]. Representative images of histogram showing the range of scores obtained for cytoplasmic and nuclear tumour HIF-1α (1) expression and distribution pattern of data [B].

7.3.2.2 Association of HIF-1α (1) with clinical outcome in ER-positive patients

Kaplan-Meier survival estimates for HIF-1α (1) are presented in Figure 7.2. The P-value reported on the Figures is from the log-rank test. When patients were split into two groups based on low and high HIF-1α (1), there was statistically significant poorer DFS (P = 0.032), and OS (P = 0.002) with high level of cytoplasmic HIF-1α (1) (Figure 7.2C, E). However, high cytoplasmic HIF-1α (1) expression did not attain statistical significance in predicting decreased RFS in ER-positive breast cancer (P = 0.552) (Figure 7.2A). Similarly, high nuclear HIF-1α (1) expression was associated with worse survival outcomes in term of DFS (P = 0.009), and OS (P = 0.002) (Figure 7.2D, F). There was no significant association between high nuclear HIF-1α (1) expression and RFS (P = 0.541) (Figure 7.2B). Based on text life table analysis, the 10-year DFS of patients with high cytoplasmic HIF-1α (1) expression was 7% versus 31% with low HIF-1α (1) expression (P = 0.887), and the 10-year OS of patients with high cytoplasmic HIF-1α (1) expression was 9% versus 35% with low HIF-1α (1) expression (P = 0.244). Also, the 10-year DFS of patients with high nuclear HIF-1α (1) expression was 13% versus 26% with low HIF-1α (1) expression (P = 0.220), and the 10-year OS of patients with high nuclear HIF-1α (1) expression was 15% versus 31% with low HIF-1α (1) expression (P = 0.052) as summarized in Table 7.2.

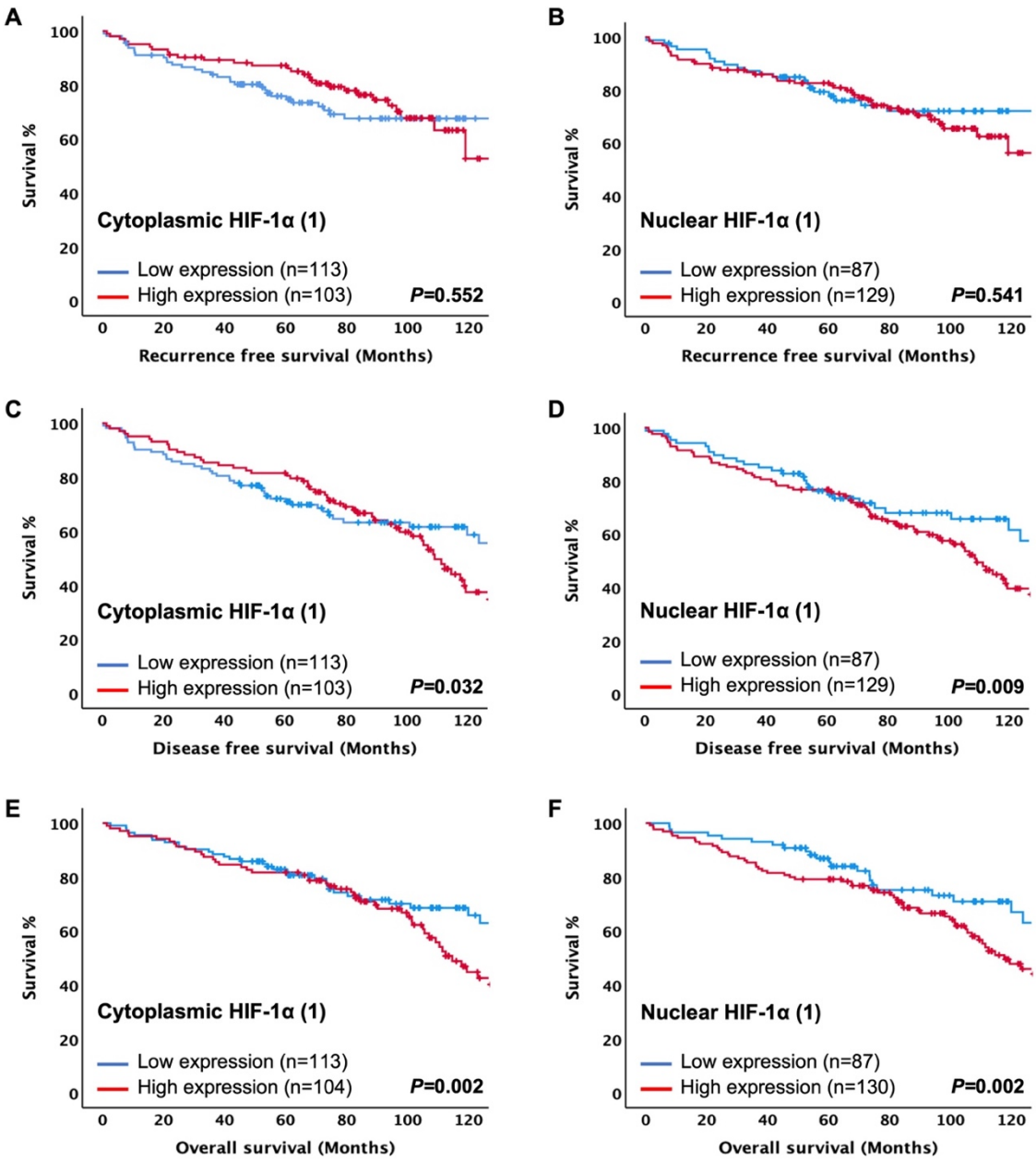

Figure 7.2 Expression of HIF-1α (1) and clinical outcome in the entire ER-positive breast cancer.

Kaplan-Meier curves showing associations between cytoplasmic and nuclear HIF-1α (1) with recurrence free survival [A, B], disease-free survival [C, D], and overall survival [E, F].

Table 7.2 Association between hypoxic markers and survival in ER-positive breast cancer patients (n = 285)

Markers	Recurrence free survival (RFS)						Disease-free survival (DFS)						Overall survival (OS)					
	Cytoplasmic			Membrane/Nuclear			Cytoplasmic			Membrane/Nuclear			Cytoplasmic			Membrane/Nuclear		
	n (%)	10yr-RFS (SE)	P-value	n (%)	10yr-RFS (SE)	P-value	n (%)	10yr-DFS (SE)	P-value	n (%)	10yr-DFS (SE)	P-value	n (%)	10yr-OS (SE)	P-value	n (%)	10yr-OS (SE)	P-value
HIF-1α (1)			0.552			0.541			**0.032**			**0.009**			**0.002**			**0.002**
Low	113(52)	51(10)		87(40)	50(14)		113(52)	31(9)		87(40)	26(10)		113(52)	35(9)		87(40)	31(10)	
High	103(48)	59(7)		129(60)	59(6)		103(48)	7(4)		129(60)	13(5)		104(48)	9(4)		130(60)	15(5)	
HIF-1α (2)			0.495			0.825			**0.023**			0.132			**0.005**			0.078
Low	23(8)	53(16)		32(11)	53(13)		23(8)	23(14)		32(11)	35(12)		23(8)	35(16)		32(11)	32(11)	
High	261(92)	52(8)		252(89)	50(8)		261(92)	13(4)		252(89)	11(4)		262(92)	15(4)		253(89)	14(4)	
HIF-2α			0.239			0.469			0.554			0.923			0.949			0.561
Low	44(16)	47(10)		36(13)	49(12)		44(16)	11(8)		36(13)	9(9)		45(16)	16(9)		37(13)	9(8)	
High	236(84)	52(8)		244(87)	52(8)		236(84)	15(4)		244(87)	15(4)		236(84)	18(4)		244(87)	19(4)	
CAIX			**0.014**			0.379			**0.008**			0.612			0.118			0.344
Low	182(72)	56(10)		238(94)	54(8)		182(72)	13(5)		238(94)	15(4)		183(72)	17(5)		239(94)	18(4)	
High	71(28)	36(11)		15(6)	17(21)		71(28)	13(7)		15(6)	0(0)		71(28)	16(7)		15(6)	0(0)	

Table showing the number of patients and associations with survival for each hypoxic marker in ER-positive cohort.

Univariate analysis with the use of the Cox proportional hazard model showed the same statistical tendency as that obtained with the use of the log-rank test. In term of DFS, both cytoplasmic and nuclear HIF-1α (1) had prognostic value. However, when entered into multivariate analysis and comparing them directly against DFS, nuclear but not cytoplasmic HIF-1α (1) retained an independent prognostic value (HR = 1.85, 95% CI: 1.10–3.11, P = 0.019) when combined with tumour size, lymph node status, NPI, Ki67, and molecular subtype in the entire cohort (Table 7.3).

Table 7.3 Univariate and multivariate analysis for disease-free survival of HIF-1α (1) and clinicopathological characteristics in the entire ER-positive cohort (n=285)

Clinicopathological characteristics	Univariate analysis		Multivariate analysis	
	HR (95% CI)	P-value	HR (95% CI)	P-value
Age (<50/>50)	1.57 (0.93–2.65)	0.089	-	-
Size (≤20/21–50/>50 mm)	1.65 (1.24–2.21)	**0.001**	2.11 (1.36–3.28)	**0.001**
Grade (I/II/III)	1.25 (0.99–1.59)	0.066	-	-
Lymph node (negative/positive)	1.69 (1.19–2.40)	**0.004**	1.16 (0.64–2.12)	0.622
NPI (<3.5/3.5–5.5/>5.5)	1.63 (1.27–2.09)	**<0.001**	1.25 (0.84–1.86)	0.273
PR (negative/positive)	0.78 (0.56–1.09)	0.152	-	-
Her-2 (negative/positive)	0.86 (0.42–1.76)	0.682	-	-
Ki67 (proliferative index) (low/high)	1.83 (1.24–2.70)	**0.002**	1.14 (0.26–4.93)	0.860
Molecular subtype (lum A/lum B)	1.69 (1.16–2.46)	**0.007**	1.99 (1.23–3.24)	**0.005**
Adjuvant chemotherapy (no/yes)	0.99 (0.65–1.51)	0.964	-	-
Adjuvant radiotherapy (no/yes)	0.78 (0.54–1.13)	0.189	-	-
Cytoplasmic HIF-1α (1) (low/high)	1.54 (1.04–2.29)	**0.032**	0.89 (0.43–1.87)	0.774
Nuclear HIF-1α (1) (low/high)	1.75 (1.14–2.68)	**0.006**	1.85 (1.10–3.11)	**0.019**

Multivariate Cox regression model was adjusted for age, tumour size, grade, lymph node, NPI, PR status, Her-2 status, Ki67, molecular subtype, adjuvant chemotherapy, and adjuvant radiotherapy.

Similar to DFS, when entered into multivariate analysis, nuclear HIF-1α (1) was superior to cytoplasmic HIF-1α (1) in predicting OS in the entire cohort (HR = 1.85, 95% CI: 1.08–3.19, P = 0.026) when combined with patient's age, tumour size, lymph node status, NPI, Ki67, and molecular subtype (Table 7.4).

Table 7.4 Univariate and multivariate analysis for overall survival of HIF-1α (1) and clinicopathological characteristics in the entire ER-positive cohort (n = 285)

Clinicopathological characteristics	Univariate analysis		Multivariate analysis	
	HR (95% CI)	P-value	HR (95% CI)	P-value
Age (<50/>50)	3.02 (1.54–5.95)	**0.001**	3.69 (1.14–11.97)	**0.030**
Size (≤20/21–50/>50 mm)	1.71 (1.27–2.32)	**0.001**	1.96 (1.22–3.14)	**0.005**
Grade (I/II/III)	1.26 (0.98–1.61)	0.073	-	-
Lymph node (negative/positive)	1.64 (1.14–2.38)	**0.008**	1.39 (0.83–2.34)	0.212
NPI (<3.5/3.5–5.5/>5.5)	1.56 (1.20–2.04)	**0.001**	1.15 (0.69–1.89)	0.591
PR (negative/positive)	0.83 (0.59–1.17)	0.290	-	-
Her-2 (negative/positive)	1.05 (0.51–2.15)	0.891	-	-
Ki67 (proliferative index) (low/high)	1.65 (1.10–2.48)	**0.016**	0.79 (0.18–3.47)	0.756
Molecular subtype (lum A/lum B)	1.57 (1.06–2.32)	**0.026**	2.08 (1.25–3.45)	**0.005**
Adjuvant chemotherapy (no/yes)	0.93 (0.59–1.46)	0.737	-	-
Adjuvant radiotherapy (no/yes)	0.75 (0.50–1.12)	0.157	-	-
Cytoplasmic HIF-1α (1) (low/high)	1.92 (1.26–2.93)	**0.002**	1.27 (0.60–2.69)	0.530
Nuclear HIF-1α (1) (low/high)	2.06 (1.29–3.28)	**0.002**	1.85 (1.08–3.19)	**0.026**

Multivariate Cox regression model was adjusted for age, tumour size, grade, lymph node, NPI, PR status, Her-2 status, Ki67, molecular subtype, adjuvant chemotherapy, and adjuvant radiotherapy.

.

7.3.2.3 Associations between nuclear HIF-1α (1) expression and clinicopathological characteristics of ER-positive patients

Chi-squared analysis was performed in order to determine whether expression of nuclear HIF-1α (1) was associated with any clinicopathological characteristics of the patients in the ER-positive cohort. As shown in Table 7.5, high expression of nuclear HIF-1α (1) was associated with increasing patient's age (P = 0.004), tumour size (P = 0.017), and positive PR status (P = 0.033).

Table 7.5 Association between nuclear HIF-1α (1) expression and clinicopathological characteristics in the entire ER-positive cohort (n = 285)

Clinicopathological characteristics	**Nuclear HIF-1α (1)**		
	Low n = 69 (26%)	High n = 199 (74%)	P-value
Age (≤50/>50 years)	25(29)/61(71)	17(13)/113(87)	**0.004**
Tumour size (≤20/21–50/>50 mm)	29(37)/43(54)/7(9)	64(50)/61(48)/3(2)	**0.017**
Grade (I/II/III)	13(15)/45(52)/28(33)	31(25)/58(46)/36(29)	0.177
Lymph node (negative/positive)	33(40)/49(60)	61(51)/58(49)	0.123
NPI (<3.5/3.5–5.5/>5.5)	19(25)/38(51)/18(24)	40(35)/54(48)/19(17)	0.101
PR status (negative/positive)	40(46)/46(54)	40(32)/85(68)	**0.033**
Her-2 status (negative/positive)	81(93)/6(7)	119(92)/10(8)	0.813
Ki67 (proliferative index) (low/high)	58(76)/18(24)	88(75)/30(25)	0.784
Molecular subtype (lum A/lum B)	55(72)/21(28)	83(70)/35(30)	0.760
Adjuvant chemotherapy (no/yes)	60(69)/27(31)	103(79)/27(21)	0.088
Adjuvant radiotherapy (no/yes)	59(68)28(32)	93(72)/37(28)	0.558

Multivariate Cox regression model was adjusted for age, tumour size, grade, lymph node, NPI, PR status, Her-2 status, Ki67, molecular subtype, adjuvant chemotherapy, and adjuvant radiotherapy.

7.3.2.4 Expression of nuclear HIF-1α (1) and clinical outcome in different luminal subtypes

In order to determine whether nuclear expression of HIF-1α (1) was associated with clinical outcome in specific ER-positive subtype, the cohort was subdivided into luminal A and luminal B tumours. The Kaplan-Meier survival curves for nuclear HIF-1α (1) expression were plotted, and log-rank test was performed to compare between groups. High nuclear HIF-1α (1) was significantly associated with poorer DFS (P = 0.013), and OS (P = 0.003) in luminal A (Figure 7.3A, C). In contrast, no association was found with luminal B disease for DFS, and OS (P = 0.587, 0.210, respectively) (Figure 7.3B, D).

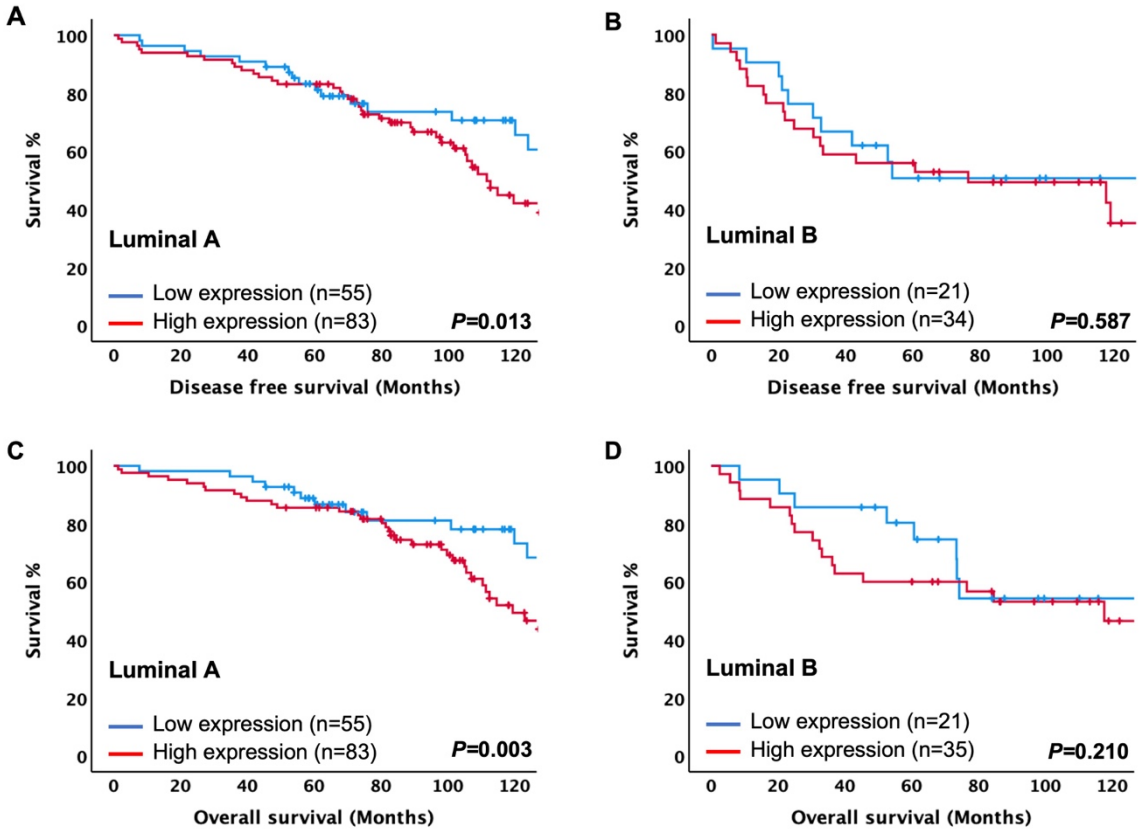

Figure 7.3 Expression of nuclear HIF-1α (1) and survival in ER-positive breast cancer subtypes.

Kaplan-Meier curves showing associations between nuclear HIF-1α (1) expression and patients' survival in luminal A disease [A, C], and in luminal B disease [B, D].

Multivariate analysis suggested that nuclear expression of HIF-1α (1) was an independent unfavourable prognostic marker for DFS (HR = 1.98, 95% CI: 1.02–3.83, P = 0.042) when combined with NPI in luminal A tumour (Table 7.6).

Table 7.6 Univariate and multivariate analysis for disease-free survival of nuclear HIF-1α (1) and clinicopathological characteristics in luminal A tumours (n = 169)

Clinicopathological characteristics	Luminal A			
	Univariate analysis		Multivariate analysis	
	HR (95% CI)	P-value	HR (95% CI)	P-value
Age (<50/>50)	1.97 (0.91–4.27)	0.087	-	-
Size (≤20/21–50/>50 mm)	1.34 (0.90–1.99)	0.151	-	-
Grade (I/II/III)	1.07 (0.76–1.49)	0.714	-	-
Lymph node (negative/positive)	1.43 (0.92–2.23)	0.117	-	-
NPI (<3.5/3.5–5.5/>5.5)	1.42 (1.02–1.99)	**0.040**	1.64 (1.07–2.51)	**0.023**
PR status (negative/positive)	0.92 (0.59–1.43)	0.705	-	-
Adjuvant chemotherapy (no/yes)	0.94 (0.49–1.79)	0.853	-	-
Adjuvant radiotherapy (no/yes)	0.64 (0.38–1.06)	0.085	-	-
Nuclear HIF-1α (1) (low/high)	2.04 (1.15–3.62)	**0.013**	1.98 (1.02–3.83)	**0.042**

Multivariate Cox regression model was adjusted for age, tumour size, grade, lymph node, NPI, PR status, adjuvant chemotherapy, and adjuvant radiotherapy.

Similarly, in multivariate logistic regression analysis, nuclear HIF-1α (1) expression was independent prognostic marker for OS (HR = 2.08, 95% CI: 1.11–3.89, P = 0.022) when combined with patient's age in luminal A tumour (Table 7.7).

Table 7.7 Univariate and multivariate analysis for overall survival of nuclear HIF-1α (1) and clinicopathological characteristics in luminal A tumours (n = 169)

Clinicopathological characteristics	Luminal A			
	Univariate analysis		Multivariate analysis	
	HR (95 % CI)	P-value	HR (95% CI)	P-value
Age (<50/>50)	3.29 (1.20–9.04)	**0.020**	6.18 (0.84–45.49)	0.074
Size (≤20/21–50/>50 mm)	1.37 (0.90–2.09)	0.139	-	-
Grade (I/II/III)	1.08 (0.76–1.54)	0.658	-	-
Lymph node (negative/positive)	1.30 (0.82–2.07)	0.264	-	-
NPI (<3.5/3.5–5.5/>5.5)	1.36 (0.95–1.94)	0.092	-	-
PR status (negative/positive)	0.95 (0.59–1.51)	0.824	-	-
Adjuvant chemotherapy (no/yes)	0.89 (0.44–1.82)	0.766	-	-
Adjuvant radiotherapy (no/yes)	0.69 (0.40–1.19)	0.180	-	-
Nuclear HIF-1α (1) (low/high)	2.49 (1.34–4.65)	**0.003**	2.08 (1.11–3.89)	**0.022**

Multivariate Cox regression model was adjusted for age, tumour size, grade, lymph node, NPI, PR status, adjuvant chemotherapy, and adjuvant radiotherapy.

7.3.3 Expression of HIF-1α (2)

7.3.3.1 Immunohistochemistry of HIF-1α (2)

The expression of HIF-1α (2) was analysed in 285 patients from ER-positive cohort. HIF-1α (2) was clearly expressed in the nuclei and cytoplasm of tumour cells. An example of immunostaining of low and high expression of HIF-1α (2) is shown in Figure 7.4A. The histoscore for cytoplasmic expression of HIF-1α (2) ranged from 0 to 300 with a mean score of 127.42, and the histoscore for nuclear expression of HIF-1α (2) ranged from 0 to 260 with a mean score of 216.33 and data were relatively normally distributed as shown in histogram plot (Figure 7.4B). There was good correlation between observers with an ICCC score of 0.996 for cytoplasmic and 0.910 nuclear HIF-1α (2).

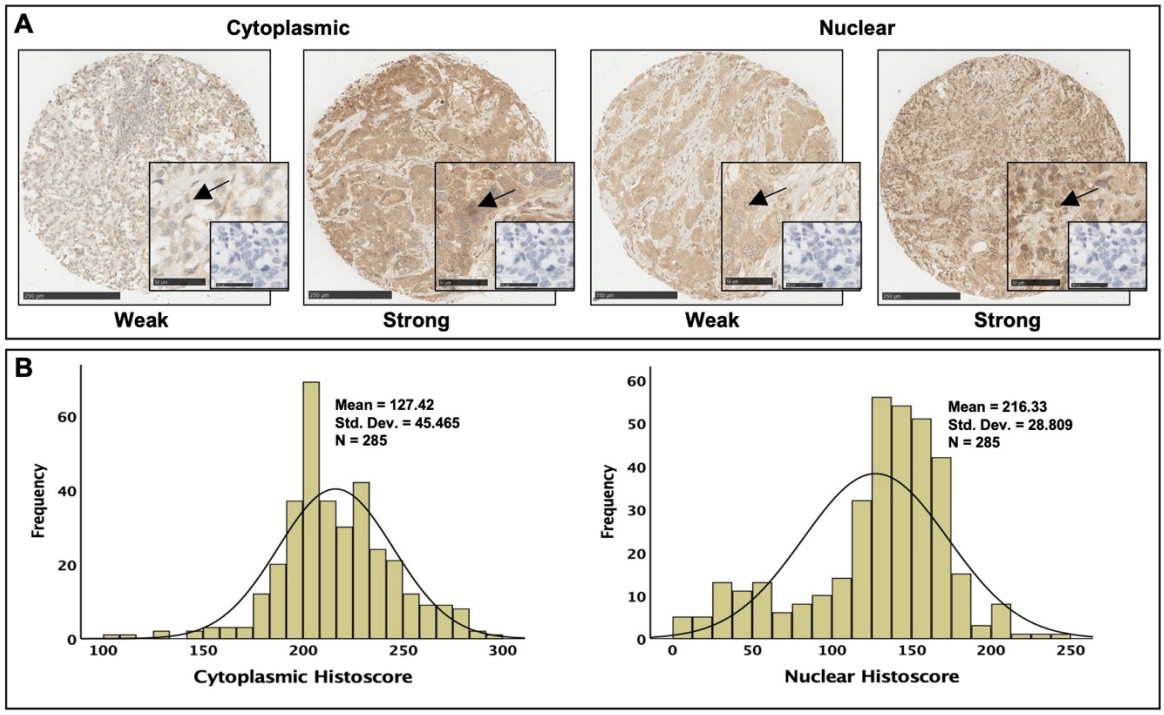

Figure 7.4 Representative immunohistochemical images and scoring distribution for HIF-1α (2).

Representative images of weak and strong cytoplasmic and nuclear staining of HIF-1α (2) [A]. Representative images of histogram showing the range of scores obtained for cytoplasmic and nuclear tumour HIF-1α (2) expression and distribution pattern of data [B].

7.3.4 Expression of HIF-2α

7.3.4.1 Immunohistochemistry of HIF-2α

The expression of HIF-2α was analysed in 281 (99%) of the patients from the ER-positive cohort (n = 285). In 4 (1%) patients, there was a tissue core missing and so HIF-2α staining could not be carried out, and they were excluded from the analysis. HIF-2α was clearly expressed in the nuclei and cytoplasm of tumour cells (Figure 7.5A). Histograms showing the distribution of histoscores for cytoplasmic HIF-2α ranged from 0 to 290 with a mean score of 219.33 and for nuclear ranged from 0 to 215 with a mean score of 143.53 and data were relatively normally distributed as shown in histogram plot (Figure 7.5B). A correlation coefficient of 0.773 and 0.792 for cytoplasmic and nuclear HIF-2α, respectively, was obtained between two observers. The threshold values were obtained from previous cohort in order to subdivide the HIF-2α into low and high expression. The optimal threshold determined was 113 and 173 for cytoplasmic and nuclear HIF-2α expression, respectively. Based on R threshold, low cytoplasmic HIF-2α expression of malignant cell was only observed in 45 (16%) and high cytoplasmic protein was 236 (84%). Low nuclear HIF-2α expression was detected in 37 (13%), and 244 patients (87%) with high protein expression.

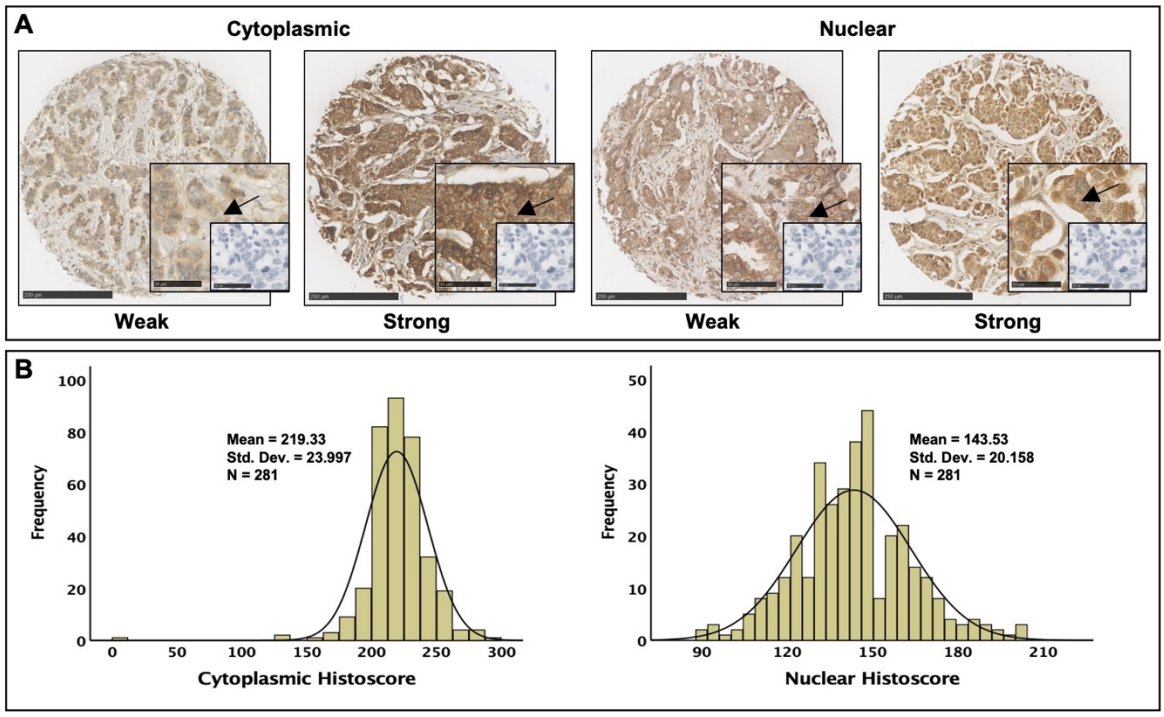

Figure 7.5 Representative immunohistochemical images and scoring distribution for HIF-2α.

Representative images of weak and strong cytoplasmic and nuclear staining of HIF-2α [A]. Representative images of histogram showing the range of scores obtained for cytoplasmic and nuclear tumour HIF-2α expression and distribution pattern of data [B].

7.3.4.2 Association of HIF-2α with clinical outcome in ER-positive patients

Survival analyses by the Kaplan-Meier method were compared by log-rank test. Cytoplasmic HIF-2α expression was not associated with ER-positive patient survival in term of RFS (P = 0.239), DFS (P = 0.554), and OS (P = 0.949) (Figure 7.6A, C, E). Similarly, nuclear HIF-2α expression failed to demonstrate any association with RFS (P = 0.469), DFS (P = 0.923), and OS (P = 0.561) in ER-positive breast cancer patients (Figure 7.6B, D, F). Because there was no survival end point significant, HIF-2α was not be investigated further.

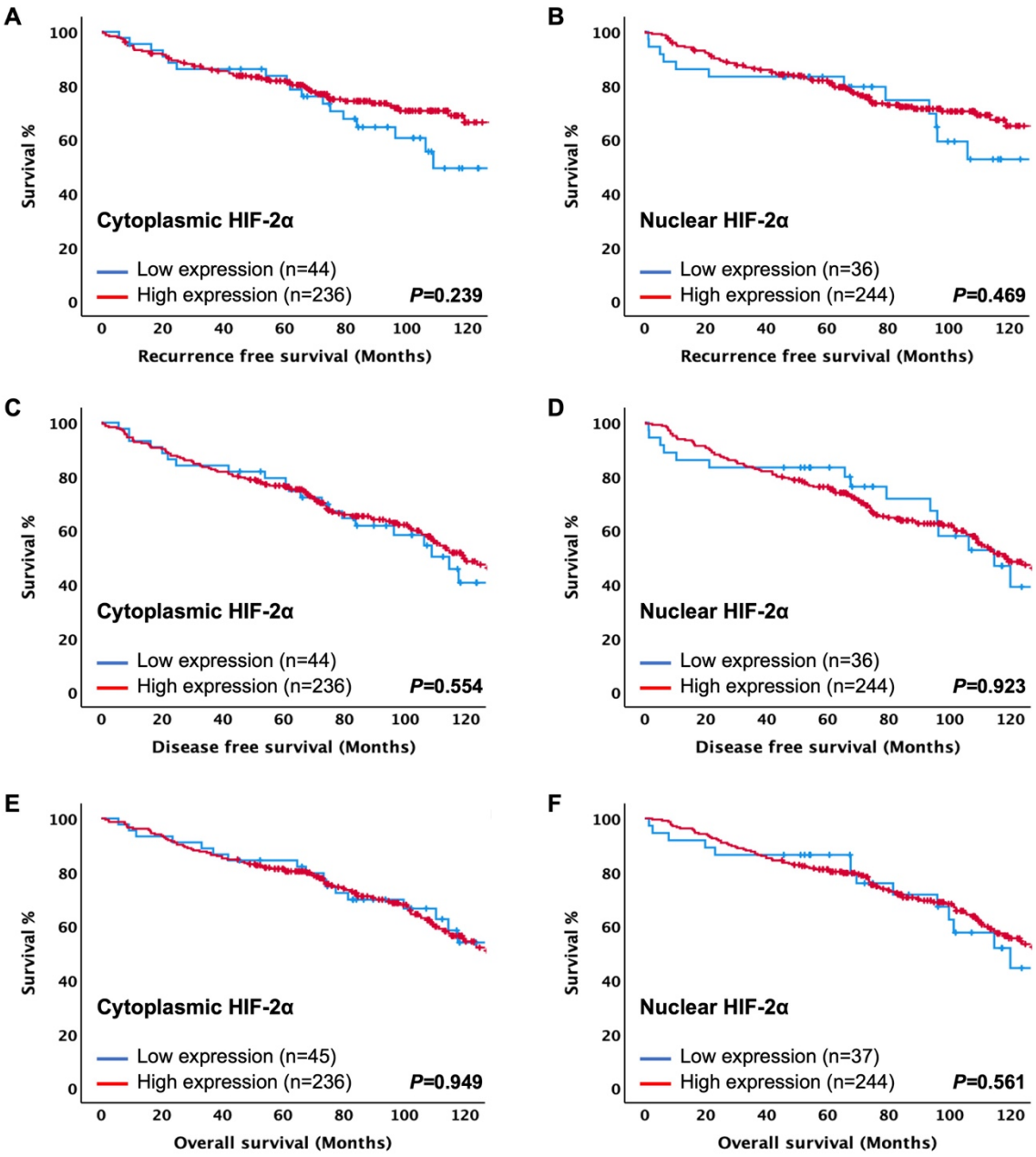

Figure 7.6 Expression of HIF-2α and clinical outcome in the entire ER-positive breast cancer.

Kaplan-Meier curves showing associations between cytoplasmic and nuclear HIF-2α with recurrence free survival [A, B], disease-free survival [C, D], and overall survival [E, F].

7.3.5 Expression of CAIX

7.3.5.1 Immunohistochemistry of CAIX

Of the 285 patients, 31 (11%) had a tissue core missing and so CAIX staining could not be carried out, and they were excluded from the analysis. Therefore, the expression of CAIX was assessed in 254 patients. CAIX was clearly expressed in the cytoplasm and membrane of tumour cells (Figure 7.7A). Weighted Histoscores for cytoplasmic CAIX expression ranged from 0 to 220 with a mean score of 19.57, and for membranous scores ranged from 0 to 145 with a mean score of 5.98. A histogram was plotted to visualise the range of scores and data showed a positively skewed pattern (Figure 7.7B). An ICCC of 0.889 for cytoplasmic and 0.840 for membranous CAIX was obtained between observers' scores. Using threshold values obtained from previous cohort (18 for cytoplasmic and 30 for membranous CAIX), 71 patients had high cytoplasmic expression and 183 patients had low cytoplasmic expression. 15 patients had high membranous expression and 239 patients had low membranous expression.

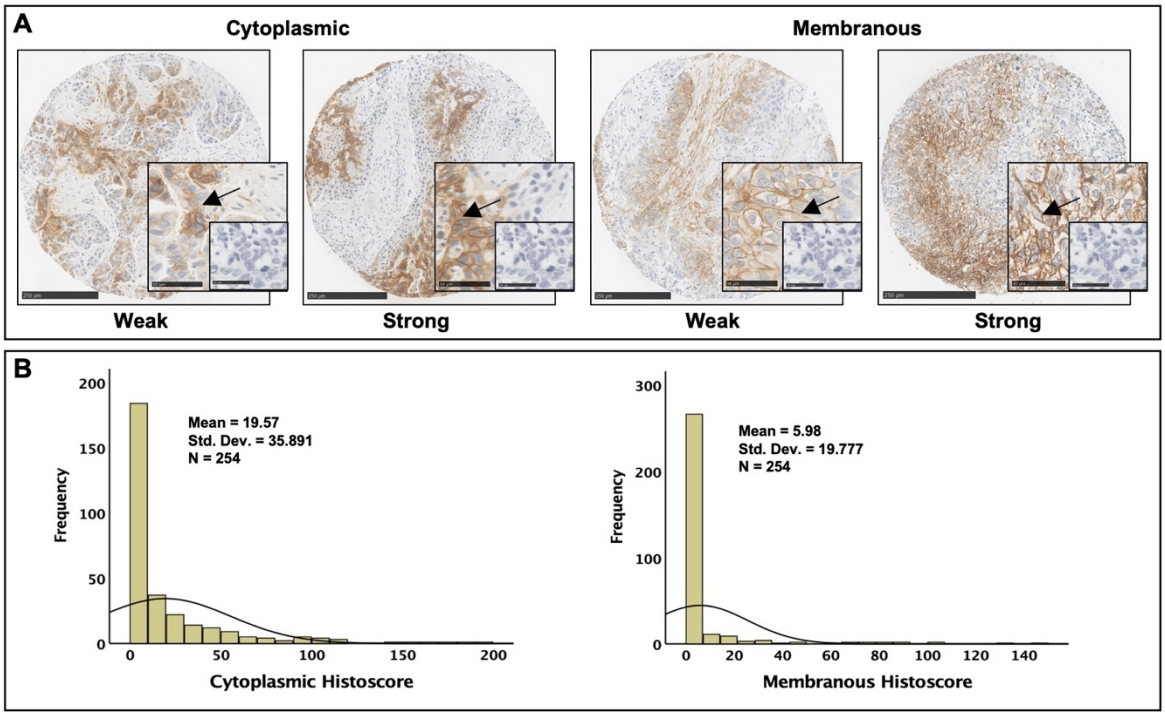

Figure 7.7 Representative immunohistochemical images and scoring distribution for CAIX.

Representative images of weak and strong cytoplasmic and membranous staining of CAIX [A]. Representative images of histogram showing the range of scores obtained for cytoplasmic and membranous tumour CAIX expression and distribution pattern of data [B].

7.3.5.2 Association of CAIX with clinical outcome in patients with ER-positive breast cancer

To determine whether CAIX expression was significantly associated with clinical outcome, Kaplan-Meier survival curves for cytoplasmic and membranous expression of CAIX were plotted and low and high expression were compared using the log-rank test. Univariate survival analysis for the entire group of patients showed association between cytoplasmic CAIX and RFS (P = 0.014), DFS (P = 0.008), however, no association was observed with OS (P = 0.118) as shown in Figure 7.8 (A, C, E). In contrast, no correlation was found with membranous CAIX protein and any clinical outcomes including RFS (P = 0.379), DFS (P = 0.612), and OS (P = 0.344) (Figure 7.8B, D F). The 10-year DFS of patients with high cytoplasmic CAIX expression compared with patients with low cytoplasmic CAIX expression was significant (P = 0.012) and 10-year OS showed borderline significant (P = 0.055) (Table 7.2).

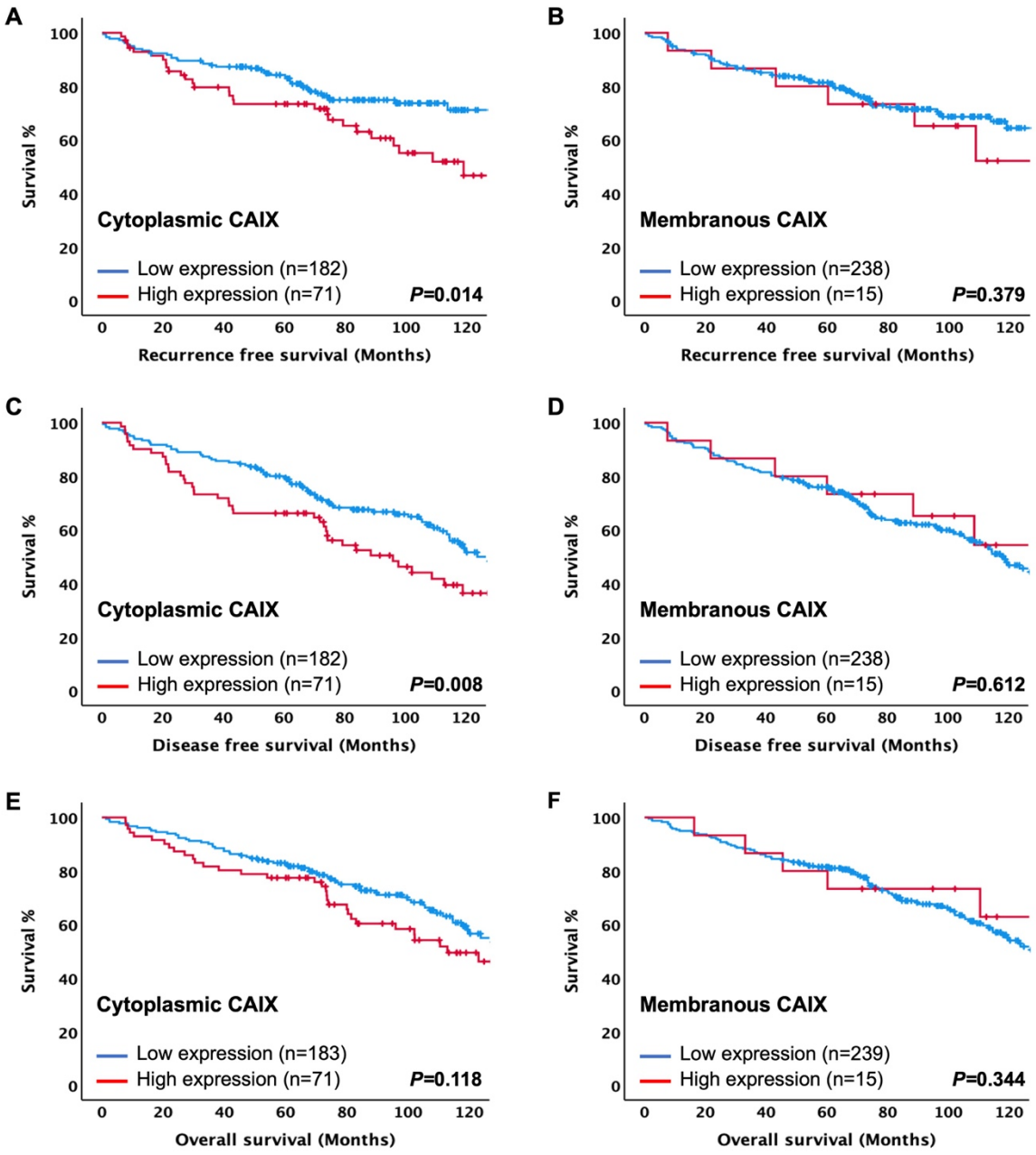

Figure 7.8 Expression of CAIX and clinical outcome in the entire ER-positive breast cancer.

Kaplan-Meier curves showing associations between cytoplasmic and membranous CAIX with recurrence free survival [A, B], disease-free survival [C, D], and overall survival [E, F].

In term of RFS, cytoplasmic CAIX has prognostic value. When entered into multivariate analysis, cytoplasmic CAIX retained an independent prognostic marker (HR = 2.09, 95% CI: 1.17–3.75, P = 0.013) when combined with tumour size, grade, lymph node status, NPI, PR status, Ki67, and molecular subtype in the entire cohort (Table 7.8).

Table 7.8 Univariate and multivariate analysis for recurrence free survival of cytoplasmic CAIX and clinicopathological characteristics in the entire ER-positive cohort (n = 285)

Clinicopathological characteristics	Cytoplasmic CAIX			
	Univariate analysis		Multivariate analysis	
	HR (95% CI)	P-value	HR (95% CI)	P-value
Age (<50/>50)	1.02 (0.58–1.79)	0.943	-	-
Size (≤20/21–50/>50 mm)	2.29 (1.59–3.29)	**<0.001**	2.56 (1.52–4.29)	**<0.001**
Grade (I/II/III)	1.72 (1.24–2.39)	**0.001**	1.04 (0.61–1.78)	0.875
Lymph node (negative/positive)	2.87 (1.71–4.81)	**<0.001**	2.14 (1.14–4.03)	**0.019**
NPI (<3.5/3.5–5.5/>5.5)	2.63 (1.84–3.76)	**<0.001**	1.19 (0.66–2.14)	0.564
PR (negative/positive)	0.64 (0.41–0.99)	**0.043**	0.71 (0.40–1.24)	0.225
Her-2 (negative/positive)	1.28 (0.56–2.95)	0.558	-	-
Ki67 (proliferative index) (low/high)	2.37 (1.46–3.86)	**0.001**	1.85 (1.04–3.28)	**0.036**
Molecular subtype (lum A/lum B)	2.29 (1.42–3.69)	**0.001**	1.10 (0.24–5.04)	0.898
Adjuvant chemotherapy (no/yes)	1.21 (0.73–1.99)	0.466	-	-
Adjuvant radiotherapy (no/yes)	0.95 (0.59–1.52)	0.838	-	-
Cytoplasmic CAIX (low/high)	1.79 (1.12–2.86)	**0.014**	2.09 (1.17–3.75)	**0.013**

Multivariate Cox regression model was adjusted for age, tumour size, grade, lymph node, NPI, PR status, Her-2 status, Ki67, molecular subtype, adjuvant chemotherapy, and adjuvant radiotherapy.

Similar to RFS, when entered into multivariate analysis, cytoplasmic CAIX was an independent prognostic marker for DFS (HR = 1.74, 95% CI: 1.08–2.82, P = 0.023) when combined with tumour size, lymph node status, NPI, Ki67, and molecular subtype in the entire cohort (Table 7.9).

Table 7.9 Univariate and multivariate analysis for disease-free survival of cytoplasmic CAIX and clinicopathological characteristics in the entire ER-positive cohort (n = 285)

Clinicopathological characteristics	Cytoplasmic CAIX			
	Univariate analysis		Multivariate analysis	
	HR (95% CI)	P-value	HR (95% CI)	P-value
Age (<50/>50)	1.57 (0.93–2.65)	0.089	-	-
Size (≤20/21–50/>50 mm)	1.65 (1.24–2.21)	**0.001**	1.84 (1.25–2.69)	**0.002**
Grade (I/II/III)	1.25 (0.99–1.59)	0.066	-	-
Lymph node (negative/positive)	1.69 (1.19–2.40)	**0.004**	1.40 (0.91–2.15)	0.123
NPI (<3.5/3.5–5.5/>5.5)	1.63 (1.27–2.09)	**<0.001**	1.07 (0.69–1.64)	0.759
PR (negative/positive)	0.78 (0.56–1.09)	0.152	-	-
Her-2 (negative/positive)	0.86 (0.42–1.76)	0.682	-	-
Ki67 (proliferative index) (low/high)	1.83 (1.24–2.70)	**0.002**	1.65 (1.06–2.57)	**0.026**
Molecular subtype (lum A/lum B)	1.69 (1.16–2.46)	**0.007**	1.03 (0.24–4.39)	0.974
Adjuvant chemotherapy (no/yes)	0.99 (0.65–1.51)	0.964	-	-
Adjuvant radiotherapy (no/yes)	0.78 (0.54–1.13)	0.189	-	-
Cytoplasmic CAIX (low/high)	1.64 (1.14–2.37)	**0.008**	1.74 (1.08-2.82)	**0.023**

Multivariate Cox regression model was adjusted for age, tumour size, grade, lymph node, NPI, PR status, Her-2 status, Ki67, Molecular subtype, adjuvant chemotherapy, and adjuvant radiotherapy.

7.3.5.3 Associations between cytoplasmic CAIX expression and clinicopathological characteristics of ER-positive patients

A significant association was found between high cytoplasmic CAIX expression in tumour cells and patient's age (P = 0.027) using Chi-square test as shown in Table 7.10.

Table 7.10 Association between cytoplasmic CAIX expression and clinicopathological characteristics in the entire ER-positive cohort (n = 285)

Clinicopathological characteristics	Cytoplasmic CAIX		
	Low n = 183 (72%)	High n = 71 (28%)	P-value
Age (≤50/>50 years)	27(15)/156(85)	19(27)/51(73)	**0.027**
Tumour size (≤20/21–50/>50 mm)	78(44)/90(51)/8(5)	36(55)/26(39)/4(6)	0.304
Grade (I/II/III)	33(18)/96(54)/51(28)	18(28)/28(43)/19(29)	0.403
Lymph node (negative/positive)	81(47)/93(53)	30(48)/33(52)	0.884
NPI (<3.5/3.5–5.5/>5.5)	52(32)/79(48)/34(20)	19(35)/26(47)/10(18)	0.886
PR status (negative/positive)	66(37)/112(63)	28(41)/40(59)	0.555
Her-2 status (negative/positive)	172(95)/10(5)	63(90)/7(10)	0.218
Ki67 (proliferative index) (low/high)	120(76)/38(24)	45(71)/18(29)	0.489
Molecular subtype (lum A/lum B)	114(72)/44(28)	42(67)/21(33)	0.422
Adjuvant chemotherapy (no/yes)	141(78)/41(22)	52(73)/19(27)	0.481
Adjuvant radiotherapy (no/yes)	129(71)54(29)	52(73)/19(27)	0.663

Chi-squared table of associations for cytoplasmic CAIX expression and clinical prognostic factors including age, tumour size, grade, lymph node, NPI, PR status, Her-2 status, Ki67, molecular subtype, adjuvant chemotherapy, and adjuvant radiotherapy.

7.3.5.4 Expression of CAIX and clinical outcome in different luminal subtypes

In order to determine whether CAIX expression was associated with clinical outcome in specific ER-positive subtype, the cohort was subdivided into luminal A and luminal B tumours. Kaplan-Meier survival curves were constructed, and the log-rank test was used to assess any differences in survival time between CAIX levels. Univariate survival analysis revealed that high levels of cytoplasmic CAIX were correlated strongly with shortened RFS

(P = 0.018), DFS (P = 0.001) and OS (P = 0.003) in patients with luminal B but not with luminal A disease (P = 0.586, 0.814, 0.494, respectively) as shown in Figure 7.9 (A-F).

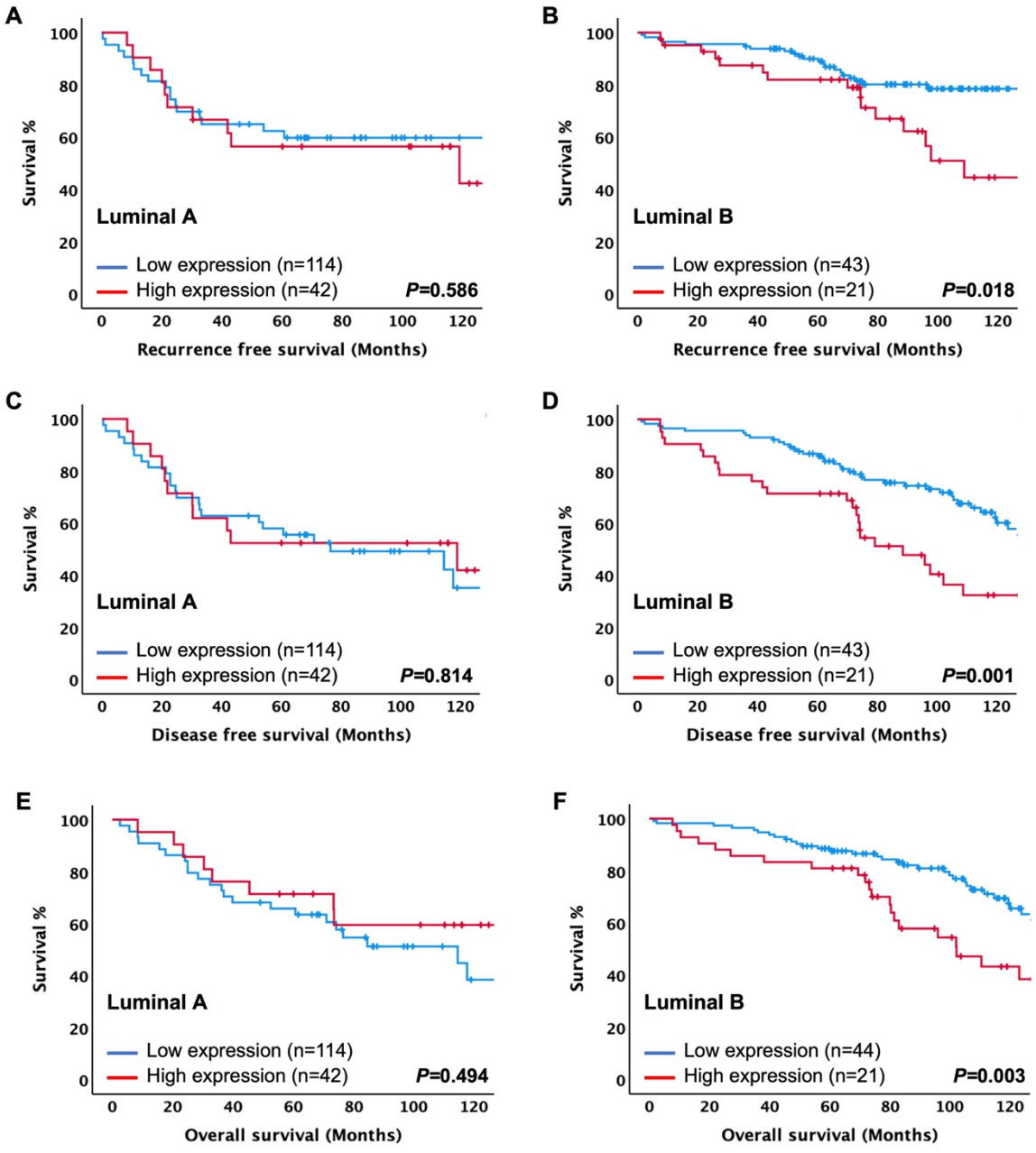

Figure 7.9 Expression of cytoplasmic CAIX and survival in ER-positive breast cancer subtypes.

Kaplan-Meier curves showing associations between cytoplasmic CAIX expression and patients' survival in luminal A disease [A, C, E], and in luminal B disease [B, D, F].

Multivariate analysis suggested that cytoplasmic expression of CAIX was an independent prognostic marker for RFS (HR = 2.57, 95% CI: 1.29–5.12, P = 0.007) when combined with tumour size in luminal B tumour (Table 7.11).

Table 7.11 Univariate and multivariate analysis for recurrence free survival of cytoplasmic CAIX and clinicopathological characteristics in luminal B tumours (n = 69)

Clinicopathological characteristics	Luminal B			
	Univariate analysis		Multivariate analysis	
	HR (95% CI)	P-value	HR (95% CI)	P-value
Age (<50/>50)	1.49 (0.56–3.96)	0.420	-	-
Size (≤20/21–50/>50 mm)	2.64 (1.41–4.95)	**0.003**	2.41 (1.31–4.43)	**0.005**
Grade (I/II/III)	1.06 (0.56–1.99)	0.860	-	-
Lymph node (negative/positive)	2.21 (0.82–5.99)	0.117	-	-
NPI (<3.5/3.5–5.5/>5.5)	1.83 (0.90–3.71)	0.094	-	-
PR status (negative/positive)	0.51 (0.24–1.07)	0.076	-	-
Her-2 status (negative/positive)	0.64 (0.26–1.57)	0.328	-	-
Ki67 (proliferative index) (low/high)	1.23 (0.37–4.10)	0.731	-	-
Adjuvant chemotherapy (no/yes)	0.66 (0.29–1.46)	0.301	-	-
Adjuvant radiotherapy (no/yes)	1.11 (0.50–2.46)	0.792	-	-
Cytoplasmic CAIX (low/high)	2.17 (1.12–4.18)	**0.018**	2.57 (1.29–5.12)	**0.007**

Multivariate Cox regression model was adjusted for age, tumour size, grade, lymph node, NPI, PR status, Her-2 status, Ki67, adjuvant chemotherapy, and adjuvant radiotherapy.

Similar to RFS, when entered into multivariate analysis, cytoplasmic CAIX expression was an independent prognostic marker for DFS (HR = 2.75, 95% CI: 1.66–4.55, P<0.001) when combined with tumour size in luminal B tumour (Table 7.12).

Table 7.12 Univariate and multivariate analysis for disease-free survival of cytoplasmic CAIX and clinicopathological characteristics in luminal B tumours (n = 69)

Clinicopathological characteristics	Luminal B			
	Univariate analysis		Multivariate analysis	
	HR (95% CI)	P-value	HR (95% CI)	P-value
Age (<50/>50)	1.73 (0.67–4.46)	0.259	-	-
Size (≤20/21–50/>50 mm)	2.38 (1.34–4.21)	**0.003**	2.26 (1.26–4.06)	**0.006**
Grade (I/II/III)	0.95 (0.55–1.63)	0.847	-	-
Lymph node (negative/positive)	2.25 (0.97–5.19)	0.058	-	-
NPI (<3.5/3.5–5.5/>5.5)	1.63 (0.90–2.95)	0.106	-	-
PR status (negative/positive)	0.73 (0.39–1.37)	0.324	-	-
Her-2 status (negative/positive)	0.49 (0.22–1.08)	0.078	-	-
Ki67 (proliferative index) (low/high)	1.42 (0.50–4.03)	0.507	-	-
Adjuvant chemotherapy (no/yes)	0.67 (0.34–1.33)	0.256	-	-
Adjuvant radiotherapy (no/yes)	1.01 (0.50–2.02)	0.984	-	-
Cytoplasmic CAIX (low/high)	2.23 (1.38–3.61)	**0.001**	2.75 (1.66–4.55)	**<0.001**

Multivariate Cox regression model was adjusted for age, tumour size, grade, lymph node, NPI, PR status, Her-2 status, Ki67, adjuvant chemotherapy, and adjuvant radiotherapy.

On multivariate analysis, cytoplasmic CAIX expression was an independent prognostic marker for OS (HR = 2.28, 95% CI: 1.36–3.84, P = 0.002) when combined with patient's age, tumour size and lymph node in luminal B tumours (Table 7.13).

Table 7.13 Univariate and multivariate analysis for overall survival of cytoplasmic CAIX and clinicopathological characteristics in luminal B tumours (n = 69)

Clinicopathological characteristics	Luminal B			
	Univariate analysis		Multivariate analysis	
	HR (95% CI)	P-value	HR (95% CI)	P-value
Age (<50/>50)	4.86 (1.16–20.27)	**0.030**	3.66 (0.86–15.51)	0.078
Size (≤20/21–50/>50 mm)	2.49 (1.38–4.51)	**0.003**	2.26 (1.26–4.06)	**0.006**
Grade (I/II/III)	0.87 (0.49–1.55)	0.631	-	-
Lymph node (negative/positive)	3.21 (1.22–8.48)	**0.018**	2.75 (1.04–7.25)	**0.041**
NPI (<3.5/3.5-5.5/>5.5)	1.58 (0.85–2.95)	0.148	-	-
PR status (negative/positive)	0.93 (0.47–1.82)	0.826	-	-
Her-2 status (negative/positive)	0.67 (0.30–1.48)	0.322	-	-
Ki67 (proliferative index) (low/high)	1.12 (0.39–3.20)	0.826	-	-
Adjuvant chemotherapy (no/yes)	0.82 (0.39–1.68)	0.582	-	-
Adjuvant radiotherapy (no/yes)	0.79 (0.37–1.67)	0.533	-	-
Cytoplasmic CAIX (low/high)	2.09 (1.27–3.43)	**0.003**	2.28 (1.36–3.84)	**0.002**

Multivariate Cox regression model was adjusted for age, tumour size, grade, lymph node, NPI, PR status, Her-2 status, Ki67, adjuvant chemotherapy, and adjuvant radiotherapy.

7.3.6 Association between hypoxia regulated proteins in patients with ER-positive breast cancer

Chi-square analysis was used to examine possible association between markers. There was a significant association between cytoplasmic HIF-1α (1) and membranous CAIX expression in tumour cells (P = 0.035). Also, there was a significant association between cytoplasmic and nuclear HIF-1α (1) (P<0.001) and cytoplasmic and membranous CAIX (P<0.001) (Table 7.14).

Table 7.14 Association between hypoxic markers in ER-positive cohort

Hypoxic markers	Nuclear HIF-1α (1)	Cytoplasmic CAIX	Membranous CAIX
Cytoplasmic HIF-1α (1)	**<0.001**	0.366	**0.035**
Nuclear HIF-1α (1)	-	0.432	0.071
Cytoplasmic CAIX	-	-	**<0.001**

Chi-squared table of associations between hypoxic markers including cytoplasmic/nuclear HIF-1α (1), and cytoplasmic/membranous CAIX.

7.4 Discussion

It was observed in the previous chapter that high expression of both cytoplasmic HIF-1α (1), HIF-2α was a poor prognostic biomarker for luminal B tumour, and Her-2 disease, respectively, and high expression of cytoplasmic CAIX was an unfavourable prognostic marker for the entire cohort of mixed breast cancer subtype and in luminal B tumour, and Her-2 disease. Therefore, these hypoxic markers were investigated in ER-positive cohort with different molecular subtypes (luminal A and luminal B) using pre-defined thresholds for mixed breast cancer cohort (chapter 6).

In the current study, there were differences in survival associated with nuclear HIF-1α (1) and cytoplasmic CAIX expression seen between luminal A and luminal B patients. High expression of HIF-1α (1) in the tumour cells was a consistent significant factor with the presence of high nuclear HIF-1α (1) retaining independent prognostic significance for DFS and OS in the entire cohort and in luminal A subtypes. Cytoplasmic CAIX expression was a consistent independent prognosticator for RFS and DFS in the entire cohort and in luminal B disease. These differences in the clinical outcomes between luminal A and B types might reflect difference in the biology between luminal A and luminal B. However, it may also reflect that luminal B breast cancer subtypes are associated with greater tumour aggressiveness and with significantly worse prognosis than the luminal A subtypes (15, 409). Also, luminal B subtypes have high expression of Ki67 (high proliferation rate) (410).

The observation that nuclear HIF-1α (1) is correlated with poor survival may be explained by its role in inducing therapy resistance. Previous results link HIF-1α to a worse outcome with tamoxifen resistance in breast cancer patients (328). Recent meta-analysis showed that HIF-1α overexpression are predictive of poor prognosis in breast cancer patients (357). A previous study of 187 patients reported an association between HIF-1α expression and poorer DFS in ER-positive but not ER-negative patients (246). This larger study confirms the prognostic significance of HIF-1α and shows the independent prognostic value of HIF-1α (1) in ER-positive breast cancer. These findings suggest that the nuclear expression of HIF-1α (1) may be a hallmark of malignancy and associated with the progression of ER-positive breast carcinoma. However, further molecular and mechanistic investigations are needed to fully elucidate the role of HIF-1α protein in ER-positive.

In the present chapter, although cytoplasmic CAIX expression was elevated in approximately 28% of ER-positive breast cancer patients, this percentage was low and associated with poor prognosis of luminal B breast cancers. These results are consistent with

previous studies. Ivanova et al. evaluated breast cancer samples of more than 3000 breast cancer patients and showed that a high CAIX level was significantly associated with lower OS in luminal B but not in luminal A (385). Moreover, Generali et al. reported that in breast cancer patients treated with epirubicin and tamoxifen, CAIX expression was associated with lower DFS and OS (258). CAIX is functionally involved in diverse aspects of cancer progression. CAIX is important for hypoxic tumour cell survival by regulating acidification of the external TME, allowing cancer cells to adapt and metastasise to other tissues (411).

Although membranous CAIX expression in our patients was significantly associated with cytoplasmic expression of HIF-1α (1), there was no significant association between nuclear HIF-1α (1) and cytoplasmic CAIX. This absence of an association is consistent with other reports (307, 386, 387). This further supports that HIF-1α may not be an exclusive candidate marker for breast cancer. Previous findings have demonstrated that HIF-1α was undetectable within 5 minutes after re-oxygenation (360), suggesting that CAIX possibly activates hypoxic condition independently of HIF-1α. Thus, CAIX as a biomarker for hypoxia could be more suitable as it is more stable and persists longer than HIF-1α. However, there was a consistent association between cytoplasmic and nuclear HIF-1α (1), and between cytoplasmic and membranous CAIX indicating reliable methodology.

Recently, diagnostic and therapeutic agents targeting HIF-1α and CAIX have been developed (412). Hypoxia-associated biomarkers profiling in advanced breast cancer may provide additional information for staging, clinical decision, prognosis, and potentially have an important part in the development of personalized therapeutic drugs. Indeed, HIF-1α targeting is considered as a novel therapeutic modality for management of breast cancer patients and improving their prognosis which could be used in combination with currently used therapies. Many small molecules have been reported as HIF-1α inhibitors (194). Knockdown of HIF-1α expression has been reported to cause complete inhibition of the hypoxic induction in breast cancer stem cells (238). Also, CAIX is under consideration by both academic and pharmaceutical entities, as a potential target for intervention in breast carcinoma (398). Assessment of CAIX in tumours before or during therapy may represent a more powerful prognostic and predictive biomarker as well as important targets for breast cancer especially in luminal B which warrants further investigation.

The main limitation of this chapter was the relatively small number of patient samples analysed limiting the power of the present analysis and so further confirmation of the present results is required. Compared with CAIX protein which relatively stable (232), the HIF

proteins undergo a rapid degradation (307), and this may have impacted on the results obtained.

In conclusion, the data from this chapter show that nuclear HIF-1α (1) was an independent prognostic factor for DFS and OS in the entire cohort and in luminal A disease, and cytoplasmic CAIX was an independent prognosticator for both RFS and DFS in the entire cohort and in the patient subpopulation of luminal B disease. This finding suggests that HIF-1α (1) and CAIX are biomarkers with potentially important therapeutic implications, which may help clinician to refine the treatment plan including therapeutic options of luminal B patients.

Taken together these data, coupled with results from previous chapters, suggest patients with CAIX expressing tumours would be an important prognostic marker in breast cancer patients. CAIX in particular appears to have prognostic power in ER-positive breast cancer but what CAIX represents in ER-negative breast cancer particularly TNBC unknown. This will be further investigated in an independent cohort in the following chapter of this thesis.

Chapter 8 The role of hypoxic markers in predicting survival in patients with triple negative breast cancer

8.1 Introduction

TNBC is a heterogeneous breast cancer subtype characterized by lack of expression of ER, PR and Her-2 (13). Most of the TNBCs about 75% are BLBCs; however, not all BLBCs are TNBCs (413). TNBC accounts for approximately 15–20% of all breast cancer cases (20). It is often seen in younger and premenopausal women and more frequently in African American women. It has early relapse, lower OS, and frequent distant metastasis rather than other breast cancer subtypes (414). The lack of targeted therapies and the poor prognosis of TNBC patients have contributed to significant efforts to discover potential molecular targets for the treatment of TNBC patients (136).

Interrogation of TMAs has revealed associations between CAIX overexpression and specific tumour categories. In breast cancer, the expression levels of CAIX vary depending on the intrinsic subtype, and they are increased in TNBC compared to other subtypes (235, 248, 264, 265). Neumeister and co-workers reported that elevated CAIX protein was associated with a BRCA1 mutant signature and loss of BRCA1 function (309). Several studies have also reported that higher CAIX expression in TNBC patients is associated with adjuvant chemotherapy and radiotherapy resistance and poorer survival (258, 264, 265). It is important to develop new treatment regimens and discover potential therapeutic targets to aid in the development of effective therapies.

It was previously demonstrated that high expression of CAIX was associated with poorer clinical outcomes within cohort of mixed breast cancer subtype (chapter 6). Therefore, an independent TNBC cohort was utilised to validate the finding results and to describe the association of CAIX expression with survival, and clinicopathological characteristics in TNBC patients.

8.2 Material and methods

8.2.1 Patient cohort

A TNBC cohort was examined, and the characteristics are described in chapter 2. FFPE tissue was obtained from 207 TNBC patients, who underwent surgery at the Greater Glasgow and Clyde, between 2011 and 2019. Only invasive ductal TNBC female patients were included in the study (n = 177) while those with history of neoadjuvant chemotherapy were excluded (n = 41), thus 136 patients remained for downstream analysis as showed in chapter 2.

The follow up for the selected patients ranged from 0–112 months and a median follow up time was 54 months (range 38.75–68.68 months). There were 112 patients alive at the last follow up, and median follow up was 63.70 months (range 48.60–73.50 months). Clinicopathological data including patient's age, tumour size, grade, lymph node status and treatment the patient received was available.

8.2.2 TMA slide staining and scanning

IHC analysis was performed with the TMA technique. Stained slides were scanned using Hamamatsu slide scanner and visualised using NDP serve 3 image viewer platform system as described previously in chapter 2.

8.2.3 Scoring of CAIX

Cytoplasmic CAIX expression within the tumour cell was scored digitally using QuPath platform whereas membranous expression was assessed using the weighted Histoscore method as described in chapter 2. QuPath was unable to accurately score the membrane CAIX staining, therefore it was assessed using the manual weighted Histoscore method.

8.2.4 Statistical analysis

The threshold value for CAIX determined from the previous Glasgow breast cohort in chapter 5 was applied in this cohort. Analysis of associations with clinicopathological characteristics and with survival outcomes was carried out as described in chapter 2.

8.3 Results

8.3.1 Clinicopathological characteristics of TNBC

A total of 136 patients who presented with TNBC were included in the study. Table 8.1 shows clinicopathological characteristics of patients. The majority of patients were over 50 years of age (74%), had tumour size 21–50 (51%), had grade III carcinoma (96%), and had negative lymph nodes (78%). 92 (68%) patient received adjuvant chemotherapy, 102 (75%) received adjuvant radiotherapy, and 78 (57%) received both adjuvant chemotherapy and radiotherapy. 101 (76%) patients had no recurrence, and 33 (24%) patients experienced recurrences. Of these patients, 3 (2%) had bilateral recurrence. The median follow-up of survivors was 54 months with 33 cancer-associated deaths and 8 non-cancer deaths.

Table 8.1 The clinicopathological characteristics of TNBC patients (n = 136)

Clinicopathological characteristics	Patients, n (%)
Age (≤50/>50 years)	36(26)/100(74)
Size (≤20/21–50/>50 mm)	60(45)/68(51)/6(4)
Grade (I/II/III)	0(0)/5(4)/131(96)
Lymph node (negative/positive)	104(78)/30(22)
Adjuvant chemotherapy (no/yes)	44(32)/92(68)
Adjuvant radiotherapy (no/yes)	34(25)/102(75)
Combined adjuvant chemotherapy and radiotherapy (no/yes)	58(43)/78(57)
Alive/cancer death/non-cancer death	95(70)/33(24)/8(6)
No recurrence/recurrence/bilateral	101(76)/30(22)/3(2)

Table showing the number of patients with clinical characteristics and survival outcomes in patients from TNBC cohort including age, tumour size, grade, lymph node, adjuvant chemotherapy and adjuvant radiotherapy.

8.3.2 Expression of CAIX

8.3.2.1 Immunohistochemistry of CAIX

To determine whether CAIX expression at the protein level played a role in TNBC, TMA comprised of 136 patient tumour samples were stained for CAIX expression. CAIX expression was detected in the cytoplasm and membrane of tumour cells (Figure 8.1A). Weighted Histoscores for cytoplasmic expression ranged from 0 to 220 with a mean score of 19.25, and for membranous scores ranged from 0 to 221.7 with a mean score of 23.57. A histogram was plotted to visualise the range of scores and data showed a positively skewed pattern (Figure 8.1B). An ICCC of 0.942 for cytoplasmic and 0.864 for membranous CAIX was obtained between the 2 estimations. The previously established R threshold levels (18, 30) were applied for cytoplasmic and membranous CAIX analysis, respectively. Low cytoplasmic CAIX expression was observed in 102 (75%) samples, while 34 (25%) samples had high cytoplasmic expression. 98 (72%) patients showed low, and 38 (28%) showed high membranous CAIX expression.

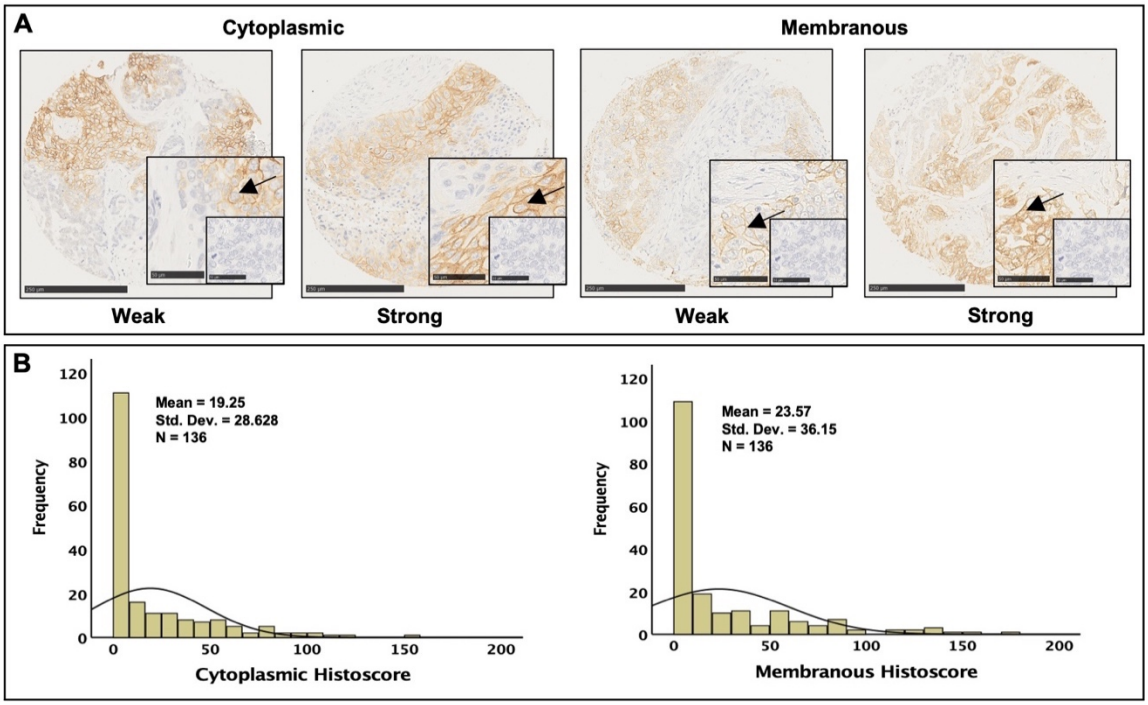

Figure 8.1 Representative immunohistochemical images and scoring distribution for CAIX.

Representative images of weak and strong cytoplasmic and membranous staining of CAIX [A]. Representative images of histogram showing the range of scores obtained for cytoplasmic and membranous tumour CAIX expression and distribution pattern of data [B].

8.3.2.2 Association of CAIX with clinical outcome in TNBC patients

The prognostic value of CAIX expression levels was evaluated in 136 TNBC cases using Kaplan-Meier analysis and the log-rank test. TNBC patients that had high cytoplasmic expression of CAIX had shorter RFS (P = 0.038) while no association was found with DFS (P = 0.407) and OS (P = 0.398) (Figure 8.2A, C, E). In contrast, in membranous cases, there was no significant association with RFS (P = 0.258), DFS (P = 0.528), and OS (P = 0.580) (Figure 8.2B, D, F).

Based on text life table analysis, the 10-year RFS of patients with high cytoplasmic CAIX expression was 68% versus 89% with low cytoplasmic CAIX expression (P = 0.066) as summarized in Table 8.2.

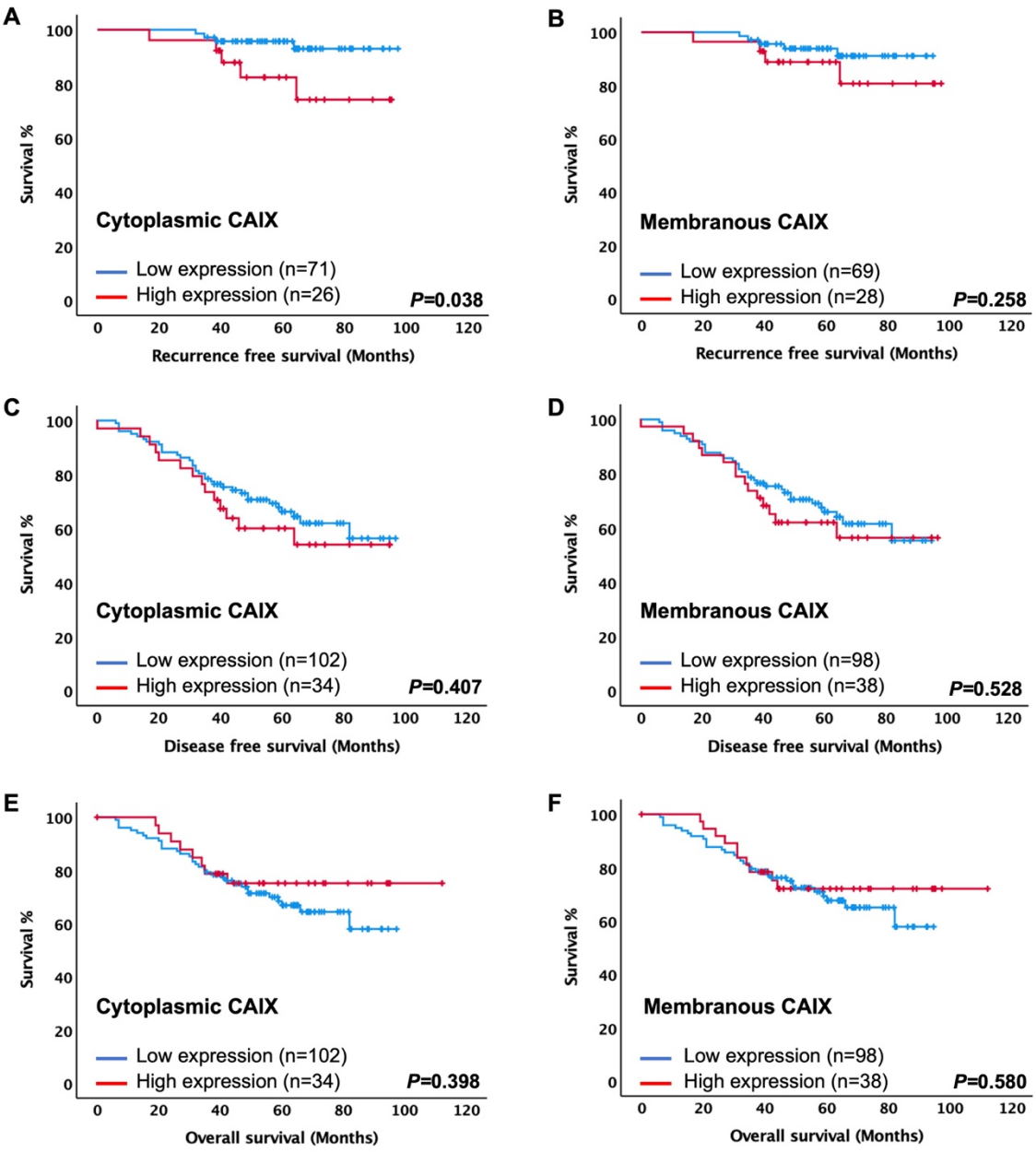

Figure 8.2 Expression of CAIX and clinical outcome in TNBC cohort.

Kaplan-Meier curves showing associations between cytoplasmic and membranous CAIX with recurrence free survival [A, B], disease-free survival [C, D], and overall survival [E, F].

Table 8.2 Association between CAIX expression and survival in TNBC patients (n = 136)

Markers	Recurrence free survival (RFS)						Disease-free survival (DFS)						Overall survival (OS)					
	Cytoplasmic			Membranous			Cytoplasmic			Membranous			Cytoplasmic			Membranous		
	n (%)	10yr-RFS (SE)	P-value	n (%)	10yr-RFS (SE)	P-value	n (%)	10yr-DFS (SE)	P-value	n (%)	10yr-DFS (SE)	P-value	n (%)	10yr-OS (SE)	P-value	n (%)	10yr-OS (SE)	P-value
CAIX			**0.038**			0.258			0.407			0.528			0.398			0.580
Low	71(73)	89(5)		69(71)	86(6)		102(75)	50(6)		98(72)	50(6)		102(75)	52(6)		98(72)	53(6)	
High	26(27)	68(12)		28(29)	75(11)		34(25)	42(10)		38(28)	44(10)		34(25)	61(11)		38(28)	57(10)	

Table showing the number of patients and associations with survival for CAIX marker in TNBC cohort.

To examine the independent prognostic significance of clinicopathological variables and markers expression, multivariate analysis was performed. Only variables with significant (P<0.05) univariate impact were used in the multivariate analysis. Multivariate analysis showed that cytoplasmic CAIX remained as factor contributing significantly to RFS (HR = 6.59, 95% CI: 1.47–29.58, P = 0.014) for patients with TNBC along with tumour size, and Klintrup-Mäkinen grade (Table 8.3).

Table 8.3 Univariate and multivariate analysis for recurrence free survival of CAIX and clinicopathological characteristics in TNBC (n = 136)

Clinicopathological characteristics	Univariate analysis		Multivariate analysis	
	HR (95%CI)	P-value	HR (95%CI)	P-value
Age (≤50/>50years)	4.11 (0.51–33.15)	0.184	-	-
Tumour size (≤ 20/21–50/>50 mm)	3.49 (1.12–10.89)	**0.032**	3.92 (0.92–16.62)	0.064
Grade (I/II/III)	0.32 (0.04–2.59)	0.287	-	-
Lymph node (negative/positive)	3.49 (0.93–13.07)	0.063	-	-
Lymphatic vessel invasion (no/yes)	1.32 (0.33–5.28)	0.696	-	-
Blood vessel invasion (no/yes)	1.32 (0.33–5.28)	0.696	-	-
Tumour necrosis (low/high)	0.56 (0.14–2.25)	0.416	-	-
Klintrup-Mäkinen grade (0/1/2/3)	0.27 (0.09–0.75)	**0.012**	0.26 (0.09–0.74)	**0.012**
Tumour stroma percentage (low/high)	1.52 (0.36–6.35)	0.570	-	-
Adjuvant chemotherapy (no/yes)	0.37 (0.09–1.38)	0.137	-	-
Adjuvant radiotherapy (no/yes)	0.27 (0.07–1.02)	0.053	-	-
Cytoplasmic CAIX (low/high)	3.67 (0.98–13.69)	**0.038**	6.59 (1.47–29.58)	**0.014**

Multivariate Cox regression model was adjusted for age, tumour size, grade, lymph node, lymphatic vessel invasion, blood vessel invasion, tumour necrosis, Klintrup-Mäkinen grade, tumour stroma percentage, adjuvant chemotherapy and adjuvant radiotherapy.

8.3.2.3 Associations between cytoplasmic CAIX expression and clinicopathological characteristics in TNBC patients

Chi-square analysis was performed in order to determine whether expression of cytoplasmic CAIX was associated with any clinicopathological characteristics of the patients in TNBC cohort. Significant association was found between CAIX positivity in tumour cells and patients who received adjuvant radiotherapy (P<0.001) in Table 8.4.

Table 8.4 Association between cytoplasmic CAIX expression and clinicopathological characteristics in TNBC cohort (n = 136)

Clinicopathological characteristics	Cytoplasmic CAIX		
	Low expression n = 102 (75%)	High expression n = 34 (25%)	P-value
Age (≤50/>50 years)	28(27)/74(73)	8(23)/26(77)	0.651
Tumour size (≤ 20/21−50/>50 mm)	48(48)/47(47)/6(5)	12(36)/21(64)/0(0)	0.652
Grade (I/II/III)	0(0)/4(4)/98(96)	1(3)/33(97)	0.793
Lymph node (negative/positive)	78(78)/22(22)	26(77)/8(23)	0.854
Lymphatic vessel invasion (no/yes)	11(11)/88(90)	4(13)/27(87)	0.788
Blood vessel invasion (no/yes)	64(63)/37(37)	26(77)/8(23)	0.152
Tumour necrosis (low/high)	46(46)/54(54)	14(45)/17(55)	0.935
Klintrup-Mäkinen grade (0/1/2/3)	13(13)/39(40)/32(33)/14(14)	4(13)/14(47)/9(30)/3(10)	0.541
Tumour stroma percentage (low/high)	69(70)/30(30)	22(71)/9(29)	0.893
Adjuvant chemotherapy (no/yes)	31(30)/71(70)	13(38)/21(62)	0.402
Adjuvant radiotherapy (no/yes)	18(18)/84(82)	16(47)/18(53)	**<0.001**

Chi-squared table of associations for cytoplasmic CAIX expression and clinical prognostic factors including age, tumour size, grade, lymph node, lymphatic vessel invasion, blood vessel invasion, tumour necrosis, Klintrup-Mäkinen grade, tumour stroma percentage, adjuvant chemotherapy and adjuvant radiotherapy.

8.4 Discussion

The findings of the previous chapters suggested a possible prognostic role of CAIX in mixed breast cancer cases and in ER-positive patients. The results of the present chapter in a small historical cohort showed that tumour cytoplasmic CAIX expression was independently associated with RFS in patients with TNBC. If this observation was confirmed in larger contemporaneous cohorts, then it may that cytoplasmic CAIX expression would be a useful therapeutic target in patients with TNBC.

Due to the lack of hormonal and Her-2 receptor expression, TNBC often do not respond to standard breast cancer treatments and have poor prognosis (415-417). Therefore, it is of great clinical importance to identify new molecular biomarker that could be used for prognosis and for selecting appropriate therapeutic schedules (418). The overexpression of CAIX in cancer cells compared to healthy tissues has made it a promising target for cancer therapy (305, 419). There are several inhibitors of the CAIX being examined in the clinical trials that show promising results as therapeutic as well as diagnostic agents in solid tumours including the pancreatic and colorectal cancer (420). It was previously shown that hypoxia could be specifically linked with TNBC (421). High levels of CAIX expression have been reported in TNBC (378, 385). Neumeister et al. (309) reported that CAIX was expressed in about one-fourth of TNBCs and significantly associated with the triple negative phenotype. Moreover, Lou et al (308) reporting that 51% of BLBCs are CAIX positive by IHC, whereas only 8% of luminal A, 11% luminal B and 33% of Her-2 tumours are CAIX positive. Tan et al. (264) showing that BLBCs were nine times more likely to be associated with CAIX expression. Indeed, TNBC frequently shows morphological features which are characteristic of hypoxia, such as the presence of fibrotic and necrotic areas (100).

Many researchers have studied CAIX expression in a plethora of human malignancies and reported that it was associated with poor patient's outcome, however, the importance of this protein as prognostic marker, especially in TNBC, has been little examined. It has been previously reported that hyperactivity of CAIX in TNBC is significantly associated with worse prognosis (264, 265, 385). However, the absence of correlation of CAIX expression with survival was reported by other studies (309, 311). This discrepancy between studies could be explained by different number of patients, variable technique of staining and different antibody clone which gives diverse results.

There are multiple theories which could explain the association between high CAIX expression and poor patients' prognosis in breast cancer. CAIX expression is associated with

tumour tissue hypoxia and acidosis and its upregulation is a step-in tumour cells adaptation to survive under hypoxic conditions (422). CAIX is linked to cancer hypoxia and stimulates cancer cell invasion and metastasis. Cancers with activation of CAIX could be able to maintain their intracellular but it increased acidification in extracellular space, which leads to extracellular matrix breakdown which could increase cancer cell's invasive ability (423, 424). In fact, silencing of CAIX decreased invasiveness and self-renewal capacity under hypoxic conditions and had a synergistic effect with doxorubicin on reducing the spheroid-forming efficiency in TNBC cells (385). Additionally, CAIX could influence breast cancer stem cells growth and survival under hypoxic conditions (425). CAIX may be a surrogate marker of TNBC and has attracted the attention of the scientific and pharmaceutical community. Since tumour hypoxia can negatively influence treatment outcome, its targeting CAIX could be of particular importance in managing this aggressive cancer and improving patient's prognosis.

Therapeutically targeting CAIX in hypoxic solid tumours with the particular small-molecule, SLC-0111 inhibits tumour growth and metastases in preclinical models of breast tumour (308, 350). SLC-0111 has now entered clinical assessment and has been found to be well tolerated (426).

The present chapter showed no association between CAIX expression and clinicopathological characteristics. However, an association with patients who received radiotherapy was observed. A recent clinical study showing that CAIX overexpression was significantly associated with poor survival in TNBC patients treated with radiotherapy, which suggests a correlation between CAIX expression and response to radiotherapy (265).

There are limitations in the present chapter. The present cohort of TNBC was consisted of a relatively small number of patients (n = 136). Therefore, further studies in large numbers of patients are required to confirm the present observations.

In conclusion, the results of the present chapter showed independent prognostic role of cytoplasmic CAIX expression with RFS in TNBC patients. In the following chapter, further investigation into gene expression profiling associated with cytoplasmic CAIX in ER-negative breast cancer will be carried out which might result in the identification of new targeted therapeutics.

Chapter 9 Differential gene expression profiles associated with CAIX expression in patients with ER-negative breast cancer

9.1 Introduction

Results from previous chapters have highlighted a prognostics role of cytoplasmic CAIX in different breast cancer subtypes. Here we aim to unravel any differences in the underlying transcriptomic signatures associated with high cytoplasmic CAIX expression in ER-negative disease. A better understanding of the transcriptomic and protein pathways associated with the CAIX may identify potential therapeutic targets against this aggressive phenotype.

The samples available to use were FFPE, however tissue fixation may result in formaldehyde modification of RNA leading to degradation and fragmentation during extraction. However, in the current chapter TempO-Seq, a targeted sequencing technology based on probe hybridisation (BioSpyder. Tempo-Seq Workflow, BioClavis. TempO-Seq 2020), was employed as this was developed to overcome the problems associated with the performance of RNAseq on FFPE cancer specimens.

In recent years, prognosis-based gene signature identification has been of immense interest for the prediction of outcome or for evaluation of the course of breast cancer (427). Therefore, in this chapter TempO-Seq was employed to identify DEGs profiles for tumours with low versus high cytoplasmic CAIX. A small pilot study was carried out, using this technique, to investigate the difference in transcriptomic signatures between ER-negative cancers with high compared to those with low tumour cytoplasmic CAIX, and to evaluate TempO-Seq technology in this setting.

9.2 Materials and methods

9.2.1 Cohort selection

The Glasgow breast cohort was used as this was the cohort for which tissue blocks were available for cutting of a previously constructed TMA. Only patients with ER-negative disease (n = 50) were utilised for TempO-Seq analysis. From these 50 samples, 37 had cytoplasmic CAIX data available, 16 samples had high expression and 21 samples had low expression (as described in chapter 2). Because of heterogenous population, the 20-lymph node negative patients' samples were selected specifically to search for a prognostic signature in their gene expression profiles.

9.2.2 Slide preparation

Prior to transfer to BioClavis, tissue sections were cut and fixed as described in chapter 2. Sections were labelled with the TMA ID only to maintain anonymity while allowing data to be linked back to the main database.

9.2.3 RNA sequencing using TempO-Seq®

RNA sequencing was carried out at BioClavis using the protocol described in chapter 2.

9.2.4 Data pre-processing

Raw sequencing data in form of FASTQ files were initially analysed and aligned with human whole transcriptome by BioClavis using the TempO-Seq data analysis program (BioSpyder Technologies, Inc., Carlsbad, CA, United States).

9.2.5 Differential expression analysis and clustering

Prior to performing differential expression analysis, the mean gene count was calculated where multiple probes were used to detect a single gene. The finalised gene count matrix, therefore, had a single gene count value for each gene per patient sample. Next, the raw read counts were normalised using DESeq2, which divided the number of reads per gene by the geometric mean of the gene across all samples. DEGs were identified using R Studio Team (2020) (RStudio: Integrated Development for R. RStudio, PBC, Boston, MA). The targeted RNA sequencing methods focused on assessment of DEGs between tumours with high and low cytoplasmic CAIX expression. Differential expression analysis was visualised using volcano plots and MA plots. Significance was set to the adjusted P-value (padj) <0.10 and log2 fold change (log2 FC) of either >1 or <-1. Cluster analysis was then used to group the DEGs into clusters based on the similarity in their expression profiles using R Studio. Principal component analysis (PCA). The heatmap was performed using ComplexHeatmap in R Studio to visualise the patterns of gene expression for the top 20 most significant DEGs. The R code used for analysis is shown in appendix.

9.2.6 Gene Ontology and pathway enrichment analyses

To determine functional enrichment analysis, the search tool for the retrieval of interacting genes (STRING) version 11.5 (295) was used by inputting the gene name of DEGs and

exporting the results. The DEGs were analysed and categorised into the three categories, including cellular component, biological process, and molecular function.

STRING database and Gene Ontology (GO) were utilised to identify biological pathways associated with DEGs in the high cytoplasmic CAIX expression group. The GO is a system for unification of biology, including cellular component, biological process, and molecular function (428). For enhanced graphical representation, bar plots and cnet plots were constructed using GO enrichment analysis.

9.2.7 Protein-protein interaction network construction

A protein-protein interaction (PPI) network was constructed to investigate the interrelationship of the DEGs and visualised using STRING online database (295) with a required interaction score of >0.4 (medium confidence), a false discovery rate (FDR) <0.05 and PPI enrichment P-value <0.05 (296). Maximum number of interactors to show the first shell was limited to no more than 10 interactions.

9.3 Results

9.3.1 ER-negative cohort

9.3.1.1 Clinicopathological characteristics of ER-negative cohort

There was a significant difference in lymph node involvement between specimens with high and low cytoplasmic CAIX expression (P = 0.023). However, no significant difference between expression groups in terms of patients age (P = 0.469), tumour size (P = 0.538), tumour grade (P = 0.660), PR status (P = 0.191), and Her-2 status (P = 0.615) (Table 9.1).

Table 9.1 Association between cytoplasmic CAIX expression and clinicopathological characteristics in ER-negative cohort (n = 37)

Clinicopathological characteristics	Cytoplasmic CAIX		
	Low (n = 21)	High (n = 16)	P-value
Age (<50/>50)	9(43)/12(57)	5(31)/11(69)	0.469
Size (≤ 20/21-50/>50 mm)	6(29)/13(62)/2(9)	6(38)/9(56)/1(6)	0.538
Grade (I/II/III)	1(5)/5(24)/15(71)	1(6)/2(13)/13(81)	0.660
Lymph node (negative/positive)	8(38)/13(62)	12(75)/4(25)	**0.023**
PR (negative/positive)	21(100)/0(0)	15(94)/1(6)	0.191
Her-2 (negative/positive)	16(76)/5(24)	11(69)/5(31)	0.615

Chi-squared table of associations for cytoplasmic CAIX expression and clinical prognostic factors including age, tumour size, grade, lymph node, PR status, and Her-2 status.

9.3.1.2 Differentially expressed genes in tumours with high versus low cytoplasmic CAIX expression

The gene counts and sample sheet files were loaded into R Studio (RStudio, Boston, MA, USA) and DESeq2 analysis was performed to generate a table of DEGs relative to the high or low cytoplasmic CAIX expression groups. Significance was set to padj <0.10 and a log2 FC >+1 or <-1. A total of 18,629 DEGs between low and high expression of cytoplasmic CAIX were identified. Despite the low sample size, 3 genes were significantly differentially expressed, named OR8B2, SERHL2, and KRT6A, with padj <0.05 (Table 9.2). An additional 7 genes were significantly associated with high tumour CAIX when significance was defined as P<0.10, namely MMP7, SPINK8, TMEM150C, CEACAM6, MUCL1, PITX2, and GALNT6 as shown in volcano plot and MA plot which were constructed using ggplot in R Studio (RStudio, Boston, MA, USA) (Figure 9.1A, B, respectively). In view of the small sample size, all 10 of these genes were felt to be of interest. Three genes were down-regulated in high CAIX tumours while the other 7 genes were up-regulated (Table 9.2).

Table 9.2 The top 20 differential expression genes comparing high and low cytoplasmic CAIX expression in ER-negative cohort

Gene name	Gene description	log2 Fold change	Adjusted P-value
OR8B2	Olfactory receptor family 8 subfamily B member 2	-18.52133276	**8.14221E-06**
SERHL2	Serine hydrolase-like protein 2	4.512067996	**1.33351E-05**
KRT6A	Keratin 6A	-3.864480196	**0.000133005**
MMP7	Matrix metalloproteinase 7	-2.396251083	**0.051437738**
SPINK8	Serine peptidase inhibitor kazal type 8	4.56278643	**0.051437738**
TMEM150C	Transmembrane protein 150C	3.057561702	**0.056140876**
CEACAM6	Carcinoembryonic antigen cell adhesion molecule 6	5.048945946	**0.087775933**
MUCL1	Mucin like 1	3.943601762	**0.087775933**
PITX2	Paired like homeodomain 2	5.377563312	**0.087775933**
GALNT6	Polypeptide N-Acetyl galactosaminyl transferase 6	2.404459373	**0.088597392**
ACTA2	Actin alpha 2, smooth muscle	-1.819614515	0.163515345
OR51B2	Olfactory receptor family 51 subfamily B member 2	5.273790568	0.199261887
ACTG2	Actin gamma 2 smooth muscle	-2.656233588	0.199261887
NPRL2	NPR2 like, gator1 complex subunit	0.86487402	0.201298362
ZNF620	Zinc finger protein 620	4.830953325	0.231360705
FGFR4	Fibroblast growth factor receptor 4	2.66290296	0.231360705
DUSP4	Dual specificity phosphatase 4	1.638628628	0.231360705
PRR15	Proline rich 15	2.129102068	0.231360705
FAM151A	Family with sequence similarity 151 member A	6.610181692	0.231360705
PALM2-AKAP2	Ficolin 2	-1.157764709	0.231360705

Note: The top 20 Genes are arranged in the order of adjusted P-value regardless of adjusted log2 FC. Padj <0.10 are highlighted in bold. Gene names are taken from www.genecards.org.

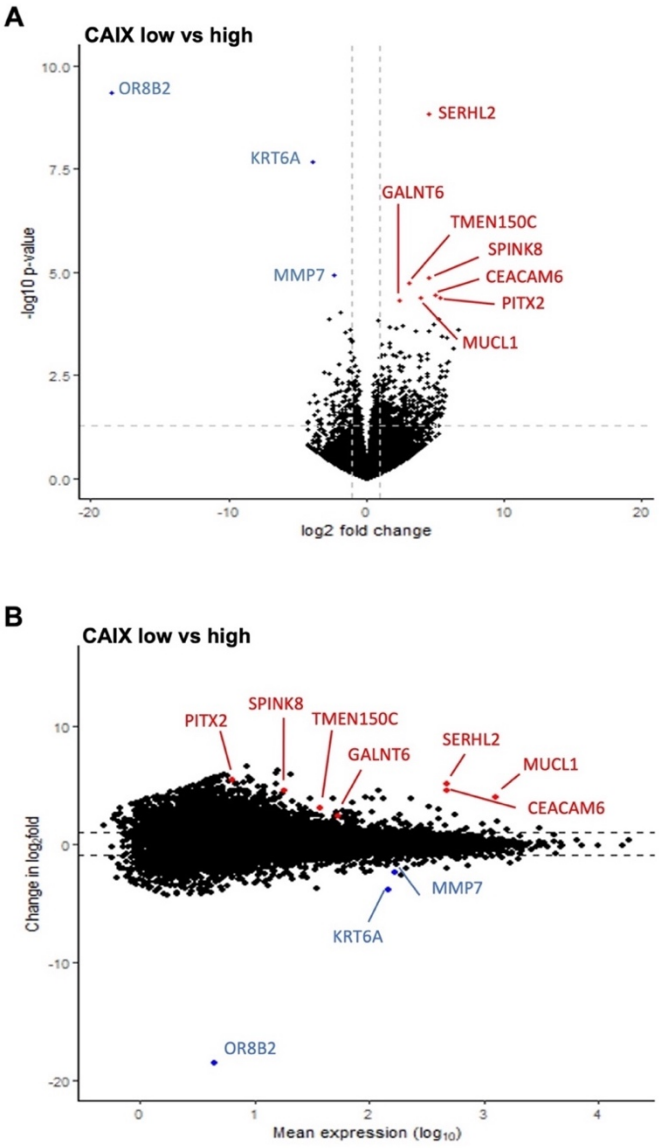

Figure 9.1 Differential gene expression analysis on the full cohort relative to CAIX group.

The volcano plot describes log2 FC in the X-axis and logarithmic adjusted P-value in the Y-axis. The lines parallel to the Y-axis represent a value of FC = 1. The line parallel to the X-axis represents a value of padj = 0.10. A gene was identified as significantly changed if the FC was greater than 1 (up or down) and the padj was less than 0.10 [A]. MA plot depicts the logarithmic scale of the FCs in the Y-axis, and the count mean expression in the X-axis [B]. Red dots illustrate upregulated genes, and blue dots represent downregulated genes. Gene counts were obtained from full transcriptome sequencing performed by TempO-Seq in a subset of ER-negative cohort. Plots were constructed by Dr Gerard Lynch.

9.3.1.3 Cluster analysis of tumour with high versus low expression of cytoplasmic CAIX

PCA plot was generated to determine whether samples in each group (high versus low cytoplasmic CAIX expression) clustered with each other or other groups. Principal component 1 (PC1) and principal component 2 (PC2) were identified by variance stabilizing transformation in DESeq2. The percentage of variance indicates how much variance was explained by PC1 and PC2. 35 patients were included in analysis after excluding 2 outliers. There was potential clustering of gene expression observed between CAIX groups with not much difference between low and high groups when PCA was performed (Figure 9.2A). A scree plot displays how much variation each principal component captures from the data. The plot in Figure 9.2B, suggesting that PC1 and PC2 be used to capture the variability in the data.

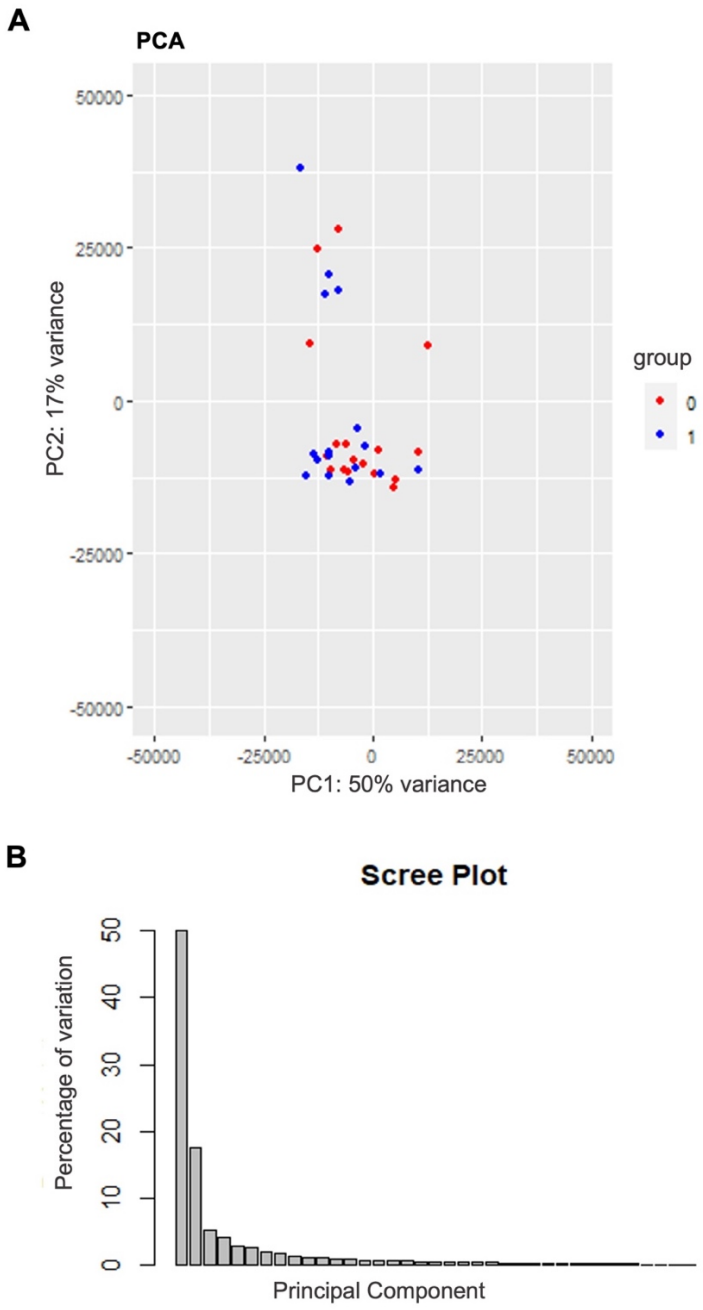

Figure 9.2 Principal component analysis scatter plots and scree plots for ER-negative cohort.

PCA plots of DEGs identified between tumour with high (blue) and low (red) expression of cytoplasmic CAIX. Two outliers were excluded from the plot [A]. A scree plot of the PC against percentage of variation. The X-axis displays the PC, and the Y-axis shows percentage of variance explained [B]. Gene counts were obtained from full transcriptome sequencing performed by TempO-Seq in a subset of the ER-negative cohort. Plots were constructed by Dr Gerard Lynch.

The heatmap of normalised expression values across samples was performed using ComplexHeatmap in R Studio (RStudio, Boston, MA, USA) to visualise the patterns of gene expression for the top 20 most significantly DEGs (Figure 9.3). Expressional status of cytoplasmic CAIX is shown with colour bars at the top of the heatmap. Each row represents a single gene, and each column represents a tumour sample. As shown in the colour bar, orange indicates up-regulation and purple represents down-regulation. There was clear pattern in the gene expression profile between tumours with high and low CAIX expression when only the top 20 DEGs were considered.

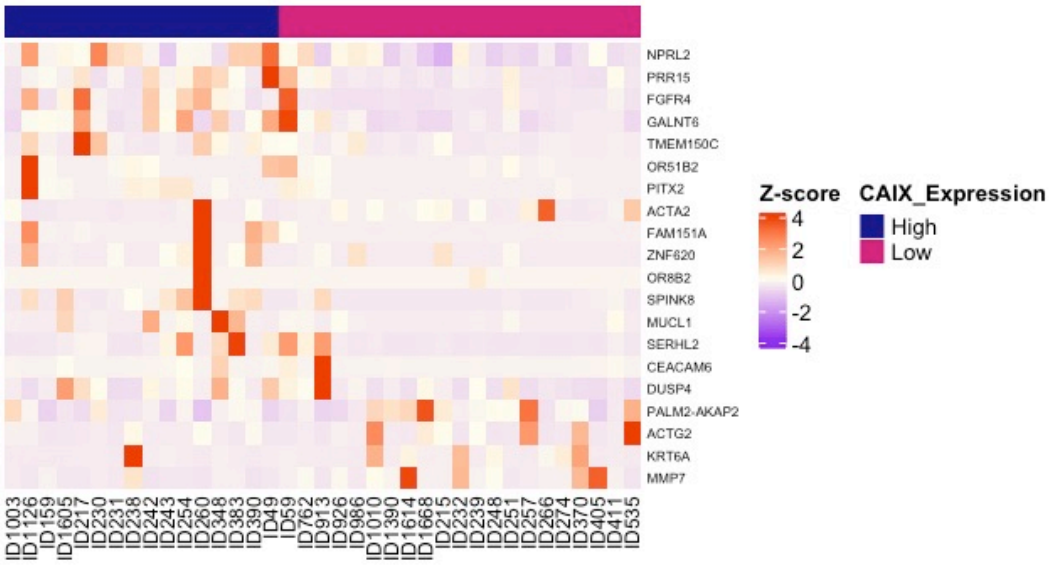

Figure 9.3 Heatmap of gene expression data from microarray analysis in ER-negative cohort.

Heatmap of the top 20 DEGs of cytoplasmic CAIX expression groups. Each row represents a single gene and each column represent a tumour sample. The scale bar shows the relative gene expression levels corresponding to the colours in the heatmap. As shown in the colour bar, orange indicates up-regulation and purple represent down-regulation. Plot was constructed by Phimmada Hatthakarnkul.

9.3.1.4 Enrichment analyses of differential expression genes

The DEGs were analysed using STRING to provide information for ten DEGs which were categorised into the three categories, including cellular component, biological process, and molecular function. STRING database demonstrated that cell component enrichment analysis of DEGs mainly located in the extracellular region, and Golgi lumen/apparatus (Table 9.3).

Table 9.3 Functional enrichments for cellular components

Cellular component	Matched proteins	FDR
Golgi lumen	MUCL1	0.00015
Golgi apparatus	MUCL1, GALNT6	0.0092
Extracellular space	MMP7, KRT6A, CEACAM6	0.0377
Extracellular region	SPINK8, MMP7, MUCL1, KRT6A, CEACAM6	0.0051

The functional enrichments regarding biological process are shown in Table 9.4. The up-regulated genes, PITX2 is associated with odontogenesis, cell migration, tissue development, and anatomical structure morphogenesis, and CEACAM6 is associated with cell migration, and cell adhesion. However, the down-regulated genes, MMP7 is associated with extracellular matrix organization, and KRT6A gene is associated with tissue development, and anatomical structure morphogenesis.

Table 9.4 Functional enrichments for biological process

Biological process	Matched proteins	FDR
Odontogenesis	PITX2	0.0171
Extracellular matrix organization	MMP7	0.0090
Cell migration	CEACAM6, PITX2	0.0385
Cell adhesion	CEACAM6	0.0385
Tissue development	PITX2, KRT6A	0.0090
Anatomical structure morphogenesis	PITX2, KRT6A	0.0090

The functional enrichments regarding molecular function are shown in Table 9.5. The down-regulated gene, MMP7 is associated with glycosaminoglycan binding.

Table 9.5 Functional enrichments for molecular function

Molecular function	Matched proteins	FDR
Glycosaminoglycan binding	MMP7	0.0204

9.3.1.5 Protein-protein interaction network construction

PPI of ten DEGs, OR8B2, SERHL2, KRT6A, MMP7, SPINK8, TMEM150C, CEACAM6, MUCL1, PITX2, and GALNT6 was analysed based on STRING online database. Within a PPI network, only 2 of the 10 genes analysed could be linked. There was significant interaction between MUCL1 and GALNT6 proteins. However, there were 8 proteins that did not have interactions with other proteins (Figure 9.4A). A total of 10 proteins were added to show a network around the input proteins and showed 20 nodes and 42 edges, with the PPI enrichment P-value of 1.12e-06. MMP7, PITX2, and CEACAM6 were demonstrated to interact with their partner proteins which were added from the STRING database (Figure 9.4B). Each node represents a gene, the edges indicate the interaction between nodes, and each colour represents their response molecular function. However, there were three white nodes as unidentified functions based on the STRING online database.

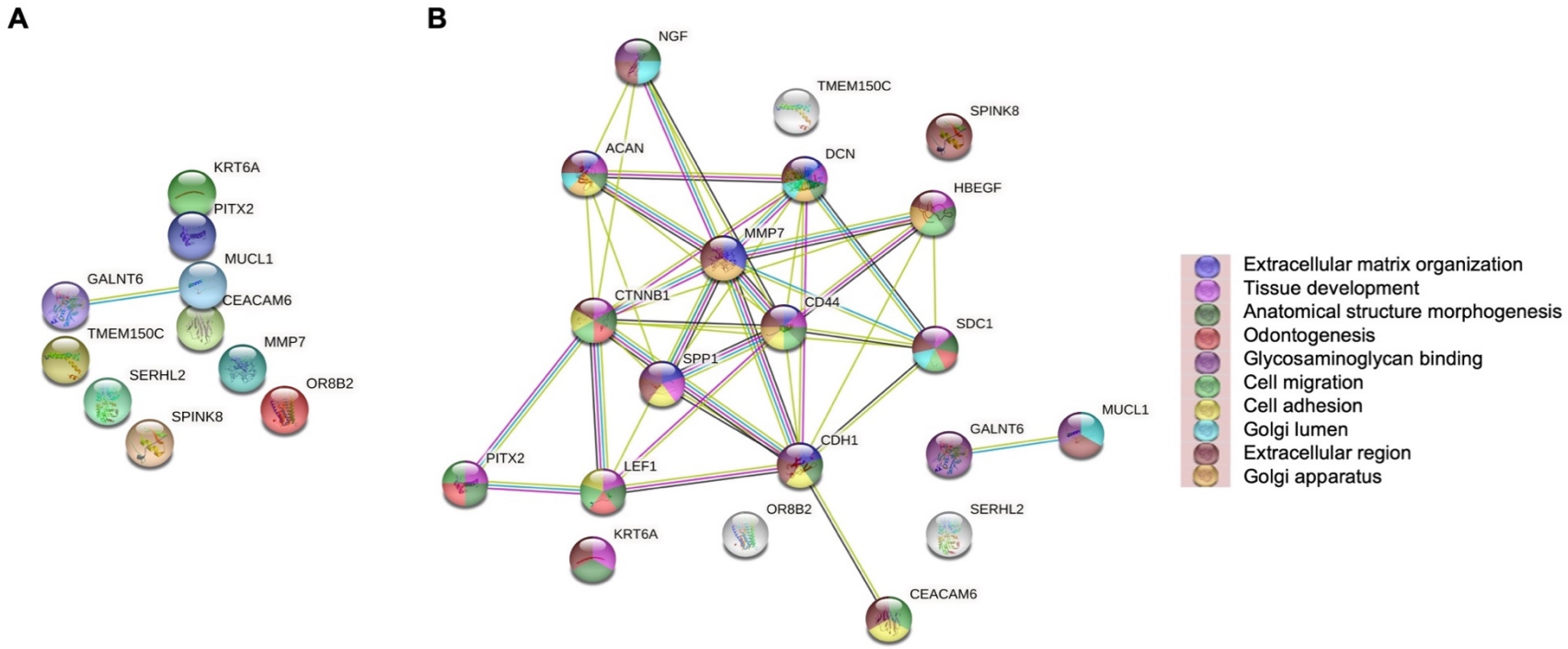

Figure 9.4 String map of differential expression genes in ER-negative cohort.

String interaction network diagram showing relationships between the DEGs from whole transcriptome analysis on a subset of the ER-negative cohort. PPI network analysis for ten proteins [A], PPI network analysis for extra added 10 proteins [B].

9.3.1.6 Pathway enrichment analyses

To determine biological pathways associated with DEGs in the high cytoplasmic CAIX expression group, the STRING online database was used. The down-regulated MMP7 gene was linked with KEGG pathway. Besides MMP7, CEACAM6 and MUCL1 were linked with Reactome pathway (Table 9.6).

Table 9.6 Pathway's enrichment analysis

Pathway enrichment	Matching proteins	FDR
WNT signalling pathway (KEGG)	MMP7	0.0332
Extracellular matrix organization (Reactome)	MMP7, CEACAM6	6.51e-05
Degradation of extracellular matrix (Reactome)	MMP7	4.78e-05
Disease of glycosylation (Reactome)	MUCL1	0.0476

GO was also performed on the top 10 significant genes to view the biological pathways linked with DEGs in the high cytoplasmic CAIX expression group. The genes were selected from the GO analysis data using their Entrez ID with a P-value <0.1 was set as the threshold criterion. Gene enrichment analysis is shown in Table 9.7.

Table 9.7 Top 10 set of genes in the dataset

Gene name	Entrez ID
OR8B2	26595
SERHL2	253190
KRT6A	3853
MMP7	4316
SPINK8	646424
TMEM150C	441027
CEACAM6	4680
MUCL1	118430
PITX2	5308
GALNT6	11226

A bar plot of top 10 DEGs was constructed for cytoplasmic CAIX to demonstrate the differences in gene expression. A total of 10 pathways were enriched by the target genes, including O-glycan processing, cellular response to mechanical stimulus, protein O-linked glycosylation, response to mechanical stimulus, cardiac neural crest cell differentiation involved in heart development, adenohypophysis development, estrous cycle, left/right axis specification, and protein glycosylation (Figure 9.5). In the GO pathway enrichment analysis, gene sets associated with cellular response to mechanical stimulus and protein glycosylation signalling appeared to be the most enriched pathways with the largest number of significantly enriched genes.

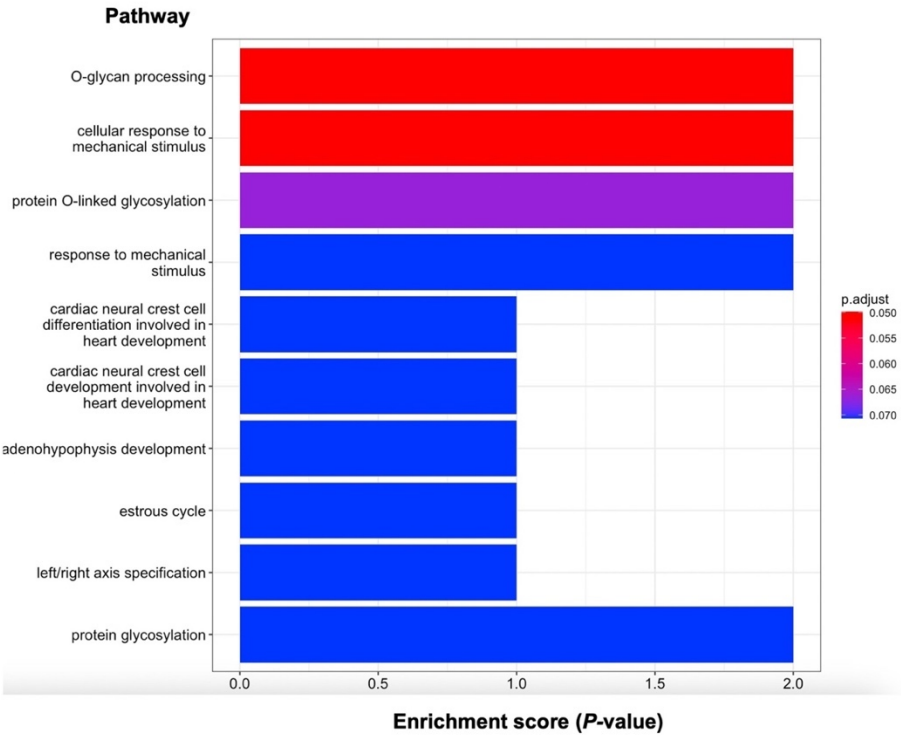

Figure 9.5 Genomes signalling pathway enrichment of target genes.

Bar plot diagram to demonstrate pathway analysis outcomes of DEGs. The X-axis indicates enrichment scores (P-value) of the significant enrichment genes, and the Y-axis indicates the pathway term name. Plot was constructed by Molly McKenzie.

The bar plot only displayed most significant or selected enriched terms. However, to investigate the enriched genes with the corresponding enriched pathways a cnet plot was constructed. As shown in Figure 9.6, five proteins including PITX2, TMEM150C, MMP7, GALNT6 and MUCL1 are the only ones that are associated with significantly enriched gene sets, and the other 5 proteins are less significant. MUCL1 and GALNT6 genes associated

with protein O-linked glycosylation, and O-glycan processing pathways. MMP7 and TMEM150C genes associated with cellular response to mechanical stimulus pathway. PITX2 gene associated with cardiac neural crest cell development involved in heart development.

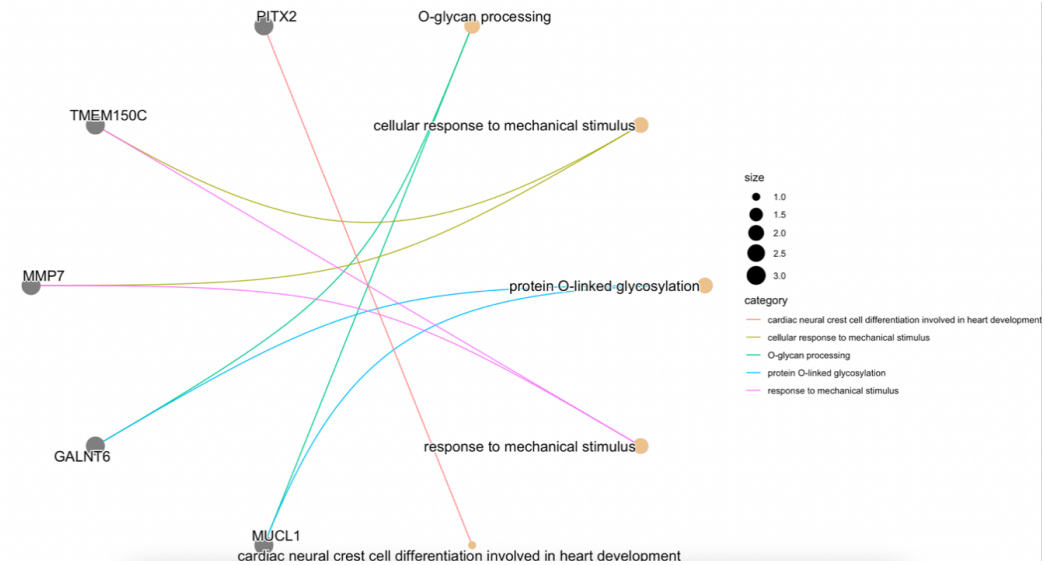

Figure 9.6 Enrichment cnet plot for differential expression genes.

Cnet plot depicts relationships of enriched genes with the corresponding enriched pathways. Relationships as a network diagram with associated data to colour nodes. Plot was constructed by Molly McKenzie.

9.3.2 Node negative group

Because cytoplasmic CAIX was negatively associated with lymph node involvement (P = 0.023), sub-analysis of node negative subset of ER-negative breast cancer cohort was used to establish biological processes, and key pathways related to cytoplasmic CAIX expression.

9.3.2.1 Differentially expressed genes in tumour with high versus low expression of cytoplasmic CAIX

In order to look at a more homogenous group of specimens and to identify if cytoplasmic CAIX was important in lymph node negative disease, analysis of transcriptomic data was performed relative to lymph node negative groups using DESeq 2 package. DEGs were considered significant with padj of <0.10 and log2 FC >+1 or <-1. A total 18,170 DEGs between low and high expression of cytoplasmic CAIX were identified. 3 genes were significantly differentially expressed, PCSK1N, SERHL2, and SPNS2 (Table 9.8). Two genes were up-regulated in high CAIX tumours while one gene was down-regulated as shown in volcano plot and MA plot which were constructed using ggplot in R Studio (RStudio, Boston, MA, USA) (Figure 9.7A, B, respectively).

Table 9.8 The top 10 differential expression genes comparing high and low cytoplasmic expression of CAIX in node negative group

Gene name	Gene description	log2 FC	Adjusted P-value
PCSK1N	Proprotein convertase subtilisin/kexin type 1 inhibitor	-4.204870921	**0.019622676**
SERHL2	Serine hydrolase-like protein 2	4.003706191	**0.019622676**
SPNS2	Sphingolipid transporter 2	1.483867408	**0.057847213**
KLHL17	Kelch like family member 17	-3.771946076	0.529928807
TMEM150C	Transmembrane protein 150c	3.469885701	0.529928807
ZNF689	Zinc finger protein 689	1.67546516	0.529928807
STK35	Serine/threonine kinase 35	-5.624161304	0.793427612
FLNA	Filamin A	-1.189853683	0.793427612
CANT1	Calcium activated nucleotidase 1	1.104507616	0.793427612
PYROXD2	Pyridine nucleotide-disulphide oxidoreductase domain2	1.30757317	0.793427612

Note: The top 10 DEGs are arranged in the order of adjusted P-value regardless of adjusted log2 FC. Padj <0.10 are highlighted in bold. Gene names are taken from www.genecards.org.

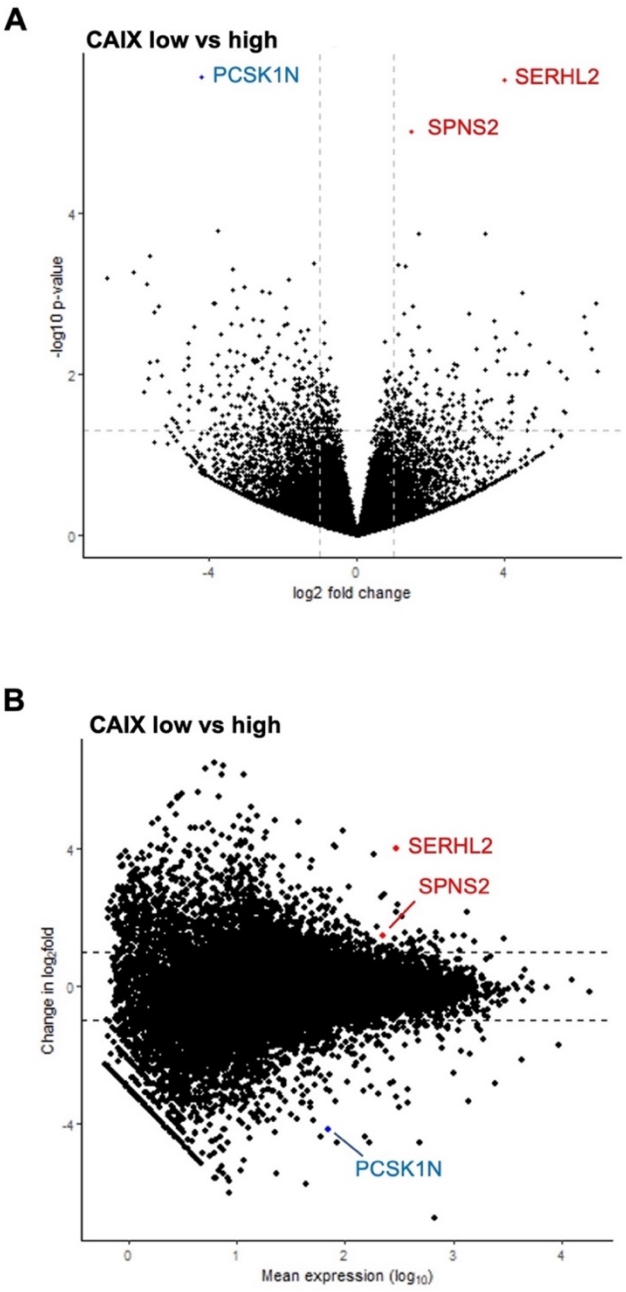

Figure 9.7 Differential gene expression analysis on lymph node negative patients relative to CAIX group.

The volcano plot describes log2 FC in the X-axis and logarithmic adjusted P-value in the Y-axis. The lines parallel to the Y-axis represent a value of FC = 1. The line parallel to the X-axis represents a value of padj = 0.10. A gene was identified as significantly changed if the FC was greater than 1 (up or down) and the padj was less than 0.10 [A]. MA plot depicts the logarithmic scale of the FCs in the Y-axis, and the count mean expression in the X-axis [B]. Red dots illustrate up-regulated genes, blue dots represent down-regulated genes. Plots were constructed by Dr Gerard Lynch.

9.3.2.2 Cluster analysis in tumour with high versus low expression of cytoplasmic CAIX

PCA plot was performed using DESeq2 to determine whether lymph node negative samples in each group (high versus low cytoplasmic CAIX expression) clustered with each other or other groups. 20 patients were included in analysis. PCA revealed no clustering of gene expression (Figure 9.8A). A scree plot shows how much variation each principal component captures from the data. The plot in Figure 9.8B, suggesting that PC1 and PC2 be used to capture the variability in the data.

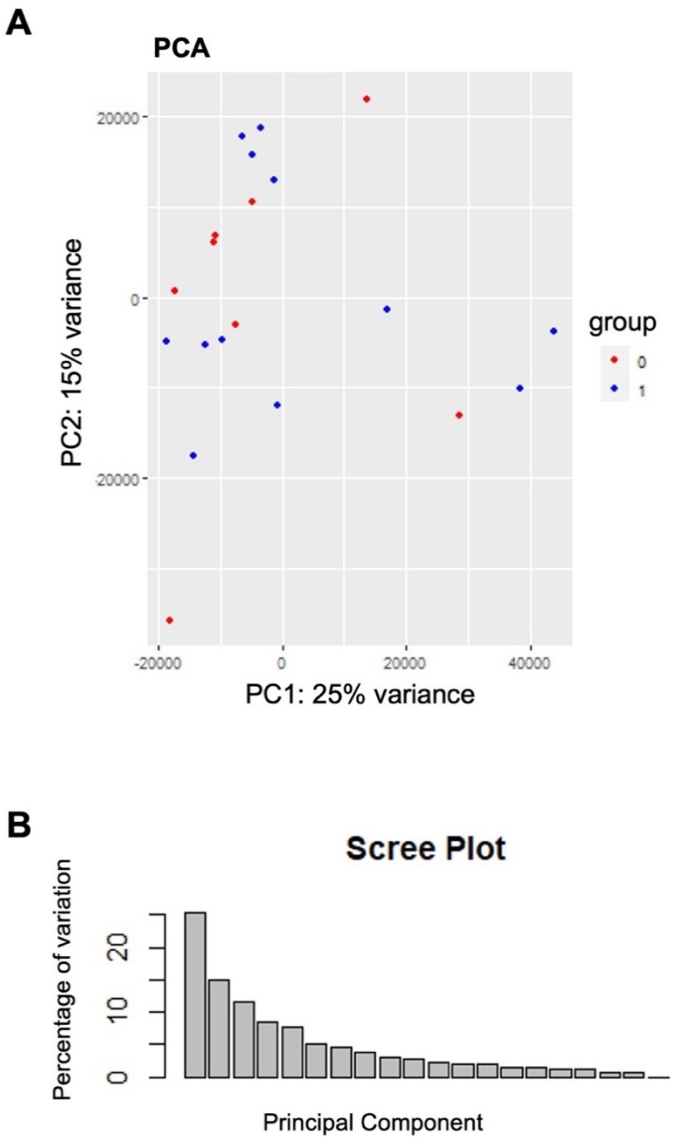

Figure 9.8 Principal component analysis scatter plots and scree plots in node negative group.

PCA plots of DEGs identified between tumour with high (blue) and low (red) expression of cytoplasmic CAIX [A]. A scree plot of the PC against percentage of variation. The X-axis displays the PC, and the Y-axis shows percentage of variance explained [B]. Plots were constructed by Dr Gerard Lynch.

Next, a heatmap was constructed to visualise the patterns of the top 20 DEGs amongst node negative patient samples using ComplexHeatmap in R Studio (RStudio, Boston, MA, USA) (Figure 9.9). Expressional status of cytoplasmic CAIX is shown with colour bars at the top of the heatmap. Each row represents a single gene, and each column represents a tumour sample. As shown in the colour bar, orange indicates up-regulation and purple represents down-regulation. There was clear pattern in the gene expression profile between tumours with low expression than those tumours with high expression.

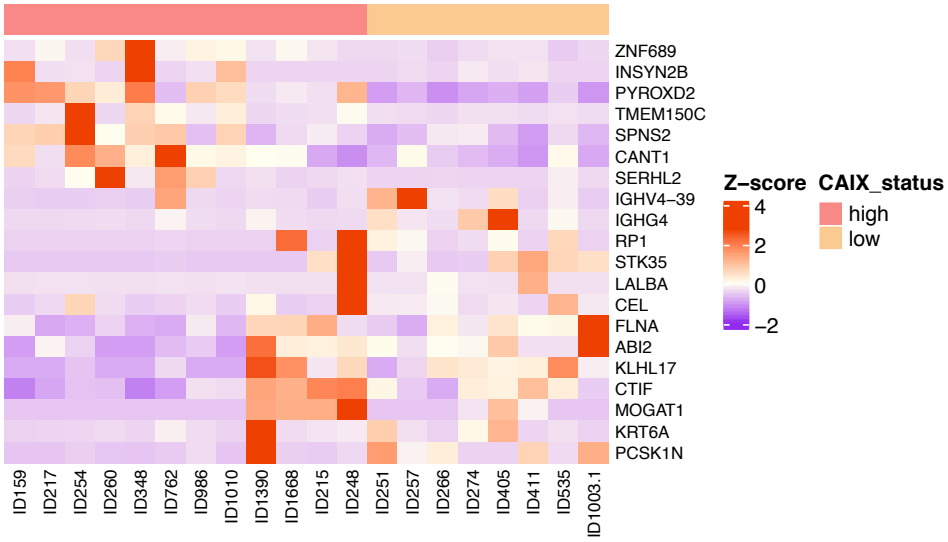

Figure 9.9 Heatmap of gene expression data from microarray analysis in node negative group.

Heatmap of the top 20 DEGs of cytoplasmic CAIX expression groups. Each row represents a single gene and each column represent a tumour sample. The scale bar shows the relative gene expression levels corresponding to the colours in the heatmap. As shown in the colour bar, orange indicates up-regulation and purple represents down-regulation. Plot was constructed by Phimmada Hatthakarnkul.

9.3.2.3 Enrichment analyses

The DEGs were analysed using STRING online method to provide information for three DEGs. The DEGs were analysed and categorised into the three categories, including cellular component, biological process, and molecular function. The functional gene set enrichments of the cellular component are shown in Table 9.9. These include cytoplasmic vesicle, secretory granule, and endomembrane system.

Table 9.9 Functional enrichments for cellular components

Cellular component	Matched proteins	FDR
Cytop lasmic vesicle	SPNS2, SERHL2, PCSK1N	0.00037
Secretory granule	PCSK1N	0.0072
Endomembrane system	SPNS2, PCSK1N	0.0264

The functional enrichments regarding biological process are shown in Table 9.10. SPNS2 is associated with G protein-coupled receptor signalling pathway, and sphingosine 1-phosphate receptor signalling pathway.

Table 9.10 Functional enrichments for biological process

Biological process	Matched proteins	FDR
G protein-coupled receptor signalling pathway	SPNS2, PCSK1N	0.00064
Peptide hormone processing	PCSK1N	6.11e-07
Sphingosine 1-phosphate receptor signalling pathway	SPNS2	6.80e-07

9.3.2.4 Protein-protein interaction network construction

Protein interactions among the DEGs, including PCSK1N, SERHL2, SPNS2 were predicted with STRING tools. The results showed no significant interaction between these proteins within a PPI network as presented in Figure 9.10A. A total of 10 proteins were added to show a network around the input proteins. A total of 13 nodes and 22 edges were involved

in the PPI network with the PPI enrichment P-value of 0.0009. SPNS2 showed interaction with their partner proteins, SphK1, SphK2, and S1PR2 which were added from the STRING database (Figure 9.10B).

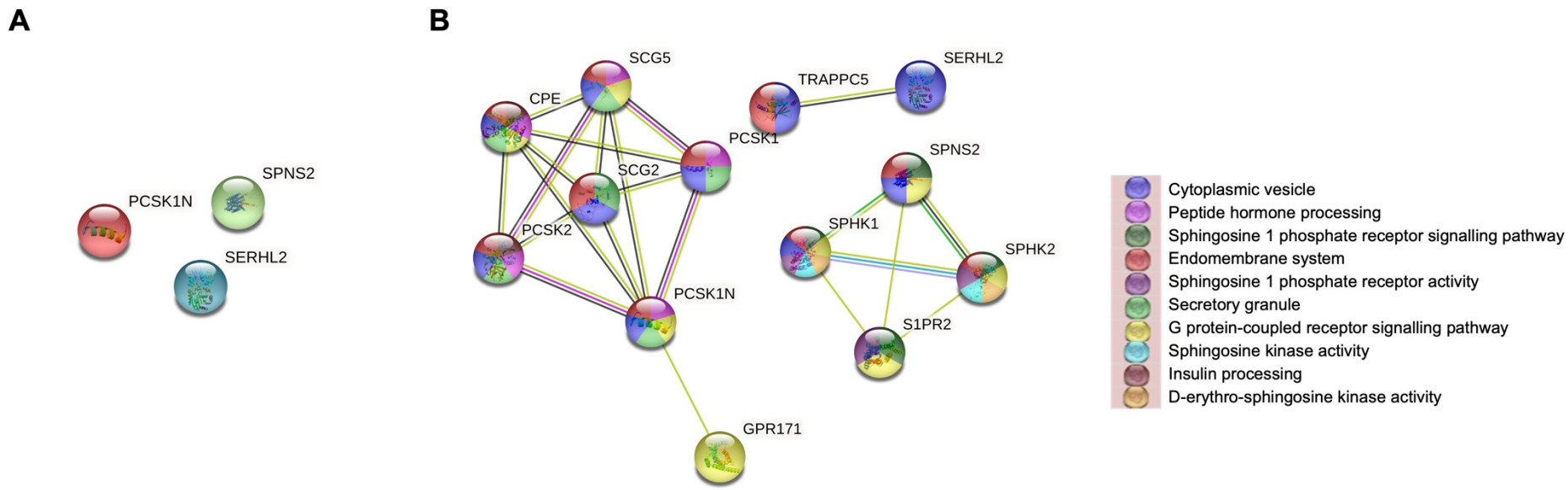

Figure 9.10 String map of differential expression genes in node negative group.

String interaction network diagram showing relationships between the differentially expressed genes from whole transcriptome analysis on a subset of node negative group. PPI network analysis for three proteins [A], PPI network analysis for extra added 10 proteins [B].

9.3.2.5 Pathway enrichment analyses

To determine biological pathways associated with DEGs in the high cytoplasmic CAIX expression in node negative group, the STRING online database was used. SPNS2 and PCSK1N genes were linked with Reactome pathway as shown in Table 9.11.

Table 9.11 Pathway's enrichment analysis

Pathway enrichment	Matching proteins	FDR
Sphingolipid de novo biosynthesis (Reactome)	SPNS2	0.0277
Insulin processing (Reactome)	PCSK1N	0.0160

9.3.2.6 Validation of SPNS2 using tissue microarrays

As the node negative data implicated the sphingosine kinase signalling being associated with hypoxia, the protein level was considered to investigate the effect of sphingosine kinase on hypoxia pathway. Our lab has performed the IHC test for sphingosine kinase pathway on ER-negative patients (429). With this dataset, we attempted to investigate the correlation of this pathway with hypoxia. No significant correlations were observed between sphingosine kinase pathway and CAIX protein but there was an association between cytoplasmic sphingosine kinase-1 (SphK1) and cytoplasmic HIF-1α (1) protein (Table 9.12).

Table 9.12 Association between SphK1, S1P4, CAIX and HIF-1α (2) proteins expression in ER-negative cohort

Markers	Membranous SphK1	Cytoplasmic SphK1	Nuclear SphK1	Membranous S1P4	Cytoplasmic S1P4	Nuclear S1P4
Cytoplasmic CAIX	0.575	0.965	0.781	0.320	0.152	0.124
Cytoplasmic HIF-1α (1)	0.289	**0.017**	0.328	0.415	0.992	0.397

Chi-squared table of associations between hypoxic markers [cytoplasmic CAIX, and HIF-1α (1)] and sphingosine kinase markers [membranous, cytoplasmic, nuclear SphK1 and S1P4].

9.4 Discussion

This exploratory pilot study of 37 ER-negative breast cancer used gene expression profiling to better understand total changes in gene expression in various endogenous biochemical processes and during tumour development. In particular, the TempO-Seq platform was used to identify DEG profiles for tumours with low versus high cytoplasmic CAIX, including those with node negative disease.

In ER-negative tumours, the majority of DEGs in high expression of cytoplasmic CAIX were up-regulated, however few of these genes reached statistical significance. 10 significant genes were identified namely OR8B2, SERHL2, KRT6A, MMP7, SPINK8, TMEM150C, CEACAM6, MUCL1, PITX2, and GALNT6 which warrant further investigation. In contrast, in those patients with node negative disease only 3 genes were significantly differentially expressed PCSK1N, SERHL2 and SPNS2. Therefore, different genes are differentially expressed in more advanced disease and that only SERHL2 remained differentially expressed (log2 FC increase approximately 4) with disease progression.

SERHL2 (Serine hydrolase-like protein 2) belongs to the serine hydrolase family (430). Suppression of SERHL2 showed moderately increased progression of ductal carcinoma *in situ* to invasive breast cancer (431). SERHL2 identified in TNBC for predicting chemotherapeutic response (432). According to a recent study in the LAR subtype, the most shortened 3′UTR (3' untranslated region) was SERHL2, which was associated with 4 mRNAs (433). However, from the literature, the present study is the first to document the association of SERHL2 with cancer hypoxia. Moreover, due to its function and that it is consistently overexpressed independent of disease ER-α stage, it may prove to be a useful therapeutic target.

Identification of PPI networks is a crucial step in finding the signal transduction pathways that interact. In ER-negative patients, the result from the PPI networks of the tumours with high cytoplasmic CAIX expression demonstrated that two proteins GALNT6 and MUCL1 had significant interactions with each other.

GALNT6 (Polypeptide N-acetylgalactosaminyltransferase 6) is an enzyme for O-glycosylation and its expression is increased in some human cancers including breast cancer (434). In addition, GALNT6-mediated mucin-type O-glycosylation can increase nuclear translocation of ERα in breast cancer (435). Previously, it has been suggested that GALNT6 as a marker for breast cancer progression and metastasis (436) by catalysing mucin-type O-

glycosylation-mediated stabilization of mucin 1 and fibronectin in breast cancer cells (437). High GALNT6 expression was significantly related to advanced tumour stage and associated with poor OS in breast cancer (438). Therefore, the present results confirm the association of GALNT6 with more advanced stage in patients with ER-negative breast cancer and suggest that hypoxia is a significant driver of GALNT6 expression in these patients.

MUCL1 (Mucin like 1) is a type of secretory protein, which belongs to the mucin family (439). It is a breast specific gene which is highly expressed in most breast tumours, developing an important role in the proliferation of cancer cells (440). Many studies have shown that MUCL1 expression strongly associates with higher tumour grade (440), TNM staging and lymph node metastasis (441, 442). MUCL1 has the potential to enhance migration and invasion of breast cancer cells via promoting EMT (443), and serve as a specific marker for hematogenous metastasis of breast cancer (442). High expression of MUCL1 was associated with poorer RFS in Her-2 disease (444), and in TNBC (445). Therefore, the present results confirm the association of MUCL1 with more advanced stage in patients with ER-negative breast cancer and suggest that hypoxia is a significant driver of MUCL1 expression in these patients. To our knowledge, the relationship between such expression of GALNT6 and MUCL1 and tumour hypoxia in ER-negative breast cancer has not been previously documented and therefore such work requires confirmation in further studies.

From the other DEGs input proteins, MMP7, PITX2, and CEACAM6 were demonstrated to interact with their partner proteins, which were added from the STRING database. Among these proteins, MMP7 showed a potential link and target for tumour therapy.

MMP7 (Matrix metalloproteinase 7) is a proteolytic enzyme which belongs to the family of MMP (446). It is recognised to degrade various extracellular matrix (ECM) substrates (447), and cleave non-ECM proteins, such as E-cadherin and Fas ligand (448). In addition, MMP7 promotes cancer progression by inhibiting the apoptosis of tumour cells (449), reducing cell adhesion (450), and stimulating angiogenesis (448). With reference to breast cancer, MMP7 was highly expressed in BLBC/TNBC compared with other breast cancer subtypes (451). Previous studies have suggested that MMP7 expression in breast cancer may be positively regulated by Her-2 implying that MMP7 might be an important factor in the growth and metastasis of Her-2 breast cancers (452, 453). Breast cancer patients that developed bone metastasis were found to have higher levels of circulating MMP7 than patients without such metastasis (454). Inverse association between MMP7 expression and tumour grade was reported (455). Associations between MMP7 overexpression and breast cancer prognosis are

less consistent. Two studies found significant associations with survival (456, 457) but one study found no association (455). Hypoxia was known to regulate a cohort of genes, including members of the MMP family and genes that modulate EMT, and thus to promote cancer migration and invasion (458). Under hypoxic conditions, HIF-1α promotes the expression of MMP7 and invasion in TNBC (459). The MMP7 mRNA expression in hepatocellular carcinoma has a significant correlation with HIF-1α mRNA (460).

PITX2 (Paired like homeodomain 2) is involved in pituitary specific gene regulation and left-right patterning during embryonic and organogenic development (461). Patients with aberrant methylation of PITX2 promoter show a significantly higher risk of breast cancer progression (462). IHC for PITX2 determination showed a significant association between PITX2 protein and ER/PR expression, indicating that PITX2 may be useful prognostic markers in invasive breast cancer (463). PITX2 demonstrated a predictive value in preclinical cancer models (464), tamoxifen treated node negative patients (465), and TNBC patients (466). However, to date, there have been no reports of investigations of the prognostic significance of PITX2 expression and cancer hypoxia, and the present study is the first to document the association of PITX2 with tumour hypoxia.

CEACAM6 (Carcinoembryonic antigen cell adhesion molecule 6) is a member of carcinoembryonic antigen family. It has a role in tumorigenesis, disruption of cell polarity (467). In a cohort study of 840 invasive breast carcinoma and a validation cohort of 300 invasive breast cancers, CEACAM6 expression was found in 37% patients (468). Poola et al. reported that overexpression of CEACAM6 is associated with breast cancer progression (469) which leads to invasion and migration in breast cancer cells (470). Regarding its expression in metastasis, CEACAM6 was highly expressed among breast cancer lymph node metastasis but was not expressed in unaffected lymph nodes or surrounding tissue (471). Expression of CEACAM6 also serves as an indicator of response to therapy in breast cancer. CEACAM6 overexpression reflected trastuzumab-resistant Her-2-positive (472), and tamoxifen-resistance ER-positive breast cancer (473). In a multivariate analysis, high CEACAM6 expression was an independent predictor of breast cancer recurrence (474). Antibody studies have revealed possible therapeutic potential of CEACAM6 in breast cancer (475). However, the association of CEACAM6 with tumour hypoxia is yet to be explained, and the present study is the first to document the association of CEACAM6 with cancer hypoxia.

Taken together the present results on MMP7, PITX2, and CEACAM6 suggest a variety of interactions and association among these proteins that influence breast cancer progression.

For example, the STRING database demonstrated that cell component enrichment analysis showed that MMP7 was located in extracellular space and associated with glycosaminoglycan binding, which are essential for tumour metastasis (476). MMP7 was significantly enriched in three pathways, including WNT signalling pathway, ECM organization, and degradation of ECM which are known to be directly involved in breast cancer progression (477, 478). This result was consistent with the report from previous studies. TNBC patients displaying dysregulated WNT/β-catenin signalling is more likely to develop lung and brain secondary metastases with high expression of MMP7, a transcriptional target of WNT pathway (479). Furthermore, Han and colleagues have proposed that a FOXC1-WNT5A-MMP7 signalling axis plays an essential role in the migration, invasion, and distant metastasis of TNBC cells (480). Furthermore, this result has identified CEACAM6 as a critical gene in the regulation of cell adhesion and in cell migration. CEACAM6 has been found to be associated with migration, invasion and adhesion (470), steps which are important in the metastasis to secondary tissue sites other than lymph nodes (481). Indeed, anti-adhesive molecules that disrupt cell-matrix and cell-cell adhesion have been proposed as potential cancer therapeutics based on their ability to interfere with motility, adhesion, and metastatic progression (475).

Clinically, nodal status remains an important prognostic factor and therefore, gene expression analysis was compared between the whole cohort and those patients who were node negative. With reference to the node negative tumours, STRING online method demonstrated no significant interaction between expressed proteins. SPNS2 showed interaction with their partner proteins which were added from the STRING database including SphK1, SphK2, and S1PR2. These results suggest a variety of interactions and association among these proteins that influence breast cancer progression.

SPNS2 (Sphingolipid transporter 2) encodes for SPNS2, a member of the major facilitator superfamily, regulates sphingosine 1-phosphate (S1P) release and modulates S1P activity as an S1P transporter (482). S1P is a lipid mediator derived from sphingosine and is catalysed by two sphingosine kinases (SphK1and SphK2) (483). The S1P formed by these enzymes can either be exported from the cells (through transporter proteins such as SPNS2) and act as a ligand on a family of five S1P-specific G protein coupled receptors (S1P1−5) (484) or can bind to specific intracellular target proteins (485). S1P has been implicated as a tumour-derived factor that stimulates both angiogenesis and lymphangiogenesis in breast cancer (486). High S1P expression by tumour was associated with lymph node metastasis (487), indicating that S1P enhances cancer metastasis by affecting TME in human breast cancer.

Evidence is accumulating to support a role for SphK1 in human cancers including breast cancer (488). Studies revealed that SphK1 mRNA expression was higher in TNBC cells and enhanced metastasis, and invasion compared to non-TNBC cell lines (489, 490). Furthermore, SphK1 expression had a role in breast cancer cells' survival. High expression of SphK1 in ER-positive breast cancer was associated reduced patient survival (491, 492) and increased resistance to tamoxifen (493, 494). Silencing of SphK1 enhanced cytotoxic effects of fluorouracil and doxorubicin in TNBC cells (495). S1P receptors are also involved in cancer progression. It stimulates the proliferation of ER-positive and ER-negative breast cancer cells (496). High expression of S1P1 or S1P3 by ER-positive breast cancer cells correlated with poor prognosis (494). SPNS2 showed a promoting effect in the genesis, apoptosis and migration of cancer, through S1P/S1PRs pathways activating downstream signalling such as STAT3, AKT, ERK, Ras and Rac (497).

In this chapter, the STRING online method showed SPNS2 mainly located in the cytoplasmic vesicle and endomembrane system and associated with G protein-coupled receptor signalling pathway, S1PR signalling pathway, and sphingolipid de novo biosynthesis pathway. A similar conclusion has also been reported previously. S1P released from cells functions to stimulate a family of G protein-coupled receptors, the S1P receptors (S1P1−5) (484). In ER-negative breast cancer cells, S1P binding to S1P4 stimulates activation of ERK1/2 pathway and correlated with poor prognosis (429), and this is depending on Her-2 (498). ER-positive breast cancer cells responded to S1P via S1P3 to co-ordinately regulate EGFR localization and signalling (499). Functionally, SphK1 was exhibited to regulate the levels of notch signalling target gene Hes1 via S1P3-mediated up-regulation of notch intracellular domain (495). Migration of ER-negative breast cancer cells involves S1P derived from both SphK1 and SphK2 (500). Inhibition of SphK1 results in cell death in human breast cancer cells (488), indicating that tumour SphK1/S1P signalling plays vital roles in growth/proliferation. However, such data is hard to interpret and therefore it is important to validate at protein level. SPNS2 was validated by IHC via our lab (429). For a given gene at protein level, a statistically significant correlation between HIF-1α (1) and cytoplasmic SphK1 expressions was observed in node negative group ($P = 0.017$). In line with this chapter result, the previous *in vitro* experiments (501), suggested that SphK1 has been identified as a key mediator of the adaptive response to hypoxia in various cancer cell models including breast cancer cell lines. Studies demonstrated that SphK1 promoter has two hypoxia-inducible factor-responsive elements and both HIF-1α and HIF-2α have been involved in the transcriptional regulation of SphK1 (502, 503). It has also been reported that SphK1/S1P signalling is also involved regulating the expression of HIF-2α, which can drive

aggressive tumour (504). Therefore, siRNA knockdown of SphK1/S1P was associated with a decreased HIF-2α protein expression and co-overexpression of HIFs and SphK1 may be a biomarker in node-negative breast cancer.

Taken together, the present chapter showed that although a variety of genes were expressed in hypoxia mediated by high CAIX in ER-negative cohort, only three genes were expressed in node negative group. This finding supports the idea that apparent difference in DEGs between two patients' groups could be required to include representation of specific pathways that might be involved in breast cancer progression. In fact, SPNS2 has the superior performance compared with other DEGs. Interestingly, SPNS2 pathway was dependent on HIF activity. Hypoxia stimulates endothelial cell migration (502) and increases production and release of S1P from glioma cells (503). Adenocarcinoma cells show hypoxia dependent induction of SphK2 expression and S1P release (505). Sustained hypoxia stimulates SphK1 and SphK2 expression in proliferating human pulmonary smooth muscle cells (506).

Finally, genes implicated in these analyses generate valuable information for future pathway studies, with the potential to identify new targets that might contribute to improved treatment and better understanding of genes that are related to tumour progression and metastasis. The present study has provided further evidence that co-expression of HIF-1α (1), and SphK1 in this cohort of patients with node-negative breast cancer may allow for the rational use of molecules blocking the HIF molecular cascade for a novel target of drug development.

Limitations of this study include a limited sample size which increase the risk of bias and therefore further studies are required to confirm the present results. In particular, the unique observation that SERHL2 was differentially expressed requires confirmation on other studies.

In conclusion, data from this chapter has identified 10 genes significantly associated with tumour CAIX in ER-negative cohort. However, due to heterogenous population, subsequent analysis of lymph node negative patients was performed with SPNS2 of particular interest. This gene profile was validated at protein level, and it was highly informative and could provide a powerful tool to identify subgroups of patients with node negative breast cancer who most likely to respond to therapy directed toward hypoxic tumour and preventing overtreatment in substantial numbers of patients. If validated in larger cohorts, the recommendation of hypoxia targeted therapy in patients with lymph node negative primary breast cancer could be guided by this prognostic signature.

Because ER-negative is a heterogenous cohort with combined tumour and stromal cells, the spatial transcriptomic study was therefore carried out to consider tumour and stroma compartment independently. This will be further investigated in the following chapter on TNBC patients.

Chapter 10 Spatial transcriptomic analysis of tumour with high and low CAIX expression in TNBC tissue samples using GeoMx™ RNA assay

10.1 Introduction

Data from chapter 8 has highlighted the prognostic role for CAIX in TNBC cohort, however the underlying genomics driving these phenotypes not yet known and may be of importance. In the previous chapter we employed bulk RNAseq method to identify DEGs in ER-negative tumours. However, there were several limitations with this approach including the heterogeneity of ER-negative tumours and being unable to differentiate if expression profiles were from tumour or stromal cells. Therefore, we have aimed to address these issues in the current chapter by limiting the tumours to only TNBC and by performing spatial profiling allowing us to determine if the signal was from the tumour or stromal cells.

In addition, in previous IHC chapter 6, expression of CAIX showed a prognostic association within Her-2 subtype. However, due to time restriction, these finding requires future work including spatial transcriptomics study.

High-plex spatial profiling of tumours enables characterization of diversity in the breast TME, which can holistically illuminate the biology of tumour growth, dissemination, and response to therapy. There is an urgent need to identify biomarkers which accurately predict of metastatic behaviours in TNBC and response to treatment (507). Bioinformatics methods can be used to interrogate the mutational and gene expression profiles that underlie TNBC and elucidate the molecular mechanism that drive pathogenesis (508). GeoMx digital spatial profiler (DSP) is an innovative new technique that, for the first time, allows the analysis in patients with breast cancer. Previously, the TME of breast cancer was analysed using DSP, but mainly for protein expression (509).

Although there is an increasing awareness that tumour and stromal interactions contribute to tumour progression, previous studies have not addressed how changes occurring in tumour hypoxia affect disease outcome. In this study, GeoMx DSP was used to explore potential biomarkers of hypoxic TNBC. We identify genes corresponding to good and poor outcome in TNBC associated with cytoplasmic CAIX protein expression that have not been previously recognized and correlate the presence of overlapping genes with transcriptomic data in previous chapter. Such insight is essential to open new windows for the discovery of new therapeutics targeting hypoxic tumour cells and hypoxic microenvironment.

10.2 Materials and methods

The present study was performed in two steps: (1) spatially analyse RNA transcripts in TNBC tissue samples. (2) validation of identified genes at protein level by IHC.

10.2.1 Tissue microarray and patient cohorts

GeoMx data analysis was conducted using archival FFPE microarray data from TNBC samples. The sample cohort representing a population-based retrospective collection that was obtained at the department of pathology at Queen Elizabeth University Hospital. From 207 TNBC samples, 98 cores were selected from more than 1 core from each patient and then the results were averaged leaving 52 patients (155 AOI) were utilised for GeoMx DSP analysis. The use of the epithelial cell-specific marker, pan-cytokeratin, assists pathologic identification of breast tumour tissue within a sample. Within these specifications, 73 pan-cytokeratin positive (PanCK-positive) and 82 pan-cytokeratin negative (PanCK-negative) as described in chapter 2.

10.2.2 GeoMx digital spatial profiling

10.2.2.1 Preparation of slides

Briefly, 2.5µm FFPE TMA sections of archival surgically resected patient TNBC were put on glass slides, dewaxed, target retrieved, digested with proteinase K, and then incubated with GeoMx RNA detection probes overnight. Stringent washes were performed followed by *in situ* hybridization probes for RNA via an ultraviolet (UV)-photocleavable linker. Slides were stained with fluorescently labelled antibodies against pan-cytokeratin (PanCK, tumour cell marker) and CD45 (lymphocyte marker) which served as visualization markers to distinguish the tumour cells from their immune infiltrate stromal cells and a fluorescent DNA dye (SYTO 13).

10.2.2.2 Region of interest selection (ROI)

TMA cores were then selected for future analysis based on successful 3-plex immunofluorescence staining of SYTO 13, PanCK and CD45 to obtain regions of interest. Circular ROIs were selected on the basis of fluorescently labelled anti-PanCK. PanCK-positive used to select tumour-rich regions that were enriched for PanCK, and PanCK-negative to identify stroma-rich regions that were enriched for CD45 and lacked PanCK staining. After ROIs were selected, the GeoMx platform employs an automatically

controlled UV laser to illuminate each ROI in turn, specifically cleaving barcodes within the ROI but not in surrounding tissue. A microcapillary collection system collected the liberated barcodes from each region and plated them into an individual well on a microtiter plate. This process was repeated in turn for each ROI before processing using NanoString MAX/FLEX nCounter system as detailed in chapter 2.

10.2.2.3 nCounter hybridization assay for photocleaved oligo counting

Gene expression values within each ROI were quantified by the GeoMx DSP platform by counting the unique indexing oligos assigned to each target with the NanoString nCounter instrument (510).

10.2.2.4 GeoMx data analysis

Raw data of all the samples were normalized with negative probes using the geometric mean. The GeoMx data analysis suite provides a range of native software tools for analysis. For comparing two groups of tissues (tumour and stroma), with multiple ROIs/segments per tissue, linear mixed models (LMMs) statistical test was used. Data analysis was performed to identify differences in gene expression between high and low CAIX tumours. DEGs were performed using the GeoMx analysis suite, which utilises the GeoMxTools R package (tool: 'mixedModelDE' in R package 'lmerTest'). The DEGs screened out with the criteria of log2 FC > ± (0.25 and 0.3) for tumour and stromal compartment, respectively, and P-value <0.05. The number of genes assessed in the RNA panel was 84 genes. Volcano plots were created using a plugin script, available at: (https://github.com/NanostringBiostats/DSPPlugins/tree/master/DSPPlugVolcanoPlot). Heatmaps comparing the low and high CAIX groups were performed by loading the counts and sample sheet files to ComplexHeatmap package in R Studio (RStudio, Boston, MA, USA).

10.2.3 Protein level validation of DSP gene expression by Immunohistochemistry

TMAs were prepared from TNBC cohort from all representative areas of tumour and tumour rich stroma when present to validate identified genes. IHC staining of CD68, CD3, BCL2, and HIF-1α (1) was used to measure macrophages, lymphocytes and evaluate apoptosis and hypoxia in included cases. All samples had a negative control slide (no primary antibody) to assess the degree of non-specific staining.

10.2.4 Scanning and visualisation of slides

Stained slides were digitally scanned using a Hamamatsu NanoZoomer Digital Slide Scanner (Hamamatsu Photonics K.K., Shizuoka, Japan), at 20x magnification high resolution images and viewed using SlidePath and NDP serve 3 image viewer platform system.

10.2.5 Pathological scoring of immunohistochemistry

Assessment of IHC stained sections by the presence of brown coloured reaction in the nucleus and/or cytoplasm was considered a positive reaction. Different scoring methods were required to be most appropriate to the biomarker. Expression of protein levels was assessed at each cellular compartment separately, cytoplasmic and nuclear HIF-1α (1) in tumour nests and cytoplasmic BCL2 in TME were scored using QuPath digital pathology software v. 0.2.3 (QuPath, Edinburgh, UK). Also, the number of cytoplasmic CD3 staining cells was recorded as percentage in tumour nests, TME and total lymphocytes separately using QuPath. However, QuPath method was inappropriate to score macrophages due to shape irregularity. Therefore, cytoplasmic CD68 staining cells were quantified manually in separate tumour nests, TME and total TAM (sum of both).

Expression of each marker within the cohort was assessed in the three separate tumour/ stroma sites. Then, the mean number of triplicate cores from each tumour/stroma cores was calculated for the macrophages and used to separate “high-” from “low-” expressing tumours as previously described in chapter 2.

10.2.6 Statistical analyses

Survival probabilities were studied by the Kaplan-Meier method, and differences in survival time were analysed with a log-rank test. Qualitative data were compared using Chi-squared statistics. All statistical analyses were conducted using IBM SPSS software v. 28 (SPSS Inc., Chicago, IL, USA). All tests were two-sided, and $P<0.05$ was regarded as significant. The optimal threshold for each marker in each cellular compartment was defined using R Studio (RStudio, Boston, MA, USA). Threshold values for nuclear and cytoplasmic HIF-1α (1) included in this cohort were chosen as previously described for the Glasgow breast cohort in chapter 5.

10.3 Results

To determine the correlation of gene expression data with high and low cytoplasmic CAIX expression within PanCK-positive and PanCK-negative samples, the GeoMx DSP was used. DEGs were identified in a comparison of high and low CAIX expression groups by using R Studio (R Studio, Boston, MA, USA).

10.3.1 Identification of differentially expressed genes with cytoplasmic CAIX expression in tumour compartment

The DEGs were filtered according to log2 FC > ± 0.25 and 0.3 for tumour and stromal compartment, respectively, and $P<0.05$. Volcano maps were plotted, within PanCK-positive cells, high CAIX expression group had significantly higher expression of three genes, including CD68, HIF1A, VSIR, and lower expression of one gene, pan-melanocyte (Table 10.1).

Table 10.1 The significant genes comparing high and low cytoplasmic CAIX expression in pan-cytokeratin positive group

Gene name	Gene description	Categories	Log2 FC	P-value
CD68	CD68 molecule	Macrophage	- 0.371574835	**0.008896029**
HIF1A	Hypoxia inducible factor 1 alfa	Tumour, cytokine, and chemokine signalling	- 0.274447855	**0.011833749**
pan-melanocyte	Pan-melanocyte	Melanoma	0.245326804	**0.016388306**
VSIR	V-Set immunoregulatory receptor	Myeloid activation, macrophage, myeloid checkpoint	- 0.097641803	**0.029824509**

Volcano plot was plotted using ggplot to visualize the FC and determine the statistically significance differences between the high and low cytoplasmic CAIX expression groups (Figure 10.1).

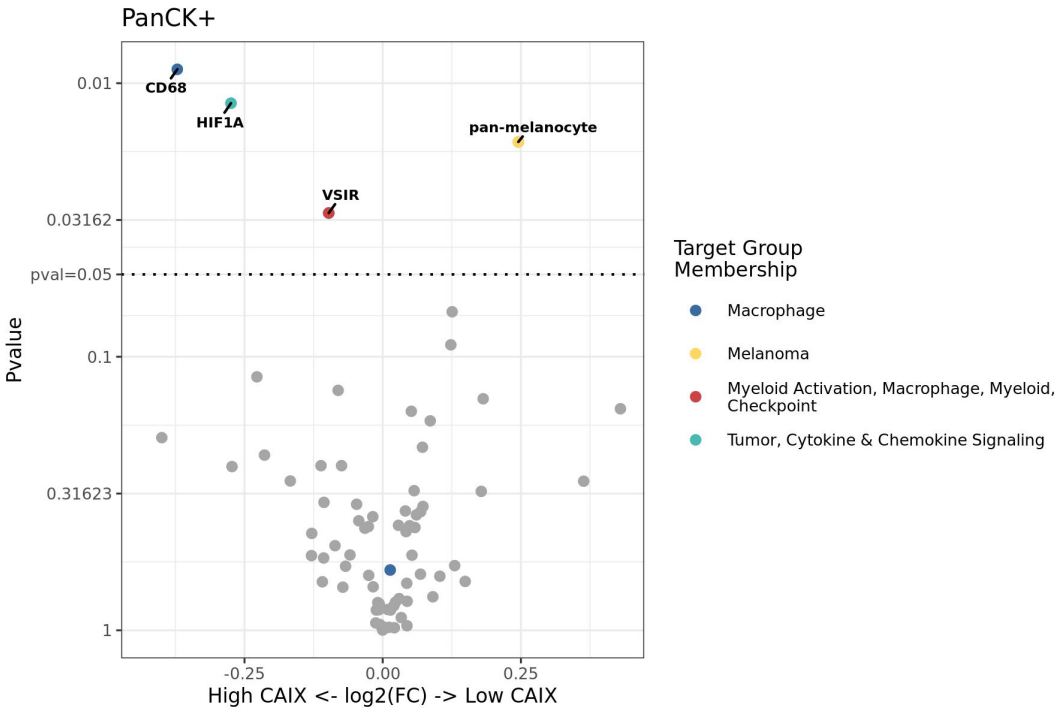

Figure 10.1 Volcano plot of differentially expressed genes in pan-cytokeratin positive tumour with high and low cytoplasmic CAIX expression groups.

The volcano plot describes log2 FC in the X-axis and P-value in the Y-axis. The line parallel to the X-axis represents a value of P = 0.05. P-value<0.05 was considered significant. Plot was constructed with the assistance of Phimmada Hatthakarnkul.

In addition, within tumour-rich region (PanCK-positive compartment), the heatmap for the significantly DEGs between high and low cytoplasmic CAIX expression groups was generated with ComplexHeatmap package in R Studio. There was no clear pattern associated with CAIX expression levels (Figure 10.2).

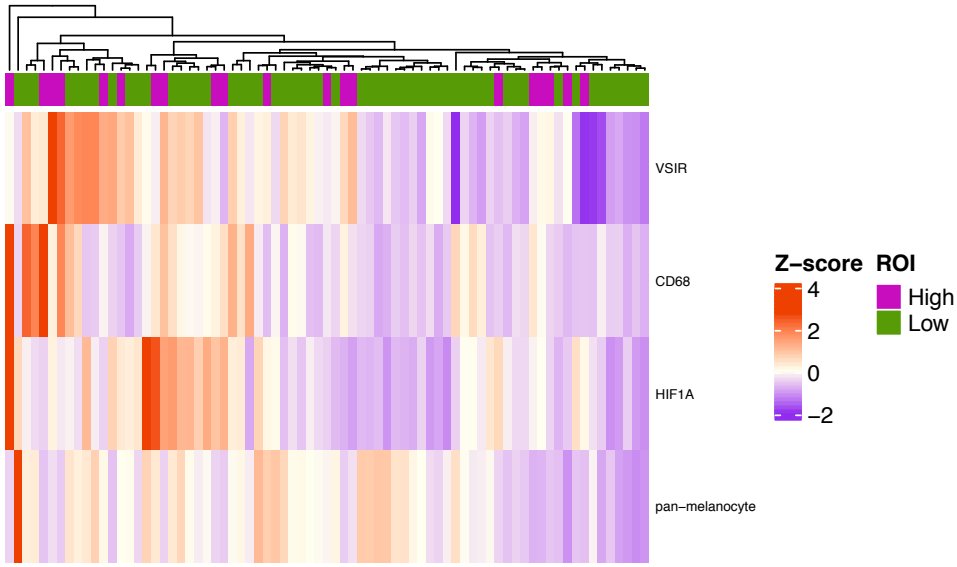

Figure 10.2 Hierarchical clustering heatmap showing the most significant differentially expressed genes in pan-cytokeratin positive tumour with high and low cytoplasmic CAIX expression groups.

Hierarchical clustering analysis and heatmap of the DEGs. Each row represents a single gene and each column represent a tumour sample. The scale bar shows the relative gene expression levels corresponding to the colours in the heatmap. As shown in the colour bar, orange indicates up-regulation and purple represents down-regulation. Plot was constructed with the assistance of Phimmada Hatthakarnkul.

10.3.2 Identification of DEGs with cytoplasmic CAIX expression in stromal compartment

Based on stromal compartment (PanCK-negative segments), low cytoplasmic CAIX expression had significantly higher expression of 8 genes, including CD86, CD3E, MS4A1, BCL2, CCL5, NKG7, PTPRC, and CD27, and a trend towards significance was observed with FAS gene (P = 0.053) (Table 10.2). Genes ordered by P-value, regardless of log2 FC.

Table 10.2 The significant genes comparing low and high cytoplasmic CAIX expression in pan-cytokeratin negative group

Gene name	Gene description	Categories	Log2 FC	P-value
CD86	CD86 molecule	T cell activation, myeloid checkpoint	0.194619932	**0.000425023**
CD3E	CD3E molecule	T cells	0.300552796	**0.005474011**
MS4A1	Membrane spanning 4-domains A1	B cells	0.22399975	**0.007014351**
BCL2	B-cell lymphoma-2	Apoptosis	0.194899023	**0.008449576**
CCL5	C-C motif chemokine ligand 5	Cytokine and chemokine signalling	0.35022514	**0.012321049**
NKG7	Natural killer cell granule protein 7	Cytotoxicity	0.19508988	**0.024832855**
PTPRC	Protein tyrosine phosphatase receptor type C	Total immune	0.32467447	**0.035836939**
CD27	CD27 molecule	T cells	0.169683196	**0.041806309**
FAS	Cell surface death receptor	Apoptosis, cytokine, and chemokine signalling	0.119141511	**0.053309814**

Volcano plot was used to determine the statistically significance differences between the high and low cytoplasmic CAIX expression groups (Figure 10.3).

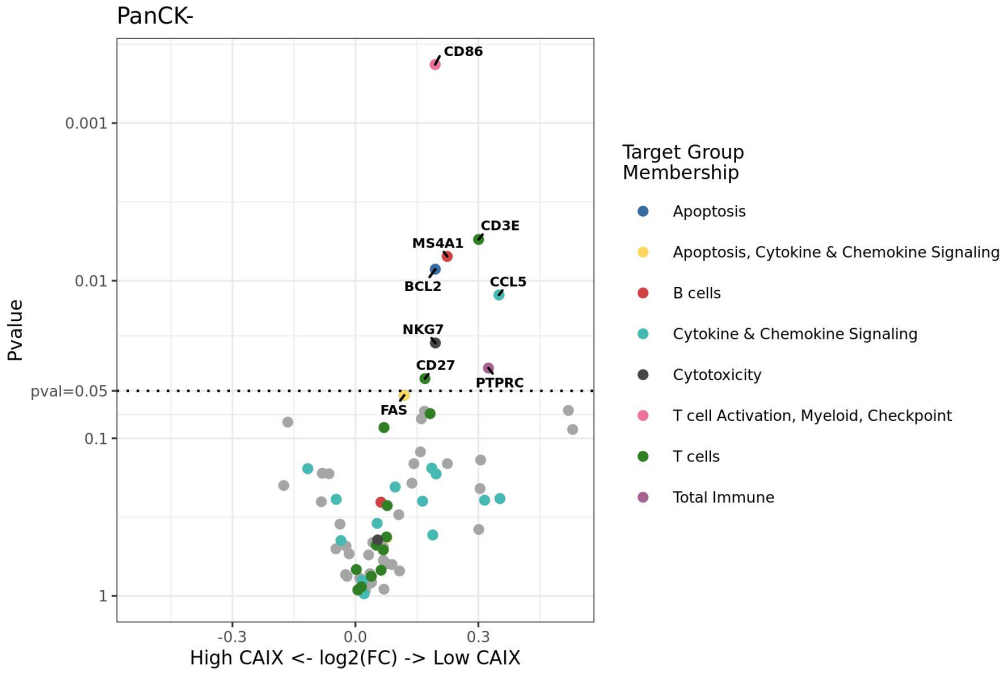

Figure 10.3 Volcano plot of differentially expressed genes in pan-cytokeratin negative tumour with high and low cytoplasmic CAIX expression groups.

The volcano plot describes log2 FC in the X-axis and P-value in the Y-axis. The line parallel to the X-axis represents a value of P = 0.05. P-value<0.05 were considered significant. Plot was constructed by Phimmada Hatthakarnkul.

Correspondingly, for grouping comparisons based on the CAIX expression in PanCK-negative, the heatmap demonstrated noticeable gene expression differences when the high CAIX group was compared to the low group. Most of high expression genes were shown in low CAIX expression group as shown in Figure 10.4.

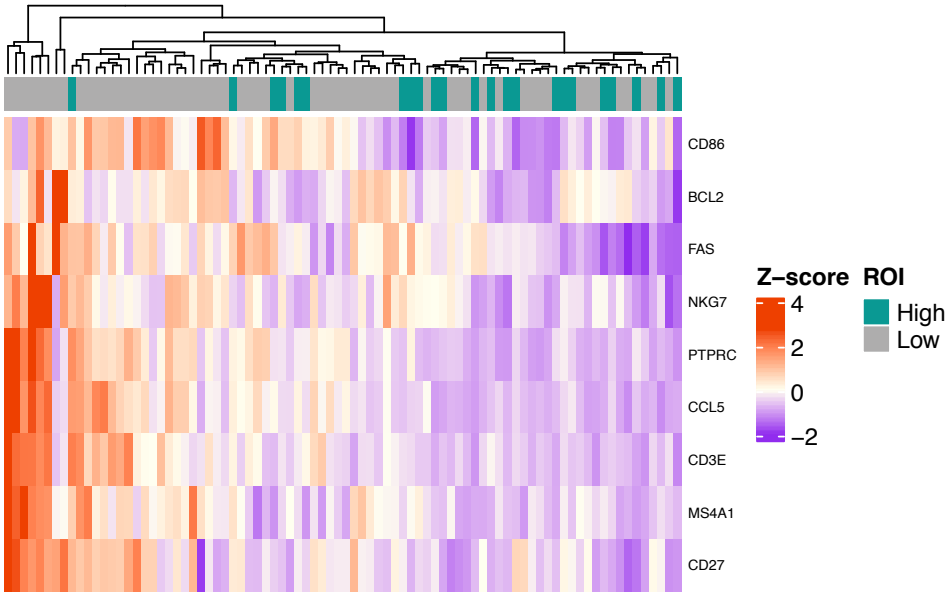

Figure 10.4 Hierarchical clustering heatmap showing the most significant differentially expressed genes in pan-cytokeratin negative tumour with high and low cytoplasmic CAIX expression groups.

Comparison of gene expression data of TNBC in PanCK-negative group based on cytoplasmic CAIX expression levels. Genes are shown in rows, and cases are shown in columns in the heatmap (green; high expression, grey; low expression). The scale bar shows the relative gene expression levels corresponding to the colours in the heatmap. As shown in the colour bar, orange indicates up-regulation and purple represents down-regulation. Plot was constructed by Phimmada Hatthakarnkul.

10.3.3 Validation of the identified genes in the microarray TNBC samples

To evaluate the significance of the four selected genes HIF1A in tumour cells, BCL2, CD68, and CD3 in immune stromal cells, their expression patterns were validated by IHC at protein level with respect to hypoxic marker CAIX, in the microarray TNBC datasets as descried in chapter 2. Most of the proteins selected to study in this work have a well-established role in breast prognosis (357, 511-513). In addition, antibodies are in routine clinical use in most pathology laboratories.

10.3.3.1 Immunohistochemical analysis of tissue microarrays

10.3.3.1.1 HIF-1α (1) immunostaining

From 136 patients, in 3 (2%) patients there was a tissue core missing and HIF-1α (1) staining could not be carried out and were excluded from the analysis. Therefore, expression of HIF-1α (1) was assessed in 133 patients. Representative images of cytoplasmic and nuclear HIF-1α (1) staining are shown in Figure 10.5 (A, B). 113 (85%) tumours with low cytoplasmic expression, and 20 (15%) with high expression. In contrast, 31 (23%) patients with low nuclear expression and 102 (77%) with high nuclear expression (Table 10.3). An ICCC of 0.887 and 0.827 for cytoplasmic and nuclear HIF-1α (1), respectively was obtained between QuPath and manual scores.

10.3.3.1.2 BCL2 immunostaining

Of the 136 patients, 6 (4%) had a tissue core missing and so BCL2 staining could not be carried out, and they were excluded from the analysis. Therefore, expression of BCL2 was assessed in 130 patients. As shown in Figure 10.5 (C, D), BCL2 protein was mainly localized in the cytoplasm of tumour and immune cells, respectively. However, its expression was assessed in immune cells where 104 (80%) showed low expression and 26 of 130 (20%) tumours showed high BCL2 immunoreactivity (Table 10.3). There was good correlation between QuPath and manual scores with ICCC score of 0.937.

10.3.3.1.3 CD68 immunostaining

Expression of CD68 was examined in 128 from 136 patients. 8 (6%) of patients were excluded from analysis due to a tissue core missing or inadequate quality for scoring. Macrophages observed in both tumour and stroma of breast cancer with a predominantly

diffuse pattern (Figure 10.5E, F). Tumour-infiltrating macrophages were large irregular cells with oval to round nuclei with strong cytoplasmic staining but no nuclear staining for CD68. CD68 have been assessed in tumour nests, TME and combined both (Table 10.3). Scores were also rechecked randomly by a second observer (A.A). Excellent ICCC was found for CD68 in tumour nests and in TME (0.888 and 0.910, respectively).

10.3.3.1.4 CD3 immunostaining

A total of 135 tumours was available for CD3 IHC staining after the exclusion of missing cores. The infiltration pattern was mainly diffuse in the tumour, and stromal cells. CD3 protein was predominantly located in cell cytoplasm of lymphocytes in tumour nests and TME as shown in Figure 10.5G, H. CD3 T cells have been assessed in tumour nests, TME and combined both locations (total) (Table 10.3). An ICCC of 0.989, 0.984 and 0.983 for CD3 score in tumour nests, TME and total, respectively was obtained between QuPath and manual scores.

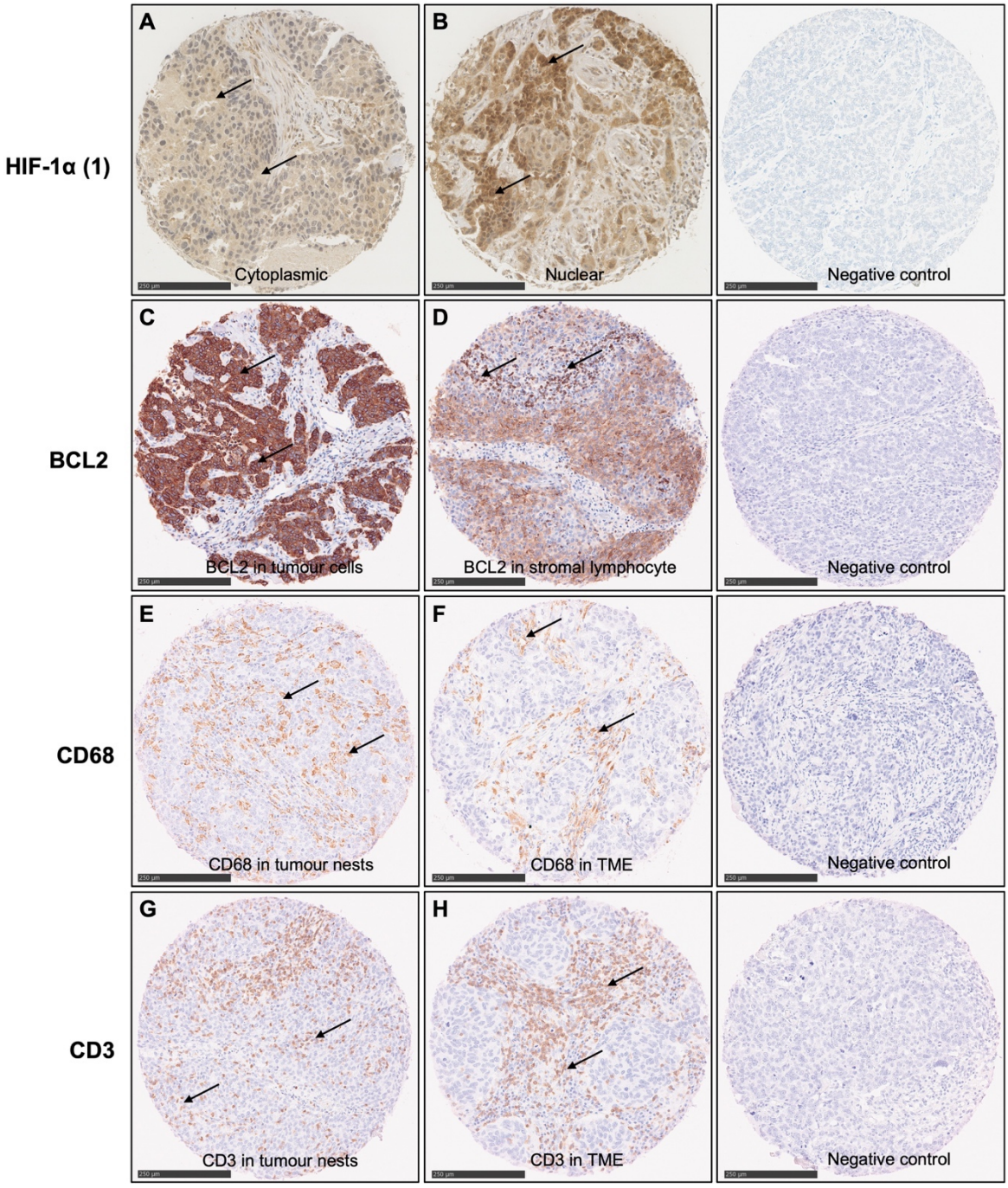

Figure 10.5 Representative images of immunohistochemistry staining of examined markers in TNBC samples.

Cytoplasmic and nuclear HIF-1α (1) expression [A, B], cytoplasmic BCL2 expression in tumour cells and immune cells [C, D], cytoplasmic CD68 are noted in tumour nests and TME [E F], cytoplasmic CD3 infiltration of both tumour nests and TME [G, H]. Negative control antibody was used in the breast cancer TMA to rule out nonspecific staining in the last column. Magnification at 250μm.

Table 10.3 Protein markers expression in TNBC cohort (n = 136)

Markers	Cytoplasmic n (%)	Nuclear n (%)	Missing cases n (%)
HIF-1α (1)			
Low expression	113 (85)	31 (23)	3 (2)
High expression	20 (15)	102 (77)	
BCL2			
Low expression	26 (20)	-	6 (4)
High expression	104 (80)		
CD68			
Tumour nests			
Low expression	47 (37)	-	8 (6)
High expression	81 (63)		
TME			
Low expression	33 (26)	-	8 (6)
High expression	95 (74)		
Total			
Low expression	25 (19)	-	8 (6)
High expression	103 (81)		
CD3			
Tumour nests			
Low expression	13 (10)	-	1 (0.7)
High expression	122 (90)		
TME			
Low expression	21 (16)	-	1 (0.7)
High expression	114 (84)		
Total			
Low expression	13 (10)	-	1 (0.7)
High expression	115 (90)		

Table showing the number of patients and the percentage for each marker included in the analysis.

10.3.3.2 Association of CAIX protein expression with immunohistochemical staining markers

To assess the interrelationship between CAIX protein expression, HIF-1α (1), BCL2 and immune markers, Chi-squared test was done as summarized in Table 10.4. High cytoplasmic CAIX expression correlated positively with cytoplasmic HIF-1α (1) (P = 0.010) and cytoplasmic CD68 protein expression in tumour nests (P = 0.039) and negatively with cytoplasmic BCL2 protein expression (P = 0.033). No other associations were found.

Table 10.4 Association between cytoplasmic CAIX expression and protein markers in TNBC cohort

Markers	Cytoplasmic CAIX
Cytoplasmic HIF-1α (1)	**0.010**
Nuclear HIF-1α (1)	0.355
Cytoplasmic BCL2	**0.033**
CD68 in tumour nests	**0.039**
CD68 in TME	0.728
Total CD68	0.865
CD3 in tumour nests	0.853
CD3 in TME	0.153
Total CD3	0.126

Chi-squared table of associations for cytoplasmic CAIX expression and protein markers including HIF-1α (1), BCL2, CD68, and CD3.

10.3.3.3 Association of proteins expression with survival

Kaplan-Meier analysis and log-rank test indicated a strong association of high cytoplasmic HIF-1α (1) with RFS (P = 0.048) but not with DFS and OS (P = 0.147, 0.594, respectively) (Figure 10.6A, C, E). High nuclear HIF-1α (1) expression was correlated with reduced DFS (P = 0.003) and OS (P = 0.016), however, no significant difference in RFS was observed between low and high expression groups (Figure 10.6B, D, F).

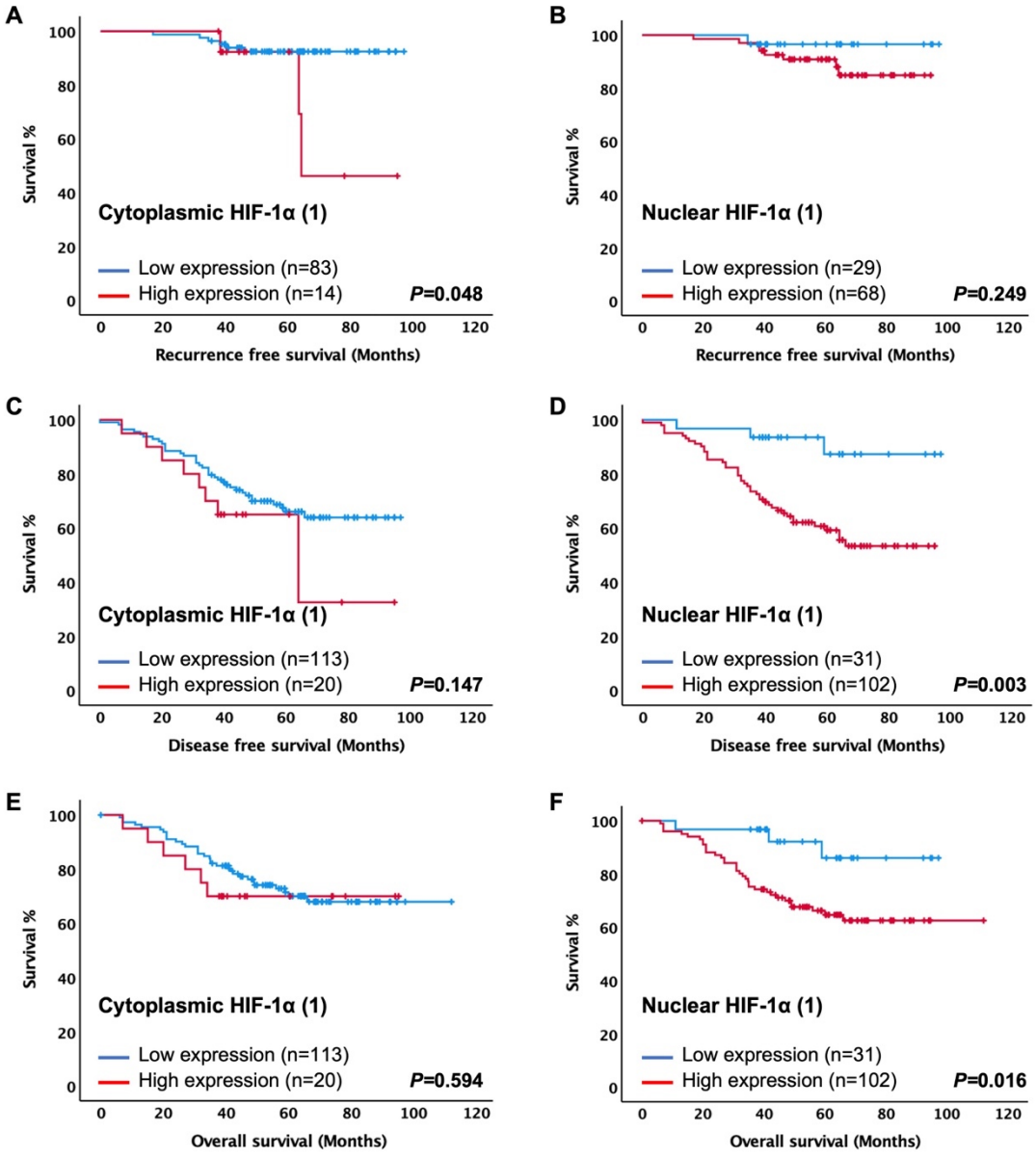

Figure 10.6 Expression of HIF-1α (1) and clinical outcome in TNBC patients.

Kaplan-Meier curves showing associations between cytoplasmic and nuclear HIF-1α (1) with recurrence free survival [A, B], disease-free survival [C, D], and overall survival [E, F].

In addition, at protein level, the patients with lower cytoplasmic BCL2 expression levels had unfavourable outcomes compared to those with higher expression level group by using Kaplan-Meier plotter analysis. Lower expression of BCL2 was associated with poorer RFS and DFS (P = 0.001, 0.009, respectively). However, low BCL2 expression did not show significant association with OS (P = 0.359) (Figure 10.7A-C).

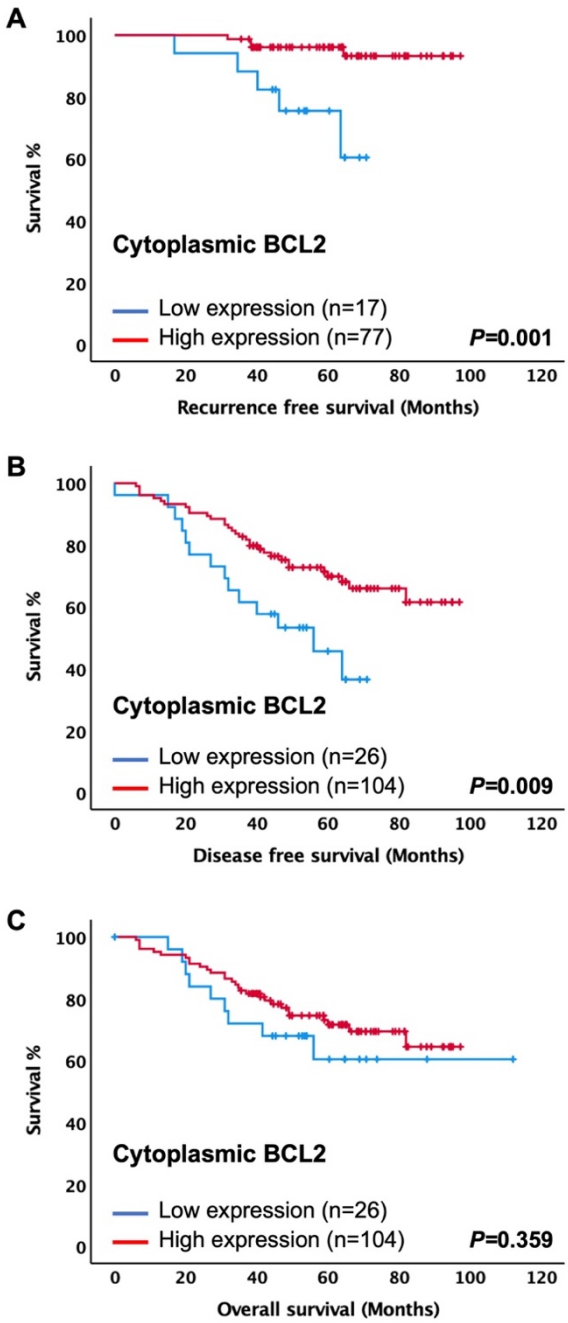

Figure 10.7 Expression of BCL2 and clinical outcome in TNBC patients.

Kaplan-Meier curves showing associations between cytoplasmic BCL2 with recurrence free survival [A], disease-free survival [B], and overall survival [C].

The prognostic significance of CD68 infiltration levels according to the different histologic locations was also investigated. Kaplan-Meier analysis and log-rank test showed that high levels of infiltration of tumour nests, TME, and total CD68 was correlated with shorter DFS ($P = 0.049$, 0.048, 0.039, respectively) (Figure 10.8D-F). A similar correlation was found between higher tumour nests, TME, and total CD68 infiltration with shorter OS ($P = 0.043$, 0.030, 0.018, respectively) (Figure 10.8G-I). However, no correlation between CD68 in tumour nests, TME, and total CD68 and RFS was detected in this chapter ($P = 0.599$, 0.263, 0.957, respectively) (Figure 10.8A-C).

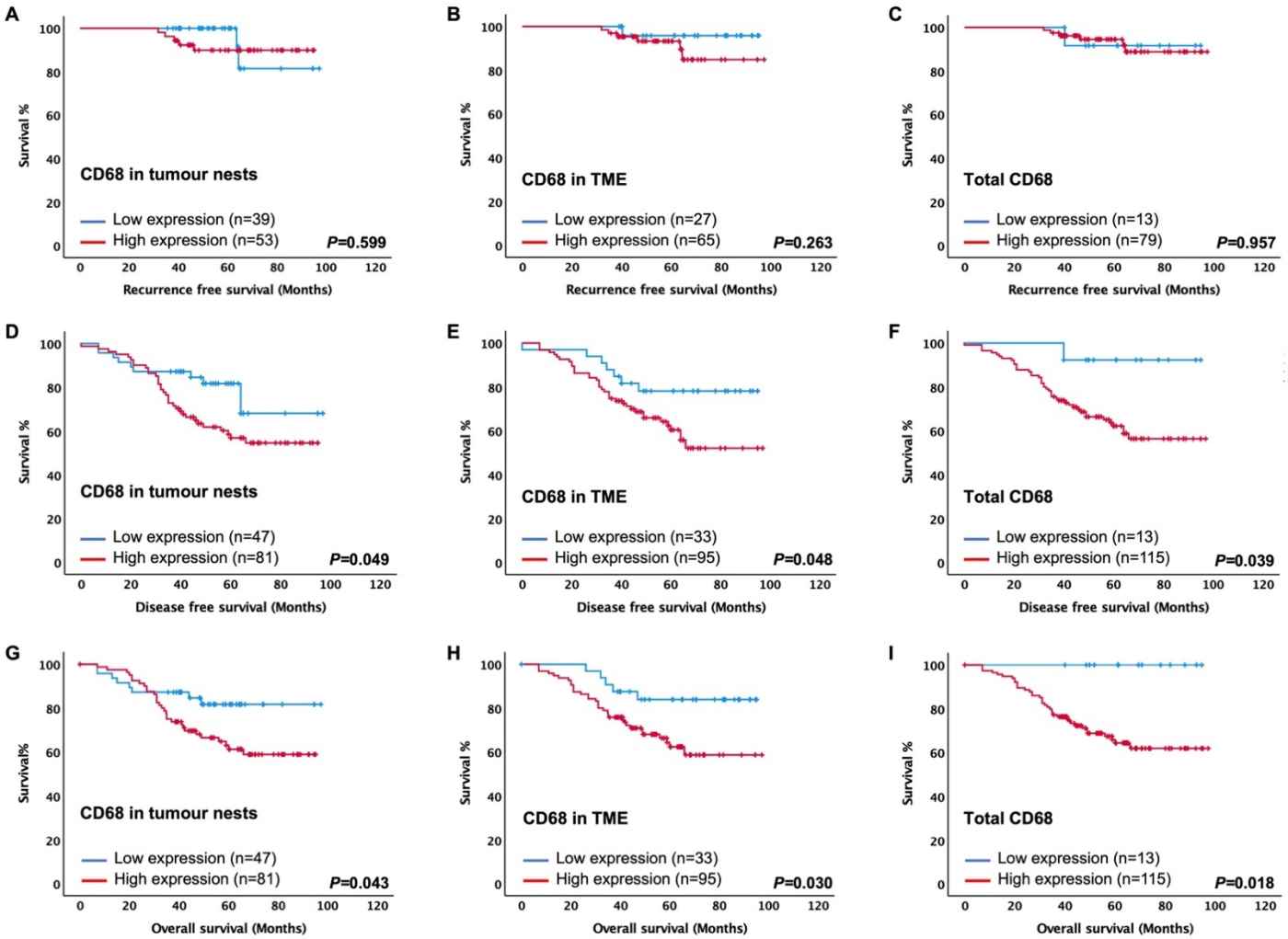

Figure 10.8 Expression of CD68 and clinical outcome in TNBC patients.

Kaplan-Meier curves showing associations of CD68 in tumour nests, TME, and total CD68 with recurrence free survival [A-C], disease-free survival [D-F], and overall survival [G-I].

Moreover, univariate Kaplan-Meier analysis showed that lower CD3 expression levels in tumour nests, TME, and total CD3 were associated with poor RFS (log-rank, P = 0.020, 0.002, 0.013, respectively) (Figure 10.9A-C). However, lower CD3 infiltration levels in tumour nests, TME, and total CD3 did not predict DFS (P = 0.928, 0.426, 0.447) and OS in this chapter (P = 0.263, 0.348, 0.501), respectively.

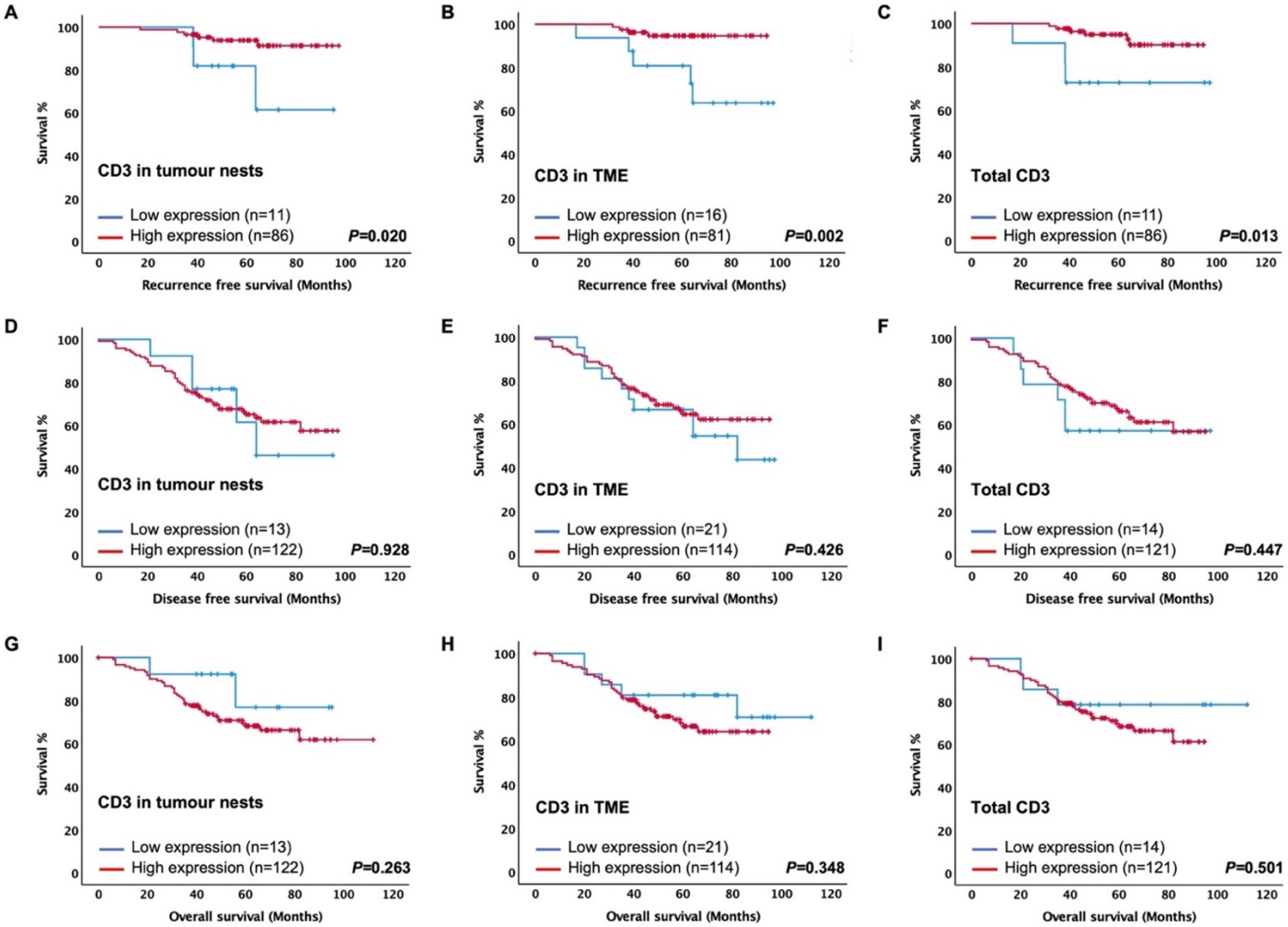

Figure 10.9 Expression of CD3 and clinical outcome in TNBC patients.

Kaplan-Meier curves showing associations of CD3 in tumour nests, TME, and total CD3 with recurrence free survival [A-C], disease-free survival [D-F], and overall survival [G-I].

To examine the independent prognostic significance of clinicopathological variables and markers expression, multivariate analysis was performed. High CD68 in tumour nests (HR = 2.42, 95% CI: 1.05–5.59, P = 0.038), and in TME (HR = 3.34, 95% CI: 1.28–8.69, P = 0.014) tissue expression were factors of poorer OS along with tumour necrosis, and adjuvant radiotherapy (Table 10.5).

Table 10.5 Univariate and multivariate analysis for overall survival of protein markers and clinicopathological characteristics in TNBC (n = 136)

Clinicopathological characteristics	Univariate analysis		Multivariate analysis	
	HR (95%CI)	P-value	HR (95%CI)	P-value
Age (≤50/>50 years)	2.13 (0.94–4.81)	0.070	-	-
Tumour size (≤2/2.1–5/>5cm)	2.07 (1.24–3.46)	**0.005**	1.01 (0.99–1.03)	0.562
Grade (I/II/III)	1.51 (0.21–10.97)	0.686	-	-
Lymph node (negative/positive)	1.38 (0.69–2.77)	0.363	-	-
Lymphatic vessel invasion (no/yes)	1.24 (0.44–3.49)	0.686	-	-
Blood vessel invasion (no/yes)	1.68 (0.91–3.12)	0.099	-	-
Tumour necrosis (low/high)	0.386 (0.19–0.75)	**0.005**	0.41 (0.19–0.84)	**0.016**
Klintrup-Mäkinen grade (0/1/2/3)	0.87 (0.61–1.24)	0.443	-	-
Tumour stroma percentage (low/high)	1.29 (0.67–2.49)	0.442	-	-
Adjuvant chemotherapy (no/yes)	0.37 (0.20–0.68)	**0.001**	0.67 (0.31–1.45)	0.308
Adjuvant radiotherapy (no/yes)	0.45 (0.24–0.85)	**0.014**	0.39 (0.20–0.78)	**0.007**
Nuclear HIF-1α (1) (low/high)	3.83 (1.17–12.45)	**0.026**	3.01 (0.91–10.01)	0.072
CD68 in tumour nests (low/high)	2.19 (1.01–4.79)	**0.049**	2.42 (1.05–5.59)	**0.038**
CD68 in TME (low/high)	2.72 (1.06–6.99)	**0.037**	3.34 (1.28–8.69)	**0.014**
Total CD68 (low/high)	24.93 (0.38–1629.6)	0.132	-	-

Multivariate Cox regression model was adjusted for age, tumour size, grade, lymph node, lymphatic vessel invasion, blood vessel invasion, tumour necrosis, Klintrup-Mäkinen grade, tumour stroma percentage, adjuvant chemotherapy and adjuvant radiotherapy.

10.4 Discussion

Transcriptomic RNAseq analysis in previous chapter identified 10 significant genes between high and low expression of cytoplasmic CAIX in ER-negative breast cancer. To compare these genes with genes expression in TNBC, the present chapter generated preliminary data, using high-plex profiling and specially combining proteomic and transcriptomic data on TNBC tissue section, comparing high and low CAIX expression in tumour and stromal/ immune cells. To best of our knowledge, this is the first such study in patients with TNBC in a broad tumour and immune context, therefore paving the way to the identification of reliable predictive biomarkers and design of innovative therapies when properly correlated with clinical outcomes.

Preliminary data comparing high and low CAIX expression in pan-cytokeratin rich regions identified 4 genes, CD68, HIF-1A, pan-melanocyte and VSIR, three of which were significantly down-regulated, and one was up-regulated by low CAIX expression group. In contrast, GeoMx analysis of RNA expression within PanCK-negative samples identified 8 significant microenvironment-related genes, CD86, CD3E, MS4A1, BCL2, CCL5, NKG7, PTPRC, and CD27 with low compared to high CAIX expression groups. These common genes are signatures of stromal and immune cells, which play critical roles in the TME.

CD68 mRNA was overexpressed with high CAIX expression (log2 FC - 0.372, P = 0.009, Table 10.1). CD68 gene encodes a 110 kD transmembrane glycoprotein that is highly expressed by human monocytes and tissue macrophages. CD68 is recognized as a pan-macrophage marker in various cancer types including breast cancer (514, 515). Several studies suggested that tumour cells stimulate macrophages to produce various factors that in turn stimulate tumour growth and survival (516, 517). It was particularly noteworthy that the infiltration of macrophages was mainly associated with hormone receptor negativity and basal phenotype (515). These results suggested that TAM infiltration might be more closely associated with TNBC. This chapter demonstrated high levels of CD68 infiltration in all histological locations were associated with shorter DFS and OS. Other studies have demonstrated similar results (518), especially in the high infiltrated group (160, 518). Patients with high CD68 infiltration express higher levels of IL-6 and CCL5 (160), which are well known to correlate with poor prognosis. However, little direct evidence reported the significance of the histological location of CD68 in breast cancers except for a few studies (152, 515, 519). The TAMs have different effects on tumour progression according to their histologic location. Ch'ng et al. suggested that stromal TAM influence tubular architecture

and, finally, tumour grade, while tumour TAMs have a closer relationship with hypoxia-induced angiogenesis by secreting angiogenic cytokines such as VEGF and TNF-α (519). It may be possible that the central tumour area becomes more hypoxic as tumours outgrow their blood supply, and then, TAMs in tumour nests which are recruited by hypoxia-induced tumour necrosis become more active in angiogenesis and cancer progression. Therefore, TAMs in tumour nests, as well as their TME counterpart, appear to play an important role in tumour progression.

Another surprising finding in this chapter was overexpression of HIF-1A gene in tumour compartment with high CAIX expression (log2 FC - 0.274, P = 0.012, Table 10.1). HIF-1A gene encodes HIF-1α protein, a transcriptional regulator in response to intratumoural hypoxia (520, 521), which plays an important role in cellular functions including apoptosis, cell proliferation, erythropoiesis, glucose metabolism, iron metabolism and angiogenesis. HIF-1α levels are significantly higher in invasive and poorly differentiated breast cancers as compared to well-differentiated cancers (240). Specifically, increased levels of HIF-1α mRNA and the core hypoxic transcriptional response are associated with hormone receptor negative breast cancers (240). High expression of HIF-1α contributes to breast cancer metastasis and malignant progression (522, 523) by acting at multiple levels of the metastatic cascade (212). It was suggested that targeting this pathway might provide a new therapeutic option for TNBC patients (212). Consistent with a recent meta-analysis, the results of this chapter shown that overexpression of HIF-1α in breast tumours predict poor outcomes. As determined by Chi-squared test, the expression of cytoplasmic HIF-1α (1) was significantly associated with cytoplasmic CAIX in this chapter. Results have been variable in other studies. CAIX expression has correlated with HIF-1α expression in one study (262), but not in others (387). When hypoxic environment advances, HIF-1α is overexpressed and promoting upregulation of various target genes, including CAIX allowing breast cancer cells to undergo metabolic adaptation to hypoxia (235, 236).

Within the tumour compartment, the resulting heatmap did not clearly differentiate between low and high CAIX expression groups. This might be due to the same tumour had TMA cores for stroma and for tumour sample that were stained together then scored separately and an average score was taken.

In addition, within PanCK-negative samples, CD3E showed high level by a log2 FC of 0.30, P = 0.005 (Table 10.2) in low CAIX tumours compared to high CAIX tumours. CD3E protein, encodes by CD3E gene, is one of the subunits of CD3, and associated with severe immune deficiency and is frequently used as protein target of CD3 antibody (524). Studies

have found that cancer patients with low CD3E mRNA levels tend to have poor prognosis (525). A recent study found that CD3E gene might be considered as novel and potential biomarkers of TNBC (526). The location of CD3, whether in the tumour nests or in TME is important. In this chapter, higher infiltration of CD3 were observed in both tumour nests and TME of TNBC, which were uniformly significantly associated with favourable RFS. In line with previous results, this chapter has shown that patients with high CD3 infiltration predicted better survival than patients with low lymphocytic infiltration (512, 527). We found TME CD3 to be a superior parameter. Based on this finding, we hypothesised that the stromal compartment plays the main role in antitumour activity. Studies of early-stage TNBC showed that the TIL level in the stromal compartment of TNBC tumours was higher than that in lower-grade tumours and could improve the outcome, which supported our results (137, 528). A purified anti-CD3E nanobody effectively inhibited the growth of breast cancer *in vivo* (529), and suppressed angiogenesis and tumour cell proliferation in a breast cancer mouse model (530). In context of hypoxia, extracellular acidosis in tumours which is a consequence of acceleration of glycolysis opposes antitumour immune responses (531). Studies have reported that breast cancer patients with poor outcomes had high HIF-1α and low expression of CD3E (532), suggesting that hypoxia could reflect more aggressive disease and a more immunosuppressive TME. Indeed, higher CAIX expression was significantly associated with lower expression of CD3E gene in basal-like breast cancer, and it was associated with worse OS (533). Observations in this chapter were consistent with these results.

BCL2 (B-cell lymphoma-2) was overexpression of with low tumour CAIX (log2 FC 0.19, P = 0.008, Table 10.2). BCL2 protein, coded by the BCL2 gene, plays an anti-apoptotic role and inhibits cell death (534), resulting in prolonged cell survival (535). BCL2 is overexpressed in many cancers and contributes to tumour initiation, progression, and therapy resistance (536). With reference to breast cancer, BCL2 is overexpressed in approximately 41% of TNBC cases (537), and was independent predictor of poor prognosis (538). On the other hand, the reverse was observed in the present chapter that high BCL2 expression was significantly associated with improved survival rates in TNBC patients. As extensively reviewed by Bouchalova et al (513), most clinical studies have shown that increased expression of BCL2 is connected with better survival for TNBC (539-541). The favourable clinical outcome in BCL2 positive cases is surprising considering the anti-apoptotic nature of BCL2. BCL2 functions not only in apoptosis, but also in the cell cycle where cell line studies have shown that its expression hinder G1 progression and G1-S transition. This is due to it extending the G0 phase (542). BCL2 expression has also been found to be associated

with markers of better prognosis in breast carcinoma. In fact, BCL2 is inversely correlated with Ki67 and Her-2 overexpression (543). Therefore, BCL2 plays an anti-proliferative role despite its anti-apoptotic effect (544), resulting in a more favourable outcome compared to that of breast cancer with BCL2-negative expression. Also, a variety of studies have suggested that it may undergo conversion from protector to killer under some circumstances. For example, proteolytic removal of N-terminal sequences by caspase-mediated cleavage reverses the phenotype of BCL2 (545). Furthermore, this role may be explained by its interactions with other members of the BCL2 family of apoptotic regulators, especially with pro-apoptotic proteins (546). HIF-1α can initiate hypoxia mediated apoptosis by increasing the expression of BCL2 binding proteins (BNIP3 and NIX), thereby inhibiting the anti-apoptotic effect of BCL2, or by stabilising wild-type p53 if the cell already has a p53 gene mutation. Also, the severity of hypoxia determines whether cells become apoptotic or adapt to hypoxia and survive (547).

In PanCK-negative compartment, heatmap shown most of high expression genes were shown in low CAIX expression group.

In the present chapter, it was apparent that tumour hypoxia has an essential role in regulating tumour inflammatory cell functions in addition to regulating immune cell recruitment. The epithelial and stromal genes expression was readily delineated by CAIX expression in TNBC. Analysis of genes expression in tumour cells showed hypoxia increased expression of CD68 which contribute to tumour progression and are associated with poor tumour prognosis. In contrast, analysis of genes expression in stroma showed down-regulation of CD3, and BCL2 with high CAIX expression.

Extracellular acidification is primarily considered to be due to secretion of H^+ produced by glycolysis. Tumour cells decrease extracellular pH by activation of HIF-1α target genes encoding CAIX protein which catalyses the reversible hydration of $CO_2 + H_2O$ to $H^+ + HCO_3^-$ and acting in concert with HCO_3^- transporters, contributes to net efflux of H^+ from tumour cells (231). Acidification of the microenvironment enhances the tumour cell invasion, migration, and the radio-resistance (548) and reduces antitumour immunity in many ways. Increased levels of H^+ and lactate decrease the capacity of T cells to produce interleukin-2 (IL-2), interferon-γ (IFNγ), granzyme B and perforin and that of monocytes to release tumour necrosis factor (TNF) in a dose-dependent manner. The acidic microenvironment also decreases the activity of NK cells. Thus, hypoxia-driven tumour acidification is a formidable barrier to immune cell function (549, 550). The data from the present chapter highlight hypoxia and inflammation as critical modulators of the immune

microenvironment of solid tumours. Hypoxia increases the cellular plasticity and tumour heterogeneity and cancer cells immune suppression (551).

Finally, comparing with transcriptomic RNAseq analysis in previous chapter 9, there was no overlap between these two analyses in terms of targeted genes. Dissimilarity may indicate differences in the cohorts. In particular, bulk RNAseq, ER-negative patients with tumour and stromal cells mixed together were used while in spatial transcriptomic the analysis was performed on TNBC patients and consider tumour cells and stromal cells separately.

Well-controlled future studies are required to overcome the limitations of the present study. These include studies with a larger sample size of TNBC tissues. Also, some of the patients are represented by multiple cores across the TMAs sections, further validation using full tissue sections would enable insight into any spatial heterogeneity of CAIX-signature across each patient. Furthermore, whole transcriptome profiling is warranted. Finally, the high expression of CD68 in the PanCK-positive AOIs in the transcriptomic analysis highlights a key limitation of the approach. Presumably this reflects the lack of single cell resolution to distinguish between tumour and immune cells within tumour nests as high CAIX expression is positively correlated with CD68 staining in tumour nests and not the TME. Therefore, newer technology such as CosMx could be used to investigate gene and protein expression at the single cell level.

In conclusion, based on GeoMx DSP, the current chapter highlight a specific mRNA signature associated with hypoxia within tumour and stromal compartments was identified in TNBC, and that may influence tumour development, and thus represent potential targets for novel intervention strategies. 4 DEGs were identified in tumour compartment and 9 DEGs in the stromal compartment in comparison of high and low CAIX expression groups. 4 genes were selected to validated by IHC at protein level in microarray TNBC datasets. IHC staining showed tumour infiltrating macrophage can predict the progression of TNBC, and the involvement of BCL2 and lymphocyte in tumour protection. IHC proteins expression were associated with a different prognosis in TNBC. High HIF-1α (1), and CD68 expression in tumour were linked to poorer survival while high levels of CD3 and BCL2 expression within stroma were associated with improved patient's survival. In addition, high density CD68 in both tumour nests and TME were independently predictive of OS. Among the four markers tested, HIF-1α (1) and CD68 protein expression had a significant positive association with CAIX expression whereas BCL2 expression showed significant inverse association with CAIX expression.

These results demonstrate that even from a small number of samples, GeoMx profiling can be used as an efficient tool to identify potential prognostic biomarkers that may have clinical relevance, however, further functional analysis of these results is warranted. Any further investigation would also require patients with different breast cancer subtypes to identify the particular signature for each subtype in relation to expression of cytoplasmic CAIX.

Chapter 11 General discussion

11.1 General discussion

The progression and metastasis of tumours mainly depend on the bidirectional interaction between tumour cells and their microenvironment. The TME comprises endothelial cells, immune cells, mesenchymal stem cells, extracellular matrix, blood vessels, and cytokines. Hypoxia is closely related to the TME (552). The effect of extracellular microenvironment such as hypoxia and pH has been regarded as a key hallmark in cancer progression. The limitation of oxygen diffusion and the disordered vascular system prevent rapidly growing tumours from acquiring sufficient oxygen, resulting in a hypoxic microenvironment (553). An increasing number of studies have reported that hypoxia is associated with tumour progression (554, 555).

Considering the relevance of hypoxia at the TME, this thesis has therefore focussed on the association of hypoxic markers, HIF-1α, HIF-2α, and CAIX in breast cancer tissue cohorts in correlation with clinicopathological parameters and predicting survival outcomes. Also, to identify DEGs profiles, and to establish key biological processes and pathways related to high cytoplasmic CAIX expression in ER-negative and a node-negative subset of ER-negative breast cancer patients using TempO-Seq. Further, to identify the mRNA signature associated with CAIX within tumour and stromal compartments in TNBC, a spatial transcriptomic platform was employed (NanoString).

For antibody specificity, although no result has been found for HIF antibodies after several Western blot experiments, they appeared specific in the cell pellet experiments. This possibly could be because these antibodies are not suitable for Westerns, or because of that HIF-1α degrades rapidly resulting in it being undetectable within minutes following re-oxygenation, while CAIX expression remained even after 2−3 days of re-oxygenation (307) so is more stable. Conversely, CAIX antibody in experiments were acquired, supporting the specificity of this antibody and as a reliable marker of hypoxia in breast cancer.

Because HIF-1α (2) was not fully specific, it would not be investigated in further IHC chapters. IHC was employed on a TMA of patients in chapter 6, which investigated a cohort of mixed breast cancer subtypes. In this cohort, overexpression of HIF-1α (1), HIF-2α was not consistently associated with survival outcomes. This further supports that HIFs may not be an exclusive candidate marker for breast cancer. However, high cytoplasmic CAIX expression was a consistent independent prognosticator in the entire cohort, in luminal B and Her-2-enriched diseases. These results demonstrate CAIX was a superior predictor of survival in patients with invasive ductal breast cancer and may be a useful independent

indicator of clinical outcome in these patients. This result was in line with the results of a recent meta-analysis of 23 studies (380). Previous clinical studies in invasive breast cancer have also demonstrated the association of CAIX with poor outcome (248, 259, 310, 336) suggesting that CAIX expression is linked to an aggressive phenotype. Furthermore, large studies on breast cancer samples showed that a high CAIX level was significantly associated with poor survival in luminal B disease (249, 385). Generali et al. also concluded that high CAIX expression was associated with lower survival in breast cancer patients treated with epirubicin and tamoxifen (258). Contrary to our expectations, however, the CAIX score was not associated with TNBC subtype survival outcome. This may at least partially be explained by limited patients' size and low statistical power. Irrespective, the present results indicate a need for further work to understand the prognostic value of hypoxic markers in subgroups of breast cancer.

The clinical significance of these hypoxic biomarkers was further validated in a cohort of ER-positive breast cancer patients in chapter 7. The result of this cohort has provided evidence of a prognostic role for nuclear HIF-1α (1) expression in the whole cohort and in luminal A tumours and the prognostic role for cytoplasmic CAIX expression in the whole cohort and in luminal B breast cancers. These finding corresponds to the previous studies that demonstrated high expression of HIF-1α was associated with poorer survival in ER-positive breast cancer (246, 556, 557). Consistent to the cohort of mixed breast cancer subtypes, cytoplasmic expression of CAIX was associated with poor clinical outcome in term of DFS in luminal B tumours.

This thesis demonstrates differences in outcomes conditions of HIF-1α (1) in Glasgow breast cohort and in ER-positive cohort. While cytoplasmic HIF-1α (1) overexpression was correlated with better OS in the Glasgow breast cohort, it was correlated with poorer OS in ER-positive cohort. It has been reported that HIF-1α is broadly expressed in breast cancer and is associated with shorter OS (235, 328). In this thesis, however, interpretation of the prognostic effect of HIF-1α (1) expression on two cohorts is less straightforward. One likely explanation of this discrepancy is consistent with the observation that different regulation pathways of HIF-1α overexpression exist in breast cancer, first, hypoxia induced, perinecrotic HIF-1α overexpression with robust expression of hypoxia associated genes, which is correlated with a poor prognosis; and further, diffuse HIF-1α overexpression lacking main hypoxia associated downstream effects, resulting in a more favourable prognosis (327). Since TMAs were randomly sampled from the tumour tissue in this thesis, they are expected to represent diffuse rather than localized expression of HIF-1α in Glasgow

breast cohort. Furthermore, these observations could be in part attributed to patient numbers. This further supports the understanding of breast cancer as a heterogenous disease with subtypes which behave differently and respond to different treatments.

Although CAIX is known target gene of HIF-1α as part of the metabolic process, its association with HIF-1α protein expression in the present study showed different results on three cohorts. While it failed to demonstrate an association with cytoplasmic HIF-1α in Glasgow breast cohort, and in ER-positive cohort, it was correlated with HIF-1α (1) in TNBC cohort. The lack of association was reported in other studies (236, 264, 307, 386, 387). This discrepancy could be due to biological and methodological explanations for this lack of association. Previous IHC study of solid tumours showed that in perinecrotic area, CAIX is expressed without HIF-1α being detected (386), such as at perinecrotic area, which is often avoided during IHC sectioning due to unpredictable immunoreactivity of epitopes in that region (558). Other possible explanation is the difference in the half lives of HIF-1α and CAIX (559). CAIX protein is relatively stable and persisted much longer than HIF-1α (391). Therefore, cells that had been hypoxic and then were reoxygenated may stain for CAIX but not HIF-1α (302). Furthermore, when cells or tissue have only recently become hypoxic, they may stain positive for HIF-1α but not CAIX, because those cells may have been analysed before the full onset of CAIX expression (302). Suggesting that CAIX possibly activates hypoxic condition independently of HIF-1α, as CAIX protein persists longer than HIF-1α. Also, tumour tissues used in this study were obtained through standard clinical practice and without special attention to assure preservation of labile proteins. Therefore, differences in tissue processing may contribute to artifact variability in HIF-1α levels. In contrast, CAIX protein is relatively stable and less subject to variability due to tumour tissue handling procedures. Besides, the degree of hypoxia required to stimulate HIF-1α may be lower than that required to enhance CAIX expression as previously suggested (560). Therefore, CAIX expression may represent tumours with a greater degree and/or duration of hypoxia and consistently a more aggressive malignant potential. Another possible explanation is that the expression of CAIX may be regulated by other factors rather than being regulated by HIF-1α. CAIX is known to be activated by PI3K pathway (366, 392) and by the mitogen-activated protein kinase (MAPK) pathway during both normoxia and hypoxia (393, 561). Therefore, CAIX may be a better biomarker for tumour hypoxia and that HIF-1α may not be an exclusive candidate marker for breast cancer.

With reference to CAIX, as the previous two chapters have investigated its prognostic role in primary operable mixed breast cancer and in ER-positive breast cancer, therefore, going

forward it would seem sensible to focus further on TNBC, rather than breast cancer across all subtypes to better understand the role of CAIX in TNBC (Chapter 8). The work in this chapter, an IHC-based TMA study of TNBC patients (n = 136) evaluating CAIX protein, demonstrated that the expression of cytoplasmic CAIX was independent indicator of poorer RFS. This result was in agreement with other studies (264, 265, 385), suggesting that CAIX expression is linked to an aggressive phenotype. Evidence gained from this study, TNBC cases supports the observation reported in the literature that detection of the cytoplasmic CAIX expression on TMA can be used as a poor prognostic factor in TNBC.

Since cytoplasmic CAIX was the most consistent prognostic feature in the Glasgow breast cohort and was independent prognostic factor in ER-positive cohort, and in TNBC cohort, gene expression levels were established in a subset of ER-negative patients and node negative group (chapter 9). With the aim of gaining a better understanding of the transcriptomic and protein pathways associated with CAIX. A small pilot study was carried out for which transcriptomic analysis was performed to compare the transcriptome of patients with high cytoplasmic CAIX to those with low CAIX in a subset of ER-negative patients. Despite the small sample size (n = 37, due to financial limitations), 10 DEGs in ER-negative tumours and 3 DEGs in node negative patients between low and high cytoplasmic CAIX expression were identified. Of particular interest, 6 DEGs (SERHL2, GALNT6, MUCL1, MMP7, PITX2, and CEACAM6) in ER-negative cohort and 2 DEGs (SERHL2, SPNS2) in node negative group were considered as justifying further investigation. SERHL2 gene was overexpressed in high CAIX in both ER-negative breast cancer and in node negative patients. It was previously identified in TNBC for predicting chemotherapeutic response (432). Since it is consistently overexpressed regardless of disease stage, it might be promising therapeutic target in these two patient groups.

STRING analysis identified a variety of interactions among these DEGs. In ER-negative breast cancer, GALNT6 and MUCL1 had significant interactions, as did PITX2, CEACAM6, and MMP7. One of particular interest is the GALNT6 gene was overexpressed in high CAIX ER-negative breast cancer. High GALNT6 expression was associated with poor prognosis in breast cancer (438). It promotes breast cancer metastasis through β-catenin/MUC1-C signalling pathway (562). The other gene is MUCL1 gene which was highly expressed in high CAIX expressing ER-negative breast cancer. High MUCL1 expression was associated with worse TNBC survival (445), and may be significant in EMT. Next, we observed up-regulation of PITX2 in tumours with high cytoplasmic CAIX. It has previously been demonstrated that reduced PITX2 DNA methylation status was associated

with shorter time to progression in treated TNBC patients (466). Expression of PITX2 was associated with risk for early breast cancer recurrence (461). CEACAM6 was up-regulated in high cytoplasmic CAIX group. This gene encodes the protein that has been reported to important biomarker of breast cancer metastasis (470). However, the association of these genes with tumour hypoxia is yet to be explained as the present study is the first to document their association with cancer hypoxia and therefore requires confirmation in further studies. The other important gene is MMP7 which was under expressed in high CAIX tumours. Its expression was correlated with poor prognosis in breast cancer (563). With regards to hypoxia, there is evidence that HIF-1α promotes MMP7 expression in breast cancer cells (564) and in TNBC (459). It may be that targeting of these genes could lead to reduced tumour hypoxia and improved prognosis. However, much more work is required to establish this hypothesis and funding is currently being sought for further research in this area.

With reference to the node negative tumours, a PPI network construction showed interaction of SPNS2 with their partner proteins which were added from the STRING database including SphK1, SphK2, and S1PR2. SPNS2, a S1P transporter, stimulating genesis, apoptosis and migration of cancer, through S1P/S1PRs pathways activating downstream signalling such as STAT3, AKT, ERK, Ras and Rac (497). A bioactive lipid mediator, S1P, which is produced by SphK1 stimulates angiogenesis in breast cancer (486), and that SphK1 stimulates node metastasis in breast cancer (487). Inhibitor of SphK1 suppresses angiogenesis and lymphangiogenesis which lead to reduction of tumour metastasis in murine breast cancer model (486). High expression of SphK1, S1P1 and S1P3 is associated with decreased survival in ER-positive breast cancer patients (491, 494). S1P binding to S1P3 promotes functional regulation of SphK1 (491). Furthermore, knockdown of SphK1 decreases S1P3 expression and ERK-1/2 activation in response to S1P, indicating that SphK1 and S1P3 function in an amplification loop to stimulate ER-positive breast cancer progression (491). Therefore, SphK1 regulates S1P3 expression, and this enables ER-positive breast cancer cells to potentially match S1P released into the microenvironment with the required effector response. Moreover, SphK1 and S1P4 are functionally linked in ER-negative breast cancer as S1P stimulation of the ERK-1/2 pathway mediated by S1P4 is blocked by SphK1 inhibitors (429). It has demonstrated that oncogenic Her-2 functionally interacts with S1P4 in ER-negative breast cancer cells (498). In fact, high S1P4 expression in ER-negative breast cancer was also correlated with lymph node positivity suggesting a role for S1P4 in metastasis (429). A functional link between S1P2 and S1P4 receptors in ER-negative breast cancer cells was also identified (565). SPNS2 was validated by IHC in our lab (429). One principle finding of this thesis was the association between cytoplasmic HIF-1α (1) and

cytoplasmic SphK1 expression at protein level providing further evidence for the role of hypoxic microenvironment in tumour progression. Further supporting evidence was that SphK1 promoter has two hypoxia inducible factor-responsive elements and both HIF-1α and HIF-2α have been involved in the transcriptional regulation of SphK1 (502, 503). These results are consistent with those of other studies (501), which suggested that SphK1 acts as a modulator of HIF-1α in various cancer cell models including breast cancer cell lines. In a recent study, it has reported that S1P and SphK2 in the nucleus are linked to the regulation of HIF-1α/-2α functions associated with progression of breast cancer particularly TNBC subtype (566).

In the present thesis, while several genes were expressed by cytoplasmic CAIX-mediated hypoxia in ER-negative patients, only three genes were expressed in the node negative group. This finding supports the idea that the apparent DEG differences between the two patient groups may be necessary to involve certain pathways that may be involved in the progression of breast cancer. SPNS2 is of particular interest compared to other DEGs and its pathway was dependent on HIF activity. This genetic profile was validated at the protein level and was very informative and represents a powerful tool for identifying subgroups of node negative breast cancer patients most likely to respond to hypoxic tumour-targeted therapy, thereby, it may avoid significant overtreatment of patients.

Although the findings of previous work in chapter 9 have focused on analysis of gene expression signatures from whole tissue consisting of combined tumour epithelial cells and the surrounding stromal cells in ER-negative breast cancer, most prognostic gene expression signatures and predictors have been derived from tissue consisting of a separate tumour and stroma compartment. In chapter 10, further spatial transcriptomic studies to consider tumour and stroma compartment separately were done with high and low cytoplasmic CAIX expression in TNBC samples. In this chapter, GeoMx DSP has identified 4 genes in tumour compartment (CD68, HIF1A, pan-melanocyte and VSIR), and 9 genes in the stromal compartment (CD86, CD3E, MS4A1, BCL2, CCL5, NKG7, PTPRC, CD27 and FAS) in comparison of high and low cytoplasmic CAIX expression groups. It further validated four identified genes, HIF-1A, BCL2, CD68, and CD3, at protein level by IHC using TNBC samples. Here, this shows that high expression of CD68 gene was associated with high cytoplasmic CAIX protein expression. A higher total macrophage number in tumour nests and in TME was an independent prognostic factor in TNBC patient. Our results are supported by other studies who showed an association between CD68 expression and an unfavourable prognosis in TNBC patients (160, 518). TAMs upregulate HIFs expression,

which is important for their adaptation to the hypoxic TME. In this context, a significant association between CD68 and HIF-1α expression in non-small cell lung cancer was found (567). Hypoxia-induced inflammation has been established in clinical aspects. Recently, Mirchandani et al. (568) have found hypoxemia and monocytopenia in patients with acute respiratory distress syndrome within the first 48 hours after ventilation. Monocytopenia has also been observed in mouse models of hypoxic acute lung injury, which leads to a decrease in monocyte-derived macrophages and stimulated neutrophil-mediated inflammation in the lungs. Similarly, our results demonstrate that high HIF-1α gene expression in tumour compartment was associated with high cytoplasmic CAIX expression. HIF-1α (1) protein levels are significantly associated with poor survival in TNBC patients. These findings are consistent with the recent meta-analysis which concludes that high HIF-1α expression is an indicator of poor prognosis, even though significant heterogeneity did exist in this meta-analysis (357). In this chapter, HIF-1α (1) and CAIX proteins expression were well correlated with each other. A similar observation was reported by Brennan and co-workers (262). CAIX is a well-known downstream effector of HIF-1α, and its expression in relationship to exogenous markers of hypoxia is well documented (235) suggesting that expression of CAIX may be induced in a hypoxia-dependent manner and explain the effect on survival.

Conversely, within the stroma compartment, higher CAIX expression was associated with decreased expression of CD3E gene in the tumours of these patients. Recently, Li et al have found that CD3E gene might be considered as novel and potential biomarkers of TNBC (526). Then, we further demonstrate that patients with higher densities of CD3 immune cells in the stromal compartment had significantly better survival. The finding is in keeping with another study which reported better breast cancer outcomes with higher expression of CD3 (569). The broader implications that CAIX expression is negatively correlated with the expression of CD3 across TNBC, strengthen the rationale for combining CAIX inhibition with immunotherapy to improve immune activity clinically. In context of hypoxia, studies have reported that breast cancer patients with poor prognosis had higher HIF-1α and lower CD3 expression (532), suggesting that hypoxia contributes to decrease immune activity and more aggressive disease. Furthermore, it was interesting that increased CAIX expression was associated with reduced BCL2 gene expression within the TME in TNBC patients considering that, in this thesis, BCL2 was a good prognostic factor. This is supported by a study which reported an association between BCL2 expression and improved survival in breast cancer (570). In cooperation to hypoxia, an inverse association between HIF-1α and BCL2 was found in breast cancer (571). Indeed, increased HIF-1α levels and decreased

BCL2 levels are potentially associated with more aggressive tumours such as TNBC. However, under hypoxia, studies found that overexpression of the anti-apoptotic and pro-survival protein BCL2 in breast carcinoma cells, enhances HIF-1α protein expression and HIF-1 activity consequently leading to angiogenesis through VEGF (572).

11.2 Further work

Although the IHC work in this thesis has the strength that it was carried out in a large cohort of patients, this is not a geographical diverse cohort, with all patients diagnosed living within the Glasgow area. Future studies should aim to validate the associations with survival of CAIX in other cohorts, particularly geographically diverse and more contemporary cohorts. The data in this study suggests that differences in prognosis of the two cohorts, mixed and ER-positive breast cancer are evident by 10 years of follow up, so it should be possible to power a study with shorter follow up than the cohorts in this thesis. Following this, the prognostic performance of CAIX in TNBC tumour sample requires validation in adequate number of patients as lack of statistical power may affect results in this subtype.

Dual IHC staining for HIF-1α and CAIX proteins to show their expression in the same cells within Glasgow breast cohort and ER-positive cohort.

Mechanistic cell line studies will also be required to gain a better understanding of the associations observed in the clinical studies. CAIX inhibition should also be investigated. CAIX is upregulated in hypoxic TNBC, where it is a marker for poor RFS. Therefore, depletion of CAIX expression or pharmacologic inhibition of its activity significantly inhibits TNBC growth and recurrence in pre-clinical breast tumour models.

To identify potential therapeutic targets for patients with ER-negative breast cancer and high tumour CAIX expression, a group with a particularly poor prognosis, further work to identify genes associated with CAIX is required. The pilot study in this thesis identified 10 genes of potential interest in ER-negative group and 3 genes in node negative group. Funding is being sought to carry out a larger study having verified TempO-Seq as an appropriate technique for this work. Also, gene expression will need to be validated at the protein level in ER-negative cohort and in node negative group.

Spatial transcriptomic was conducted on a limited number of TNBC patient samples and identified 9 up-regulated microenvironment-related genes and 4 genes in tumour compartment with high cytoplasmic CAIX group. The data indicates that quantification of

hypoxia-related genes in TNBC can have potential prognostic value. Thereby, this should be further explored in a larger cohort to further investigate these results. Also, further validation using full TNBC sections would enable insight into any spatial heterogeneity of CAIX-signature across each patient, and whole transcriptome profiling is warranted. The lack of single cell resolution to distinguish between tumour and immune cells within tumour nests. Therefore, it may be possible to examine gene and protein expression at the single cell level using more recent technology like CosMx. Finally, it is important that the clinical relevance of the remaining seven hypoxia-linked gene signatures to be validated at protein level in independent studies with larger TNBC tumour samples. Further spatial transcriptomic analyses in Her-2 disease to identify the mRNA signature associated with cytoplasmic CAIX.

11.3 Conclusion

Collectively, this thesis aimed to investigate the impact of hypoxic markers on breast cancer patient's prognosis. Cytoplasmic CAIX has an independent prognostic role in the entire Glasgow breast cohort, luminal B and Her-2 subtypes, in the entire ER-positive cohort and luminal B disease and in TNBC cohort. Furthermore, nuclear HIF-1α (1) is independently associated with poorer outcome in the entire ER-positive cohort and in luminal A disease. This finding suggests a potential independent prognosticator role of cytoplasmic CAIX particularly in aggressive subtypes of breast cancer with worst prognosis. It is a straightforward and low-cost method to stratify risk and could have a role in decisions regarding adjuvant treatment.

Since these results demonstrate cytoplasmic CAIX appears to be a significant hypoxia inducible molecular marker and increased CAIX protein levels are independently associated with poor survival in breast cancer, we further hypothesised that it may associated with DEGs among tumours. Therefore, TempO-Seq was utilized on FFPE ER-negative specimens to identify DEG profiles associated with high versus low cytoplasmic CAIX expression. Identification of CAIX-linked ten gene signatures and its relationship with functional enrichments further support the implication and influence of hypoxia-mediated CAIX expression in ER-negative TME. However, due to the heterogenous population, an analysis was subsequently performed of node negative patients in which the SPNS2 gene was of particular importance. At the protein level, cytoplasmic SphK1 was statistically significant associated with cytoplasmic HIF-1α (1). The identification of the 10 genes

associated with cytoplasmic CAIX could be a step forward to test for hypoxia in ER-negative breast cancer and possibly improve patients' treatment regimen and prognosis.

One of the most novel findings from this thesis was identifying CAIX-linked gene signatures, that have not been previously reported, within tumour and stromal compartments in TNBC by using spatial transcriptomic technology. 4 genes were selected to validated by IHC at protein level in TMA TNBC datasets. High HIF-1α (1), and CD68 proteins expression in TNBC were linked to poorer survival while high levels of CD3 and BCL2 proteins expression were associated with improved patient's survival. In addition, high density CD68 in both tumour nests and TME were independently predictive of OS in TNBC patients. Also, most interesting finding was a significant positive association between HIF-1α (1) and CD68 expression with CAIX expression while BCL2 expression showed significant inverse association with CAIX expression. These results demonstrate that even from a small number of samples, spatial transcriptomic profiling using the GeoMx DSP can be used to stratify patients in terms of prognosis, predict benefit from hypoxia-modifying therapies and increase understanding of the complexities of hypoxia biology.

Overall, the results from this thesis provide sufficient evidence to further investigate in a cohort of adequate number of samples to fully define the role of CAIX in breast cancer particularly in TNBC.

List of References

1. Society AC. Breast cancer facts & figures 2005–2006. American Cancer Society Atlanta, GA; 2005.
2. Houthuijzen J, Jonkers J. Cancer-associated fibroblasts as key regulators of the breast cancer tumor microenvironment. Cancer and Metastasis Reviews. 2018;37(4):577-97.
3. Stolnicu. Practical Atlas of Breast Pathology
. 2018.
4. Sung H, Ferlay J, Siegel RL, Laversanne M, Soerjomataram I, Jemal A, et al. Global cancer statistics 2020: GLOBOCAN estimates of incidence and mortality worldwide for 36 cancers in 185 countries. CA: a cancer journal for clinicians. 2021;71(3):209-49.
5. Lei S, Zheng R, Zhang S, Wang S, Chen R, Sun K, et al. Global patterns of breast cancer incidence and mortality: A population-based cancer registry data analysis from 2000 to 2020. Cancer Communications. 2021;41(11):1183-94.
6. Siegel RL, Miller KD, Fuchs HE, Jemal A. Cancer statistics, 2021. CA: a cancer journal for clinicians. 2021;71(1):7-33.
7. CRUK. [July 2020]. Available from: https://www.cancerresearchuk.org/health-professional/cancer-statistics/statistics-by-cancer-type/breast-cancer#heading-Zero.
8. Haussmann J, Corradini S, Nestle-Kraemling C, Bölke E, Njanang FJD, Tamaskovics B, et al. Recent advances in radiotherapy of breast cancer. Radiation Oncology. 2020;15(1):1-10.
9. Gote V, Nookala AR, Bolla PK, Pal D. Drug resistance in metastatic breast cancer: tumor targeted nanomedicine to the rescue. International journal of molecular sciences. 2021;22(9):4673.
10. Howlader N, Cronin KA, Kurian AW, Andridge R. Differences in breast cancer survival by molecular subtypes in the United States. Cancer Epidemiology, Biomarkers & Prevention. 2018;27(6):619-26.
11. Norum J, Andersen K, Sørlie T. Lessons learned from the intrinsic subtypes of breast cancer in the quest for precision therapy. Journal of British Surgery. 2014;101(8):925-38.
12. Puig-Vives M, Sanchez M, Sanchez-Cantalejo J, Torrella-Ramos A, Martos C, Ardanaz E, et al. Distribution and prognosis of molecular breast cancer subtypes defined by immunohistochemical biomarkers in a Spanish population-based study. Gynecologic oncology. 2013;130(3):609-14.
13. Fragomeni SM, Sciallis A, Jeruss JS. Molecular subtypes and local-regional control of breast cancer. Surgical Oncology Clinics. 2018;27(1):95-120.
14. van Maaren MC, de Munck L, Strobbe LJA, Sonke GS, Westenend PJ, Smidt ML, et al. Ten-year recurrence rates for breast cancer subtypes in the Netherlands: A large population-based study. International journal of cancer. 2019;144(2):263-72.
15. Creighton CJ. The molecular profile of luminal B breast cancer. Biologics: targets & therapy. 2012;6:289.
16. Dai X, Li T, Bai Z, Yang Y, Liu X, Zhan J, et al. Breast cancer intrinsic subtype classification, clinical use and future trends. American journal of cancer research. 2015;5(10):2929-43.
17. Nassar A, Khoor A, Radhakrishnan R, Radhakrishnan A, Cohen C. Correlation of HER2 overexpression with gene amplification and its relation to chromosome 17 aneuploidy: a 5-year experience with invasive ductal and lobular carcinomas. International journal of clinical and experimental pathology. 2014;7(9):6254.

18. Mueller C, Haymond A, Davis JB, Williams A, Espina V. Protein biomarkers for subtyping breast cancer and implications for future research. Expert review of proteomics. 2018;15(2):131-52.
19. Leitzel K, Teramoto Y, Konrad K, Chinchilli VM, Volas G, Grossberg H, et al. Elevated serum c-erbB-2 antigen levels and decreased response to hormone therapy of breast cancer. Journal of Clinical Oncology. 1995;13(5):1129-35.
20. Prat A, Lluch A, Albanell J, Barry W, Fan C, Chacon J, et al. Predicting response and survival in chemotherapy-treated triple-negative breast cancer. British journal of cancer. 2014;111(8):1532-41.
21. Heitz F, Harter P, Lueck H-J, Fissler-Eckhoff A, Lorenz-Salehi F, Scheil-Bertram S, et al. Triple-negative and HER2-overexpressing breast cancers exhibit an elevated risk and an earlier occurrence of cerebral metastases. European journal of cancer. 2009;45(16):2792-8.
22. Perou CM. Molecular stratification of triple-negative breast cancers. The oncologist. 2010;15:39-48.
23. Kreike B, van Kouwenhove M, Horlings H, Weigelt B, Peterse H, Bartelink H, et al. Gene expression profiling and histopathological characterization of triple-negative/basal-like breast carcinomas. Breast cancer research : BCR. 2007;9(5):R65-R.
24. Millikan RC, Newman B, Tse C-K, Moorman PG, Conway K, Smith LV, et al. Epidemiology of basal-like breast cancer. Breast cancer research and treatment. 2008;109(1):123-39.
25. Phipps AI, Chlebowski RT, Prentice R, McTiernan A, Stefanick ML, Wactawski-Wende J, et al. Body size, physical activity, and risk of triple-negative and estrogen receptor–positive breast cancer. Cancer Epidemiology and Prevention Biomarkers. 2011;20(3):454-63.
26. Aebi S, Sun Z, Braun D, Price K, Castiglione-Gertsch M, Rabaglio M, et al. Differential efficacy of three cycles of CMF followed by tamoxifen in patients with ER-positive and ER-negative tumors: long-term follow up on IBCSG Trial IX. Annals of oncology. 2011;22(9):1981-7.
27. Ballinger T, Kremer J, Miller K. Triple negative breast cancer-Review of current and emerging therapeutic strategies. 2016.
28. Ishitha G, Manipadam MT, Backianathan S, Chacko RT, Abraham DT, Jacob PM. Clinicopathological Study of Triple Negative Breast Cancers. Journal of clinical and diagnostic research. 2016;10(9):EC05-EC9.
29. Gonçalves Jr H, Guerra MR, Duarte Cintra JR, Fayer VA, Brum IV, Bustamante Teixeira MT. Survival study of triple-negative and non–triple-negative breast cancer in a Brazilian Cohort. Clinical Medicine Insights: Oncology. 2018;12:1179554918790563.
30. Dent R, Trudeau M, Pritchard KI, Hanna WM, Kahn HK, Sawka CA, et al. Triple-negative breast cancer: clinical features and patterns of recurrence. Clinical cancer research. 2007;13(15):4429-34.
31. Lin NU, Claus E, Sohl J, Razzak AR, Arnaout A, Winer EP. Sites of distant recurrence and clinical outcomes in patients with metastatic triple-negative breast cancer: high incidence of central nervous system metastases. Cancer. 2008;113(10):2638-45.
32. Salpeter SR, Malter DS, Luo EJ, Lin AY, Stuart B. Systematic review of cancer presentations with a median survival of six months or less. Journal of palliative medicine. 2012;15(2):175-85.
33. Pogoda K, Niwinska A, Murawska M, Olszewski W, Nowecki Z. The outcome of special histologic types of triple-negative breast cancer (TNBC). Journal of clinical oncology. 2014;32(15_suppl):1122-.
34. Dreyer G, Vandorpe T, Smeets A, Forceville K, Brouwers B, Neven P, et al. Triple negative breast cancer: clinical characteristics in the different histological subtypes. The Breast. 2013;22(5):761-6.

35. Zhao S, Ma D, Xiao Y, Jiang Y-Z, Shao Z-M. Clinicopathologic features and prognoses of different histologic types of triple-negative breast cancer: A large population-based analysis. European journal of surgical oncology. 2018;44(4):420-8.
36. Mills MN, Yang GQ, Oliver DE, Liveringhouse CL, Ahmed KA, Orman AG, et al. Histologic heterogeneity of triple negative breast cancer: A National Cancer Centre Database analysis. European journal of cancer (1990). 2018;98:48-58.
37. Lehmann BD, Pietenpol JA. Identification and use of biomarkers in treatment strategies for triple-negative breast cancer subtypes. The Journal of pathology. 2014;232(2):142-50.
38. Lehmann BD, Jovanović B, Chen X, Estrada MV, Johnson KN, Shyr Y, et al. Refinement of triple-negative breast cancer molecular subtypes: implications for neoadjuvant chemotherapy selection. PloS one. 2016;11(6):e0157368.
39. Roseweir AK, McCall P, Scott A, Liew B, Lim Z, Mallon EA, et al. Phosphorylation of androgen receptors at serine 515 is a potential prognostic marker for triple negative breast cancer. Oncotarget. 2017;8(23):37172.
40. Ferrer J, Neyro JL, Estevez A. Identification of risk factors for prevention and early diagnosis of a-symptomatic post-menopausal women. Maturitas. 2005;52:7-22.
41. Newman LA, Reis-Filho JS, Morrow M, Carey LA, King TA. The 2014 Society of Surgical Oncology Susan G. Komen for the cure symposium: triple-negative breast cancer. Annals of surgical oncology. 2015;22(3):874-82.
42. Haynes B, Gajan A, Nangia-Makker P, Shekhar MP. RAD6B is a major mediator of triple negative breast cancer cisplatin resistance: Regulation of translesion synthesis/Fanconi anemia crosstalk and BRCA1 independence. Biochimica et Biophysica Acta (BBA)-Molecular Basis of Disease. 2020;1866(1):165561.
43. Buys SS, Sandbach JF, Gammon A, Patel G, Kidd J, Brown KL, et al. A study of over 35,000 women with breast cancer tested with a 25-gene panel of hereditary cancer genes. Cancer. 2017;123(10):1721-30.
44. Meyer P, Landgraf K, Högel B, Eiermann W, Ataseven B. BRCA2 mutations and triple-negative breast cancer. PLoS One. 2012;7(5):e38361.
45. Fostira F, Tsitlaidou M, Papadimitriou C, Pertesi M, Timotheadou E, Stavropoulou AV, et al. Prevalence of BRCA1 mutations among 403 women with triple-negative breast cancer: implications for genetic screening selection criteria: a Hellenic Cooperative Oncology Group Study. Breast cancer research and treatment. 2012;134(1):353-62.
46. Anderson KN, Schwab RB, Martinez ME. Reproductive risk factors and breast cancer subtypes: a review of the literature. Breast cancer research and treatment. 2014;144(1):1-10.
47. Ma H, Wang Y, Sullivan-Halley J, Weiss L, Marchbanks PA, Spirtas R, et al. Use of four biomarkers to evaluate the risk of breast cancer subtypes in the women's contraceptive and reproductive experiences study. Cancer research. 2010;70(2):575-87.
48. Ma H, Ursin G, Xu X, Lee E, Togawa K, Duan L, et al. Reproductive factors and the risk of triple-negative breast cancer in white women and African-American women: a pooled analysis. Breast Cancer Research. 2017;19(1):6.
49. Mørch LS, Skovlund CW, Hannaford PC, Iversen L, Fielding S, Lidegaard Ø. Contemporary hormonal contraception and the risk of breast cancer. New England Journal of Medicine. 2017;377(23):2228-39.
50. Lodha RS, Nandeshwar S, Pal D, Shrivastav A, Lodha K, Bhagat VK, et al. Risk factors for breast cancer among women in Bhopal urban agglomerate: a case-control study. Asian Pac J Cancer Prev. 2011;12(8):2111-5.
51. Li L, Zhong Y, Zhang H, Yu H, Huang Y, Li Z, et al. Association between oral contraceptive use as a risk factor and triple-negative breast cancer: A systematic review and meta-analysis. Molecular and clinical oncology. 2017a;7(1):76-80.

52. Dolle JM, Daling JR, White E, Brinton LA, Doody DR, Porter PL, et al. Risk factors for triple-negative breast cancer in women under the age of 45 years. Cancer Epidemiology and Prevention Biomarkers. 2009;18(4):1157-66.
53. Holmberg L, Anderson H. HABITS (hormonal replacement therapy after breast cancer—is it safe?), a randomised comparison: trial stopped. The Lancet. 2004;363(9407):453-5.
54. Kenemans P, Bundred NJ, Foidart J-M, Kubista E, von Schoultz B, Sismondi P, et al. Safety and efficacy of tibolone in breast-cancer patients with vasomotor symptoms: a double-blind, randomised, non-inferiority trial. The lancet oncology. 2009;10(2):135-46.
55. Go Y, Chung M, Park Y. Dietary patterns for women with triple-negative breast cancer and dense breasts. Nutrition and cancer. 2016;68(8):1281-8.
56. Shams-White MM, Brockton NT, Mitrou P, Romaguera D, Brown S, Bender A, et al. Operationalizing the 2018 World Cancer Research Fund/American Institute for Cancer Research (WCRF/AICR) cancer prevention recommendations: a standardized scoring system. Nutrients. 2019;11(7):1572.
57. Merten JW, Parker A, Williams A, King JL, Largo-Wight E, Osmani M. Cancer risk factor knowledge among young adults. Journal of Cancer Education. 2017;32(4):865-70.
58. Cancer CGoHFiB. Alcohol, tobacco and breast cancer–collaborative reanalysis of individual data from 53 epidemiological studies, including 58 515 women with breast cancer and 95 067 women without the disease. British journal of cancer. 2002;87(11):1234.
59. Gago-Dominguez M, Castelao JE, Gude F, Fernandez MP, Aguado-Barrera ME, Ponte SM, et al. Alcohol and breast cancer tumor subtypes in a Spanish Cohort. Springerplus. 2016;5(1):39.
60. Zhao M, Howard EW, Parris AB, Guo Z, Zhao Q, Yang X. Alcohol promotes migration and invasion of triple-negative breast cancer cells through activation of p38 MAPK and JNK. Molecular carcinogenesis. 2017a;56(3):849-62.
61. Liu Y, Tobias DK, Sturgeon KM, Rosner B, Malik V, Cespedes E, et al. Physical activity from menarche to first pregnancy and risk of breast cancer. International journal of cancer. 2016;139(6):1223-30.
62. Ma H, Xu X, Clague J, Lu Y, Togawa K, Wang SS, et al. Recreational physical activity and risk of triple negative breast cancer in the California Teachers Study. Breast Cancer Research. 2016;18(1):1-16.
63. Almansour N. Triple-Negative Breast Cancer: A Brief Review About Epidemiology, Risk Factors, Signaling Pathways, Treatment and Role of Artificial Intelligence. Frontiers in Molecular Biosciences. 2022:32.
64. Ashcraft KA, Warner AB, Jones LW, Dewhirst MW, editors. Exercise as adjunct therapy in cancer. Seminars in radiation oncology; 2019: Elsevier.
65. Suzuki R, Orsini N, Saji S, Key TJ, Wolk A. Body weight and incidence of breast cancer defined by estrogen and progesterone receptor status—a meta-analysis. International journal of cancer. 2009;124(3):698-712.
66. Cakar B, Muslu U, Erdogan AP, Ozisik M, Ozisik H, Dalgic CT, et al. The role of body mass index in triple negative breast cancer. Oncology research and treatment. 2015;38(10):518-22.
67. Dietze EC, Chavez TA, Seewaldt VL. Obesity and triple-negative breast cancer: disparities, controversies, and biology. The American journal of pathology. 2018;188(2):280-90.
68. Fitzgibbons HD, Hutter RV. Benign breast changes and the risk for subsequent breast cancer: an update of the 1985 consensus statement. 1998.
69. Page DL, Dupont WD, Rogers LW, Rados MS. Atypical hyperplastic lesions of the female breast. A long-term follow-up study. Cancer. 1985;55(11):2698-708.

70. Hartmann LC, Radisky DC, Frost MH, Santen RJ, Vierkant RA, Benetti LL, et al. Understanding the Premalignant Potential of Atypical Hyperplasia through Its Natural History: A Longitudinal Cohort Study is. Cancer prevention research (Philadelphia, Pa). 2014;7(2):211-7.
71. Newman LA, Stark A, Chitale D, Pepe M, Longton G, Worsham MJ, et al. Benign Breast Disease in White/Caucasian American and African American Women and Subsequent Triple Negative Breast Cancer. JAMA oncology. 2017;3(8):1102-6.
72. Cianfrocca M, Goldstein LJ. Prognostic and Predictive Factors in Early-Stage Breast Cancer. The oncologist (Dayton, Ohio). 2004;9(6):606-16.
73. Bastiaannet E, Liefers GJ, de Craen AJ, Kuppen PJ, van de Water W, Portielje JE, et al. Breast cancer in elderly compared to younger patients in the Netherlands: stage at diagnosis, treatment and survival in 127,805 unselected patients. Breast Cancer Res Treat. 2010;124(3):801-7.
74. Fredholm H, Eaker S, Frisell J, Holmberg L, Fredriksson I, Lindman H. Breast cancer in young women: poor survival despite intensive treatment. PLoS One. 2009;4(11):e7695.
75. Li C-Y, Zhang S, Zhang X-B, Wang P, Hou G-F, Zhang J. Clinicopathological and prognostic characteristics of triple-negative breast cancer (TNBC) in Chinese patients: a retrospective study. Asian Pacific Journal of Cancer Prevention. 2013a;14(6):3779-84.
76. Agarwal G, Nanda G, Lal P, Mishra A, Agarwal A, Agrawal V, et al. Outcomes of triple-negative breast cancers (TNBC) compared with non-TNBC: does the survival vary for all stages? World journal of surgery. 2016;40(6):1362-72.
77. Bloom H, Richardson W. Histological grading and prognosis in breast cancer: a study of 1409 cases of which 359 have been followed for 15 years. British journal of cancer. 1957;11(3):359.
78. Elston CW, Ellis IO. Pathological prognostic factors in breast cancer. I. The value of histological grade in breast cancer: experience from a large study with long-term follow-up. Histopathology. 1991;19(5):403-10.
79. Galea MH, Blamey RW, Elston CE, Ellis IO. The Nottingham Prognostic Index in primary breast cancer. Breast cancer research and treatment. 1992;22(3):207-19.
80. Yao Y, Chu Y, Xu B, Hu Q, Song Q. Risk factors for distant metastasis of patients with primary triple-negative breast cancer. Bioscience Reports. 2019;39(6).
81. Yin L, Shuang H, Sheng C, Liang H, Sun X-J, Yang W-T, et al. The Prognostic Value of Nodal Staging in Triple-Negative Breast Cancer—A Cohort from China. Scientific reports. 2018;8(1):1-7.
82. Hernandez-Aya LF, Chavez-MacGregor M, Lei X, Meric-Bernstam F, Buchholz TA, Hsu L, et al. Nodal status and clinical outcomes in a large cohort of patients with triple-negative breast cancer. Journal of clinical oncology. 2011;29(19):2628.
83. de Azambuja E, Cardoso F, de Castro G, Jr., Colozza M, Mano MS, Durbecq V, et al. Ki-67 as prognostic marker in early breast cancer: a meta-analysis of published studies involving 12,155 patients. Br J Cancer. 2007;96(10):1504-13.
84. Wang W, Wu J, Zhang P, Fei X, Zong Y, Chen X, et al. Prognostic and predictive value of Ki-67 in triple-negative breast cancer. Oncotarget. 2016a;7(21):31079.
85. Penault-Llorca F, Radosevic-Robin N. Ki67 assessment in breast cancer: an update. Pathology. 2017;49(2):166-71.
86. Tan AC, Li BT, Nahar K, Danieletto S, Fong ES, Currer T, et al. Correlating Ki67 and other prognostic markers with Oncotype DX recurrence score in early estrogen receptor-positive breast cancer. Asia-Pacific Journal of Clinical Oncology. 2018;14(2):e161-e6.
87. Zhu X, Chen L, Huang B, Wang Y, Ji L, Wu J, et al. The prognostic and predictive potential of Ki-67 in triple-negative breast cancer. Scientific reports. 2020;10(1):1-10.

88. Zhou Q, Li W. Prognostic value of Ki-67 in patients with triple-negative breast cancer receiving neo-adjuvant or adjuvant chemotherapy: A systematic review and meta-analysis. Annals of Oncology. 2019;30:iii15.
89. De Mascarel I, MacGrogan G, Debled M, Sierankowski G, Brouste V, Mathoulin-Pélissier S, et al. D2-40 in breast cancer: should we detect more vascular emboli? Modern Pathology. 2009;22(2):216-22.
90. Ahn KJ, Park J, Choi Y. Lymphovascular invasion as a negative prognostic factor for triple-negative breast cancer after surgery. Radiation oncology journal : ROJ. 2017;35(4):332-9.
91. Liao G-S, Hsu H-M, Chu C-H, Hong Z-J, Fu C-Y, Chou Y-C, et al. Prognostic role of lymphovascular invasion and lymph node status among breast cancer subtypes. J Med Sci. 2018;38(2):54-61.
92. Urru SAM, Gallus S, Bosetti C, Moi T, Medda R, Sollai E, et al. Clinical and pathological factors influencing survival in a large cohort of triple-negative breast cancer patients. BMC cancer. 2018;18(1):1-11.
93. Mohammed RA, Martin SG, Gill MS, Green AR, Paish EC, Ellis IO. Improved methods of detection of lymphovascular invasion demonstrate that it is the predominant method of vascular invasion in breast cancer and has important clinical consequences. The American journal of surgical pathology. 2007;31(12):1825-33.
94. Golstein P, Kroemer G. Cell death by necrosis: towards a molecular definition. Trends in biochemical sciences (Amsterdam Regular ed). 2007;32(1):37-43.
95. Proskuryakov SY, Gabai VL. Mechanisms of tumor cell necrosis. Current pharmaceutical design. 2010;16(1):56-68.
96. Karsch-Bluman A, Feiglin A, Arbib E, Stern T, Shoval H, Schwob O, et al. Tissue necrosis and its role in cancer progression. Oncogene. 2019;38(11):1920-35.
97. Leek RD, Landers RJ, Harris AL, Lewis CE. Necrosis correlates with high vascular density and focal macrophage infiltration in invasive carcinoma of the breast. British journal of cancer. 1999;79(5-6):991-5.
98. Colpaert C, Vermeulen P, Van Beest P, Goovaerts G, Weyler J, Van Dam P, et al. Intratumoral hypoxia resulting in the presence of a fibrotic focus is an independent predictor of early distant relapse in lymph node-negative breast cancer patients. Histopathology. 2001;39(4):416-25.
99. Maiorano E, Regan MM, Viale G, Mastropasqua MG, Colleoni M, Castiglione-Gertsch M, et al. Prognostic and predictive impact of central necrosis and fibrosis in early breast cancer: results from two International Breast Cancer Study Group randomized trials of chemoendocrine adjuvant therapy. Breast cancer research and treatment. 2010;121(1):211-8.
100. Livasy CA, Karaca G, Nanda R, Tretiakova MS, Olopade OI, Moore DT, et al. Phenotypic evaluation of the basal-like subtype of invasive breast carcinoma. Modern pathology. 2006;19(2):264-71.
101. Foulkes WD, Smith IE, Reis-Filho JS. Triple-negative breast cancer. New England journal of medicine. 2010;363(20):1938-48.
102. Wahba HA, El-Hadaad HA. Current approaches in treatment of triple-negative breast cancer. Cancer biology & medicine. 2015;12(2):106.
103. Dusowitz E. An Analysis on Various Treatment Options for Triple-Negative Breast Cancer. The Science Journal of the Lander College of Arts and Sciences. 2022;15(2):10-5.
104. Zhai Z, Zheng Y, Yao J, Liu Y, Ruan J, Deng Y, et al. Evaluation of adjuvant treatments for T1 N0 M0 triple-negative breast cancer. JAMA network open. 2020;3(11):e2021881-e.
105. Sioshansi S, Ehdaivand S, Cramer C, Lomme MM, Price LL, Wazer DE. Triple negative breast cancer is associated with an increased risk of residual invasive carcinoma after lumpectomy. Cancer. 2012;118(16):3893-8.

106. Zhang Y, Wang M, Liu W, Wang CY, Xie XF, Chen X, Dong JF, Li M. Enhanced autophagy reveals vulnerability of P-gp mediated epirubicin resistance in triple negative breast cancer cells. . 2016.
107. Park JH, Ahn J-H, Kim S-B. How shall we treat early triple-negative breast cancer (TNBC): from the current standard to upcoming immuno-molecular strategies. ESMO open. 2018;3:e000357.
108. Ghahremanloo A, Soltani A, Modaresi SMS, Hashemy SI. Recent advances in the clinical development of immune checkpoint blockade therapy. Cellular Oncology. 2019;42(5):609-26.
109. Li X, Li M, Lian Z, Zhu H, Kong L, Wang P, et al. Prognostic role of programmed death ligand-1 expression in breast cancer: a systematic review and meta-analysis. Targeted oncology. 2016a;11(6):753-61.
110. Kwa MJ, Adams S. Checkpoint inhibitors in triple-negative breast cancer (TNBC): Where to go from here. Cancer. 2018;124(10):2086-103.
111. García-Teijido P, Cabal ML, Fernández IP, Pérez YF. Tumor-Infiltrating Lymphocytes in Triple Negative Breast Cancer: The Future of Immune Targeting. Clinical Medicine Insights: Oncology. 2016;2016(Suppl. 1):31-9.
112. Nanda R, Chow LQM, Dees EC, Berger R, Gupta S, Geva R, et al. Pembrolizumab in Patients With Advanced Triple-Negative Breast Cancer: Phase Ib KEYNOTE-012 Study. Journal of clinical oncology. 2016;34(21):2460-7.
113. Budhathoki N, Dhakal A, Opyrchal M. Immune checkpoint inhibitors in triple negative breast cancer. Theranostics Can Res. 2017;1:1-4.
114. Gluz O, Liedtke C, Gottschalk N, Pusztai L, Nitz U, Harbeck N. Triple-negative breast cancer—current status and future directions. Annals of Oncology. 2009;20(12):1913-27.
115. Hanahan D, Weinberg RA. Hallmarks of cancer: the next generation. cell. 2011;144(5):646-74.
116. Hanahan D, Coussens LM. Accessories to the crime: functions of cells recruited to the tumor microenvironment. Cancer cell. 2012;21(3):309-22.
117. Dittmer J, Leyh B, editors. The impact of tumor stroma on drug response in breast cancer. Seminars in cancer biology; 2015: Elsevier.
118. Yu T, Di G. Role of tumor microenvironment in triple-negative breast cancer and its prognostic significance. Chinese Journal of Cancer Research. 2017;29(3):237.
119. Koontongkaew S. The tumor microenvironment contribution to development, growth, invasion and metastasis of head and neck squamous cell carcinomas. Journal of Cancer. 2013;4(1):66.
120. Lotfinejad P, Asghari Jafarabadi M, Abdoli Shadbad M, Kazemi T, Pashazadeh F, Sandoghchian Shotorbani S, et al. Prognostic role and clinical significance of tumor-infiltrating lymphocyte (TIL) and programmed death ligand 1 (PD-L1) expression in triple-negative breast cancer (TNBC): a systematic review and meta-analysis study. Diagnostics. 2020;10(9):704.
121. Sahin Ozkan H, Ugurlu MU, Yumuk PF, Kaya H. Prognostic role of immune markers in triple negative breast carcinoma. Pathology & Oncology Research. 2020;26(4):2733-45.
122. Loi S, Michiels S, Salgado R, Sirtaine N, Jose V, Fumagalli D, et al. Tumor infiltrating lymphocytes are prognostic in triple negative breast cancer and predictive for trastuzumab benefit in early breast cancer: results from the FinHER trial. Annals of oncology. 2014;25(8):1544-50.
123. Denkert C, von Minckwitz G, Darb-Esfahani S, Lederer B, Heppner BI, Weber KE, et al. Tumour-infiltrating lymphocytes and prognosis in different subtypes of breast cancer: a pooled analysis of 3771 patients treated with neoadjuvant therapy. The lancet oncology. 2018;19(1):40-50.

124. Matsumoto H, Koo S-l, Dent R, Tan PH, Iqbal J. Role of inflammatory infiltrates in triple negative breast cancer. Journal of clinical pathology. 2015;68(7):506-10.
125. Lehmann BD, Bauer JA, Chen X, Sanders ME, Chakravarthy AB, Shyr Y, et al. Identification of human triple-negative breast cancer subtypes and preclinical models for selection of targeted therapies. The Journal of clinical investigation. 2011;121(7):2750-67.
126. Safonov A, Jiang T, Bianchini G, Győrffy B, Karn T, Hatzis C, et al. Immune gene expression is associated with genomic aberrations in breast cancer. Cancer research. 2017;77(12):3317-24.
127. Romero-Cordoba S, Meneghini E, Sant M, Iorio MV, Sfondrini L, Paolini B, et al. Decoding immune heterogeneity of triple negative breast cancer and its association with systemic inflammation. Cancers. 2019;11(7):911.
128. Ishida Y, Agata Y, Shibahara K, Honjo T. Induced expression of PD-1, a novel member of the immunoglobulin gene superfamily, upon programmed cell death. The EMBO journal. 1992;11(11):3887-95.
129. Mittendorf EA, Philips AV, Meric-Bernstam F, Qiao N, Wu Y, Harrington S, et al. PD-L1 expression in triple-negative breast cancer. Cancer immunology research. 2014;2(4):361-70.
130. Li Z, Dong P, Ren M, Song Y, Qian X, Yang Y, et al. PD-L1 expression is associated with tumor FOXP3+ regulatory T-cell infiltration of breast cancer and poor prognosis of patient. Journal of Cancer. 2016b;7(7):784.
131. Mediratta K, El-Sahli S, D'Costa V, Wang L. Current progresses and challenges of immunotherapy in triple-negative breast cancer. Cancers. 2020;12(12):3529.
132. Stanton SE, Disis ML. Clinical significance of tumor-infiltrating lymphocytes in breast cancer. Journal for immunotherapy of cancer. 2016;4(1):59.
133. Ku YJ, Kim HH, Cha JH, Shin HJ, Baek SH, Lee HJ, et al. Correlation between MRI and the level of tumor-infiltrating lymphocytes in patients with triple-negative breast cancer. American Journal of Roentgenology. 2016;207(5):1146-51.
134. Lee J, Kim D-M, Lee A. Prognostic role and clinical association of tumor-infiltrating lymphocyte, programmed death ligand-1 expression with neutrophil-lymphocyte ratio in locally advanced triple-negative breast cancer. Cancer Research and Treatment: Official Journal of Korean Cancer Association. 2019;51(2):649-63.
135. Yu H, Meng X, Chen H, Han X, Fan J, Gao W, et al. Correlation between mammographic radiomics features and the level of tumor-infiltrating lymphocytes in patients with triple-negative breast cancer. Frontiers in Oncology. 2020;10:412.
136. Bianchini G, Balko JM, Mayer IA, Sanders ME, Gianni L. Triple-negative breast cancer: challenges and opportunities of a heterogeneous disease. Nature reviews Clinical oncology. 2016;13(11):674-90.
137. Salgado R, Denkert C, Demaria S, Sirtaine N, Klauschen F, Pruneri G, et al. The evaluation of tumor-infiltrating lymphocytes (TILs) in breast cancer: recommendations by an International TILs Working Group 2014. Annals of oncology. 2015;26(2):259-71.
138. Hendry S, Salgado R, Gevaert T, Russell PA, John T, Thapa B, et al. Assessing tumor infiltrating lymphocytes in solid tumors: a practical review for pathologists and proposal for a standardized method from the International Immuno-Oncology Biomarkers Working Group: Part 1: Assessing the host immune response, TILs in invasive breast carcinoma and ductal carcinoma in situ, metastatic tumor deposits and areas for further research. Advances in anatomic pathology. 2017;24(5):235.
139. Gu-Trantien C, Loi S, Garaud S, Equeter C, Libin M, De Wind A, et al. CD4+ follicular helper T cell infiltration predicts breast cancer survival. The Journal of clinical investigation. 2013;123(7):2873-92.
140. Oshi M, Asaoka M, Tokumaru Y, Yan L, Matsuyama R, Ishikawa T, et al. CD8 T cell score as a prognostic biomarker for triple negative breast cancer. International journal of molecular sciences. 2020;21(18):6968.

141. Ono M, Tsuda H, Shimizu C, Yamamoto S, Shibata T, Yamamoto H, et al. Tumor-infiltrating lymphocytes are correlated with response to neoadjuvant chemotherapy in triple-negative breast cancer. Breast cancer research and treatment. 2012;132(3):793-805.
142. Sanchez K, Page D, McArthur HL. Immunotherapy in breast cancer: an overview of modern checkpoint blockade strategies and vaccines. Current problems in cancer. 2016;40(2-4):151-62.
143. Boieri M, Malishkevich A, Guennoun R, Marchese E, Kroon S, Trerice KE, et al. CD4+ T helper 2 cells suppress breast cancer by inducing terminal differentiation. Journal of Experimental Medicine. 2022;219(7):e20201963.
144. Xiao Y, Huang Y, Jiang J, Chen Y, Wei C. Identification of the prognostic value of Th1/Th2 ratio and a novel prognostic signature in basal-like breast cancer. Hereditas. 2023;160(1):1-14.
145. Bohling SD, Allison KH. Immunosuppressive regulatory T cells are associated with aggressive breast cancer phenotypes: a potential therapeutic target. Modern Pathology. 2008;21(12):1527-32.
146. Stovgaard ES, Nielsen D, Hogdall E, Balslev E. Triple negative breast cancer–prognostic role of immune-related factors: a systematic review. Acta Oncologica. 2018;57(1):74-82.
147. Song IH, Heo S-H, Bang WS, Park HS, Park IA, Kim Y-A, et al. Predictive value of tertiary lymphoid structures assessed by high endothelial venule counts in the neoadjuvant setting of triple-negative breast cancer. Cancer research and treatment: official journal of Korean Cancer Association. 2017;49(2):399.
148. Mohammed Z, Going J, Edwards J, Elsberger B, McMillan D. The relationship between lymphocyte subsets and clinico-pathological determinants of survival in patients with primary operable invasive ductal breast cancer. British journal of cancer. 2013;109(6):1676-84.
149. Mantovani A, Sozzani S, Locati M, Allavena P, Sica A. Macrophage polarization: tumor-associated macrophages as a paradigm for polarized M2 mononuclear phagocytes. Trends in immunology. 2002;23(11):549-55.
150. Qian B-Z, Pollard JW. Macrophage diversity enhances tumor progression and metastasis. Cell. 2010;141(1):39-51.
151. DeNardo DG, Barreto JB, Andreu P, Vasquez L, Tawfik D, Kolhatkar N, et al. CD4+ T cells regulate pulmonary metastasis of mammary carcinomas by enhancing protumor properties of macrophages. Cancer cell. 2009;16(2):91-102.
152. Medrek C, Pontén F, Jirström K, Leandersson K. The presence of tumor associated macrophages in tumor stroma as a prognostic marker for breast cancer patients. BMC cancer. 2012;12(1):306.
153. Mohammed ZM, Going JJ, Edwards J, McMillan DC. The role of the tumour inflammatory cell infiltrate in predicting recurrence and survival in patients with primary operable breast cancer. Cancer treatment reviews. 2012;38(8):943-55.
154. Stewart DA, Yang Y, Makowski L, Troester MA. Basal-like breast cancer cells induce phenotypic and genomic changes in macrophages. Molecular Cancer Research. 2012;10(6):727-38.
155. Zhang X, Zeng Y, Qu Q, Zhu J, Liu Z, Ning W, et al. PD-L1 induced by IFN-γ from tumor-associated macrophages via the JAK/STAT3 and PI3K/AKT signaling pathways promoted progression of lung cancer. International journal of clinical oncology. 2017;22(6):1026-33.
156. Schalper KA. PD-L1 expression and tumor-infiltrating lymphocytes: revisiting the antitumor immune response potential in breast cancer. Oncoimmunology. 2014;3(6):e29288.
157. Singh S, Kumar S, Srivastava RK, Nandi A, Thacker G, Murali H, et al. Loss of ELF5–FBXW7 stabilizes IFNGR1 to promote the growth and metastasis of triple-negative breast cancer through interferon-γ signalling. Nature cell biology. 2020;22(5):591-602.

158. Liubomirski Y, Lerrer S, Meshel T, Rubinstein-Achiasaf L, Morein D, Wiemann S, et al. Tumor-stroma-inflammation networks promote pro-metastatic chemokines and aggressiveness characteristics in triple-negative breast cancer. Frontiers in immunology. 2019;10:757.
159. Santoni M, Romagnoli E, Saladino T, Foghini L, Guarino S, Capponi M, et al. Triple negative breast cancer: Key role of Tumor-Associated Macrophages in regulating the activity of anti-PD-1/PD-L1 agents. Biochimica et Biophysica Acta (BBA)-Reviews on Cancer. 2018;1869(1):78-84.
160. Wang J, Chen H, Chen X, Lin H. Expression of tumor-related macrophages and cytokines after surgery of triple-negative breast cancer patients and its implications. Medical science monitor: international medical journal of experimental and clinical research. 2016b;22:115.
161. Hartman ZC, Poage GM, Den Hollander P, Tsimelzon A, Hill J, Panupinthu N, et al. Growth of triple-negative breast cancer cells relies upon coordinate autocrine expression of the proinflammatory cytokines IL-6 and IL-8. Cancer research. 2013;73(11):3470-80.
162. Jin K, Pandey NB, Popel AS. Crosstalk between stromal components and tumor cells of TNBC via secreted factors enhances tumor growth and metastasis. Oncotarget. 2017;8(36):60210.
163. Mi Z, Bhattacharya SD, Kim VM, Guo H, Talbot LJ, Kuo PC. Osteopontin promotes CCL5-mesenchymal stromal cell-mediated breast cancer metastasis. Carcinogenesis. 2011;32(4):477-87.
164. Ryan D, Sinha A, Bogan D, Davies J, Koziol J, ElShamy WM. Correction: A niche that triggers aggressiveness within BRCA1-IRIS overexpressing triple negative tumors is supported by reciprocal interactions with the microenvironment. Oncotarget. 2017;8(68):113294.
165. Juliá EP, Mordoh J, Levy EM. Cetuximab and IL-15 promote NK and dendritic cell activation in vitro in triple negative breast cancer. Cells. 2020;9(7):1573.
166. Park IH, Yang HN, Lee KJ, Kim T-S, Lee ES, Jung S-Y, et al. Tumor-derived IL-18 induces PD-1 expression on immunosuppressive NK cells in triple-negative breast cancer. Oncotarget. 2017;8(20):32722.
167. de Kruijf EM, van Nes JG, van de Velde CJ, Putter H, Smit VT, Liefers GJ, et al. Tumor–stroma ratio in the primary tumor is a prognostic factor in early breast cancer patients, especially in triple-negative carcinoma patients. Breast cancer research and treatment. 2011;125(3):687-96.
168. Kramer C, Vangangelt K, Van Pelt G, Dekker T, Tollenaar R, Mesker W. The prognostic value of tumour–stroma ratio in primary breast cancer with special attention to triple-negative tumours: a review. Breast cancer research and treatment. 2019;173(1):55-64.
169. Mao Y, Keller ET, Garfield DH, Shen K, Wang J. Stromal cells in tumor microenvironment and breast cancer. Cancer and Metastasis Reviews. 2013;32(1-2):303-15.
170. Chen Y, Zou L, Zhang Y, Chen Y, Xing P, Yang W, et al. Transforming growth factor-β1 and α-smooth muscle actin in stromal fibroblasts are associated with a poor prognosis in patients with clinical stage I–IIIA nonsmall cell lung cancer after curative resection. Tumor Biology. 2014;35:6707-13.
171. Magesh P, Thankachan S, Venkatesh T, Suresh PS. Breast cancer fibroblasts and cross-talk. Clinica Chimica Acta. 2021;521:158-69.
172. Wang M, Zhang J, Huang Y, Ji S, Shao G, Feng S, et al. Cancer-associated fibroblasts autophagy enhances progression of triple-negative breast cancer cells. Medical science monitor: international medical journal of experimental and clinical research. 2017a;23:3904.

173. Takai K, Le A, Weaver VM, Werb Z. Targeting the cancer-associated fibroblasts as a treatment in triple-negative breast cancer. Oncotarget. 2016;7(50):82889.
174. Zhu X, Wang K, Zhang K, Xu F, Yin Y, Zhu L, et al. Galectin-1 knockdown in carcinoma-associated fibroblasts inhibits migration and invasion of human MDA-MB-231 breast cancer cells by modulating MMP-9 expression. Acta Biochim Biophys Sin. 2016;48(5):462-7.
175. Niemiec JA, Adamczyk A, Ambicka A, Mucha-Malecka A, Wysocki WM, Rys J. Triple-negative, basal marker-expressing, and high-grade breast carcinomas are characterized by high lymphatic vessel density and the expression of podoplanin in stromal fibroblasts. Applied Immunohistochemistry & Molecular Morphology. 2014;22(1):10-6.
176. Brauer HA, Makowski L, Hoadley KA, Casbas-Hernandez P, Lang LJ, Romàn-Pèrez E, et al. Impact of tumor microenvironment and epithelial phenotypes on metabolism in breast cancer. Clinical Cancer Research. 2013;19(3):571-85.
177. Zhou J, Wang X-H, Zhao Y-X, Chen C, Xu X-Y. Cancer-associated fibroblasts correlate with tumor-associated macrophages infiltration and lymphatic metastasis in triple negative breast cancer patients. Journal of Cancer. 2018;9(24):4635.
178. Huang T, Bao H, Meng Y-h, Zhu J-l, Chu X-d, Chu X-l, et al. Tumour budding is a novel marker in breast cancer: the clinical application and future prospects. Annals of Medicine. 2022;54(1):1303-12.
179. Okcu O, Öztürk Ç, Şen B, Arpa M, Bedir R. Tumor Budding is a reliable predictor for death and metastasis in invasive ductal breast cancer and correlates with other prognostic clinicopathological parameters. Annals of diagnostic pathology. 2021;54:151792.
180. Li X, Wei B, Sonmez C, Li Z, Peng L. High tumor budding count is associated with adverse clinicopathologic features and poor prognosis in breast carcinoma. Human Pathology. 2017b;66:222-9.
181. Kumarguru B, Ramaswamy AS, Shaik S, Karri A, Srinivas VS, Prashant B. Tumor budding in invasive breast cancer-An indispensable budding touchstone. Indian Journal of Pathology and Microbiology. 2020;63(5):117.
182. Righi A, Sarotto I, Casorzo L, Cavalchini S, Frangipane E, Risio M. Tumour budding is associated with hypoxia at the advancing front of colorectal cancer. Histopathology. 2015;66(7):982-90.
183. Vaupel P. Hypoxia and aggressive tumor phenotype: implications for therapy and prognosis. The oncologist. 2008;13(S3):21-6.
184. Vaupel P, Mayer A. Hypoxia in cancer: significance and impact on clinical outcome. Cancer and Metastasis Reviews. 2007a;26(2):225-39.
185. Lundgren K, Holm C, Landberg G. Hypoxia and breast cancer: prognostic and therapeutic implications. Cell Mol Life Sci. 2007;64(24):3233-47.
186. Denny WA. The role of hypoxia-activated prodrugs in cancer therapy. The lancet oncology. 2000;1(1):25-9.
187. Vaupel P, Harrison L. Tumor hypoxia: causative factors, compensatory mechanisms, and cellular response. The oncologist. 2004;9(S5):4-9.
188. Semenza GL. Hypoxia-inducible factors in physiology and medicine. Cell. 2012a;148(3):399-408.
189. Weidemann A, Johnson R. Biology of HIF-1 α. Cell Death & Differentiation. 2008;15(4):621-7.
190. Wang GL, Jiang B-H, Rue EA, Semenza GL. Hypoxia-inducible factor 1 is a basic-helix-loop-helix-PAS heterodimer regulated by cellular O2 tension. Proceedings of the national academy of sciences. 1995;92(12):5510-4.
191. Kallio PJ, Okamoto K, O'Brien S, Carrero P, Makino Y, Tanaka H, et al. Signal transduction in hypoxic cells: inducible nuclear translocation and recruitment of theCBP/p300 coactivator by the hypoxia-induciblefactor-1α. The EMBO journal. 1998;17(22):6573-86.

192. Albadari N, Deng S, Li W. The transcriptional factors HIF-1 and HIF-2 and their novel inhibitors in cancer therapy. Expert opinion on drug discovery. 2019;14(7):667-82.
193. Semenza GL, Wang GL. A nuclear factor induced by hypoxia via de novo protein synthesis binds to the human erythropoietin gene enhancer at a site required for transcriptional activation. Molecular and cellular biology. 1992;12(12):5447-54.
194. Wigerup C, Påhlman S, Bexell D. Therapeutic targeting of hypoxia and hypoxia-inducible factors in cancer. Pharmacology & therapeutics. 2016;164:152-69.
195. Ema M, Taya S, Yokotani N, Sogawa K, Matsuda Y, Fujii-Kuriyama Y. A novel bHLH-PAS factor with close sequence similarity to hypoxia-inducible factor 1α regulates the VEGF expression and is potentially involved in lung and vascular development. Proceedings of the National Academy of Sciences. 1997;94(9):4273-8.
196. Hu C-J, Wang L-Y, Chodosh LA, Keith B, Simon MC. Differential roles of hypoxia-inducible factor 1α (HIF-1α) and HIF-2α in hypoxic gene regulation. Molecular and cellular biology. 2003;23(24):9361-74.
197. Vaupel P, Mayer A, Briest S, Höckel M. Hypoxia in Breast Cancer. Oxygen Transport to Tissue XXVI. 2005:333-42.
198. Loboda A, Jozkowicz A, Dulak J. HIF-1 and HIF-2 transcription factors—similar but not identical. Molecules and cells. 2010;29(5):435-42.
199. Keith B, Johnson RS, Simon MC. HIF1α and HIF2α: sibling rivalry in hypoxic tumour growth and progression. Nature Reviews Cancer. 2012;12(1):9-22.
200. Gu Y-Z, Moran SM, Hogenesch JB, Wartman L, Bradfield CA. Molecular characterization and chromosomal localization of a third α-class hypoxia inducible factor subunit, HIF3α. Gene Expression The Journal of Liver Research. 1998;7(3):205-13.
201. Makino C, Svensson K, Bertilsson G, Asman M, Tanaka H, Cao Y, Berkenstam A, Poellinger L. Inhibitory PAS domain protein is a negative regulator of hypoxia-inducible gene expression. 2001.
202. Semenza GL. Regulation of mammalian O2 homeostasis by hypoxia-inducible factor 1. Annual review of cell and developmental biology. 1999;15(1):551-78.
203. Hirose K, Morita M, Ema M, Mimura J, Hamada H, Fujii H, et al. cDNA cloning and tissue-specific expression of a novel basic helix-loop-helix/PAS factor (Arnt2) with close sequence similarity to the aryl hydrocarbon receptor nuclear translocator (Arnt). Molecular and cellular biology. 1996;16(4):1706-13.
204. Bedogni B, Powell MB. Hypoxia, melanocytes and melanoma–survival and tumor development in the permissive microenvironment of the skin. Pigment cell & melanoma research. 2009;22(2):166-74.
205. Dengler VL, Galbraith MD, Espinosa JM. Transcriptional regulation by hypoxia inducible factors. Critical reviews in biochemistry and molecular biology. 2014;49(1):1-15.
206. Masoud GN, Li W. HIF-1α pathway: role, regulation and intervention for cancer therapy. Acta Pharmaceutica Sinica B. 2015;5(5):378-89.
207. Shi Y, Chang M, Wang F, Ouyang X, Jia Y, Du H. Role and mechanism of hypoxia-inducible factor-1 in cell growth and apoptosis of breast cancer cell line MDA-MB-231. Oncology letters. 2010;1(4):657-62.
208. Saggar JK, Yu M, Tan Q, Tannock IF. The tumor microenvironment and strategies to improve drug distribution. Frontiers in oncology. 2013;3:154.
209. Denko NC, Fontana LA, Hudson KM, Sutphin PD, Raychaudhuri S, Altman R, et al. Investigating hypoxic tumor physiology through gene expression patterns. Oncogene. 2003;22(37):5907-14.
210. Chi J-T, Wang Z, Nuyten DSA, Rodriguez EH, Schaner ME, Salim A, et al. Gene expression programs in response to hypoxia: cell type specificity and prognostic significance in human cancers. PLoS medicine. 2006;3(3):e47.
211. Ye IC, Fertig EJ, DiGiacomo JW, Considine M, Godet I, Gilkes DM. Molecular portrait of hypoxia in breast cancer: a prognostic signature and novel HIF-regulated genes. Molecular Cancer Research. 2018;16(12):1889-901.

212. Liu Z-j, Semenza GL, Zhang H-f. Hypoxia-inducible factor 1 and breast cancer metastasis. Journal of Zhejiang University-SCIENCE B. 2015;16(1):32-43.
213. Robey IF, Lien AD, Welsh SJ, Baggett BK, Gillies RJ. Hypoxia-inducible factor-1α and the glycolytic phenotype in tumors. Neoplasia (New York, NY). 2005;7(4):324.
214. Selak MA, Armour SM, MacKenzie ED, Boulahbel H, Watson DG, Mansfield KD, et al. Succinate links TCA cycle dysfunction to oncogenesis by inhibiting HIF-α prolyl hydroxylase. Cancer cell. 2005;7(1):77-85.
215. Semenza GL. HIF-1: upstream and downstream of cancer metabolism. Current opinion in genetics & development. 2010;20(1):51-6.
216. Ippolito L, Morandi A, Giannoni E, Chiarugi P. Lactate: a metabolic driver in the tumour landscape. Trends in biochemical sciences. 2019;44(2):153-66.
217. Doe MR, Ascano JM, Kaur M, Cole MD. Myc posttranscriptionally induces HIF1 protein and target gene expression in normal and cancer cells. Cancer research. 2012;72(4):949-57.
218. Zhong H, Chiles K, Feldser D, Laughner E, Hanrahan C, Georgescu M-M, et al. Modulation of hypoxia-inducible factor 1α expression by the epidermal growth factor/phosphatidylinositol 3-kinase/PTEN/AKT/FRAP pathway in human prostate cancer cells: implications for tumor angiogenesis and therapeutics. Cancer research. 2000;60(6):1541-5.
219. Yuan G, Nanduri J, Khan S, Semenza GL, Prabhakar NR. Induction of HIF-1α expression by intermittent hypoxia: involvement of NADPH oxidase, Ca2+ signaling, prolyl hydroxylases, and mTOR. Journal of cellular physiology. 2008a;217(3):674-85.
220. Laughner E, Taghavi P, Chiles K, Mahon PC, Semenza GL. HER2 (neu) signaling increases the rate of hypoxia-inducible factor 1α (HIF-1α) synthesis: novel mechanism for HIF-1-mediated vascular endothelial growth factor expression. Molecular and cellular biology. 2001;21(12):3995-4004.
221. Benej M, Svastova E, Banova R, Kopacek J, Gibadulinova A, Kery M, et al. CA IX stabilizes intracellular pH to maintain metabolic reprogramming and proliferation in hypoxia. Frontiers in oncology. 2020;10:1462.
222. Potter C, Harris A. Diagnostic, prognostic and therapeutic implications of carbonic anhydrases in cancer. British journal of cancer. 2003;89(1):2-7.
223. Pastoreková S, Závadová Z, Košťál M, Babušíková O, Závada J. A novel quasi-viral agent, MaTu, is a two-component system. Virology. 1992;187(2):620-6.
224. Mboge MY, Mahon BP, McKenna R, Frost SC. Carbonic anhydrases: role in pH control and cancer. Metabolites. 2018a;8(1):19.
225. Saarnio J, Parkkila S, Parkkila A-K, Waheed A, Casey MC, Zhou XY, et al. Immunohistochemistry of carbonic anhydrase isozyme IX (MN/CA IX) in human gut reveals polarized expression in the epithelial cells with the highest proliferative capacity. Journal of Histochemistry & Cytochemistry. 1998;46(4):497-504.
226. Liao S-Y, Aurelio ON, Jan K, Zavada J, Stanbridge EJ. Identification of the MN/CA9 protein as a reliable diagnostic biomarker of clear cell carcinoma of the kidney. Cancer research. 1997;57(14):2827-31.
227. De Simone G, Supuran CT. Carbonic anhydrase IX: Biochemical and crystallographic characterization of a novel antitumor target. Biochimica et Biophysica Acta (BBA)-Proteins and Proteomics. 2010;1804(2):404-9.
228. Mahon BP, Pinard MA, McKenna R. Targeting carbonic anhydrase IX activity and expression. Molecules. 2015;20(2):2323-48.
229. Švastová E, Žilka N, Zat'ovičová M, Gibadulinová A, Čiampor F, Pastorek J, et al. Carbonic anhydrase IX reduces E-cadherin-mediated adhesion of MDCK cells via interaction with β-catenin. Experimental cell research. 2003;290(2):332-45.
230. Ditte P, Dequiedt F, Svastova E, Hulikova A, Ohradanova-Repic A, Zatovicova M, et al. Phosphorylation of carbonic anhydrase IX controls its ability to mediate extracellular acidification in hypoxic tumors. Cancer research. 2011;71(24):7558-67.

231. Swietach P, Wigfield S, Cobden P, Supuran CT, Harris AL, Vaughan-Jones RD. Tumor-associated carbonic anhydrase 9 spatially coordinates intracellular pH in three-dimensional multicellular growths. Journal of Biological Chemistry. 2008;283(29):20473-83.
232. Švastová E, Hulíková A, Rafajová M, Zat'ovičová M, Gibadulinová A, Casini A, et al. Hypoxia activates the capacity of tumor-associated carbonic anhydrase IX to acidify extracellular pH. FEBS letters. 2004;577(3):439-45.
233. Pastorekova S, Gillies RJ. The role of carbonic anhydrase IX in cancer development: Links to hypoxia, acidosis, and beyond. Cancer and Metastasis Reviews. 2019;38(1):65-77.
234. Sedlakova O, Svastova E, Takacova M, Kopacek J, Pastorek J, Pastorekova S. Carbonic anhydrase IX, a hypoxia-induced catalytic component of the pH regulating machinery in tumors. Frontiers in physiology. 2014;4:400.
235. Choi J, Jung W-H, Koo JS. Metabolism-related proteins are differentially expressed according to the molecular subtype of invasive breast cancer defined by surrogate immunohistochemistry. Pathobiology. 2013;80(1):41-52.
236. Chen C-L, Chu J-S, Su W-C, Huang S-C, Lee W-Y. Hypoxia and metabolic phenotypes during breast carcinogenesis: expression of HIF-1α, GLUT1, and CAIX. Virchows Archiv. 2010;457(1):53-61.
237. McDonald PC, Dedhar S. Carbonic Anhydrase IX (CAIX) as a Mediator of Hypoxia-Induced Stress Response in Cancer Cells. In: Frost SC, McKenna R, editors. Carbonic Anhydrase: Mechanism, Regulation, Links to Disease, and Industrial Applications. Dordrecht: Springer Netherlands; 2014. p. 255-69.
238. Conley SJ, Gheordunescu E, Kakarala P, Newman B, Korkaya H, Heath AN, et al. Antiangiogenic agents increase breast cancer stem cells via the generation of tumor hypoxia. Proceedings of the National Academy of Sciences. 2012;109(8):2784-9.
239. Talks KL, Turley H, Gatter KC, Maxwell PH, Pugh CW, Ratcliffe PJ, et al. The expression and distribution of the hypoxia-inducible factors HIF-1α and HIF-2α in normal human tissues, cancers, and tumor-associated macrophages. The American journal of pathology. 2000;157(2):411-21.
240. Yamamoto Y, Ibusuki M, Okumura Y, Kawasoe T, Kai K, Iyama K, et al. Hypoxia-inducible factor 1α is closely linked to an aggressive phenotype in breast cancer. Breast cancer research and treatment. 2008;110(3):465-75.
241. Dales JP, Garcia S, Meunier-Carpentier S, Andrac-Meyer L, Haddad O, Lavaut MN, et al. Overexpression of hypoxia-inducible factor HIF-1α predicts early relapse in breast cancer: Retrospective study in a series of 745 patients. International journal of cancer. 2005;116(5):734-9.
242. Schito L, Rey S, Konopleva M. Integration of hypoxic HIF-alpha signaling in blood cancers. Oncogene. 2017a;36(38):5331-40.
243. Schindl M, Schoppmann SF, Samonigg H, Hausmaninger H, Kwasny W, Gnant M, et al. Overexpression of hypoxia-inducible factor 1α is associated with an unfavorable prognosis in lymph node-positive breast cancer. Clinical Cancer Research. 2002;8(6):1831-7.
244. Bos R, Van der Groep P, Greijer AE, Shvarts A, Meijer S, Pinedo HM, et al. Levels of hypoxia-inducible factor-1α independently predict prognosis in patients with lymph node negative breast carcinoma. Cancer: Interdisciplinary International Journal of the American Cancer Society. 2003;97(6):1573-81.
245. Giatromanolaki A, Koukourakis MI, Simopoulos C, Polychronidis A, Gatter KC, Harris AL, et al. c-erbB-2 related aggressiveness in breast cancer is hypoxia inducible factor-1α dependent. Clinical cancer research. 2004;10(23):7972-7.
246. Generali D, Berruti A, Brizzi MP, Campo L, Bonardi S, Wigfield S, et al. Hypoxia-inducible factor-1α expression predicts a poor response to primary chemoendocrine

therapy and disease-free survival in primary human breast cancer. Clinical Cancer Research. 2006a;12(15):4562-8.
247. Kronblad Å, Jirström K, Rydén L, Nordenskjöld B, Landberg G. Hypoxia inducible factor-1α is a prognostic marker in premenopausal patients with intermediate to highly differentiated breast cancer but not a predictive marker for tamoxifen response. International journal of cancer. 2006;118(10):2609-16.
248. Trastour C, Benizri E, Ettore F, Ramaioli A, Chamorey E, Pouysségur J, et al. HIF-1α and CA IX staining in invasive breast carcinomas: prognosis and treatment outcome. International journal of cancer. 2007;120(7):1451-8.
249. Shamis SA, Quinn J, Mallon EE, Edwards J, McMillan DC. The Relationship Between the Tumor Cell Expression of Hypoxic Markers and Survival in Patients With ER-positive Invasive Ductal Breast Cancer. Journal of Histochemistry & Cytochemistry. 2022:00221554221110280.
250. Badowska-Kozakiewicz AM, Budzik MP. Triple-Negative Breast Cancer: Expression of Hypoxia-Inducible Factor 1α in Triple-Negative Breast Cancer with Metastasis to Lymph Nodes. Breast Cancer and Surgery. 2018.
251. Yan M, Rayoo M, Takano E, Thorne H, Fox S. BRCA1 tumours correlate with a HIF-1 α phenotype and have a poor prognosis through modulation of hydroxylase enzyme profile expression. British journal of cancer. 2009;101(7):1168-74.
252. Ali MJM, AL-Khafaji HAR, Hassoon AF. Immunohistochemical Expression of Hypoxia-Inducible Factor-1α in Triple Negative Breast Cancer. Medical Journal of Babylon. 2015;12(4):902-15.
253. Bharti SK, Mironchik Y, Wildes F, Penet M-F, Goggins E, Krishnamachary B, et al. Metabolic consequences of HIF silencing in a triple negative human breast cancer xenograft. Oncotarget. 2018;9(20):15326.
254. Network CGA. Comprehensive molecular portraits of human breast tumours. Nature. 2012;490(7418):61.
255. Semenza GL. The hypoxic tumor microenvironment: A driving force for breast cancer progression. Biochimica et Biophysica Acta (BBA)-Molecular Cell Research. 2016;1863(3):382-91.
256. Helczynska K, Larsson A-M, Mengelbier LH, Bridges E, Fredlund E, Borgquist S, et al. Hypoxia-inducible factor-2α correlates to distant recurrence and poor outcome in invasive breast cancer. Cancer research. 2008;68(22):9212-20.
257. Wykoff CC, Beasley NJ, Watson PH, Turner KJ, Pastorek J, Sibtain A, et al. Hypoxia-inducible expression of tumor-associated carbonic anhydrases. Cancer research. 2000;60(24):7075-83.
258. Generali D, Fox SB, Berruti A, Brizzi MP, Campo L, Bonardi S, et al. Role of carbonic anhydrase IX expression in prediction of the efficacy and outcome of primary epirubicin/tamoxifen therapy for breast cancer. Endocrine-related cancer. 2006b;13(3):921-30.
259. Hussain S, Ganesan R, Reynolds G, Gross L, Stevens A, Pastorek J, et al. Hypoxia-regulated carbonic anhydrase IX expression is associated with poor survival in patients with invasive breast cancer. British journal of cancer. 2007;96(1):104-9.
260. Span P, Bussink J, Manders P, Beex L, Sweep C. Carbonic anhydrase-9 expression levels and prognosis in human breast cancer: association with treatment outcome. British journal of cancer. 2003;89(2):271-6.
261. Ward C, Meehan J, Mullen P, Supuran C, Dixon JM, Thomas JS, et al. Evaluation of carbonic anhydrase IX as a therapeutic target for inhibition of breast cancer invasion and metastasis using a series of in vitro breast cancer models. Oncotarget. 2015;6(28):24856.
262. Brennan DJ, Jirstrom K, Kronblad Å, Millikan RC, Landberg G, Duffy MJ, et al. CA IX is an independent prognostic marker in premenopausal breast cancer patients with one to three positive lymph nodes and a putative marker of radiation resistance. Clinical cancer research. 2006;12(21):6421-31.

263. Chia SK, Wykoff CC, Watson PH, Han C, Leek RD, Pastorek J, et al. Prognostic significance of a novel hypoxia-regulated marker, carbonic anhydrase IX, in invasive breast carcinoma. Journal of Clinical Oncology. 2001;19(16):3660-8.
264. Tan EY, Yan M, Campo L, Han C, Takano E, Turley H, et al. The key hypoxia regulated gene CAIX is upregulated in basal-like breast tumours and is associated with resistance to chemotherapy. British journal of cancer. 2009;100(2):405-11.
265. Jin M-S, Lee H, Park IA, Chung YR, Im S-A, Lee K-H, et al. Overexpression of HIF1α and CAXI predicts poor outcome in early-stage triple negative breast cancer. Virchows Archiv. 2016;469(2):183-90.
266. Jing Y, Han Z, Zhang S, Liu Y, Wei L. Epithelial-Mesenchymal Transition in tumor microenvironment. Cell & bioscience. 2011;1(1):1-7.
267. Moreno-Bueno G, Portillo F, Cano A. Transcriptional regulation of cell polarity in EMT and cancer. Oncogene. 2008;27(55):6958-69.
268. Wong CC-L, Gilkes DM, Zhang H, Chen J, Wei H, Chaturvedi P, et al. Hypoxia-inducible factor 1 is a master regulator of breast cancer metastatic niche formation. Proceedings of the National Academy of Sciences. 2011;108(39):16369-74.
269. Saatci O, Kaymak A, Raza U, Ersan PG, Akbulut O, Banister CE, et al. Targeting lysyl oxidase (LOX) overcomes chemotherapy resistance in triple negative breast cancer. Nature communications. 2020;11(1):1-17.
270. Gatenby RA, Gillies RJ. Why do cancers have high aerobic glycolysis? Nature reviews cancer. 2004;4(11):891-9.
271. Warburg OH. Uber den stoffwechsel der tumoren. 1926.
272. Semenza GL, Artemov D, Bedi A, Bhujwalla Z, Chiles K, Feldser D, et al., editors. The metabolism of tumours': 70 years later. Novartis Foundation Symposium; 2001: Wiley Online Library.
273. Vaupel P. Metabolic microenvironment of tumor cells: a key factor in malignant progression. Exp Oncol. 2010;32(3):125-7.
274. Zheng J. Energy metabolism of cancer: Glycolysis versus oxidative phosphorylation. Oncology letters. 2012;4(6):1151-7.
275. Tateishi U, Yamaguchi U, Seki K, Terauchi T, Arai Y, Hasegawa T. Glut-1 expression and enhanced glucose metabolism are associated with tumour grade in bone and soft tissue sarcomas: a prospective evaluation by [18 F] fluorodeoxyglucose positron emission tomography. European journal of nuclear medicine and molecular imaging. 2006;33(6):683.
276. Pelicano H, Zhang W, Liu J, Hammoudi N, Dai J, Xu R-H, et al. Mitochondrial dysfunction in some triple-negative breast cancer cell lines: role of mTOR pathway and therapeutic potential. Breast cancer research. 2014;16(5):434.
277. Diers AR, Vayalil PK, Oliva CR, Griguer CE, Darley-Usmar V, Hurst DR, et al. Mitochondrial bioenergetics of metastatic breast cancer cells in response to dynamic changes in oxygen tension: effects of HIF-1α. PloS one. 2013;8(6):e68348.
278. Maxwell PH, Pugh CW, Ratcliffe PJ. Activation of the HIF pathway in cancer. Current opinion in genetics & development. 2001;11(3):293-9.
279. Maxwell P, Dachs G, Gleadle J, Nicholls L, Harris A, Stratford I, et al. Hypoxia-inducible factor-1 modulates gene expression in solid tumors and influences both angiogenesis and tumor growth. Proceedings of the National Academy of Sciences. 1997;94(15):8104-9.
280. Semenza GL, editor Regulation of cancer cell metabolism by hypoxia-inducible factor 1. Seminars in cancer biology; 2009: Elsevier.
281. Swietach á, Hulikova A, Vaughan-Jones R, Harris A. New insights into the physiological role of carbonic anhydrase IX in tumour pH regulation. Oncogene. 2010;29(50):6509-21.

282. Gilreath C, Boerma M, Qin Z, Hudson MK, Wang S. The hypoxic microenvironment of breast cancer cells promotes resistance in radiation therapy. Frontiers in Oncology. 2021;10:629422.
283. Jawhar NM. Tissue microarray: a rapidly evolving diagnostic and research tool. Annals of Saudi medicine. 2009;29(2):123-7.
284. Muñoz-Sánchez J, Chánez-Cárdenas ME. The use of cobalt chloride as a chemical hypoxia model. Journal of Applied Toxicology. 2019;39(4):556-70.
285. Lan A-P, Xiao L-C, Yang Z-L, Yang C-T, Wang X-Y, Chen P-X, et al. Interaction between ROS and p38MAPK contributes to chemical hypoxia-induced injuries in PC12 cells. Molecular Medicine Reports. 2012;5(1):250-5.
286. Li F, Huang L, Su X-L, Gu Q-H, Hu C-P. Inhibition of nuclear factor-κB activity enhanced chemosensitivity to cisplatin in human lung adeno-carcinoma A549 cells under chemical hypoxia conditions. Chinese medical journal. 2013b;126(17):3276-82.
287. Kirkegaard T, Edwards J, Tovey S, McGlynn L, Krishna S, Mukherjee R, et al. Observer variation in immunohistochemical analysis of protein expression, time for a change? Histopathology. 2006;48(7):787-94.
288. Wu L, Yi B, Wei S, Rao D, He Y, Naik G, et al. Loss of FOXP3 and TSC1 accelerates prostate cancer progression through synergistic transcriptional and posttranslational regulation of c-MYC. Cancer research. 2019;79(7):1413-25.
289. Bankhead P, Loughrey MB, Fernández JA, Dombrowski Y, McArt DG, Dunne PD, et al. QuPath: Open source software for digital pathology image analysis. Scientific reports. 2017;7(1):1-7.
290. Davis BW, Gelber R, Goldhirsch A, Hartmann WH, Hollaway L, Russell I, et al. Prognostic significance of peritumoral vessel invasion in clinical trials of adjuvant therapy for breast cancer with axillary lymph node metastasis. Human pathology. 1985;16(12):1212-8.
291. Koo TK, Li MY. A guideline of selecting and reporting intraclass correlation coefficients for reliability research. Journal of chiropractic medicine. 2016;15(2):155-63.
292. Yeakley JM, Shepard PJ, Goyena DE, VanSteenhouse HC, McComb JD, Seligmann BE. A trichostatin A expression signature identified by TempO-Seq targeted whole transcriptome profiling. PloS one. 2017;12(5):e0178302.
293. Dobin A, Davis CA, Schlesinger F, Drenkow J, Zaleski C, Jha S, et al. STAR: ultrafast universal RNA-seq aligner. Bioinformatics. 2013;29(1):15-21.
294. Love MI, Huber W, Anders S. Moderated estimation of fold change and dispersion for RNA-seq data with DESeq2. Genome biology. 2014;15(12):1-21.
295. Szklarczyk D, Gable AL, Nastou KC, Lyon D, Kirsch R, Pyysalo S, et al. The STRING database in 2021: customizable protein–protein networks, and functional characterization of user-uploaded gene/measurement sets. Nucleic acids research. 2021;49(D1):D605-D12.
296. Mering Cv, Huynen M, Jaeggi D, Schmidt S, Bork P, Snel B. STRING: a database of predicted functional associations between proteins. Nucleic acids research. 2003;31(1):258-61.
297. Li X, Wang C-Y. From bulk, single-cell to spatial RNA sequencing. International Journal of Oral Science. 2021a;13(1):36.
298. Erpolat O, Gocun P, Akmansu M, Ozgun G, Akyol G. Hypoxia-related molecules HIF-1α, CA9, and osteopontin. Strahlentherapie und Onkologie. 2013;189(2):147-54.
299. Lee G-W, Go SI, Cho YJ, Jeong YY, Kim H-C, Lee JD, et al. Hypoxia-inducible factor-1α and excision repair cross-complementing 1 in patients with small cell lung cancer who received front-line platinum-based chemotherapy: a retrospective study. Journal of Thoracic Oncology. 2012;7(3):528-34.
300. Gruber G, Greiner RH, Hlushchuk R, Aebersold DM, Altermatt HJ, Berclaz G, et al. Hypoxia-inducible factor 1 alpha in high-risk breast cancer: an independent prognostic parameter? Breast Cancer Research. 2004;6(3):R191.

301. Huang C-J, Lian S-L, Hou M-F, Chai C-Y, Yang Y-H, Lin S-F, et al. SNP 1772 C> T of HIF-1α gene associates with breast cancer risk in a Taiwanese population. Cancer cell international. 2014;14(1):1-7.
302. Kaluz S, Kaluzová M, Liao S-Y, Lerman M, Stanbridge EJ. Transcriptional control of the tumor-and hypoxia-marker carbonic anhydrase 9: A one transcription factor (HIF-1) show? Biochimica et Biophysica Acta (BBA)-Reviews on Cancer. 2009;1795(2):162-72.
303. Tafreshi NK, Tafreshi NK, Lloyd MC, Lloyd MC, Proemsey JB, Proemsey JB, et al. Evaluation of CAIX and CAXII Expression in Breast Cancer at Varied O2 Levels: CAIX is the Superior Surrogate Imaging Biomarker of Tumor Hypoxia. Molecular imaging and biology. 2016;18(2):219-31.
304. Li Y, Wang H, Oosterwijk E, Tu C, Shiverick KT, Silverman DN, et al. Expression and activity of carbonic anhydrase IX is associated with metabolic dysfunction in MDA-MB-231 breast cancer cells. Cancer investigation. 2009;27(6):613-23.
305. Pastorek J, Pastorekova S, editors. Hypoxia-induced carbonic anhydrase IX as a target for cancer therapy: from biology to clinical use. Seminars in cancer biology; 2015: Elsevier.
306. Pinheiro C, Sousa B, Albergaria A, Paredes J, Dufloth R, Vieira D, et al. GLUT1 and CAIX expression profiles in breast cancer correlate with adverse prognostic factors and MCT1 overexpression. 2011.
307. Tomes L, Emberley E, Niu Y, Troup S, Pastorek J, Strange K, et al. Necrosis and Hypoxia in Invasive Breast Carcinoma. Breast cancer research and treatment. 2003;81(1):61-9.
308. Lou Y, McDonald PC, Oloumi A, Chia S, Ostlund C, Ahmadi A, et al. Targeting tumor hypoxia: suppression of breast tumor growth and metastasis by novel carbonic anhydrase IX inhibitors. Cancer research. 2011;71(9):3364-76.
309. Neumeister VM, Sullivan CA, Lindner R, Lezon-Geyda K, Li J, Zavada J, et al. Hypoxia-induced protein CAIX is associated with somatic loss of BRCA1 protein and pathway activity in triple negative breast cancer. Breast cancer research and treatment. 2012;136(1):67-75.
310. Beketic-Oreskovic L, Ozretic P, Rabbani ZN, Jackson IL, Sarcevic B, Levanat S, et al. Prognostic significance of carbonic anhydrase IX (CA-IX), endoglin (CD105) and 8-hydroxy-2′-deoxyguanosine (8-OHdG) in breast cancer patients. Pathology & Oncology Research. 2011;17(3):593-603.
311. Ozretic P, Alvir I, Sarcevic B, Vujaskovic Z, Rendic-Miocevic Z, Roguljic A, et al. Apoptosis regulator Bcl-2 is an independent prognostic marker for worse overall survival in triple-negative breast cancer patients. The International journal of biological markers. 2018;33(1):109-15.
312. Alves WEFM, Bonatelli M, Dufloth R, Kerr LM, Carrara GFA, da Costa RFA, et al. CAIX is a predictor of pathological complete response and is associated with higher survival in locally advanced breast cancer submitted to neoadjuvant chemotherapy. BMC cancer. 2019;19(1):1173.
313. Zhao Z, Liao G, Li Y, Zhou S, Zou H, Fernando S. Prognostic value of carbonic anhydrase IX immunohistochemical expression in renal cell carcinoma: a meta-analysis of the literature. PloS one. 2014;9(11):e114096-e.
314. Peridis S, Pilgrim G, Athanasopoulos I, Parpounas K. Carbonic anhydrase-9 expression in head and neck cancer: a meta-analysis. European archives of oto-rhino-laryngology. 2011;268(5):661-70.
315. Tierney JF, Stewart LA, Ghersi D, Burdett S, Sydes MR. Practical methods for incorporating summary time-to-event data into meta-analysis. Trials. 2007;8(1):16.
316. Higgins JP, Thompson SG, Deeks JJ, Altman DG. Measuring inconsistency in meta-analyses. Bmj. 2003;327(7414):557-60.

317. Nie C, Lv H, Bie L, Hou H, Chen X. Hypoxia-inducible factor 1-alpha expression correlates with response to neoadjuvant chemotherapy in women with breast cancer. Medicine. 2018;97(51).
318. Cui J, Jiang H. Prediction of postoperative survival of triple-negative breast cancer based on nomogram model combined with expression of HIF-1α and c-myc. Medicine. 2019;98(40).
319. Shi L, Zhao C, Pu H, Zhang Q. FBP1 expression is associated with basal-like breast carcinoma. Oncology Letters. 2017;13(5):3046-56.
320. Dong M, Wan X-b, Yuan ZY, Wei L, Fan XJ, Wang T-t, et al. Low expression of Beclin 1 and elevated expression of HIF-1α refine distant metastasis risk and predict poor prognosis of ER-positive, HER2-negative breast cancer. Medical oncology. 2013;30(1):355.
321. Marton I, Knežević F, Ramić S, Milošević M, Tomas D. Immunohistochemical expression and prognostic significance of HIF-1α and VEGF-C in neuroendocrine breast cancer. Anticancer research. 2012;32(12):5227-32.
322. Peurala E, Koivunen P, Bloigu R, Haapasaari K-M, Jukkola-Vuorinen A. Expressions of individual PHDs associate with good prognostic factors and increased proliferation in breast cancer patients. Breast cancer research and treatment. 2012;133(1):179-88.
323. Koo JS, Jung W. Alteration of REDD1-mediated mammalian target of rapamycin pathway and hypoxia-inducible factor-1α regulation in human breast cancer. Pathobiology. 2010;77(6):289-300.
324. Chen HH, Su W-C, Lin P-W, Guo H-R, Lee W-Y. Hypoxia-inducible factor-1α correlates with MET and metastasis in node-negative breast cancer. Breast cancer research and treatment. 2007;103(2):167-75.
325. Tan EY, Campo L, Han C, Turley H, Pezzella F, Gatter KC, et al. BNIP3 as a progression marker in primary human breast cancer; opposing functions in in situ versus invasive cancer. Clinical Cancer Research. 2007;13(2):467-74.
326. Schoppmann SF, Fenzl A, Schindl M, Bachleitner-Hofmann T, Nagy K, Gnant M, et al. Hypoxia inducible factor-1α correlates with VEGF-C expression and lymphangiogenesis in breast cancer. Breast cancer research and treatment. 2006;99(2):135-41.
327. Vleugel M, Greijer A, Shvarts A, Van Der Groep P, Van Berkel M, Aarbodem Y, et al. Differential prognostic impact of hypoxia induced and diffuse HIF-1α expression in invasive breast cancer. Journal of clinical pathology. 2005;58(2):172-7.
328. Jögi A, Ehinger A, Hartman L, Alkner S. Expression of HIF-1α is related to a poor prognosis and tamoxifen resistance in contralateral breast cancer. Plos one. 2019;14(12):e0226150.
329. Li M, Xiao D, Zhang J, Qu H, Yang Y, Yan Y, et al. Expression of LPA2 is associated with poor prognosis in human breast cancer and regulates HIF-1α expression and breast cancer cell growth. Oncology Reports. 2016c;36(6):3479-87.
330. Laurinavicius A, Green AR, Laurinaviciene A, Smailyte G, Ostapenko V, Meskauskas R, et al. Ki67/SATB1 ratio is an independent prognostic factor of overall survival in patients with early hormone receptor-positive invasive ductal breast carcinoma. Oncotarget. 2015;6(38):41134.
331. Rajkovic-Molek K, Mustac E, Hadžisejdic I, Jonjic N. The prognostic importance of nuclear factor κB and hypoxia-inducible factor 1α in relation to the breast cancer subtype and the overall survival. Applied Immunohistochemistry & Molecular Morphology. 2014;22(6):464-70.
332. Ni X, Zhao Y, Ma J, Xia T, Liu X, Ding Q, et al. Hypoxia-induced factor-1 alpha upregulates vascular endothelial growth factor C to promote lymphangiogenesis and angiogenesis in breast cancer patients. Journal of Biomedical Research. 2013;27(6):478.

333. Malfettone A, Saponaro C, Paradiso A, Simone G, Mangia A. Peritumoral vascular invasion and NHERF1 expression define an immunophenotype of grade 2 invasive breast cancer associated with poor prognosis. BMC cancer. 2012;12(1):106.
334. Lancashire LJ, Powe D, Reis-Filho J, Rakha E, Lemetre C, Weigelt B, et al. A validated gene expression profile for detecting clinical outcome in breast cancer using artificial neural networks. Breast cancer research and treatment. 2010;120(1):83-93.
335. Crabb SJ, Bajdik CD, Leung S, Speers CH, Kennecke H, Huntsman DG, et al. Can clinically relevant prognostic subsets of breast cancer patients with four or more involved axillary lymph nodes be identified through immunohistochemical biomarkers? A tissue microarray feasibility study. Breast cancer research. 2008;10(1):R6.
336. Aomatsu N, Yashiro M, Kashiwagi S, Kawajiri H, Takashima T, Ohsawa M, et al. Carbonic anhydrase 9 is associated with chemosensitivity and prognosis in breast cancer patients treated with taxane and anthracycline. BMC cancer. 2014;14(1):400.
337. Noh S, Kim J-Y, Koo JS. Metabolic differences in estrogen receptor-negative breast cancer based on androgen receptor status. Tumor Biology. 2014;35(8):8179-92.
338. Currie MJ, Beardsley BE, Harris GC, Gunningham SP, Dachs GU, Dijkstra B, et al. Immunohistochemical analysis of cancer stem cell markers in invasive breast carcinoma and associated ductal carcinoma in situ: relationships with markers of tumor hypoxia and microvascularity. Human pathology. 2013;44(3):402-11.
339. Betof A, Rabbani Z, Hardee M, Kim S, Broadwater G, Bentley R, et al. Carbonic anhydrase IX is a predictive marker of doxorubicin resistance in early-stage breast cancer independent of HER2 and TOP2A amplification. British journal of cancer. 2012;106(5):916-22.
340. Kaya A, Gunel N, Benekli M, Akyurek N, Buyukberber S, Tatli H, et al. Hypoxia inducible factor-1 alpha and carbonic anhydrase IX overexpression are associated with poor survival in breast cancer patients. J buon. 2012;17(4):663-8.
341. Jubb AM, Soilleux EJ, Turley H, Steers G, Parker A, Low I, et al. Expression of vascular notch ligand delta-like 4 and inflammatory markers in breast cancer. The American journal of pathology. 2010;176(4):2019-28.
342. Kyndi M, Sørensen FB, Knudsen H, Alsner J, Overgaard M, Nielsen HM, et al. Carbonic anhydrase IX and response to postmastectomy radiotherapy in high-risk breast cancer: a subgroup analysis of the DBCG82 b and c trials. Breast Cancer Research. 2008;10(2):R24.
343. Wang W, He Y-F, Sun Q-K, Wang Y, Han X-H, Peng D-F, et al. Hypoxia-inducible factor 1α in breast cancer prognosis. Clinica chimica acta. 2014a;428:32-7.
344. Kalemkerian GP, Narula N, Kennedy EB, Biermann WA, Donington J, Leighl NB, et al. Molecular testing guideline for the selection of patients with lung cancer for treatment with targeted tyrosine kinase inhibitors: American society of clinical oncology endorsement of the college of american pathologists/international association for the study of lung cancer/association for molecular pathology clinical practice guideline update. Journal of clinical oncology: official journal of the American Society of Clinical Oncology. 2018;36(9):911.
345. Semenza GL. Targeting HIF-1 for cancer therapy. Nature reviews cancer. 2003;3(10):721-32.
346. Nalwoga H, Ahmed L, Arnes JB, Wabinga H, Akslen LA. Strong expression of hypoxia-inducible factor-1α (HIF-1α) is associated with Axl expression and features of aggressive tumors in african breast cancer. PLoS One. 2016;11(1):e0146823.
347. Cai F-F, Xu C, Pan X, Cai L, Lin X-Y, Chen S, et al. Prognostic value of plasma levels of HIF-1a and PGC-1a in breast cancer. Oncotarget. 2016;7(47):77793.
348. Peng J, Wang X, Ran L, Song J, Luo R, Wang Y. Hypoxia-inducible factor 1α regulates the transforming growth factor β1/SMAD family member 3 pathway to promote breast cancer progression. Journal of breast cancer. 2018;21(3):259-66.

349. Vaupel P, Höckel M, Mayer A. Detection and characterization of tumor hypoxia using pO2 histography. Antioxidants & redox signaling. 2007b;9(8):1221-36.
350. Lock F, McDonald P, Lou Y, Serrano I, Chafe S, Ostlund C, et al. Targeting carbonic anhydrase IX depletes breast cancer stem cells within the hypoxic niche. Oncogene. 2013;32(44):5210-9.
351. Proescholdt MA, Merrill MJ, Stoerr E-M, Lohmeier A, Pohl F, Brawanski A. Function of carbonic anhydrase IX in glioblastoma multiforme. Neuro-oncology. 2012;14(11):1357-66.
352. Gieling WK. Carbonic anhydrase IX as a target for metastatic disease. 2013.
353. Wykoff CC, Beasley N, Watson PH, Campo L, Chia SK, English R, et al. Expression of the hypoxia-inducible and tumor-associated carbonic anhydrases in ductal carcinoma in situ of the breast. The American journal of pathology. 2001;158(3):1011-9.
354. Dittrich C, Zandvliet A, Gneist M, Huitema A, King A, Wanders J. A phase I and pharmacokinetic study of indisulam in combination with carboplatin. British journal of cancer. 2007;96(4):559-66.
355. Pastorekova S, Ratcliffe PJ, Pastorek J. Molecular mechanisms of carbonic anhydrase IX-mediated pH regulation under hypoxia. BJU international. 2008;101:8-15.
356. Buller F, Steiner M, Frey K, Mircsof D, Scheuermann Jr, Kalisch M, et al. Selection of carbonic anhydrase IX inhibitors from one million DNA-encoded compounds. ACS chemical biology. 2011;6(4):336-44.
357. Shamis SA, McMillan DC, Edwards J. The relationship between hypoxia-inducible factor 1α (HIF-1α) and patient survival in breast cancer: systematic review and meta-analysis. Critical reviews in oncology/hematology. 2021:103231.
358. Hoffmann C, Mao X, Brown-Clay J, Moreau F, Al Absi A, Wurzer H, et al. Hypoxia promotes breast cancer cell invasion through HIF-1α-mediated up-regulation of the invadopodial actin bundling protein CSRP2. Scientific reports. 2018;8(1):10191.
359. Kim Y-J, Zhao Y, Myung JK, Yi JM, Kim M-J, Lee S-J. Suppression of breast cancer progression by FBXL16 via oxygen-independent regulation of HIF1α stability. Cell Reports. 2021;37(8).
360. Galbán S, Gorospe M. Factors interacting with HIF-1α mRNA: novel therapeutic targets. Current pharmaceutical design. 2009;15(33):3853-60.
361. Kim BW, Cho H, Chung J-Y, Conway C, Ylaya K, Kim J-H, et al. Prognostic assessment of hypoxia and metabolic markers in cervical cancer using automated digital image analysis of immunohistochemistry. Journal of translational medicine. 2013;11(1):1-11.
362. Vordermark D. Hypoxia-specific targets in cancer therapy: role of splice variants. BMC medicine. 2010;8(1):45.
363. Luo W, Wang Y. Epigenetic regulators: multifunctional proteins modulating hypoxia-inducible factor-α protein stability and activity. Cellular and Molecular Life Sciences. 2018;75(6):1043-56.
364. Chun Y-S, Choi E, Kim T-Y, Kim M-S, Park J-W. A dominant-negative isoform lacking exons 11 and 12 of the human hypoxia-inducible factor-1α gene. Biochemical Journal. 2002;362(1):71-9.
365. Harrison H, Rogerson L, Gregson HJ, Brennan KR, Clarke RB, Landberg G. Contrasting hypoxic effects on breast cancer stem cell hierarchy is dependent on ER-α status. Cancer Research. 2013;73(4):1420-33.
366. Chu C-Y, Jin Y-T, Zhang W, Yu J, Yang H-P, Wang H-Y, et al. CA IX is upregulated in CoCl2-induced hypoxia and associated with cell invasive potential and a poor prognosis of breast cancer. International journal of oncology. 2016;48(1):271-80.
367. Altman DG, Lausen B, Sauerbrei W, Schumacher M. Dangers of using "optimal" cutpoints in the evaluation of prognostic factors. JNCI: Journal of the National Cancer Institute. 1994;86(11):829-35.

368. Ray P, Manach YL, Riou B, Houle TT, Warner DS. Statistical evaluation of a biomarker. The Journal of the American Society of Anesthesiologists. 2010;112(4):1023-40.
369. Bao B, Azmi AS, Ali S, Ahmad A, Li Y, Banerjee S, et al. The biological kinship of hypoxia with CSC and EMT and their relationship with deregulated expression of miRNAs and tumor aggressiveness. Biochimica et Biophysica Acta (BBA)-Reviews on Cancer. 2012;1826(2):272-96.
370. Wolff M, Kosyna FK, Dunst J, Jelkmann W, Depping R. Impact of hypoxia inducible factors on estrogen receptor expression in breast cancer cells. Archives of biochemistry and biophysics. 2017;613:23-30.
371. Semenza GL. Life with oxygen. Science. 2007;318(5847):62-4.
372. Supuran CT. Carbonic anhydrases: novel therapeutic applications for inhibitors and activators. Nature reviews Drug discovery. 2008;7(2):168-81.
373. Dales J-P, Beaufils N, Silvy M, Picard C, Pauly V, Pradel V, et al. Hypoxia inducible factor 1α gene (HIF-1α) splice variants: potential prognostic biomarkers in breast cancer. BMC medicine. 2010;8(1):44.
374. Kong D, Park EJ, Stephen AG, Calvani M, Cardellina JH, Monks A, et al. Echinomycin, a small-molecule inhibitor of hypoxia-inducible factor-1 DNA-binding activity. Cancer research. 2005;65(19):9047-55.
375. Wang H, Qin C, Han F, Wang X, Li N. HIF-2alpha as a prognostic marker for breast cancer progression and patient survival. Genet Mol Res. 2014b;13(2):2817-26.
376. Stock C, Schwab A. Protons make tumor cells move like clockwork. Pflügers Archiv-European Journal of Physiology. 2009;458(5):981-92.
377. Parks SK, Chiche J, Pouyssegur J. pH control mechanisms of tumor survival and growth. Journal of cellular physiology. 2011;226(2):299-308.
378. Chen Z, Ai L, Mboge MY, Tu C, McKenna R, Brown KD, et al. Differential expression and function of CAIX and CAXII in breast cancer: A comparison between tumorgraft models and cells. PLoS One. 2018;13(7):e0199476.
379. Mboge MY, Chen Z, Wolff A, Mathias JV, Tu C, Brown KD, et al. Selective inhibition of carbonic anhydrase IX over carbonic anhydrase XII in breast cancer cells using benzene sulfonamides: Disconnect between activity and growth inhibition. PLoS One. 2018b;13(11):e0207417.
380. Shamis SA, Edwards J, McMillan DC. The relationship between carbonic anhydrase IX (CAIX) and patient survival in breast cancer: systematic review and meta-analysis. Diagnostic Pathology. 2023;18(1):1-16.
381. Giatromanolaki A, Sivridis E, Fiska A, Koukourakis MI. Hypoxia-inducible factor-2α (HIF-2α) induces angiogenesis in breast carcinomas. Applied Immunohistochemistry & Molecular Morphology. 2006;14(1):78-82.
382. Urruticoechea A, Smith IE, Dowsett M. Proliferation marker Ki-67 in early breast cancer. Journal of clinical oncology. 2005;23(28):7212-20.
383. Brahimi-Horn MC, Chiche J, Pouysségur J. Hypoxia and cancer. Journal of molecular medicine. 2007;85(12):1301-7.
384. Kurebayashi J, Otsuki T, Moriya T, Sonoo H. Hypoxia reduces hormone responsiveness of human breast cancer cells. Japanese journal of cancer research. 2001;92(10):1093-101.
385. Ivanova L, Zandberga E, Siliņa K, Kalniņa Z, Ābols A, Endzeliņš E, et al. Prognostic relevance of carbonic anhydrase IX expression is distinct in various subtypes of breast cancer and its silencing suppresses self-renewal capacity of breast cancer cells. Cancer chemotherapy and pharmacology. 2015;75(2):235-46.
386. Sobhanifar S, Aquino-Parsons C, Stanbridge EJ, Olive P. Reduced expression of hypoxia-inducible factor-1α in perinecrotic regions of solid tumors. Cancer research. 2005;65(16):7259-66.

387. Kuijper A, van der Groep P, van der Wall E, van Diest PJ. Expression of hypoxia-inducible factor 1 alpha and its downstream targets in fibroepithelial tumors of the breast. Breast cancer research. 2005;7(5):1-11.
388. Ravi R, Mookerjee B, Bhujwalla ZM, Sutter CH, Artemov D, Zeng Q, et al. Regulation of tumor angiogenesis by p53-induced degradation of hypoxia-inducible factor 1α. Genes & development. 2000;14(1):34-44.
389. Maxwell PH, Wiesener MS, Chang G-W, Clifford SC, Vaux EC, Cockman ME, et al. The tumour suppressor protein VHL targets hypoxia-inducible factors for oxygen-dependent proteolysis. Nature. 1999;399(6733):271-5.
390. Vleugel MM, Shvarts D, van der Wall E, van Diest PJ. p300 and p53 levels determine activation of HIF-1 downstream targets in invasive breast cancer. Human pathology. 2006;37(8):1085-92.
391. Rafajová M, Zatovicová M, Kettmann R, Pastorek J, Pastoreková S. Induction by hypoxia combined with low glucose or low bicarbonate and high posttranslational stability upon reoxygenation contribute to carbonic anhydrase IX expression in cancer cells. International journal of oncology. 2004;24(4):995-1004.
392. Kaluz S, Kaluzová M, Chrastina A, Olive PL, Pastoreková S, Pastorek J, et al. Lowered oxygen tension induces expression of the hypoxia marker MN/carbonic anhydrase IX in the absence of hypoxia-inducible factor 1α stabilization: a role for phosphatidylinositol 3′-kinase. Cancer research. 2002;62(15):4469-77.
393. Kopacek J, Barathova M, Dequiedt F, Sepelakova J, Kettmann R, Pastorek J, et al. MAPK pathway contributes to density-and hypoxia-induced expression of the tumor-associated carbonic anhydrase IX. Biochimica et Biophysica Acta (BBA)-Gene Structure and Expression. 2005;1729(1):41-9.
394. Nakamura J, Kitajima Y, Kai K, Hashiguchi K, Hiraki M, Noshiro H, et al. Expression of hypoxic marker CA IX is regulated by site-specific DNA methylation and is associated with the histology of gastric cancer. The American journal of pathology. 2011;178(2):515-24.
395. Zhang X, Lin Y, Gillies RJ. Tumor pH and its measurement. Journal of Nuclear Medicine. 2010;51(8):1167-70.
396. Webb BA, Chimenti M, Jacobson MP, Barber DL. Dysregulated pH: a perfect storm for cancer progression. Nature Reviews Cancer. 2011;11(9):671-7.
397. Estrella CT, Lloyd M, Wojtkowiak J, Cornnell HH, Ibrahim-Hashim A, Bailey K, Balagurunathan Y, Rothberg JM, Sloane BF, Johnson Acidity Generated by the Tumor Microenvironment Drives Local Invasion. 2013.
398. Supuran CT, Winum J-Y. Designing carbonic anhydrase inhibitors for the treatment of breast cancer. Expert opinion on drug discovery. 2015;10(6):591-7.
399. Ditte Z, Ditte P, Labudova M, Simko V, Iuliano F, Zatovicova M, et al. Carnosine inhibits carbonic anhydrase IX-mediated extracellular acidosis and suppresses growth of HeLa tumor xenografts. BMC cancer. 2014;14(1):1-13.
400. Castoria G, Migliaccio A, Giovannelli P, Auricchio F. Cell proliferation regulated by estradiol receptor: Therapeutic implications. Steroids. 2010;75(8-9):524-7.
401. Lumachi F, Luisetto G, MM Basso S, Basso U, Brunello A, Camozzi V. Endocrine therapy of breast cancer. Current medicinal chemistry. 2011;18(4):513-22.
402. Sainsbury R. The development of endocrine therapy for women with breast cancer. Cancer treatment reviews. 2013;39(5):507-17.
403. Liu C-Y, Wu C-Y, Petrossian K, Huang T-T, Tseng L-M, Chen S. Treatment for the endocrine resistant breast cancer: current options and future perspectives. The Journal of Steroid Biochemistry and Molecular Biology. 2017;172:166-75.
404. Wang M, Zhao J, Zhang L, Wei F, Lian Y, Wu Y, et al. Role of tumor microenvironment in tumorigenesis. Journal of Cancer. 2017b;8(5):761.
405. Gilkes DM, Semenza GL, Wirtz D. Hypoxia and the extracellular matrix: drivers of tumour metastasis. Nature Reviews Cancer. 2014;14(6):430-9.

406. Muz B, de la Puente P, Azab F, Azab AK. The role of hypoxia in cancer progression, angiogenesis, metastasis, and resistance to therapy. Hypoxia. 2015;3:83.
407. Jia X, Hong Q, Lei L, Li D, Li J, Mo M, et al. Basal and therapy-driven hypoxia-inducible factor-1α confers resistance to endocrine therapy in estrogen receptor-positive breast cancer. Oncotarget. 2015;6(11):8648.
408. Yang J, AlTahan A, Jones DT, Buffa FM, Bridges E, Interiano RB, et al. Estrogen receptor-α directly regulates the hypoxia-inducible factor 1 pathway associated with antiestrogen response in breast cancer. Proceedings of the National Academy of Sciences. 2015;112(49):15172-7.
409. Ades F, Zardavas D, Bozovic-Spasojevic I, Pugliano L, Fumagalli D, De Azambuja E, et al. Luminal B breast cancer: molecular characterization, clinical management, and future perspectives. Journal of Clinical Oncology. 2014;32(25):2794-803.
410. Zhang MH, Man HT, Zhao XD, Dong N, Ma SL. Estrogen receptor-positive breast cancer molecular signatures and therapeutic potentials. Biomedical reports. 2014;2(1):41-52.
411. Semenza GL. Molecular mechanisms mediating metastasis of hypoxic breast cancer cells. Trends in molecular medicine. 2012b;18(9):534-43.
412. Ward C, Langdon SP, Mullen P, Harris AL, Harrison DJ, Supuran CT, et al. New strategies for targeting the hypoxic tumour microenvironment in breast cancer. Cancer treatment reviews. 2013;39(2):171-9.
413. Prat A, Adamo B, Cheang MC, Anders CK, Carey LA, Perou CM. Molecular characterization of basal-like and non-basal-like triple-negative breast cancer. The oncologist. 2013;18(2):123-33.
414. Ovcaricek T, Frkovic S, Matos E, Mozina B, Borstnar S. Triple negative breast cancer-prognostic factors and survival. Radiology and oncology. 2011;45(1):46-52.
415. Lee A, Djamgoz MB. Triple negative breast cancer: emerging therapeutic modalities and novel combination therapies. Cancer treatment reviews. 2018;62:110-22.
416. M Ali A, AK Ansari J, M Abd El-Aziz N, N Abozeed W, M Abdel Warith A, Alsaleh K, et al. Triple negative breast cancer: a tale of two decades. Anti-Cancer Agents in Medicinal Chemistry (Formerly Current Medicinal Chemistry-Anti-Cancer Agents). 2017;17(4):491-9.
417. Kansara S, Pandey V, Lobie PE, Sethi G, Garg M, Pandey AK. Mechanistic involvement of long non-coding RNAs in oncotherapeutics resistance in triple-negative breast cancer. Cells. 2020;9(6):1511.
418. Beketic-Oreskovic L, Maric P, Ozretic P, Oreskovic D, Ajdukovic M, Levanat S. Assessing the clinical significance of tumor markers in common neoplasms. Front Biosci (Elite Ed). 2012;4(7):2558-78.
419. Rogez-Florent T, Meignan S, Foulon C, Six P, Gros A, Bal-Mahieu C, et al. New selective carbonic anhydrase IX inhibitors: synthesis and pharmacological evaluation of diarylpyrazole-benzenesulfonamides. Bioorganic & medicinal chemistry. 2013;21(6):1451-64.
420. Kazokaitė J, Aspatwar A, Parkkila S, Matulis D. An update on anticancer drug development and delivery targeting carbonic anhydrase IX. PeerJ. 2017;5:e4068.
421. O'Reilly EA, Gubbins L, Sharma S, Tully R, Guang MHZ, Weiner-Gorzel K, et al. The fate of chemoresistance in triple negative breast cancer (TNBC). BBA clinical. 2015;3:257-75.
422. Debreova M, Csaderova L, Burikova M, Lukacikova L, Kajanova I, Sedlakova O, et al. CAIX regulates invadopodia formation through both a pH-dependent mechanism and interplay with actin regulatory proteins. International journal of molecular sciences. 2019;20(11):2745.
423. Thiry A, Dogne J-M, Masereel B, Supuran CT. Targeting tumor-associated carbonic anhydrase IX in cancer therapy. Trends in pharmacological sciences. 2006;27(11):566-73.

424. Müller V, Riethdorf S, Rack B, Janni W, Fasching PA, Solomayer E, et al. Prospective evaluation of serum tissue inhibitor of metalloproteinase 1 and carbonic anhydrase IX in correlation to circulating tumor cells in patients with metastatic breast cancer. Breast Cancer Research. 2011;13(4):1-11.
425. Gibadulinova A, Bullova P, Strnad H, Pohlodek K, Jurkovicova D, Takacova M, et al. CAIX-mediated control of LIN28/let-7 axis contributes to metabolic adaptation of breast cancer cells to hypoxia. International journal of molecular sciences. 2020;21(12):4299.
426. McDonald PC, Swayampakula M, Dedhar S. Coordinated regulation of metabolic transporters and migration/invasion by carbonic anhydrase IX. Metabolites. 2018;8(1):20.
427. Manjang K, Tripathi S, Yli-Harja O, Dehmer M, Glazko G, Emmert-Streib F. Prognostic gene expression signatures of breast cancer are lacking a sensible biological meaning. Scientific Reports. 2021;11(1):156.
428. Ashburner M, Ball CA, Blake JA, Botstein D, Butler H, Cherry JM, et al. Gene ontology: tool for the unification of biology. Nature genetics. 2000;25(1):25-9.
429. Ohotski J, Long J, Orange C, Elsberger B, Mallon E, Doughty J, et al. Expression of sphingosine 1-phosphate receptor 4 and sphingosine kinase 1 is associated with outcome in oestrogen receptor-negative breast cancer. British journal of cancer. 2012;106(8):1453-9.
430. Sadusky T, Kemp T, Simon M, Carey N, Coulton G. Identification of Serhl, a new member of the serine hydrolase family induced by passive stretch of skeletal muscle in vivo. Genomics. 2001;73(1):38-49.
431. Lee S, Stewart S, Nagtegaal I, Luo J, Wu Y, Colditz G, et al. Differentially expressed genes regulating the progression of ductal carcinoma in situ to invasive breast cancer. Cancer research. 2012;72(17):4574-86.
432. Cheng J, Greshock J, Painter J, Lin X, Lee K, Zheng S, et al. Predicting breast cancer chemotherapeutic response using a novel tool for microarray data analysis. Journal of integrative bioinformatics. 2012;9(2):80-7.
433. Wang L, Lang G-T, Xue M-Z, Yang L, Chen L, Yao L, et al. Dissecting the heterogeneity of the alternative polyadenylation profiles in triple-negative breast cancers. Theranostics. 2020;10(23):10531.
434. Patani N, Jiang W, Mokbel K. Prognostic utility of glycosyltransferase expression in breast cancer. Cancer genomics & proteomics. 2008;5(6):333-40.
435. Deng B, Tarhan YE, Ueda K, Ren L, Katagiri T, Park J-H, et al. Critical role of estrogen receptor alpha O-glycosylation by N-acetylgalactosaminyltransferase 6 (GALNT6) in its nuclear localization in breast cancer cells. Neoplasia. 2018;20(10):1038-44.
436. Freire T, Berois N, Sónora C, Varangot M, Barrios E, Osinaga E. UDP-N-acetyl-d-galactosamine: polypeptide N-acetylgalactosaminyltransferase 6 (ppGalNAc-T6) mRNA as a potential new marker for detection of bone marrow-disseminated breast cancer cells. International journal of cancer. 2006;119(6):1383-8.
437. Park J-H, Katagiri T, Chung S, Kijima K, Nakamura Y. Polypeptide N-acetylgalactosaminyltransferase 6 disrupts mammary acinar morphogenesis through O-glycosylation of fibronectin. Neoplasia. 2011;13(4):320-IN10.
438. Liu C, Li Z, Xu L, Shi Y, Zhang X, Shi S, et al. GALNT6 promotes breast cancer metastasis by increasing mucin-type O-glycosylation of α2M. Aging (Albany NY). 2020;12(12):11794.
439. Becker T, Dziadek S, Wittrock S, Kunz H. Synthetic glycopeptides from the mucin family as potential tools in cancer immunotherapy. Current cancer drug targets. 2006;6(6):491-517.
440. Conley S, Bosco E, Tice D, Hollingsworth R, Herbst R, Xiao Z. HER2 drives Mucin-like 1 to control proliferation in breast cancer cells. Oncogene. 2016;35(32):4225-34.

441. Liu Z-Z, Xie X-D, Qu S-X, Zheng Z-D, Wang Y-K. Small breast epithelial mucin (SBEM) has the potential to be a marker for predicting hematogenous micrometastasis and response to neoadjuvant chemotherapy in breast cancer. Clinical & experimental metastasis. 2010;27(4):251-9.
442. Zhang Y, Lun X, Guo W. Expression of TRPC1 and SBEM protein in breast cancer tissue and its relationship with clinicopathological features and prognosis of patients. Oncology Letters. 2020;20(6):1-.
443. Li QH, Liu ZZ, Ge YN, Liu X, Xie XD, Zheng ZD, et al. Small breast epithelial mucin promotes the invasion and metastasis of breast cancer cells via promoting epithelial-to-mesenchymal transition. Oncology Reports. 2020;44(2):509-18.
444. Jia L, Ling Y, Li K, Zhang L, Wang Y, Kang H. A 10-Gene Signature for Predicting the Response to Neoadjuvant Trastuzumab Therapy in HER2-Positive Breast Cancer. Clinical Breast Cancer. 2021.
445. Liu L, Liu Z, Qu S, Zheng Z, Liu Y, Xie X, et al. Small breast epithelial mucin tumor tissue expression is associated with increased risk of recurrence and death in triple-negative breast cancer patients. Diagnostic pathology. 2013;8(1):1-10.
446. Gaire M, Magbanua Z, McDonnell S, McNeil L, Lovett DH, Matrisian LM. Structure and expression of the human gene for the matrix metalloproteinase matrilysin. Journal of Biological Chemistry. 1994;269(3):2032-40.
447. Tan RJ, Liu Y. Matrix metalloproteinases in kidney homeostasis and diseases. American journal of physiology-renal physiology. 2012;302(11):F1351-F61.
448. Ii M, Yamamoto H, Adachi Y, Maruyama Y, Shinomura Y. Role of matrix metalloproteinase-7 (matrilysin) in human cancer invasion, apoptosis, growth, and angiogenesis. Experimental biology and medicine. 2006;231(1):20-7.
449. Wang W-S, Chen P-M, Wang H-S, Liang W-Y, Su Y. Matrix metalloproteinase-7 increases resistance to Fas-mediated apoptosis and is a poor prognostic factor of patients with colorectal carcinoma. Carcinogenesis. 2006;27(5):1113-20.
450. Von Bredow D, Nagle R, Bowden G, Cress A. Cleavage of β4 integrin by matrilysin. Experimental cell research. 1997;236(1):341-5.
451. Kim G-E, Lee JS, Choi Y-D, Lee K-H, Lee JH, Nam JH, et al. Expression of matrix metalloproteinases and their inhibitors in different immunohistochemical-based molecular subtypes of breast cancer. BMC cancer. 2014;14(1):1-10.
452. Yuan G, Qian L, Shi M, Lu F, Li D, Hu M, et al. HER2-dependent MMP-7 expression is mediated by activated STAT3. Cellular signalling. 2008b;20(7):1284-91.
453. Yuan G, Qian L, Song L, Shi M, Li D, Yu M, et al. Heregulin-β promotes matrix metalloproteinase-7 expression via HER2-mediated AP-1 activation in MCF-7 cells. Molecular and cellular biochemistry. 2008c;318(1):73-9.
454. Voorzanger-Rousselot N, Juillet F, Mareau E, Zimmermann J, Kalebic T, Garnero P. Association of 12 serum biochemical markers of angiogenesis, tumour invasion and bone turnover with bone metastases from breast cancer: a crossectional and longitudinal evaluation. British journal of cancer. 2006;95(4):506-14.
455. Mylona E, Kapranou A, Mavrommatis J, Markaki S, Keramopoulos A, Nakopoulou L. The multifunctional role of the immunohistochemical expression of MMP-7 in invasive breast cancer. Apmis. 2005;113(4):246-55.
456. Jiang WG, Davies G, Martin TA, Parr C, Watkins G, Mason MD, et al. Targeting matrilysin and its impact on tumor growth in vivo: the potential implications in breast cancer therapy. Clinical Cancer Research. 2005;11(16):6012-9.
457. Vizoso F, Gonzalez L, Corte M, Rodriguez J, Vazquez J, Lamelas M, et al. Study of matrix metalloproteinases and their inhibitors in breast cancer. British journal of cancer. 2007;96(6):903-11.
458. Gilkes DM, Semenza GL. Role of hypoxia-inducible factors in breast cancer metastasis. Future oncology. 2013;9(11):1623-36.

459. Mahara S, Lee PL, Feng M, Tergaonkar V, Chng WJ, Yu Q. HIFI-α activation underlies a functional switch in the paradoxical role of Ezh2/PRC2 in breast cancer. Proceedings of the National Academy of Sciences. 2016;113(26):E3735-E44.
460. Dai C-X, Gao Q, Qiu S-J, Ju M-J, Cai M-Y, Xu Y-F, et al. Hypoxia-inducible factor-1 alpha, in association with inflammation, angiogenesis and MYC, is a critical prognostic factor in patients with HCC after surgery. BMC cancer. 2009;9(1):418.
461. Pillai SG, Dasgupta N, Siddappa CM, Watson MA, Fleming T, Trinkaus K, et al. Paired-like Homeodomain Transcription factor 2 expression by breast cancer bone marrow disseminated tumor cells is associated with early recurrent disease development. Breast Cancer Research and Treatment. 2015;153(3):507-17.
462. Yin A, Zhang X, Wu J, Du L, He T, Zhang X. Screening significantly hypermethylated genes in fetal tissues compared with maternal blood using a methylated-CpG island recovery assay-based microarray. BMC medical genomics. 2012;5(1):1-8.
463. Rahman WFWA, Fauzi MH, Jaafar H. Expression of DNA methylation marker of paired-like homeodomain transcription factor 2 and growth receptors in invasive ductal carcinoma of the breast. Asian Pacific Journal of Cancer Prevention. 2014;15(19):8441-5.
464. Gu F, Hsu H-K, Hsu P-Y, Wu J, Ma Y, Parvin J, et al. Inference of hierarchical regulatory network of estrogen-dependent breast cancer through ChIP-based data. BMC systems biology. 2010;4(1):1-15.
465. Harbeck N, Nimmrich I, Hartmann A, Ross JS, Cufer T, Grützmann R, et al. Multicenter study using paraffin-embedded tumor tissue testing PITX2 DNA methylation as a marker for outcome prediction in tamoxifen-treated, node-negative breast cancer patients. Journal of clinical oncology. 2008;26(31):5036-42.
466. Absmaier M, Napieralski R, Schuster T, Aubele M, Walch A, Magdolen V, et al. PITX2 DNA-methylation predicts response to anthracycline-based adjuvant chemotherapy in triple-negative breast cancer patients. International Journal of Oncology. 2018;52(3):755-67.
467. Ilantzis C, Demarte L, Screaton RA, Stanners CP. Deregulated expression of the human tumor marker CEA and CEA family member CEACAM6 disrupts tissue architecture and blocks colonocyte differentiation. Neoplasia. 2002;4(2):151-63.
468. Tsang J, Kwok YK, Chan KW, Ni Y-B, Chow WNV, Lau KF, et al. Expression and clinical significance of carcinoembryonic antigen-related cell adhesion molecule 6 in breast cancers. Breast cancer research and treatment. 2013;142(2):311-22.
469. Poola I, Shokrani B, Bhatnagar R, DeWitty RL, Yue Q, Bonney G. Expression of carcinoembryonic antigen cell adhesion molecule 6 oncoprotein in atypical ductal hyperplastic tissues is associated with the development of invasive breast cancer. Clinical cancer research. 2006;12(15):4773-83.
470. Lewis-Wambi JS, Cunliffe HE, Kim HR, Willis AL, Jordan VC. Overexpression of CEACAM6 promotes migration and invasion of oestrogen-deprived breast cancer cells. European journal of cancer. 2008;44(12):1770-9.
471. Tafreshi NK, Bui MM, Bishop K, Lloyd MC, Enkemann SA, Lopez AS, et al. Noninvasive detection of breast cancer lymph node metastasis using carbonic anhydrases IX and XII targeted imaging probes. Clinical Cancer Research. 2012;18(1):207-19.
472. Khoury T, Kanehira K, Wang D, Ademuyiwa F, Mojica W, Cheney R, et al. Breast carcinoma with amplified HER2: a gene expression signature specific for trastuzumab resistance and poor prognosis. Modern Pathology. 2010;23(10):1364-78.
473. Beauchemin N, Arabzadeh A. Carcinoembryonic antigen-related cell adhesion molecules (CEACAMs) in cancer progression and metastasis. Cancer and Metastasis Reviews. 2013;32(3):643-71.
474. Maraqa L, Cummings M, Peter MB, Shaaban AM, Horgan K, Hanby AM, et al. Carcinoembryonic antigen cell adhesion molecule 6 predicts breast cancer recurrence following adjuvant tamoxifen. Clinical Cancer Research. 2008;14(2):405-11.

475. Blumenthal RD, Hansen HJ, Goldenberg DM. Inhibition of adhesion, invasion, and metastasis by antibodies targeting CEACAM6 (NCA-90) and CEACAM5 (Carcinoembryonic Antigen). Cancer research. 2005;65(19):8809-17.
476. Afratis N, Gialeli C, Nikitovic D, Tsegenidis T, Karousou E, Theocharis AD, et al. Glycosaminoglycans: key players in cancer cell biology and treatment. The FEBS journal. 2012;279(7):1177-97.
477. Pohl S-G, Brook N, Agostino M, Arfuso F, Kumar AP, Dharmarajan A. Wnt signaling in triple-negative breast cancer. Oncogenesis. 2017;6(4):e310-e.
478. Oskarsson T. Extracellular matrix components in breast cancer progression and metastasis. The Breast. 2013;22:S66-S72.
479. Dey N, Barwick BG, Moreno CS, Ordanic-Kodani M, Chen Z, Oprea-Ilies G, et al. Wnt signaling in triple negative breast cancer is associated with metastasis. BMC cancer. 2013;13(1):1-15.
480. Han B, Zhou B, Qu Y, Gao B, Xu Y, Chung S, et al. FOXC1-induced non-canonical WNT5A-MMP7 signaling regulates invasiveness in triple-negative breast cancer. Oncogene. 2018;37(10):1399-408.
481. Nathanson SD. Insights into the mechanisms of lymph node metastasis. Cancer. 2003;98(2):413-23.
482. Saier Jr MH, Beatty JT, Goffeau A, Harley KT, Heijne W, Huang S-C, et al. The major facilitator superfamily. J Mol Microbiol Biotechnol. 1999;1(2):257-79.
483. Zheng X, Li W, Ren L, Liu J, Pang X, Chen X, et al. The sphingosine kinase-1/sphingosine-1-phosphate axis in cancer: Potential target for anticancer therapy. Pharmacology & therapeutics. 2019;195:85-99.
484. Blaho VA, Hla T. An update on the biology of sphingosine 1-phosphate receptors. Journal of lipid research. 2014;55(8):1596-608.
485. Pyne S, Adams DR, Pyne NJ. Sphingosine 1-phosphate and sphingosine kinases in health and disease. 2016.
486. Nagahashi M, Ramachandran S, Kim EY, Allegood JC, Rashid OM, Yamada A, et al. Sphingosine-1-phosphate produced by sphingosine kinase 1 promotes breast cancer progression by stimulating angiogenesis and lymphangiogenesis. Cancer research. 2012;72(3):726-35.
487. Tsuchida J, Nagahashi M, Nakajima M, Moro K, Tatsuda K, Ramanathan R, et al. Breast cancer sphingosine-1-phosphate is associated with phospho-sphingosine kinase 1 and lymphatic metastasis. journal of surgical research. 2016;205(1):85-94.
488. Sarkar S, Maceyka M, Hait NC, Paugh SW, Sankala H, Milstien S, et al. Sphingosine kinase 1 is required for migration, proliferation and survival of MCF-7 human breast cancer cells. FEBS letters. 2005;579(24):5313-7.
489. Datta A, Loo SY, Huang B, Wong L, Tan SS, Tan TZ, et al. SPHK1 regulates proliferation and survival responses in triple-negative breast cancer. Oncotarget. 2014;5(15):5920.
490. Acharya S, Yao J, Li P, Zhang C, Lowery FJ, Zhang Q, et al. Sphingosine kinase 1 signaling promotes metastasis of triple-negative breast cancer. Cancer research. 2019;79(16):4211-26.
491. Long JS, Edwards J, Watson C, Tovey S, Mair KM, Schiff R, et al. Sphingosine kinase 1 induces tolerance to human epidermal growth factor receptor 2 and prevents formation of a migratory phenotype in response to sphingosine 1-phosphate in estrogen receptor-positive breast cancer cells. Molecular and cellular biology. 2010a;30(15):3827-41.
492. Ruckhäberle E, Rody A, Engels K, Gaetje R, von Minckwitz G, Schiffmann S, et al. Microarray analysis of altered sphingolipid metabolism reveals prognostic significance of sphingosine kinase 1 in breast cancer. Breast cancer research and treatment. 2008;112(1):41-52.

493. Sukocheva O, Wang L, Verrier E, Vadas MA, Xia P. Restoring endocrine response in breast cancer cells by inhibition of the sphingosine kinase-1 signaling pathway. Endocrinology. 2009;150(10):4484-92.
494. Watson C, Long JS, Orange C, Tannahill CL, Mallon E, McGlynn LM, et al. High expression of sphingosine 1-phosphate receptors, S1P1 and S1P3, sphingosine kinase 1, and extracellular signal-regulated kinase-1/2 is associated with development of tamoxifen resistance in estrogen receptor-positive breast cancer patients. The American journal of pathology. 2010;177(5):2205-15.
495. Wang S, Liang Y, Chang W, Hu B, Zhang Y. Triple negative breast cancer depends on sphingosine kinase 1 (SphK1)/sphingosine-1-phosphate (S1P)/sphingosine 1-phosphate receptor 3 (S1PR3)/notch signaling for metastasis. Medical science monitor: international medical journal of experimental and clinical research. 2018;24:1912.
496. Goetzl EJ, Dolezalova H, Kong Y, Zeng L. Dual mechanisms for lysophospholipid induction of proliferation of human breast carcinoma cells. Cancer research. 1999;59(18):4732-7.
497. Fang L, Hou J, Cao Y, Shan J-J, Zhao J. Spinster homolog 2 in cancers, its functions and mechanisms. Cellular Signalling. 2021;77:109821.
498. Long JS, Fujiwara Y, Edwards J, Tannahill CL, Tigyi G, Pyne S, et al. Sphingosine 1-phosphate receptor 4 uses HER2 (ERBB2) to regulate extracellular signal regulated kinase-1/2 in MDA-MB-453 breast cancer cells. Journal of Biological Chemistry. 2010b;285(46):35957-66.
499. Sukocheva O, Wadham C, Xia P. Estrogen defines the dynamics and destination of transactivated EGF receptor in breast cancer cells: Role of S1P3 receptor and Cdc42. Experimental cell research. 2013;319(4):455-65.
500. Hait NC, Bellamy A, Milstien S, Kordula T, Spiegel S. Sphingosine kinase type 2 activation by ERK-mediated phosphorylation. Journal of Biological Chemistry. 2007;282(16):12058-65.
501. Ader I, Brizuela L, Bouquerel P, Malavaud B, Cuvillier O. Sphingosine kinase 1: a new modulator of hypoxia inducible factor 1α during hypoxia in human cancer cells. Cancer research. 2008;68(20):8635-42.
502. Schwalm S, Döll F, Römer I, Bubnova S, Pfeilschifter J, Huwiler A. Sphingosine kinase-1 is a hypoxia-regulated gene that stimulates migration of human endothelial cells. Biochemical and biophysical research communications. 2008;368(4):1020-5.
503. Anelli V, Gault CR, Cheng AB, Obeid LM. Sphingosine kinase 1 is up-regulated during hypoxia in U87MG glioma cells: role of hypoxia-inducible factors 1 and 2. Journal of Biological Chemistry. 2008;283(6):3365-75.
504. Bouquerel P, Gstalder C, Müller D, Laurent J, Brizuela L, Sabbadini R, et al. Essential role for SphK1/S1P signaling to regulate hypoxia-inducible factor 2α expression and activity in cancer. Oncogenesis. 2016;5(3):e209-e.
505. Schnitzer SE, Weigert A, Zhou J, Brüne B. Hypoxia enhances sphingosine kinase 2 activity and provokes sphingosine-1-phosphate-mediated chemoresistance in A549 lung cancer cells. Molecular Cancer Research. 2009;7(3):393-401.
506. Ahmad M, Long JS, Pyne NJ, Pyne S. The effect of hypoxia on lipid phosphate receptor and sphingosine kinase expression and mitogen-activated protein kinase signaling in human pulmonary smooth muscle cells. Prostaglandins & other lipid mediators. 2006;79(3-4):278-86.
507. Li G, Hu J, Hu G. Biomarker studies in early detection and prognosis of breast cancer. Translational Research in Breast Cancer. 2017:27-39.
508. Li M-X, Jin L-T, Wang T-J, Feng Y-J, Pan C-P, Zhao D-M, et al. Identification of potential core genes in triple negative breast cancer using bioinformatics analysis. OncoTargets and therapy. 2018;11:4105.

509. Stewart RL, Matynia AP, Factor RE, Varley KE. Spatially-resolved quantification of proteins in triple negative breast cancers reveals differences in the immune microenvironment associated with prognosis. Scientific reports. 2020;10(1):1-8.
510. Zollinger DR, Lingle SE, Sorg K, Beechem JM, Merritt CR. GeoMx™ RNA assay: High multiplex, digital, spatial analysis of RNA in FFPE tissue. In Situ Hybridization Protocols: Springer; 2020. p. 331-45.
511. Ni C, Yang L, Xu Q, Yuan H, Wang W, Xia W, et al. CD68-and CD163-positive tumor infiltrating macrophages in non-metastatic breast cancer: a retrospective study and meta-analysis. Journal of Cancer. 2019;10(19):4463.
512. Rathore AS, Kumar S, Konwar R, Makker A, Negi M, Goel MM. CD3+, CD4+ & CD8+ tumour infiltrating lymphocytes (TILs) are predictors of favourable survival outcome in infiltrating ductal carcinoma of breast. The Indian journal of medical research. 2014;140(3):361.
513. Bouchalova K, Kharaishvili G, Bouchal J, Vrbkova J, Megova M, Hlobilkova A. Triple negative breast cancer-BCL2 in prognosis and prediction. Review. Current drug targets. 2014;15(12):1166-75.
514. Zhao X, Qu J, Sun Y, Wang J, Liu X, Wang F, et al. Prognostic significance of tumor-associated macrophages in breast cancer: a meta-analysis of the literature. Oncotarget. 2017b;8(18):30576.
515. Mahmoud S, Lee A, Paish E, Macmillan R, Ellis I, Green A. Tumour-infiltrating macrophages and clinical outcome in breast cancer. Journal of clinical pathology. 2012;65(2):159-63.
516. Bingle L, Brown N, Lewis CE. The role of tumour-associated macrophages in tumour progression: implications for new anticancer therapies. The Journal of Pathology: A Journal of the Pathological Society of Great Britain and Ireland. 2002;196(3):254-65.
517. Huang S, Van Arsdall M, Tedjarati S, McCarty M, Wu W, Langley R, et al. Contributions of stromal metalloproteinase-9 to angiogenesis and growth of human ovarian carcinoma in mice. Journal of the National Cancer Institute. 2002;94(15):1134-42.
518. Yuan Z-Y, Luo R-Z, Peng R-J, Wang S-S, Xue C. High infiltration of tumor-associated macrophages in triple-negative breast cancer is associated with a higher risk of distant metastasis. OncoTargets and therapy. 2014;7:1475.
519. Ch'ng ES, Tuan Sharif SE, Jaafar H. In human invasive breast ductal carcinoma, tumor stromal macrophages and tumor nest macrophages have distinct relationships with clinicopathological parameters and tumor angiogenesis. Virchows Archiv. 2013;462(3):257-67.
520. Hayashi Y, Yokota A, Harada H, Huang G. Hypoxia/pseudohypoxia-mediated activation of hypoxia-inducible factor-1α in cancer. Cancer science. 2019;110(5):1510-7.
521. Akanji MA, Rotimi D, Adeyemi OS. Hypoxia-inducible factors as an alternative source of treatment strategy for cancer. Oxidative medicine and cellular longevity. 2019;2019.
522. Wyss CB, Duffey N, Peyvandi S, Barras D, Usatorre AM, Coquoz O, et al. Gain of HIF1 activity and loss of miRNA let-7d promote breast cancer metastasis to the brain via the PDGF/PDGFR axis. Cancer Research. 2021;81(3):594-605.
523. Ebright RY, Zachariah MA, Micalizzi DS, Wittner BS, Niederhoffer KL, Nieman LT, et al. HIF1A signaling selectively supports proliferation of breast cancer in the brain. Nature communications. 2020;11(1):1-13.
524. Iizuka A, Nonomura C, Ashizawa T, Kondou R, Ohshima K, Sugino T, et al. A T-cell–engaging B7-H4/CD3-bispecific Fab-scFv antibody targets human breast cancer. Clinical Cancer Research. 2019;25(9):2925-34.
525. Lecerf C, Kamal M, Vacher S, Chemlali W, Schnitzler A, Morel C, et al. Immune gene expression in head and neck squamous cell carcinoma patients. European Journal of Cancer. 2019;121:210-23.

526. Li L, Huang H, Zhu M, Wu J. Identification of Hub Genes and Pathways of Triple Negative Breast Cancer by Expression Profiles Analysis. Cancer Management and Research. 2021;13:2095.
527. Wang Q, Li P, Wu W. A systematic analysis of immune genes and overall survival in cancer patients. BMC cancer. 2019;19(1):1-9.
528. Blackley EF, Loi S. Targeting immune pathways in breast cancer: review of the prognostic utility of TILs in early stage triple negative breast cancer (TNBC). The Breast. 2019;48:S44-S8.
529. Moradi-Kalbolandi S, Sharifi-K A, Darvishi B, Majidzadeh-A K, Sadeghi S, Mosayebzadeh M, et al. Evaluation the potential of recombinant anti-CD3 nanobody on immunomodulatory function. Molecular immunology. 2020;118:174-81.
530. Khatibi AS, Roodbari NH, Majidzade-A K, Yaghmaei P, Farahmand L. In vivo tumor-suppressing and anti-angiogenic activities of a recombinant anti-CD3ε nanobody in breast cancer mice model. Immunotherapy. 2019;11(18):1555-67.
531. Calcinotto A, Filipazzi P, Grioni M, Iero M, De Milito A, Ricupito A, et al. Modulation of Microenvironment Acidity Reverses Anergy in Human and Murine Tumor-Infiltrating T LymphocytespH and T-Cell Anergy. Cancer research. 2012;72(11):2746-56.
532. Serganova I, Cohen IJ, Vemuri K, Shindo M, Maeda M, Mane M, et al. LDH-A regulates the tumor microenvironment via HIF-signaling and modulates the immune response. PLoS One. 2018;13(9):e0203965.
533. Chafe SC, McDonald PC, Saberi S, Nemirovsky O, Venkateswaran G, Burugu S, et al. Targeting hypoxia-induced carbonic anhydrase IX enhances immune-checkpoint blockade locally and systemically. Cancer immunology research. 2019;7(7):1064-78.
534. Vaux DL, Cory S, Adams JM. Bcl-2 gene promotes haemopoietic cell survival and cooperates with c-myc to immortalize pre-B cells. Nature. 1988;335(6189):440-2.
535. McDonnell TJ, Deane N, Platt FM, Nunez G, Jaeger U, McKearn JP, et al. bcl-2-immunoglobulin transgenic mice demonstrate extended B cell survival and follicular lymphoproliferation. Cell. 1989;57(1):79-88.
536. Kirkin V, Joos S, Zörnig M. The role of Bcl-2 family members in tumorigenesis. Biochimica et Biophysica Acta (BBA)-Molecular Cell Research. 2004;1644(2-3):229-49.
537. Merino D, Lok S, Visvader J, Lindeman G. Targeting BCL-2 to enhance vulnerability to therapy in estrogen receptor-positive breast cancer. Oncogene. 2016;35(15):1877-87.
538. Bouchalova K, Svoboda M, Kharaishvili G, Vrbkova J, Bouchal J, Trojanec R, et al. BCL2 is an independent predictor of outcome in basal-like triple-negative breast cancers treated with adjuvant anthracycline-based chemotherapy. Tumor Biology. 2015;36(6):4243-52.
539. Kallel-Bayoudh I, Hassen HB, Khabir A, Boujelbene N, Daoud J, Frikha M, et al. Bcl-2 expression and triple negative profile in breast carcinoma. Medical Oncology. 2011;28(1):55-61.
540. Rhee J, Han S-W, Oh D-Y, Kim JH, Im S-A, Han W, et al. The clinicopathologic characteristics and prognostic significance of triple-negativity in node-negative breast cancer. BMC cancer. 2008;8(1):1-8.
541. Abdel-Fatah T, Perry C, Dickinson P, Ball G, Moseley P, Madhusudan S, et al. Bcl2 is an independent prognostic marker of triple negative breast cancer (TNBC) and predicts response to anthracycline combination (ATC) chemotherapy (CT) in adjuvant and neoadjuvant settings. Annals of oncology. 2013;24(11):2801-7.
542. Zinkel S, Gross A, Yang E. BCL2 family in DNA damage and cell cycle control. Cell Death & Differentiation. 2006;13(8):1351-9.
543. Joensuu H, Pylkkänen L, Toikkanen S. Bcl-2 protein expression and long-term survival in breast cancer. The American journal of pathology. 1994;145(5):1191.
544. Mitrović O, Čokić V, Đikić D, Budeč M, Vignjević S, Subotički T, et al. Correlation between ER, PR, HER-2, Bcl-2, p53, proliferative and apoptotic indexes with

HER-2 gene amplification and TOP2A gene amplification and deletion in four molecular subtypes of breast cancer. Targeted oncology. 2014;9(4):367-79.
545. Cheng EH-Y, Kirsch DG, Clem RJ, Ravi R, Kastan MB, Bedi A, et al. Conversion of Bcl-2 to a Bax-like death effector by caspases. Science. 1997;278(5345):1966-8.
546. Redondo M. Bcl-2, an antiapoptotic gene indicator of good prognosis in breast cancer: The paradox. J Carcinogene Mutagene. 2013;4(02):134.
547. Greijer A, Van der Wall E. The role of hypoxia inducible factor 1 (HIF-1) in hypoxia induced apoptosis. Journal of clinical pathology. 2004;57(10):1009-14.
548. Corbet C, Feron O. Tumour acidosis: from the passenger to the driver's seat. Nature Reviews Cancer. 2017;17(10):577-93.
549. Wang T, Liu G, Wang R. The intercellular metabolic interplay between tumor and immune cells. Frontiers in immunology. 2014c;5:358.
550. Dietl K, Renner K, Dettmer K, Timischl B, Eberhart K, Dorn C, et al. Lactic acid and acidification inhibit TNF secretion and glycolysis of human monocytes. The Journal of Immunology. 2010;184(3):1200-9.
551. Terry S, Faouzi Zaarour R, Hassan Venkatesh G, Francis A, El-Sayed W, Buart S, et al. Role of hypoxic stress in regulating tumor immunogenicity, resistance and plasticity. International journal of molecular sciences. 2018;19(10):3044.
552. Meng W, Hao Y, He C, Li L, Zhu G. Exosome-orchestrated hypoxic tumor microenvironment. Molecular cancer. 2019;18(1):1-14.
553. Chen P-S, Chiu W-T, Hsu P-L, Lin S-C, Peng I-C, Wang C-Y, et al. Pathophysiological implications of hypoxia in human diseases. Journal of biomedical science. 2020;27:1-19.
554. Farina AR, Cappabianca L, Sebastiano M, Zelli V, Guadagni S, Mackay AR. Hypoxia-induced alternative splicing: the 11th Hallmark of Cancer. Journal of Experimental & Clinical Cancer Research. 2020;39(1):1-30.
555. Mo Z, Yu L, Cao Z, Hu H, Luo S, Zhang S. Identification of a hypoxia-associated signature for lung adenocarcinoma. Frontiers in genetics. 2020;11:647.
556. Bennett L, Quinn J, McCall P, Mallon EA, Horgan PG, McMillan DC, et al. High IKKα expression is associated with reduced time to recurrence and cancer specific survival in oestrogen receptor (ER)-positive breast cancer. Int J Cancer. 2017;140(7):1633-44.
557. Espinoza-Sanchez NA, Gyorffy B, Fuentes-Panana EM, Gotte M. Differential impact of classical and non-canonical NF-kappaB pathway-related gene expression on the survival of breast cancer patients. J Cancer. 2019;10(21):5191-211.
558. True LD. Quality control in molecular immunohistochemistry. Histochemistry and cell biology. 2008;130(3):473-80.
559. Jiang B-H, Semenza GL, Bauer C, Marti HH. Hypoxia-inducible factor 1 levels vary exponentially over a physiologically relevant range of O2 tension. American Journal of Physiology-Cell Physiology. 1996;271(4):C1172-C80.
560. Hedley D, Pintilie M, Woo J, Morrison A, Birle D, Fyles A, et al. Carbonic anhydrase IX expression, hypoxia, and prognosis in patients with uterine cervical carcinomas. Clinical Cancer Research. 2003;9(15):5666-74.
561. Shafee N, Kaluz S, Ru N, Stanbridge EJ. PI3K/Akt activity has variable cell-specific effects on expression of HIF target genes, CA9 and VEGF, in human cancer cell lines. Cancer letters. 2009;282(1):109-15.
562. Mao Y, Zhang Y, Fan S, Chen L, Tang L, Chen X, et al. GALNT6 promotes tumorigenicity and metastasis of breast cancer cell via β-catenin/MUC1-C signaling pathway. International Journal of Biological Sciences. 2019;15(1):169.
563. Sizemore ST, Sizemore GM, Booth CN, Thompson CL, Silverman P, Bebek G, et al. Hypomethylation of the MMP7 promoter and increased expression of MMP7 distinguishes the basal-like breast cancer subtype from other triple-negative tumors. Breast cancer research and treatment. 2014;146(1):25-40.

564. Fu O-Y, Hou M-F, Yang S-F, Huang S-C, Lee W-Y. Cobalt chloride-induced hypoxia modulates the invasive potential and matrix metalloproteinases of primary and metastatic breast cancer cells. Anticancer research. 2009;29(8):3131-8.
565. Ohotski J, Rosen H, Bittman R, Pyne S, Pyne NJ. Sphingosine kinase 2 prevents the nuclear translocation of sphingosine 1-phosphate receptor-2 and tyrosine 416 phosphorylated c-Src and increases estrogen receptor negative MDA-MB-231 breast cancer cell growth: The role of sphingosine 1-phosphate receptor-4. Cellular signalling. 2014;26(5):1040-7.
566. Hait NC, Maiti A, Xu P, Qi Q, Kawaguchi T, Okano M, et al. Regulation of hypoxia-inducible factor functions in the nucleus by sphingosine-1-phosphate. The FASEB Journal. 2020;34(3):4293-310.
567. Jeong H, Kim S, Hong B-J, Lee C-J, Kim Y-E, Bok S, et al. Tumor-associated macrophages enhance tumor hypoxia and aerobic glycolysis. Cancer research. 2019;79(4):795-806.
568. Mirchandani AS, Jenkins SJ, Bain CC, Sanchez-Garcia MA, Lawson H, Coelho P, et al. Hypoxia shapes the immune landscape in lung injury and promotes the persistence of inflammation. Nature Immunology. 2022:1-13.
569. Sun X, Zhai J, Sun B, Parra ER, Jiang M, Ma W, et al. Effector memory cytotoxic CD3+/CD8+/CD45RO+ T cells are predictive of good survival and a lower risk of recurrence in triple-negative breast cancer. Modern Pathology. 2022;35(5):601-8.
570. Hwang KT, Woo JW, Shin HC, Kim HS, Ahn SK, Moon HG, et al. Prognostic influence of BCL2 expression in breast cancer. International journal of cancer. 2012;131(7):E1109-E19.
571. Bos R, van Diest PJ, van der Groep P, Shvarts A, Greijer AE, van der Wall E. Expression of hypoxia-inducible factor-1α and cell cycle proteins in invasive breast cancer are estrogen receptor related. Breast Cancer Research. 2004;6(4):1-10.
572. Biroccio A, Candiloro A, Mottolese M, Sapora O, Albini A, Zupi G, et al. Bcl-2 overexpression and hypoxia synergistically act to modulate vascular endothelial growth factor expression and in vivo angiogenesis in a breast carcinoma line. The FASEB Journal. 2000;14(5):652-60.

Appendix

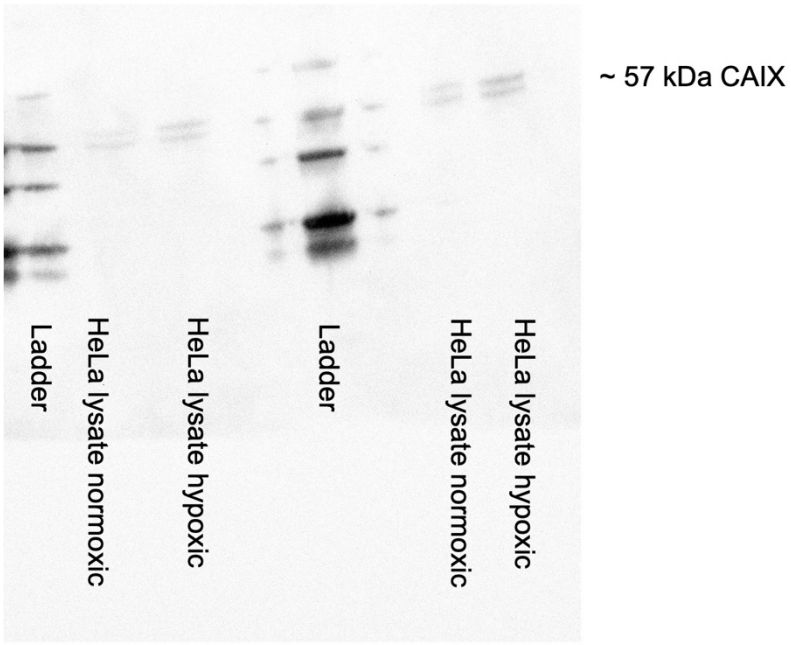
~ 57 kDa CAIX
HeLa lysate hypoxic
HeLa lysate normoxic
Ladder
HeLa lysate hypoxic
HeLa lysate normoxic
Ladder

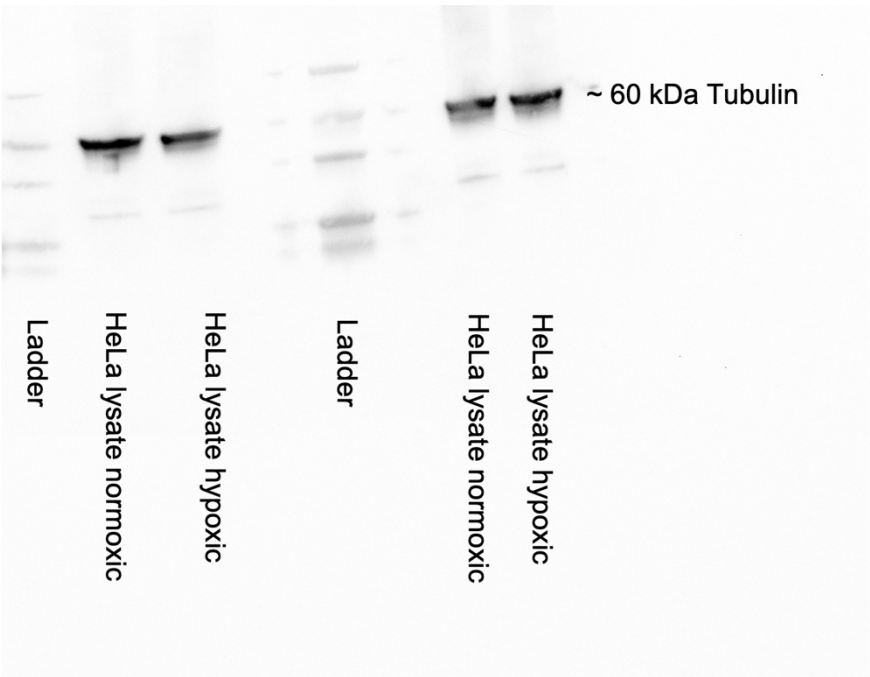
~ 60 kDa Tubulin
HeLa lysate hypoxic
HeLa lysate normoxic
Ladder
HeLa lysate hypoxic
HeLa lysate normoxic
Ladder

```
#Install counts and ss files
sample_sheet = read.table("/gl93v/Desktop/Suad Transcriptomic data/CAIX_Sample_Sheet.csv",
header=TRUE, row.names=1, sep=',')
counts =read.table ("/gl93v/Desktop/Suad Transcriptomic data/CAIX_new_counts.csv",
header=TRUE, row.names=, sep=',')

#Parse sample_sheet
sample_sheet=na.omit(sample_sheet)

#creating master
counts=t(counts)

merged_tables = merge(counts, sample_sheet, by=0)
master = merged_tables
row.names(master)=master[,1]

# sort by CAIX status
master = master[order(master[,"CAIX_Status"]),]

#new counts table removing samples which status is unknown
counts=master[,2:19702]
counts=t(counts)

#new sample sheet to remove samples with no corresponding gene counts
sample_sheet=master[,-(2:19702)]

#write.table(sample_sheet, file="/gl93v/Desktop/Batch1 TempOSeq/KRAS/SS_KRAS.csv",
row.names=FALSE, sep="\t",quote=FALSE)

#Filter read to remove non-expressed genes
counts = subset(counts,apply(counts, 1, mean) >=1)
nrow(counts)
counts=as.matrix(counts)

#Prepare sample information
colnames(sample_sheet)=c("Sample_IDs", "CAIX_Status")
sample_group=factor(sample_sheet$CAIX_Status)

sample_data=data.frame(row.names=colnames(counts), sample_group)

#Running DESeq2
dds = DESeqDataSetFromMatrix(countData=counts, colData=sample_data,
design=~sample_group)
dds=DESeq(dds)

#Extract results from dds
norm_counts=as.data.frame(counts(dds, normalized=TRUE))
```

```
norm_counts=round(norm_counts,2)

#Save to Disk
norm_counts_out=data.frame(row.names(norm_counts))
names(norm_counts_out)="id"
norm_counts_out=cbind(norm_counts_out,norm_counts)
#write.table(norm_counts_out, file="/gl93v/Desktop/Suad Transcriptomic data/EM_CAIX.tsv",
row.names=FALSE, sep="\t", quote=FALSE)
em=norm_counts_out
em=em[,-1]

#Extract differential info from DESeq2
de=results(dds, c("sample_group","0","1"))
de_table=as.data.frame(de)

#Clean up de_table
de_out=de_table
de_out=de_out[order(de_out$padj),]
de_out$id=row.names(de_out)
de_out=de_out[,c(7,2,5,6)]
colnames(de_out)=c("id","log2fold","p","p.adj")
#write.table(de_out, file="/gl93v/Desktop/Suad Transcriptomic data/DE_CAIX.tsv",
row.names=FALSE, sep="\t",quote=FALSE)

#creating master
de=de_out[,-1]
merged_tables = merge(em,de,by=0)
master = merged_tables
row.names(master)=master[,1]

names(master)[1]="Genes"
master=na.omit(master)

#Sort master by p-value
order(master[,"p"], decreasing=FALSE)
order(master[,"log2fold"], decreasing=FALSE)
sorted_order = order(master[,"p"], decreasing=FALSE)
master = master [sorted_order,]
master=master[,-1]

#Making a new column in your master table for mean expression
master$meanvalue = rowMeans(master[,1:37])

#Add a column for -log10p to the master table
master$mlog10p=-log10(master $p)
master

#new column flagging significance to the master table
master$sig = as.factor(master$p.adj < 0.1 & abs(master$log2fold) > 1.0)
master$Log2fold_up_down = as.factor(abs(master$log2fold) >1.0)
```

```
#gene IDs for expression table
em_symbols=master[,1:37]

#Make a scaled expression matrix
em_scaled = data.frame(t(scale(t(em_symbols))))
em_scaled = na.omit(em_scaled)

#List of sig genes
master_sig = subset(master, p.adj<0.1 & abs(master$log2fold)>1)
sig_genes = row.names (master_sig)
master_sig_up = subset(master,p.adj<0.1 & log2fold>1)
master_sig_down = subset(master, p.adj<0.1 & log2fold< -1)

#Make expression tables of significant genes only
em_symbols_sig = em_symbols[sig_genes,]

#Make em_symbols
em_symbols_20=em_symbols[1:20,]

#Make scaled expression value table
em_scaled_sig = em_scaled[sig_genes,]

#Write master table
write.table(em_symbols_20, file="/gl93v/Desktop/Suad Transcriptomic data/EM_symbols_20.tsv",
row.names=TRUE, sep="\t",quote=FALSE)

#Write master table
write.table(master, file="/gl93v/Desktop/Suad Transcriptomic data/CAIX_master.tsv",
row.names=TRUE, sep="\t",quote=FALSE)

#Volcano plot
ggp = ggplot(master, aes(x=log2fold, y=mlog10p)) +
  geom_point(data=master, colour="black", size=1)+
  geom_point(data=master_sig_up, colour="red", size=1)+
  geom_point(data=master_sig_down, colour="blue", size=1)+
  labs(title="Volcano plot, CAIX Low vs High", x="log2 fold change", y="-log10 p-value")+
  theme_classic()+
  geom_vline(xintercept=-1, linetype="dashed", colour="grey", size=0.5)+
  geom_hline(yintercept=-log10(0.05), linetype="dashed", colour="grey", size=0.5)+
  geom_vline(xintercept=1, linetype="dashed", colour="grey", size=0.5)+
  xlim(c(-19,19))+
  ylim(c(0,10))+

## adds the text labels for top 5 genes
#geom_text(data=master_sig_up, aes(label=x, colour = "red" , hjust=-0.1, vjust=-0.1,
show.legend=FALSE)
#geom_text(data=master_sig_down, aes(label=gene_symbol), colour = "blue", hjust=1, vjust=-0.1,
show.legend=FALSE)
```

```
png("/gl93v/Desktop/Suad Transcriptomic data/volcanoplot_CAIX.png", height=400, width=400)
print(ggp)
dev.off()
```

##-- MA --##

```
# make plot
ggp = ggplot(master, aes(x=log10(meanvalue), y=log2fold)) +

  # adds the dots
  geom_point(colour = "black") +
geom_point(data=master_sig_up, colour = "red") +
geom_point(data=master_sig_down, colour = "blue") +

# adds the fancy lines
geom_hline(yintercept=1,linetype="dashed") +
geom_hline(yintercept=-1,linetype="dashed") +

# adds the theme and axis titles
theme_classic() +
labs(title = "MA plot, CAIX Low vs High", x=expression("Mean expression (log"[10]*")"),
y=expression("Change in log"[2]*"fold"))+

  ylim(c(-20,15))
png("/gl93v/Desktop/Suad Transcriptomic data/MA_CAIX.png", height=400, width=400)
print(ggp)
dev.off()


#load sample sheet
#ss1 = read.table("/gl93v/Desktop/Batch1 TempOSeq/KRAS/KRASstatus_SS.csv",
header=TRUE, sep=',')
#colnames(ss1)=c("Sample","Sample_group")
```

##-- PCA plot for PC1 vs PC2--##

```
#Casting the expression matrix data table into a numeric matrix
EM.nm = as.matrix(sapply(em_symbols, as.numeric))

#prcomp() function n.b. works by column not row so we need to transpose.
pca = prcomp(t(EM.nm))

#Extract component data
pca_coordinates = data.frame(pca$x)

#Secree plot of variation
pca.var = pca$sdev^2
pca.var.per = round(pca.var/sum(pca.var)*100,1)
barplot(pca.var.per, main="Scree Plot", xlab="Principal Component", ylab="Percent Variation")
```

#Defining x and y axis %

```
vars = apply(pca$x, 2, var)
prop_x = round(vars["PC1"] / sum(vars),4) * 100
prop_y = round(vars["PC2"] / sum(vars),4) * 100
x_axis_label = paste("PC1", "(",prop_x,"%)", sep="")
y_axis_label = paste("PC2 ","(",prop_y,"%)", sep="")
```

#adding colour to dots

```
ggp= ggplot(pca_coordinates, aes(x=PC1, y=PC2, colour = sample_group))+
  geom_point()+
  scale_colour_manual(values=c("red","blue"))+
  labs(title = "PCA", x= x_axis_label, y= y_axis_label)+
  theme_gray()+
xlim(c(-0.5e+5,0.5e+5))+
 ylim(c(-0.5e+5,0.5e+5))

write.table(pca_coordinates, file="/gl93v/Desktop/Suad Transcriptomic data/pca_coordinates.tsv",
row.names=TRUE, sep="\t",quote=FALSE)

png(paste("/gl93v/Desktop/Suad Transcriptomic
data/PCAplot_CAIX_v3",".png",sep=""),height=400,width=400)
print(ggp)
dev.off()
```